PHYTOPATHOGENIC AND POST-HARVEST FUNGI ON SELECTED ECONOMICALLY FRUITS IN NORTHERN THAILAND

ALIREZA ARMAND

DOCTER OF PHILOSOPHY

IN

BIOLOGICAL SCIENCE

SCHOOL OF SCIENCE

MAE FAH LUANG UNIVERSITY

2024

©COPYRIGHT BY MAE FAH LUANG UNIVERSITY

PHYTOPATHOGENIC AND POST-HARVEST FUNGI ON SELECTED ECONOMICALLY FRUITS IN NORTHERN THAILAND

ALIREZA ARMAND

THIS DISSERTATION IS A PARTIAL FULFILLMENT OF THE REQUIREMENTS FOR THE DEGREE OF DOCTOR OF PHILOSOPHY IN BIOLOGICAL SCIENCE

SCHOOL OF SCIENCE
MAE FAH LUANG UNIVERSITY
2024
©COPYRIGHT BY MAE FAH LUANG UNIVERSITY

DISSERTATION APPROVAL

MAE FAH LUANG UNIVERSITY

FOR

DOCTOR OF PHILOSOPHY IN BIOLOGICAL SCIENCE

Dissertation Title: Phytopathogenic and Post-harvest Fungi on Selected Economically Fruits in Northern Thailand

Author: Alireza Armand

Examination Committee:

Professor Sajeewa Sandeshya Nilukana Maharachchikumbura, Ph. D.	Chairperson
Assistant Professor Kitiphong Khongphinitbunjong, Ph. D.	Member
Adjunct Professor Kevin David Hyde, Ph. D.	Member
Mahamarakkalage Mary Ruvishika Shehali Jayawardena, Ph. D.	Member
Thilini Chethana Kandawatte Wedaralalage, Ph. D.	Member
Ishara Sandeepani Manawasinghe, Ph. D.	Member

Advisors:

Kitiphong .....Advisor

(Assistant Professor Kitiphong Khongphinitbunjong, Ph. D.)

.....Co-Advisor

(Adjunct Professor Kevin David Hyde, Ph. D.)

.....Co-Advisor

(Mahamarakkalage Mary Ruvishika Shehali Jayawardena, Ph. D.)

Dean:

.....

(Professor Surat Laphookhieo, Ph. D.)

ACKNOWLEDGEMENTS

Firstly, I would like to express my deepest appreciation to my advisor, Arjan Dr. Kitiphong Khongphinitbunjong for his invaluable help and encouragement throughout my research work. I'm extremely grateful to my co-advisors, Emeritus Prof. Dr. Kevin David Hyde and Assoc. Prof. Dr. Ruvishika Shehali Jayawardena who gave me the opportunity to do research and provide invaluable guidance throughout my research work. I would not have achieved this far and this thesis would not have been completed without all the support that I have always received from them. I am grateful to my thesis committee for their valuable feedback and support, which inspired me to expand my research from multiple aspects. I would also like to thank Mushroom Research Foundation (MRF), Chiang Rai Province, Thailand for providing Postgraduate Scholarship. I extend my profound gratitude to Office of Postgraduate Studies, School of Science, Mae Fah Luang University, Thailand, for providing me the Thesis and Dissertation Writing Grant.

A special word of gratitude is due to Prof. Dr. Rasoul Zare and Assoc. Prof. Dr. Mounes Bakhshi for introducing me to Prof. Hyde and facilitating the process to carry out the research work in Thailand. I would like to thank Digvijayini Bundhun, my mentor for teaching me all the basic knowledge of mycology when I started my study. I would like to express my gratitude to Dr. Thilini, Dr. Saranyaphat Boonmee, Dr. Chitrabhanu Sharma Bhunjun, Prof. Sajeewa, Prof. Uwe Braun, Prof. Paul Taylor, Dr. Erick McKenzie, Dr. Indunil Chinthani Senanayake, Dr. Roberto Farias, Mr. Tony Arttapon, Prof. Yong Wang, Dr. Dong Wei, Dr. Ishara Sandeepani Manawasinghe, Dr. Maryam Fallahi, Dr. Mohammad Javad Pourmoghaddam, Ms. Lin Li, and Dr. Achala Rathnayaka for their valuable suggestions and help. My warmest special thanks to Ms. Sahar Absalan for encouraging, supporting, and giving me all the help and strength during these years. My sincere thanks go to Dr. Binu Samarakoon for her unwavering support and encouragement.

I would like to thank Dr. Shaun Pennycook for helping with the nomenclatural clarification of the new species. I would like to extent my gratitude to the staffs, colleagues and friends in the Center of Excellence in Fungal Research, Mae Fah Luang

University, Chiang Rai, Thailand. I would like to thank Mr. Sornram Sukpisit, Ms. Wilawan Punyaboon, Ms. Naruemon huanraluek, and Mr. Kasiphat Limsakul for their invaluable assistance, suggestions and great help during my studies.

Last but not the least, I wish to express my heartfelt gratitude to my father, mother, and brothers for their unwavering spiritual support and for being my source of strength throughout my Ph.D. journey and my life.

Alireza Armand

Dissertation Title	Phytopathogenic and Post-harvest Fungi on Selected Economically Fruits in Northern Thailand
Author	Alireza Armand
Degree	Doctor of Philosophy (Biological Science)
Advisor	Assistant Professor Kitiphong Khongphinitbunjong, Ph. D.
Co-Advisor	Adjunct Professor Kevin David Hyde, Ph. D. Mahamarakkalage Mary Ruvishika Shehali Jayawardena, Ph. D.

ABSTRACT

Thailand is a leading global producer of tropical fruit crops, renowned for its diverse and high-quality produce, including mangoes, durians, rambutans, longans, and pineapples. These fruit crops are integral to the country's economy, contributing significantly to export revenues and local livelihoods. Cultivation of fruit crops supports the agricultural sector, employing millions of farmers and fostering rural development. Beyond economic value, these fruits hold cultural and nutritional significance, forming a vital component of traditional diets and health practices.

Despite Thailand’s favourable climate and fertile soils, fungal diseases pose a serious threat to fruit production, both pre- and post-harvest. Pre-harvest infections by pathogenic fungi, associated with symptoms such as anthracnose, fruit rot, and leaf blight, often manifest or worsen during post-harvest handling, storage, and transportation, leading to significant losses in fruit quality and marketability. Isolation and identification of these fungi are essential to understand their diversity, pathogenicity, and infection mechanisms. Accurate identification using morphological and molecular techniques enables the development of targeted management strategies, including resistant cultivars, biological control agents, and integrated disease management practices. Post-harvest disease management, focusing on early detection, fungicidal treatments, and optimized storage conditions, is equally critical to ensuring fruit quality and extending shelf life.

The comprehensive survey of fungal pathogens associated with diverse tropical fruit crops in northern Thailand aimed to expand the understanding of fungal diversity, host-pathogen relationships, taxonomic novelties and new host or geographical records of pathogenic species and their potential impacts on the crops. Fresh samples of main tropical crops and economically important plants exhibiting specific symptoms were collected across local markets and orchards from multiple locations, including Chiang Mai, Chiang Rai, Lamphun, and Phayao Provinces, followed by the application of a polyphasic identification approach that combined morphological assessments with multi-locus phylogenetic analysis. Furthermore, pathogenicity assays were conducted on selected crops, including avocado, mango, and pineapple.

This study identified numerous fungal species associated with a range of symptoms, including leaf blight, dieback, fruit rot, and anthracnose, affecting key economic crops such as mango, avocado, durian, pineapple, longan, rambutan, langsat, guava, mangosteen, lychee, and papaya. Additionally, various fungal species were found to be associated with symptoms such as leaf blight, leaf spots, and dieback on ornamental plants. Herbarium specimens of the fungi described in the thesis were deposited in the Mae Fah Luang University (MFLU) Fungarium, Chiang Rai, Thailand. Living cultures were deposited in the Culture Collection of Mae Fah Luang University (MFLUCC). The obtained DNA sequences were verified, submitted to GenBank, and made available for public reference.

Pathogenicity assessment revealed that most of the strains isolated from mango (91.6%) were pathogenic to mango fruits and leaves, although their levels of virulence varied significantly. The pathogenic genera tested against mango included *Botryosphaeria*, *Colletotrichum*, *Diaporthe*, *Neofusicoccum*, *Neopestalotiopsis*, *Neoscytalidium*, *Pestalotiopsis*, *Pseudopallidocercospora*, and *Zasmidium*. Pathogenicity tests conducted on *Colletotrichum endophyticum*, *C. fructicola*, *C. siamense*, and *C. henanense* isolated from avocado indicated that these species were pathogenic to avocado fruits and leaves, exhibiting varying degrees of aggressiveness. Furthermore, pathogenicity tests on pineapple leaves demonstrated that *Colletotrichum fructicola* strains were pathogenic to the leaves. The study identified the main post-

harvest fungal species associated with mango and avocado, and assessed their virulence.

A total of 260 potentially pathogenic isolates were obtained, all belonging to ascomycetes. This study identified 20 genera, including *Albonectria*, *Bisifusarium*, *Botryosphaeria*, *Cercospora*, *Colletotrichum*, *Diaporthe*, *Fusarium*, *Lasiodiplodia*, *Lasmenia*, *Neocosmospora*, *Neofusicoccum*, *Neopestalotiopsis*, *Neoscytalidium*, *Paramyrothecium*, *Pestalotiopsis*, *Phyllosticta*, *Pseudocercospora*, *Pseudopallidocercospora* gen. nov., *Pseudoplagiostoma*, and *Zasmidium*. The 260 isolates were classified into 82 taxa, 10 families (*Apoharknessiaceae*, *Botryosphaeriaceae*, *Diaporthaceae*, *Glomerellaceae*, *Mycosphaerellaceae*, *Nectriaceae*, *Phyllostictaceae*, *Pseudoplagiostomataceae*, *Sporocadaceae*, *Stachybotryaceae*), and six orders (*Amphisphaeriales*, *Botryosphaeriales*, *Diaporthales*, *Glomerellales*, *Hypocreales*, *Mycosphaerellales*) in *Dothideomycetes* and *Sordariomycetes*, comprising 22 new species and 60 previously known species. This research also revealed 19 new geographical records and 80 new host records, the majority associated with main crops.

The newly described species are *Albonectria durionigenum*, *A. lansii*, *Bisifusarium mangiferae*, *B. thailandica*, *Cercospora alocasiicola*, *Colletotrichum durionigenum*, *C. thasutense*, *Diaporthe capsicicola*, *D. durionis*, *D. lansii*, *D. perseae-americanae*, *D. tamarindi*, *N. iridicola*, *N. iridis*, *N. litchii*, *N. litchiicola*, *N. mangiferae*, *N. mangifericola*, *N. mangiferigena*, *Paramyrothecium amorphophalli*, *Pseudopallidocercospora mangiferae*, and *Zasmidium mangiferae*. Additionally, *Pseudopallidocercospora* was illustrated as a new genus, associated with leaf spots of *Mangifera indica*. All these species were illustrated and described with confirmed morphology and molecular phylogeny.

The morpho-molecular data revealed the occurrence of 16 *Colletotrichum* species *viz. C. asianum*, *C. brevisporum*, *C. durionigenum*, *C. endophyticum*, *C. fructicola*, *C. gigasporum*, *C. gloeosporioides*, *C. guajavae*, *C. henanense*, *C. musae*, *C. musicola*, *C. plurivorum*, *C. siamense*, *C. thasutense*, and *C. tropicicola*, *C. truncatum* in northern Thailand. The species were associated with anthracnose, leaf blight, leaf spots, and fruit rot. This study provides an update information of occurrence

and distribution of main *Colletotrichum* species associated with important crops in Thailand. Moreover, *Colletotrichum* was identified as the most frequent genus representing 91 (35%) strains, and *Colletotrichum siamense* was the dominant species showing a wide host range, isolated from more than 15 plant genera. This study revealed Twenty-eight new host records of *Colletotrichum* species *viz. C. endophyticum* (from *Psidium guajava* and *Theobroma cacao*), *C. fructicola* (*Sapodilla sapote, Bauhinia* sp., *Ficus religiosa,* and *Piper nigrum*), *C. gigasporum* (from *Durio zibethinus*), *C. guajavae* (from *Mangifera indica*), *C. henanense* (from *Persea americana*), *C. musicola* (from *Lagerstroemia* sp.), *C. siamense* (from *Asplenium nidus, Dendrobium* sp., *Durio zibethinus, Dracaena fragrans, Morinda citrifolia, Polyscias balfouriana, Diospyros virginiana, Solanum lycopersicum, Sphagneticola trilobata, Hibiscus rosa-sinensis, Dimocarpus longan, Chamaedorea seifrizii, Syzygium jambos, Vanilla planifolia,* and *Lansium domesticum*), *C. thasutense* (from *Theobroma cacao*), and *C. truncatum* (from *Ficus religiosa* and *Durio zibethinus*). Twelve new geographical records of *Colletotrichum* species were also discovered in this research *viz. C. endophyticum* (from *Persea americana*), *C. fructicola* (from *Persea americana*), *C. gigasporum* (from *Mangifera indica*), *C. musae* (from *Mangifera indica*), *C. plurivorum* (from *Mangifera indica*), and *C. siamense* (from *Anthurium andraeanum, Artocarpus heterophyllus, Bauhinia* sp., *Ficus* sp., *Litchi chinensis, Piper nigrum,* and *Psidium guajava*).

This study was also the first comprehensive study documenting and illustrating species diversity of *Diaporthe* associated with crop diseases in Thailand. Thirteen species were obtained and identified using a morpho-molecular approach *viz. D. arecae, D. capsicicola, D. discoidispora, D. durionis, D. lansii, D. perseae-americanae, D. pterocarpi, D. rosae, D. siamensis, D. sojae, D. tamarindi, D. thunbergiicola,* and *D. tulliensis*. The species were associated with leaf blight, die back, canker, and fruit rot of crops *viz. Mangifera indica, Durio zibethinus, Capsicum annuum, Lansium domesticum, Psidium guajava, Persea americana, Ziziphus mauritiana, Dimocarpus longan, Tamarindus indica, Nephelium lappaceum, Litchi chinensis,* and *Solanum lycopersicum. Diaporthe* was the second most frequently obtained genus, representing 49 (19%) strains.

The present study revealed a high species diversity of *Neopestalotiopsis* associated with major tropical crops, namely: *Cocos nucifera*, *Lansium domesticum*, *Mangifera indica*, *Persea americana*, *Nephelium lappaceum*, *Garcinia mangostana*, *Psidium guajava*, and *Litchi chinensis*. Thirteen species of *Neopestalotiopsis* were identified in this study *viz. N. chrysea*, *N. rosicola*, N. *cubana*, *N. dendrobii*, *N. hydeana*, *N. iridicola*, *N. litchii*, *N. litchiicola*, *N. mangiferae*, *N. mangifericola*, *N. mangiferigena*, *N. psidii*, and *N. rhododendri*, associated with leaf spots, leaf blight, and fruit rot. *Neopestalotiopsis* was the third most frequently obtained genus, representing 39 (15%) strains. This study represented fifteen new host records of *Neopestalotiopsis* species *viz. N. chrysea* (from *Mangifera indica*), *N. cubana* (from *Lansium domesticum*, *Nephelium lappaceum*, *Garcinia mangostana*, *Mangifera indica*, *Nyssa sylvatica*, *Persea americana*, *Psidium guajava*), *N. dendrobii* (from *Mangifera indica*) *N. hydeana* (from *Persea americana*), *N. neomaricae* (from *Casearia lasiophylla*), *N. psidii* (from *Mangifera indica*), *N. rhododendri* (from *Mangifera indica*), *N. rosicola* (from *Cocos nucifera*), and *N. samarangensis* (from *Garcinia mangostana*).

Lasiodiplodia was obtained with 18 (7%) strains and *Fusarium* with 15 (6%) strains, majority reported from important tropical crops for the first time worldwide. Different *Lasiodiplodia* species *viz. L. brasiliensis*, *L. chonburiensis*, *L. pseudotheobromae*, and *L. theobromae* were discovered from different symptoms such as dieback, canker, leaf blight, and fruit rot. The present study expant our knowledge on species diversity of *Lasiodiplodia* in Thailand, discovering six new host reports from *Durio zibethinus*, *Morinda citrifolia*, *Iris pseudacorus*, *Elaeagnus pungens*, *Litchi chinensis*, and one new geographical record of *Lasiodiplodia theobromae* associated with *Musa* sp. fruit rot. *Fusarium* species were discovered for the first time worldwide associated with symptomatic tissues viz. *F. coffeibaccae* (*Psidium guajava*), *F. endophyticum* (from *Citrus* sp., and *Dimocarpus longan*), *F. fujikuroi* (from *Persea americana*), *F. hainanense* (from *Mangifera indica*), *F. pernambucanum* (from *Persea americana* and *Carica papaya*), *F. pseudocircinatum* (from *Citrus* sp., *Spathiphyllum* sp., and *Carica papaya*), *F. sulawesiense* (from *Dimocarpus longan*, and *Carica papaya*), and one new geographical record of *F. sacchari* from *Musa* sp.

Other species and new records reveaded in This study include *Botryosphaeria fabicerciana* (from *Mangifera indica*), *B. scharifii* (from *Mangifera indica*), *Neocosmospora diminuta* (from *Durio zibethinus*), *N. metavorans* (from *Persea americana*), *Neofusicoccum parvum* (from *Persea americana*), *N. sinoeucalypti* (from *Mangifera indica*), *Phyllosticta capitalensis* (from *Diospyros virginiana*, *Brassica oleracea*, *Psidium guajava*, and *Dimocarpus longan*), *Pseudocercospora terengganuensis* (from *Hymenocallis littoralis*), *Pseudoplagiostoma perseae* (from *Persea americana*), *Neoscytalidium dimidiatum* (from *Mangifera indica*), *Pestalotiopsis humicola* (from *Mangifera indica*), and *P. menhaiensis* (from *Mangifera indica*).

These results underscore the need for comprehensive surveillance and targeted management strategies to mitigate the potential impact of these fungi on agriculture and horticulture. The study's outcomes enhance understanding of fungal distribution, species diversity, pathogenicity, and potential threats to plant health, aiding in future diagnostic and control efforts.

Keywords: Agriculture, Anthracnose, Multi-gene Phylogeny, Pathogenicity, Phytopathogenic Fungi, Post-harvest Disease, Taxonomy

TABLE OF CONTENTS

CHAPTER	Page
1 INTRODUCTION	**1**
1.1 Importance of Agriculture Sector in Thailand	1
1.2 Phytopathogenic Fungi: A Global Threat to Agriculture and Food Security	3
2 LITERATURE REVIEW	**8**
2.1 Global Impact of Plant Pathogenic Fungi on Agriculture and Ecosystems	8
2.2 The Historical Progression of Plant Pathogenic Fungi Research	8
2.3 Previous Related Studies and Research Gaps in Thailand	9
3 *Paramyrothecium amorphophalli* sp. nov., A CAUSAL AGENT OF LEAF BLIGHT ON ELEPHANT FOOT YAM IN NORTHEN THAILAND	**14**
3.1 Introduction	14
3.2 Materials & Methods	15
3.3 Results	19
3.4 Discussion	25
4 FIRST REPORT OF *Colletotrichum fructicola* CAUSING FRUIT ROT AND LEAF-TIP DIEBACK ON PINEAPPLE IN NORTHERN THAILAND	**27**
4.1 Introduction	27
4.2 Materials & Methods	29
4.3 Results	35
4.4 Discussion	42
5 IDENTIFICATION AND CHARACTERIZATION OF *Colletotrichum* SPECIES ASSOCIATED WITH DURIAN FRUIT IN NORTHERN THAILAND	**44**

TABLE OF CONTENTS

CHAPTER	Page
5.1 Introduction	44
5.2 Materials & Methods	45
5.3 Results	47
5.4 Discussion	62
5.5 Conclusion	65
6 MORPHOMOLECULAR IDENTIFICATION AND PATHOGENICITY OF *Colletotrichum* SPECIES ASSOCIATED WITH AVODADO ANTHRACNOSE IN NORTHERN THAILAND	**66**
6.1 Introduction	66
6.2 Materials & Methods	68
6.3 Results	71
6.4 Discussion	89
7 NEW SPECIES AND NEW RECORDS OF PLANT PATHOGENIC FUNGI FROM NORTHERN THAILAND	**91**
7.1 Introduction	91
7.2 Materials & Methods	92
7.3 Results	93
7.4 Discussion	120
8 MANGO MICROCOSM: UNVEILING THE SPECIES DIVERSITY AND PATHOGENIC POTENTIAL OF FUNGI ISOLATED FROM MANGO (*Mangifera indica*) IN NORTHERN THAILAND	**124**
8.1 Introduction	124
8.2 Materials & Methods	126
8.3 Results	131
8.4 Discussion	211

TABLE OF CONTENTS

CHAPTER		Page
9	**FUNGAL FOOTPRINTS IN THE TROPICS: AN UPDATE ON SPECIES DIVERSITY LINKED TO DISEASED FRUIT CROPS AND ORNAMENTALS IN NORTHERN THAILAND**	**214**
9.1	Introduction	214
9.2	Materials & Methods	216
9.3	Results	218
9.4	Discussion	293
10	**CONCLUSIONS**	**298**
10.1	Overall Conclusions	298
10.2	Research Advances	302
10.3	Future Directions	303
10.4	Publications Generated from the Dissertation	304
REFERENCES		**306**
APPENDICES		**357**
APPENDIX A	IDENTIFICATION AND CHARACTERIZATION OF *Colletotrichum* SPECIES ASSOCIATED WITH DURIAN FRUIT IN NORTHERN THAILAND	357
APPENDIX B	MORPHOMOLECULAR IDENTIFICATION AND PATHOGENICITY OF *Colletotrichum* SPECIES ASSOCIATED WITH AVODADO ANTHRACNOSE IN NORTHERN THAILAND	367
APPENDIX C	STATISTICAL ANAYSES OF PATHOGENICITY TESTS ON AVOCADO FRUITS AND LEAVES	373
APPENDIX D	NEW SPECIES AND NEW RECORDS OF PLANT PATHOGENIC FUNGI FROM NORTHERN THAILAND	381

TABLE OF CONTENTS

APPENDICES		**Page**
APPENDIX E	MANGO MICROCOSM: UNVEILING THE SPECIES DIVERSITY AND PATHOGENIC POTENTIAL OF FUNGI ISOLATED FROM MANGO (*Mangifera indica*) IN NORTHERN THAILAND	385
APPENDIX F	FUNGAL FOOTPRINTS IN THE TROPICS: AN UPDATE ON SPECIES DIVERSITY LINKED TO DISEASED FRUIT CROPS AND ORNAMENTALS IN NORTHERN THAILAND	409
APPENDIX G	PUBLICATIONS	429
CURRICULUM VITAE		**434**

LIST OF TABLES

Table		Page
2.1	Pathogenic fungal species reported from crops in Thailand	11
3.1	Taxa with their respective GenBank accession numbers used in the phylogenetic analyses	18
3.2	Blast search results of the GenBank nucleotide database using the ITS, *cmdA*, *rpb2* and *tub2*	19
4.1	Primers used in this study	30
4.2	Taxa and their GenBank accession numbers used in the phylogenetic analysis	31
4.3	Base pair differences between *C. fructicola* (ICMP 18581) and two newly isolated strains	38
5.1	Primers used in the study	47
5.2	Base pair differences between *C. durionigenum* and *C. magnisporum* (CBS 398.84)	49
6.1	Base pair difference between *C. endophyticum* (MFLUCC 13-0418) and strains isolated in this study	75
6.2	Base pair difference between *C. siamense* (ICMP 18578) and *C. pandanicola* (MFLUCC 17-0571), *C. parvisporum* (YMF1.06942), and *C. siamense* strains	83
7.1	Base pair differences comparison between three loci of *Neopestalotiopsis iridis* and its closely-related species	119

LIST OF FIGURES

Figure		Page
3.1	Phylogram of *Paramyrothecium* revealed by RAxML analysis	20
3.2	Morphology of *Paramyrothecium amorphophalli* (holotype, MFLU22-0145; ex-type, MFLUCC 22-0085)	23
3.3	Pathogenicity test results of *Paramyrothecium amorphophalli* on elephant foot yam	24
4.1	Phylogram of *Colletotrichum gloeosporioides* species complex generated from maximum likelihood analysis	37
4.2	Morphology of *Colletotrichum fructicola* (MFLU 22-0302)	39
4.3	Morphology of *Colletotrichum fructicola* (MFLUCC 22-0182)	40
4.4	Pathogenicity assay on leaf of pineapple	41
5.1	Phylogram of *Colletotrichum gigasporum* species complex generated by maximum parsimony analysis	50
5.2	Morphology of *Colletotrichum durionigenum* (MFLU 22-0194, holotype)	53
5.3	The PHI test of *Colletotrichum durionigenum* and closely related species	54
5.4	Morphology of *Colletotrichum gigasporum* (MFLUCC 22-0108)	56
5.5	Phylogram of the *Colletotrichum gloeosporioides* species complex generated by maximum parsimony	57
5.6	Morphology of *Colletotrichum pandanicola* (MFLU 22-0193)	59
5.7	Phylogram of the *Colletotrichum truncatum* species complex generated by maximum parsimony	60
5.8	Phylogram of the *Colletotrichum truncatum* (MFLU 22-0191)	62
6.1	Phylogram of the *Colletotrichum gloeosporioides* species complex based on maximum likelihood	72
6.2	Morphology of *Colletotrichum endophyticum* (MFLU 23-0060); (MFLU 23-0061)	74

LIST OF FIGURES

Figure	Page
6.3 Morphology of *Colletotrichum fructicola* (MFLU 23-0062)	77
6.4 Morphology of *Colletotrichum henanense* (MFLU 23-0055)	79
6.5 Morphology of *Colletotrichum siamense* (MFLU 23-0058); (MFLU 23-0057); (MFLU 23-0056)	82
6.6 Pairwise homoplasy index (PHI) test of *C. pandanicola, C. parvisporum*, and *C. siamense*	83
6.7 Pathogenicity tests of different isolates of *Colletotrichum* on avocado fruit	85
6.8 Pathogenicity tests of different isolates on avocado leaves	87
6.9 Disease progression *Colletotrichum* strains on avocado leaves and fruits	88
7.1 Phylogram of the *Colletotrichum gloeosporioides* species complex	95
7.2 Morphology of *Colletotrichum fructicola* (MFLU 24-0212)	98
7.3 Morphology of *Colletotrichum musae* (MFLU 24-0213)	100
7.4 Morphology of *Colletotrichum siamense* (MFLU 24-0215)	102
7.5 Phylogram of the *Colletotrichum orchidearum* and *Colletotrichum magnum* species complexes	103
7.6 Morphology of *Colletotrichum musicola* (MFLU 24-0214)	105
7.7 Phylogram of the *Colletotrichum dracaenophilum* species complex	106
7.8 Morphology of *Colletotrichum tropicicola* (MFLU 24-0216)	108
7.9 Phylogram of the *Colletotrichum truncatum* species complex	109
7.10 Morphology of *Colletotrichum truncatum* (MFLU 24-0217)	111
7.11 *Lasiodiplodia theobromae* (MFLU 24-0218)	113
7.12 Phylogram of *Lasiodiplodia* generated by maximum likelihood analysis of	114
7.13 Morphology of *Neopestalotiopsis iridis* (MFLU 24-0219, holotype)	117
7.14 Phylogenetic tree obtained from maximum likelihood analysis of *Neopestalotiopsis*	118

LIST OF FIGURES

Figure	Page
8.1 Prevailing symptoms associated with mango fruits, leaves, and branches examined in the present study	127
8.2 Frequency of the genera obtained in this study	132
8.3 Morphology of *Botryosphaeria fabicerciana* (MFLU 24-0422)	134
8.4 The maximum likelihood (ML) tree of *Botryosphaeria*	135
8.5 Morphology of *Botryosphaeria scharifii* (MFLU 24-0423)	137
8.6 Morphology of *Colletotrichum asianum* (MFLU 24-0424)	140
8.7 Maximum likelihood (ML) tree of *Colletotrichum gloeosporioides* species complex	141
8.8 Maximum likelihood (ML) tree of *Colletotrichum gigasporum* species complex	143
8.9 Morphology of *Colletotrichum guajavae* (MFLU 24-0425)	145
8.10 Maximum likelihood (ML) tree of *Colletotrichum acutatum* species complex	146
8.11 Morphology of *Colletotrichum musae* (MFLU 24-0426)	148
8.12 Morphology of *Colletotrichum plurivorum* (MFLU 24-0427)	150
8.13 Maximum Likelihood (ML) tree of *Colletotrichum orchidearum* species complex	151
8.14 Morphology of *Colletotrichum siamense* (MFLU 24-0428)	153
8.15 Morphology of *Diaporthe arecae* (MFLU 24-0429)	155
8.16 Maximum likelihood tree of *Diaporthe arecae*, *D. longicolla*, *D. siamensis*, and *D. sojae* species complexes	156
8.17 Morphology of *Diaporthe rosae* (MFLU 20-0430)	160
8.18 Morphology of *Diaporthe sojae* (MFLU 24-0432)	162
8.19 Morphology of *Diaporthe* sp. (MFLU 24-0433)	164
8.20 Morphology of *Diaporthe thunbergiicola* (MFLU 24-0434)	166
8.21 Morphology of *Neofusicoccum sinoeucalypti* (MFLU 24-0435)	168

LIST OF FIGURES

Figure		Page
8.22	Maximum Likelihood (ML) tree of *Neofusicoccum*	169
8.23	Morphology of *Neopestalotiopsis chrysea* (MFLU 24-0436)	171
8.24	Maximum likelihood (ML) tree of *Neopestalotiopsis*	172
8.25	Morphology of *Neopestalotiopsis cubana* (MFLU 24-0437)	174
8.26	Morphology of *Neopestalotiopsis dendrobii* (MFLU 24-0438)	176
8.27	Morphology of *Neopestalotiopsis mangiferae* (MFLU 24-0439 holotype)	178
8.28	Morphology of *Neopestalotiopsis mangifericola* (MFLU 24-0440 holotype)	181
8.29	Morphology of *Neopestalotiopsis mangiferigena* (MFLU 24-0441 holotype)	183
8.30	Morphology of *Neopestalotiopsis psidii* (MFLU 24-0442)	185
8.31	Morphology of *Neopestalotiopsis rhododendri* (MFLU 24-0443)	186
8.32	Morphology of *Neopestalotiopsis* sp. 1 (MFLU 24-0444)	188
8.33	Morphology of *Neopestalotiopsis* sp. 2 (MFLU 24-0445)	190
8.34	Morphology of *Neoscytalidium dimidiatum* (MFLU 24-0446)	192
8.35	Maximum Likelihood (ML) tree of *Neoscytalidium*	193
8.36	Morphology of *Pestalotiopsis humicola* (MFLU 24-0447)	195
8.37	Maximum Likelihood (ML) tree of *Pestalotiopsis*	196
8.38	Morphology of *Pestalotiopsis menhaiensis* (MFLU 24-0448)	198
8.39	Morphology of *Parapseudocercospora mangiferae* (MFLU 24-0449 holotype)	201
8.40	Maximum likelihood (ML) tree of *Pseudopallidocercospora*, *Zasmidium*, and allied genera	202
8.41	Morphology of *Zasmidium mangiferae* (MFLU 24-0450, holotype)	205
8.42	Haplotype network generated for the ITS sequences data	206

LIST OF FIGURES

Figure		Page
8.43	Pathogenicity testing on mango fruits, photographed 7 days post-incubation	208
8.44	Pathogenicity testing on mango leaves, photographed 7 days post-incubation	209
8.45	Lesion area (mm) progression of the tested strains on mango fruits at 7 days post-inoculation	210
8.46	Lesion area (mm) progression of the tested strains on mango leaves at 7 days post-inoculation	210
9.1	Morphology of *Albonectria durionigenum* (MFLU 25-0048 holotype)	224
9.2	The most parsimonious tree of *Fusarium* and allied genera	225
9.3	Morphology of *Albonectria lansii* (MFLU 25-0049 holotype)	228
9.4	Morphology of *Bisifusarium mangiferae* (MFLU 25-0050 holotype)	230
9.5	Morphology of *Bisifusarium thailandica* (MFLU 25-0051 holotype)	232
9.6	Morphology of *Cercospora alocasiicola* (MFLU 25-0052 holotype)	234
9.7	The maximum likelihood (ML) tree of *Cercospora*	235
9.8	Morphology of *Cercospora malloti* (MFLU 25-0053)	238
9.9	The maximum likelihood (ML) tree of *Colletotrichum gloeosporioides* species complex	240
9.10	The maximum likelihood (ML) tree of *Diaporthe*	245
9.11	*Diaporthe capsicicola* (MFLU 25-0054 holotype)	247
9.12	The pairwise homoplasy index (PHI) test of new *Diaporthe* species	248
9.13	Morphology of *Diaporthe durionis* (MFLU 25-0055 holotype)	251
9.14	Morphology of *Diaporthe lansii* (MFLU 25-0056 holotype)	253
9.15	Morphology of *Diaporthe perseae-americanae* (MFLU 25-0057 holotype)	255
9.16	Morphology of *Diaporthe tamarindi* (MFLU 25-0058 holotype)	259
9.17	The maximum likelihood (ML) tree of *Lasiodiplodia*	265

LIST OF FIGURES

Figure	Page
9.18 The maximum likelihood (ML) tree of *Neofusicoccum*	270
9.19 Morphology of *Neopestalotiopsis cubana* (MFLU 25-0059)	272
9.20 The maximum likelihood (ML) tree of *Neopestalotiopsis*	273
9.21 Morphology of *Neopestalotiopsis hydeana* (MFLU 25-0060)	275
9.22 Morphology of *Neopestalotiopsis* sp. (MFLU 25-0061)	277
9.23 *Neopestalotiopsis litchii* (MFLU 25-0062 holotype)	279
9.24 Morphology of *Neopestalotiopsis litchiicola* (MFLU 25-0063 holotype)	281
9.25 Morphology of *Neopestalotiopsis rosicola* (MFLU 25-0064)	283
9.26 The maximum likelihood (ML) tree of *Phyllosticta*	287
9.27 *Pseudocercospora terengganuensis* (MFLU 25-0065)	289
9.28 The maximum likelihood (ML) tree of *Pseudocercospora*	290
9.29 Morphology of *Pseudoplagiostoma perseae* (MFLU 25-0066)	292
9.30 The maximum likelihood (ML) tree of *Pseudoplagiostoma*	293

ABBREVIATIONS AND SYMBOLS

AIC	Akaike Information Criterion
BLASTn	Basic Local Alignment Search Tool
CI	Consistency Index
CLA	Carnation Leaf Agar
DNA	Deoxyribonucleic acid
GTR+I+G	General Time Reversible+Proportion of invariable sites+Gamma distribution
HI	Homoplasy Index
MAFFT	Multiple alignment program for amino acid or nucleotide sequences
MCMC	Markov Chain Monte Carlo
MEA	Malt Extract Agar
MFLU	Mae Fah Laung University Herbarium
MFLUCC	Mae Fah Laung University Culture Collection
ML	Maximum Likelihood
MP	Maximum Parsimony
OA	Oatmeal Agar
PCR	Polymerase Chain Reaction
PDA	Potato Dextrose Agar
PP	Posterior Probability
RC	Rescaled Consistency Index
RI	Retention Index
SNA	Synthetic Nutrient Deficient Agar
TL	Tree Length
$\bar{x}$	Mean

CHAPTER 1

INTRODUCTION

1.1 Importance of Agriculture Sector in Thailand

Agriculture plays a crucial role in the world economy, serving as a source of business activity, a protector of the environment, and a driver of economic and social growth (Antle et al., 2020; Sarris, 2021). It is particularly important in developing countries, where it often forms the backbone of the economy (Alvarado et al., 2021). The sector's significance is further underscored by its role in ensuring food security and driving human development (Byerlee et al., 2009; Baba et al., 2010). As a nation with a significant agricultural sector, Thailand boasts a farming population comprising approximately 54.4% of its populace (Boonyanam, 2020). Nevertheless, plant-pathogenic fungi pose a persistent threat to the agricultural sector (Jantasorn et al., 2016; Ristaino et al., 2021).

Economic Significance of Tropical Fruits in Thailand

The total cultivated area of tropical fruits in Thailand covered 1.7 million ha in 2010, with production of 22.8 million tons. The quantity of fresh tropical fruit exported in 2010 was 256,172 tons worth 119.8 million US$. Thailand cultivates a diverse array of tropical and subtropical fruits including durian (*Durio zibethinus* L.), rambutan (*Nephelium lappaceum* L.), mangosteen (*Garcinia mangostana* L.), papaya (*Carica papaya* L.), guava (*Psidium guajava* L.), coconut (*Cocos nucifera* L.), and pineapple (*Ananas comosus* (L.) Murr.), each renowned for their nutritional richness alongside their delightful taste (Somsri, 2011). Additionally, in Thailand, the marketing of fresh-cut fruits such as jackfruit (*Artocarpus heterophyllus* Lam.), durian, pineapple, and papaya has been ongoing for several years, with sales of these products steadily rising in both open-air markets and supermarkets (Rattanapanone et al., 2000). Thailand plays a significant role as a primary producer and exporter of tropical fruits, such as durian, longan (*Dimocarpus longan* Lour.), and lychee (*Litchi chinensis* Sonn.), being the most significant in terms of both domestic consumption and export (Chomchalow et al.,

2008). Longan production has seen a notable rise in recent years, driven by increasing demand from both China and Thailand. Furthermore, Thai longans hold a preference in China due to their exceptional quality, resulting in a significant surge in imports by China, reaching approximately 140% in 2017 (Altendorf, 2018). In Thailand, longan cultivation spans approximately 188,574 hectares, yielding a total annual production of 1,027,298 tons. The primary production hubs in Thailand are situated in the northern region, notably in Chiang Mai, Chiang Rai, Lamphun, and Phayao Provinces (Office of Agricultural Economics 2017). Durian, acclaimed as the 'king of fruits' due to its distinctive spiny husk and remarkable flavor and odor, stands as one of Thailand's foremost economically significant exported fruits (Bampenrat et al., 2020; Li et al., 2012). Thailand holds the leading position as the primary durian producer globally, with commercial production reaching 1,111.93 thousand metric tons in 2020 (National Agricultural Big Data Center; OAE). Mango (*Mangifera indica* L.), an agro-industrial fruit belonging to the Anacardiaceae family, holds the eighth position globally in terms of productivity output (Iqbal et al. 2022). Thailand, one of the top three mango-producing countries globally, contributes approximately 7.69% to the world's mango production (Worldatlas, 2019). In Thailand, avocado (*Persea americana* Mill.) cultivation commenced approximately 90 years ago in Nan province, located in the northern region. The cultivation area of avocados in Thailand has been expanding annually, particularly in the northern and northeastern regions. Moreover, avocado holds significant importance in Thailand and is exported to various Asian countries, including Hong Kong, Japan, and Singapore (Trakunyingcharoen et al., 2015a). In Thailand, pineapple derivatives have garnered recognition as significant economic assets earmarked for international trade (Apipatpapha et al., 2022). Thailand presently stands as the second-largest provider of processed pineapple produce globally. Geographically, pineapple cultivation zones in Thailand are stratified into regions encompassing the north, northeast, central, and southern territories (Hemung et al., 2022).

1.2 Phytopathogenic Fungi: A Global Threat to Agriculture and Food Security

Phytopathogenic fungi represent a formidable challenge to agriculture and food security worldwide, precipitating notable crop and postharvest losses (Gould, 2009; Crous et al., 2016; Udayanga et al., 2020). Fungal pathogens initiate pre-harvest and post-harvest diseases that impact all anatomical structures of the crop, encompassing the roots, pseudostems, leaves, inflorescences and fruits (Vujanovic et al., 2000; Zimowska, 2008; Anuagasi et al., 2018). Employing an array of sophisticated mechanisms, these fungi adeptly colonize their host plants and instigate pathogenic manifestations, prominently characterized by the development of specialized infection structures alongside the orchestrated deployment of virulence factors (Doehlemann et al., 2017). Manifesting an extensive host range, plant pathogenic fungi exhibit a broad spectrum of parasitic behaviors, encompassing obligate as well as facultative parasitism (Capote et al., 2012). Moreover, these fungi can have devastating impacts when they spread beyond their natural range and become invasive on new hosts (Fones et al., 2017; Case et al., 2022).

1.2.1 Advancing Fungal Taxonomy: Implications for Plant Pathology and Food Security

While plant pathogenic fungi represent crucial organisms within ecosystems, comprehensive knowledge regarding most species remains limited and incomplete (Jayawardena et al., 2021a), reflecting the scarcity of available data (Hawksworth, 2001; Mueller & Schmit, 2007; Schmit & Mueller, 2007; Hawksworth & Lücking, 2017). This deficiency in fundamental taxonomic diversity information holds substantial implications for various facets of biology (Bass & Richards, 2011). Furthermore, the use of precise taxonomic names is paramount for conveying information regarding fungi, particularly in plant pathology, serving as linchpins connecting data pertaining to fungal biology, host specificity, geographic distribution, and associated risks (Crous et al., 2015a). Therefore, comprehensive sampling and in-depth studies, especially in the tropics, can help to address the uncertainties among fungal taxonomy, leading to a better understanding of fungal biology, niches,

distribution, and invasion (Crous et al., 2006a; Hawksworth, 2012; Crowther et al., 2014; Hyde et al., 2018b; Jayawardena et al., 2021a; Bhunjun et al., 2022). Additionally, the identification and delineation of plant pathogenic species assume paramount importance in fostering adept disease control strategies and ameliorating their deleterious repercussions on food stability (Rossman & Palm-Hernández, 2008; Wijayawardene et al., 2012; Crous et al., 2016; Udayanga et al., 2020; Jayawardena et al., 2021b). With the continued progression of molecular methodologies and the integration of DNA sequence information into fungal taxonomy, recent molecular investigations have unveiled that numerous pathogenic species exist as complexes, harboring multiple distinct species (Ko et al., 2011). Furthermore, molecular investigations have demonstrated that traditional methods of species identification may lack accuracy, leading to the misidentification of pathogenic species (Phoulivong et al., 2010).

1.2.2 Fungal Diseases of Economically Important Fruits in Thailand

A range of fungal diseases affect economically important fruits in Thailand. Tropical fruit crops are prone to infection by *Colletotrichum* species, commonly resulting in anthracnose disease during pre- and post-harvest stages (Zakaria, 2021, 2022). *Colletotrichum* species are accountable for anthracnose and fruit rot disease affecting various crucial fruits such as mango, lychee, papaya, dragon fruit, guava, and avocado. Consequently, they pose significant challenges in both the production and marketing of these commodities (Zakaria, 2021, 2022). *Lasiodiplodia* spp. are associated with cankers, decline, dieback and fruit rot diseases on a wide range of tropical fruits in Thailand, including avocado, mango, longan, mangosteen, strawberry, Melon (*Cucumis melo*) (Chang-ngern et al., 2010; Trakunyingcharoen et al., 2013, 2015a; Pipattanapuckdee et al., 2019; Suwannarach et al., 2020; Zakaria, 2022; Phetphan et al., 2023). The genus *Cercospora*, a destructive plant pathogen, has been found to infect a wide range of host plants in Thailand (To-Anun et al., 2011). Other important pathogenic genera reported from Thailand including *Pestalotiopsis*, *Neopestalotiopsis*, *Diaporthe*, *Pseudocercospora*, *Alternaria*, *Fusarium* (Cheewangkoon et al., 2021; Huanaluek et al., 2021; Sunpapao et al., 2022; Pongpisutta et al., 2023).

1.2.3 Advancing Phytopathogen Research in Thailand

The current knowledge of phytopathogens in Thailand is mainly based on morphologies or host-associations, leading to the use of outdated or no longer applicable names (Ko et al., 2011; Cheewangkoon et al., 2021). In numerous instances, identification procedures lacked the utilization of multiple markers, with analysis often limited to the ITS region alone. Consequently, the data acquired may not accurately represent the true causal pathogens (Zakaria, 2021). To enhance understanding of species evolutionary relationships and improvement in the field of plant pathology, a polyphasic approach that integrates molecular data is essential for species-level identification (Ko et al., 2011; Cheewangkoon et al., 2021), with an emphasis on significant fungal pathogens that impact commercial crops and plants, thereby fostering agricultural productivity and sustainability (Ko et al., 2011; Cheewangkoon et al., 2021). Furthermore, investigations pertaining to the evaluation of pathogenicity in plant pathogenic fungi within Thailand have been confined to particular fungal genera and plant species (Than et al., 2008a; Trakunyingcharoen et al., 2013; Withee et al., 2022). Consequently, there arises a necessity for inquiries into the pathogenicity assessment of pivotal fungal genera affecting economically significant plants.

1.3 Research Objectives

1.3.1 To systematically identify pathogenic fungi affecting selected fruits in northern Thailand

1.3.2 To assess the virulence of selected pathogenic fungal species from selected fruits in northern Thailand

1.3.3 To generate and update molecular data on pathogenic genera affecting fruits in northern Thailand, and their multi-gene phylogenetic analysis

1.4 Research Contents

This thesis is divided into ten chapters.

Chapter 1 is the general introduction that explains the importance of studying the taxonomy, phylogeny and pathogenicity of microfungi associated with fruit crops. It also contains the research objectives and the outline of the thesis.

Chapter 2 is literature review about global impact of pathogenic fungi on agriculture and ecosystems, the historical progression of plant pathogenic fungi research, studies and research gaps in fungi affecting fruits in Thailand, and checklist of pathogenic fungal species reported from crops in Thailand.

Chapter 3 discusses the taxonomy and phylogeny of *Paramyrothecium amorphophalli* sp. nov. isolated from elephant foot yam in northern Thailand and its multi-locus phylogenetic analysis and pathogenicity test.

Chapter 4 identifies two *Colletotrichum* strains as *C. fructicola* associated with fruit rot and leaf-tip dieback of pineapple in northern Thailand. Phylogenetic analysis and morphological examination were utilized to identify these strains for the first time worldwide on pineapple. Finally, the pathogenicity tests were conducted and discussed in this chapter.

Chapter 5 describes a comprehensive study of *Colletotrichum* species isolated from durian fruits in northern Thailand. In this chapter *Colletotrichum durionigenum* is introduced as a new species, and *C. gigasporum*, *C. pandanicola*, and *C. truncatum* are described and illustrated as new host records using both phylogenetic analysis and morphological characteristics.

Chapter 6 identifies 11 *Colletotrichun* isolates associated with avocado anthracnose and fruit rot. Phylogenetic analyses using five loci (ITS, *ACT*, *CHS-1*, *GAPDH* and *TUB2*) coupled with the morphological analysis showed that they belonged to four known species of *Colletotrichum*. *Colletotrichum endophyticum*, *C. fructicola* and *C. siamense* are illustrated as new geographical records, and *C. henanense* is characterized as a new host record. Furthermore, the pathogenicity of these species in avocado fruits and leaves (West Indian variety) has been proven.

Chapter 7 introduces one new species, *Neopestalotiopsis iridis*, through morphological and multi-gene phylogenetic analyses. Moreover, eight new fungus-host and five new geographical records are reported.

Chapter 8 represent a comprehensive study on pathogenic microfungi associated with mango fruits and leaves in northern Thailand. This chapter illustrates

and describes nine pathogenic genera, including eight known genera and one new genus, *Pseudopallidocercospora*. Moreover, reports twelve globally new host-fungus occurrences and six new geographical records. Furthermore, pathogenicity assessment of the obtained strains is discussed and haplotype analysis of *C. asianum* is illustrated.

Chapter 9 presents an update species diversity associated with diseased fruit crops in Thailand. The obtained strains belonged to 13 genera and 50 species, comprising 12 new species. Moreover, this chapter provides 68 new host records and nine new geographical records from Thailand.

Chapter 10 discusses the overall conclusions of the above-mentioned studies and suggestions for future work.

CHAPTER 2

LITERATURE REVIEW

2.1 Global Impact of Pathogenic Fungi on Agriculture and Ecosystems

A plethora of plant pathogenic genera distributed worldwide exert profound repercussions by inflicting substantial damage upon crops and natural ecosystems. Among these, *Alternaria*, a genus of phytopathogenic fungi, emerges as a formidable menace to vegetable and spice plants, eliciting significant concerns for agricultural productivity (Trkulja et al., 2020). The Magnaporthaceae family, comprising *Gaeumannomyces graminis*, *Pyricularia oryzae* and *Magnaporthe poae*, stands as a principal perpetrator of debilitating diseases in cereals and grasses, posing formidable challenges to global food security (Illana et al., 2013). Furthermore, an array of pivotal plant pathogenic genera, including but not limited to *Bipolaris*, *Botryosphaeria*, *Botrytis*, *Choanephora*, *Colletotrichum*, *Curvularia*, *Diaporthe*, *Diplodia*, *Dothiorella*, *Fusarium*, *Gilbertella*, *Lasiodiplodia*, *Mucor*, *Neofusicoccum*, *Pestalotiopsis*, *Phyllosticta*, *Phytophthora*, *Puccinia*, *Pyrenophora*, *Pythium*, *Rhizopus*, *Stagonosporopsis*, *Ustilago*, and *Verticillium*, exert significant deleterious impacts on plant health and agricultural sustainability, underscoring the complexity and diversity of phytopathogenic threats encountered worldwide (Hyde et al., 2014).

2.2 The Historical Progression of Plant Pathogenic Fungi Research

The examination of plant pathogenic fungi traces back to the 18th century, marked by the initial identification of these agents (Rapilly, 2001). However, it wasn't until the 19th century that substantial scientific progress was achieved in comprehending the origins and mechanisms of plant diseases (Yoshida et al., 2014). This era witnessed the inaugural detailed investigations into plant pathogens and the emergence of modern plant pathology. The exploration of plant pathogenic fungi has since advanced,

propelled by improvements in microscopy, genetic dissection, and genome-wide analysis techniques (Gold et al., 2001). These advancements have significantly deepened our comprehension of plant diseases and the involvement of fungi in their onset.

2.3 Studies and Research Gaps in Fungi Affecting Fruits in Thailand

In Thailand, the primary record of plant diseases in Thailand was established in 1994, primarily utilizing morphological characteristics for identification purposes (Ko et al., 2011; Cheewangkoon et al., 2021). *Colletotrichum*, mostly investigated in the past in Thailand, stands as one of the most well-studied fungal pathogenic genera, holding significance as plant pathogens responsible for anthracnose disease affecting agricultural, forestry, and native host plants (Jayawardena et al., 2016). Nonetheless, the predominant species on tropical crops and fruits were determined to be *C. acutatum* and *C. gloeosporioides* through morphological assessments (Cheewangkoon et al., 2021). However, Phoulivong et al. (2010) demonstrated that *C. gloeosporioides* is not a common pathogen in tropical fruits, based on their analysis of sequence data from 25 *Colletotrichum* isolates obtained from eight tropical fruits. Subsequent to the prior research, Udayanga and colleagues (2013) delved into the examination of prevalent *Colletotrichum* species associated with anthracnose of tropical fruits. Their study underscored the imperative of re-evaluating the evolutionary correlations among *Colletotrichum* species present in tropical fruits. However, none of the aforementioned investigations incorporated a pathogenicity evaluation as part of their research protocols.

The examination of phytopathogenic fungi in Thailand has predominantly revolved around specific crops or fungal categories (Photita et al., 2004; Than et al., 2008b; Kaewjan et al., 2012; Trakunyingcharoen et al., 2014; Sunpapao et al., 2022). In contrast, numerous economically significant fruits (e.g. Avocado, Durian, Mango, Citrus, Rambutan, Lychee, Longan, Langsat) have been overlooked in Thailand in terms of the investigation into the pathogenic fungi affecting these fruits. For instance, Pongpisutta et al.

(2023) have investigated the die-back disease of durian caused by *Fusarium* species, while other significant pathogenic fungi linked to durian diseases have yet to be explored. *Diaporthe* species exhibit a global presence and are recognized as pathogens on economically significant hosts (Norphanphoun et al., 2022). While numerous accounts of *Diaporthe* spp. exist in Thailand (Udayanga et al., 2012, 2014; Perera et al., 2018a, 2018b; Tibpromma et al., 2018; Mapook et al., 2020; Monkai et al., 2023), only a limited number of investigations have focused specifically on pathogenic species, particularly those affecting tropical fruits. Likewise, Cheewangkoon et al. (2021) discussed that scant data is accessible regarding other deleterious pathogenic genera affecting essential tropical fruits in Thailand, with many identifications relying solely on ITS sequence data. Consequently, there is a pressing need for heightened research efforts aimed at isolating and identifying poorly studied pathogenic genera affecting important fruits in Thailand. Additionally, comprehensive collection and identification endeavors employing a multi-gene approach and pathogenicity assessment from tropical fruits could aid in identifying the prevailing species infecting diverse crops and refining previous data on plant pathogenic fungi in Thailand. Therefore, this research aims to investigate phytopathogenic fungi associated with economically important fruits, focusing on mango, avocado, durian, longan, langsat, lychee, rambutan, mangosteen, papaya, and guava. The prevailing pathogenic fungi associated with important crops from Thailand are delineated in Table 2.1.

Table 2.1 Pathogenic fungal species reported from crops in Thailand

Plant host	Fungal species	Disease	Molecular data	Reference
Avocado (*Persea americana*)	*Lasiodiplodia pseudotheobromae*	Canker and dieback	ITS, *tef1*	Trakunyingcharoen et al. (2015b)
Banana (*Musa* sp.)	*Colletotrichum musae*	Anthracnose, Fruit rot	ITS, *act*, *chs-1*, *cmdA*, *gapdh*, *tub2*	Samarakoon et al. (2024)
	Colletotrichum siamense	Anthracnose, Fruit rot	ITS, *act*, *chs-1*, *cmdA*, *gapdh*, *tub2*	Samarakoon et al. (2024)
	Corynespora torulosa	Fruit speckles	ITS, LSU	Samarakoon et al. (2024)
Chilli (*Capcicum annuum*)	*Colletotrichum. asianum*	Anthracnose	—	Phoulivong et al. (2012)
Coconut (*Cocos nucifera*)	*Alternaria burnsii*	Dirty Panicle	ITS, *gapdh*, *tef1*, *rpb2*	Sunpapao et al. (2022)
	Neopestalotiopsis cocoes	Leaf blight	ITS, LSU, *tub2*, *tef1*	Hyde et al. (2016)
	Fusarium clavum	Dirty Panicle	ITS, *tef1*, *rpb2*	Sunpapao et al. (2022)
	F. tricinctum			
Dragon fruit (*Hylocerous undatus*)	*Colletotrichum fructicola*	Anthracnose	ITS, *act*, *cmdA*, *gapdh*, *gs*, *tub2*	Udayanga et al. (2013)
Durian (*Durio zibethinus*)	*Fusarium incarnatum*	Dieback	ITS, *tef1*, *rpb2*	Pongpisutta et al. (2023)
	F. solani	Dieback	ITS, *tef1*, *rpb2*	Pongpisutta et al. (2023)
	F. mangiferae	Dieback	ITS, *tef1*, *rpb2*	Pongpisutta et al. (2023)

Table 2.1 (continued)

Plant host	Fungal species	Disease	Molecular data	Reference
	Lasiodiplodia pseudotheobromae	Stem rot	ITS	Chantarasiri et al. (2021)
Jack fruit (*Artocarpus heterophyllus*)	*Pseudofusicoccum artocarpi*	Canker and dieback	ITS, *tef1*	Trakunyingcharoen et al. (2015b)
	Aplosporella artocarpi	Canker and dieback	ITS, *tef1*	Trakunyingcharoen et al. (2015b)
Jujube (*Ziziphus* sp.)	*Colletotrichum fructicola*	Anthracnose	ITS, *act*, *cmdA*, *gapdh*, *gs*, *tub2*	Udayanga et al. (2013)
Lime (*Citrus aurantifolia*)	*Colletotrichum gloeosporioides*	Anthracnose	ITS, *act*, *cmdA*, *gapdh*, *gs*, *tub2*	Udayanga et al. (2013)
Longan (*Dimocarpus longan*)	*Lasiodiplodia pseudotheobromae*	Fruit rot	ITS, *tef1*	Pipattanapuckdee et al. (2019)
	Pseudofusicoccum adansoniae	Canker and dieback	ITS, *tef1*	Trakunyingcharoen et al. (2015b)
	Colletotrichum fructicola	Anthracnose	ITS, *act*, *tub2*, *gapdh*	Phoulivong et al. (2010)
Mango (*Mangifera indica*)	*Lasiodiplodia pseudotheobromae*	Fruit and stem-end rot	ITS, *tef1*	Trakunyingcharoen et al. (2014, 2015b)
	Lasiodiplodia viticola	Fruit and stem-end rot	ITS, *tef1*	Trakunyingcharoen et al. (2014)
	Lasiodiplodia thailandica	Canker and dieback	ITS, *tef1*	Trakunyingcharoen et al. (2015b)

Table 2.1 (continued)

Plant host	Fungal species	Disease	Molecular data	Reference
	Colletotrichum acutatum	Anthracnose	ITS, *tub2*, *act*, *chs-1*	Rattanakreetakul et al. (2023)
	Colletotrichum gloeosporioides	Anthracnose	ITS, *tub2*, *act*, *chs -1*	Rattanakreetakul et al. (2023)
	Colletotrichum fructicola	Anthracnose	ITS, *act*, *tub2*, *gapdh*	Phoulivong et al. (2010)
Rose apple (*Syzygium samarangense*)	*Colletotrichum gloeosporioides*	Anthracnose	ITS, *act*, *cmdA*, *gapdh*, *gs*, *tub2*	Udayanga et al. (2013)
	Lasiodiplodia theobromae	Canker and dieback	ITS, *tef1*	Trakunyingcharoen et al. (2015b)
	Colletotrichum syzygicola	Anthracnose		Udayanga et al. (2013)
Strawberry (*Fragaria ananassa*)	*Lasiodiplodia theobromae*	Dieback	ITS, LSU	Phetphan et al. (2023)
Tomato (*Solanum lycopersicum*)	*Alternaria linariae*	Leaf spots	ITS, *gapdh*, *rpb2*, *tef*, *altA1*	Woudenberg et al. (2014)
Watermelon (*Citrullus lanatus*)	*Lasiodiplodia theobromae*	Fruit rot	ITS, *TUB*, *RPB2*, *TEF*	Khuna et al. (2024)

CHAPTER 3

Paramyrothecium amorphophalli sp. nov., A CAUSAL AGENT OF LEAF BLIGHT ON ELEPHANT FOOT YAM IN NORTHEN THAILAND

3.1 Introduction

Elephant foot yam is a tropical tuber crop that belongs to *Amorphophallus*. It is a significant edible tuberous crop extensively cultivated in tropical and subtropical regions, especially in China and India (John et al., 2014; Prasad et al., 2017). Konjac Glucomannan (KGM) extracted from the tuber of *Amorphophallus konjac*, is used as a medicinal ingredient and nutritional supplement (Yao-ling et al., 2013). Among the significant health advantages of KGMs are those related to lowering cholesterol, regulating triglyceride levels, enhancing sugar levels, and promoting human immunological and intestinal functions (Yao-ling et al., 2013). Among plant pathogens, fungi are considered devastating agents responsible for economic losses in the agriculture circle and threatening food security (Gomdola et al. 2022; Withee et al. 2022). Prasad et al. (2017) reported *Colletotrichum siamense* from India causing anthracnose on elephant foot yam. *Sclerotium rolfsii* is a devastating soil-borne disease which causes collar rot on this plant (Sahoo et al., 2016). As the correct identification is the first and vital step in disease management, it becomes imperative to consider a proper taxonomic identification and understanding of fungi to undertake appropriate strategies for managing plant diseases (Bhunjun et al., 2021b; Jayawardena et al., 2021b).

Paramyrothecium (*Stachybotryaceae*, *Hypocreales*, *Sordariomycetes*) (Wijayawardene et al. 2020) was introduced to accommodate taxa earlier included in *Myrothecium sensu lato* (Lombard et al., 2016). According to morphological characteristics and molecular analyses, Lombard et al. (2016) showed that this group of fungi is distinguished from other *Myrothecium* species and subsequently established

Paramyrothecium (Lombard et al., 2016). *Paramyrothecium* is a plant pathogenic genus and among the 20 species reported in this genus (MycoBank 2023), *Paramyrothecium foliicola* and *P. roridum* have been widely isolated from different plant hosts as leaf spot causal agents (Chen et al., 2016; Ben et al., 2017; Withee et al., 2022). *Paramyrothecium foliicola* has been reported on a variety of hosts, including melon (Sabahi et al., 2022), tomato (Huo et al., 2023) and eggplant (Aumentado & Balendres, 2022). It has also been isolated from cucumber as the causal agent of stem canker in seedlings (Huo et al., 2021). *Paramyrothecium foliicola* was also discovered in Iran as the causative agent of apple tree canker (Azizi et al., 2020). *Paramyrothecium roridum* as well as *P. breviseta* have been reported from coffee, causing leaf spots and stem rot (Wu et al., 2021; Huaman-Pilco et al., 2023). Wang et al. (2021) isolated *P. roridum* from the false dragonhead plant (*Physostegia virginiana*). Mulberry has also reportedly been infected by *P. roridum* (Pappachan et al., 2019). Moreover, the latter was isolated from muskmelon as a crown canker-causing agent (Chen Z. et al., 2018).

Paramyrothecium eichhorniae and *P. vignicola*, isolated from *Eichhornia crassipes* and *Vigna* sp. respectively, are the latest new species additions to *Paramyrothecium* (Pinruan et al., 2022; Withee et al, 2022). Both species have been reported from northern Thailand. During microfungal investigations in the same part of the country, symptomatic leaves of elephant foot yam, resulting from a fungal attack, were collected. The fungus was isolated and subjected to morpho-molecular analyses. The present study aims to introduce the new species *Paramyrothecium amorphophalli* and confirm its pathogenicity on elephant foot yam.

3.2 Materials & Methods

3.2.1 Sample Collection and Fungal Isolation

Symptomatic leaves with leaf spots were collected from living *Amorphophallus* sp. in Doi Pui Sai Khao, Phan District, Chiang Rai, Thailand, in September 2021. Fungal isolation and purification were conducted using the single-spore isolation method (Senanayake et al., 2020). The pure culture was maintained in slant cryogenic tubes and deposited in the culture collection of Mae Fah Luang University and the dried

leaf with fungal fruiting bodies was deposited in the Mae Fah Luang University herbarium. Moreover, the isolate was submitted to the Index Fungorum (IF558845), Faces of Fungi (FoF12745) and Greater Mekong Subregion webpage (Chaiwan et al., 2021).

3.2.2 DNA Extraction and PCR Amplification

Genomic DNA was extracted from fresh mycelia grown on potato dextrose agar (PDA) for 10 days using the DNA Extraction Kit (Omega Bio-tek) according to the manufacturer's instructions. The internal transcribed spacer (ITS) region, β-tubulin (*tub2*), calmodulin (*cmdA*) and RNA polymerase II second largest subunit (*rpb2*) were amplified by ITS5/ITS4 (White et al., 1990), Bt2a/Bt2b (Glass & Donaldson, 1995), CAL–CL1/CAL–CL2A (O'Donnell et al., 1998) and 5F2/7– CR (O'Donnell et al., 2007), respectively. The polymerase chain reaction was performed in a total volume of 25 µL, containing 12.5 µL of 2 × Power Taq PCR Master Mix, 1 µL of each primer (20 µM), 1 µL genomic DNA and 9.5 µL deionized water. The PCR procedure was performed using the following conditions: initial denaturation at 94 °C for 4 min; 35 cycles of denaturation for 30 s at 94 °C, annealing at 55 °C (ITS); 57 °C (*tub2*); 51 °C (*cmdA*); 58 °C (*rpb2*) for 60 s, extension at 72 °C for 60 s; and the final extension at 72 °C for 10 min. The PCR reaction system with the total reaction volume was 25 µL PCR mixture. PCR amplification was performed in an Eppendorf (Master Cycler X50s) thermal cycler. PCR products were sequenced by SolGent Co., South Korea.

3.2.3 Phylogenetic Analyses

The obtained sequences were searched using BLAST (Table 2) and related sequences were downloaded from GenBank according to BLASTn searches and recently published papers (Pinruan et al., 2022; Withee et al., 2022) (Table 1). The individual loci were manually adjusted with MAFFT v.7 using the web server (http://mafft.cbrc.jp/alignment/server) (Katoh et al., 2019). BioEdit v.7.0.9.0 was used to manually further adjust the alignment where necessary (Hall, 1999). Aligned sequences were automatically trimmed using command-based TrimAl software with the gappyout method. The alignment was converted to phylip and nexus formats using the online tool ALTER (Glez-Peña et al., 2010). *Albifimbria verrucaria* (CBS 328.52) and *A. viridis* (CBS 449.71) were used as the outgroups. The phylogeny was generated by maximum likelihood (ML) analysis using RAxML-HPC2 on XSEDE with

bootstrapping of 1000 replicates. The GTR + GAMMA model of nucleotide evolution was used for maximum likelihood analysis. The best-fit evolutionary models for each dataset were evaluated using the Akaike Information Criterion (AIC) using jModeltest 2.1.10 on the CIPRES online platform. The best-fit evolutionary models for *cmdA* and ITS were HKY+I+G, K80+I for *rpb2* and TIM2+I+G for *tub2* (Nylander 2004). The Bayesian posterior probability (BYPP) analysis was performed using a Markov Chain Monte Carlo (MCMC) algorithm with Bayesian posterior probabilities in MrBayes on XSEDE (Ronquist et al., 2012). For the BYPP analysis, four MCMC chains were run from random trees for 1,000,000 generations and sampled every 100th generation. The first 25% of the generated trees were discarded as the burn-in and the remaining trees were used for calculating posterior probabilities. Maximum parsimony (MP) analysis was carried out using PAUP XSEDE (Swofford, 2002) and gaps were treated as missing data and ambiguously aligned regions were excluded. Trees were inferred using the heuristic search option with tree bisection reconnection (TBR) branch swapping and 1,000 random sequence additions. All these analyses were performed on the CIPRES Science Gateway (https://www.phylo.org/portal2) (Miller et al., 2011). The resulting phylograms were visualized in FigTree v. 1.4.0 and annotated in Adobe Illustrator CC 22.0.0 (Adobe Systems, USA). Newly generated sequence data were deposited in GenBank (Table 1).

3.2.4 Pathogenicity Assay

Koch's postulates were used to confirm the pathogenicity of the new species on its original host (Bhunjun et al., 2021a). Four replicates of both the wounded and non-wounded assays using conidial suspension and mycelial plugs were examined. The leaves of elephant foot yam were first surface sterilized by washing in 70% ethanol for 1 minute, then in 2% sodium hypochlorite for 1 minute, followed by three times washing with sterile distilled water and laminar air drying. A conidial suspension (1×10^6 conidia/mL) was applied to four wounded and four non-wounded leaves while a sterilized water inoculation was used for the control leaves. Mycelial plugs were obtained from colonies grown on PDA (10-day colonies). Control inoculations were performed using uncolonized PDA plugs. The inoculated and the control leaves were incubated in a moist chamber at 28 °C with 80% relative humidity. Koch's postulates

were confirmed by re-isolating the fungus from the infected leaves. The re-isolated fungus was identified based on cultural and morphological characteristics.

Table 3.1 Taxa with their respective GenBank accession numbers used in the phylogenetic analyses

Taxa	Strains	GenBank accession numbers			
		ITS	***cmdA***	***tub2***	***rpb2***
Albifimbria verrucaria	CBS 328.52^{T}	KU845893	KU845875	KU845969	KU845931
A. viridis	CBS 449.71^{T}	KU845898	KU845879	KU845974	KU845936
Paramyrothecium acadiense	CBS 123.96^{T}	KU846288	-	KU846405	KU846350
P. amorphophalli	**MFLUCC 22-0085^{T}**	OP279643	OP434479	OP434480	OP434481
P. breviseta	CBS 544.75^{T}	KU846289	KU846262	KU846406	KU846351
P. cupuliforme	CBS 127789^{T}	KU846291	KU846264	KU846408	KU846353
P. eichhorniae	TBRC 10637^{T}	MT973996	MT975319	MT975317	MT977540
P. eichhorniae	KKFC 474	MT973995	MT975318	MT975316	MT977541
P. foeniculicola	CBS 331.51^{T}	KU846292	-	KU846409	KU846354
P. foliicola	CBS 113121^{T}	KU846294	KU846266	KU846411	-
P. guiyangense	HGUP 2016-8002^{T}	KY126418	KY196193	KY196201	-
P. humicola	CBS 127295^{T}	KU846295	-	KU846412	KU846356
P. nigrum	CBS 116537^{T}	KU846296	KU846267	KU846413	KU846357
P. pituitipietianum	CBS 146817^{T}	MW175358	MW173100	MW173139	-
P. parvum	CBS 257.35^{T}	KU846298	-	KU846415	KU846359
P. roridum	CBS 357.89^{T}	KU846300	KU846270	KU846417	KU846361
P. roridum	CBS 372.50	KU846301	KU846271	KU846418	KU846362
P. salvadorae	CBS 147074^{T}	MZ064453	-	MZ078277	MZ078210
P. sinense	CGMCC 3.19212^{T}	MH793296	MH885437	MH793313	MH818824
P. tellicola	CBS 478.91^{T}	KU846302	KU846272	KU846419	KU846363
P. terrestris	CBS 564.86^{T}	KU846303	KU846273	KU846420	KU846364
P. verruridum	HGUP 2016-8006^{T}	KY126422	KY196197	KY196205	-
P. vignicola	SDBR-CMU376^{T}	MZ373242	OM810412	ON009015	ON033778
P. vignicola	SDBR-CMU377	MZ373244	OM810413	ON009016	ON033779

Table 3.1 (continued)

Taxa	Strains	GenBank accession numbers			
		ITS	***cmdA***	***tub2***	***rpb2***
P. viridisporum	CBS 873.85^{T}	KU846308	KU846278	KU846425	KU846369

Note "^{T}" indicates type species and the newly generated sequence is in bold

3.3 Results

3.3.1 Phylogenetic Analyses

The phylogram (Figure 3.1) was constructed based on a concatenated *cmdA* – ITS – *rpb2* – *tub2* alignment comprising sequence data from 25 taxa and the outgroup taxa (Table 1). The matrix comprised 2322 characters. The concatenated alignment was subjected to ML, MP and BYPP analyses. However, as the tree topology resulting from all three analyses was similar, hence the ML tree is illustrated herein (Figure 3.1).

The best-scoring RAxML tree with final optimization had a likelihood value of -10252.351870. The matrix consisted of 690 distinct alignment patterns, with 14.14% gaps and undetermined characters. Estimated base frequencies were as follows: A = 0.232961, C = 0.280953, G = 0.256616, T = 0.229470, with substitution rates AC = 1.287563, AG = 5.379673, AT = 1.231938, CG = 1.290010, CT = 8.976371, GT = 1.000000. The gamma distribution shape parameter = 0.179871 and the tree-length = 1.020557. The maximum parsimonious dataset comprised 1621 conserved characters while 137 characters were variable. The parsimony analysis resulted in two equally parsimonious trees (tree length = 1475, Consistency Index (CI) = 0.647, Retention Index (RI) = 0.752, Rescaled Consistency index (RC) = 0.487 and Homoplasy Index (HI) = 0.353).

Table 3.2 Blast search results of the GenBank nucleotide database using the ITS, *cmdA*, *rpb2* and *tub2*.

Gene	Taxon	Identities	Gaps
ITS	*Paramyrothecium* sp. (MZ373249)	562/563(99%)	1/563(0%)
cmdA	*Paramyrothecium eichhorniae* (OM810415)	661/673(98%)	1/673(0%)

Table 3.2 (continued)

Gene	Taxon	Identities	Gaps
rpb2	*Paramyrothecium eichhorniae* (ON033785)	959/967(99%)	2/967(0%)
tub2	*Paramyrothecium eichhorniae* (ON033772)	312/316(99%)	0/316(0%)

The phylogenetic tree constructed from the combined dataset showed that the isolated strain (MFLUCC 22-0085) formed a distinct lineage, clustering sister to two strains of *P. eichhorniae* (TBRC 10637 and KKFC 474) (Figure 3.1), with high statistical support (100% ML, 97% MP, 0.99 BYPP).

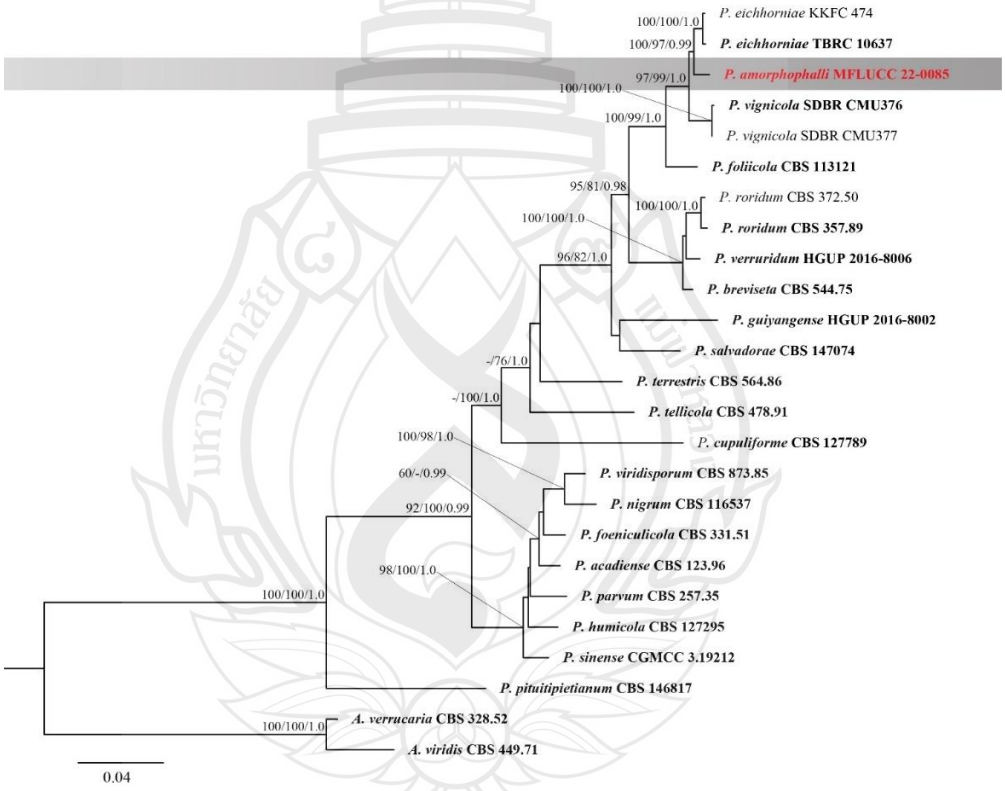

Note Maximum likelihood (left) and maximum parsimony (middle) bootstrap support values ≥ 60% and Bayesian posterior probabilities (right) ≥ 0.98 are indicated near the nodes. The tree is rooted with *Albifimbria verrucaria* (CBS 328.52) and *A. viridis* (CBS 449.71). The type strains are in bold and the newly generated sequence is highlighted in red.

Figure 3.1 Maximum likelihood tree of *Paramyrothecium* revealed by RAxML analyses of combined *cmdA* – ITS – *rpb2* – *tub2* sequences

3.3.2 Taxonomy

Paramyrothecium amorphophalli Armand & Jayawardena. sp. nov.

Figure 3.2

Index Fungorum number: IF558845; Facesoffungi number: FoF12745

Etymology – The species epithet refers to *Amorphophallus*, the plant genus from which the fungus was isolated.

Holotype – MFLU 22-0145

Pathogenic, causing leaf blight on *Amorphophallus* sp. Sexual morph: Not observed. Asexual morph: *Sporodochia* irregularly shaped, stromatic, superficial, with setose fringe, surrounded by olivaceous to dark green slimy mass of conidia. *Stroma* poorly developed, hyaline to sub-hyaline, made up of textura angularis. *Conidiophores* arising from the basal stroma, hyaline or slightly olivaceous, consisting of a stipe and penicillately branched conidiogenous apparatus. *Stipes* 11–20 × 2–2.5 µm, unbranched, hyaline, sometimes olivaceous, septate, smooth; primary branches 7–12 × 1.8–2 µm, aseptate, unbranched, smooth; secondary branches 8–15 × 1.5–2 µm, aseptate, unbranched, smooth, bearing 3–6 conidiogenous cells in a whorl. *Conidiogenous cells* 10.5–14.7 × 1.6–2 µm ($\overline{x}$ = 12 × 2 µm, n = 20), phialidic, cylindrical to subcylindrical, hyaline or olivaceous, smooth. *Conidia* two types: cylindrical conidia 5–6.4 × 1.5–2 µm ($\overline{x}$ = 5 × 1.8 µm, n = 30), abundant, aseptate, hyaline, smooth, rounded at both ends or narrowed at one end; ellipsoidal conidia 6–7 × 3–3.5 µm ($\overline{x}$ = 6.4 × 3.3 µm, n = 4) rarely observed, aseptate, hyaline.

Culture characteristics – Colonies reaching 20 mm in diameter after 7 days (25–28 °C) on PDA, with compact mycelia, white in color, becoming light saffron in the center; sporodochia forming superficially on the aerial mycelia, scattered, solitary to gregarious, surrounded by slimy olivaceous green to dark green conidial masses, reverse on PDA luteous to rosy buff, without exudate into the medium.

Material examined – Thailand, Doi Pui Sai Khao, Phan District, Chiang Rai, on leaf of *Amorphophallus* sp., 27 September 2021, Alireza Armand, T42 (MFLU 22-0145, holotype); extype living culture MFLUCC 22-0085.

Notes – The new species *Paramyrothecium amorphophalli* is phylogenetically close to *P. eichhorniae* (TBRC 10637) and *P. vignicola* (SDBR-CMU376). *Paramyrothecium amorphophalli* is morphologically similar to *P. eichhorniae* in

having stromatic, superficial sporodochia with an irregularly shaped outline and surrounding setose fringe, scattered or aggregated on the media (Pinruan et al., 2022). Moreover, the two taxa are similar in producing green to dark green slimy masses of conidia and both have aseptate, hyaline, smooth, cylindrical to ellipsoidal conidia (Pinruan et al., 2022). However, *P. amorphophalli* differs from *P. eichhorniae* in lacking setae on sporodochia and producing thick ellipsoidal conidia with completely rounded ends which are not observed in *P. eichhorniae*. It also produces shorter conidiophores (11–20 µm in *P. amorphophalli* vs. 15–40 µm in *P. eichhorniae*) and grows more slowly on media (20 mm after 7 days in *P. amorphophalli* vs. 90 mm after 14 days in *P. eichhorniae*) (Pinruan et al., 2022). *Paramyrothecium amorphophalli* can be recognized from *P. vignicola* by producing relatively smaller conidia (5–6.4 µm in *P. amorphophalli* vs. 5–7 µm in *P. vignicola*), smaller conidiophores (11–20 µm in *P. amorphophalli* µm vs. 40–60 µm in *P. vignicola*) and absence of setae associated with sporodochia (Withee et al., 2022). Following the recommendations of Chethana et al. (2021) and Jayawardena et al. (2021b), we used a polyphasic approach to confirm that our isolate is a new species.

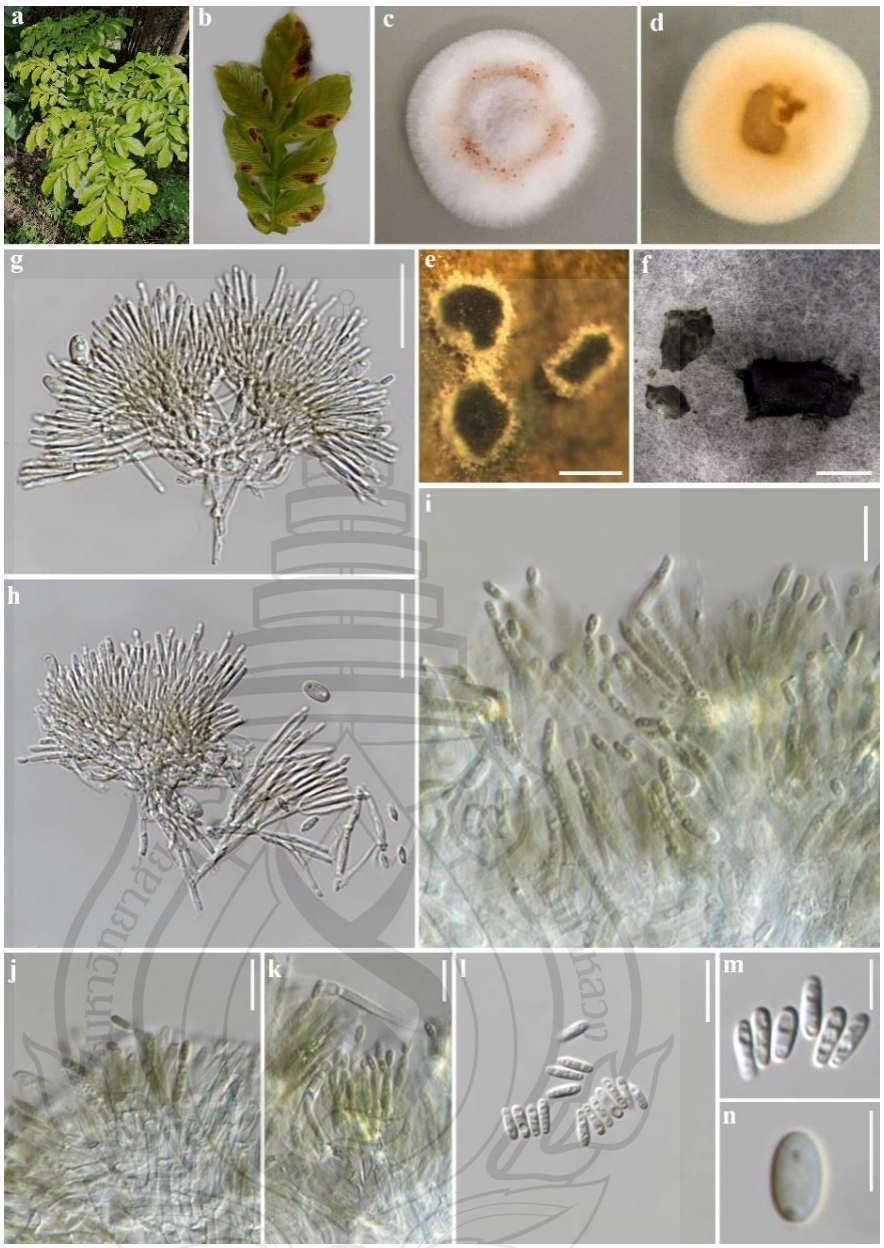

Note **a** Host plant. **b** Symptomatic leaves. **c**, **d** Upper and reverse sides of the colony on PDA (7 days old). **e** Sporodochia. **f** Conidial masses on PDA. **g**, **h** Conidiogenous cells and conidial attachment. **i-k** Conidiogenous cells and conidia. **l**, **m** Cylindrical conidia. **n** Ellipsoidal conidium. Scale bars: **e**, **f** = 500 µm, **g**, **h** = 20 µm, **i-l** = 10 µm, **m**, **n** = 5 µm.

Figure 3.2 *Paramyrothecium amorphophalli* (**g**, **h**, **n** holotype, MFLU22-0145; **i-n** ex-type, MFLUCC 22-0085)

3.3.3 Pathogenicity Assay

Paramyrothecium amorphophalli was isolated from the leaf blight of elephant foot yam which appeared mostly around the leaf margins. The pathogenicity tests have been conducted by both conidial suspension and mycelial plug on wounded leaves showed that the fungus can cause disease on the host leaves (Figure 3.3). The wounded leaves inoculated with conidial suspension showed symptoms after 24 hours of incubation, whereas the wounded leaves treated with mycelial plugs showed symptoms 48 hours later. The symptoms continued to spread in the leaves for 7 days, after which most of the leaves started to rot. After 10 days of incubation, sporodochia were observed on the symptomatic areas of the wounded leaves. The symptoms and sporodochia that appeared on the leaves during the pathogenicity test were similar to those symptoms and sporodochia formed on the host leaves in nature (Figure 3.3). The re-isolated fungus was identified as the same species according to the morphological characteristics of its sporodichia and conidia. The negative controls (wounded and non-wounded leaves) did not show any symptoms during the test. Interestingly, no symptoms were observed on the non-wounded leaves incubated with conidial suspension or mycelial plugs.

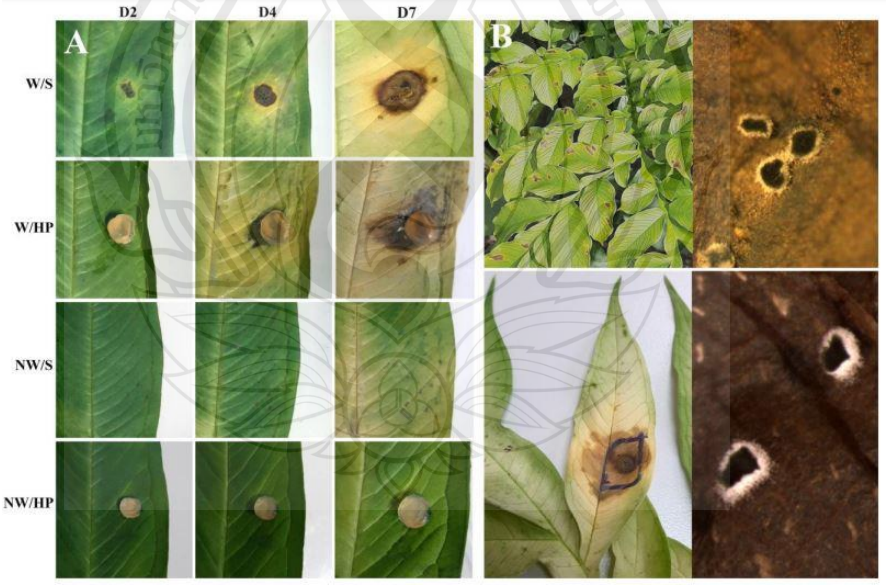

Note Symptoms on days 2 (D2), 4 (D4) and 7 (D7) post incubation are shown (W: Wounded, NW: Non-wounded, S: Conidial suspension, HP: Mycelial plug). B Symptoms and sporodochia on the leaves in nature (up); symptoms and sporodochia on the leaves after incubation in the laboratory (bottom).

Figure 3.3 The pathogenicity test results on elephant foot yam's leaves

3.4 Discussion

A morphological and multi-locus phylogenetic study revealed that *Paramyrothecium amorphophalli* isolated from elephant foot yam is a new species of *Paramyrothecium*. *Paramyrothecium amorphophalli* was found in a separate lineage from *P. eichhorniae* and *P. vignicola*. Based on the morphological characters, it can be distinguished from *P. vignicola* in that it produces slightly smaller conidia (5–6.4 µm in *P. amorphophalli*; 5–7 µm in *P. vignicola*) (Withee et al., 2022). *Paramyrothecium amorphophalli* differs from both *P. eichhorniae* (Pinruan et al., 2022) and *P. vignicola* as observed from the absence of setae associated with sporodochia and producing smaller conidiophores (11–20 µm in *P. amorphophalli*; 15–40 µm in *P. eichhorniae*; 40–60 µm in *P. vignicola*). Moreover, it has a slower growth rate on PDA as compared to *P. eichhorniae*. We found that *P. amorphophalli* (MFLU22-0145) rarely produces robust ellipsoidal conidia that have never been described from *Paramyrothecium*. The ellipsoidal conidia, however, were not observed in the culture. The base pair differences between *P. amorphophalli* and *P. eichhorniae* (TBRC 10637) for ITS, *cmdA*, *rpb2* and *tub2* were 0.5% (3/583 bp), 2.3% (16/694 bp), 0.5% (4/700 bp) and 1.4% (5/340 bp) respectively.

Pathogenicity tests have shown that *Paramyrothecium amorphophalli* can cause disease in the host from which it was originally isolated. Additionally, the symptoms that appeared throughout the pathogenicity tests conducted under laboratory conditions were similar to the blight symptoms observed on the leaves in nature. Interestingly, the results also showed that *P. amorphophalli* can only infect wounded leaves. It can be hypothesized that the taxon requires wounds to penetrate and infect the host.

Many species of *Myrothecium sensu lato* (including those later transferred to *Paramyrothecium*) were earlier identified based on morphology. Later, taxonomic revision of the genus based on molecular study brought about the establishment of several new genera (Lombard et al., 2016). Since *Paramyrothecium* species have overlapping morphological characteristics, identification based only on morphology is not recommended (Lombard et al., 2016). Additionally, many studies have proven the importance of multi-gene phylogenetic identification, particularly in phytopathogens

(Jayawardena et al., 2016, 2019; Phoulivong et al., 2010). Therefore, it becomes imperative to support morphological studies with multi-gene phylogenetic data (Cai et al., 2009; Bhunjun et al., 2021b; Hyde et al., 2018b). Even though many species of *Paramyrothecium* have been isolated from Thailand, their distribution, host specificity and diversity remained inconclusive (Withee et al., 2022). Hence, extensive sampling from different hosts using a morpho-molecular approach is recommended. The *Myrothecium* group presently comprises 87 species (MycoBank 2023), and many of these species have been synonymized and are scattered into different genera.

Moreover, only a few phylogenetic studies have been carried out that included *Myrothecium* species (Lombard et al., 2016). Recent studies on the *Myrothecium* group showed their high diversity (Liang et al., 2019; Withee et al., 2022) and more species are likely to be found, indicating that these speciose genera and groups of fungi are likely to comprise more new taxa (Bhunjun et al., 2022; Calabon et al., 2022; Senanayake et al., 2022).

CHAPTER 4

FIRST REPORT OF *Colletotrichum fructicola* CAUSING FRUIT ROT AND LEAF-TIP DIEBACK ON PINEAPPLE IN NORTHERN THAILAND

4.1 Introduction

Pineapple (*Ananas comosus* (L.) Merr.) is one of the edible and nutritious fruits of the Bromeliaceae, grown in tropical and subtropical countries (Sapak et al., 2021). Asia, South Central America, and Africa are the world's leading areas producing this fruit (Altendorf & Major, 2018). Pineapple is the second largest tropical crop in the world (Altendorf & Major, 2018) and the third most consumed fruit worldwide (Baruwa, 2013). Brazil, China, Costa Rica, India, the Philippines, and Thailand are the top pineappleproducing countries (Sapak et al., 2021). Pineapple could be eaten as a fresh fruit or selected as a basic raw ingredient used in the confectionery industry (Hossain et al., 2015; Sodjinou et al., 2022; Umi et al., 2020). The fruit contains immense nutrients and is abundant in vitamins A, C, B1, and B6 (Joy, 2010; Kader et al., 2010; Williams et al., 2017). It also has proteins, carbohydrates, fiber, copper, manganese, and several minerals (Hasan et al., 2022; Sodjinou et al., 2022).

In Thailand, pineapple products have been regarded as economic commodities for export (Apipatpapha et al., 2022). Thailand is currently the second-largest supplier of processed pineapple fruit in the world. Production areas for pineapple in Thailand have been divided into northern, northeastern, central, and southern parts (Hemung et al., 2022). Most cultivated areas are in Prachuap Khiri Khan, Rayong, Ratchaburi, and Chonburi provinces (Apipatpapha et al., 2022). Pineapple is classified into five groups based on the morphology of the leaf and fruit, namely Abacaxi, Cayenne, Maipure or Perolera, Queen, and Spanish (Py et al., 1987). Among these, Cayenne, Queen, and Spanish are cultivated in Thailand (Popluechai et al., 2007). Nang Lae district in Chiang Rai province is the most pineapple-cultivating area, and Nang Lae (Cayenne group) and

Phu Lae (Queen group) are the most common varieties in northern Thailand (http://www.doa.go.th/; https://www.saio.co.th/; accessed on 12 December 2022). The pineapple-growing area in Thailand is around 72,656 hectares, with an annual production of 1,680,884 metric tons. The total canned pineapples exported from Thailand were 290,524 metric tons in 2020, valued at about 345 million US dollars (International Trade Centre Trade Map; https: //www.trademap.org).

Diseases are the key elements of significant yield losses in pineapples across the world (Sapak et al., 2021). Among fungal pathogens, *Colletotrichum* species are the most important fungi responsible for the diseases of tropical and sub-tropical fruits (Jayawardena et al., 2016). Many *Colletotrichum* species have been reported from different hosts in Thailand such as *C. aenigma* (Meetum et al., 2015), *C. aeschynomenes* (Sangpueak et al., 2018), *C. artocarpicola* (Bhunjun et al., 2019), *C. asianum* (Noor & Zakaria, 2018; Phoulivong et al., 2012; Wang et al., 2020; Weir et al., 2012), *C. boninense* (Hyde et al., 2018b; Sangpueak et al., 2018), *C. brevisporum* (Chai et al., 2018; Damm et al., 2019; Hou et al., 2016; Jayawardena et al., 2016), *C. chiangraiense* (Hyde et al., 2018b; Ma et al., 2018), *C. cordylinicola* (Jayawardena et al., 2016; Phoulivong et al., 2010; Weir et al., 2012), *C. endophyticum* (Diao et al., 2017; Liu F. et al., 2015; Manamgoda et al., 2013; Sharma et al., 2014), *C. orchidearum* (Damm et al., 2019; Hyde et al., 2018b), *C. orchidophilum* (Hyde et al., 2018b), *C. plurivorum* (De Silva et al., 2019), and *C. siamense* (Hyde et al., 2018b; Jayawardena et al., 2016; Sharma et al., 2017; Suwannarat et al., 2017; Weir et al., 2012), majority belonging to gloeosporioides species complex. *Colletotrichum fructicola* is one of the most invasive species and has been reported as the causal agent of anthracnose, leaf spots and bitter rots in more than 90 plant species (Bragard et al., 2021). It was originally isolated from *Coffea arabica* in northern Thailand (Prihastuti et al., 2009). It has also been reported from *Capsicum annuum* (Hyde et al., 2018b), *Carica papaya* (Noor & Zakaria, 2018; Phoulivong et al., 2012; Wang et al., 2020; Weir et al., 2012), *Cymbopogon citratus* (Hyde et al., 2018b; Jayawardena et al., 2016), *Dendrobium* sp. (Hyde et al., 2018b), *Dimocarpus longan* (Hyde et al., 2018b; Phoulivong et al., 2010, 2012), *Freycinetia* sp. (Hyde et al., 2018b), *Pandanus* sp. Hyde et al., 2018b, *Pennisetum purpureum* (Hyde et al., 2018b; Jayawardena et al., 2016) in Thailand. Mealybug wilt-associated virus, bacterial heart rot, fruit collapse, butt rot, fruitlet core rot, black rot, yeasty, and

fusariosis are the main diseases of pineapple, discussed by Sapak et al. (2021). Despite the importance of pineapple in Thailand, studies for the isolation and identification of fungal pathogens associated with pineapple have not been conducted in Thailand.

4.2 Materials & Methods

4.2.1 Sample Collection, Examination and Isolation

In order to isolate the fungal pathogens associated with pineapple plants, pineapple leaves with diebacks and leaf spots, and rotting fruits were considered. In total, 10 symptomatic leaves and 12 rotting pineapple fruit were collected during June–July 2022 from organic farms in Ban Du and Nang Lae sub-districts, Mueang Chiang Rai district, Chiang Rai province, northern Thailand. The samples were kept in plastic bags containing the information of collection date, collection site, host name and disease type, and subsequently were transferred to the laboratory for further examination. The fruiting bodies on natural substrates were observed and photographed using a stereo-microscope (OLYMPUS-SZX16). Morphological features were observed using a LEICA-EZ4 stereo-microscope and photographed with an optical microscope equipped with a Nikon DS-Ri2 camera. The photo plates were made by the Adobe Photoshop v.21.1.2 software, and the scales were measured by the Tarosoft (R) Image Frame Work software.

Direct isolation and indirect isolation (tissue isolation) were used to obtain cultures (White et al., 1990). For tissue isolation, 30 mm^2 leaf fragments were cut from the margin of lesions and healthy part sterilized by submerging in 70% ethanol for 2 mins, 10% sodium hypochlorite solution for 60s followed by 3 times rinsing in sterile distilled water for 60s (Manamgoda et al., 2013). Following the procedures outlined by Senanayake et al. (2020), single spore isolation and hyphal tip isolation were done to purify the isolates. Finally, the pure cultures were deposited in Mae Fah Luang University Culture Collection (MFLUCC), Chiang Rai, Thailand. Specimens were deposited in the herbarium of the Center of Excellence in Fungal Research (CEFR), Mae Fah Luang University (MFLU).

4.2.2 DNA Extraction and PCR Amplification

Using a DNA Extraction Kit (Omega Biotek) in accordance with the manufacturer's instructions, genomic DNA was extracted from fresh mycelia cultured on potato dextrose agar (PDA) for 14 days. The internal transcribed spacer (ITS), actin (*ACT*), chitin synthase (*CHS-1*), glyceraldehyde-3-phosphate dehydrogenase (*GAPDH*) and β-tubulin (*TUB2*) were amplified using primers ITS5/ITS4, ACT-512F/ACT-783R, CHS-79F/CHS-345R, GDF/GDR and BT-2Fd/BT-4Rd, respectively (Table 4.1). The polymerase chain reaction was carried out in a total volume of 25 µL, including 12.5 µL of 2 × Power Taq PCR Master Mix, 1 µL of each primer (20 µM), 1 µL genomic DNA and 9.5 µL deionized water. The PCR procedure was done under the following conditions: Initial denaturation at 95 °C for 5 min, followed by 40 cycles of denaturation for 30 s at 95 °C; annealing at 53 ℃ for 60 s (ITS), 55 °C for 50 s (*ACT*), 58 °C for 30 s (*CHS-1*); 58 °C for 50 s (*GAPDH*), 58 ℃ for 90 s (*TUB2*); extension at 72 °C for 60 s; and the final extension at 72 °C for 10 min. PCR amplification was performed in an Eppendorf (Master cycler X50s) thermal cycler. PCR products were sequenced by SolGent company, South Korea.

Table 4.1 Primers used in this study

Gene	Primer	Sequence (5'→3')	References
ITS	ITS 5 ITS 4	GGA AGT AAA AGT CGT AAC AAG G TCC TCC GCT TAT TGA TAT GC	Carbone &Kohn (1999)
ACT	ACT-512F ACT-783R	ATG TGC AAG GCC GGT TTC GC TAC GAG TCC TTC TGG CCC AT	Templeton et al. (1992)
CHS-1	CHS-79F CHS-345R	TGG GGC AAG GAT GCT TGG AAG AAG TGG AAG AAC CAT CTG TGA GAG TTG	Templeton et al. (1992)
TUB2	BT-2Fd BT-4Rd	GTB CAC CTY CAR ACC GGY CAR TG CCR GAY TGR CCR AAR ACR AAG TTG TC	Katoh et al. (2019)

Table 4.2 Taxa and their GenBank accession numbers used in the phylogenetic analysis

Taxa	**Strains**	**GenBank accession numbers**				
		ITS	***GAPDH***	***CHS-1***	***ACT***	***TUB***
Colletotrichum acidae	MFLUCC 17-2659*	MG996505	MH003691	MH003694	MH003697	MH003700
C. aenigma	ICMP 18608*	JX010244	JX010044	JX009774	JX009443	JX010389
C. aeschynomenes	ICMP 17673*, ATCC 201874	JX010176	JX009930	JX009799	JX009483	JX010392
C. alatae	CBS 304.67*, ICMP 17919	JX010190	JX009990	JX009837	JX009471	JX010383
C. alienum	ICMP 12071*	JX010251	JX010028	JX009882	JX009572	JX010411
C. aotearoa	ICMP 18537*	JX010205	JX010005	JX009853	—	JX010420
C. arecicola	CGMCC 3.19667*	MK914635	—	MK935541	MK935374	MK935498
C. artocarpicola	MFLUCC 18-1167*	MN415991	MN435568	MN435569	MN435570	MN435567
C. asianum	ICMP 18580*, CBS 130418	JX010196	JX010053	JX009867	JX009584	JX010406
C. analogum	YMF1.06943*	OK030860	OK513663	OK513559	OK513599	OK513629
C. camelliae	CGMCC 3.14925, LC1364*	KJ955081	KJ954782	MZ799255	KJ954363	KJ955230
C. cangyuanensis	YMF1.05001*	OK030864	OK513667	OK513563	OK513603	OK513633
C. changpingense	CGMCC 3.17582*, SA0016, MFLUCC 15-0022	KP683152	KP852469	KP852449	KP683093	KP852490
C. chiangmaiense	MFLUCC 18-0945*	MW346499	MW548592	MW623653	MW655578	—
C. chrysophilum	URM 7368, CMM4268*	KX094252	KX094183	KX094083	KX093982	KX094285
C. ciggaro	ICMP 18539*	JX010230	JX009966	JX009800	JX009523	JX010434
C. clidemiae	ICMP 18658*	JX010265	JX009989	JX009877	JX009537	JX010438
C. cobbittiense	BRIP 66219*	MH087016	MH094133	MH094135	MH094134	MH094137
C. conoides	LC6226*	KP890168	KP890162	KP890156	KP890144	KP890174

Table 4.2 (continued)

Taxa	Strains	GenBank accession numbers				
		ITS	***GAPDH***	***CHS-1***	***ACT***	***TUB***
C. cordylinicola	MFLUCC 090551*, ICMP 18579	JX010226	JX009975	JX009864	HM470234	JX010440
C. dimorphum	YMF1.07309*	OK030867	OK513670	OK513566	OK513606	OK513636
C. dracaenigenum	MFLUCC 19-0430*	MN921250	MT215577	MT215575	MT313686	—
C. endophytica	MFLUCC 13-0418, LC0324*	KC633854	KC832854	MZ799261	KF306258	MZ673954
C. fici-septicae	MFLU 19-2770*	MW114367	MW183774	MW177701	MW151585	—
C. fructicola	ICMP 18581*, CBS 130416	JX010165	JX010033	JX009866	FJ907426	JX010405
C. fructicola	MFLUCC 17-0555	MG646969	MG646936	MG646932	MG646944	MG646928
C. fructicola	MFLUCC 17-0613	MG646968	MG646935	MG646933	MG646939	MG646927
C. fructicola	**P76, MFLUCC 22-0181**	**OQ048649**	**OQ067350**	**OQ067349**	**OQ067348**	**OQ067351**
C. fructicola	**P76-3, MFLUCC 22-0182**	**OQ048650**	**OQ067354**	**OQ067353**	**OQ067352**	**OQ067355**
C. fructivorum	Coll1414, BPI 884103, CBS133125*	JX145145	MZ664047	MZ799259	MZ664126	JX145196
C. gloeosporioides	IMI 356878*, ICMP 17821, CBS 112999	JQ005152	JQ005239	JQ005326	JQ005500	JQ005587
C. gracile	YMF1.06939*	OK030868	OK513671	OK513567	OK513607	OK513637
C. grevilleae	CBS 132879, CPC 15481*	KC297078	KC297010	KC296987	KC296941	KC297102
C. grossum	CAUG7, LC6227*	KP890165	KP890159	KP890153	KP890141	KP890171

Table 4.2 (continued)

Taxa	Strains	GenBank accession numbers				
		ITS	***GAPDH***	***CHS-1***	***ACT***	***TUB***
C. hebeiense	MFLUCC 13-0726*	KF156863	KF377495	KF289008	KF377532	KF288975
C. hederiicola	MFLU 15-0689*	MN631384	—	MN635794	MN635795	—
C. helleniense	CBS 142418, CPC 26844*	KY856446	KY856270	KY856186	KY856019	KY856528
C. henanense	LC3030, CGMCC 3.17354, LF238*	KJ955109	KJ954810	MZ799256	KM023257	KJ955257
C. horii	NBRC 7478*, ICMP 10492, MTCC 10841	GQ329690	GQ329681	JX009752	JX009438	JX010450
C. hystricis	CBS 142411, CPC 28153*	KY856450	KY856274	KY856190	KY856023	KY856532
C. jiangxiense	CGMCC 3.17363*	KJ955201	KJ954902	—	KJ954471	KJ955348
C. kahawae	IMI 319418*, ICMP 17816	JX010231	JX010012	JX009813	JX009452	JX010444
C. makassarense	CBS 143664*	MH728812	MH728820	MH805850	MH781480	MH846563
C. musae	CBS 116870*, ICMP 19119, MTCC 11349	HQ596292	HQ596299	JX009896	HQ596284	HQ596280
C. nanhuaensis	YMF1.04993*	OK030870	OK513673	OK513569	OK513609	OK513639
C. nullisetosum	YMF1.06946*	OK030872	OK513675	OK513571	OK513611	OK513641
C. nupharicola	CBS 470.96*, ICMP 18187	JX010187	JX009972	JX009835	JX009437	JX010398
C. oblongisporum	YMF1.06938*	OK030874	OK513677	OK513573	—	OK513643
C. parvisporum	YMF1.06942*	OK030876	OK513679	OK513575	OK513613	OK513645
C. pandanicola	MFLUCC 17-0571*	MG646967	MG646934	MG646931	MG646938	MG646926

Table 4.2 (continued)

Taxa	Strains	GenBank accession numbers				
		ITS	***GAPDH***	***CHS-1***	***ACT***	***TUB***
C. perseae	CBS 141365*, GA100	KX620308	KX620242	MZ799260	KX620145	KX620341
C. proteae	CBS 132882*	KC297079	KC297009	KC296986	KC296940	KC297101
C. pseudotheobromicola	MFLUCC 18-1602*	MH817395	MH853675	MH853678	MH853681	MH853684
C. psidii	CBS 145.29*, ICMP 19120	JX010219	JX009967	JX009901	JX009515	JX010443
C. queenslandicum	ICMP 1778*	JX010276	JX009934	JX009899	JX009447	JX010414
C. rhexiae	Coll1026, BPI 884112, CBS 133134*	JX145128	MZ664046	MZ799258	MZ664127	JX145179
C. salsolae	ICMP 19051*	JX010242	JX009916	JX009863	JX009562	JX010403
C. siamense	ICMP 18578*, CBS 130417	FJ972613	FJ972575	JX009865	FJ907423	FJ907438
C. syzygiicola	DNCL021, MFLUCC 10-0624*	KF242094	KF242156	—	KF157801	KF254880
C. tainanense	CBS 143666*	MH728818	MH728823	MH805845	MH781475	MH846558
C. temperatum	CBS 133122*, Coll883, BPI 884100	JX145159	MZ664045	MZ799254	MZ664125	JX145211
C. tengchongense	YMF 1.04950*	OL842169	OL981264	OL981290	OL981238	—
C. theobromicola	CBS 124945*, ICMP 18649	JX010294	JX010006	JX009869	JX009444	JX010447
C. ti	ICMP 4832*	JX010269	JX009952	JX009898	JX009520	JX010442
C. tropicale	CBS 124949*, ICMP 18653, MTCC 11371	JX010264	JX010007	JX009870	JX009489	JX010407
C. truncatum	CBS 151.35*	GU227862	GU228254	GU228352	GU227960	GU228156
C. viniferum	GZAAS 5.08601*, yg1	JN412804	JN412798	—	JN412795	JN412813

Table 4.2 (continued)

Taxa	Strains	GenBank accession numbers				
		ITS	***GAPDH***	***CHS-1***	***ACT***	***TUB***
C. vulgaris	YMF 1.04940*	OL842170	OL981265	OL981291	OL981239	—
C. wuxiense	CGMCC 3.17894*	KU251591	KU252045	KU251939	KU251672	KU252200
C. xanthorrhoeae	BRIP 45094*, ICMP 17903, CBS 127831	JX010261	JX009927	JX009823	JX009478	JX010448
C. xishuangbannaense	MFLUCC.19-0107*	MW346469	MW537586	MW660832	MW652294	—
C. yulongense	CFCC.50818*	MH751507	MK108986	MH793605	MH777394	MK108987
C. yunajiangensis	YMF1.04996*	OK030885	OK513686	OK513583	OK513620	OK513649

Note Type strains are indicated with "*". The isolates sequenced in this study are in bold

4.3 Results

4.3.1 Morphological Studies

Following 7–14 days of incubation, morphological features including culture (color and growth rate) and microscopic features (conidiogenous cells and conidial measurements, appressoria measurements) were recorded for P76 (MFLU 22-0302) and P76-3 (MFLU 22- 0303). The two strains, P76 and P76-3 were isolated from rotting pineapple fruit and leaf dieback, respectively. Morphological comparisons of P76 and P76-3 were performed on 14-day-old cultures grown on PDA at 25 ˚C ± 2 ˚C. There were minor differences in size of conidia and conidiogenous cells and also in appressoria shape which are very common in a specific species within the C. gloeosporioides species complex. Finally, these two isolates were identified as *C. fructicola* based on morpho-molecular evidence.

4.3.2 Phylogenetic Analyses

The five-locus (ITS, *ACT*, *GAPDH*, *CHS-1*, and *TUB2*) phylogenetic analysis included 73 reference isolates (Jayawardena et al., 2020, 2021a; Liu et al., 2022). The phylogenetic tree consisted of 71 ingroup and two outgroup taxa (*Colletotrichum truncatum* (CBS 151.35) and *C. acidae* (MFLUCC 17-2659)). The data matrix contained a total of 1670 characters, of which 269 were parsimony-uninformative and 384 were parsimony-informative. The most parsimonious tree (Tree Length (TL) = 1321, Consistency Index (CI) = 0.673, Retention Index (RI) = 0.824, Rescaled Consistency Index (RC) = 0.554, Homoplasy Index (HI) = 0.327) was presented (Figure 1). The ML, MP and BYPP trees were identical in topology. The best-scoring RAxML tree with final optimization showed a likelihood value of -9834.854352. The dataset comprised 754 distinct alignment patterns, with 5.31% of characters being gaps or undetermined. Estimated base frequencies were as follows: A = 0.229261, C = 0.299900, G = 0.241493, T = 0.229347, with substitution rates AC = 1.133302, AG = 2.907494, AT = 1.290422, CG = 0.902726, CT = 4.957643, GT = 1.000000. The gamma distribution shape parameter is 0.422238 and the tree length is 0.963648. Based on the phylogenetic analysis, strains P76 and P76-3 clustered with *C. fructicola*, showing 86%/77%/0.99 (ML/MP/PP) bootstrap support, respectively (Figure 4.3). The base pair differences between these two strains and the ex-type of *C. fructicola* (ICMP 18581) were shown (Table 4.3).

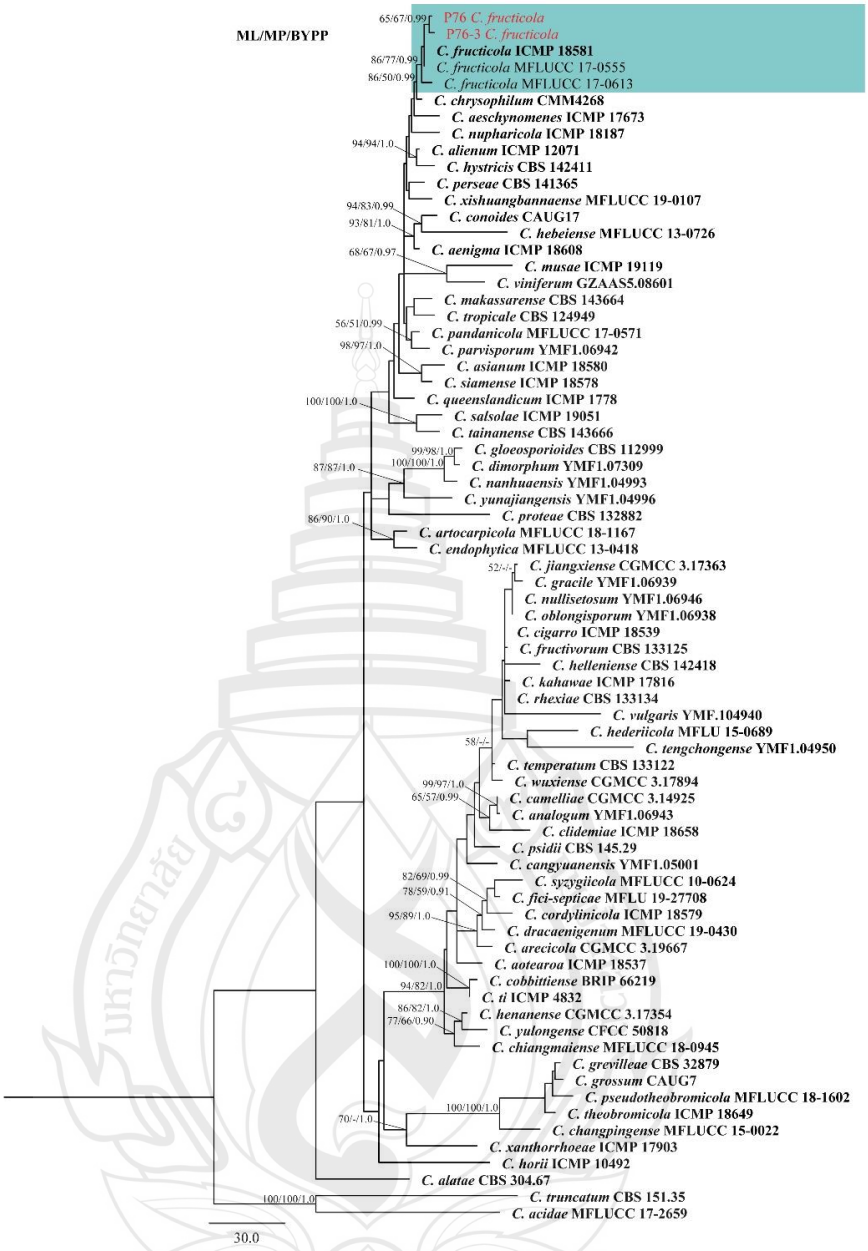

Note The tree was rooted with *Colletotrichum truncatum* (CBS 151.35) and *Colletotrichum acidae* (MFLUCC 17.2659). Maximum likelihood and maximum parsimony bootstrap values ≥ 50% and bayesian posterior probabilities ≥ 0.90 are shown near the nodes, respectively. Type strains are in bold and the newly generated isolates are in red.

Figure 4.1 Maximum parsimony tree of the *Colletotrichum gloeosporioides* species complex obtained from a combined ITS, *ACT*, *CHS-1*, *GAPDH*, and *TUB2* sequence data

Table 4.3 Base pair differences between *C. fructicola* (ICMP 18581) and two newly isolated strains

Isolate	ITS	*ACT*	*CHS-1*	*GAPDH*	*TUB2*
P76	2/511 bp	0/256 bp	0/241 bp	0/248 bp	1/402 bp
P76-3	3/511 bp	1/256 bp	0/241 bp	0/248 bp	0/402 bp

4.3.3 Taxonomy

Colletotrichum fructicola Prihast., L. Cai & K.D. Hyde 2009 (Figures 4.2, 4.3)

Index fungorum number: IF 515409; Faces of Fungi number: FoF 06767

Associated with pineapple fruit rot and leaf dieback. Sexual morph: Not observed. Asexual morph: *Vegetative hyphae* hyaline, smooth-walled, septate, branched. *Conidiomata* acervular, dark brown, bearing conidial mass, and setae. *Setae* brown to dark brown, smooth-walled, 2–4 septate, 38–83 µm long ($\bar{x}$ = 59.5 µm, n = 6), base cylindrical, 3–5 µm diam. ($\bar{x}$ = 4.5 µm, n = 6), tip acute or obtuse. *Conidiophores* rarely observed, hyaline, septate, branched, cylindrical to inflated. *Conidiogenous cells* hyaline, cylindrical or clavate, 12–25 × 3–4.5 µm ($\bar{x}$ = 18 × 3.5 µm, n = 20). *Conidia* hyaline, aseptate, smooth-walled, cylindrical, rounded at apex, sub-acute at base, guttulate, 12.5–19 × 4.5–6 µm ($\bar{x}$ = 16 × 5 µm, n = 30). *Appressoria* produced on slide culture, brown to dark brown, irregular in shape, undulate, 7–9 × 4.5–6 µm ($\bar{x}$ = 7.8 × 5 µm, n = 15), producing on hyphae and conidia.

Culture characteristics: Colonies on PDA 65–85 mm in diam. after 7 days at 28°C, velvety, circular, undulate; surface pale grey in center and white in margin, becoming grey with age, reverse same color. Colonies on OA 60–71 mm in diam. after 7 days, cottony, slightly raised, entire, surface white to whitish grey, reverse same color.

Material examined: Thailand, Chiang Rai Province, Mueang Chiang Rai District, Ban Du Sub-district. On pineapple rotting fruit, 27 June 2022, A. Armand, P76 (MFLU 22-0302), living culture, MFLUCC 22-0181. On pineapple leaf dieback, 27 June 2022, A. Armand, P76-3 (MFLU 22-0303), living culture, MFLUCC 22-0182.

Notes: The species within gloeosporioides species complex are mainly distinguished by producing cylindrical conidia with rounded ends tapering slightly towards the base (Jayawardena et al., 2016). The strain P76 was isolated directly from pineapple rotting fruit, whereas P76-3 has been obtained by tissue isolation from a

young fresh leaf with tip dieback symptoms. Based on the phylogenetic tree (Figure 4.1), isolates P76 (MFLUCC 22-0182) and P76-3 (MFLU 22-0303) clustered with *C. fructicola* strains with 86/ 77/ 0.99 ML, MP and BYPP values, respectively. Morphologically, P76 and P76-3 are similar. However, P76 produced slightly larger conidia than P76-3 (13–19 × 4.5–6 µm in P76 vs. 12.5–17.5 × 4–6 µm in P76-3). The conidial shape was slightly different as P76 produced conidia with obtuse ends, whereas P76-3 mostly produced rounded ends conidia. However, morphological comparison with the ex-type of *C. fructicola* revealed no significant differences between the type strain and our isolates (P76, P76-3) (Jayawardena et al., 2020).

Note **a**, **b** Rotting pineapple fruit **c** Acervuli on the fruit **d** Setae **e** Conidiophores **f** Conidiogenous cells and conidial attachment **g** Conidia **h** Appressoria **i** Upper and reverse view of colony on PDA. Scale bars: **c** = 200 µm, **d** = 20 µm, **e**–**h** = 10 µm.

Figure 4.2 *Colletotrichum fructicola* P76 (MFLU 22-0302)

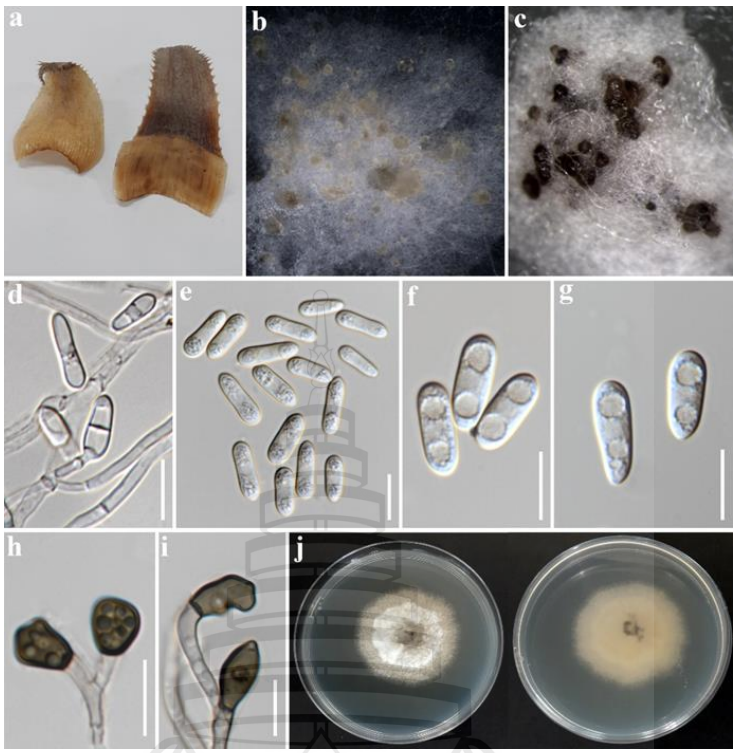

Note **a** Symptomatic leaves **b** Conidial masses on PDA **c** Acervuli on PDA **d** Conidial attachment **e**–**g** Conidia **h**, **i** Appressoria **j** Upper and reverse view of colony on PDA. Scale bars: **d**–**i** 10 µm.

Figure 4.3 *Colletotrichum fructicola* P76-3 (MFLUCC 22-0182)

4.3.4 Pathogenicity Assay

Pathogenicity test results related to strain P76 showed that this strain can cause disease on both wounded and non-wounded host leaves. The wounded leaves inoculated with P76 showed dieback symptoms 4 days after the inoculation, whereas those of non-wounded leaves showed symptoms 6 days after inoculation. However, the symptoms continued to spread in both wounded and non-wounded leaves after 10 days. After 11 days, aerial mycelia started to grow on the surface of the symptomatic area in both wounded and non-wounded leaves. (Figure 4.4, P76/W, P76/NW).

The strain P76-3 was proven that can cause disease only on wounded leaves. The symptoms on the wounded leaves treated with P76-3 appeared 6 days after inoculation, limited to the mycelial plug margins and could not spread through the leaf (Figure 4.4, P76-3/W). The non-wounded leaves inoculated with P76-3 remained asymptomatic during the test (Figure 4.4, P76-3/NW) along with the negative control

treatments. The re-isolated fungi were identified as *C. fructicola* according to morphological characteristics.

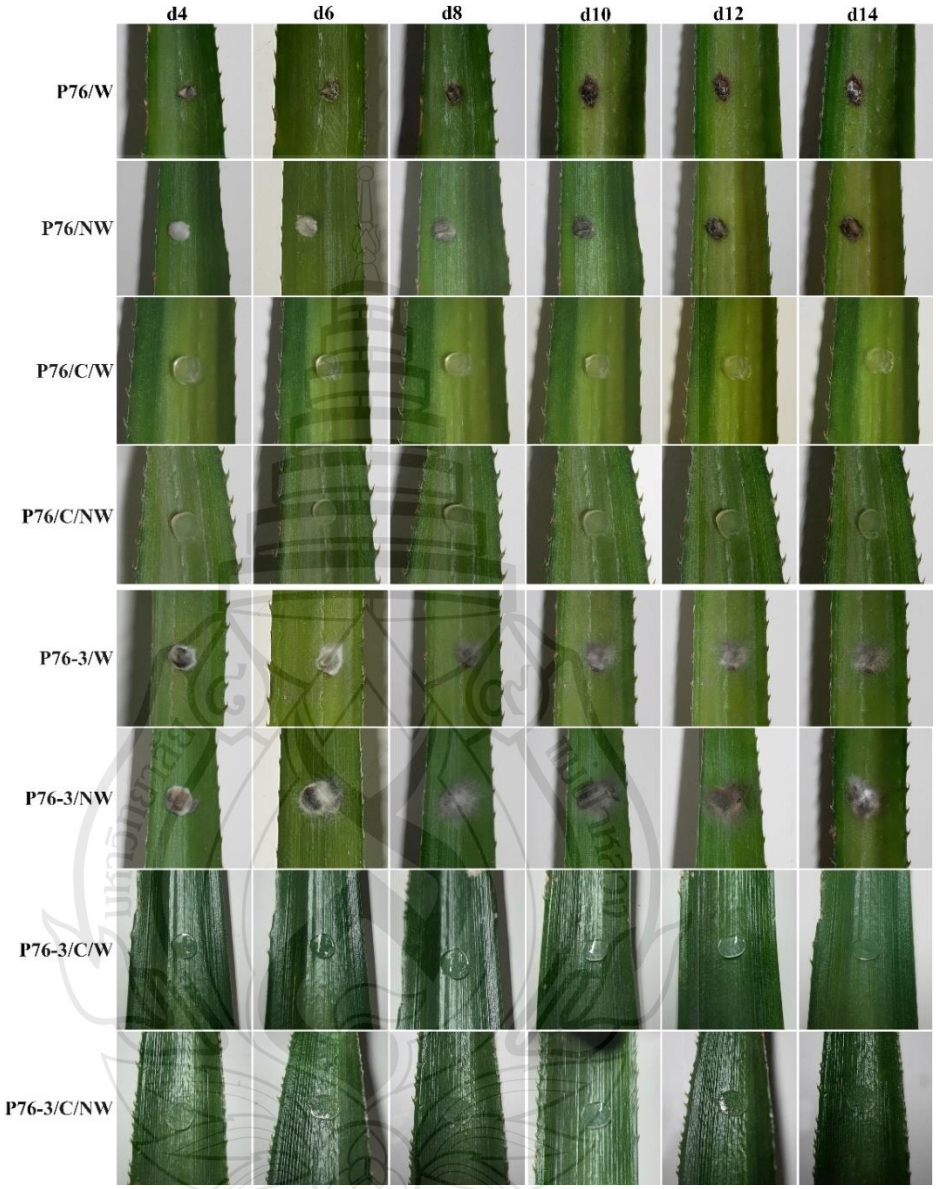

Note Symptoms (dieback) on days 4 (**d4**), 6 (**d6**), 8 (**d8**), 10 (**d10**), 12 (**d12**) and 14 (**d14**) after inoculation are shown. **C**: Control, **W**: Wounded, **NW**: Non-wounded.

Figure 4.4 Pathogenicity assay on leaf of pineapple

4.4 Discussion

In this study, the diseased leaves showing dieback symptoms and rotting fruits of pineapple were collected in Chiang Rai province, northern Thailand. Based on a direct isolation from the fruiting bodies (Figure 4.2) and indirect isolation of infected leaves via tissue culture (Figure 4.3), we obtained two *Colletotrichum* isolates. Jayawardena et al. (2021b) recommended using a poly-phasic approach to identify *Colletotrichum* species (Jayawardena et al., 2021b). We used both morphological examination and multi-loci molecular analysis for species-level identification. The phylogenetic analysis of a combined dataset of ITS, *ACT*, *CHS-1*, *GAPDH* and *TUB2* showed that the two isolates of *Colletotrichum* associated with pineapple belong to *C. fructicola* (Figure 4.1). Morphological studies also confirmed the phylogenetic results. *Colletotrichum* species have a wide host range and geographical distribution worldwide (Jayawardena et al., 2016; Liu et al., 2022). However, the occurrence of *Colletotrichum* species on pineapple has not so far been reported in Thailand. In the USDA host fungal database, there are 12 records of *Colletotrichum* species on *Ananas* sp. (Cannon et al., 2012). *Colletotrichum ananas* was reported in India (Farr & Rossman, 2022), while *C. truncatum* was reported to cause leaf-tip dieback in Malaysia (Cannon et al., 2012). *Colletotrichum gloeosporioides* was recorded as causing anthracnose in China and USA on pineapple (Cannon et al., 2012). *Colletotrichum gloeosporioides* was also recorded from *Ananas* sp. in Brazil from pineapple leaves. *Colletotrichum* sp. was identified from Cuba, India, Korea, Panama and West Indies (Garud, 1968) However, these species were identified based only on morphology.

In the last decades, identification based on morphology has led to misidentifying of fungal pathogens (Jayawardena et al., 2021b). In plant pathology, correct identification of fungal species is a fundamental step which links information concerning biology, host range, distribution, pathogenicity and food security (Jayawardena et al., 2021b), indicating importance of species identification to barricade future afflictions provoked by these pathogens (Bhunjun et al., 2022). Moreover, emerging pathogens have also been increasing threats during the last decades (Castro et al., 2023). *Colletotrichum*, being a complex genus, shares overlapping morphological

characteristics among species. *Colletotrichum fructicola* belongs to the *C. gloeosporioides* species complex which is comprising fruit rots and post-harvest pathogens. Since this species complex is the most confusing complex within the *Colletotrichum* genus, morphological identification alone cannot be trusted to identify the species correctly. It follows that, the use of a poly-phasic approach in plant pathology is crucial for the precise identification and naming of fungi, which will advance the management and control of both recognized and newly emerging diseases. (Jayawardena et al., 2021b). Furthermore, poly-phasic approach poly-phasic approach using molecular analyses is an effective tool to identify cryptic species and to stimate species diversity (Bhunjun et al., 2022).

Among *Colletotrichum* species in the gloeosporioides species complex, *C. fructicola* has a very broad host range, isolated from more than eight plant families as endophytes and plant pathogens (Johnston, 1960). It has been reported from America, Asia, Africa, Europe and Oceania (Chen et al., 2022). In This study, we isolated and illustrated *C. fructicola* as the first report of *Colletotrichum* species associated with pineapple in Thailand, based on molecular and morphological analyses. Furthermore, the pathogenicity tests of P76 and P76-3 isolates proved that *C. fructicola* isolated from pineapple is pathogenic to the host (Figure 4.4).

The results of the present study can be useful for pathologists, understanding the fungal pathogen diversity associated with pineapple, disease management and quarantine purposes. Many new *Colletotrichum* species have been introduced in 2022 (MycoBank, accessed 08 December 2022), and still there are potentially many novel species of *Colletotrichum* remained undiscovered (Bhunjun et al., 2022; Castro et al., 2023). Additionally, many studies reported new hosts for existing *Colletotrichum* species (Li L. et al., 2022; Nigar et al., 2022; Pacheco-Esteva et al., 2022; Senanayake et al., 2020; Wang et al., 2023; Wei et al., 2023; Yu et al., 2023; Zhang Y. et al., 2023; Zhu et al., 2023), broadening their host and geographical ranges. Therefore, more investigations on the isolation and identification of *Colletotrichum* associated with pineapple can improve our knowledge about fungal diversity and host range, and will potentially discover novel species of *Colletotrichum*.

CHAPTER 5

IDENTIFICATION AND CHARACTERIZATION OF *Colletotrichum* SPECIES ASSOCIATED WITH DURIAN IN NORTHERN THAILAND

5.1 Introduction

Durian (*Durio* sp., Malvaceae) is a tropical fruit native to Southeast Asia and one of the most popular fruits in Thailand (Teh et al., 2017). This fruit is known as the 'king of fruits' for its formidable spiny husk, unique overwhelming flavor and odor (Bampenrat et al., 2020; Li et al., 2012). The three leading durian-producing countries are Thailand, Malaysia, and Indonesia. Thailand is the main durian producer in the world. Thailand's commercial durian production was 1,111.93 thousand metric tons in 2020 (National Agricultural Big Data Center; OAE 2021).

Durian is one of the most economically important exported fruits in Thailand (Charoensumran et al., 2021). Thailand's most popular cultivars for consumption and export include 'Chanee', 'Gaan Yaow', 'Gradumtong', 'Nok Yib', 'Puang Mani' and 'Monthong' (Lim & Sangchote, 2003). Sweeter cultivars with a mild odor are popular in Thailand (Monthong), whereas pungent and bitter varieties are popular in Malaysia and Singapore (Musang King) (Teh et al., 2017). The complexity of different cultivars and distinctive odors is due to differences in sulfur volatiles, esters, alcohol, and acid percentages (Siriphanich, 2011). A draft genome assembly of *D. zibethinus* was provided by Teh et al. (2017).

Durian is also subjected to different kinds of fungal diseases: fruit rots, stem cankers and root rots, resulting in low yield and quality. Among these diseases, fruit rots are a serious problem in durian production for domestic consumption and export (Siriphanich, 2011). *Colletotrichum* includes important plant pathogens, endophytes, saprobes, and human pathogens (Jayawardena et al., 2021a). As plant pathogens, *Colletotrichum* is a member of the family *Glomerellaceae* (Glomerellales,

Sordariomycetes) (Wijayawardene et al., 2020), and the species are known to cause anthracnose disease, fruit rots, crown rots, leaf spots, and stem end rots in pre- and postharvest (Cannon et al., 2012; Jayawardena et al., 2021a). Two hundred and eighty species with molecular data are accepted in this genus with 16 species complexes and 15 singleton species (Liu et al., 2022). The use of polyphasic approaches has enabled the correct identification of *Colletotrichum* species (Bhunjun et al., 2021b; Damm et al., 2019; Hyde et al., 2014; Liu et al., 2022). However, knowledge of the overall species diversity and host distribution is largely incomplete (Jayawardena et al., 2021a; Bhunjun et al., 2022; Liu et al., 2022). Hence, to fill this gap, this study aims to identify *Colletotrichum* species associated with durian in Thailand based on morphology and phylogenetic analyses.

5.2 Materials & Methods

5.2.1 Sample Collection, Examination, and Isolation

Fresh samples of durian fruit were collected from orchards in Chiang Rai province, Thailand, from 2021 to 2022. Samples were brought to the laboratory in Zip-lock plastic bags for examination. The fruiting bodies on natural substrates were observed and photographed using a stereo-microscope (OLYMPUS-SZX16). Morphological characters were observed using a LEICA-EZ4 stereomicroscope and photographed with an optical microscope equipped with a Nikon DS-Ri2 camera. The photo plates were made by Adobe Photoshop v. 21.1.2 software. Measurements were done using the Tarosoft (R) Image Frame Work software.

Single spore isolation was employed to obtain pure cultures, following the methods described by Senanayake et al. (2020). The pure cultures were deposited in the Mae Fah Luang University Culture Collection (MFLUCC), Chiang Rai, Thailand. Specimens were deposited in the herbarium of Mae Fah Luang University (MFLU). Faces of Fungi (FoF) and Index Fungorum numbers were acquired for the new species as described in Jayasiri et al. (2015). Moreover, the novel species was submitted to the GMS webpage (Chaiwan et al., 2021). Based on the recommendations provided by

Chethana et al. (2021) and Jayawardena et al. (2021b), the new species has been confirmed.

5.2.2 DNA Extraction, PCR Amplification, and Sequencing

Genomic DNA was extracted from fresh mycelia grown on potato dextrose agar (PDA) for 10 days using the DNA Extraction Kit (Omega Bio-Tek) according to the manufacturer's instructions. The internal transcribed spacer (ITS), actin (*ACT*), chitin synthase (*CHS-1*), glyceraldehyde-3- phosphate dehydrogenase (*GAPDH*), and β-tubulin (*TUB2*) were amplified using primers given in Table 5.1. The polymerase chain reaction was performed in a total volume of 25 µL, containing 12.5 µL of 2 × Power Taq PCR Master Mix, 1 µL of each primer (20 µM), 1 µL genomic DNA, and 9.5 µL deionized water. The PCR procedure was performed using the following conditions: initial denaturation at 95 °C for 5 min, followed by 40 cycles of denaturation for 30 s at 95 °C; annealing at 53 °C for 60 s (ITS), 55 °C for 50 s (*ACT*), 58 °C for 30 s (*CHS-1*); 58 °C for 50 s (*GAPDH*), 58 °C for 90 s (*TUB2*); extension at 72 °C for 60 s; and the final extension at 72 °C for 10 min. PCR amplification was performed in an Eppendorf (Master cycler X50s) thermal cycler. PCR products were sequenced by the SolGent Co, Republic of Korea.

5.2.3 Phylogenetic Analyses

The retrieved sequences were BLAST-searched, and comparable reference sequences were downloaded from GenBank (Table A1) in accordance with the results of those searches and recently published papers on Colletotrichum (Jayawardena et al., 2020, 2021a; Liu et al., 2022). Utilizing MAFFT v.7 under the web server (http://mafft.cbrc.jp/alignment/server), the individual loci were manually adjusted (Katoh et al., 2019). Where necessary, the alignment was further adjusted using BioEdit v. 7.0.9.0 (Hall, 1999). Command-based TrimAl software and the gappyout approach were used to trim aligned sequences automatically. Maximum likelihood (ML) analysis with the GTR + GAMMA model of nucleotide evolution was carried out using RAxML-HPC2 on XSEDE with bootstrapping of 1000 replicates. The Bayesian analysis was conducted using a Markov Chain Monte Carlo (MCMC) algorithm with Bayesian posterior probabilities (BYPP) using MrBayes on XSEDE (Ronquist et al., 2012). On the CIPRES online platform, the best-fit evolutionary models for each dataset were assessed using jModeltest 2.1.10 through the Akaike Information Criterion

(AIC). Four MCMC chains were run from random trees for 1,000,000 generations and sampled every 100th generation. The first 25% of the generated trees were discarded as burn-in, and the remaining trees were used for calculating posterior probabilities. Using PAUP XSEDE (Swofford, 2002), a maximum parsimony (MP) analysis was performed. Gaps were deemed to be missing data, and ambiguously aligned areas were discarded. The analyses were performed on the CIPRES Science Gateway (https://www.phylo.org/portal2) (Miller et al., 2011). A multi-locus concatenated sequence dataset (ITS, *ACT*, *CHS-1*, *GAPDH*, and *TUB2*) of closely related species was used for a pairwise homoplasy index (PHI) test using Splits Tree 4 (version 4.14.2) to determine the recombination level (Fu et al., 2019). The phylograms were visualized in FigTree v. 1.4.0 and annotated in Adobe Illustrator CC 22.0.0 (Adobe Systems, San Jose, CA, USA).

Table 5.1 Primers used in the study

Gene	Primer	Sequence (5'-3')	References
ITS	ITS 5	GGA AGT AAA AGT CGT AAC AAG G	White et al. (1990)
	ITS 4	TCC TCC GCT TAT TGA TAT GC	
ACT	ACT-512F	ATG TGC AAG GCC GGT TTC GC	Carbone and Kohn
	ACT-783R	TAC GAG TCC TTC TGG CCC AT	(1999)
CHS-1	CHS-79F	TGG GGC AAG GAT GCT TGG AAG AAG	Carbone and Kohn
	CHS-345R	TGG AAG AAC CAT CTG TGA GAG TTG	(1999)
GAPDH	GDF	GCC GTC AAC GAC CCC TTC ATT GA	Templeton et al. (1992)
	GDR	GGG TGG AGT CGT ACT TGA GCA TGT	
TUB2	BT-2Fd	GTB CAC CTY CAR ACC GGY CAR TG	Woudenberg et al.
	BT-4Rd	CCR GAY TGR CCR AAR ACR AAG TTG TC	(2009)

5.3 Results

5.3.1 Multi-locus Phylogeny

Phylogenetic analyses were performed based on a five-locus concatenated alignment of ITS, *ACT*, *CHS-1*, *GAPDH*, and *TUB2*. We constructed three phylograms separately for the *C. gigasporum*, *C. gloeosporioides*, and *C. truncatum* species complexes. The concatenated alignments for each complex were subjected to ML, MP, and BYPP analyses.

The dataset for the *C. gigasporum* species complex comprised 35 taxa and 1708 characters, including gaps, with two outgroup taxa (*C. crousii* LC13858 and *C. crousii* LC13860). Parsimony analysis revealed the presence of 1318 constant characters (proportion = 0.771663), 104 uninformative characters, and 286 parsimony-informative characters. A single most parsimonious tree (Tree Length (TL) = 690, Consistency Index (CI) = 0.696, Retention Index (RI) = 0.861, Rescaled Consistency (RC) = 0.599, Homoplasy Index (HI) = 0.304) was obtained by the parsimony analysis (Figure 5.1).

The data matrix for the *C. gloeosporioides* species complex included 72 taxa and 1636 characters, including gaps, with two outgroup taxa (*C. acidae* MFLUCC 17-2659 and *C. truncatum* CBS:151.35). Parsimony analysis showed 987 constant characters (proportion = 0.603301), 267 variable characters, and 382 parsimony-informative characters. The most parsimonious tree (TL = 1296, CI = 0.676, RI = 0.812, RC = 0.549, HI = 0.324) was shown (Figure 5.5).

The dataset for the *C. truncatum* species complex consisted of 13 taxa and 1637 characters, including gaps, with one outgroup (*C. arxii* CBS 132511). Parsimony analysis indicated 1240 constant characters (proportion = 0.757483), 214 variable characters, and 183 parsimony-informative characters. The most parsimonious tree (TL = 532, CI = 0.889, RI = 0.914, RC = 0.813, HI = 0.111) constructed by parsimony analysis was shown (Figure 5.7).

The phylogenetic tree showed that two isolates belong to the *Colletotrichum gigasporum* species complex clade. Of these, one isolate clustered with *C. gigasporum*, representing 100% ML, 100% MP and 100% BYPP values (Figure 5.1). Another obtained isolate made a separate branch from *C. magnisporum* with 73% ML, 74% MP, and 94% BYPP values and introduced as a new species, namely *Colletotrichum durionigenum* (Figure 5.1). *Colletotrichum durionigenum* differs from *C. magnisporum* (CBS 398.84) by a 0.96% bp difference in ITS, 1.51% bp difference in *ACT*, 1.68% bp difference in *CHS-1*, 9.02% bp difference in *GAPDH*, and 4.602% bp difference in *TUB2* (Table 5.2). Since more strains of *C. magnisporum* were not available, we compared only the type strain with our species. A pairwise homoplasy index (PHI) test indicated no significant recombination (Φw = 1.0) between *C. durionigenum* and its closely related taxa (Figure 5.3). *CHS-1* and *TUB2* sequences were not available for *C. jishouense* (GZU_HJ3_J5), hence it has not been included in the PHI test. Phylogenetic

analyses showed that one obtained isolate fell into the *C. gloeosporioides* species complex and clustered with *C. pandanicola*, showing 99% BYPP. Finally, this isolate was identified as *C. pandanicola* based on the phylogenetic result and morphological comparison (Figure 5.5).

One isolate belongs to the *Colletotrichum truncatum* species complex, clustering with *C. truncatum* strains with 100% ML, 100%, MP, and 100% BYPP. We identified this isolate as *C. truncatum* based on morpho-molecular results (Figure 5.7).

Table 5.2 Base pair differences between *C. durionigenum* and *C. magnisporum* (CBS 398.84)

Taxon	**Gene regions**				
	ITS	***ACT***	***CHS-1***	***GAPDH***	***TUB2***
C. magnisporum (CBS 398.84)	5/519 bp	4/264 bp	5/298 bp	12/133 bp	22/478 bp

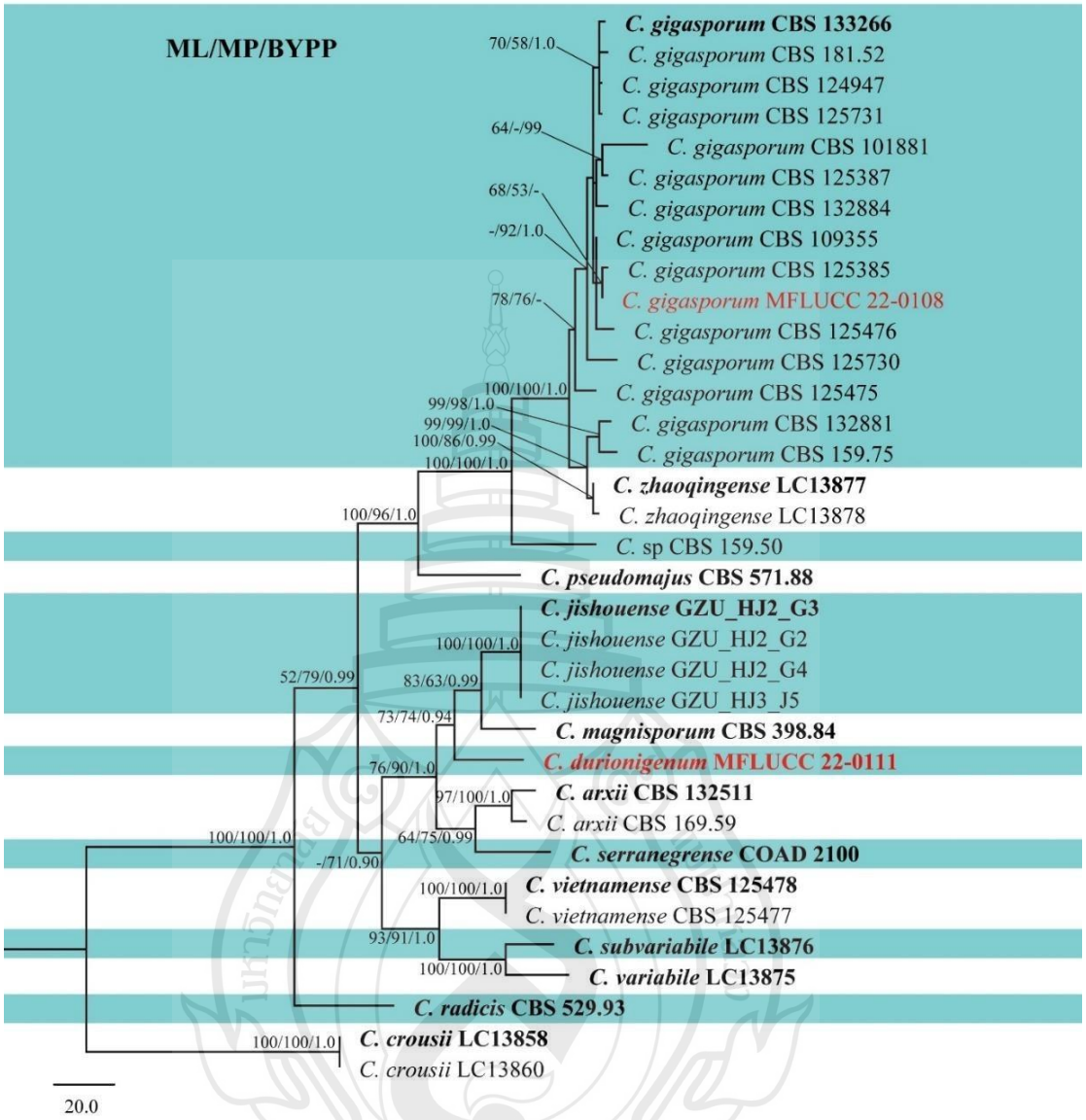

Note The tree was rooted with *Colletotrichum crousii* (LC13858) and *Colletotrichum crousii* (LC13860). Maximum likelihood and maximum parsimony bootstrap support values ≥50% (BT) as well as bayesian posterior probabilities ≥0.90 (PP) are shown respectively near the nodes. Type strains are in bold, and the newly generated isolates are in red.

Figure 5.1 Phylogenetic tree of the *Colletotrichum gigasporum* species complex generated by maximum parsimony analysis of combined ITS, *ACT*, *CHS-1*, *GAPDH* and *TUB2* sequence data

Colletotrichum durionigenum A. Armand, Jayawar. & K.D. Hyde, sp. nov.

Figure 5.2

Index Fungorum number: IF559996; Facesoffungi number: FoF13362

Etymology – "*durio*" refers to the plant genus from which the fungus was isolated, and "*durionigenum*" is a Latin combination meaning "Durio-borne"

Holotype – MFLU 22-0194

Associated with durian fruit rot. Sexual morph: Not observed. Asexual morph: *Vegetative hyphae* hyaline to brown, smooth-walled, septate, branched. *Conidiomata* acervular, dark brown, bearing conidial masses and setae. *Setae* brown to dark brown, smooth-walled, 2–5-septate, 107–176 µm ($\overline{x}$ = 135.5 µm, n = 10) long, base conic or inflated, 8.5–12.5 µm diam. ($\overline{x}$ = 10.5 µm, n = 10), tip acute or obtuse. *Conidiophores* medium brown to brown, septate, branched. *Conidiogenous cells* hyaline to pale brown, cylindrical or clavate, 18.5–39 × 6.5–10 µm ($\overline{x}$ = 28.5 × 8 µm, n = 30). *Conidia* hyaline or pale purple, aseptate, smooth-walled, cylindrical with rounded ends, guttulate, 29–40 × 8.5–11.5 µm ($\overline{x}$ = 35 × 10 µm, n = 30). *Appressoria* not observed.

Culture characteristics – Colonies on PDA 56–60 mm in diam. after 7 days, velvety, medium sparse, flat with undulated margin, circular. Surface olivaceous-grey in the centre, becoming olivaceous black after 30 days; reverse olivaceous-grey to olivaceous-black. Colonies on OA 59–65 mm in diam. after 7 days, flat with entire margins; surface olivaceous-grey, reverse iron-grey.

Material examined – Thailand, Chiang Rai Province, Wiang Chiang Rung District, Thung Ko Sub-district, associated with durian fruit rot, 4 July 2022, A. Armand, P132-2 (MFLU 22-0194, holotype), ex-type living culture, MFLUCC 22-0111.

GenBank numbers – (P132-2, MFLUCC 22-0111); ITS: OP740244, *act*: OP744503, *chs-1*: OP744504, *gapdh*: OP744505, *tub2*: OP744506.

Notes – Phylogenetically, *C. magnisporum* (CBS 398.84) is the closest taxon to *Colletotrichum durionigenum*. However, *C. durionigenum* (MFLU 22-0194) can be differentiated from *C. magnisporum* based on phylogenetic analyses and morphological features. The base pair differences between these two species were 48 bp in all five gene regions (48 bp/1676 bp). *Colletotrichum durionigenum* differs from *C. magnisporum* by producing non-verruculose setae that are considerably bigger than

those of *C. magnisporum* (107–176 µm in *C. durionigenum* vs. 42.5–105 µm in *C. magnisporum*). Moreover, *C. durionigenum* is distinguishable by producing longer conidiogenous cells (18.5–39 × 6.5–10 µm in *C. durionigenum* vs. 18–33.5 × 5.5–10 µm in *C. magnisporum*). Although the two species produce conidia with a same shape, the conidia of *C. durionigenum* are slightly larger than those of *C. magnisporum* (29–40 × 8.5–11.5 µm in *C. durionigenum* vs. 28–39 × 8.5– 10.5 µm in *C. magnisporum*). Additionally, *C. durionigenum* (MFLU 22-0194) produces conidia with pale purple pigments which have not been described in *C. magnisporum* (Liu et al. 2014). The pairwise homoplasy index (PHI) test for *C. durionigenum* and its closely related species yielded a p-value (Φw) of 1.0, indicating no significant recombination among the species examined (Figure 5.3).

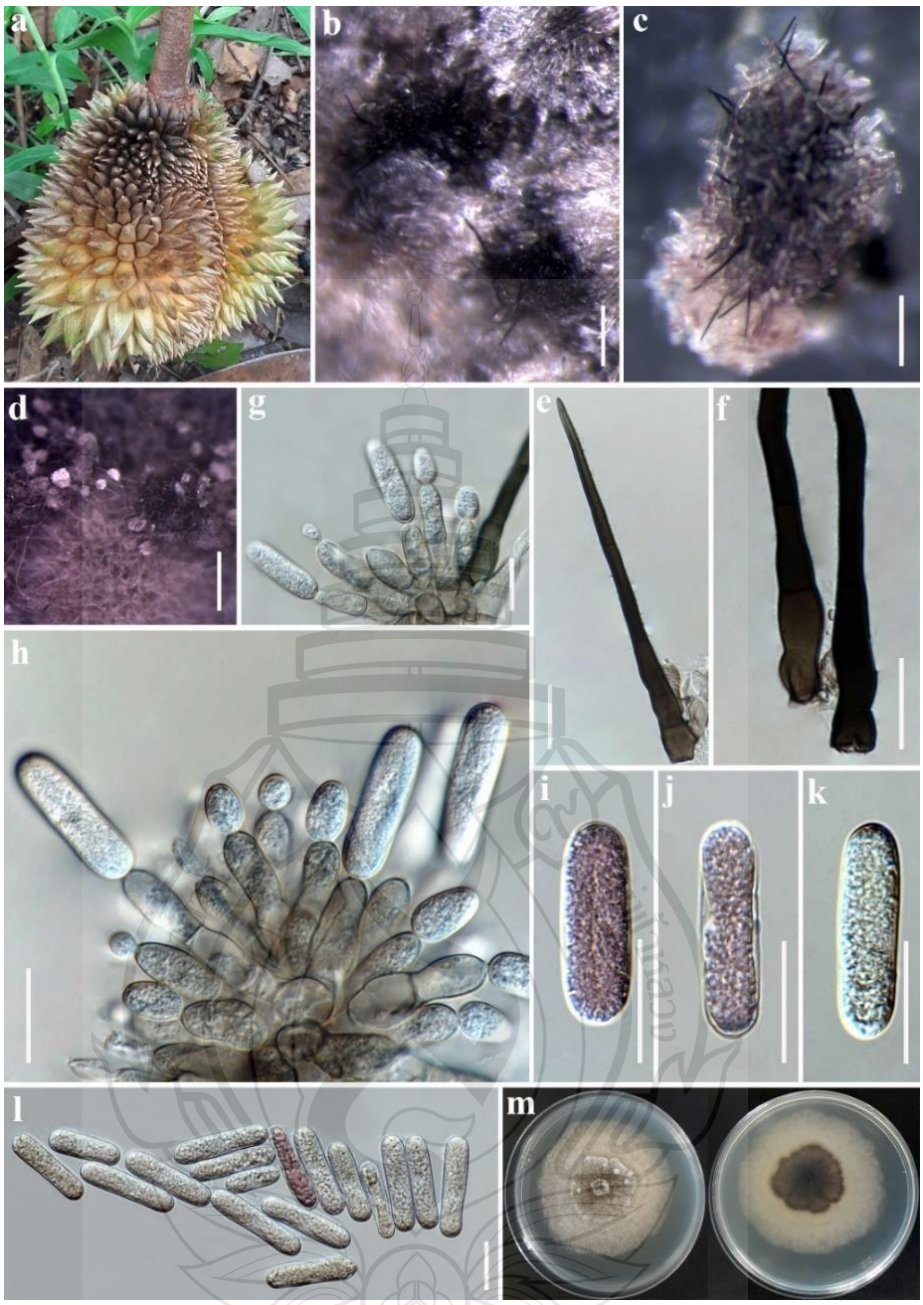

Note **a** Rotting durian fruit **b** Acervuli on the host **c** Acervulus and conidial mass in water drop **d** Acervuli and conidial masses on the PDA **e**, **f** Setae **g**, **h** Conidiophores, conidiogenous cells, and conidial attachment **i**–**l** Conidia **m** Upper and reverse view of culture on PDA. Scale bars: **b**–**d** = 100 μm, **e**–**l** = 20 μm

Figure 5.2 *Colletotrichum durionigenum* (MFLU 22-0194, holotype)

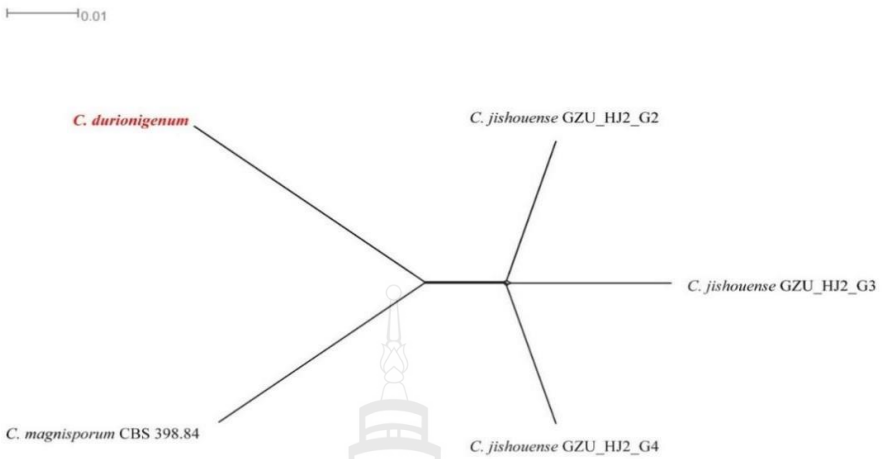

Note Pairwise homoplasy index (PHI) test conducted using both LogDet transformation and splits decomposition. PHI test results (Φw) <0.05 indicate significant recombination among the species

Figure 5.3 The PHI test of *Colletotrichum durionigenum* and closely related species

Colletotrichum gigasporum E.F. Rakotoniriana & Munaut 2013

Figure 5.4

Index Fungorum number: IF800175; Facesoffungi number: FoF10777

Associated with durian fruit rot. Sexual morph: Not observed. Asexual morph: *Vegetative hyphae* hyaline to brown, smooth-walled, septate, branched. *Conidiomata* acervular, dark brown, bearing conidial masses and setae. *Setae* brown to dark brown, smooth-walled to verruculose, 2–4- septate, 95–145 µm ($\overline{x}$ = 127.5 µm, n = 10) long, base cylindrical, 6–7.5 µm diam. ($\overline{x}$ = 6.5 µm, n = 10), tip obtuse to acute. *Conidiophores* pale brown to brown, septate, branched. *Conidiogenous cells* hyaline to pale brown, cylindrical or clavate, 15–27 × 5–7.5 µm ($\overline{x}$ = 19 × 6.5 µm, n = 30). *Conidia* hyaline, aseptate, smooth-walled, cylindrical with rounded ends, guttulate, 25–30.5 × 7–8.5 µm ($\overline{x}$ = 28 × 8 µm, n = 30). Appressoria produced on slide culture, pale brown to brown, undulated to strongly lobate, irregular in shape, 9.5–17.5 × 6.5–8 µm ($\overline{x}$ = 12.5 × 7.5 µm, n = 10), produced directly from mycelia.

Culture characteristics – Colonies on PDA 45–67 mm in diam. after 7 days, velvety, circular, entire in margins; surface olivaceous-grey, reverse olivaceous-grey to olivaceous-black. Colonies on OA 50–65 mm in diam. after 7 days. entire in margins, surface white to pale olivaceous-grey, reverse iron-grey.

Material examined – Thailand, Chiang Rai Province, Mueang Chiang Rai District, Huai Sak Sub-district. On rotting durian fruit, 27 June 2022, A. Armand, P103 (MFLU 22-0192), living culture, MFLUCC 22-0108.

Notes – Strains of *C. gigasporum* clustered together with our strain in a distinct clade with the highest bootstrap values (Figure 5.1). The base pair differences between *C. gigasporum* (MFLUCC 22- 0108) and *C. gigasporum* (CBS 133266, holotype) revealed no difference in ITS, 0.7% (2/298 bp) in *CHS-1*, 2.2% (3/133 bp) in *GAPDH*, and 0.4% (2/478) in *TUB2*. Actin's sequences were not available for the type strain. Morphologically, *C. gigasporum* (MFLU 22-0192) is similar to *C. gigasporum* (CBS 133266, holotype). However, it produced slightly smaller conidia (25–30.5 × 7–8.5 µm in *C. gigasporum* (MFLU 22-0192) vs. (22)25–29(32) × (6)7–9 µm in *C. gigasporum* (CBS 133266, holotype)) and longer setae (95–145 µm in *C. gigasporum* (MFLU 22-0192) vs. 90–140 µm in *C. gigasporum* (CBS 133266, holotype)) (Rakotoniriana et al., 2013).

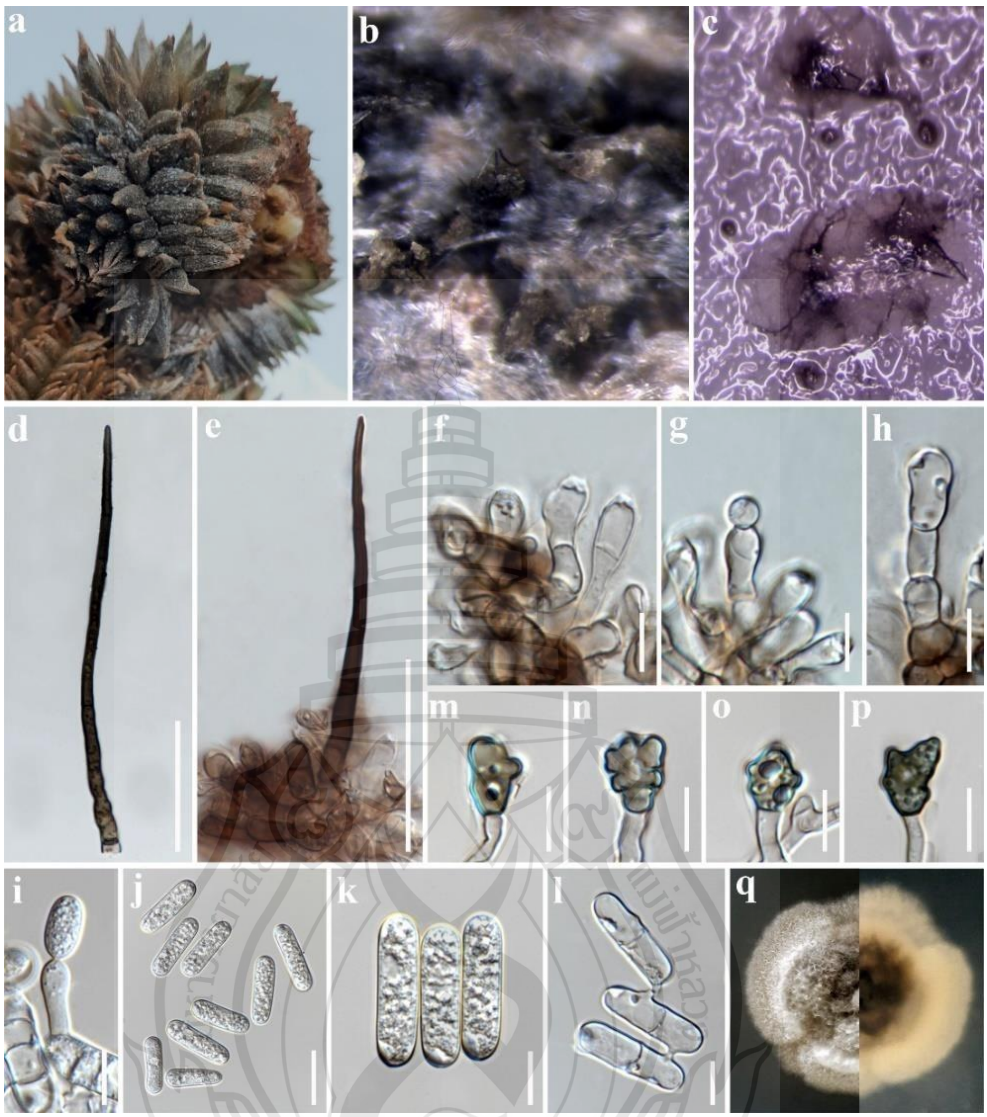

Note **a** Rotting durian fruit **b** Acervuli on the host **c** Acervuli on the PDA **d**, **e** Setae **f**–**h** Conidiophores and conidiogenous cells **i** Conidial attachment **j**, **k** Conidia **l** Conidial anastomosis **m**–**p** Appressoria **q** Upper and reverse view of culture on PDA. Scale bars: **d**, **e** = 50 µm, **f**–**i** = 10 µm, **j** = 20 µm, **k**–**p** = 10 µm.

Figure 5.4 *Colletotrichum gigasporum* (MFLUCC 22-0108)

Note The tree was rooted with *Colletotrichum acidae* (MFLUCC 17-2659) and *Colletotrichum truncatum* (CBS:151.35). Maximum likelihood and maximum parsimony bootstrap support values ≥50% (BT) as well as bayesian posterior probabilities ≥0.90 (PP) are shown respectively near the nodes. Type strains are in bold, and the newly generated isolate is in red

Figure 5.5 Phylogenetic tree of the Colletotrichum gloeosporioides species complex generated by maximum parsimony analysis of combined ITS, *ACT*, *CHS-1*, *GAPDH* and *TUB2* sequence data

Colletotrichum pandanicola Tibpromma & K.D. Hyde 2018

Figure 5.6

Index Fungorum number: IF823841; Facesoffungi number: FoF03906

Associated with durian fruit. Sexual morph: Not observed. Asexual morph: *Vegetative hyphae* hyaline to pale brown, smooth-walled, septate, branched. *Conidiomata* acervular, dark brown, bearing conidial masses. *Setae* not observed. *Conidiophores* hyaline, smooth-walled, cylindrical to inflated. *Conidiogenous cells* hyaline, cylindrical, 13.5–19 × 2.7–3 µm ($\overline{x}$ = 16.5 × 3.3 µm, n = 25). *Conidia* hyaline, aseptate, smooth-walled, cylindrical with rounded ends tapering slightly towards the base, guttulate, 14–17.5 × 4.5–5.5 µm ($\overline{x}$ = 15.5 × 5 µm, n = 30). Appressoria produced on slide culture, pale brown to dark brown, non-rounded, undulated to lobate, irregular in shape, 6–11 × 4.5–6 µm ($\overline{x}$ = 8.5 × 5 µm, n = 10), produced directly from mycelia.

Culture characteristics – Colonies on PDA 63–65 mm in diam. after 7 days, velvety, circular, entire in margins; surface white to olivaceous-grey, reverse same color. Colonies on OA 57–67 mm in diam. after 7 days. entire in margins, aerial mycelia abundant, surface white to whitish grey, reverse same color.

Material examined – Thailand, Chiang Rai Province, Mueang Chiang Rai District, Huai Sak Sub-district. On rotting durian fruit, 27 June 2022, A. Armand, P103-2 (MFLU 22-0193), living culture, MFLUCC 22-0109.

Notes – Based on the phylogenetic tree, *C. pandanicola* (MFLUCC 22-0109) clustered with *C. pandanicola* (MFLUCC 17-0571, ex-holotype) with a high bayesian posterior probabilities value (0.99) (Figure 5.5). The base pair differences between *C. pandanicola* (MFLUCC 22-0109) and the type strain revealed 0.4% (2/511 bp) differences in ITS, 0.8 (2/254 bp) differences in *ACT*, 1.4% (3/215 bp) differences in *CHS-1*, no difference in *GAPDH* and *TUB2*. Morphologically, *C. pandanicola* (MFLU 22-0193) is similar to *C. pandanicola* (MFLU 18-0003, holotype). However, the type strain produces slightly larger conidia (14–17.5 × 4.5–5.5 µm in *C. pandanicola* (MFLU 22-0193) vs. 9– 18 × 4–8 µm in *C. pandanicola* (MFLU 18-0003, holotype)) (Tibpromma et al., 2018).

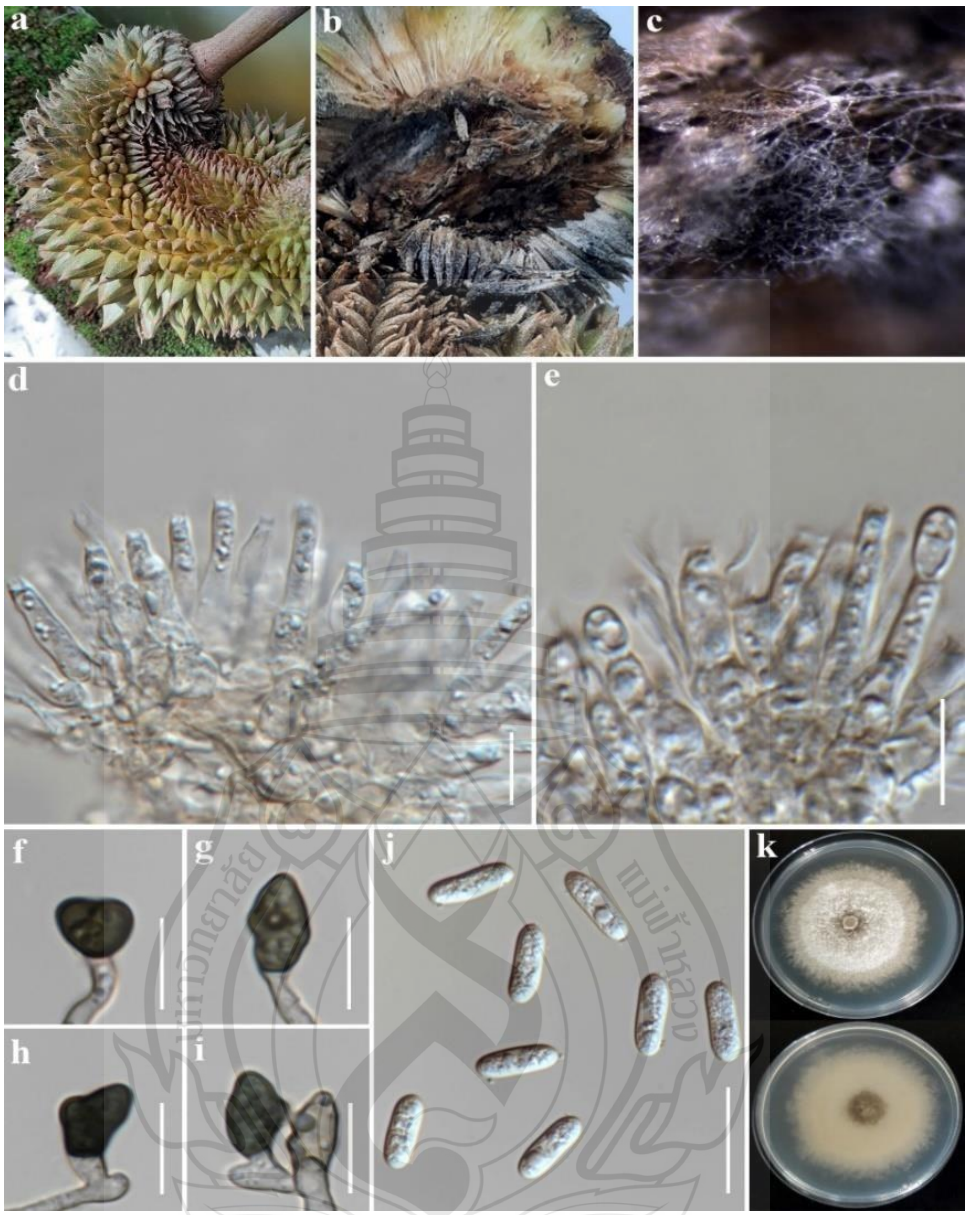

Note **a**, **b** Rotting durian fruit **c** Acervuli on the host **d**, **e** Conidiophores, conidiogenous cells and conidial attachment **i** Conidial attachment **f–i** Appressoria **j** Conidia **k** Upper and reverse view of culture on PDA. Scale bars: **d–i** = 10 µm, **j** = 20 µm.

Figure 5.6 *Colletotrichum pandanicola* (MFLU 22-0193)

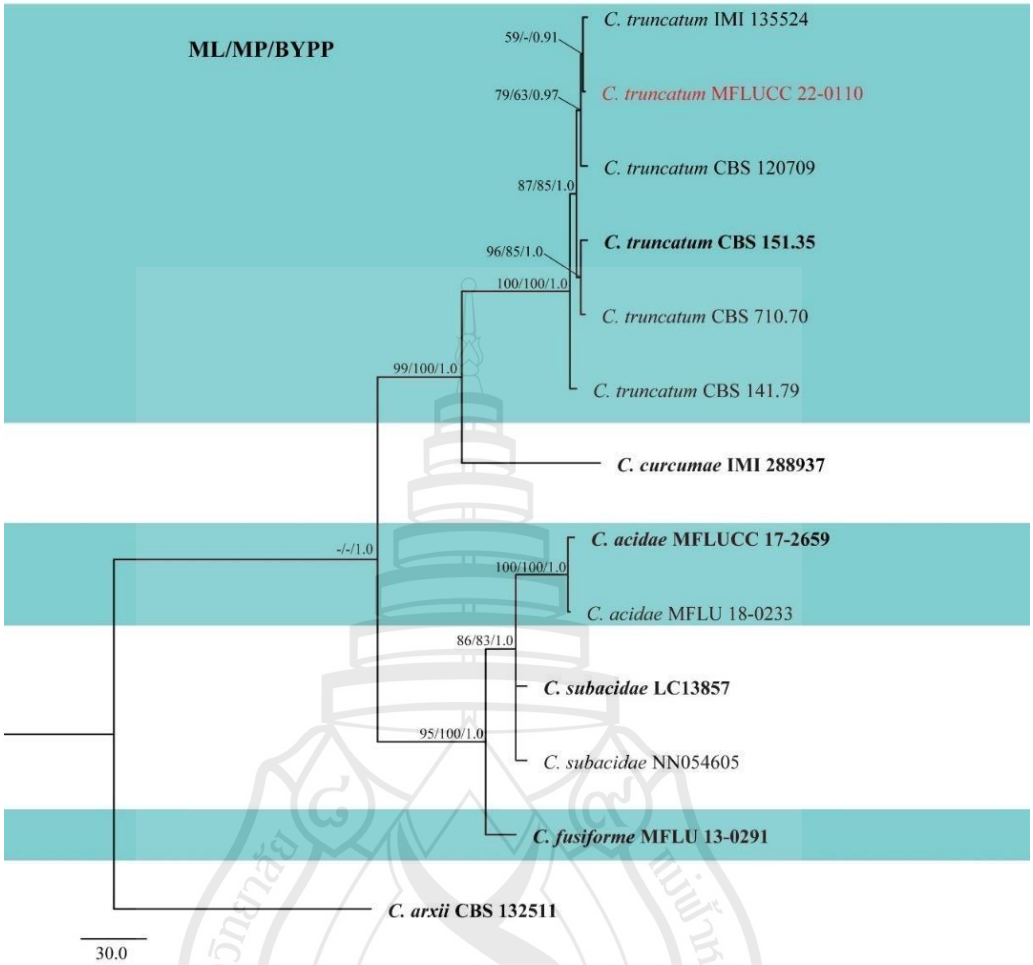

Note The tree was rooted with *Colletotrichum arxii* (CBS 132511). Maximum likelihood and maximum parsimony bootstrap support values ≥50% (BT) as well as bayesian posterior probabilities ≥0.90 (PP) are shown respectively near the nodes. Type strains are in bold, and the newly generated isolate is in red.

Figure 5.7 Phylogenetic tree of the Colletotrichum truncatum species complex generated by maximum parsimony analysis of combined ITS, *ACT*, *CHS-1*, *GAPDH* and *TUB2* sequence data

Colletotrichum truncatum (Schwein.) Andrus & W.D. Moore 1935

Figure 5.8

Index Fungorum number: IF280780; Facesoffungi number: FoF03827

Associated with durian fruit rot. Sexual morph: Not observed. Asexual morph: *Vegetative hyphae* hyaline, smooth-walled, septate, branched. *Conidiomata* acervular, dark brown, bearing conidial masses and setae. *Setae* brown to dark brown, smooth to

verruculose, 2–4 septate, 125–175 µm long ($\overline{x}$ = 155.5 µm, n = 10), base cylindrical, 4–7 µm diam ($\overline{x}$ = 5 µm, n = 10), acute at the apex. *Conidiophores* hyaline, densely clustered. *Conidiogenous cells* hyaline, cylindrical, 18–30 × 2.5–4 µm ($\overline{x}$ = 23.5 × 3 µm, n = 30), collarette not visible. *Conidia* hyaline, smooth-walled, aseptate, curved with parallel walls at the middle part, round and truncate at the base, tapering towards the acute and curved apex, guttulate, 27.5–31 × 3.3–4.4 µm ($\overline{x}$ = 29 × 3.8 µm, n = 30). *Appressoria* produced on slide culture, pale brown to brown, circular or undulated, non-lobate, 4.5–9 µm in diam. ($\overline{x}$ = 6.5 µm, n = 20), produced from both mycelia and conidia.

Culture characteristics – Colonies on PDA 30 mm in diam. after 7 days, with pigment diffusion into PDA, flat, undulated; surface buff; reverse pale luteous. Colonies on OA 25 mm in diam. after 7 days. flat with entire in margins; surface buff, reverse buff to pale olivaceous-grey.

Material examined – Thailand, Chiang Rai Province, Wiang Chiang Rung District, Thung Ko Sub-district. On durian fruit, 04 July 2022, A. Armand, P130 (MFLU 22-0191), living culture, MFLUCC 22-0110.

Notes – Strains of *C. truncatum* clustered together with our strain in a distinct clade with the highest bootstrap value (Fig. 5.7). The base pair differences between *C. truncatum* (MFLUCC 22- 0110) and *C. truncatum* (CBS:151.35, ex-epitype) revealed no difference in ITS and *TUB2*, 0.9% (2/224 bp) in *ACT*, 1.8% (4/225 bp) in *CHS-1*, and 1.3% (3/231 bp) in *GAPDH*. Morphologically, *C. truncatum* (MFLU 22-0191) is similar to *C. truncatum* (CBS:151.35). However, it produced considerably longer setae (125–175 µm in *C. truncatum* (MFLU 22-0191) vs 80–150 µm in *C. truncatum* (CBS:151.35)), longer conidiogenous cells (18–30 in *C. truncatum* (MFLU 22-0191) vs 6–20 in *C. truncatum* (CBS:151.35)) and longer conidia (27.5–31 µm in *C. truncatum* (MFLU 22- 0191) vs 20–23.5 (–26) µm in *C. truncatum* (CBS:151.35)) (Damm et al., 2009).

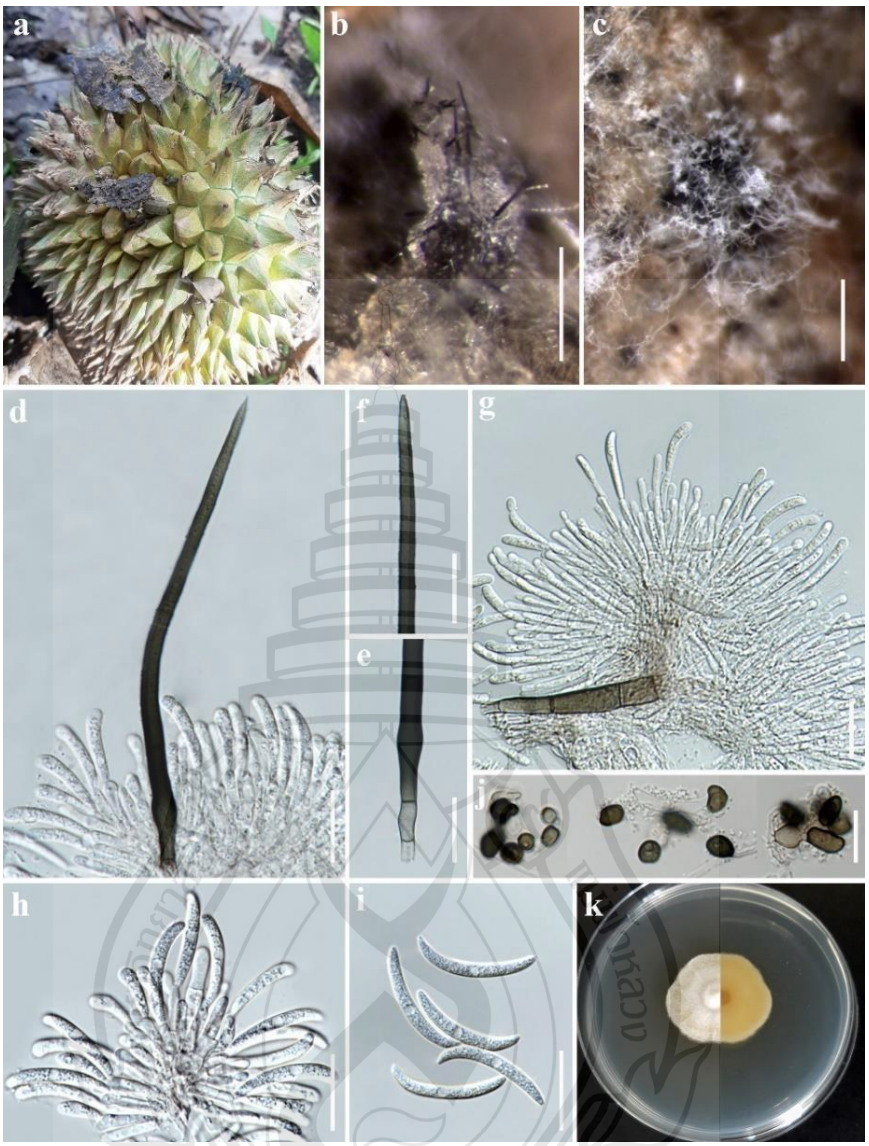

Note **a** Rotting durian fruit **b**, **c** Acervuli on the host **d**–**f** Setae **g**, **h** Conidiogenous cells and conidial attachment **i** Conidia **j** Appressoria **k** Upper and reverse view of culture on PDA. Scale bars: **b** = 200 µm, **c** = 250 µm, **d**–**i** = 20 µm, **j** = 10 µm

Figure 5.8 *Colletotrichum truncatum* (MFLU 22-0191)

5.4 Discussion

Fresh durian fruits with rot symptoms were collected from northern Thailand and examined. A combined morpho-molecular approach was adopted to identify

Colletotrichum species associated with durian. To understand the species phylogenetic relationships in C. gigasporum, C. gloeosporioides and C. truncatum species complexes, we constructed three separate phylograms with ML, MP, and BYPP analyses based on five loci, including ITS, *ACT*, *CHS-1*, *GAPDH*, and *TUB2*.

According to the MP distance tree (Figure 5.1), *Colletotrichum durionigenum* is a new species with a distinct lineage with 73%/74%/0.94 ML, MP, and BYPP bootstrap support, respectively, and is basal for *C. magnisporum* and *C. jishouense*. Moreover, morphological comparison confirmed the phylogenetic results. *Colletotrichum durionigenum* differs from *C. magnisporum* in having larger setae, conidia and producing longer conidiogenous cells (Liu et al., 2014). Although conidial pigmentation is not a strong morphological feature, producing pale purple pigments in conidia of *C. durionigenum* (MFLU 22-0194, holotype) is worthy of documentation. *Colletotrichum durionigenum* was directly isolated from fresh durian fruit with rotting symptoms, as it was well developed and produced fruiting bodies on the fruit. However, *Colletotrichum magnisporum* was introduced from an unknown host (Liu et al., 2014), collected before 1984, and it was the only report of *C. magnisporum* in nature. Talhinhas & Baroncelli. (2021) speculated that this species might be extinct and suggested further studies for the assurance of its occurrence in nature.

The phylogenetic tree showed that *Colletotrichum gigasporum* strains clustered together, indicating high genetic variations within the species (Figure 5.1). Morphological comparison revealed some minor differences between our strain (MFLUCC 22-0108) and *C. gigasporum* (CBS 133266, holotype) in the size of conidia and setae which are not surprising due to their high genetic variations. *Colletotrichum gigasporum* was introduced in 2013 from Stylo (*Stylosanthes guianensis*) and Kodavan (*Centella asiatica*) (Rakotoniriana et al., 2013). It has also been described from Thailand on Taro (*Alocasia* sp.) and Chinese Hibiscus (*Hibiscus rosa-sinensis*) (Liu et al., 2014). This study illustrated *C. gigasporum* as a new host record, associated with durian fruit rot.

Most species within the C. gloeosporioides species complex such as *C. asianum*, *C. fructicola*, *C. gloeosporioides*, *C. musae*, *C. siamense*, *C. tropicale*, and *C. viniferum* were originally isolated from tropical and sub-tropical fruits. *Colletotrichum pandanicola* was described on *Pandanus* sp. (Pandanaceae) from Thailand as an

endophyte (Tibpromma et al., 2018). In this study, we described and illustrated *C. pandanicola* as a new record association with durian fruit. Phylogenetic analyses (Figure 5.5) and morphological comparison both confirmed the identification accuracy.

Based on the phylogenetic tree (Figure 5.7), *C. truncatum* strains clustered together with type strain and showed high genetic variations within the species. The morphological comparison confirmed the phylogenetic results. However, we found differences in the size of setae, conidiogenous cells, and conidia between *C. truncatum* (MFLU 22-0191) and *C. truncatum* (CBS 151.35) which can authenticate inter-specific variations. *Colletotrichum truncatum* has been reported on different plant hosts, including *Glycine ma*x (Giatgong, 1978), *Glycine ussuriensis* (Lenne, 1990), *Solanum melongena* (Richardson, 1990), *Capsicum* sp. (Shenoy et al., 2007) and *Manihot esculenta* (Sangpueak et al., 2018) from Thailand. This is the first report of *C. truncatum* being associated with durian fruit in Thailand. Among *Colletotrichum* species recorded in Thailand, only *C. gloeosporioides* has been reported on durian as a fruit rot causal agent based on morphology alone (Sangchote et al., 2012). However, it is probably not a correct identification as it lacked molecular data.

Earlier, *Colletotrichum* species were identified based on morphology, cultural features, and pathogenicity studies (Cannon et al., 2000; Johnson et al., 1997; Sutton, 1980). However, *Colletotrichum* species cannot be reliably identified due to changes in morphology and conidial shape and size with changes in substrate, host, and repetition of subculture. Besides, species identification based on host specificity is not reliable because of the possibility of more than one species occurring on the same host, leading to misidentification of the species. Damm et al. (2012) also indicated that more than one *Colletotrichum* species can colonize a single host based on a polyphasic approach and morphology. The present study supports this result, as four *Colletotrichum* species belonging to three complexes were isolated from durian fruits. Later, Weir et al. (2012) colleagues showed that the species earlier identified as *C. gloeosporioides* belonged to different distinct lineages (some remained as *C. gloeosporioides sensu stricto*) using molecular markers. Additionally, Udayanga et al. (2013) observed that, despite *C. gloeosporioides sensu stricto*'s rather narrow host range, numerous species in the C. gloeosporioides species complex comprise the predominant anthracnose pathogens in tropical Asia, emphasizing the use of molecular approaches for *Colletotrichum* species

identification. However, two species within the C. gloeosporioides species complex, namely *C. siamense* and *C. gloeosporioides*, are the species associated with the largest number of host species worldwide (Talhinhas & Baroncelli, 2021). *Colletotrichum* is a speciose genus with 247 accepted species (Bhunjun et al., 2021b; Jayawardena et al., 2020). During 2022, 49 new species of *Colletotrichum* have been introduced from different host plants (MycoBank 2023), and one new species from durian fruit is introduced in this study. However, much more species remained undiscovered in such speciose genera, according to Bhunjun et al. (2022). Therefore, it is clear that we are a long way from discovering all *Colletotrichum* species and having a deep understanding of species diversity, biology, host range, and distribution. Current research on *Colletotrichum* in tropical Asia has revealed a surprising species diversity present on a broad variety of hosts, producing significant fungal infections on fruits, vegetables, ornamentals, and other crops. Consequently, precise detection of pre- and postharvest diseases supported by molecular data has a significant influence on farming, biosecurity, and quarantine (Hyde et al., 2013; Phoulivong et al., 2010; Sharma et al., 2013; Udayanga et al., 2013).

5.5 Conclusion

This study proposed a new species (*C. durionigenum*) and recorded durian fruit as a new host to three known species (*C. gigasporum*, *C. pandanicola*, and *C. truncatum*), belonging to three complexes. The discovery of new species and new host records can provide a better understanding of fungal biodiversity, phylogenetic relationships, biology, and lifecycle, leading to enhancement of potential usages and functions. However, we did not conduct pathogenicity studies to confirm their pathogenicity on the durian fruits. Hence, future studies are recommended in this aspect.

CHAPTER 6

MORPHOMOLECULAR IDENTIFICATION AND PATHOGENICITY OF *Colletotrichum* SPECIES ASSOCIATED WITH AVODADO ANTHRACNOSE IN NORTHERN THAILAND

6.1 Introduction

The commercial avocado (*Persea americana*) is a member of the flowering plant family Lauraceae (Chen et al., 2020) and is divided into Mexican, Guatemalan and West Indian landraces (Nath et al., 2022). Mexican types are small and cold-hardy, whereas the West Indian race is not cold-hardy (Marais, 2004). It is one of the most economically important crops in the tropical and subtropical regions as an export fruit (Geremu et al., 2022; Perkins et al., 2019; Sharma et al., 2017). Avocado was deemed a “heart-healthy” food and was recommended as a dietary source of monounsaturated fatty acids by the Australian Heart Foundation. As a unique fruit, it contains excellent nutrients, oils, proteins, vitamins and carbohydrates (Daiuto et al., 2013; Pérez-Jiménez, 2008). Avocado is cultivated in more than 60 countries in the world, with 33 major avocado-producing countries, including Mexico, the United States, the Dominican Republic, Brazil, Israel, Indonesia, Haiti, Venezuela, Colombia, South Africa and Australia (Marais, 2004; Pérez-Jiménez, 2008). The world production of avocados was estimated at around 5,924,398 tonnes in 2017 (http://www.fao.org/).

In Thailand, avocado plants were initially cultivated in Nan province in the northern part about 90 years ago, and the planted area of avocado in Thailand increases every year, concentrated in the northern and north-eastern regions. It is an important fruit in Thailand and is exported to other Asian countries, including Hong Kong, Japan and Singapore (Trakunyingcharoen et al., 2015).

Avocado trees are attacked by various fungal pathogens that cause serious damage to roots, leaves, fruits, branches and trunks (Fuentes-Aragón et al., 2020a; Guarnaccia et al., 2019). Anthracnose is a destructive disease that affects avocados worldwide, occurring in the orchard, and the symptoms appear after fruit ripening (Bustamante et al., 2022). The causal agents of avocado anthracnose are *Colletotrichum* species (Cannon et al., 2012). Species of this genus are widely known as pathogens of economically important crops worldwide (Cannon et al., 2012; Jayawardena et al., 2016); however, these species can also occur as endophytes and saprobes in nature (Damm et al., 2009; Hyde et al., 2009; Manamgoda et al., 2013). To date, 20 species of *Colletotrichum* have been reported from avocado, belonging to five different species complexes: gloeosporioides, acutatum, boninense, gigasporum and magnum (Bustamante et al., 2022; Cannon et al., 2012; Hofer et al., 2021).

Numerous studies have been carried out in Thailand to identify *Colletotrichum* species associated with various hosts (Ma et al., 2018; Manamgoda et al., 2013; Photita et al., 2005; Prihastuti et al., 2009; Than et al., 2008a). Understanding the diversity of *Colletotrichum* species associated with a specific host is crucial for the implementation of efficient management strategies, as different species have different abilities to adapt to their environment (Chen S. et al., 2018; Fuentes-Aragón et al., 2020a). Several studies have been conducted to identify *Colletotrichum* species associated with avocado in different countries, including Australia (Giblin et al., 2018), Brazil (Soares et al., 2021), Chile (Bustamante et al., 2022), China (Li M. et al., 2022), Taiwan (Wu et al., 2023), Italy (Guarnaccia et al., 2016), Mexico (Ayvar-Serna et al., 2021; Fuentes-Aragón et al., 2020a), New Zealand (Hofer et al., 2021) and Sri Lanka (Dissanayake et al., 2021; Hunupolagama et al., 2015). However, a comprehensive study investigating the diversity, phylogeny and pathogenicity of *Colletotrichum* species associated with avocado in Thailand is lacking. To address this research gap, the present study aims to conduct phylogenetic identification, morphological illustration and pathogenicity assessments of *Colletotrichum* species associated with avocado in northern Thailand.

6.2 Materials & Methods

6.2.1 Sample Collection, Examination and Isolation

Twenty-five avocado leaves and fruits showing anthracnose symptoms were collected from markets and different orchards in Chiang Rai, Thailand, during November 2021–September 2022. The specimens were kept in plastic bags containing collection and sample details and were transferred to the laboratory for examination. The fungal structures and fruiting bodies on natural substrates were photographed using an SZX16 stereomicroscope (Olympus). Morphological characters were observed using an EZ4 stereomicroscope (Leica) and photographed with an optical microscope equipped with a DS-Ri2 camera (Nikon). The photo plates were made with the Adobe Photoshop v. 21.1.2 software and measured with the Tarosoft (R) Image Frame Work software. Guidelines and recommendations from Chethana et al. (2021) and Jayawardena et al. (2021b) were used to define the *Colletotrichum* species in this study.

In order to obtain the cultures, direct culture and tissue culture methods were used (Senanayake et al., 2020). Single-spore and hyphal tip isolations were used to purify the isolates following the methods described by Senanayake et al. (2020). The culture characteristics were examined on potato dextrose agar (PDA) and oatmeal agar (OA) incubated at room temperature for 7 days. The pure cultures were deposited in the Mae Fah Luang University Culture Collection (MFLUCC), Chiang Rai, Thailand. Specimens were deposited in the herbarium of Mae Fah Luang University (MFLU).

6.2.2 DNA Extraction, PCR Amplification and Sequencing

Genomic DNA was extracted from 10-day-old mycelia cultured on PDA using a DNA Extraction Kit (Omega Bio-Tek) following the manufacturer's instructions. The primers ITS5/ITS4 (White et al., 1990), ACT-512F/ACT-783R (Carbone & Kohn, 1999), CHS-79F/CHS-345R (Carbone & Kohn, 1999), GDF/GDR (Templeton et al., 1992) and BT-2Fd/Bt-4Rd (Woudenberg et al., 2009) were used to amplify the rDNA internal transcribed spacer (ITS), actin (*ACT*), chitin synthase (*CHS-1*), glyceraldehyde-3-phosphate dehydrogenase (*GAPDH*) and β-tubulin (*TUB2*) genetic sequences, respectively. A reaction mixture of 25 µL included 12.5 µL of 2 × Power Taq PCR Master Mix, 1 µL of each primer (20 M), 1 µL of genomic DNA and 9.5 µL

deionized water. The PCR amplification was performed using the following conditions: initial denaturation at 95°C for 5 min; followed by 40 cycles of denaturation for 30 s at 95°C, annealing at 53°C for 60 s (ITS), 55°C for 50 s (*ACT*), 58°C for 30 s (*CHS-1*), 58°C for 50 s (*GAPDH*) or 58°C for 90 s (*TUB2*), followed by extension at 72°C for 60 s; and a final extension at 72°C for 10 min. PCR amplification was performed in a Master Cycler X50s thermal cycler (Eppendorf). The sequencing was done by SolGent Co., Republic of Korea.

6.2.3 Phylogenetic Analysis

Phylogenetic analysis was conducted for 11 isolates using the concatenated sequence data of ITS, *GAPDH*, *CHS-1*, *ACT* and *TUB2*. Related sequences of reference isolates were downloaded from GenBank based on blast-search and related publications (Jayawardena et al., 2020, 2021a; Liu et al., 2022) (Table A2). A total of 99 sequences were analysed, including 97 from ingroup and 2 from outgroup taxa (*C. truncatum* CBS 151.35; *C. acidae* 17-2659). The individual loci were manually adjusted using MAFFT v. 7 under the web server (http:// mafft.cbrc.jp/alignment/server) (Katoh et al., 2019). The alignment was adjusted using BioEdit v. 7.0.9.0 (Hall, 1999), and where necessary, the TrimAl software was used to trim aligned sequences with a 'gappyout' command. Maximum-likelihood (ML) analysis with the GTR + gamma model of nucleotide evolution was carried out using RAxML-HPC2 on XSEDE with bootstrapping of 1000 replicates. The Bayesian analysis was conducted using a Markov chain Monte Carlo (MCMC) algorithm with Bayesian posterior probabilities (BYPP) using MrBayes on XSEDE (Ronquist et al., 2012). The best-fit evolutionary models were determined using jModelTest v. 2.1.10 through the Akaike information criterion (AIC). Four MCMC chains were run from random trees for 1,000,000 generations and sampled every 100th generation. Using PAUP XSEDE, a maximum-parsimony (MP) analysis was performed (Swofford, 2002). Gaps were considered missing data, and ambiguously aligned areas were removed. The analyses were performed on the CIPRES Science Gateway (https://www. phylo.org/portal2) (Miller et al., 2011). The phylograms were visualized in FigTree v. 1.4.0 and annotated in Illustrator CC v. 22.0.0 (Adobe Systems). We followed Fu et al. (2019) to perform a pairwise homoplasy index (PHI) test using a multilocus concatenated sequencing dataset (ITS, *ACT*, *CHS-1*, *GAPDH* and *TUB2*) to

ascertain the recombination level among *C. pandanicola*, *C. parvisporum* and *C. siamense*.

6.2.4 Pathogenicity Test

According to the protocol described by Bhunjun et al. (2021a), Koch's postulates were conducted to confirm the pathogenicity of six representative fungal isolates on avocado fruits and leaves. Both wounded and unwounded methods using mycelial plug inoculation were employed. The experiment was conducted in a complete randomized design with three replications. The conidial suspension method was not used as the cultures did not produce enough conidia to make the suspension. Healthy avocado fruits and leaves (the same variety from which the isolates originated) were surface sterilized by washing in 70% ethanol for 2 min, then in 2% a.i. sodium hypochlorite for 2 min, followed by three washes with sterile distilled water and drying in a laminar air cabinet. Mycelial plugs were obtained from fresh colonies grown on PDA. Control inoculations were performed using uncolonized PDA plugs. All treatments were incubated in separate moist chambers at 28°C with 80% relative humidity. The aggressiveness of the isolates was assessed by measuring the disease progress and severity of symptoms caused by the fungal isolates over the test period. This included measuring lesion size, evaluating discolouration, observing tissue degradation (surface and inside of fruits) and considering the fungal fruiting bodies appearing on the tissues. Symptom measurements were conducted for 10 days in fruits and 15 days on leaves, providing comprehensive data on disease progression. Koch's postulates were confirmed by reisolating the fungi from the infected fruits.

6.2.5 Statistical Analysis

Statistical analyses were performed using SAS v. 9.4 (SAS Institute, 2016) and R v. 4.3.1, (R Foundation for Statistical Computing) software, and, to facilitate the understanding of the results, graphs were generated using R (R Core Team, 2014) and RStudio (RStudio Team, 2015) software. Means of symptom diameter were compared using Tukey's honestly significant difference (HSD), and $p < 0.05$ was considered significant.

6.3 Results

6.3.1 Morphological Studies

Microscopic features, including conidiogenous cells, conidia and appressoria were observed, and their size and shape were recorded. The colonies from 7-day-old cultures on PDA and OA were examined, and colony growth, texture and colour were recorded. All isolates were identified as belonging to the gloeosporioides species complex based on morphological characteristics. However, morphological characteristics were not sufficient to differentiate the isolates at the species level. Therefore, a multilocus phylogenetic analysis was carried out for all isolates to identify the species precisely (see below). Subsequently, 11 *Colletotrichum* isolates were identified from avocado fruits and leaves, belonging to four known species of *Colletotrichum*: *C. siamense*, *C. endophyticum*, *C. fructicola* and *C. henanense*. Of these, five isolates were obtained from fruits and six were discovered on leaves. *Colletotrichum siamense* was the most common species isolated from both fruits and leaves.

6.3.2 Phylogenetic Analysis

The phylogenetic analyses of the gloeosporioides species complex were performed using a concatenated dataset of ITS, *ACT*, *CHS-1*, *GAPDH* and *TUB2* sequence data from the isolates, reference isolates and the two outgroup taxa (*C. truncatum* CBS 151.35; *C. acidae* 17-2659). The aligned dataset comprised 1645 characters (including the gaps). The final aligned dataset was subjected to ML, MP and Bayesian probabilities. The best RAxML tree with a likelihood value of -10183.99 is presented (Figure 6.1). The matrix consisted of 751 distinct alignment patterns, with 14.14% gaps and undetermined characters. Estimated base frequencies were as follows: A = 0.229, C = 0.303, G = 0.241, T = 0.227, and substitution rates AC = 1.123, AG = 3.034, AT = 1.221, CG = 0.852, CT = 5.060, and GT = 1.000. The gamma distribution shape parameter α= 0.396235, and the tree-length = 1.026200.

Based on a multi-gene phylogenetic tree, the strains that were isolated in the present study were placed in four distinct clades belonging to four species: *Colletotrichum endophytica* (3 isolates), *C. fructicola* (1 isolate), *C. henanense* (1

isolate), and *C. siamense* (6 isolates). *Colletotrichum pandanicola* and *C. parvisporum* were not placed in a distinct clade, but scattered in the *C. siamense sensu lato* (Figure 6.1).

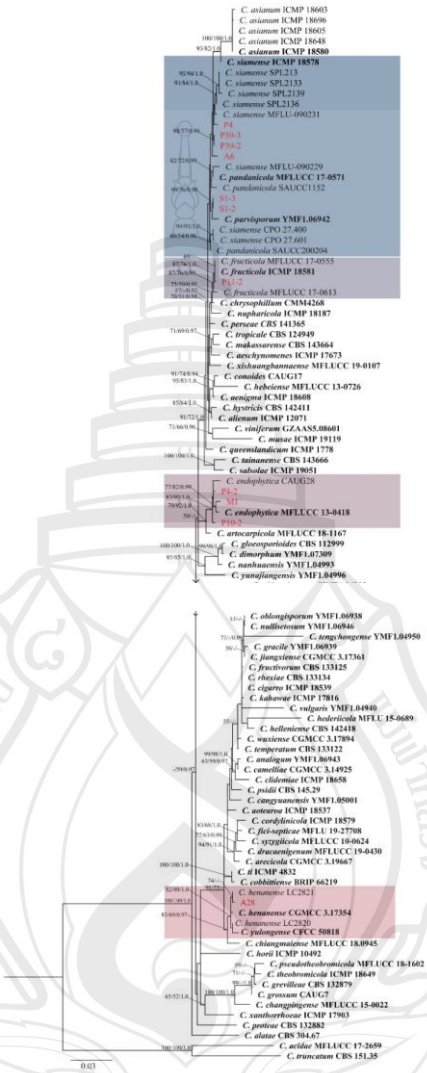

Note The tree was rooted with *Colletotrichum truncatum* (CBS 151.35) and *Colletotrichum acidae* (MFLUCC 17-2659). Maximum-likelihood and maximum-parsimony bootstrap values ≥50%, and Bayesian posterior probabilities ≥0.90 are shown near the nodes, respectively. Type strains are in bold, the new isolates from this study are in red, and the clusters into which they fall are highlighted in coloured boxes

Figure 6.1 Phylogenetic tree of the *Colletotrichum gloeosporioides* species complex based on maximum likelihood, generated by a concatenated ITS–*ACT*–*CHS-1*–*GAPDH*–*TUB2* sequences

6.3.3 Taxonomy

Colletotrichum endophyticum Manamgoda, Udayanga, L. Cai & K.D. Hyde, (2013) Figure 6.2

Index Fungorum number: IF565248; Facesoffungi number: FoF14040

Associated with anthracnose of avocado. Sexual morph: Not observed. Asexual morph: *Vegetative hyphae* hyaline to pale brown, smooth-walled, septate, branched. *Conidiomata* acervular, dark brown, bearing conidial mass. *Setae* rarely observed (M1, MFLU 23-0059), dark brown, 53–65 µm long, 4–5 µm diam. at base, 2–2.5 µm at apex. C*onidiogenous cells* hyaline, cylindrical or clavate, 15–21 × 2–3.5 µm ($\bar{x}$ = 19 × 2.4 µm, n = 30) collarette obvious. *Conidia* hyaline, aseptate, smooth-walled, cylindrical with rounded ends, sometimes slightly ovoid, guttulate, 14–17.5 (– 20) × 4.5–5.5 µm ($\bar{x}$ = 15.5 × 5 µm, n = 30). *Appressoria* produced on slide culture, brown to dark brown, non-rounded, undulate to lobate, irregular in shape, 8–13 × 5–8 µm ($\bar{x}$ = 11.5 × 6 µm, n = 20), formed directly from branched mycelia.

Culture characteristics – Colonies on PDA 60–70 mm in diam. after 7 days, velvety, slightly raised, circular, undulate. Surface white to smoke-grey, reverse same color. Colonies on OA 57–66 mm in diam. after 7 days. entire margin, surface white to whitish grey, reverse same color.

Material examined – Thailand, Chiang Rai Province, Mae Fah Luang District, Mae Salong Nok Sub-district. Associated with avocado anthracnose, 14 February 2022, A. Armand, P4-2 (MFLU 23-0060), living culture, MFLUCC 23-0011; P10-2 (MFLU 23-0061), living culture, MFLUCC 23-0013; Thailand, Chiang Rai, Mueang Chiang Rai, Nang Lae, Phat Tai market, 27 September 2021, A. Armand, M1 (MFLU 23-0059), living culture, MFLUCC 23-0009.

Notes – *Colletotrichum endophyticum* was originally isolated from *Pennisetum purpureum* as an endophytic fungus in Thailand (Manamgoda et al., 2013). We identified three isolates from avocado as *C. endophyticum*. Morphologically, isolates P4-2 and P10-2 were more similar in conidia and appressoria shape and size than those of M1. The isolate M1 produced slightly longer conidia and bigger appressoria in comparison to the other isolates. In addition, it produced dark brown setae, which were not observed in other strains (P4-2 and P10-2). However, all strains produced cylindrical conidia with rounded ends, and the colonies were similar on PDA and OA.

Morphological comparison with *C. endophyticum* (ex-holotype MFLUCC 13-0418) revealed no differences between our strains and the ex-type strain (Manamgoda et al., 2013). Strains of *C. endophyticum* clustered in a distinct clade with high support values (Figure 6.1). The number of base pair differences in gene sequences between *C. endophyticum* (MFLUCC 13-0418) and *C. endophyticum* isolates from our study is shown in Table 6.1.

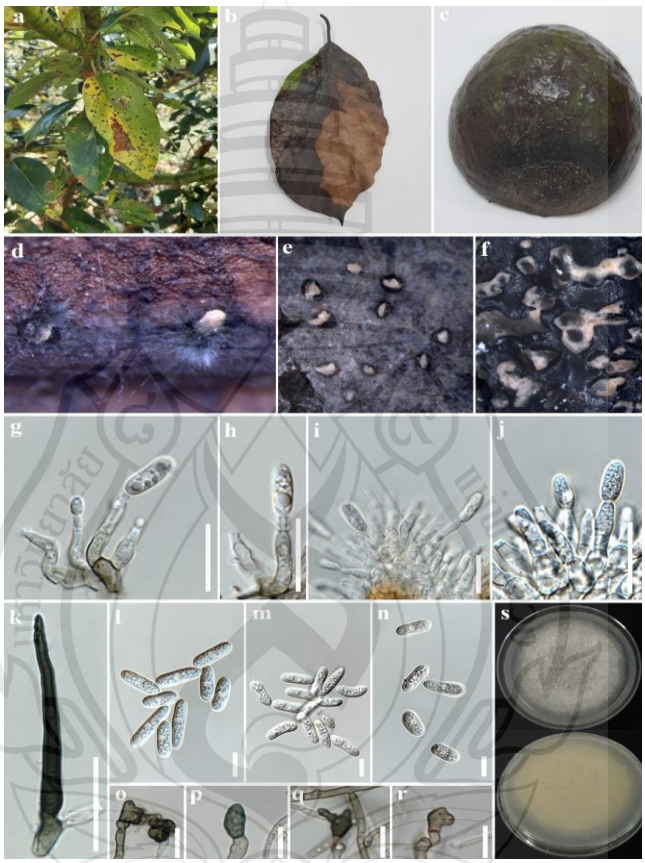

Note **a**–**c** Host tissues, **d**–**f** Fruiting bodies on the host surface, **g**–**j** Conidiogenous cells and conidial attachment, **k** Setae, **l**–**n** Conidia, **o**–**r** Appressoria, **s** Upper and reverse view of culture on PDA; Scale bars: **g**–**j** = 20 µm, **k** = 25 µm, **l**–**r** = 10 µm

Figure 6.2 *Colletotrichum endophyticum* (**a**, **d**, **g**, **h**, **n**, **o**, **s**: P4-2 (MFLU 23-0060); **b**, **e**, **i**, **m**, **q**, **r**: P10-2 (MFLU 23-0061)

Table 6.1 Base pair difference between *C. endophyticum* (MFLUCC 13-0418) and strains isolated in this study

Taxa	Gene Regions				
	ITS	***ACT***	***CHS-1***	***GAPDH***	***TUB2***
C. endophyticum P4-2	0/477	1/221	4/244	2/220	1/406
C. endophyticum M1	0/477	2/221	2/244	4/220	0/406
C. endophyticum P10-2	1/477	1/221	3/244	5/220	0/406

Colletotrichum fructicola Prihast, L. Cai & K.D. Hyde (2009)

Figure 6. 3

Index Fungorum number: IF515409; Facesoffungi number: FoF06767

Associated with avocado anthracnose. Sexual morph: *Ascomata* greyish black to black, globose to subglobose, semi-immersed or completely immersed 150–170 × 98–112 (–138). *Ascoma* 48–60 (–70) × 8–10.5 μm ($\bar{x}$ = 58 × 9.5 μm, n = 20), hyaline, thin-walled, clavate or cymbiform. *Ascospores* (13–) 15–16.5 × 3–4.5 ($\bar{x}$ = 15.7 × 3.3 μm, n=30), hyaline, one-celled, guttulate, slightly curved to curved with rounded ends. Asexual morph: *Vegetative hyphae* hyaline, smooth-walled, septate, branched. *Conidiomata* acervular, dark brown, bearing conidial masses. *Setae* not observed. *Conidiogenous cells* hyaline, aseptate, unbranched, cylindrical or clavate, 20–22 × 3.5–5 μm ($\bar{x}$ = 19.5 × 4 μm, n = 20). *Conidia* hyaline, aseptate, smooth-walled, cylindrical, rounded at the ends, guttulate, 13.5–15 × 4.5–5 μm ($\bar{x}$ = 14.7 × 4.8 μm, n = 30). *Appressoria* produced on slide culture, formed terminally from branched mycelia, brown to dark brown, irregular in shape, undulate, 7–10 × 5–7 μm ($\bar{x}$ = 9.5 × 5.5 μm, n = 20).

Culture characteristics – Colonies on PDA reaching 55–60 mm in diam. after 7 days at 28°C, velvety, flat, circular, entire in margins; Surface whitish to smoke grey in center and white in margins, becoming olivaceous grey with age, reverse same color. Colonies on OA 53–56 mm in diam. after 7 days, cottony, slightly raised, entire, surface white to whitish grey, reverse same color.

Material examined – Thailand, Chiang Rai Province, Mae Fah Luang District, Mae Salong Nok Sub-district. Associated with avocado anthracnose, 14 February 2022, A. Armand, P11-2 (MFLU 23-0062), living culture MFLUCC 23-0012.

Notes – *Colletotrichum fructicola* is characterized by producing hyaline, one-celled cylindrical conidia with obtuse to rounded ends. It was firstly described on *Coffea arabica* in Thailand (Prihastuti et al., 2009). Phylogenetic tree of multi-locus gene regions showed that our strain (MFLUCC 23-0012) is clustered with *C. fructicola* with high bootstrap values (Figure 6.1). The base pair difference between the type strain of *C. fructicola* and our strain (MFLUCC 23-0012) revealed 1/244 bp differences in *CHS-1*, and no differences in ITS, *ACT*, *GAPDH*, and *TUB2*. Morphologically, P11-2 (MFLU 23-0062) is similar to type stain of *C. fructicola* (Prihastuti et al., 2009). However, it produces slightly larger conidia (13.5–15 × 4.5–5 μm vs. 9.7–14 × 3–4.3 μm) and ascospores (15–16.5 × 3–4.5 vs. 9–14 × 3–4 μm) than the ex-type strain.

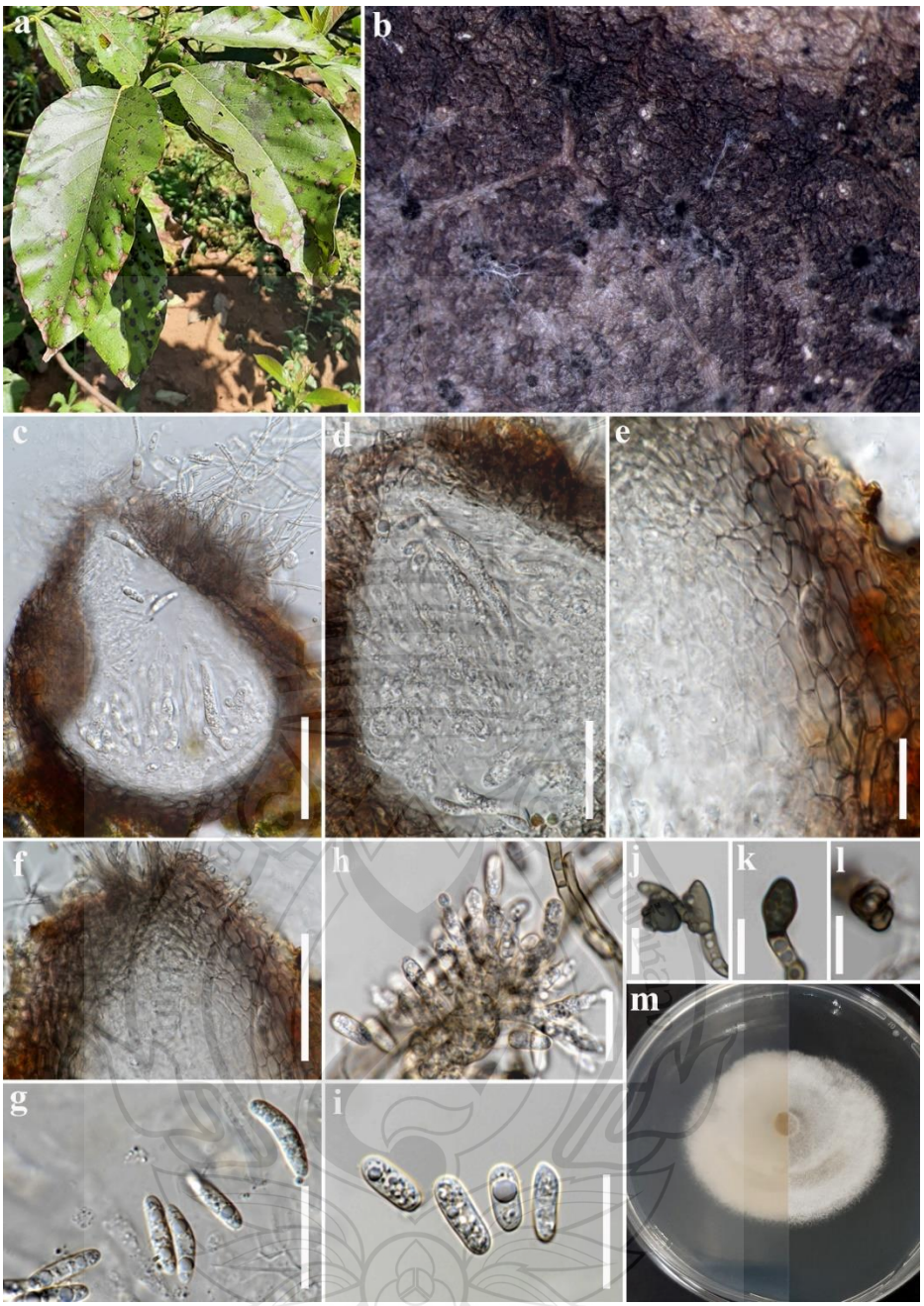

Note **a** Host leaves, **b** Fruiting bodies on the host surface, **c** Cross section of ascomata, **d** Asci in the ascomata, **e** Peridium, **f** Ostiole, **g** Ascspores, **h** Conidiogenous cells and conidial attachment, **i** Conidia, **j**–**l** Appressoria, **m** Upper and reverse view of culture on PDA; Scale bars: **c** = 50 µm, **d** = 40 µm, **e** = 20 µm, **f** = 50 µm, **g**–**i** = 20 µm, **j**–**l** = 10 µm

Figure 6.3 *Colletotrichum fructicola* (P11-2, MFLU 23-0062)

Colletotrichum henanense F. Liu & L. Cai, Persoonia 35: 80 (2015)

Figure 6.4

Index Fungorum number: IF809160; Facesoffungi number: FoF14041

Associated with anthracnose of avocado. Sexual morph: Not observed. Asexual morph: *Vegetative hyphae* hyaline to pale brown, smooth-walled, septate, branched. *Conidiomata* acervular, pale brown to brown, bearing conidial mass. *Setae* not observed. C*onidiogenous cells* hyaline, cylindrical or ampuliform, 10–14 (–16) × 2.5–3 μm ($\bar{x}$ = 13.7 × 2.7 μm, n = 30). *Conidia* hyaline, aseptate, smooth-walled, cylindrical with rounded ends, sometimes become narrower at base, guttulate, 17–20 (–20.6) × 4–5 μm ($\bar{x}$ = 19 × 4.5 μm, n = 30). *Appressoria* produced on slide culture, formed terminally from branched mycelia, brown to dark brown, irregular in shape, undulate or lobate, 5–13 × 4–8 μm ($\bar{x}$ = 11 × 6.5 μm, n = 20).

Culture characteristics – Colonies on PDA reaching 50–55 mm in diam. after 7 days at 28°C, velvety, circular, entire in margins; Surface white to pale smoke grey in center and white in margins, becoming smoke grey with age, reverse same color. Colonies on OA 50–52 mm in diam. after 7 days, velvety, slightly raised, entire, surface white to whitish grey, reverse same color.

Material examined – Thailand, Chiang Rai, Mueang Chiang Rai, Nang Lae, Phat Tai Market. Associated with avocado anthracnose, 22 March 2022, A. Armand, A28 (MFLU 23-0055), living culture MFLUCC 23-0006.

Notes – *Colletotrichum henanense* was firstly isolated from *Camellia sinensis* and *Cirsium japonicum* in China (Liu F. et al., 2015). Based on our multi-gene phylogenetic analysis, the isolate A28 (MFLUCC 23-0006) clustered with *C. henanense* with high bootstrap values (Figure 6.1). The base pair differences between type strain of *C. henanense* and *C. henanense* (MFLUCC 23-0006) revealed 1/496 base pair difference in ITS, 1/244 base pair difference in *CHS-1*, 1/220 base pair difference in *GAPDH*, 2/406 base pair differences in *TUB2*, and no differences in *ACT*. Morphological comparison with *C. henanense* (CGMCC 3.17354) revealed no significant differences between the isolate A28 and type strain. However, our strain produces larger conidiogenous cells (10–14 × 2.5–3 μm vs. 5.5–12.5 × 1–2 μm) and longer conidia (17–20 × 4–5 μm vs. 8–17 × 3–5.5 μm) than those of type strain (Liu F. et al., 2015).

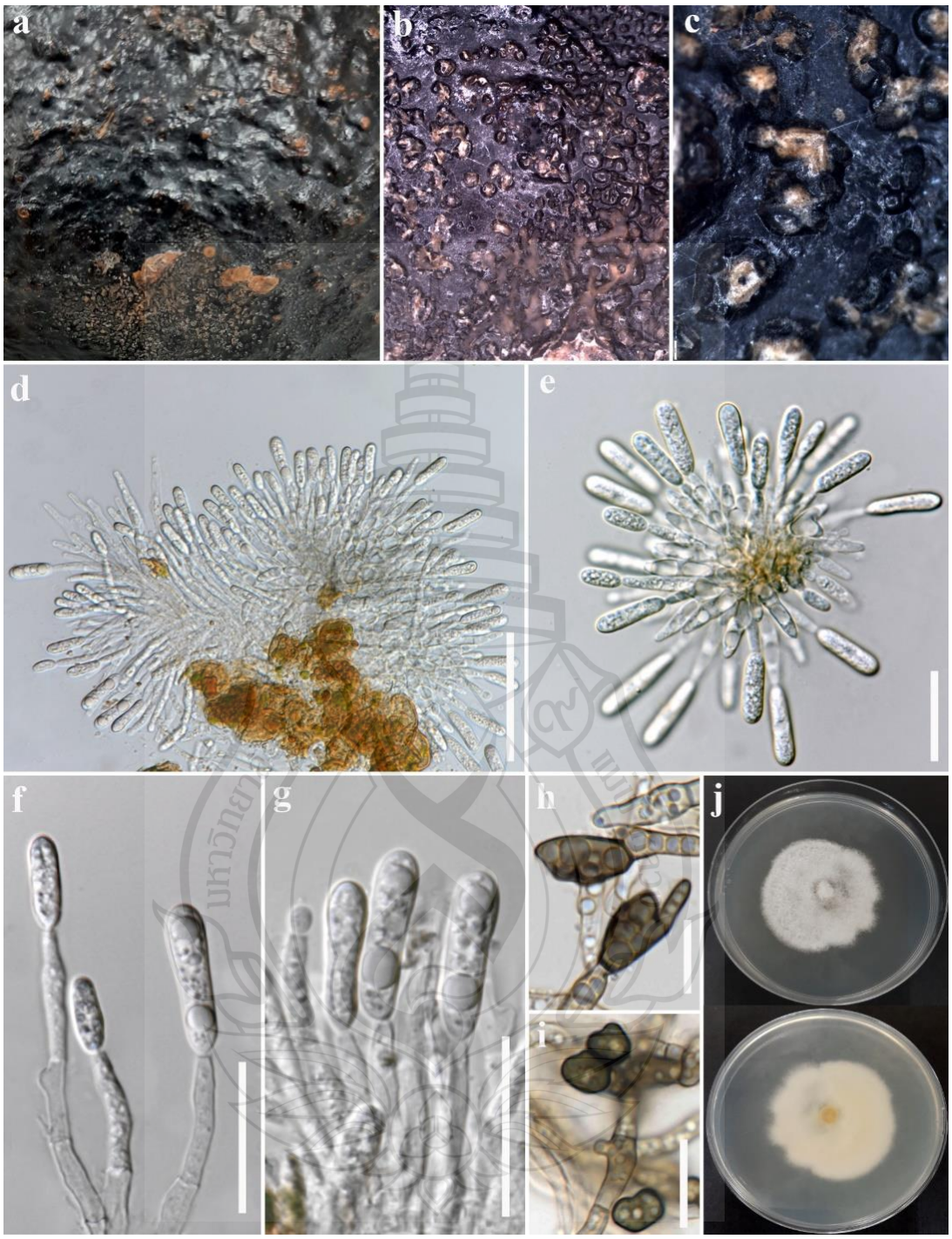

Note **a** an infected fruit, **b**, **c** Fruiting bodies on the host surface, **d**–**g** Conidiogenous cells and conidial attachment, **h**, **i** Appressoria, **j** Upper and reverse view of culture on PDA; Scale bars: **d** = 50 µm, **e**–**g** = 20 µm, **h**–**i** = 10 µm.

Figure 6.4 *Colletotrichum henanense* (A28, MFLU 23-0055)

Colletotrichum siamense Prihast, L. Cai & K.D. Hyde (2009)

Figure 6.5

Index Fungorum number: IF515410; Facesoffungi number: FoF03599

Associated with anthracnose of avocado. Sexual morph: Not observed. Asexual morph: *Vegetative hyphae* hyaline to pale brown, smooth-walled, septate, branched. *Conidiomata* acervular, brown to dark brown, bearing conidial mass. *Setae* not observed. C*onidiogenous cells* hyaline, cylindrical or ampuliform, 11.5–19 (–21) × 2–3 µm ($\bar{x}$ = 15.5 × 2.5 µm, n = 30). *Conidia* hyaline, aseptate, smooth-walled, cylindrical with rounded ends, guttulate, 13–18 × 4.5–5.5 µm ($\bar{x}$ = 14.8 × 5 µm, n = 30). *Appressoria* produced on slide culture, formed terminally from branched mycelia, brown to dark brown, irregular in shape, undulate or lobate, 4–11 × 3–6 µm ($\bar{x}$ = 8 × 4.5 µm, n = 20).

Culture characteristics – Colonies on PDA reaching 55–73 mm in diam. after 7 days at 28°C, velvety, circular, entire in margins; Surface white to pale smoke grey in center and white in margins, becoming smoke grey to olivaceous grey with age, reverse same color. Colonies on OA 50–58 mm in diam. after 7 days, velvety, slightly raised, entire, surface white to smoke grey, reverse same color.

Material examined – Thailand, Chiang Rai Province, Mae Fah Luang District, Mae Salong Nok Sub-district. Associated with avocado anthracnose, 14 February 2022, A. Armand, P39-2 (MFLU 23-0058), living culture, MFLUCC 23-0014; P4 (MFLU 23-0057), living culture, MFLUCC 23-0010; Thailand, Chiang Rai, Mueang Chiang Rai, Nang Lae, Phat Tai market, 07 February 2022, A. Armand, S1-2 (MFLU 23-0056), living culture, MFLUCC 23-0007.

Notes – In the present study, six isolates were identified as *C. siamense*, clustered in the *C. siamense* s.l. clade (Figure 6.1). The base pair differences between *C. siamense* (ICMP 18578) and *C. siamense* strains were compared as shown in Table 6.2 Morphologically, all strains were similar in producing cylindrical to ampuliform conidiogenous cells and cylindrical conidia with rounded ends. Furthermore, the strains were not considerably different in the size of conidiogenous cells and conidia, and colony appearance. Additionally, chlamydospores and setae were not observed in any of strains. However, they were different from *C. siamense* (holotype) in that they produce cylindrical conidia, whereas the type strain mostly produces fusiform conidia

with obtuse to slightly rounded ends (Prihastuti et al., 2009). Based on the morphology, *Colletotrichum pandanicola*, *C. parvisporum*, and *C. siamense* cannot be distinguished from each other due to their morphological overlap (Tibpromma et al., 2018; Yu et al., 2022). Furthermore, the base pair differences among them were not significantly high (Table 6.2). The phylogenetic tree also showed that *C. pandanicola* and *C. parvisporum* were not clustered in a distinct clade, grouped with C. *siamense*. Additionally, the PHI test indicated that there is a significant recombination ($\Phi w = 0.01$) among these three species (Figure 6.6). According to the guidelines discussed by Chethana et al. (2021) and Jayawardena et al. (2021b) on how to introduce a new species, *C. pandanicola* and *C. parvisporum* have not been supported by neither morphology nor phylogeny. Therefore, we agree with synonymizing *C. pandanicola* and *C. parvisporum* as *C. siamense.*

Note **a**, **b** Host tissues, **c**, **d** Fruiting bodies on the host surface, **e**–**g** Conidiogenous cells and conidial attachment, **h**–**j** Conidia, **k**–**n** Appressoria, **o** Upper and reverse view of culture on PDA; Scale bars: **e**–**g** = 20 µm, **h**–**n** = 10 µm.

Figure 6.5 *Colletotrichum siamense* (**a**, **c**, **e**, **h**, **k**, **l**, **o**: P39-2 (MFLU 23-0058); **f**, **i**, **n**: P4 (MFLU 23-0057); **b**, **d**, **g**, **j**, **m**: S1-2 (MFLU 23-0056)

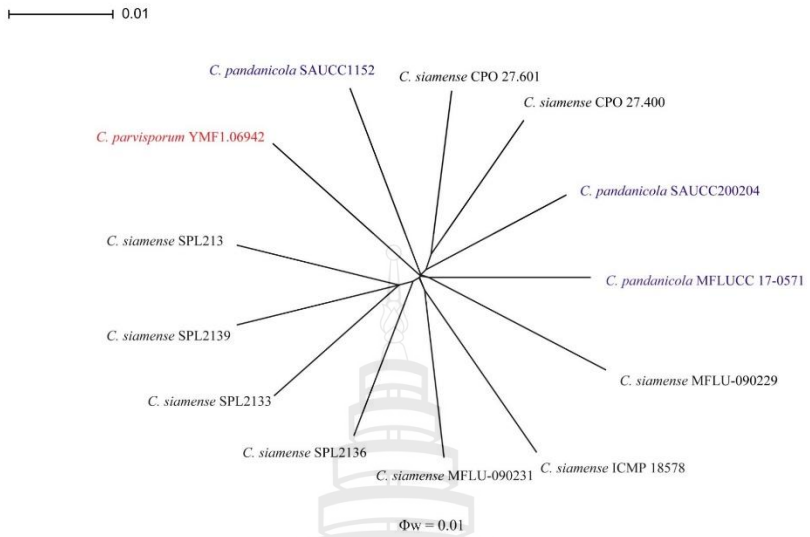

Note The PHI test conducted using using both LogDet transformation and splits decomposition. PHI test results (Φw) < 0.05 indicate significant recombination among the species

Figure 6.6 Pairwise homoplasy index (PHI) test of *C. pandanicola*, *C. parvisporum*, and *C. siamense*

Table 6.2 Base pair difference between *C. siamense* (ICMP 18578) and *C. pandanicola* (MFLUCC 17-0571), *C. parvisporum* (YMF1.06942), and *C. siamense* strains

Taxa	**Gene Regions**				
	ITS	***ACT***	***CHS-1***	***GAPDH***	***TUB2***
C. pandanicola MFLUCC 17-0571	3/475	2/240	3/244	1/217	5/366
C.parvisporum YMF1.06942	4/475	0/240	1/227	4/217	6/366
C. siamense P4	0/475	1.229	4/244	1/212	5/366
C. siamense P39-2	0/475	0/229	3/244	1/212	5/366
C. siamense P39-3	0/475	0/229	3/244	1/212	5/366
C. siamense A6	1/475	2/229	2/244	3/212	7/366
C. siamense S1-2	3/475	0/229	1/244	1/212	5/366
C. siamense S1-3	3/475	0/229	1/244	1/212	5/366

6.3.4 Pathogenicity Tests

Pathogenicity tests were performed for six isolates: *C. henanense* (A28, MFLUCC 23-006), *C. endophyticum* (M1, MFLUCC 23-009; P4- 2, MFLU 23-0060), *C. fructicola* (P11-2, MFLU 23-0062) and *C. siamense* (P39-2, MFLU 23-0058; S1-2, MFLU 23–0056). All strains exhibited pathogenicity towards avocado fruits and leaves. However, it was observed that the strains were unable to infect unwounded leaves (Figures 6.7 and 6.8). Moreover, statistical analysis using SAS software revealed a significant influence of the inoculation method on the progression and development of the disease, as indicated by the measurement of symptom diameter (mm), which varied across different strains (Figures 6.9; Table A3–Table A7). Furthermore, a t-test analysis was conducted using R software to compare the two methods across all strains throughout the entire assay period. The results revealed highly significant statistical differences between the wounded and unwounded methods, with $p = 2.15 \times 10^{-13}$ for the fruit testing and $p = 2.2 \times 10^{-16}$ for leaf testing (data and scripts available upon request). The mean disease spread and development was significantly higher in the wounded method compared to the unwounded method (Table A3, Table A4). Additionally, the results demonstrated that different strains exhibited varying abilities in disease initiation and progression, even among strains within the same species (Tables A5–Tables A7). Finally, the fungi were reisolated using the single-spore isolation technique and subsequently identified by morphological characteristics as the same species initially inoculated on the fruits. Control treatments of both wounded and unwounded fruits did not exhibit any symptoms throughout the entire duration of the experiment.

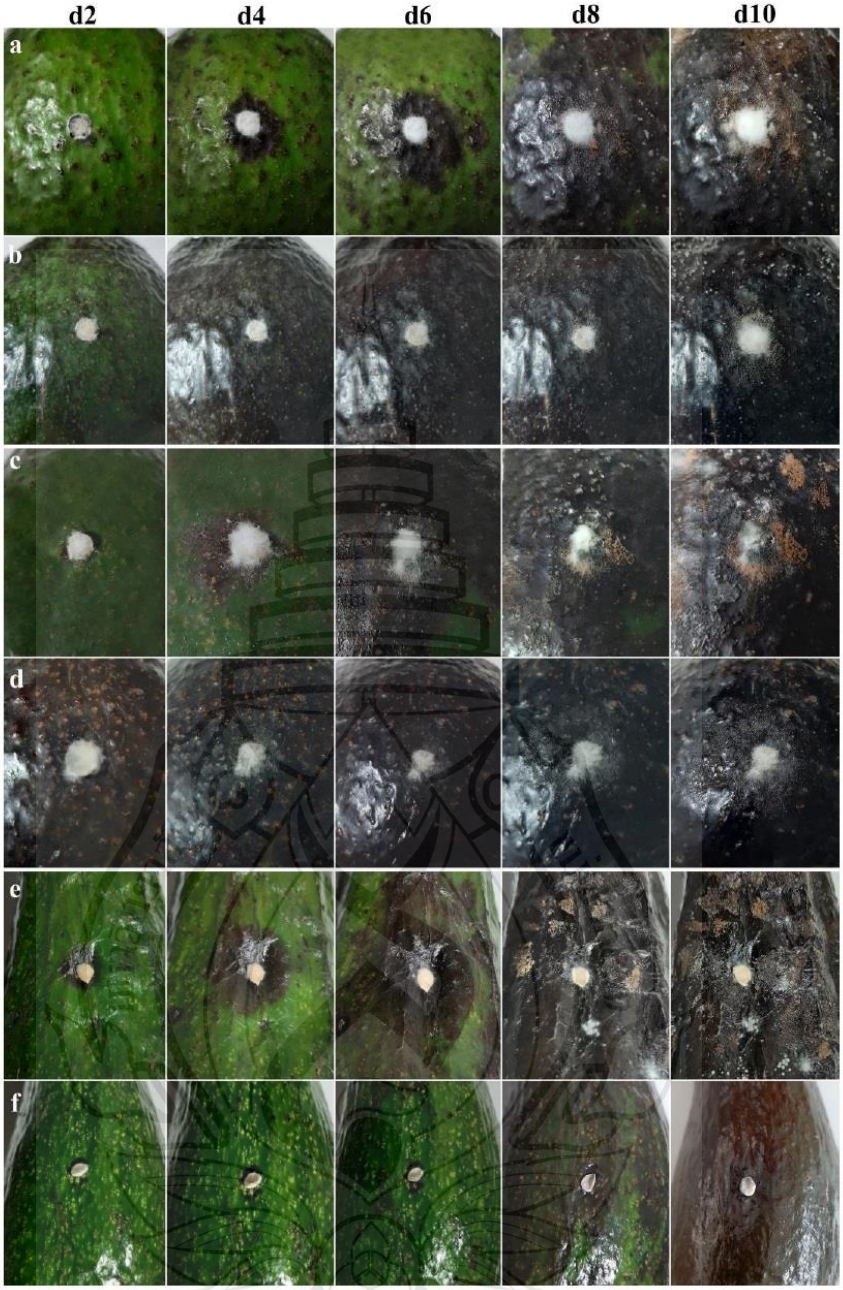

Note Fruits were inoculated using the wounded (**a**, **c**, **e**, **g**, **i**, **k**) and unwounded methods (**b**, **d**, **f**, **h**, **j**, **l**) and observed every 2 days until 10 days after inoculation. Isolates had been identified as *C. endophyticum* (M1, P4-2), *C. henanense* (A28), *C. fructicola* (P11-2) and *C. siamense* (P39-2, S1-2)

Figure 6.7 Pathogenicity tests of different isolates of *Colletotrichum* on avocado fruit. (**a**, **b**) M1, (**c**, **d**) A28, (**e**, **f**) P11-2, (**g**, **h**) P4-2, (**i**, **j**) P39-2, (**k**, **l**) S1-2

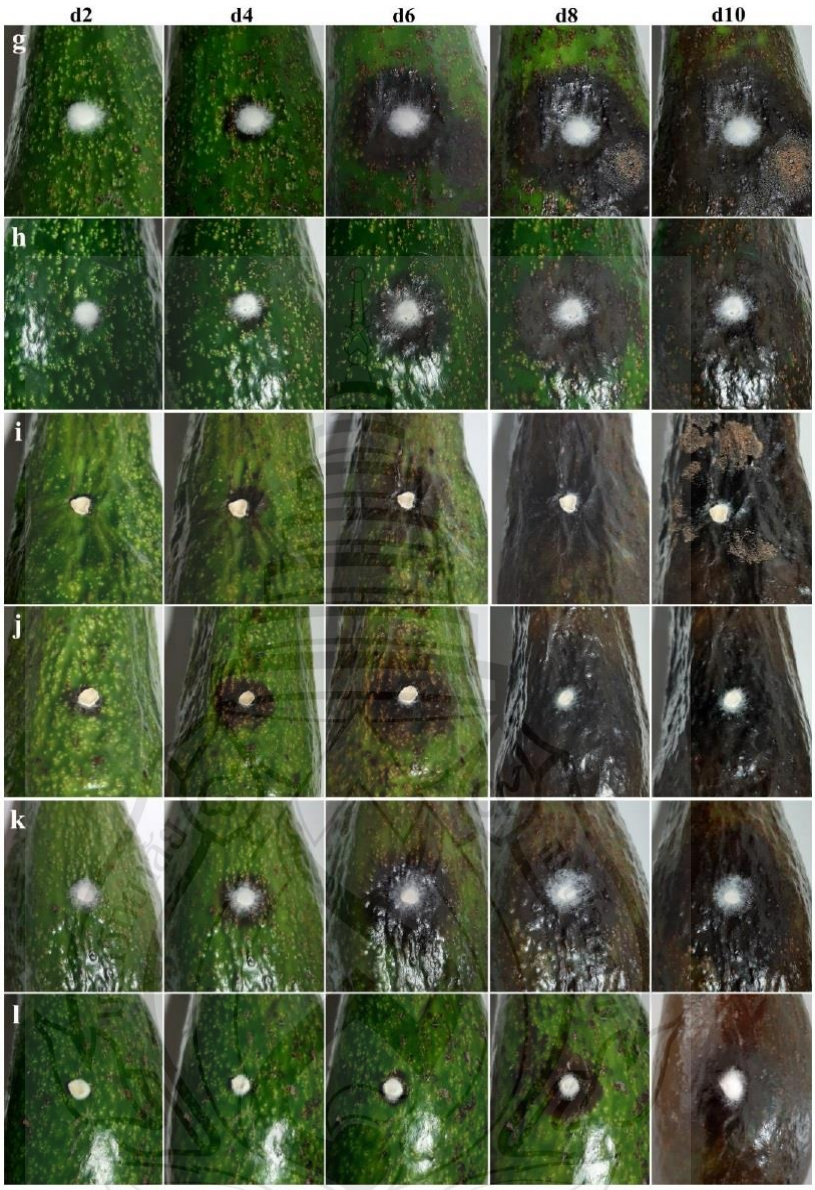

Figure 6.7 (continued)

Note Leaves were inoculated using the wounded (**a**, **c**, **e**, **g**, **i**, **k**) and unwounded methods (**b**, **d**, **f**, **h**, **j**, **l**) and observed at 2-day intervals until 15 days after inoculation. Isolates were identified as *Colletotrichum endophyticum* (M1, P4-2), *C. henanense* (A28), *C. fructicola* (P11-2) and *C. siamense* (P39-2, S1-2)

Figure 6.8 Pathogenicity tests of different isolates on avocado leaves. (**a**, **b**) M1, (**c**, **d**) A28, (**e**, **f**) P11-2, (**g**, **h**) P4-2, (**i**, **j**) P39-2, (**k**, **l**) S1-2

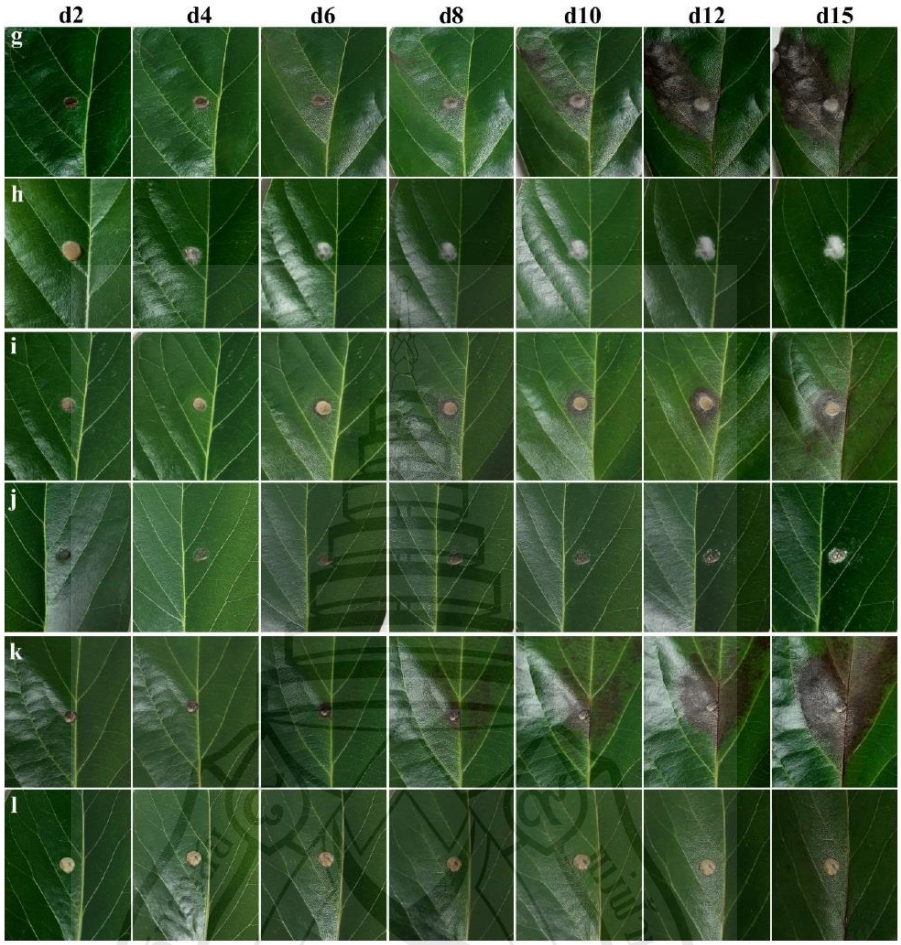

Figure 6.8 (continued)

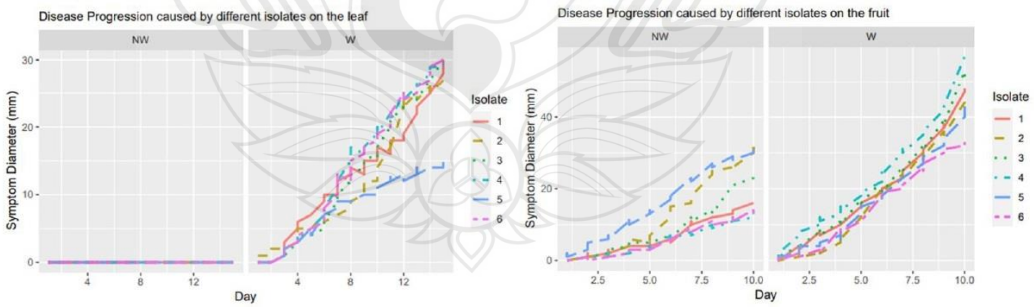

Note Isolates 1–6: M1, P4-2, A28, P11-2, P39-2 and S1-2, respectively. Isolates were identified as *Colletotrichum endophyticum* (M1, P4-2), *C. henanense* (A28), *C. fructicola* (P11-2) and *C. siamense* (P39-2, S1-2).

Figure 6.9 Disease progression of six isolates of *Colletotrichum* on avocado leaves and fruits

6.4 Discussion

Based on recommendations from previous studies (Hyde et al., 2009; Jayawardena et al., 2021b), multilocus phylogenetic analyses were employed to identify all the *Colletotrichum* isolates in this study. From our results, *C. endophyticum*, *C. fructicola* and *C. siamense* are reported as new geographical records, and the pathogenicity of *C. henanense* on avocado was identified as a new host record for this fungus.

C. fructicola and *C. siamense* have been widely reported, and their pathogenicity has been well studied on avocado (Hofer et al., 2021; Li M. et al., 2022; Wu et al., 2023). *C. siamense* was reported as the main pathogen causing anthracnose disease on avocado in Australia and Brazil (Giblin et al., 2018; Soares et al., 2021). However, no study has been conducted on strains of these species in Thailand. Based on their morphology, *C. pandanicola*, *C. parvisporum* and *C. siamense* cannot be distinguished from each other due to their morphological overlap (Tibpromma et al., 2018; Yu et al., 2022). *C. pandanicola* and *C. parvisporum* have each been introduced as new species based on a single strain. Furthermore, the species were introduced based on phylogenetic trees that included only the type strain of *C. siamense*, without any other strains of this species (Tibpromma et al., 2018; Yu et al., 2022). In the phylogenetic tree, we constructed from the multilocus sequence dataset, *C. pandanicola* and *C. parvisporum* did not sit in a distinct clade, but clustered with the *C. siamense* strains. In addition, according to the guidelines discussed by Chethana et al. (2021) and Jayawardena et al. (2021b) on how to introduce a new species, *C. pandanicola* and *C. parvisporum* have not been supported by either morphology nor phylogeny. Therefore, we agree with synonymizing *C. pandanicola* and *C. parvisporum* as *C. siamense*, as discussed by Zhang et al. (2022). In addition to *C. fructicola* and *C. siamense*, there has been only one other report of *C. endophyticum* on avocado (Dissanayake et al., 2021) and it has not been properly studied.

To address the gap in knowledge of the pathogenicity of *Colletotrichum* species on avocado in Thailand, we tested representative strains of each species we had isolated from avocado on avocado fruits and leaves. It is worth noting that all strains were able

to infect wounded and unwounded fruits. However, only wounded leaves were affected by these fungal strains. Interestingly, disease progression results showed that the fungi could spread in wounded fruits faster than in unwounded fruits. Wounding allows pathogens to attack plants and facilitates their entry into plant tissues by removing the cuticle, which acts as an effective defence barrier against pathogens, providing nutrients and energy needed by the pathogen to penetrate the plant tissue (Reina-Pinto & Yephremov, 2009; Savatin et al., 2014). The aggressiveness of different species on wounded and unwounded fruit was assessed, revealing that *C. fructicola* (P11-2) displayed the highest level of aggression on wounded fruit. Conversely, *C. siamense* (P39-2) exhibited the greatest aggressiveness on unwounded fruit. Similarly, when examining wounded leaves, *C. fructicola* (P11-2) and *C. siamense* (S1-2) were found to be the most aggressive strains. Additionally, the recently discovered species isolated from avocado fruit, *C. henanense* (A28), demonstrated a moderate level of aggressiveness on both fruit and leaf tissues. Based on the disease progression curve, it is evident that some strains exhibited greater disparities in their ability to colonize unwounded fruit compared to wounded fruit. Specifically, *C. endophyticum* (M1) and *C. endophyticum* (P4-2) displayed similar progression trends on wounded fruit, whereas their disease progression significantly diverged on unwounded fruit. These findings indicate the importance of the method of storage and protection of fruit from mechanical damage to reduce disease development. Furthermore, it is noteworthy that the maximum mean diameter of anthracnose observed in unwounded fruit 10 days after inoculation reached 31 mm. In contrast, this value represents the minimum anthracnose diameter on wounded fruit recorded during the same testing period, demonstrating the effect of mechanical damage on the speed of disease progression. The pathogenicity test of *C. endophyticum* and *C. siamense* strains isolated from avocado fruit and leaves revealed no substrate preference or specificity as these strains were able to infect both fruit and leaf.

Many pathogens are still fairly unknown and so it is crucial to discover their biology, lifestyle and distribution in order to avoid future fungal pathogen-related catastrophes (Hyde et al., 2018a). Moreover, further isolation and identification of fungi from different hosts will highlight any new occurrences of pathogenic fungi or new species in speciose pathogenic genera (Bhunjun et al., 2022).

CHAPTER 7

NEW SPECIES AND NEW RECORDS OF PLANT PATHOGENIC FUNGI FROM NORTHERN THAILAND

7.1 Introduction

Plant pathogenic fungi are a significant concern in agriculture, forestry, and natural ecosystems, causing diseases that lead to severe ecological problems and economic losses (Dayarathne et al., 2023). Determining the dynamic of interactions between plants and fungi in a particular ecological niche and creating efficient disease management plans requires an understanding of the diversity of plant pathogenic fungi (Burdon & Silk, 1997). In the tropical setting of Thailand, with its unique climatic and ecological conditions, the prevalence and impact of plant pathogenic fungi necessitate detailed investigation (Ko et al., 2011; Withee et al., 2022).

Historically, the identification and characterization of plant pathogenic fungi have relied on classical morphological methods. However, recent advancements in molecular techniques have revolutionised fungal taxonomy, enabling more accurate identification and classification (Hariharan & Prasannath, 2021). The significance of scientific exploration, encompassing the formal identification of novel taxa, resides in its pivotal role in rendering a species discernible within scientific inquiry (Chethana et al., 2021; Jayawardena et al., 2021b). Without a scientifically assigned nomenclature, a species remains imperceptible to scholarly investigation, thereby severely limiting the avenues for probing its ecological dynamics, potential applications, inherent threats, and devising strategies for conservation (Cheek et al., 2020). Despite the progress, there remains a lack of comprehensive studies on plant pathogenic fungi in specific localities, including university premises.

Mae Fah Luang University (MFU) is situated in the northern region of Thailand and boasts a diverse array of plant species encompassing ornamental, agricultural, and indigenous varieties. This diversity provides an ideal setting to explore the interactions between plants and plant pathogenic fungi (Hyde et al., 2018b). By conducting a

systematic survey, this study aims to contribute valuable data on the presence of both known and potentially new species of fungi and their occurrence within the premises.

7.2 Materials & Methods

7.2.1 Sample Collection and Fungal Isolation

Thirty fresh samples showing symptoms, including leaf and fruit anthracnose, leaf spots and leaf dieback were collected from different host plants in the Mae Fah Luang University (various places), Chiang Rai, Thailand, during 2021–2022. Samples collected from a specific host were segregated into distinct containers and transported to the laboratory for morphological examination and fungal isolation. Macro-morphological features were evaluated and documented through imaging facilitated by SZX16 (Olympus, Tokyo). Morphological characteristics were examined using an EZ4 stereomicroscope (Leica, Wetzlar, Germany), and photographed using a 600D Nikon camera (Tokyo, Japan). The dimensions of fungal characteristics were quantified employing Tarosoft (R) Image Frame Work v. 0.9.7. Visual representation was generated using Adobe Photoshop v. 21.1.2 software (Adobe Systems, San Jose, CA, USA). Fungi were isolated and purified through the single-spore isolation technique, as described by Senanayake et al. (2020), and the obtained strains were transferred to cryogenic tubes containing potato dextrose agar (PDA) and were kept at 2 °C for further examination. The culture characteristics were examined on PDA plates kept at 25±2 °C. The specimens and dried cultures were deposited in the Mae Fah Luang University Fungarium (MFLU), and living cultures were deposited in the Culture Collection (MFLUCC), Chiang Rai, Thailand.

7.2.2 DNA Extraction, PCR Amplification, and Sequencing

DNA extraction was done using the Omega DNA Extraction Kit (Bio-Tek). The PCR reactions were prepared in 25 µL volumes, comprising 9.5 µL double-distilled water, 12.5 µL 2×PCR Master Mix (PROMEGA, Madison, USA), 1 µL DNA template (10–100 ng/µL), and 1 µL of each primer (20 µM). The specific markers, corresponding primers, and amplification conditions were employed for each fungal genus in this investigation (Table A8). A Master Cycler X50s (Eppendorf) was used to conduct PCR

amplification. The sequencing service was provided by SolGent Company (Republic of Korea).

7.2.3 Alignments and Phylogenetic Analysis

The acquired genetic sequences were subjected to a BLASTn search in the NCBI. Subsequently, reference sequences were retrieved from the GenBank database. The sequences of each dataset were aligned using the MAFFT v. 7 (https://mafft.cbrc.jp/alignment/server/) (Katoh et al., 2019). The alignments were adjusted using BioEdit v. 7.0.9.0 (Hall, 1999), and were automatically trimmed using TrimAl v 1.2 (Capella-Gutiérrez et al., 2009) under the -gapthreshold (0.8) option or -gappyout option. The optimal evolutionary model for specific gene region was determined using jModelTest 2 v.2.1.6 on XSEDE, as outlined by Darriba et al. (2012).

Maximum-likelihood (ML) was carried out using RAxML-HPC2 on XSEDE and IQ-TREE 2.2.2.7 on ACCESS (Minh et al., 2020), in the CIPRES Science Gateway (https://www.phylo.org/) with the automatic substitution model selection (Kalyaanamoorthy et al., 2017) and 1000 ultrafast bootstraps. Bayesian inference (BI) was performed by MrBayes on XSEDE v.3.2.7a in the CIPRES Science Gateway portal with four independent Markov Chain Monte Carlo (MCMC) chains and four runs for 1,000,000–5,000,000 generations and sampled at every 100th generation. Maximum parsimony (MP) analysis was performed by PAUP on XSEDE (Swofford, 2002). Finally, the derived phylograms were rendered using FigTree v.1.4.0 (http://tree.bio.ed.ac.uk/software/figtree/) and were annotated in Illustrator CC v. 22.0.0 (Adobe Systems).

7.3 Results

7.3.1 Morphological Identification

Morphological characteristics, including the appearance of conidiomata, shape and size of the conidia, colour of conidia, conidial septa and appendages, shape and size of conidiophores and appearance of the colony were recorded for obtained strains. Based on morphological analysis, the obtained strains were divided into three genera: *Colletotrichum*, *Neopestalotiopsis*, and *Lasiodiplodia*. Since morphological

characteristics are insufficient to identify the species accurately, multi-gene phylogeny was conducted after that.

7.3.2 Phylogenetic Analysis

The combined sequence alignments encompassing each complex and genus were subjected to Maximum likelihood (ML), Maximum parsimony (MP), and Bayesian inference (BI) analyses. Phylogenetic analyses of *Colletotrichum* species complexes were performed using a concatenated dataset comprising ITS, *gapdh*, *chs-1*, *act*, and *tub2* gene regions. The phylogenetic relationships within *Lasiodiplodia* were resolved using a multi-locus dataset including ITS, *tef1*, *tub2*, and *rpb2*. For *Neopestalotiopsis*, evolutionary relationships were inferred based on a combined dataset of ITS, *tef1*, and *tub2* sequences. For *Neopestalotiopsis*, a combined dataset of ITS, *tef1*, and *tub2* sequence data was employed. Maximum likelihood analyses of the species complexes, namely *Colletotrichum dracaenophilum* and *C. orchidearum*, as well as for Lasiodiplodia were executed through RAxML-HPC2. Concurrently, ML analyses of the *Colletotrichum gloeosporioides* and *C. truncatum* species complex, alongside *Neopestalotiopsis*, were performed using IQ-TREE. Notably, the topology of the trees generated through ML, MP, and BI methods exhibited no significant differences. Consequently, the ML tree has been chosen and presented as the representative tree. The information related to the phylogenetic analysis and respective parameters are presented (Table A9). The details of all species and strains obtained in this study are shown (Table A10).

7.3.3 *Colletotrichum gloeosporioides* Species Complex

In the phylogenetic assessments (Figure 7.1), 12 isolates were classified within the *C. gloeosporioides* species complex. Among these, nine isolates formed a cluster within the *C. siamense* clade, and two isolates were grouped with the *C. fructicola* clade, and a single isolate was closely associated with *C. musae* (ex-type, ICMP 19119).

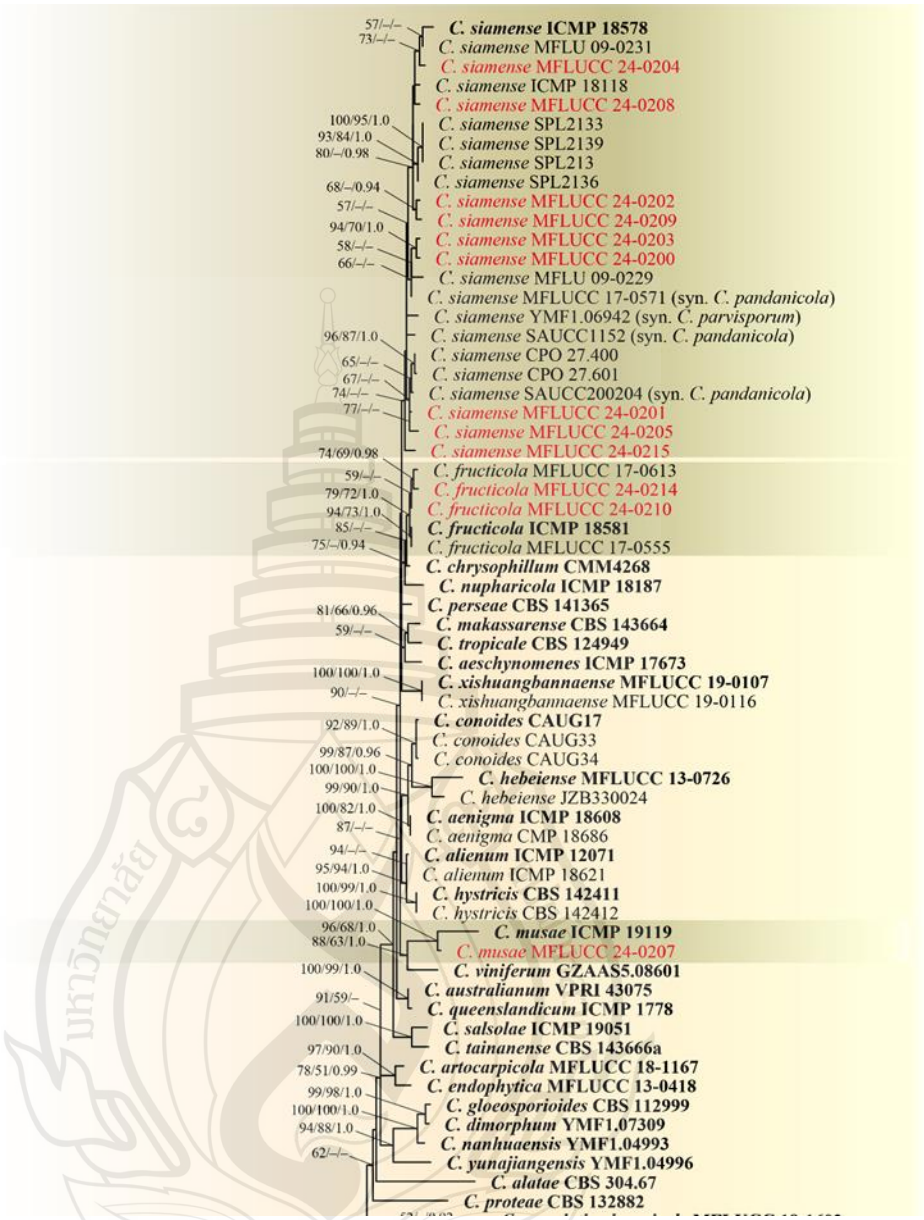

Note The tree was rooted with *Colletotrichum truncatum* (CBS 151.35). Maximum-likelihood and maximum-parsimony bootstrap values above 50%, and Bayesian posterior probabilities above 0.90 are shown near the nodes, respectively. Type strains are in bold, and the new isolates from this study are in red

Figure 7.1 Phylogenetic tree constructed using maximum likelihood analysis of the *Colletotrichum gloeosporioides* species complex, based on a combined dataset of ITS, *gapdh*, *chs-1*, *act*, *tub*2

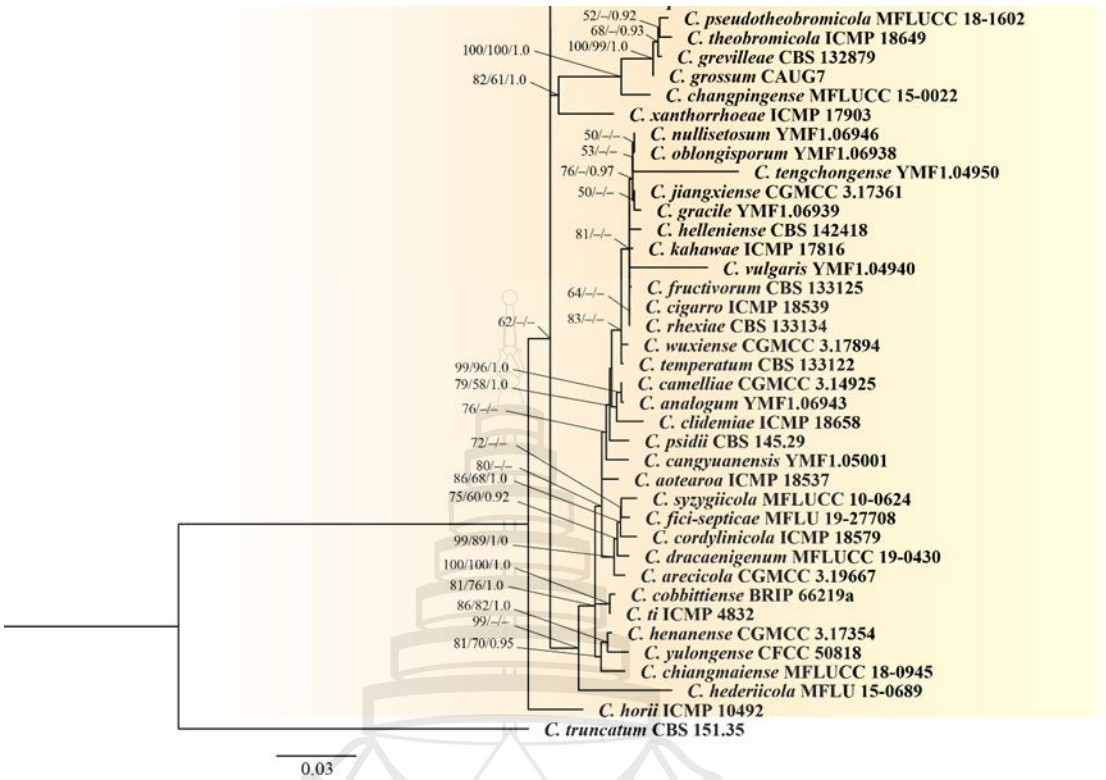

Figure 7.1 (continued)

Colletotrichum fructicola Prihast., L. Cai & K.D. Hyde (2009)

Figure 7.2

Index Fungorum Number: IF 515409; Facesoffungi Number: FoF 06767

Associated with leaf anthracnose of *Ficus religiosa*. Sexual morph: Not observed. Asexual morph: *Conidiomata* acervular and pycnidial, dark brown. *Setae* not observed. *Conidiophores* branched or solitary, septate, hyaline, cylindrical to inflated. Conidiogenous cells smooth-walled, aseptate, cylindrical or clavate, hyaline, 13–22 × 3–4 µm ($\overline{x}$ = 15 × 3 µm, n = 30). Conidia unicellular, smooth-walled, hyaline, cylindrical, apex rounded, base sub-acute, guttulate, 9–20 × 4.5–5.5 µm ($\overline{x}$ = 15 × 5 µm, n = 30). Appressoria, irregular in shape, undulate, brown to dark brown, 3–7 × 3–5 µm ($\overline{x}$ = 4 × 3.7 µm, n = 30), produced directly on both hyphae and conidia on slide culture.

Culture characteristics – Colonies on PDA 60–73 mm diam. after seven days at 28 °C, velvety, circular, entire edge; surface smoke grey in the center and white at the margin; reverse the same colour.

Material examined – Mae Fah Luang University premises, Mueang Chiang Rai District, Chiang Rai Province, Thailand, on *Ficus religiosa* (Moraceae), 19 December 2021, Alireza Armand, A9 (MFLU 24-0212), living culture, MFLUCC 24-0210; *ibid*., on *Bauhinia* sp., living culture MFLUCC 24-0214.

Two isolates designated as *C. fructicola* (MFLUCC 24-0210 and MFLUCC 24-0214) exhibited morphological uniformity, and a comparative analysis of their morphology with the ex-type strain of *C. fructicola* disclosed a lack of noteworthy distinctions between the ex-type strain and the recently isolated strains (Figure 7.2). From a phylogenetic standpoint, the two newly isolated strains were grouped with the ex-type and other strains of *C. fructicola* within a distinct clade, supported by 79%, 72%, and 1.0 support values in the ML, MP, and BI analyses (Figure 7.1). A pairwise comparison of our strains with the ex-type sequences revealed 1/229 (0.4%) bp difference in *chs-1* and 1/220 (0.4%) in *tub2* for the strain MFLUCC 24-0210. For the strain MFLUCC 24-0214, 2/217 (0.9%) bp differences were observed in *gapdh*, 2/229 (0.8%) in *chs-1*, and 2/420 (0.4%) in *tub2*. This is the first report of *C. fructicola* from *Bauhinia* sp. and *Ficus religiosa* globally.

Note **a**, **b** Symptomatic leaf of *Ficus religiosa*. **c** Pycnidia produced on the PDA. **d**, **e** Conidiophores and conidial attachment. **f**, **g** Conidia. **h** Appressoria. **i** Colony on the PDA. Scale bars: **d**, **e** = 20 µm, **f**–**h** = 10 µm

Figure 7.2 *Colletotrichum fructicola* (MFLU 24-0212)

Colletotrichum musae (Berk. & M.A. Curtis) Arx, (1957)

Figure 7.3

Index Fungorum Number: IF 295348; Facesoffungi Number: FoF 16992

Associated with the anthracnose of banana fruit. Sexual morph: Not observed. Asexual morph: *Conidiomata* acervular, pale brown, with orange conidial mass on fruit. *Setae* not observed. *Conidiophores* branched or solitary, hyaline, septate, cylindrical. *Conidiogenous cells*, smooth-walled, aseptate, hyaline, cylindrical, 7–13 × 3–4 µm ($\bar{x}$

= 11 × 3.7 µm, n = 30). *Conidia* unicellular, smooth-walled, hyaline, oval, elliptical or cylindrical with a sub-acute base and obtuse apex, guttulate, 12–15.5× 5–7 µm ($\bar{x}$ = 14 × 6.3 µm, n = 30).

Culture characteristics – Colonies on PDA 75–85 mm diam. after seven days at 28 °C, velvety, circular, entire edge; aerial mycelium sparse, surface white at the beginning, becoming salmon after conidial masses developed directly from the hyphae, reverse white at the beginning, becoming pale fulvous after conidial masses developed.

Material examined – Mae Fah Luang University premises, Mueang Chiang Rai District, Chiang Rai Province, Thailand, on the fruit skin of *Musa* sp. (Musaceae), 12 December 2021, Alireza Armand, C26 (MFLU 24-0213), living culture, MFLUCC 24-0207.

Notes – Su et al. (2011) established an epitype for *Colletotrichum musae* utilizing the specimen *C. musae* (CBS 116870) as the reference. Morphological analysis comparing our strain of *C. musae* (MFLUCC 24-0207) with *C. musae* (CBS 116870) indicated an absence of discernible distinctions in the conidial shape and size. Nevertheless, a notable prevalence of oval-shaped conidia was observed in *C. musae* (MFLUCC 24-0207) compared to *C. musae* (CBS 116870) which produced mostly cylindrical conidia. Phylogenetic analysis revealed that *C. musae* (MFLUCC 24-0207) grouped alongside the ex-type within a distinct clade, showing 100% support support in both ML and MP, as well as BI analysis (Figure 7.1). A pairwise comparison between MFLUCC 24-0207 and the ex-type sequence revealed 5/517 (0.9%) bp differences in ITS, 1/215 (0.4%) in *gapdh*, 1/210 (0.4%) in *act*, 6/405 (1.4%) in *tub2*.

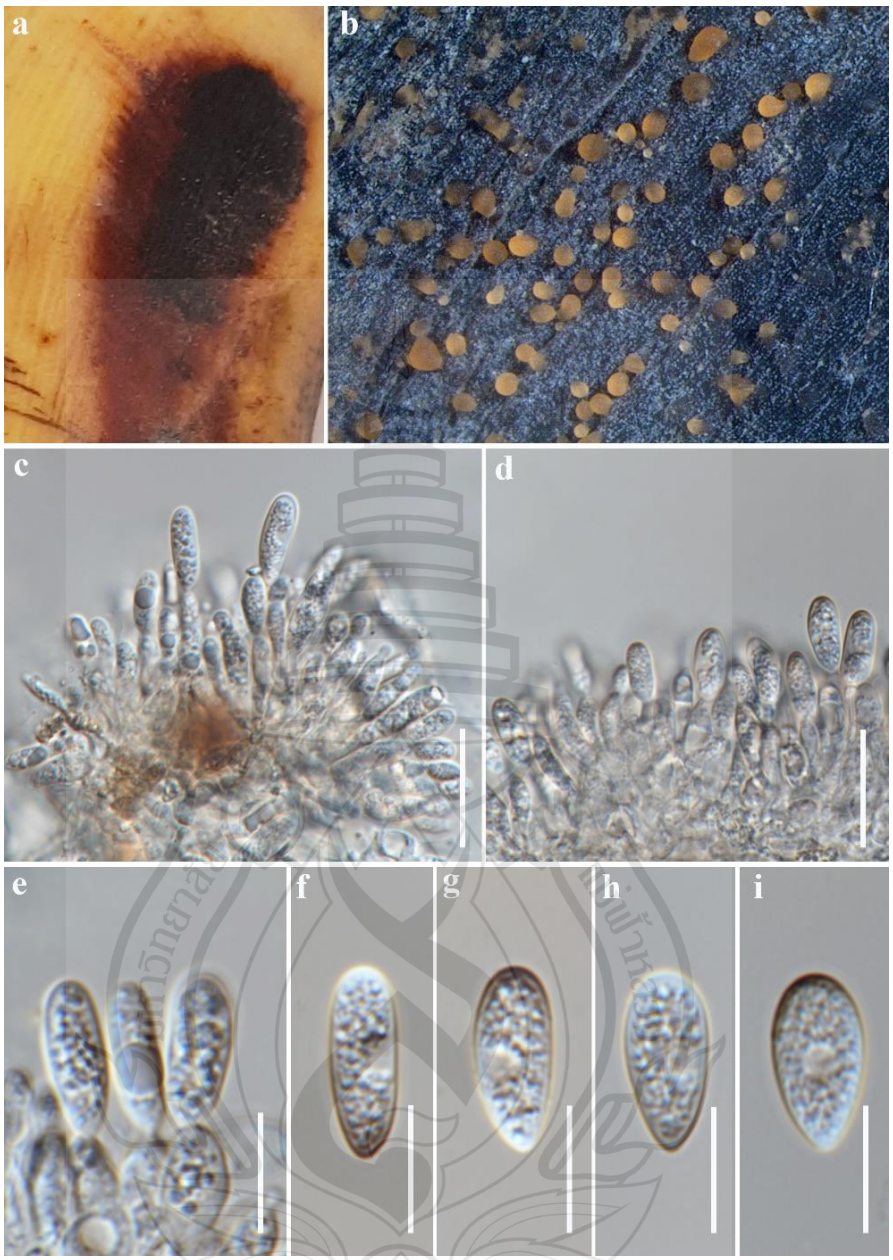

Note **a** Leision on *Musa* sp. fruit peel. **b** Fruiting bodies and conidial masses on the fruit peel. **c**, **d** Conidiophores and conidia produced on PDA. **e** Conidiophores and conidial attachment. **f**–**i** Conidia. Scale bars: **c**, **d** = 20 µm, **e**–**i** = 10 µm

Figure 7.3 *Colletotrichum musae* (MFLU 24-0213)

Colletotrichum siamense Prihast., L. Cai & K.D. Hyde (2009)

Figure 7.4

Index Fungorum Number: IF 515410; Facesoffungi Number: FoF 03599

Associated with leaf anthracnose of *Morinda citrifolia*. Sexual morph: Not observed. Asexual morph: *Conidiomata* acervular, dark brown. *Setae* not observed. *Conidiophores* branched or solitary, hyaline, septate, cylindrical to inflated. *Conidiogenous cells*, smooth-walled, aseptate, hyaline, cylindrical, 10–17 × 3–4 µm ($\bar{x}$ = 13.3 × 3.3 µm, n = 30). *Conidia* unicellular, smooth-walled, hyaline, ellipsoid or cylindrical, rounded at both ends, guttulate, 13–19× 4–5.5 µm ($\bar{x}$ = 17 × 5 µm, n = 30).

Culture characteristics – Colonies on PDA 58–70 mm diam. after seven days at 28 °C, velvety, circular, entire edge; surface white, becoming smoke grey with age; reverse the same colour.

Material examined – Mae Fah Luang University premises, Mueang Chiang Rai District, Chiang Rai Province, Thailand, on a symptomatic leaf of *Morinda citrifolia* (Rubiaceae), 03 February 2022, Alireza Armand, C36-2 (MFLU 24-0215), living culture, MFLUCC 24-0205; *ibid*., on a symptomatic leaf of *Asplenium nidus*, living culture MFLUCC 24-0203; *ibid*., on a symptomatic leaf of *Dendrobium* sp., living culture MFLUCC 24-0202; *ibid*., on a symptomatic leaf of *Anthurium andraeanum*, living culture MFLUCC 24-0200; *ibid*., on a symptomatic leaf of *Artocarpus heterophyllus*, living culture MFLUCC 24-0201; *ibid*., on a symptomatic leaf of *Dracaena fragrans*, living culture MFLUCC 24-0209; *ibid*., on a symptomatic leaf of *Bauhinia* sp., living culture MFLUCC 24-0208; *ibid*., on a symptomatic leaf of *Morinda citrifolia*, living cultures MFLUCC 24-0204, MFLUCC 24-0205; *ibid*., on a symptomatic leaf of *Ficus* sp., living cultures MFLUCC 24-0204, MFLUCC 24-0215.

Notes – Nine isolates were unequivocally identified as belonging to *Colletotrichum siamense*, obtained from different hosts (Table A10). These isolates exhibited consistent morphological characteristics, including similarities in conidiogenous cells, conidial shape and size, as well as cultural characteristics. The morphological comparison confirmed that the isolates are similar to the ex-type. Phylogenetic analyses affirmed their consistent placement within the *C. siamense* clade with 74% ML support value along with the ex-type and other strains (Fig. 1). This study reported *C. siamense* from *Asplenium nidus*, *Dendrobium* sp., *Dracaena fragrans*, and

Morinda citrifolia as new host records. Additionally, *C. siamense* was reported from *Anthurium andraeanum*, *Artocarpus heterophyllus*, *Bauhinia* sp., and *Ficus* sp., for the first time in Thailand.

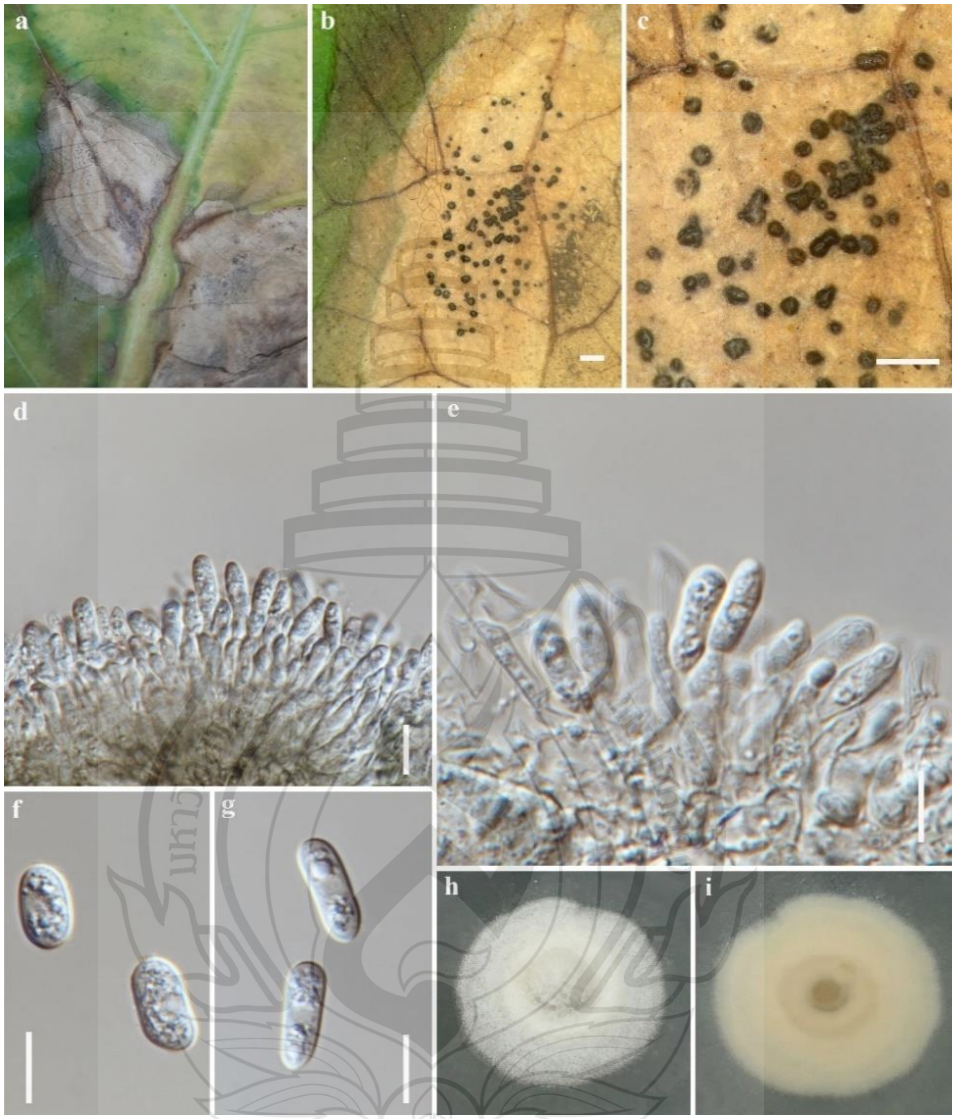

Note **a** Symptoms on leaves of *Morinda citrifolia*. **b**, **c**. Fruiting bodies on the leaves. **d**, **e** Conidiophores and conidial attachment. **f**, **g** Conidia. **h**, **i** Upper and reverse view of colony on PDA. Scale bars: **b**–**c** = 500 µm, **d**–**g** = 10 µm

Figure 7.4 *Colletotrichum siamense* (MFLU 24-0215)

7.3.4 *Colletotrichum orchidearum* Species Complex

In the phylogenetic assessments (Figure 7.5), a single isolate was identified in the *C. orchidearum* species complex, representing *C. musicola* (MFLUCC 24-0206).

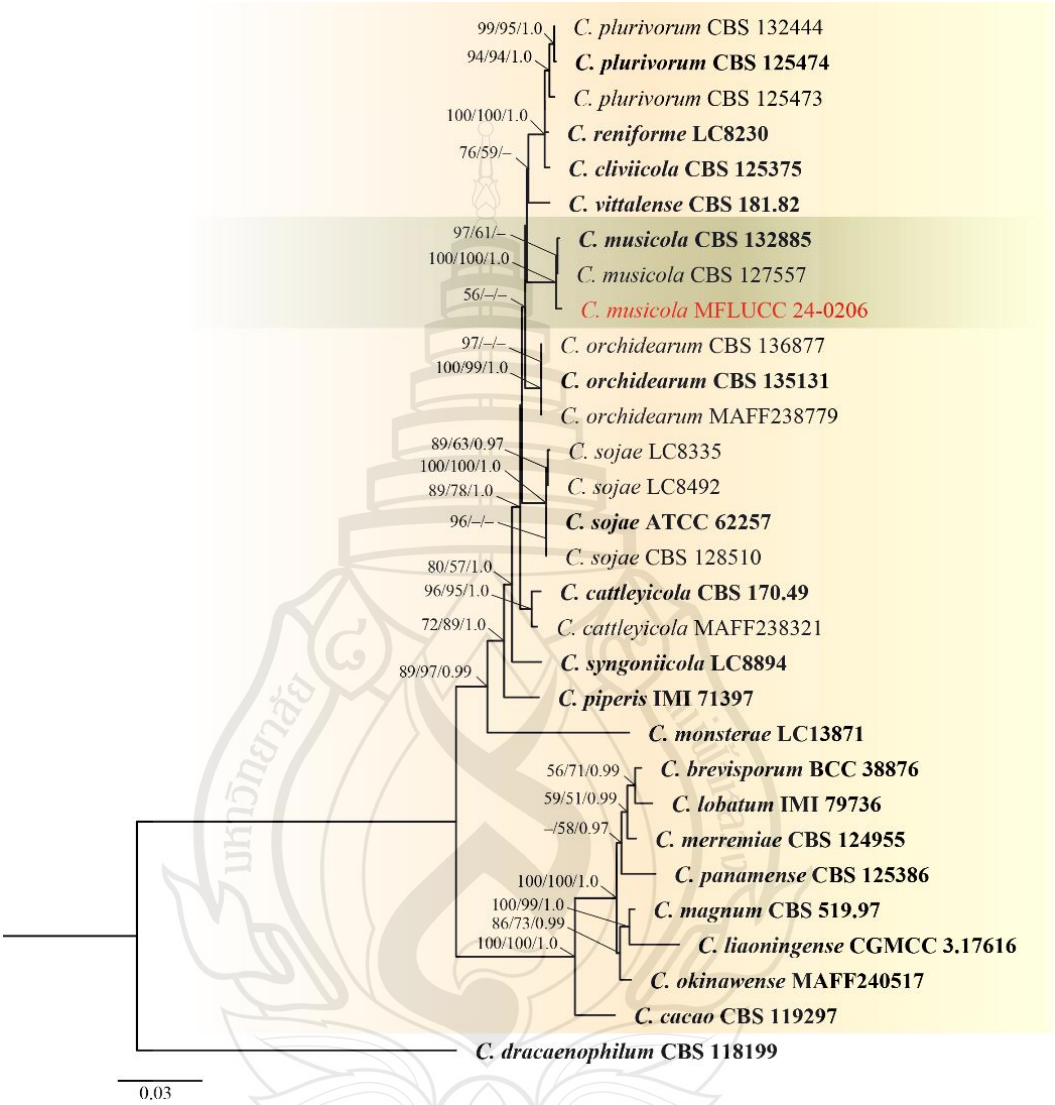

Note The tree was rooted with *Colletotrichum dracaenophilum* (CBS 118199). Maximum-likelihood and maximum-parsimony bootstrap values above 50% and Bayesian posterior probabilities above 0.90 are presented, respectively. Type strains are in bold, and the new isolates from this study are in red

Figure 7.5 Phylogenetic tree generated from maximum likelihood analysis of the *Colletotrichum orchidearum* and *Colletotrichum magnum* species complexes based on a concatenated ITS, *gapdh*, *chs-1*, *act*, *tub*2 sequence data

Colletotrichum musicola Damm (2018)

Figure 7.6

Index Fungorum Number: IF 824225; Facesoffungi Number: FoF 16993

Associated with leaf spots of *Lagerstroemia* sp. Sexual morph: Not observed. Asexual morph: *Conidiomata* acervular, dark brown. *Setae* pale to brown, verruculose, 60–100 μm long, 1–3-septate, base cylindrical to inflated. *Conidiophores* branched or solitary, hyaline, septate, cylindrical to inflated. *Conidiogenous cells*, smooth-walled, aseptate, hyaline, cylindrical, 8–18.5 × 3–4 μm ($\bar{x}$ = 14.5 × 3.5 μm, n = 30). *Conidia* unicellular, smooth-walled, hyaline or pale brown, cylindrical, rounded in the ends, straight, guttulate, (15–)17–20× 4–5.5 μm ($\bar{x}$ = 18 × 5 μm, n = 30).

Culture characteristics – Colonies on PDA 50–55 mm diam. after seven days at 28 °C, velvety, circular, entire edge; surface white, becoming smoke grey with age; reverse the same colour.

Material examined – Mae Fah Luang University premises, Mueang Chiang Rai District, Chiang Rai Province, Thailand, on a leaf of *Lagerstroemia* sp. (Lythraceae), 29 December 2021, Alireza Armand, C30 (MFLU 24-0214), living culture, MFLUCC 24-0206.

Notes – The isolate MFLUCC 24-0206 was morphologically similar to the *C. musicola* (ex-type, CBS 132885), and phylogenetically clustered with the ex-type and *C. musicola* (CBS 127557) with 100% ML, 100% MP, and 1.0 bootstrap support in BI analysis (Fig. 7.5). A pairwise comparison between our strain and the ex-type sequence showed 3/213 (1.4%) bp differences in *gapdh*, and 2/215 (0.9%) in *act*. This is a new host report of *C. musicola* associated with *Lagerstroemia* sp.

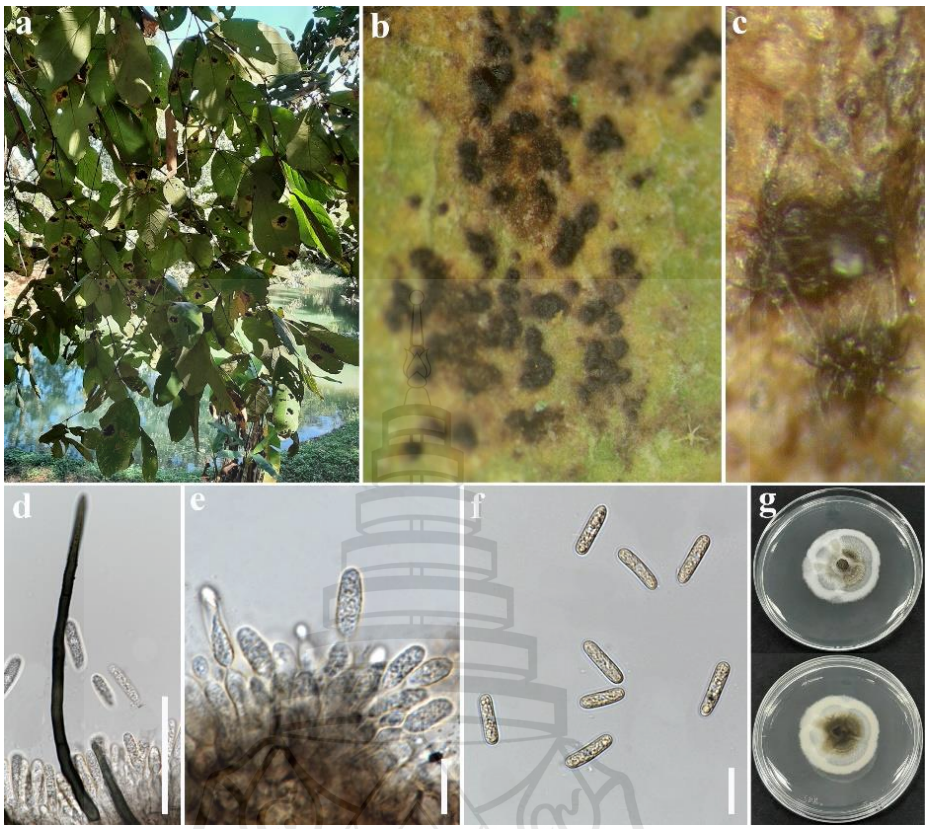

Note **a** Symptoms on leaves of *Lagerstroemia* sp. **b**, **c** Fruiting bodies on the leaf. **d** Setae. **e** Conidiophores and conidial attachment. **f** Conidia. **g** Upper and reverse view of colony on PDA. Scale bars: **d** = 50 µm, **e** = 10 µm, **f** = 20 µm

Figure 7.6 *Colletotrichum musicola* (MFLU 24-0214)

7.3.5 *Colletotrichum dracaenophilum* Species Complex

In the phylogenetic assessments (Figure 7.7), *Colletotrichum tropicicola* (MFLUCC 24-0213) was assigned to the *C. dracaenophilum* species complex, exhibiting a close clustering with its ex-type (MFLUCC 11-0114) with high support support of 91%, 96%, and 1.00 in the ML, MP, and BI analyses, respectively.

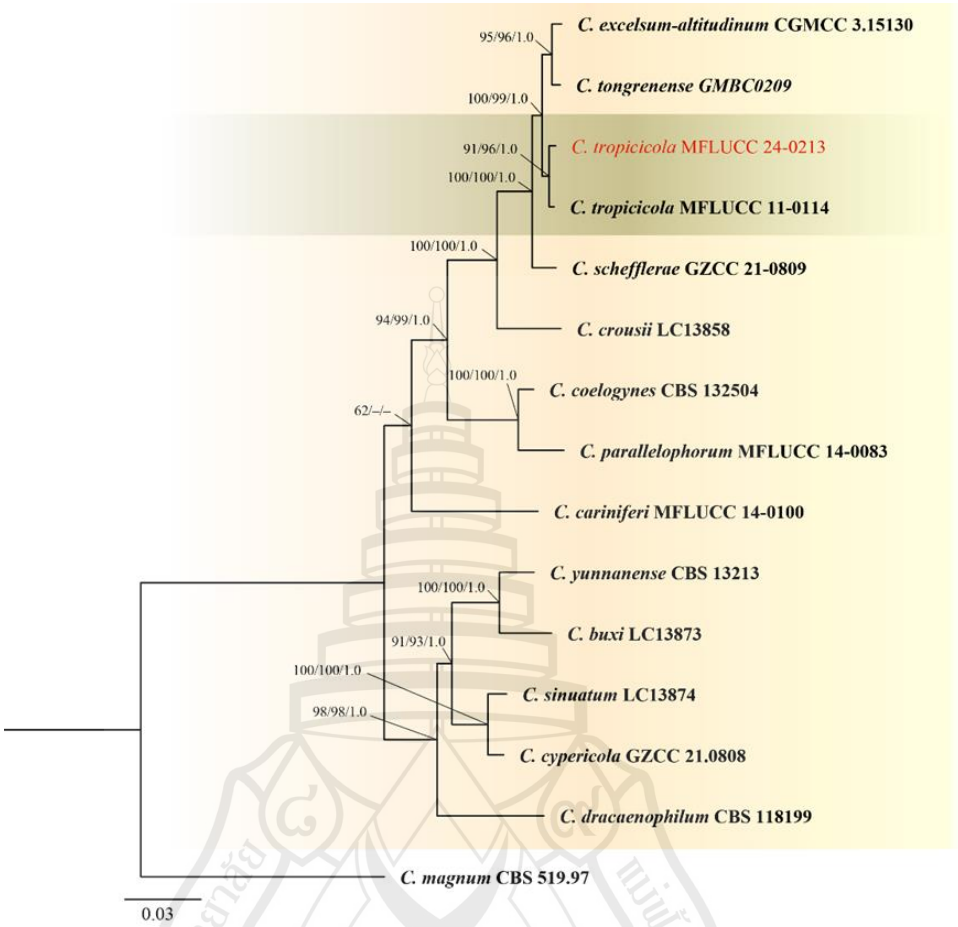

Note The tree was rooted with *Colletotrichum magnum* (CBS 519.97). Maximum-likelihood and maximum-parsimony bootstrap values above 50% and Bayesian posterior probabilities above 0.90 are shown, respectively. Type strains are in bold, and the new isolates from this study are in red

Figure 7.7 Phylogenetic tree produced through maximum likelihood analysis of the *Colletotrichum dracaenophilum* species complex based on the combined ITS, *gapdh*, *chs-1*, *act*, *tub*2 sequences

Colletotrichum tropicicola Phoulivong, Noireung, L. Cai & K.D. Hyde (2012) Figure 7.8

Index Fungorum Number: IF 564159; Facesoffungi Number: FoF 16994

Associated with leaf anthracnose and die back of *Citrus maxima*. Sexual morph: Not observed. Asexual morph: *Conidiomata* acervular, dark brown. *Setae* not observed. *Conidiophores* branched or solitary, hyaline, septate, cylindrical to inflated. *Conidiogenous cells* smooth-walled, aseptate, hyaline, cylindrical or clavate, 11–15(–

18) × 3.5–5 µm ($\bar{x}$ = 12.5 × 4.5 µm, n = 30). *Conidia* unicellular, smooth-walled, hyaline, cylindrical, rounded ends, straight or slightly curved at base, guttulate, 16.5–19.5× 5–6 µm ($\bar{x}$ = 18 × 5.3 µm, n = 30).

Culture characteristics – Colonies on PDA 70–79 mm diam. after seven days at 28 °C, fluffy, circular, entire edge; mycelia sparse, surface olivaceous; reverse olivaceous. *Appressoria* produced on slide culture, pale brown to brown, circular or undulate, non-lobate, 4–10 µm in diam. ($\bar{x}$ = 5 µm, n = 30).

Material examined – Mae Fah Luang University premises, Mueang Chiang Rai District, Chiang Rai Province, Thailand, on a leaf of *Citrus maxima* (Rutaceae), 22 February 2022, Alireza Armand, C41 (MFLU 24-0216), living culture, MFLUCC 24-0213.

Notes – *Colletotrichum tropicicola* (MFLUCC 24-0213) exhibits morphological characteristics analogous to those of the ex-type strain, and was isolated from the same host plant from which the species was initially isolated. According to the phylogenetic analyses (Figure 7.7), the strain MFLUCC 24-0213 is closely related to the ex-type strain, forming a clade supported by 91%, 96%, and 1.0 bootstrap values in the ML, MP, and BI. A pairwise comparison between our strain and the ex-type sequence revealed 2/203 (1.0%) bp differences in *gapdh*, 2/200 (1.0%) in *chs-1*, 1/210 (0.4%) in *act*, 2/400 (0.5%) in *tub2*.

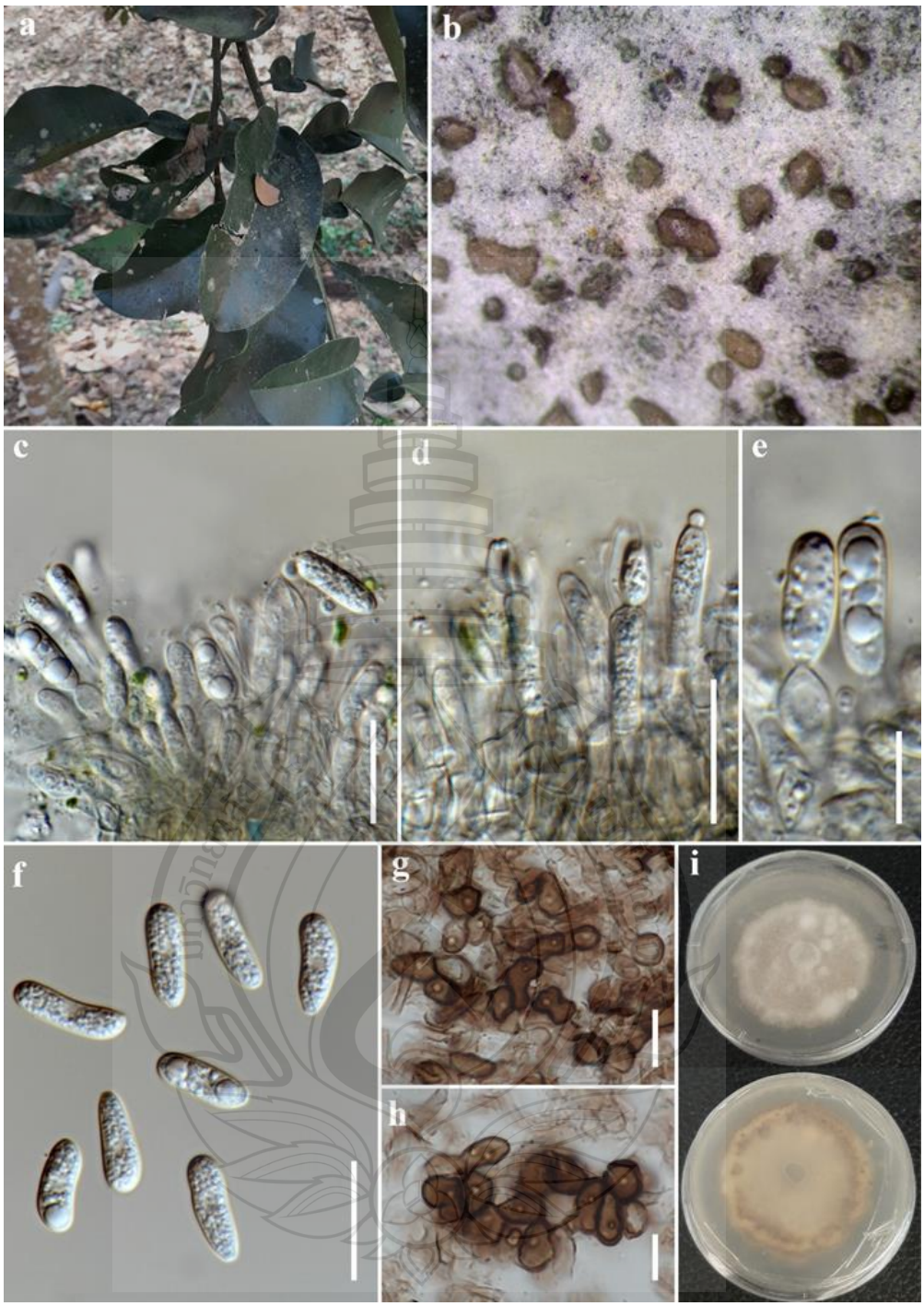

Note **a** Symptoms on leaves of *Citrus maxima*. **b** Fruiting bodies on the leaf. **c**–**e** Conidiophores and conidial attachment. **f** Conidia. **g**, **h** Appressoria. **i** Upper and reverse view of the colony on PDA. Scale bars: **c**, **d** = 20 µm, **e**–**h** = 10 µm

Figure 7.8 *Colletotrichum tropicicola* (MFLU 24-0216)

7.3.6 *Colletotrichum truncatum* Species Complex

In the phylogenetic assessments (Figure 7.9), a single isolate was identified in the *C. truncatum* species complexes, representing *C. truncatum* (MFLUCC 24-0211).

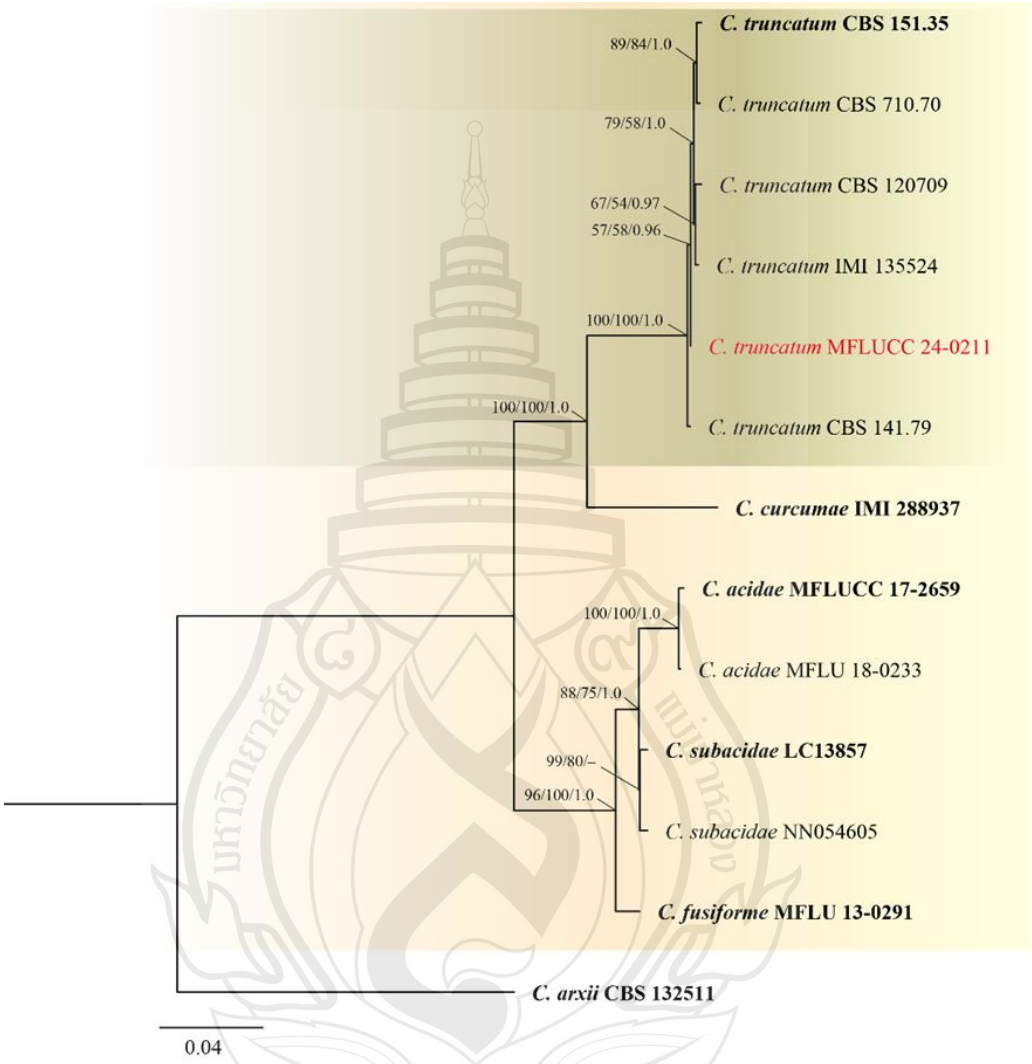

Note The tree was rooted with *Colletotrichum arxii* (CBS 132511). Maximum-likelihood and maximum-parsimony bootstrap values above 50% and Bayesian posterior probabilities above 0.90 are shown, respectively. Type strains are in bold, and the new isolates from this study are in red

Figure 7.9 Phylogenetic tree generated by maximum likelihood analysis of the *Colletotrichum truncatum* species complex based on the concatenated sequence data of ITS, *gapdh*, *chs-1*, *act*, *tub2*

Colletotrichum truncatum (Schwein.) Andrus & W.D. Moore (1935)

Figure 7.10

Index Fungorum Number: IF 280780; Facesoffungi Number: FoF 03827

Associated with leaf anthracnose of *Ficus religiosa*. Sexual morph: Not observed. Asexual morph: *Conidiomata* acervular, dark brown, bearing conidial mass and setae. *Setae* brown to dark brown, verruculose, 1–3 septate, 100–387 µm long ($\bar{x}$ = 250 µm, n = 10), base cylindrical, 6–8 µm diam. ($\bar{x}$ = 6.8 µm, n = 10), acute at the apex. *Conidiophores* branched or solitary, hyaline, septate. *Conidiogenous cells* hyaline, cylindrical, 10–15 × 2–4 µm ($\bar{x}$ = 12 × 3 µm, n = 30). *Conidia* unicellular, smooth-walled, hyaline, curved with parallel walls at the middle part, round and truncate at the base, tapering towards the acute and curved apex, guttulate, 21.5–27 × 3–4 µm ($\bar{x}$ = 24 × 3.5 µm, n = 30).

Culture characteristics – Colonies on PDA 32–35 mm in diam. after seven days at 28 °C, velvety, flat, entire edge, aerial mycelia medium dense, surface buff, reverse the same colour.

Material examined – Mae Fah Luang University premises, Mueang Chiang Rai District, Chiang Rai Province, Thailand, on a leaf of *Ficus religiosa* (Moraceae), 22 May 2022, Alireza Armand, A9-2 (MFLU 24-0217), living culture, MFLUCC 24-0211.

Notes – Morphologically, *C. truncatum* (MFLUCC 24-0211) was similar to the ex-epitype (CBS:151.35) (Damm et al., 2009). The strain (MFLUCC 24-0211) clustered with the ex-epitype and other strains in a clade with 100% ML, 100% MP, and 1.0 BI bootstrap values (Figure 7.9). A pairwise comparison between our strain and the ex-type sequences revealed 2/205 (0.9%) bp differences in *gapdh*, 1/200 (0.5%) in *chs-1*, 1/210 (0.4%) in *act*, 3/410 (0.7%) in *tub2*. This study reported *C. truncatum* from *Ficus religiosa* as a new host record.

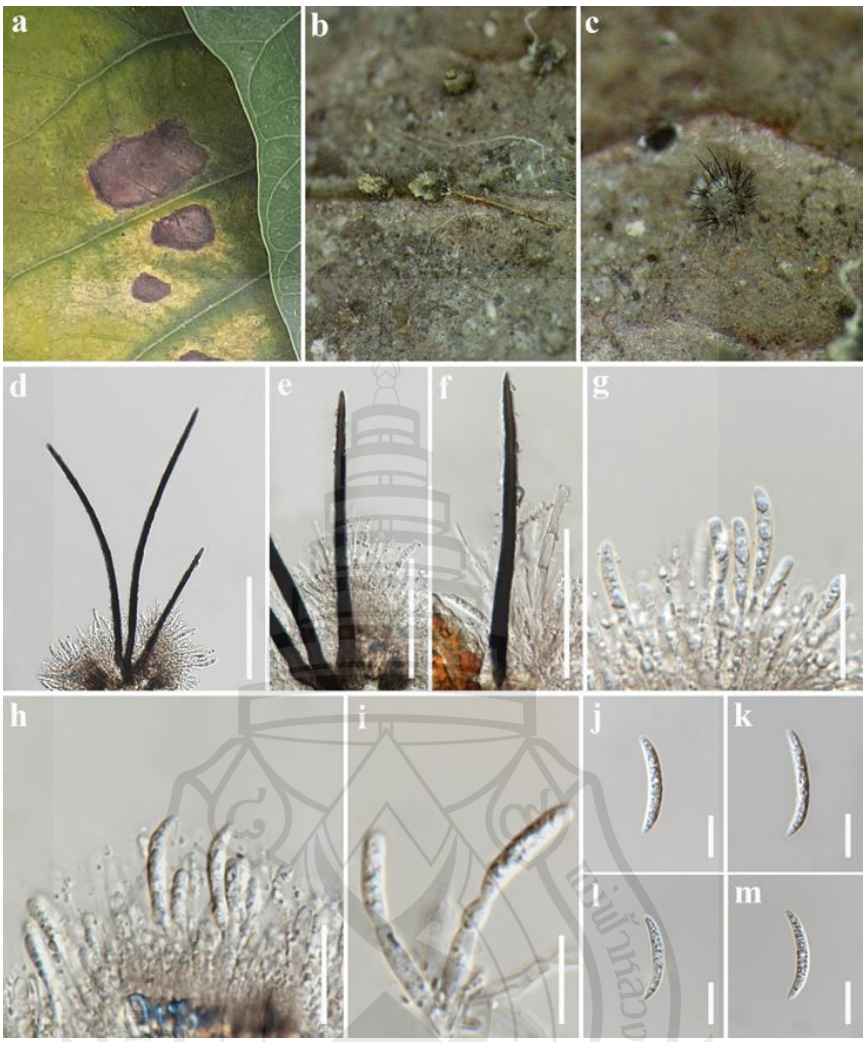

Note **a** Symptoms on leaves of *Ficus religiosa*. **b**, **c** Fruiting bodies on the leaf. **d**–**f** Setae. **g**–**i** Conidiophores and conidial attachment. **j**–**m** Conidia. Scale bars: **d** = 100 µm, **e**, **f** = 50 µm, **g**, **h** = 20 µm, **i**–**m** = 10 µm

Figure 7.10 *Colletotrichum truncatum* (MFLU 24-0217)

Lasiodiplodia theobromae (Pat.) Griffon & Maubl. (1909)

Figure 7.11

Index Fungorum Number: IF 188476; Facesoffungi Number: FoF 00167

Associated with the leaf die back of *Ficus*. Sexual morph: Not observed. Asexual morph: *Conidiomata* pycnidial, 200–350 µm high × 150–290 µm diam. ($\bar{x}$ = 283 × 220 µm, n = 10), solitary or aggregated, scattered, immersed, becoming erumpent at maturity, globose to subglobose, black. *Peridium* 17–66 µm wide, consisting of 3–6 layers, outer layer thick-walled, dark brown cells of *textura angularis* to *textura*

globulosa, inner layer thin-walled, light brown cells of *textura angularis* to *textura globulosa*. *Paraphyses* 20–60 × 2–3 μm ($\bar{x}$ = 32 × 2.2 μm, n = 30), hyaline, cylindrical, aseptate, not branched. *Conidiogenous cells* 5–11 × 3–6 μm ($\bar{x}$ = 9 × 4 μm, n = 20), hyaline, cylindrical, discrete or occasionally integrated. *Conidia* 20–26 × 12.5– 14.5 μm ($\bar{x}$ = 23 × 13 μm, n = 30), unicellular, oblong to ovoid, straight, rounded at both ends, hyaline, thick-walled, guttulate, becoming brown and 1-septate at maturity.

Culture characteristics – Colonies on PDA fast growing, reaching 80–90 mm diam. after seven days at 28 °C, circular, medium dense, flat, cottony to fluffy, white in the initial stage and become black with age, reverse the same colour.

Material examined – Mae Fah Luang University premises, Mueang Chiang Rai District, Chiang Rai Province, Thailand, on the leaf of *Ficus* sp. (Moraceae), 23 April 2022, Alireza Armand, C38 (MFLU 24-0218), living culture, MFLUCC 24-0212.

Notes – Morphological comparison of *L. theobromae* (MFLUCC 24-0212) with the neotype (MBT176098) showed similarities between these two strains (Phillips et al. 2013). The phylogenetic analysis indicated that *L. theobromae* isolate (MFLUCC 24-0212) clustered to the ex-type of *L. theobromae* with 63% ML and 0.94 BI values (Fig. 12). A pairwise comparison between our strain and the ex-type sequence revealed 1/310 (0.3%) bp difference in *tef1* and 1/370 (0.2%) in *tub2*. This is a new geographical report of *Lasiodiplodia theobromae* associated with *Ficus* sp. in Thailand.

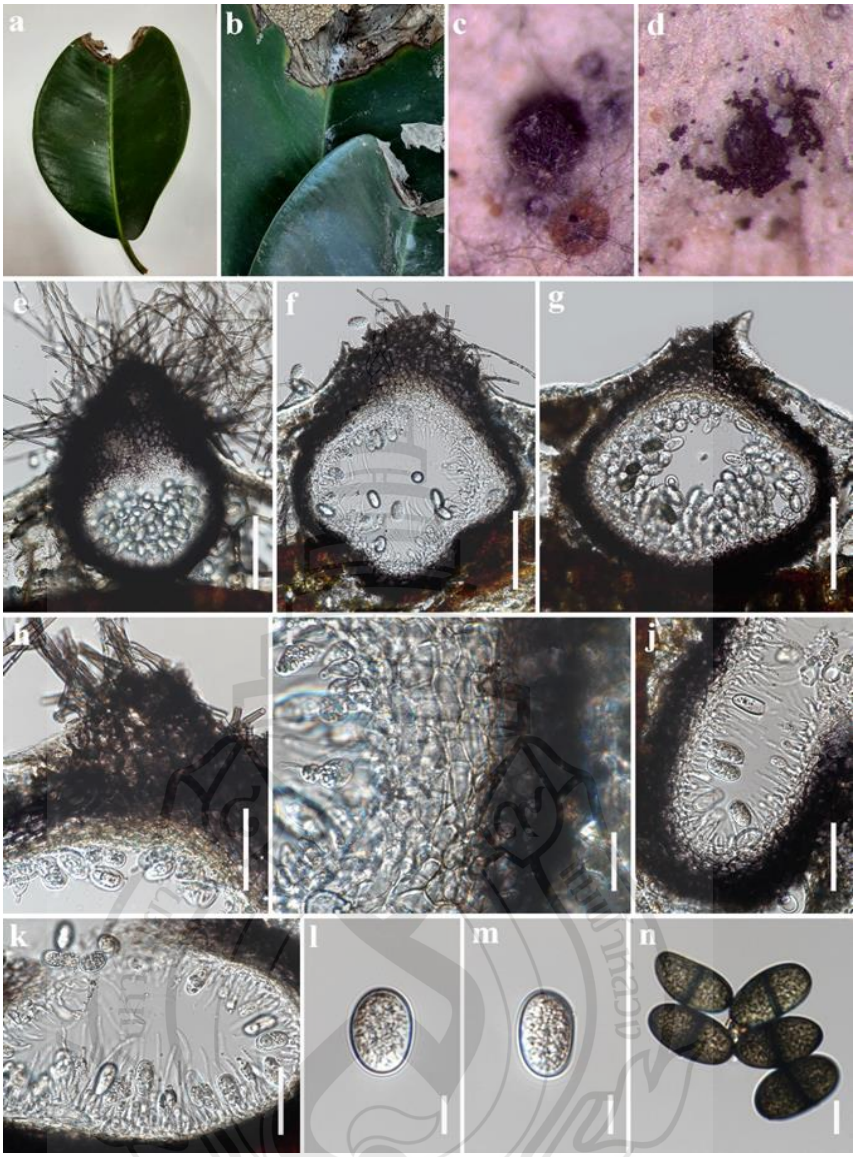

Note **a**, **b** Symptoms on leaves of *Ficus* sp. **c**, **d** Fruiting bodies on the leaf. **e**–**g** Cross section of pycnidium. **h**. Ostiole. **i**. Peridium. **j**, **k**. Conidiogenous cells and conidial arrangement inside the fruiting body. **l**, **m** Immature conidia. **n** Mature conidia. Scale bars: **c**–**d** = 200 µm, **e**–**g** = 100 µm, **h** = 50 µm, **i** = 20 µm, **j**–**k** = 50 µm, **l**–**n** = 10 µm

Figure 7.11 *Lasiodiplodia theobromae* (MFLU 24-0218)

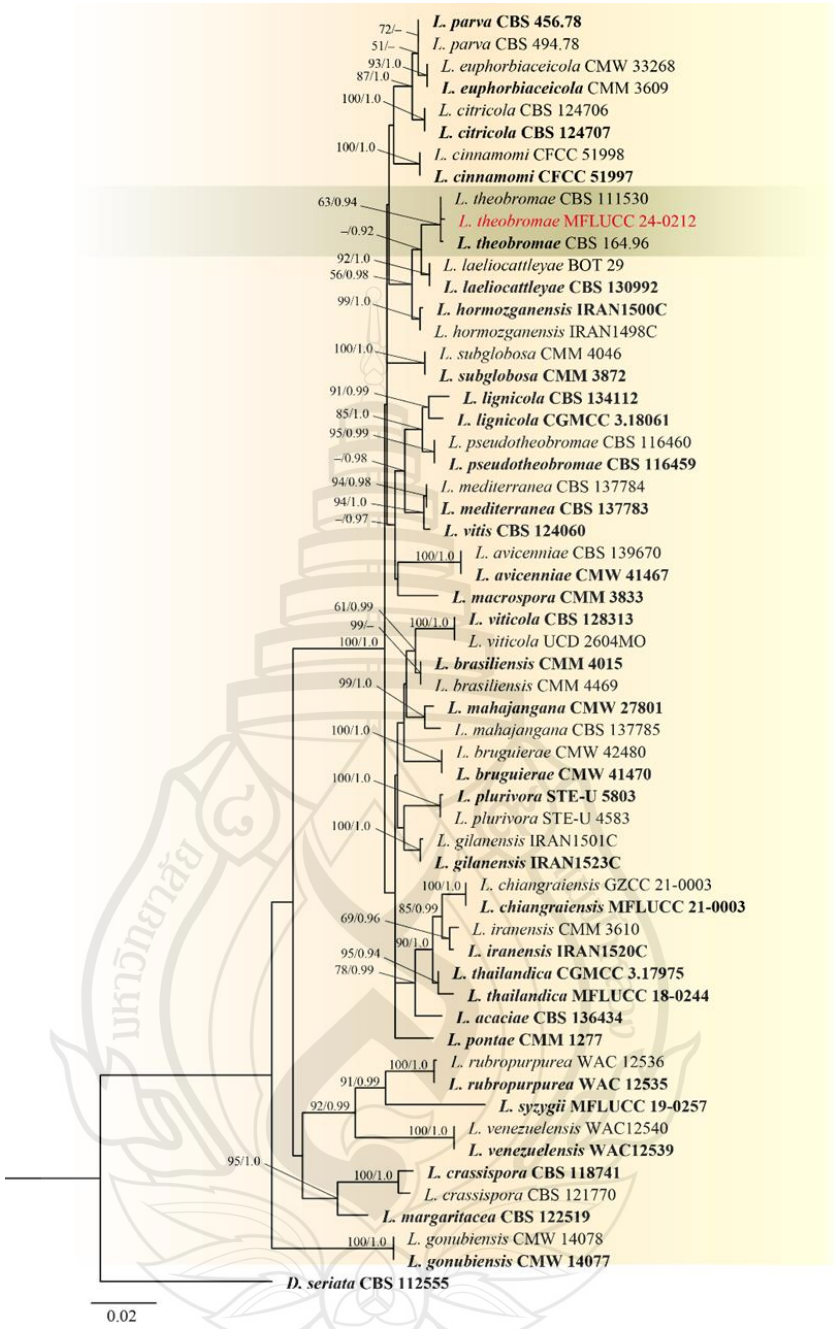

Note The tree was rooted with *Diplodia seriata* (CBS 112555). Maximum-likelihood bootstrap values above 50% and Bayesian posterior probabilities above 0.90 are shown near the nodes, respectively. Type strains are in bold, and the new isolates from this study are in red

Figure 7.12 Phylogenetic tree created by maximum likelihood analysis of *Lasiodiplodia* based on a concatenated ITS, *tef1*, *tub2*, *rpb2* sequence data

Neopestalotiopsis iridis A. Armand, Jayawar. & K.D. Hyde, sp. nov.

Figure 7.13

Etymology – The epithet refers to the plant host genus, *Iris*, from which the fungus was isolated.

Index Fungorum Number: IF 902440; Facesoffungi Number: FoF 16400

Associated with the leaf spots of *Iris pseudacorus*. Sexual morph: Not observed. Asexual morph: *Conidiomata* acervular, on PDA culture, sporodochial, solitary, scattered, black, exuding black glistening conidial masses. *Conidiophores* reduced to conidiogenous cells. *Conidiogenous cells* 5–10 × 2.6–4.5 µm ($\bar{x}$ = 8 × 3.5 µm, n = 30), discrete, cylindrical, ampulliform to flask shape, hyaline, smooth, thin-walled, annelidic, collarette visible. *Conidia* (17–)21–25 × 6–7 µm ($\bar{x}$ = 22 × 6.3 µm, n = 50), fusoid or clavate, straight or slightly curved, four-septate, smooth, septa constricted; basal cell obconic, truncate in the base, thin-walled, hyaline, (3–)4.2–5.1 µm long ($\bar{x}$ = 4 µm, n = 50); three median cells (10.2–)13–14.7(–15.5) µm long ($\bar{x}$ = 13.5 µm, n = 50), smooth-walled, brown, septa darker than the cells; second cell from the base (3.3–)4–4.7(–5.7) µm long, pale brown; third cell brown, (2.8–)3.7–4.5 µm long; fourth cell pale brown, (3.3–)4.2–5.1 µm long; with a septum between the third and fourth cell more darker than the other septa; apical cell 3–4 µm long, conic, subacute in the apex, thin-walled, smooth, hyaline, with 2–4 tubular apical appendages (mostly three), unbranched, centric, and straight or slightly bent, inserted at different loci in the apical crest, (18–)20–22.5(–26.7) × 1–1.5 µm ($\bar{x}$ = 23 × 1.2 µm, n = 50); basal appendage single, filiform, unbranched, centric, (1.5–)3.5–4(–5.3) µm long, and (0.5–)0.7–0.9(–1.1) µm wide (n = 50).

Culture characteristics – Colony on PDA 80–90 mm diam. after seven days at 28 °C, dirty white, with fluffy white aerial mycelia. Reverse pale buff.

Material examined – Mae Fah Luang University campus, Mueang Chiang Rai District, Chiang Rai Province, Thailand, on the leaf of *Iris pseudacorus* (Iridaceae), 21 September 2021, Alireza Armand, C1 (MFLU 24-0219, holotype), ex-type living culture, MFLUCC 24-0199.

Notes – *Neopestalotiopsis coffeae-arabicae* (= *Pestalotiopsis ceffeae-arabicae*) was initially isolated from *Coffea arabica* in China, where it was associated with red-brown leaf spots (Song et al., 2013). *Neopestalotiopsis thailandica* and *N. sonneratae*

were first described in association with leaf spots found on mangrove species, *Rhizophora mucronata* (Rhizophoraceae), and *Sonneronata alba* (Lythraceae) from Thailand, respectively (Norphanphoun et al., 2019). In this study, *N. iridis* was isolated from *Iris pseudacorus* (Iridaceae), which is a monocot species. *Neopestalotiopsis iridis* was identified as belonging to a distinct lineage (97% ML, 0.90 PP), positioned basally within a clade comprising three species: *N. sonneratae*, *N. thailandica*, and *N. coffeae-arabicae* (Fig. 7.14). *Neopestalotiopsis iridis* produced bigger conidiogenous cells and basal cells than those of *N. sonneratae*, *N. thailandica*, and *N. coffeae-arabicae*. Moreover, apical appendages produced by *N. iridis* were longer than those of *N. coffeae-arabicae* and *N. sonneratae*, while it was considerably shorter than those of *N. thailandica*. Base pair differences between *N. iridis* and the aforementioned closest species are provided in Table 7.1.

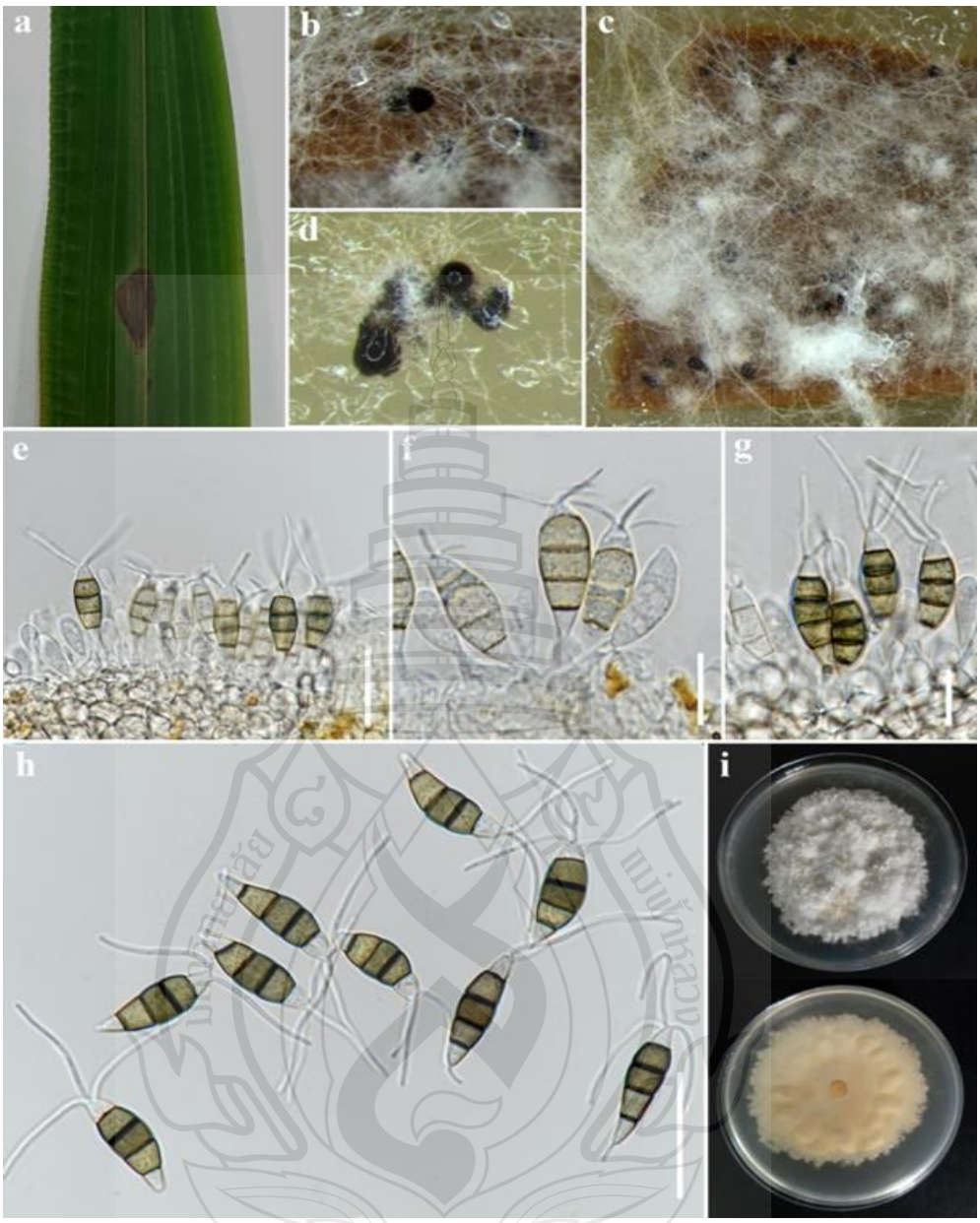

Note **a** Symptoms on the leaf of *Iris pseudacorus*. **b**–**d** Fruiting bodies produced on the host leaf scattered on PDA. **e**–**g** Conidiogenous cells and conidial attachment. **h** Conidia. **i** Upper and reverse view of the colony on the PDA. Scale bars: **e** = 20 µm, **f**, **g** = 10 µm, **h** = 20 µm

Figure 7.13 *Neopestalotiopsis iridis* (MFLU 24-0219, holotype)

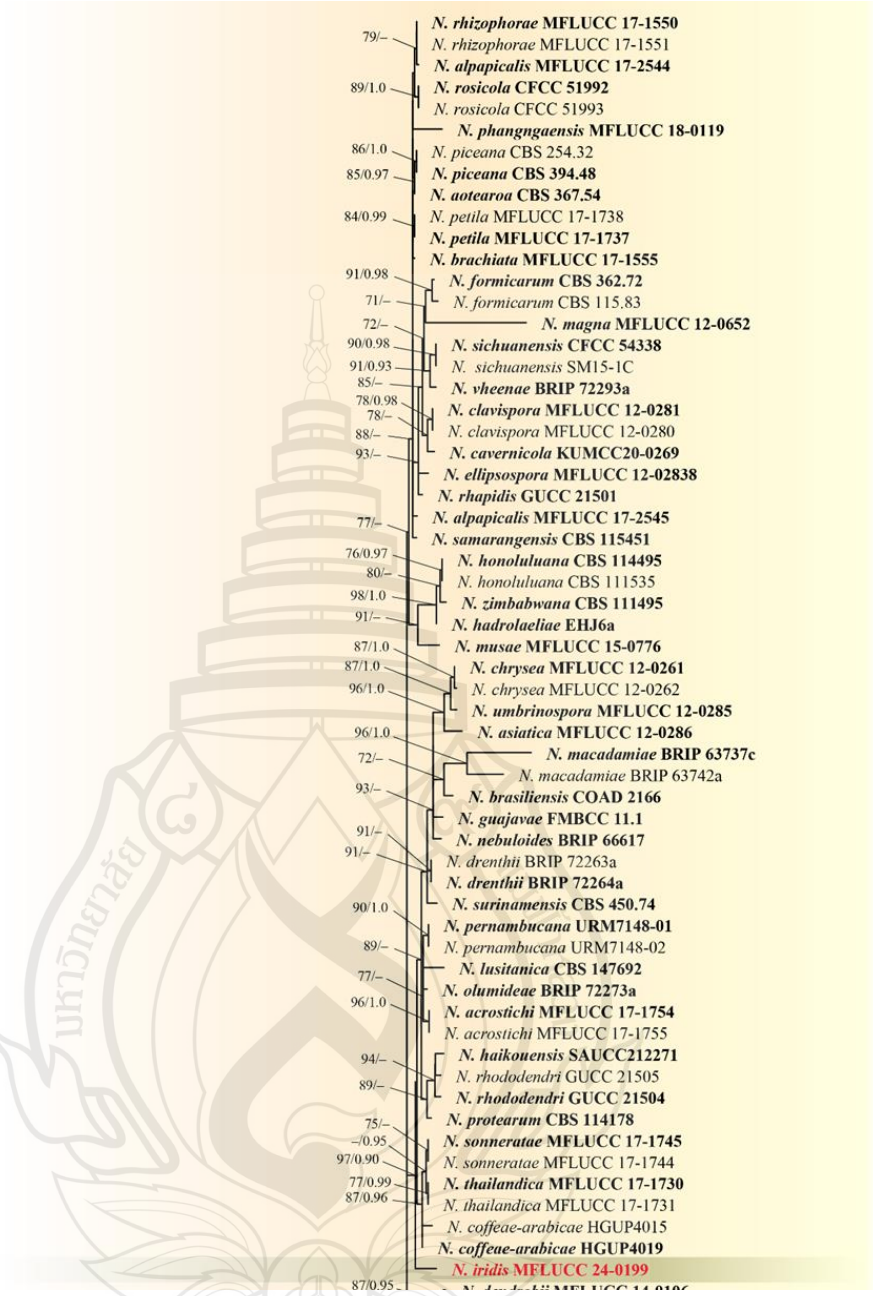

Note The tree was rooted with *Pestalotiopsis trachicarpicola* (OP068) and *P. diversiseta* (MFLUCC 12-0287). Maximum-likelihood bootstrap values above 50% and Bayesian posterior probabilities above 0.90 are presented, respectively. Type strains are in bold, and the new isolates from this study are in red

Figure 7.14 Phylogenetic tree obtained from maximum likelihood analysis of *Neopestalotiopsis*, based on a combined ITS, *tef1*, *tub2* sequences

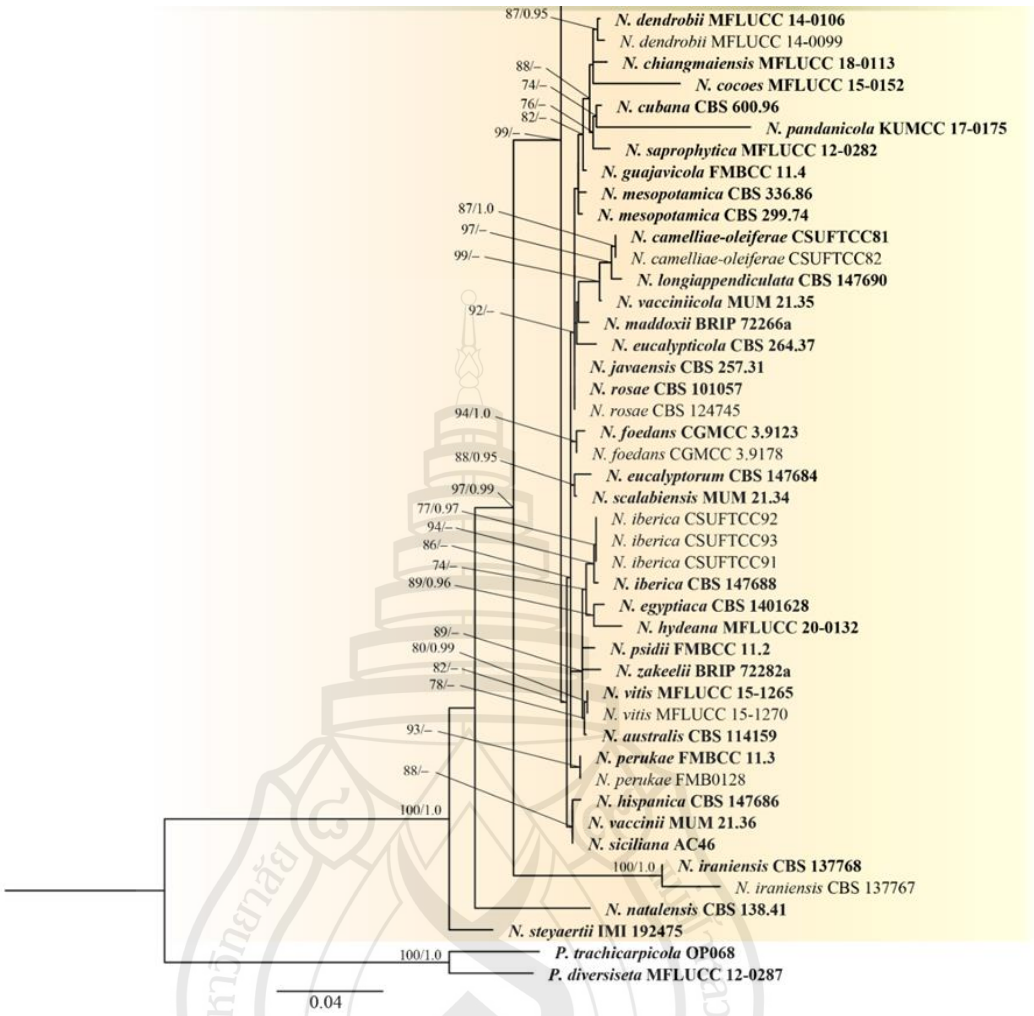

Figure 7.14 (continued)

Table 7.1 Base pair differences comparison between three loci of *Neopestalotiopsis iridis* and its closely-related species

Species	**Loci**		
	ITS	***tef1***	***tub2***
N. coffeae-arabicae (HGUP4019)	0/465 bp	2/205 bp	12/400 bp
N. thailandica (MFLUCC17-1730)	1/465 bp	3/205 bp	9/412 bp
N. sonneratae (MFLUCC17-1745)	0/465 bp	3/205 bp	9/412 bp

7.4 Discussion

Colletotrichum siamense stands out as a prominent member within the *C. gloeosporioides* species complex, having been consistently identified across a diverse range of plant hosts on a global scale (Talhinhas & Baroncelli, 2021). This species has been documented in various orchards and fruits in Thailand, including *Mangifera indica* (Rattanakreetakul et al., 2023), *Persea americana* (Armand & Jayawardena, 2024), and *Syzygium samarangense* (Khuna et al., 2023b). Moreover, it has been reported in association with both native plants and ornamentals in Thailand (Aliya et al., 2022; Khuna et al., 2023a). In this investigation, nine isolates were unequivocally identified as *Colletotrichum siamense* through meticulous morphological characterization and phylogenetic analyses of multi-gene sequence data sourced from various plant genera (Table A10).

Based on a comprehensive literature review, encompassing notable contributions such as those by Talhinhas & Baroncelli (2023), and augmented by data sourced from the USDA host-fungus database (https://fungi.ars.usda.gov/, accessed on 22 January 2024), it is evident that occurrence of *C. siamense* infection targeting *Anthurium andraeanum* has been restricted to a report from Sri Lanka (Vithanage et al., 2021). Notably, before the current study, there had been a conspicuous absence of documented instances of *C. siamense* infection in *Anthurium andraeanum* within the geographical confines of Thailand. *Colletotrichum artocarpocola* documented by Bhunjun et al. (2019) from Thailand, and *C. siamense* reported in Australia (Shivas et al., 2016) and Brazil (Borges et al., 2023), have been recognized on *Artocarpus heterophyllus* (jackfruit) as saprobe, endophyte, and pathogen, respectively. Consequently, this study represents the inaugural documentation of *C. siamense* associated with leaf spots on jackfruit as a new fungus-host record. *Morinda citrifolia* (morinda), a fruit-bearing tree belonging to the Rubiaceae family and native to Southeast Asia and Australasia (Almeida et al., 2019), has been the focus of limited investigation regarding *Colletotrichum* species. Previous studies have identified *C. gloeosporioides* in India (Kumar et al., 2012) and *C. tropicale* in Mexico from *Morinda citrifolia* (Ayvar-Serna et al., 2018). It is noteworthy, however, that both studies

substantiated species identification primarily through morphological characteristics and ITS sequence data, methodologies prone to species misidentification, as highlighted by Hyde et al. (2013), Jeewon & Hyde (2016), and Jayawardena et al. (2021b). In contrast, the current study introduces a groundbreaking revelation, identifying two strains of *C. siamense* (MFLUCC 24-0204, MFLUCC 24-0205) for the first time on a global scale, associated with anthracnose on *Morinda citrifolia*. This discovery is based on a robust analytical framework involving a five-loci phylogeny coupled with a morphological approach, thereby enhancing the accuracy and reliability of species identification in the *Colletotrichum* genus. Additionally, this study marks the first geographical record of *C. siamense* on *Bauhinia* sp. and *Ficus* sp. from Thailand. Furthermore, *C. siamense* was reported on *Asplenium nidus* (bird's-nest fern), *Dracaena fragrans*, and *Dendrobium* sp. (Orchidaceae) for the first time worldwide (Table A10).

Colletotrichum fructicola stands out as a pivotal pathogenic species predominantly distributed in tropical regions, as highlighted by Talhinhas & Baroncelli (2021). Its presence in Thailand has been documented across diverse plant species, including reports by Prihastuti et al. (2009), Phoulivong et al. (2010, 2011), and the recent contribution by Armand et al. (2023a, 2023b). *Colletotrichum siamense* from Argentina and India (Larran et al., 2015; Sharma et al., 2015) along with *C. endophyticum* and *C. gloeosporioides* from China (Li et al., 2016; Liang et al., 2023), have been isolated from *Bauhinia* spp., a genus known for its substantial biochemical properties and biotechnological applications (Cagliari et al., 2018). Intriguingly, no documented instances of *C. fructicola* have been reported on *Bauhinia* spp., neither in Thailand nor elsewhere, until the present study. Therefore, *C. fructicola* (MFLUCC 24-0214) and *C. siamense* (MFLUCC 24-0208) are illustrated as a new host record and a new geographical record from Thailand, respectively. Furthermore, *C. fructicola* (MFLUCC 24-0210) is reported as a new fungus-host record in the present study.

Colletotrichum truncatum has been documented on various plant species in Thailand, including *Capsicum* sp., *Gossypium* sp., *Manihot esculenta*, *Solanum melongena* (Hyde et al., 2018b), and *Durio zibethinus* (Armand et al., 2023b). Notably, its isolation from *Ficus religiosa* had not been reported globally until this investigation. Therefore, this study presents the inaugural documentation of the association of *C. truncatum* (MFLUCC 24-0211) with anthracnose in *Ficus religiosa*. This finding adds

a novel dimension to the host range of *C. truncatum* and contributes to a broader understanding of its ecological interactions and potential impact on diverse plant species.

Colletotrichum musicola, initially described by Damm et al. (2019), isolated from a restricted range of plant species found in Brazil and Mexico (Cavalcante et al., 2019; Vásquez-López et al., 2019; Boufleur et al., 2020). However, the present investigation has expanded its known host spectrum, revealing *C. musicola* association with *Lagerstroemia* sp. (Lythraceae) leaf spots, reported for the first time worldwide. Furthermore, the occurrence of *Lasiodiplodia theobromae* on *Ficus* spp. had not been previously documented in Thailand until the current inquiry. Herein, *L. theobromae* (MFLUCC 24-0212) was identified as a fungal pathogen associated with leaf dieback through an analysis encompassing both morphological and molecular methodologies. *Colletotrichum tropicicola* and *C. musae* were isolated from *Citrus maxima* and *Musa* sp., respectively. While *C. musae* has been extensively studied as the causal agent of banana anthracnose, this marks the second documented instance of *C. tropicicola* associated with anthracnose of *Citrus maxima* in Thailand. In the current study, *Colletotrichum* species were isolated from fruit and leaf anthracnose, leaf spots, and leaf die back across various plant families, including Moraceae, Musaceae, Lythraceae, Rubiaceae, and Rutaceae.

To justify the introduction of our strain as a new species, we conducted comprehensive morphological and phylogenetic analyses using two strains for each of the three species: *Neopestalotiopsis coffeae-arabicae*, *N. thailandica*, and *N. sonneratae*, ensuring accurate phylogenetic positioning. The analysis demonstrated that our species formed a distinct lineage separate from the type and additional strains of the closely-related species (Figure 7.14). While the ITS region, which is more conserved in the *Neopestalotiopsis* genus, showed minimal variation, significant nucleotide differences were observed in the protein-coding regions *tef1-alpha* (tef) and *beta-tubulin* (tub2) between our species and closely related species. Based on the result of both morphological and phylogenetic analysis, the isolate was introduced as a new taxon. To date, no studies have addressed fungal species diversity associated with *Iris* spp. in Thailand. Remarkably, before this investigation, the presence of *Neopestalotiopsis* species on *Iris* spp. had not been recorded

(https://fungi.ars.usda.gov/; accessed on 23 March 2024). This study isolated and characterized *Neopestalotiopsis iridis* as a novel species from leaf spots of *Iris pseudacorus* (Iridaceae).

In summary, the present study has unveiled one new species, documented eight previously unreported host records, including *C. siamense* from *Asplenium nidus*, *Dendrobium* sp., *Dracaena fragrans*, and *Morinda citrifolia*; *C. fructicola* from *Bauhinia* sp. and *Ficus religiosa*; *C. truncatum* from *Ficus religiosa*; *C. musicola* from *Lagerstroemia* sp., and identified five new geographical occurrences of plant pathogenic species in Thailand, including *C. siamense* from *Anthurium andraeanum*, *Artocarpus heterophyllus*, *Bauhinia* sp., and *Ficus* sp.; *Lasiodiplodia theobromae* from *Ficus* sp.. These observations underscore the novel contribution of the present study, shedding light on a hitherto unreported host and ecological niches for fungal species, especially *C. siamense*, thus enriching our understanding of its distribution and pathogenic potential. As such, these findings not only contribute to the specific understanding of pathogenic fungi but also provide a broader framework for comprehending the ecological dynamics of fungal species, paving the way for further investigations.

CHAPTER 8

MANGO MICROCOSM: UNVEILING THE SPECIES DIVERSITY AND PATHOGENIC POTENTIAL OF FUNGI ISOLATED FROM MANGO IN NORTHERN THAILAND

8.1 Introduction

Mango (*Mangifera indica* L.), an agro-industrial fruit in Anacardiaceae, is ranked eighth globally in terms of productivity output (Iqbal et al., 2022). It is grown in tropical and sub-tropical regions and is considered the main component of many countries' diets (Mukherjee & Litz, 2009; Phoulivong et al., 2010). India and China are the largest mango producers (Kuhn et al., 2017). More than 44,626,000 metric tonnes of mango were supplied to over 100 countries in 2018–2019 (http://www.fao.org/). Nearly 8% of the world's mango production comes from Thailand, one of the top three mango-producing countries (Worldatlas, 2019). Despite these positive statistics, the productivity of mango is threatened by numerous pathogens (Dianda et al., 2023).

Fungal diseases are the most crucial constraints to mango production in many countries (Ploetz, 2003). One of the major fungal diseases affecting the quality of mango is anthracnose caused by *Colletotrichum* species that occur in the pre- and post-harvest stages (Benatar & Wibowo, 2021; Bincader et al., 2021; Cheng et al., 2022). The disease causes blossom blight, leading to poor fruit production (Nelson, 2008). It also damages the leaves, twigs, petioles, panicles, and fruits (Honger et al., 2014). Stem-end rot disease is another important disease on mango, caused by a complex of pathogens including *Dothiorella*, *Diaporthe*, *Neofusicoccum*, *Cytosphaera*, *Alternaria*, *Lasiodiplodia*, and *Pestalotiopsis* species (Galsurker et al., 2018). This disease is considered to be the second most destructive disease after anthracnose, worldwide (Prusky et al., 2009). Other important mango diseases, including gummosis,

alternariose, blossom blight, and mango malformation disease, can reduce fruit yields significantly (Dieye et al., 2020; Ploetz, 2003).

The identification of fungal species was usually based on morphological features. However, morphological characteristics are not sufficient, and molecular techniques are required to recognise species precisely (Chethana et al., 2021; Hyde et al., 2009; Phoulivong et al., 2010). For instance, *C. gloeosporioides* and *C. acutatum* were thought to be the causes of mango anthracnose (Jayasinghe & Fernando, 2009). With advances in molecular techniques, phylogenetic analyses and poly-phasic identification have shown that various *Colletotrichum* species are responsible for mango anthracnose (Bhunjun et al., 2021b; Dela Cueva et al., 2021; Li et al., 2019; Lima et al., 2013; Mo et al., 2018; Wu et al., 2020). Many studies have been carried out worldwide to identify fungal pathogens and endophytes associated with mango (Giblin et al., 2018; Li et al., 2020; Lima et al., 2013; Slippers et al., 2005; Trakunyingcharoen et al., 2014; Viera et al., 2014). Recently, *C. asianum*, *C. gloeosporioides*, and *C. siamense* have been reported to be the causal agents of mango (cv. Nam Dork Mai See Tong) anthracnose in central Thailand (Bincader et al., 2021). Rattanakreetakul et al. (2023) reported *C. acutatum* on mango, in addition to *C. asianum*, *C. gloeosporioides*, and *C. siamense*, from central Thailand. Tamakaew et al. (2022) isolated and identified *Pseudocercospora mangiferae* causing mango leaf spot in northern Thailand. *Lasiodiplodia pseudotheobromae* and *L. viticola* have been reported to be responsible for mango stem-end rot in Thailand (Trakunyingcharoen et al., 2013). Among the pathogenic fungi threatening mango production worldwide, *Colletotrichum asianum* is the most common and widely distributed species causing anthracnose (Li et al., 2019; Talhinhas & Baroncelli, 2021, 2023). This species has been reported as the dominant pathogen on mango in Australia, Brazil, China, Colombia, India, Indonesia, Malaysia, Mexico, Panama, Peru, the Philippines, South Africa, and Thailand (Talhinhas & Baroncelli, 2021, 2023).

In spite of its economic importance, studies on the identification, species diversity, phylogeny, and pathogenicity of fungi associated with mango diseases in Thailand have been poorly studied, particularly in the northern part, and most studies have focused on a certain group of fungi (Rattanakreetakul et al., 2023; Trakunyingcharoen et al., 2013). This study aims to identify and characterise fungal

species associated with various mango symptoms, including anthracnose, leaf spots, shoot dieback, leaf blight, and fruit rot, in northern Thailand. Polyphasic approaches are employed to investigate species diversity and phylogenetic relationships among the isolated species, alongside pathogenicity assessments. Moreover, the study examines the genetic structure of globally distributed *Colletotrichum asianum* strains isolated from mango, utilising ITS sequence data.

8.2 Materials & Methods

8.2.1 Sample Collection

Sample collection was conducted from 2021 to 2023 across various mango orchards and local markets in northern Thailand, including Chiang Rai, Kalasin, Nan, and Sakon Nakhon Provinces. During this survey, different disease symptoms—such as fruit and leaf anthracnose, leaf spots, fruit rot, stem-end rot, fruit decline, leaf and stem blight, and shoot dieback (Figure 8.1)—were identified as prevalent in Thai mango orchards. Samples exhibiting these symptoms were collected to isolate the causal fungi. Specimens were placed in plastic bags labelled with sample codes and essential information such as collection date, location, substrate, and symptom description. They were then transported to the laboratory of the Centre of Excellence in Fungal Research (CEFR) at Mae Fah Luang University for further examination and fungal isolation.

Figure 8.1 Prevailing symptoms associated with mango fruits, leaves, and branches examined in the present study

8.2.2 Fungal Isolation, Purification and Morphological Identification

Symptomatic fruits and plant tissues were examined using a LEICA-EZ4 stereomicroscope, and the symptoms and fungal structures (fruiting bodies) on the surface of the plant tissues were photographed using a stereomicroscope (OLYMPUS-SZX16). Additionally, the morphological characteristics of fungi were examined and photographed using a Nikon DS-Ri2 camera-equipped optical microscope. The photo plates were made using Adobe Photoshop v. 21.1.2, and Tarosoft (R) Image Frame Work software was used for the measurements.

Direct and indirect (tissue isolation) methods were used to isolate fungi, and both single-spore isolation and hyphal-tip isolation were employed to purify fungal strains according to the protocols discussed by Senanayake et al. (2020). In brief, direct isolation was used for those specimens with clearly visible and abundant fruiting bodies on symptomatic plant tissues. To isolate the fungus, conidial suspension was made by transferring numbers of mature fruiting bodies or conidial masses to sterile water, and after obtaining ideal conidial concentration, 30–50 µl of suspension was streaked on culture media. After 18–20 hours, a single germinated spore was transferred to potato dextrose agar (PDA) (Merck, Germany) media to grow. The tissue isolation method was utilised for those symptoms without visible fungal fruiting bodies. In this method, plant tissues were cut into 5 mm^2 fragments from the margin of healthy and infected areas. The tissue fragments were surface sterilised by soaking in 70% alcohol for 1 minute and 10% NaOHCl solution for 1 minute, followed by three-time washing in sterilised distilled water for 2 minutes. Then, plant tissues were spread on sterile filter paper for 10 minutes until dried and transferred into the PDA media. After 2-3 days, when fungal mycelia were observed in the margin of planted fragments, a hyphal tip was transferred into a new media plate to obtain a pure culture. The purified cultures of those were isolated using tissue isolation and kept at room temperature (27 °C ± 2 °C) for more than a month to produce conidia. Important morphological characteristics, including conidial shape and size, presence or absence of conidial pigments, conidial ontogeny, conidiophore shape and size, presence or absence of chlamydospore, and appressoria characteristics, were taken into consideration, and subsequently the measurements were done. All the cultures were deposited in the Mae Fah Luang

University Culture Collection (MFLUCC), Chiang Rai, Thailand. The specimens were deposited in the herbarium of Mae Fah Luang University (MFLU).

8.2.3 DNA Extraction, PCR Amplification and Sequencing

The genomic DNA was extracted from 14-day-old fresh mycelia cultivated on potato dextrose agar (PDA) at room temperature (28 ± 2 °C) utilising the DNA Extraction Kit (Omega Bio-Tek), following the provided manufacturer's guidelines. The amplification procedures were conducted in a 25 µL total volume, consisting of 12.5 µL of 2 × Power Taq PCR Master Mix, 1 µL each of primers (20 µM), 9.5 µL of deionised water, and 1 µL of template DNA (5–10 ng). Polymerase chain reactions (PCR) were performed using an Eppendorf thermal cycler (Master Cycler X50s) to amplify specific gene regions required for phylogenetic analysis. Different markers with their respective primers and thermal conditions are shown in Table A11.

8.2.4 Phylogenetic Analysis

The obtained sequences underwent alignment using AliView v. 1.28 (Larsson, 2014) and were subsequently subjected to a meticulous nucleotide blast search. Following the blast search, retrieval of pertinent sequences was conducted from GenBank, informed by the blast search outcomes and relevant publications (Crous et al., 2013; Damm et al., 2012; Dissanayake et al., 2024; Jayawardena et al., 2020, 2021a; Liu et al., 2022; Razaghi et al. 2024; Si et al., 2023; Wei et al., 2023; Videira et al., 2017). Each dataset underwent rigorous independent alignment using MAFFT v. 7 (Katoh et al., 2019). The alignments were then trimmed under *gappyout* or -*gapthreshold* (0.8) (depending on datasets) using TrimAl v 1.2 (Capella-Gutiérrez et al., 2009), and finally adjusted by BioEdit v. 7.0.9.0 (Hall, 1999). Maximum-likelihood (ML) analyses were executed employing RAxML-HPC2 on XSEDE, utilising the GTR+gamma model of nucleotide evolution. Additionally, IQ-TREE 2.2.2.7 was employed on ACCESS (Minh et al., 2020) within the CIPRES Science Gateway portal (https://www.phylo.org/) with automatic substitution model selection (Kalyaanamoorthy et al., 2017). The analyses incorporated 1000 ultrafast bootstraps (Guindon et al. 2010). Bayesian inference (BI) was conducted using MrBayes 3.2.7a on XSEDE in the CIPRES Science Gateway portal. The BI analyses involved four independent Markov Chain Monte Carlo (MCMC) chains and were executed in four runs, each spanning 1,000,000–6,000,000 generations, with samples collected every

100th generation. The optimal evolutionary model for each gene region was determined using jModelTest 2 version 2.1.6 on XSEDE (Darriba et al., 2012). Furthermore, maximum-parsimony (MP) analysis was performed via PAUP on XSEDE (Swofford, 2002). The resulting phylogenetic trees were visualised using FigTree v. 1.4.0 and annotated using Illustrator CC v. 22.0.0 (Adobe Systems, USA), ensuring a comprehensive and robust representation of the evolutionary relationships within the analysed datasets.

8.2.5 Haplotype Assignment and Constructing Networks

The sequences of *Colletotrichum asianum* reported on mangoes were downloaded from GenBank. All the strains were identified in different studies using multi-locus phylogeny. Each locus (ITS, *gapdh*, *chs-1*, *act*, and *tub*) was aligned individually with MAFFT 6.864b (Katoh et al., 2019) and trimmed in trimAl v1.2 (Capella-Gutiérrez et al., 2009). Due to the significant number of missing and short sequences, *gapdh*, *chs-1*, *act*, and *tub* sequence data have been excluded from haplotype analysis. The number of haplotypes and haplotype diversity (Hd) for ITS was determined in DnaSP v. 6 (Rozas et al., 2017). The Roehl Data file (.rdf) was generated using the following parameters: Sites with gaps/missing: not considered, and invariable sites: removed. The NETWORK 10.2.0.0 was used to construct Median-joining haplotype networks for single and combined datasets (Bandelt et al., 1999, http://www.fluxus-engineering.com).

8.2.6 Pathogenicity Testing

Pathogenicity evaluations were performed using the procedures described by Mo et al. (2018) and Bhunjun et al. (2021a). All isolates were tested for pathogenicity and aggressiveness using detached leaves (for strains originally isolated from leaves) and fruits (for strains originally isolated from mango fruits, cv. Nam Doc Mai) under controlled conditions (27 °C and 80% relative humidity). Isolates were incubated on PDA for 7–14 days at 27°C ± 2. Fresh mango fruits and young leaves without visible disease, collected from Tha Sud, Mueang, Chiang Rai, were used in the experiments. The tissues were surface-sterilised with 75% ethanol for 90 seconds and 3% NaClO for 1 minute, followed by three rinses with autoclaved distilled water. After air drying, detached healthy leaves were placed in plastic containers, and ten wounds were made on the leaves in a 5-mm-diameter circle using a sterilised needle. Fresh mango fruits

were similarly wounded (ten wounds in a 5-mm-diameter circle, 2 mm deep) after washing and air drying. Mycelial plugs (5 mm in diameter) from PDA cultures were applied to the wounds, while sterile agar plugs served as control treatments.

The development of symptoms on the leaves and fruits was monitored daily up to 7 days and measured using ImageJ v.1.54g (https://imagej.net/ij/). Isolates were considered pathogenic if lesions expanded beyond the 5 mm circle of the initial wound. Aggressiveness was assessed at 7 days post-inoculation by measuring lesion diameter. According to the diameter of the disease lesions, the aggressiveness scale was classified as strongly virulent (> 2.0 cm), moderately virulent (> 1.0 to < 2.0 cm), weakly virulent (> 0.5 to < 1.0 cm), and non-virulent (0.5 < cm). The experimental design was completely randomised with three replicates per isolate. Sterile agar plugs were employed as controls. The containers were incubated in a growth chamber at 27°C with a relative humidity of 80% and a 12-hour light period.

8.2.7 Statistical Analysis

Statistical analysis was performed using SAS v.9.1 (SAS Institute, 2016), and data were subjected to analysis of variance (ANOVA), following Tukey's honest significant difference (HSD) test (Tukey, 1951) in the GLM procedure.

8.2.8 Species Identification

Species identification was done following the guidelines provided in Chethana et al. (2021), Jayawardena et al. (2021b) and Maharachchikumbura et al. (2021).

8.3 Results

8.3.1 Sample Collection and Fungal Isolation

During 2021–2023, over 250 samples of mango leaves, fruits, and branches displaying various symptoms were collected for examination and fungal isolation. A total of 140 isolates were obtained from these samples. The isolates were then purified and stored in cryogenic tubes, preserved in a refrigerator for further analysis.

8.3.2 Morphological Identification

The purified isolates underwent preliminary morphological examination to identify them at the genus level, facilitating the selection of representative isolates

within each genus for precise species-level morphological and molecular identification. Morphological examination revealed that the isolates belonged to various genera, including *Colletotrichum*, *Diaporthe*, *Neopestalotiopsis*, *Botryosphaeria*, *Neoscytalidium*, *Neofusicoccum*, *Zasmidium*, and two morphologically similar strains resembling *Pallidocercospora*. Since the majority of isolates (40%) were identified as *Colletotrichum* spp., a total of 60 isolates were selected for further analysis, based on morphological variation observed within each genus. Detailed morphological identification was conducted for the 60 isolates, with distinct morphological characteristics observed and recorded for each group. The isolates were then subjected to molecular identification to confirm accurate species-level identification.

8.3.3 Gene Amplification and Phylogenetic Analysis

Initially, the ITS region was amplified and sequenced for the 60 isolates to confirm their genus-level identification. Based on Blastn search results and morphological consistency, the genera were verified. Subsequently, the appropriate gene regions for each genus were selected and amplified, as detailed in Table A11. Phylogenetic analyses were performed using combined sequence datasets, following the parameters outlined in Table A12. The frequency of genera is represented in Figure 8.2. Species were identified using morpho-molecular approaches and respective GenBank accession numbers are listed in the Table A13.

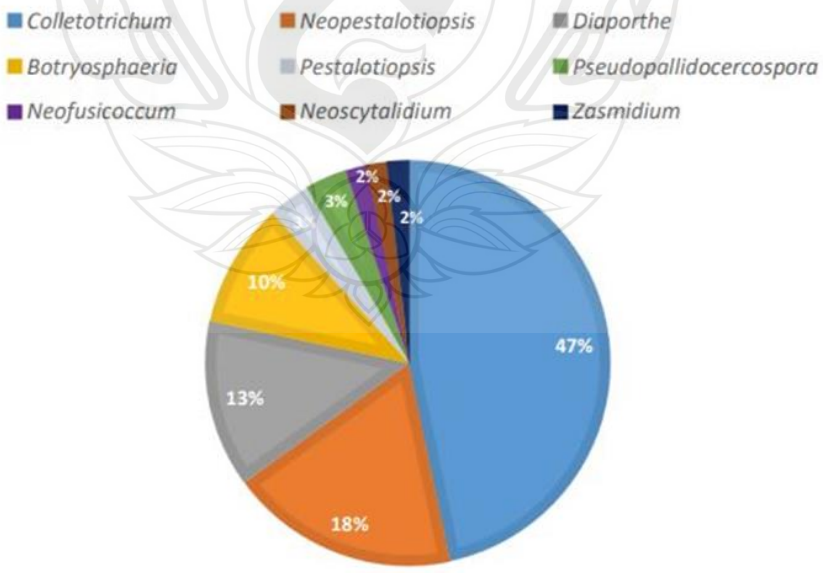

Figure 8.2 Frequency of the genera obtained in this study

8.3.4 Taxonomy

Botryosphaeria Ces. & De Not (1863)

Botryosphaeria (Botryosphaeriaceae, Botryosphaeriales, Dothideomycetes) is a species-rich genus with a cosmopolitan distribution, frequently saprobes or associated with dieback and canker diseases in economically important plantation trees across both agricultural and natural forest ecosystems (Crous et al., 2006b; Darge & Woldemariam, 2021). Many species have also been recorded as endophytes (Wang et al., 2024). Morphologically, numerous asexual morphs have been classified within *Botryosphaeria*; however, multi-locus phylogenetic analyses based on ITS, LSU, *tef1*, *tub2*, and *rpb2* sequence data have improved species resolution within the genus. As a result, several species have been synonymized, while others have been reclassified into different genera (Crous et al., 2006b; Phillips et al., 2013; Slippers et al., 2013; Zhang et al., 2021).

Botryosphaeria fabicerciana (S.F. Chen, Pavlic, M.J. Wingf. & X.D. Zhou) A.J.L. Phillips & A. Alves (2013)

Figure 8.3

Index Fungorum: IF 805457; Facesoffungi: FoF 17007

Basionym: *Fusicoccum fabicercianum* S.F. Chen, D. Pavlic, M.J. Wingf. & X.D. Zhou, Plant Pathol. 60: 746. 2011.

Description: See Chen et al. (2011), Phillips et al. (2013)

Material examined: Thailand, Chiang Rai Province, Mueang Chiang Rai District, Tha Sud, on fruit of *Mangifera indica* (Anacardiaceae), 26 April 2023, A. Armand, M10-2 (MFLU 24-0422; MFLUCC 24-0334, living culture).

Notes: Two strains of *Botryosphaeria fabicerciana* (M10, M10-2) were morphologically similar, and both were isolated from mango fruit. Phylogenetic analysis based on combined ITS, *tef1-α*, and *tub2* sequences revealed that the two strains clustered within a clade that included the ex-type strain of *B. fabicerciana* and other strains, with 85%/1.0 (ML/PP) bootstrap support (Figure 8.4). *Botryosphaeria fabicerciana* was originally described as *Fusicoccum fabicercianum* from China, isolated from twigs of *Eucalyptus* species and hybrids (Chen et al., 2011). The morphological characteristics of the two strains were consistent with those of *B. fabicerciana* (CMW 27094, ex-type culture), and no nucleotide differences were

observed in the ITS, *ef1-α*, and *tub2* regions between our strains and the ex-type strain of *B. fabicerciana*. *Botryosphaeria fabicerciana* has been reported on mangoes from Brazil (Marques et al., 2013) and China (Feng et al., 2023). To our knowledge, this is the first report of *B. fabicerciana* infesting mango from Thailand.

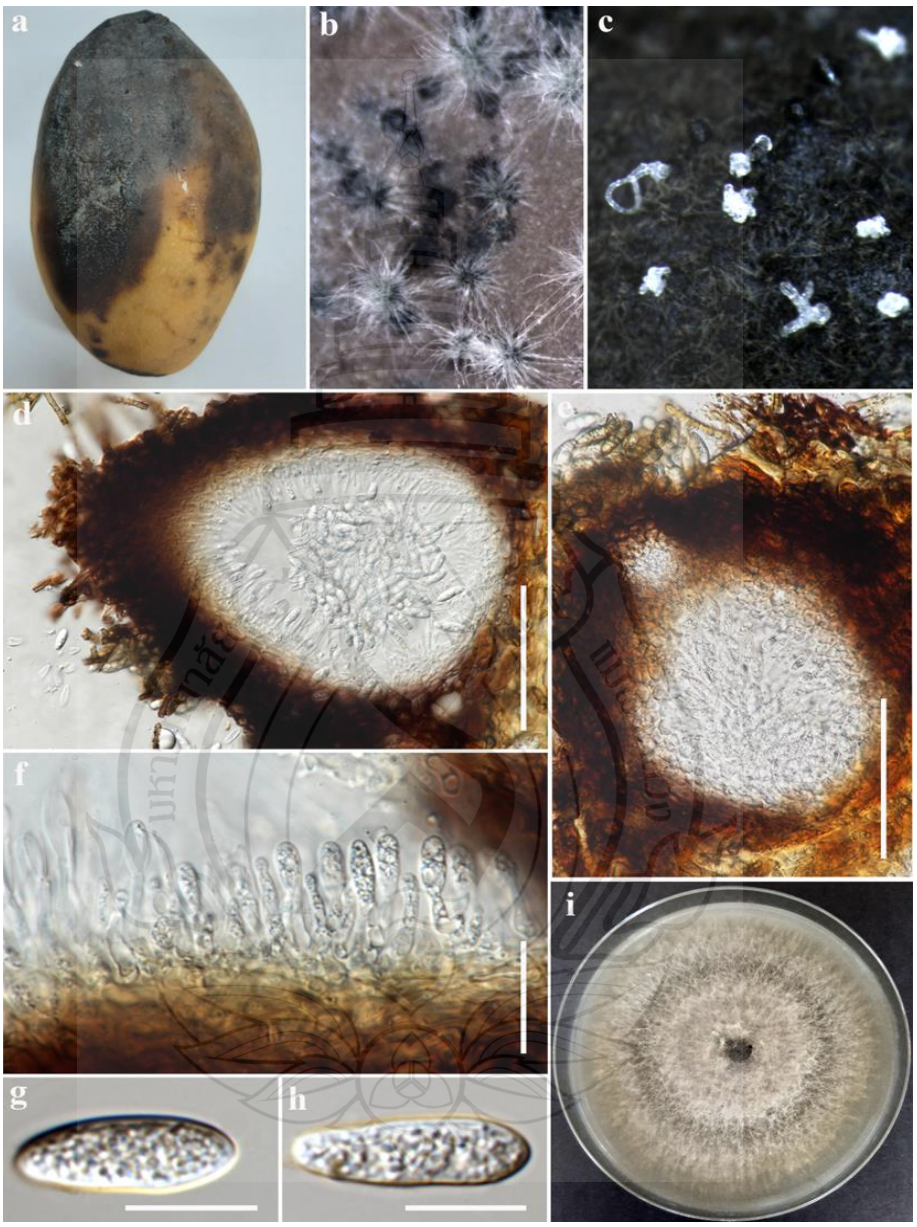

Note **a**. Infested fruit **b**. Fruiting bodies produced on the fruit surface **c**. Mass of conidia oozing from pycnidia **d**, **e**. Cross section of pycnidium **f**. Conidiogenous cells and conidial attachment **g**, **h**. Conidia **i**. Upper view of colonies on PDA; Scale bars: **d**, **e** = 100 µm, **f** = 20 µm, **g**, **h** = 10 µm

Figure 8.3 *Botryosphaeria fabicerciana* (MFLU 24-0422)

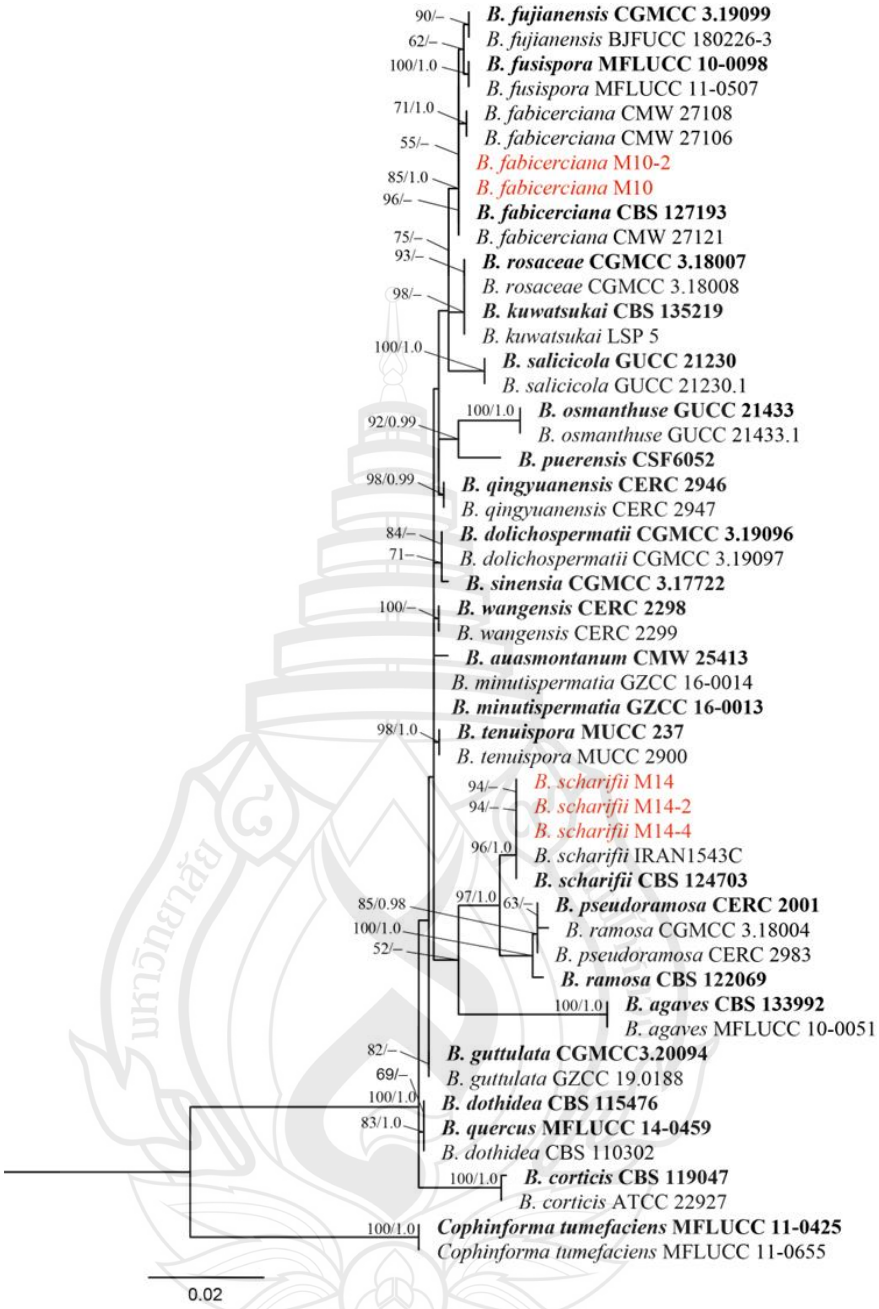

Note Maximum likelihood bootstrap values ≥ 50% and bayesian posterior probabilities ≥ 0.90 are shown near the nodes, respectively. The tree is rooted with *Cophinforma tumefaciens* (MFLUCC 11-0425) and *Cophinforma tumefaciens* (MFLUCC 11-0655). Isolates from this study are in red, and ex-type strains are in bold

Figure 8.4 The maximum likelihood (ML) tree of *Botryosphaeria* based on the combined ITS, *EF1-α*, and *Tub2* sequence dataset

Botryosphaeria scharifii Abdollahz., Zare & A.J.L. Phillips (2013)

Figure 8.5

Index Fungorum: IF 564800; Facesoffungi: FoF 17008

Description: See Abdollahzadeh et al. (2013), Phillips et al. (2013)

Material examined: Thailand, Chiang Rai Province, Mueang Chiang Rai District, Tha Sud, on fruit of *Mangifera indica* (Anacardiaceae), 29 May 2023, A. Armand, M14-4 (MFLU 24-0423; MFLUCC 24-0335, living culture).

Notes: Based on micro-morphological and culture characteristics, six isolates were identified as *Botryosphaeria* sp., while four isolates (M14, M14-2, M14-3, M14-4) were different from two other isolates (M10, M10-2) in conidial size and culture texture and colour. These four isolates, however, were similar in the morphological characteristics and ITS blast result. Finally, three isolates out of four were selected for further gene amplification and phylogenetic analysis. Phylogenetic analysis of combined ITS, *ef1-α*, and *tub2* dataset revealed that the three isolates belong to *Botryosphaeria scharifii*, grouped with the ex-type of *B. scharifii* (CBS 124703) with 96%/1.00 (ML/PP) bootstrap support (Figure 8.4). Morphological comparison with *B. scharifii* (CBS 124703) showed no differences between our strains and the ex-type strain. *Botryosphaeria scharifii* was originally described on the fruits of *Mangifera indica* from Iran (Abdollahzadeh et al., 2013). The species was also reported on mangoes from Malaysia (Li et al., 2021a). This is the first report of *B. scharifii* infesting mango in Thailand.

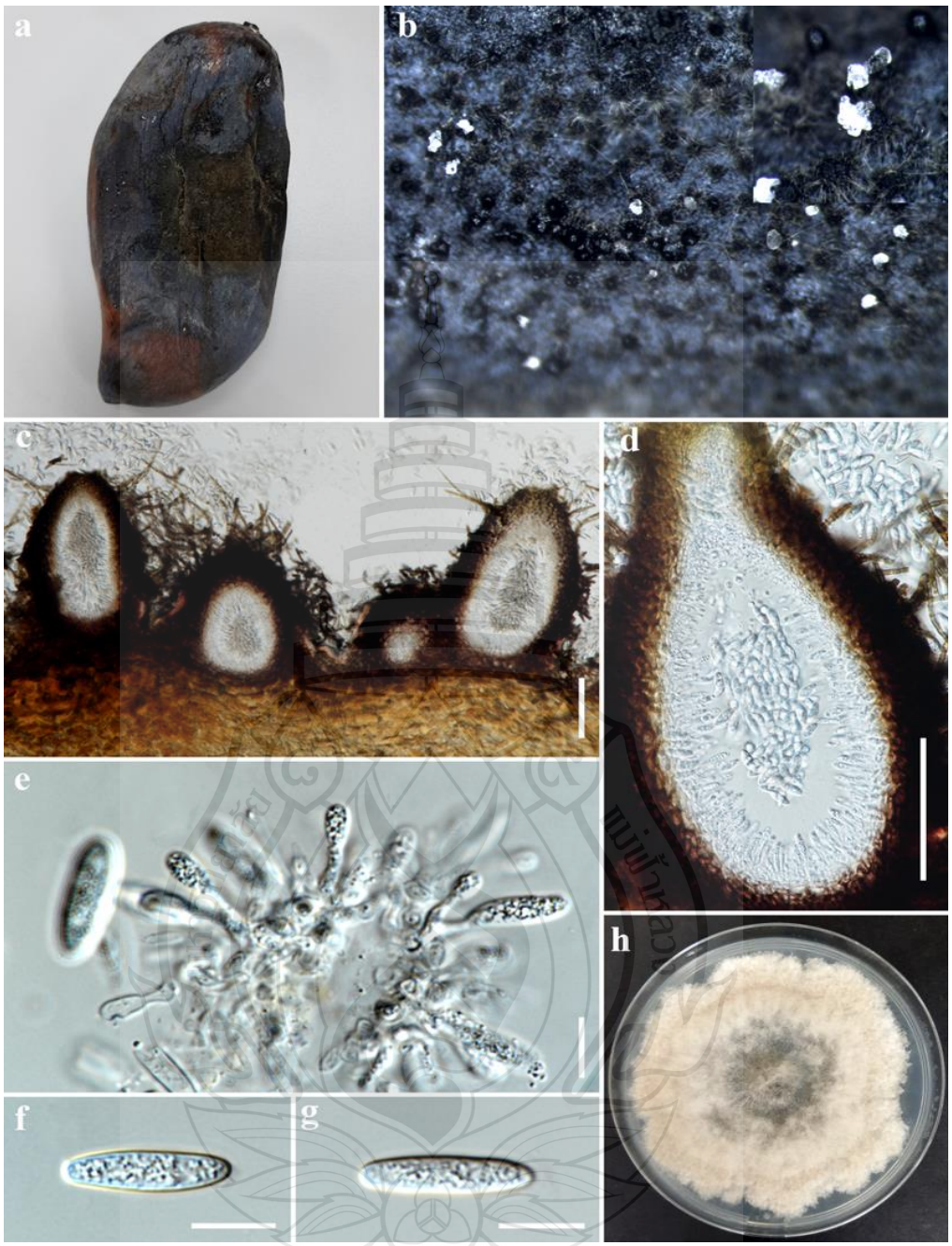

Note **a**. Infested fruit **b**. Fruiting bodies and conidial mass produced on the fruit surface **c**, **d**. Cross section of pycnidium **e**. Conidiogenous cells and conidial attachment **f**, **g**. Conidia **i**. Upper view of colonies on PDA; Scale bars: **c**, **d**= 100 µm, **e**–**g** = 10 µm

Figure 8.5 *Botryosphaeria scharifii* (MFLU 24-0423)

Colletotrichum Corda, in Sturm, Deutschl. Fl., 3 Abt. (Pilze Deutschl.) (12): 41 (1831)

Colletotrichum (Glomerellaceae, Glomerellales, Sordariomycetes) is a destructive pathogen causing anthracnose and other diseases on leaves, stems and fruits of numerous plant species, including several important crops (Huang et al., 2013; Jayawardena et al., 2016; Than et al., 2008b; Zakaria et al., 2021; Zhang Q. et al., 2023, b). However, species also occur as endophytes and saprobes (Cannon et al., 2012; Jayawardena et al., 2016, 2020; Vieira et al., 2014). Morphologically-based identification of *Colletotrichum* species has always been problematic, because there are few reliable characters and many of these characters are plastic, dependent upon methods and experimental conditions (Cai et al., 2009; Hyde et al., 2009). However, advances in molecular phylogenetic methods made it feasible to recognise the species accurately (Bhunjun et al., 2021b; Chen et al., 2022; Damm et al. 2012; Wier et al., 2012). The species of *Colletotrichum* are currently classified within 16 species complexes and 15 singletons (Jayawardena et al., 2021a, Liu et al., 2022).

Colletotrichum asianum Prihast., L. Cai & K.D. Hyde (2009)

Figure 8.6

Index Fungorum: IF 515408; Facesoffungi: FoF 10689

Description: See Prihastuti et al. (2009)

Material examined: Thailand, Chiang Rai Province, Mae Salong Nok, on leaves of *Mangifera indica* (Anacardiaceae), 14 February 2022, A. Armand, P9 (MFLU 24-0424; MFLUCC 24-0338, living culture); Thailand, Chiang Rai Province, Mae Salong Nok, on leaves of *Mangifera indica* (Anacardiaceae), 14 February 2022, A. Armand, P20 (MFLUCC 24-0349, living culture); Thailand, Chiang Rai Province, Mueang Chiang Rai District, Tha Sud, Local market, on fruit of *Mangifera indica* (Anacardiaceae), 26 April 2023, A. Armand, M4 (MFLUCC 24-0341, living culture).

Notes: *Colletotrichum asianum* is one of the most destructive species infesting mangoes worldwide (Sharma et al., 2015; Tovar-Pedraza et al., 2020). In the multi-locus phylogenetic analysis, 19 isolates clustered with the type strain of *Colletotrichum asianum* (ICMP 18580) with 100%/100%/1.00 (ML/PP/MP) values (Figure 8.7). The strains exhibited intraspecific molecular variation, as depicted in the phylogenetic tree (Figure 8.7). Morphological comparison between different strains and the ex-type

revealed differences in the shape and size of conidia, both from the type strain and among the newly isolated strains. The ex-holotype strain produced narrowly cylindrical conidia, measuring 7–12.5 μm in length, whereas the smallest conidia observed in our strains measured 12 μm in length (produced by strains P20). The newly isolated strains of *Colletotrichum asianum* varied in conidial size, ranging from 12 μm (produced by strain P20) to 22 μm (produced by strain M4) in length. Conidial shape also varied, with some being rounded at both ends, acute at one end, or acute at both ends, and conidia were either straight or slightly curved. These morphological differences were consistent with the molecular variation observed among the strains.

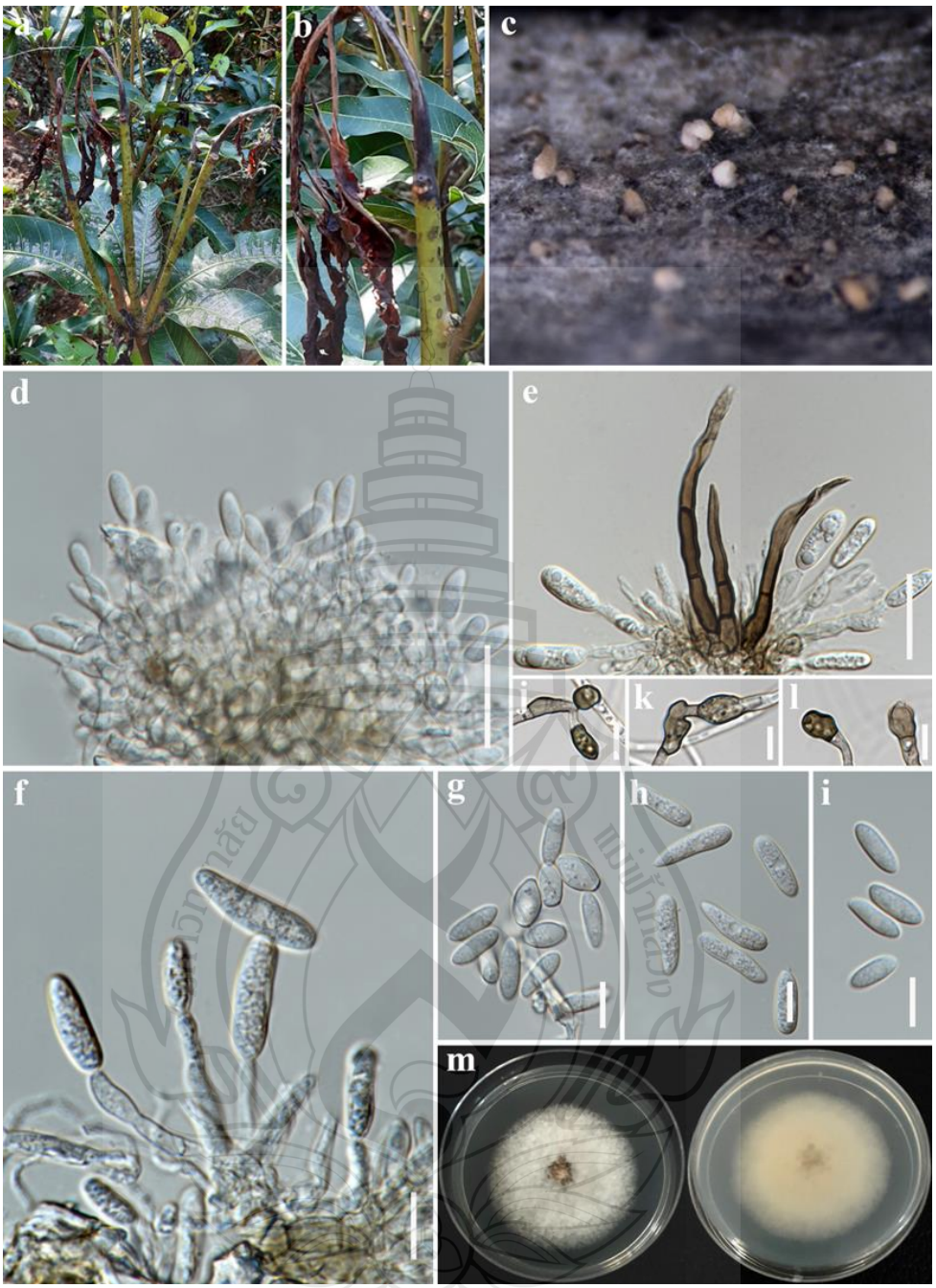

Note **a**, **b**. Symptomatic mango branches and leaves **c**. Fruiting bodies produced on the branch surface **d**. Mass of conidiophores and conidia **e**, **f**. Setae, conidiophores and conidial attachment **g–i**. Conidia **j–l**. Appressoria **m**. Upper and reverse view of colonies on PDA; Scale bars: **d**, **e** = 20 µm, **f**–**i** = 10 µm, **j**–**l** = 5 µm

Figure 8.6 *Colletotrichum asianum* (MFLU 24-0424)

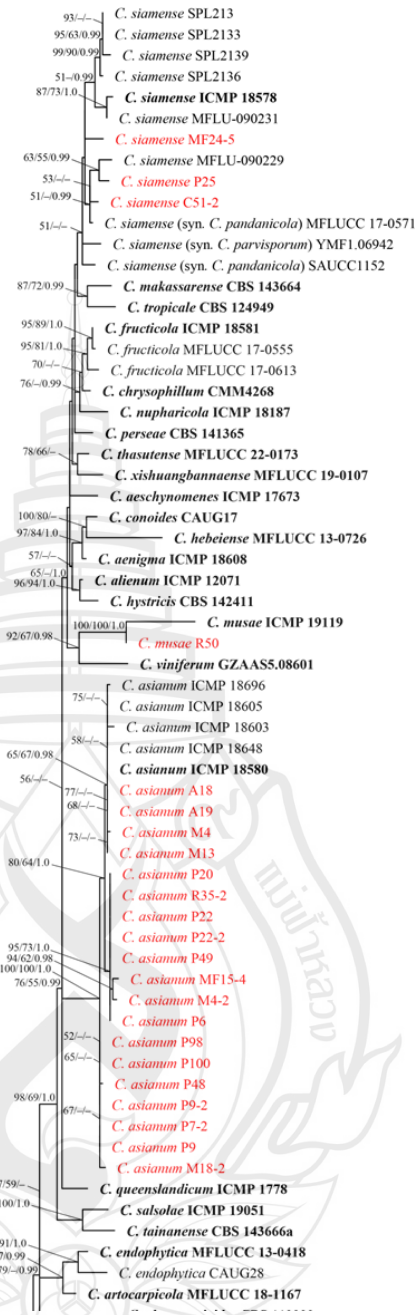

Note Maximum likelihood and maximum parsimony bootstrap support values ≥ 50% as well as bayesian posterior probabilities ≥ 0.90 are shown near the nodes, respectively. The tree is rooted with *Colletotrichum truncatum* (CBS 151.35) and *Colletotrichum acidae* (MFLUCC 17-2659). Isolates from this study are in red, and ex-type strains are in bold

Figure 8.7 Maximum likelihood (ML) tree of *Colletotrichum gloeosporioides* species complex based on the combined ITS, *gapdh*, *chs-1*, *act*, *tub2* sequence dataset

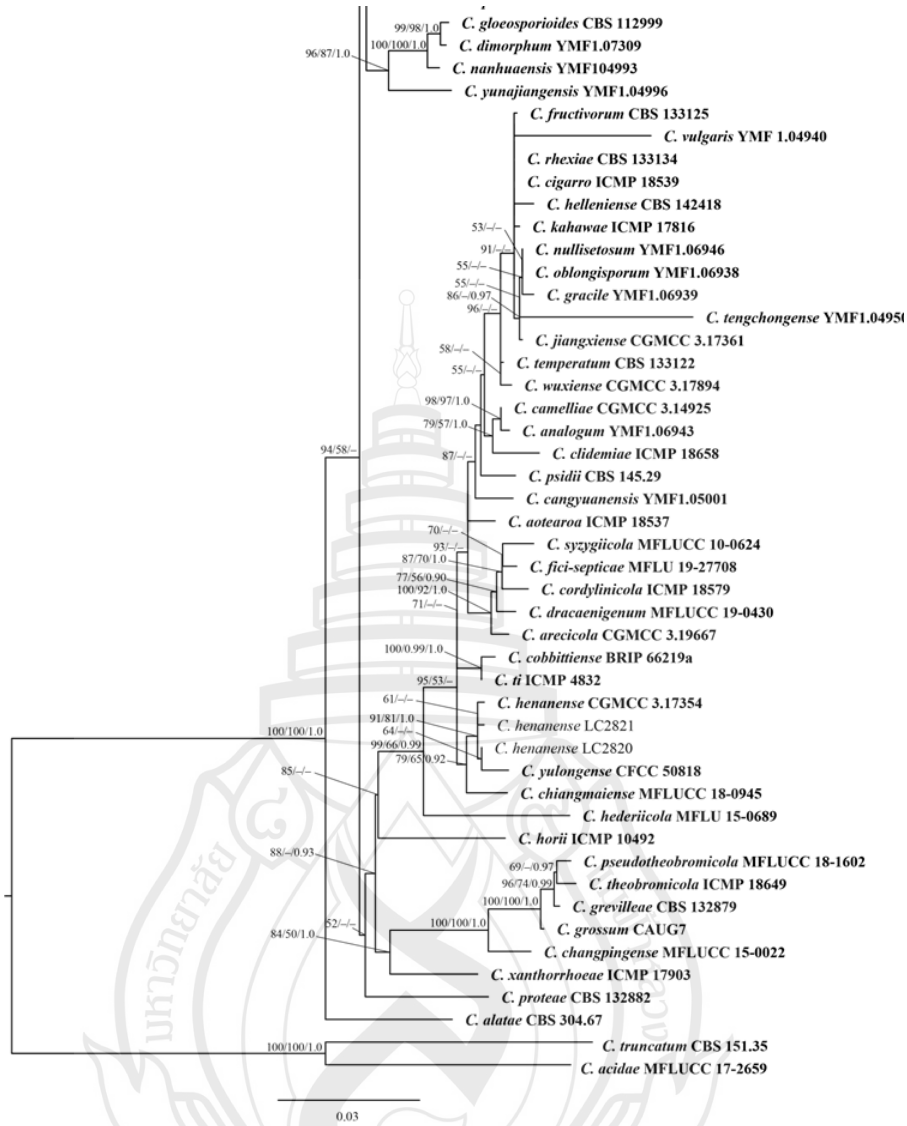

Figure 8.7 (continued)

Colletotrichum gigasporum Rakotonir. & Munaut (2012)

Index Fungorum: IF 800175; Facesoffungi: FoF 10777

Description: See Rakotoniriana et al. (2013)

Material examined: Thailand, Chiang Rai Province, Phan District, Mae Ao; on leaves of *Mangifera indica* (Anacardiaceae), 27 September 2021, A. Armand, T117-2 (MFLUCC 24-0357, living culture).

Notes: A single strain of *C. gigasporum* was obtained from symptomatic leaves of mango. The strain T117-2 (MFLUCC 24-0357) showed polymorphisms with the ex-type strain 5/232 bp (2.1%) in *gapdh*, 2/244 bp (0.8%) in *chs-1*, and 4/453 bp (0.8%) in

tub2. The newly isolated strain clustered in *C. gigasporum* clade with 100%/100%/1.00 (ML/MP/PP) support values (Figure 8.8). Morphological comparison was not feasible as the fungus remained sterile in culture. Li et al. (2019) reported *C. gigasporum* associated with mango anthracnose from China. To our knowledge, this is the first report of *C. gigasporum* infesting mangoes from Thailand.

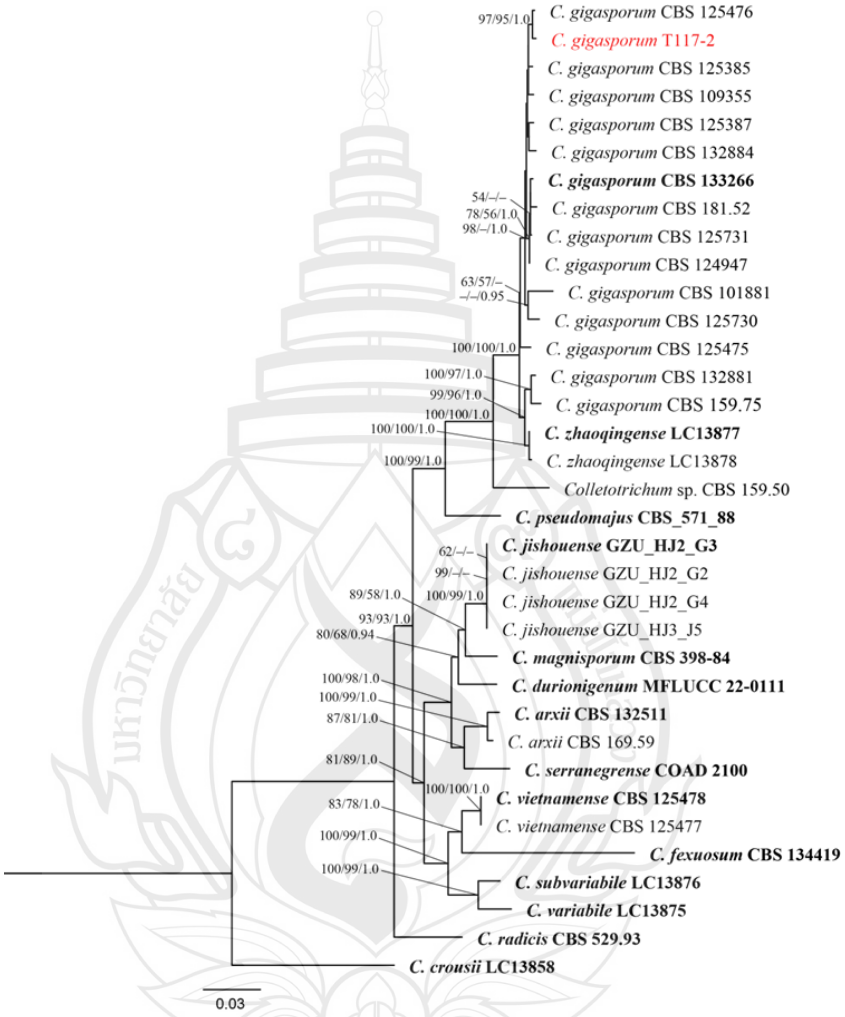

Note Maximum likelihood and maximum parsimony bootstrap support values ≥ 50% as well as bayesian posterior probabilities ≥ 0.90 are shown near the nodes, respectively. The tree is rooted with *Colletotrichum crousii* (LC13858). Isolates from this study are in red, and ex-type strains are in bold

Figure 8.8 Maximum likelihood (ML) tree of *Colletotrichum gigasporum* species complex based on the combined ITS, *gapdh*, *chs-1*, *act*, *tub2* sequence dataset

Colletotrichum guajavae Damm, P.F. Cannon & Crous (2012)

Figure 8.9

Index Fungorum: IF 800501; Facesoffungi: FoF 17009

Description: See Damm et al. (2022)

Material examined: Thailand, Chiang Rai Province, Mueang Chiang Rai District, Tha Sud, on fruit of *Mangifera indica* (Anacardiaceae), 1 February 2022, A. Armand, A20-2 (MFLU 24-0425; MFLUCC 24-0358, living culture).

Notes: *Colletotrichum guajavae* was identified by Damm et al. (2012) from *Psidium guajava* in India. The single strain of *Colletotrichum guajavae* A20-2 (MFLUCC 24-0358) exhibited similar morphological characteristics with the type strain of *C. guajavae* (IMI 350839, ex-type). However, *C. guajavae* (A20-2) is distinguished from *C. guajavae* (IMI 350839) by producing smaller conidiophores (15–25 in *C. guajavae* (A20-2) *vs.* to 30 μm long in the ex-type of *C. guajavae*), and shorter conidiogenous cells (11–17 μm in A20-2 vs. 7–19 μm in the ex-type). The strain A20-2 produces cylindrical conidia with an acute base and round apex, while *C. guajavae* (IMI 350839) produces cylindrical to fusiform conidia with acute ends (Damm et al., 2012). There are only 7 bp polymorphisms between the ex-type strain and A20-2; 2/531 bp (0.3%) in ITS, 4/215 bp (1.8%) in *gapdh*, and 1/204 bp (0.5%) in *act*. Therefore, based on morphological characteristics and phylogenetic study (Figure 8.10), the strain was identified as *Colletotrichum guajavae*. This is the first report of *C. guajavae* infesting mangoes worldwide.

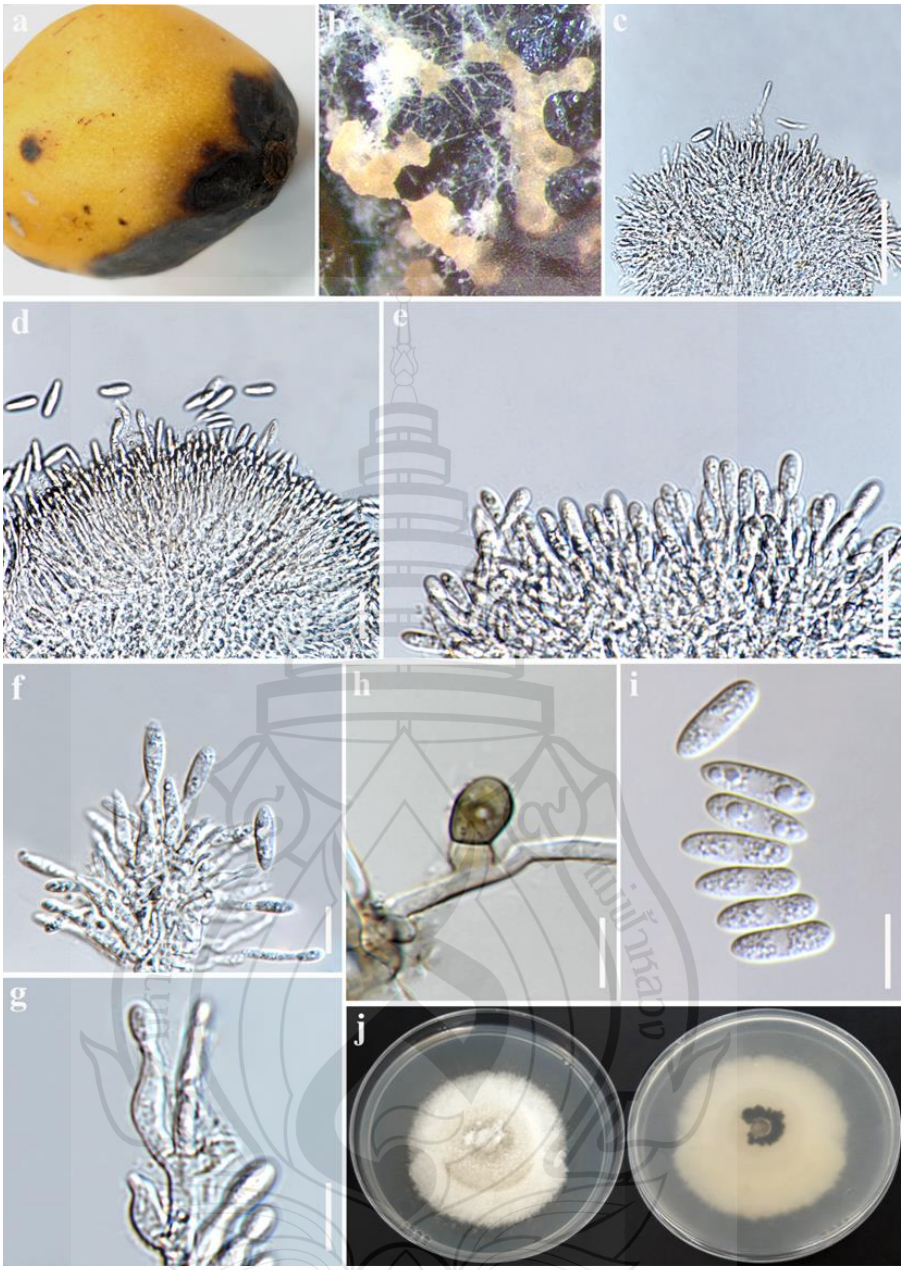

Note **a**. Infested fruit **b**. Fruiting bodies produced on the fruit surface **c**–**e**. Mass of conidiophores and conidia **f**, **g**. Conidiophores and conidial attachment **h**. Appressorium **i**. Conidia **j**. Upper and reverse view of colonies on PDA; Scale bars: **a** = 500 µm, **b** = 250 µm, **c** = 50 µm, **d**, **e** = 20 µm, **f**–**i** = 10 µm

Figure 8.9 *Colletotrichum guajavae* (MFLU 24-0425)

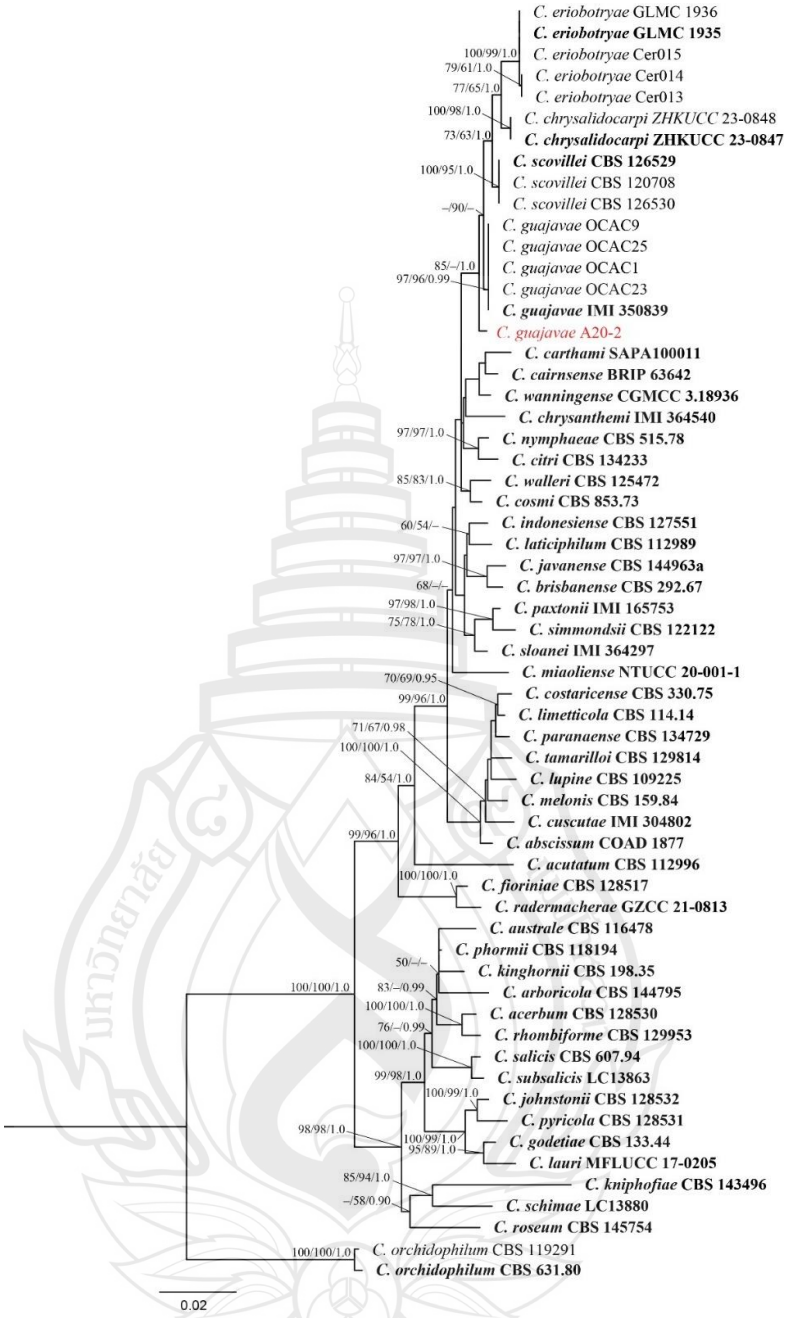

Note Maximum likelihood and maximum parsimony bootstrap support values ≥ 50% as well as bayesian posterior probabilities ≥ 0.90 are shown near the nodes, respectively. The tree is rooted with *Colletotrichum orchidophilum* (CBS 631.80) and *Colletotrichum orchidophilum* (CBS 119291). Isolates from this study are in red, and ex-type strains are in bold

Figure 8.10 Maximum likelihood (ML) tree of *Colletotrichum acutatum* species complex based on the combined ITS, *gapdh*, *chs-1*, *act*, *tub2* sequence dataset

Colletotrichum musae (Berk. & M.A. Curtis) Arx 1957

Figure 8.11

Index Fungorum: IF 295348; Facesoffungi: FoF 16992

Description: See Su et al. (2011); Samarakoon et al (2024)

Material examined: Thailand, Chiang Rai Province, Mueang Chiang Rai District, Phat Thai market, on fruit of *Mangifera indica* (Anacardiaceae), 20 June 2022, A. Armand, R50 (MFLU 24-0426; MFLUCC 24-0359, living culture).

Notes: *Colletotrichum musae* is a common agent of post-harvest disease in bananas (Balendres et al., 2020; Su et al., 2011; Udayanga et al., 2013; Weir et al., 2012). However, Li et al. (2019) reported this species involved in mango disease from China. Using the morphological and molecular approaches, this investigation reports *C. musae* as a causal agent of mango fruit anthracnose, reported for the first time from Thailand. A single strain clustered with the ex-type strain with 100%/100%/1.00 (ML/MP/PP) support support (Figure 8.7). Morphologically, it resembled *C. musae* (CBS 116870), epitypified by Su et al. (2011).

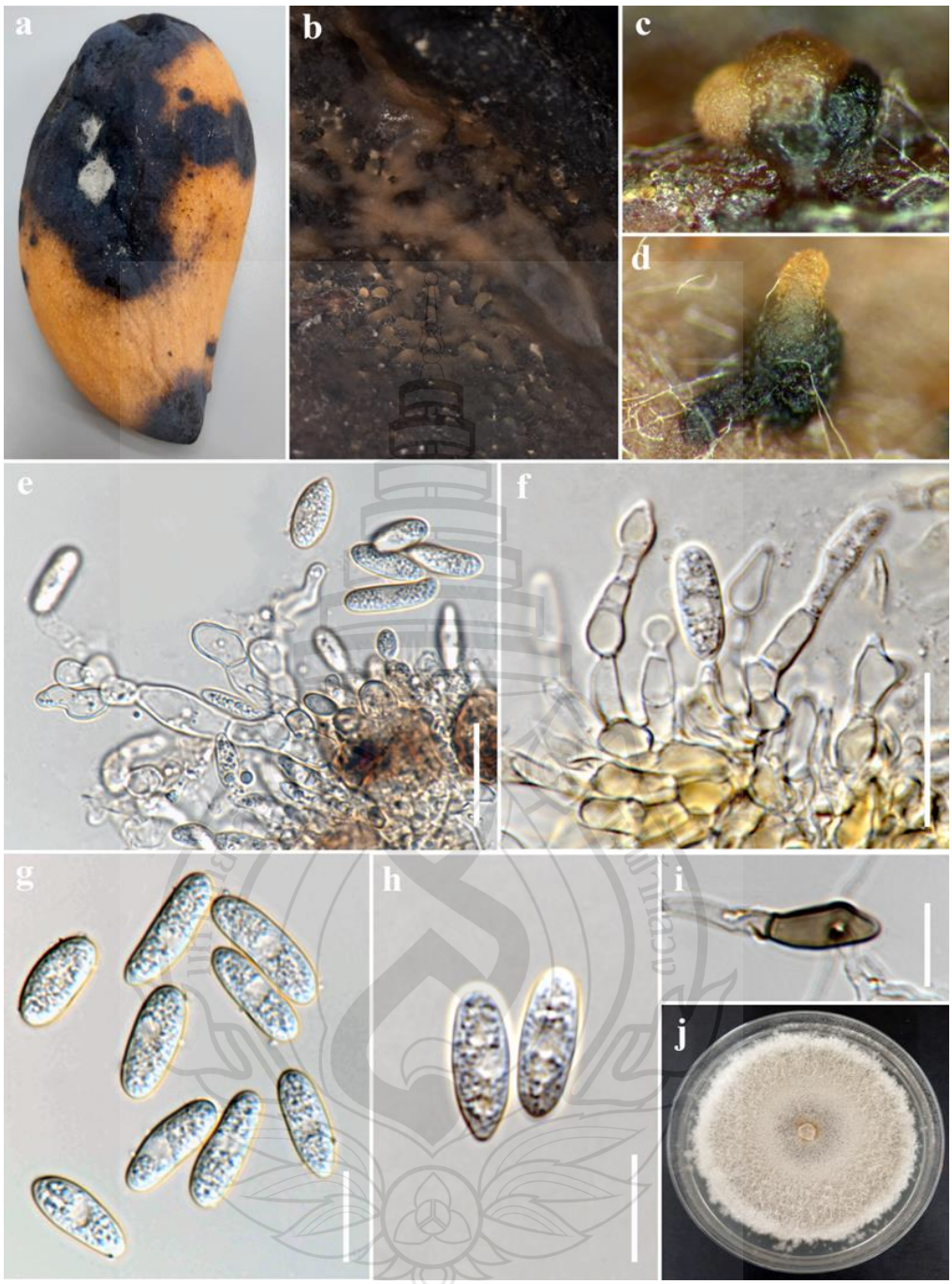

Note **a**. Infested fruit **b**. Conidial masses on the fruit surface **c**, **d**. Fruiting bodies produced on WA **e**, **g**. Conidiophores and conidia formed on natural substrate **f**, **h**. Conidiophores and conidia formed on WA **i**. Appressorium **j**. Upper view of colonies on PDA; Scale bars: **e**, **f** = 20 µm, **g**–**i** = 10 µm

Figure 8.11 *Colletotrichum musae* (MFLU 24-0426)

Colletotrichum plurivorum Damm, Alizadeh & Toy. Sato (2018)

Figure 8.12

Index Fungorum: IF 824228; Facesoffungi: FoF 10691

Material examined: Thailand, Chiang Rai Province, Mueang Chiang Rai District, Mae Fah Luang University Campus, on leaves of *Mangifera indica* (Anacardiaceae), 26 April 2023, A. Armand, AS-1 (MFLU 24-0427; MFLUCC 24-0360, living culture); Thailand, Chiang Rai Province, Mueang Chiang Rai District, Mae Fah Luang University Campus, on leaves of *Mangifera indica* (Anacardiaceae), 26 April 2023, A. Armand, AS-2 (MFLUCC 24-0361, living culture).

Notes: Based on the phylogenetic analysis of a combined dataset of ITS, *gapdh*, *chs-1*, *act*, and *tub2*, three strains clustered with the ex-type strain of *C. plurivorum*, showing 98%/95%/1.00 (ML, MP, PP) support values (Figure 8.13). Morphologically, the strains were similar and resembled the type strain of *C. plurivorum* (Damm et al., 2019). However, pairwise comparison showed nucleotide differences with the ex-type strain as follows: AS-1 (1/464 bp (0.2%) in ITS, 1/250 bp (0.4%) in *chs-1*, 2/224 bp (0.9%) in *act*, 3/468 bp (6.4%) in *tub2*), AS-2 (1/224 bp (0.44%) in *act*, 1/468 bp (0.2%) in *tub2*), T117 (1 bp in ITS, 2/197 bp (1.0%) in *gapdh*, 1/250 bp (0.4%) in *chs-1*, 3/224 bp (1.3%) in *act*, 2/468 bp (0.4%) in *tub2*). There is only one report of *Colletotrichum plurivorum* associated with mangoes recorded from Brazil (Damm et al., 2019). This study illustrated *C. plurivorum* occurrence on mango leaves using morphological characterisation and multi-gene phylogenetic analysis. This is the first report of *C. plurivorum* associated with mango anthracnose from Thailand.

Note **a**. Infested leaf **b**, **c**. Fruiting bodies produced on the leaf **d**, **e**. Setae and conidiogenous cells **f**. Conidia **g**. Upper view of colonies on PDA; Scale bars: **d** = 50 µm, **e**–**f** = 20 µm

Figure 8.12 *Colletotrichum plurivorum* (MFLU 24-0427)

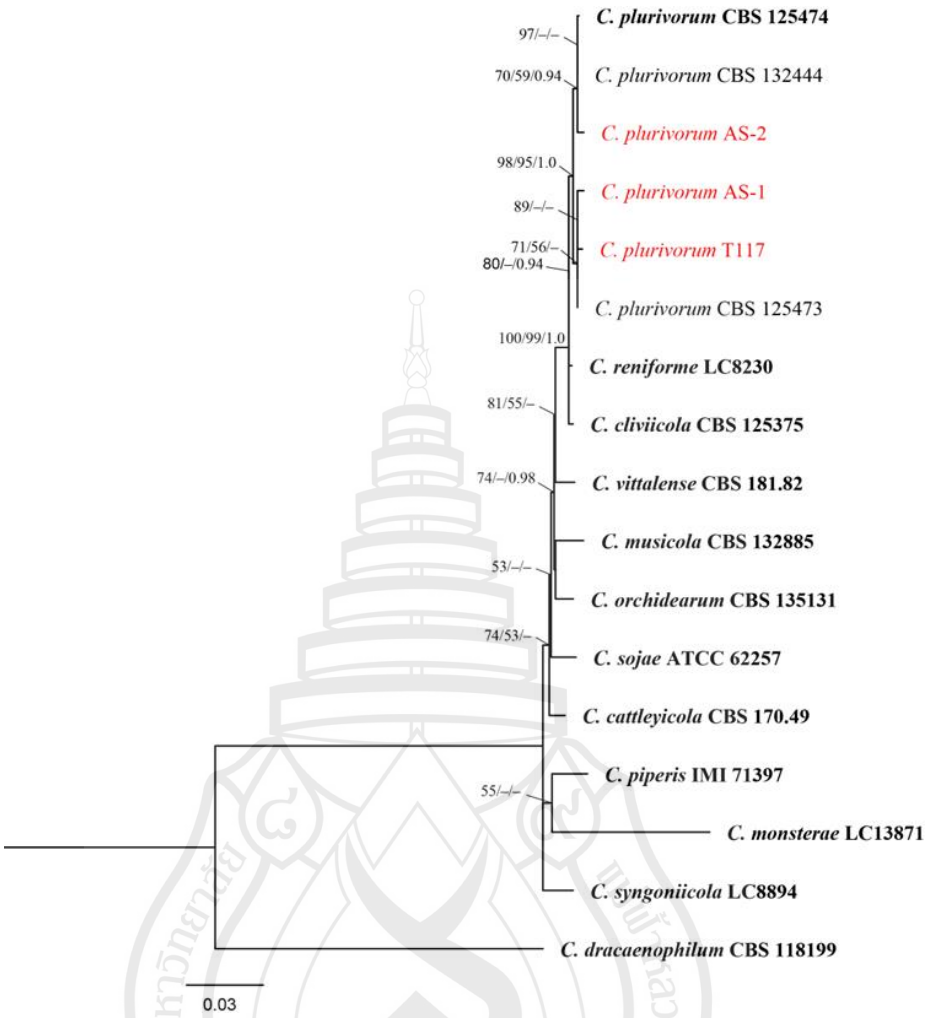

Note Maximum likelihood and maximum parsimony bootstrap support values ≥ 50% as well as bayesian posterior probabilities ≥ 0.90 are shown near the nodes, respectively. The tree is rooted with *Colletotrichum dracaenophilum* (CBS 118199). Isolates from this study are in red, and ex-type strains are in bold

Figure 8.13 Maximum Likelihood (ML) tree of *Colletotrichum orchidearum* species complex based on the combined ITS, *gapdh*, *chs-1*, *act*, *tub2* sequence dataset

Colletotrichum siamense Prihast., L. Cai & K.D. Hyde (2009)

Figure 8.14

Index Fungorum: IF 515410; Facesoffungi: FoF 03599

Description: See Prihastuti et al. (2009)

Material examined: Thailand, Chiang Rai Province, Mueang Chiang Rai District, Mae Fah Luang University Campus, on fruit of *Mangifera indica*

(Anacardiaceae), 30 May 2022, Armand A., P25 (MFLU 24-0428; MFLUCC 24-0363, living culture); Thailand, Chiang Rai Province, Mueang Chiang Rai District, Mae Fah Luang University Campus, on leaves of *Mangifera indica* (Anacardiaceae), 21 May 2022, A. Armand, C51-2 (MFLUCC 24-0364, living culture); Thailand, Chiang Rai Province, Mueang Chiang Rai District, Doi Hang, on leaves of *Mangifera indica* (Anacardiaceae), 10 December 2022, M. Fallahi, MF24-5 (MFLUCC 24-0365, living culture).

Notes: *Colletotrichum siamense* is a broad-host-range species within *C. gloeosporioides* species complex (Talhinhas & Baroncelli, 2021). This species has been isolated from mango in Australia (Giblin et al., 2018), Brazil (Jayawardena et al., 2016), China (Li et al., 2019; Liu et al., 2017; Mo et al., 2018), Colombia (Pardo-De la Hoz et al., 2016), Ghana (Honger et al., 2014), Mexico (Fuentes-Aragón et al., 2020b; Tovar-Pedraza et al., 2020), Sri Lanka (Adikaram et al., 2020), and Thailand (Jayawardena et al., 2022; Rattanakreetakul et al., 2023). In the current study, three isolates were identified as *C. siamense* using morphological and molecular analyses, isolated from mango leaves and fruits. The isolates grouped with the ex-type with 51% /–/– (ML/MP/PP) (Fig. 8. 7). Morphological comparison with the type strain showed no morphological differences (Prihastuti et al. 2009). However, the strains showed nucleotide differences with the ex-type strain as follows: P25 (3/537 bp (0.5%) in ITS, 4/259 bp (1.5%) in *act*); C51-2 (3/534 bp (0.5%) in ITS, 3/228 bp (1.3%) in *act*, 3/231 bp (1.3%) in *chs-1*, 3/228 bp (1.3%) in *gapdh*); MF24-5 (3/534 bp (0.5%) in ITS, 2/208 bp (0.9%) in *act*, 3/233 bp (1.3%) in *chs-1*, 4/224 bp (1.8%) in *gapdh*).

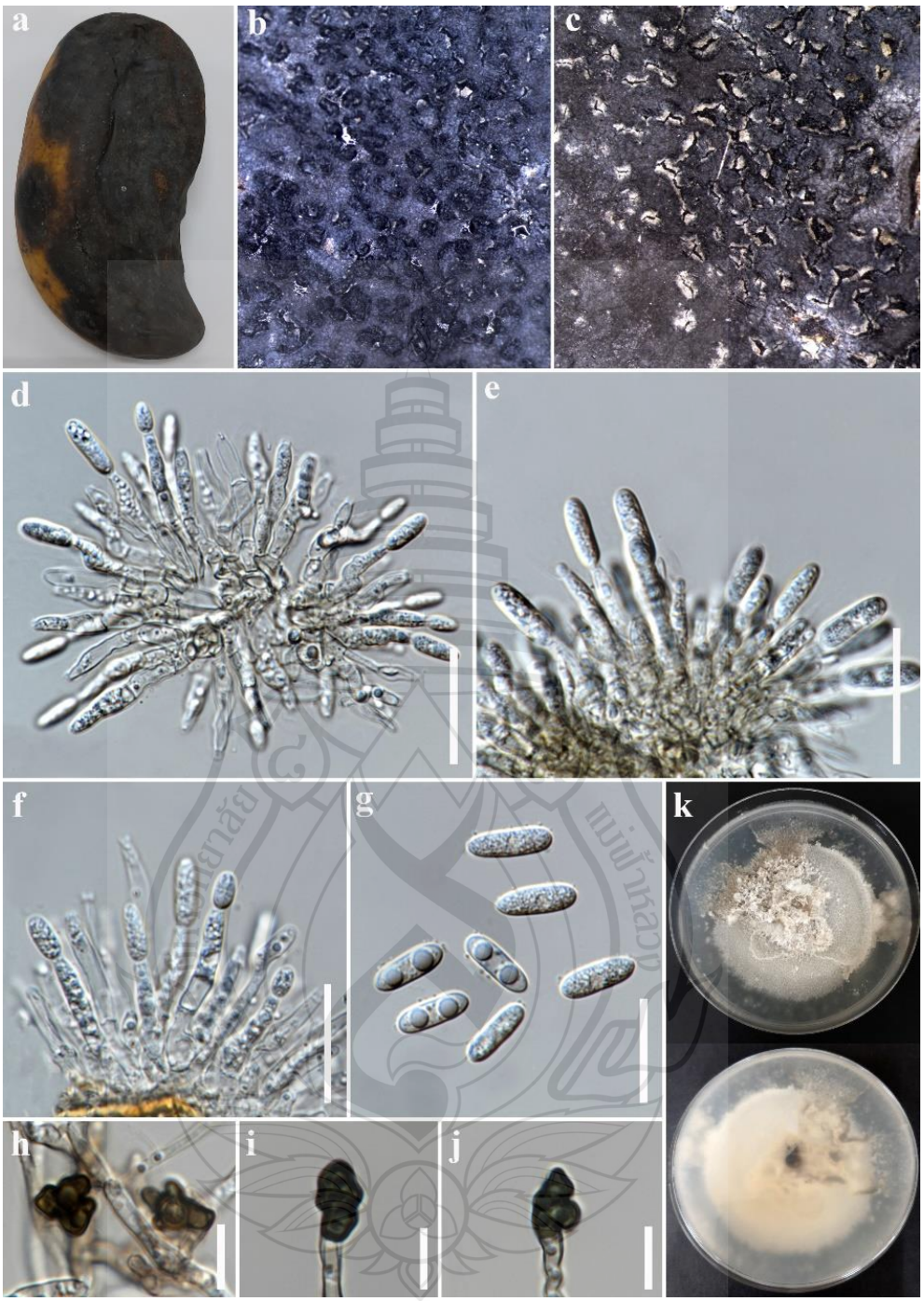

Note **a**. Infested fruit **b**, **c**. Fruiting bodies produced on the fruit surface **d**–**f**. Conidiophores and conidial attachment **g**. Conidia **h**–**j**. Appressoria **k**. Upper and reverse view of colonies on PDA; Scale bars: **d**, **e** = 25 µm, **f**, **g** = 20 µm, **h**–**j** = 10 µm

Figure 8.14 *Colletotrichum siamense* (MFLU 24-0428)

Diaporthe Nitschke, Fungi rhenani exsic., suppl., fasc. 5: no. 1988 (1867)

Diaporthe, the type genus of the family Diaporthaceae, was described by Nitschke in 1867. Species within this genus are known to exist as pathogens, endophytes, and saprobes across various host plants and regions (Dissanayake et al., 2017; Jayawardena et al., 2021a; Norphanphoun et al., 2023; Udayanga et al., 2011). Pathogenic species of *Diaporthe* have been implicated in infections of numerous economically important crops, causing significant yield losses (Manawasinghe et al., 2019). These pathogens are associated with a wide range of diseases, including blights, fruit and root rots, cankers, diebacks, wilts, and leaf spots (Jayawardena et al., 2021a).

Diaporthe arecae (H.C. Srivast., Zakia & Govindar.) R.R. Gomes, Glienke & Crous (2013)

Figure 8.15

Index Fungorum: IF 802924; Facesoffungi: FoF 08405

Description: See Gomes et al. (2013)

Material examined: Thailand, Kalasin Province, Kuchinarai District, Nong Hang; on leaves of *Mangifera indica* (Anacardiaceae), 20 February 2023, M. Fallahi, MF172-2 (MFLU 24-0429; MFLUCC 24-0366, living culture).

Notes: Three strains were clustered with different species within *Diaporthe arecae* species complex (Figure 8.16). The clade A (Figure 8.16) representing *Diaporthe arecae* species complex, was recently considered as a single species, *Diaporthe arecae* (Dissanayake et al., 2024). Therefore, the three strains were identified as *D. arecae*.

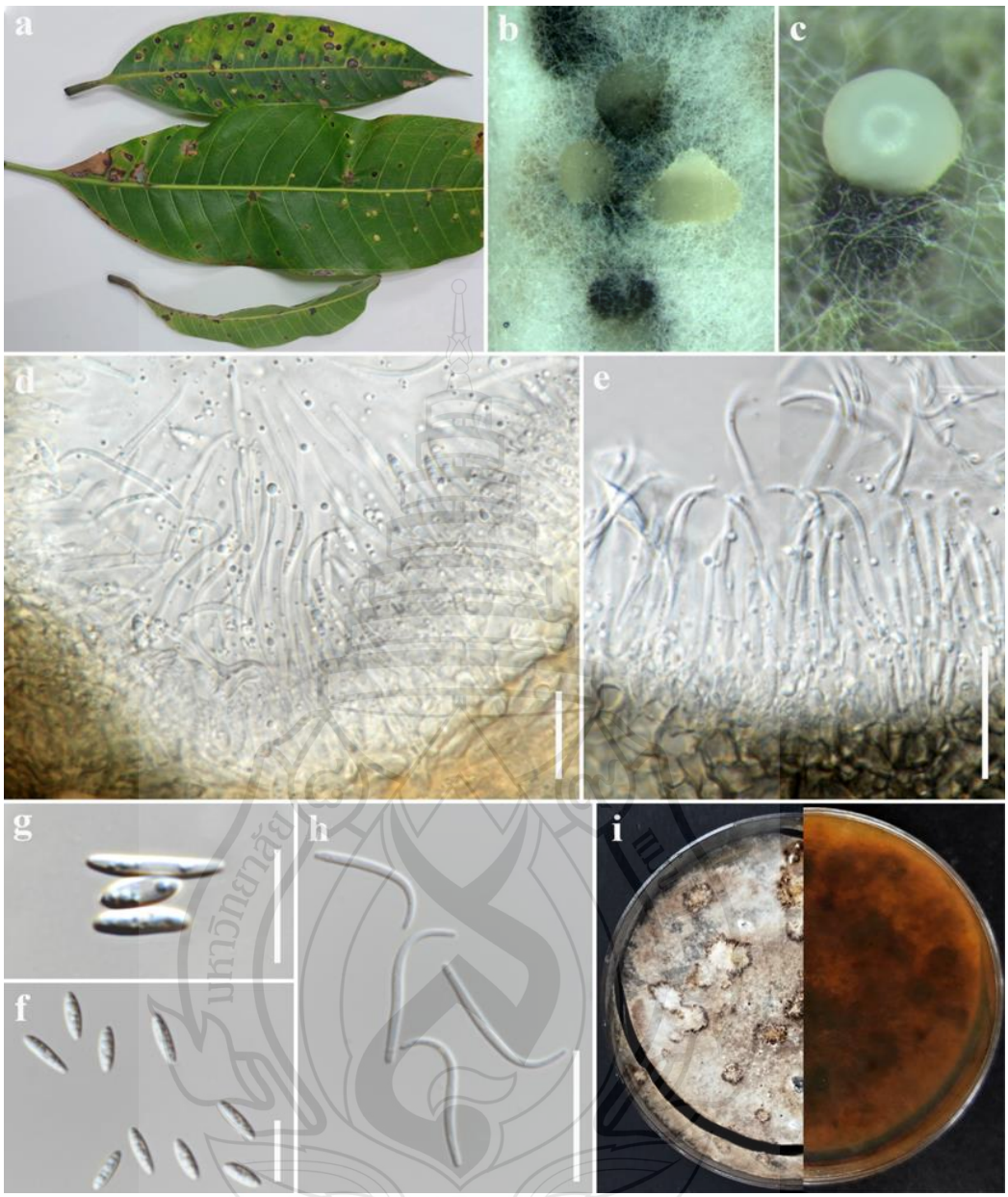

Note **a**. Symptomatic leaves **b**, **c**. Fruiting bodies and conidial mass produced on CLA (Carnation Leaf Agar) **d**, **e**. Cross section of pycnidium with conidiogenous cells and conidia inside **f**. Alpha conidia g. Alpha and gamma conidia **h**. Beta conidia **i**. Upper and reverse view of colonies on PDA; Scale bars: **d**, **e** = 20 µm, **f**, **g** = 10 µm, **h** = 20 µm

Figure 8.15 *Diaporthe arecae* (MFLU 24-0429)

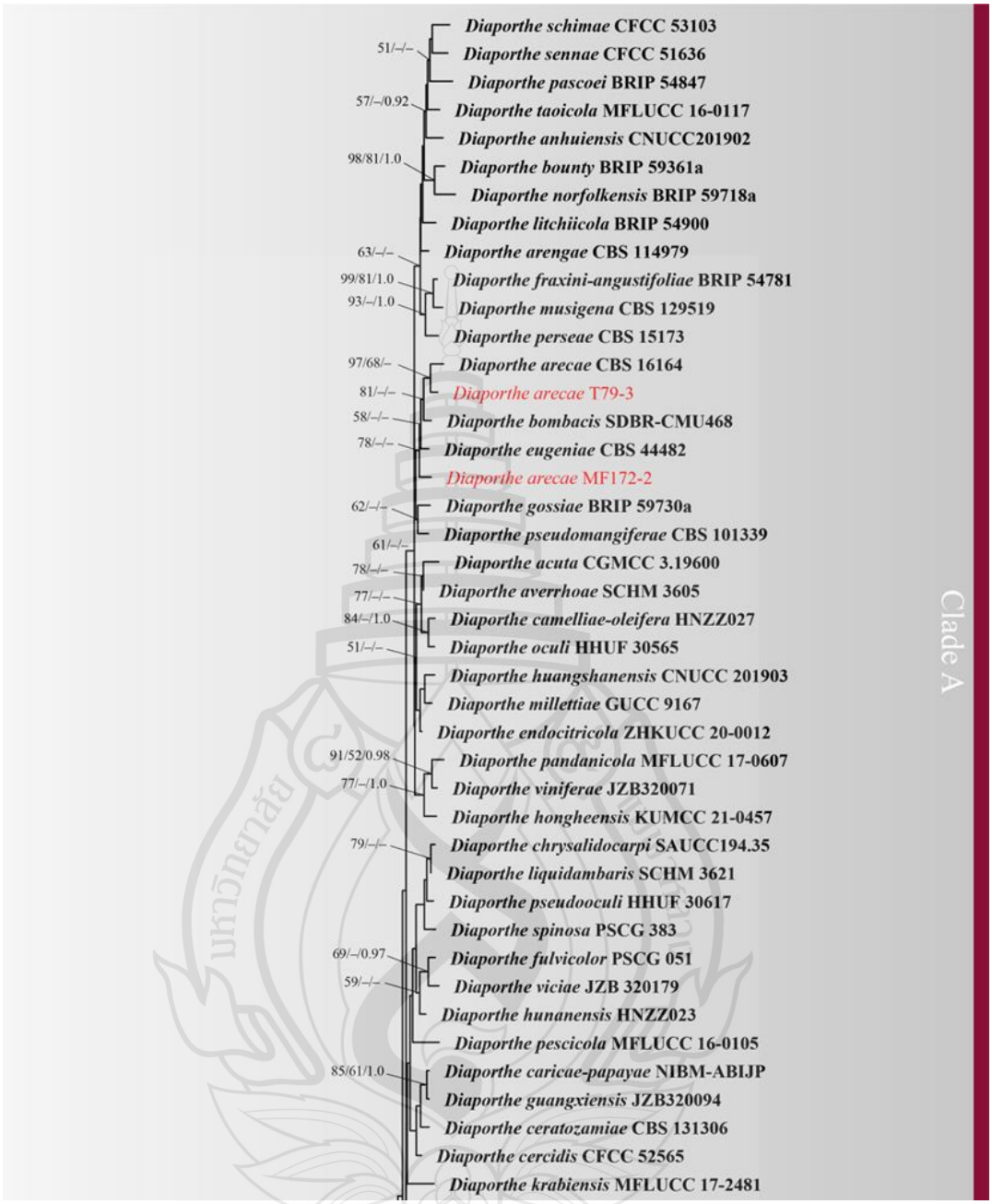

Note Maximum likelihood and maximum parsimony support values ≥ 50%, and bayesian posterior probabilities ≥ 0.90 are shown near the nodes, respectively. The tree is rooted with Diaporthella corylina (CBS 121124). Isolates from this study are in red, and ex-type strains are in bold.

Figure 8.16 Maximum likelihood (ML) tree of *Diaporthe arecae*, *D. longicolla*, *D. siamensis*, and *D. sojae* species complexes based on the combined ITS, *EF1-α*, *tub2*, *cmdA*, and *his3* sequence dataset

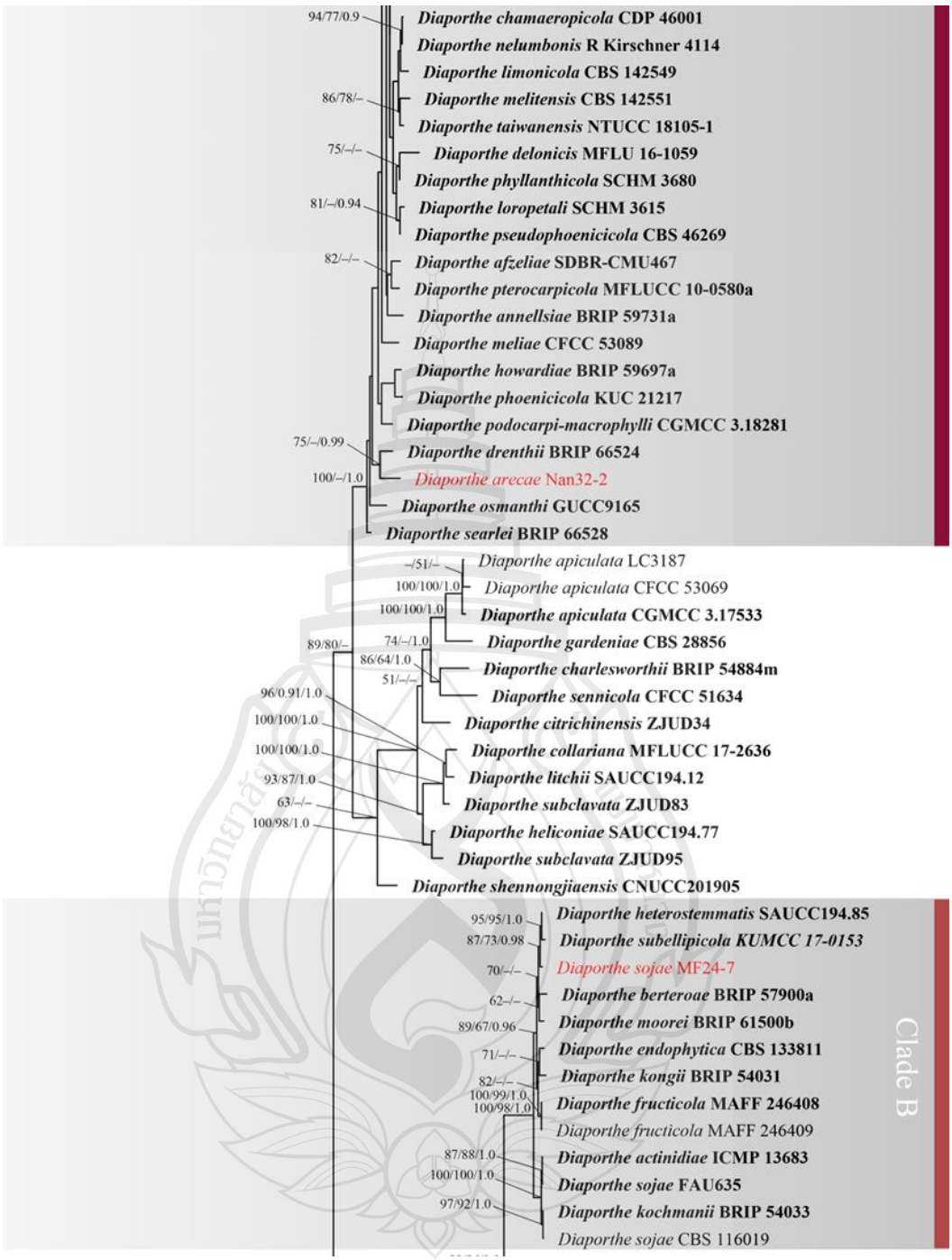

Figure 8.16 (continued)

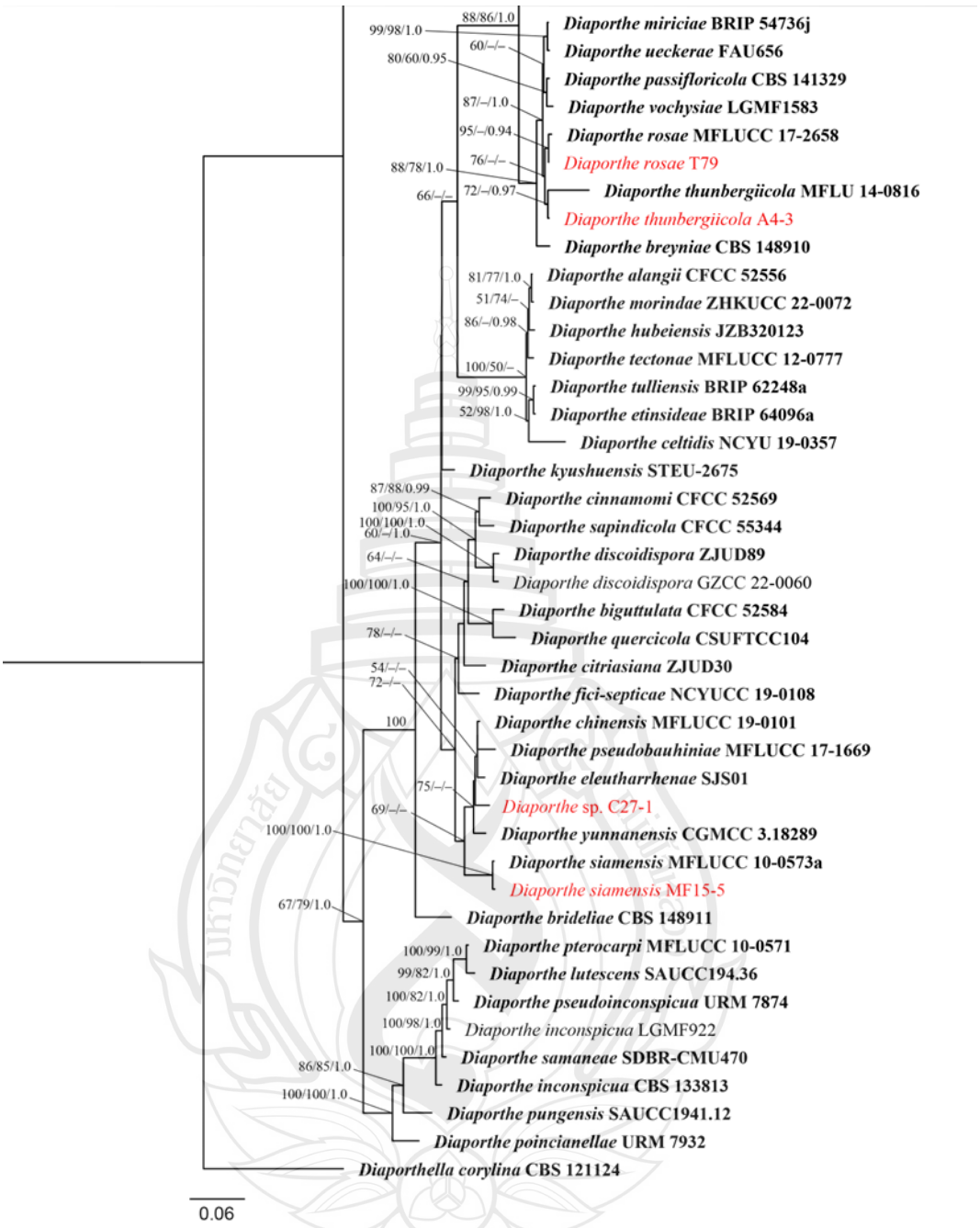

Figure 8.16 (continued)

Diaporthe rosae Samarak. & K.D. Hyde (2018)

Figure 8.17

Index Fungorum: IF 554072; Facesoffungi: FoF 03922

Description: See Wanasinghe et al. (2018)

Material examined: Thailand, Chiang Rai Province, Phan District, Mae Ao, Ang Kep Nam Huai Tonyang Reservoir; on leaves of *Mangifera indica* (Anacardiaceae), 27 September 2021, A. Armand, T79 (MFLU 24-0430; MFLUCC 24-0369, living culture).

Notes: A single strain was grouped with the type strain of *Diaporthe rosae*, showing 95%/0.94 (ML/PP) support values (Figure 8.16). Morphologically, the newly isolated strain was similar to the ex-type strain of *D. rosae* in terms of conidiogenous cells and alpha conidia (Wanasinghe et al., 2018). However, our strain did not produce beta and gamma conidia on the host nor CLA (Carnation Leaf Agar). The strain exhibited 1/436 (0.2%) nucleotide polymorphisms in ITS and 2/230 (0.6%) in *tef1-α* with the ex-type strain. The *cmdA* and *his3* are not available for the ex-type strain, and no differences were detected in the *tub2* region. To date, there is no report of *D. rosae* from mango, and this is the first report of occurring *D. rosae* on mango worldwide, causing leaf blight. This species was also reported from rambutan (*Nephelium lappaceum* L.) in Thailand (Huanraluek et al., 2022).

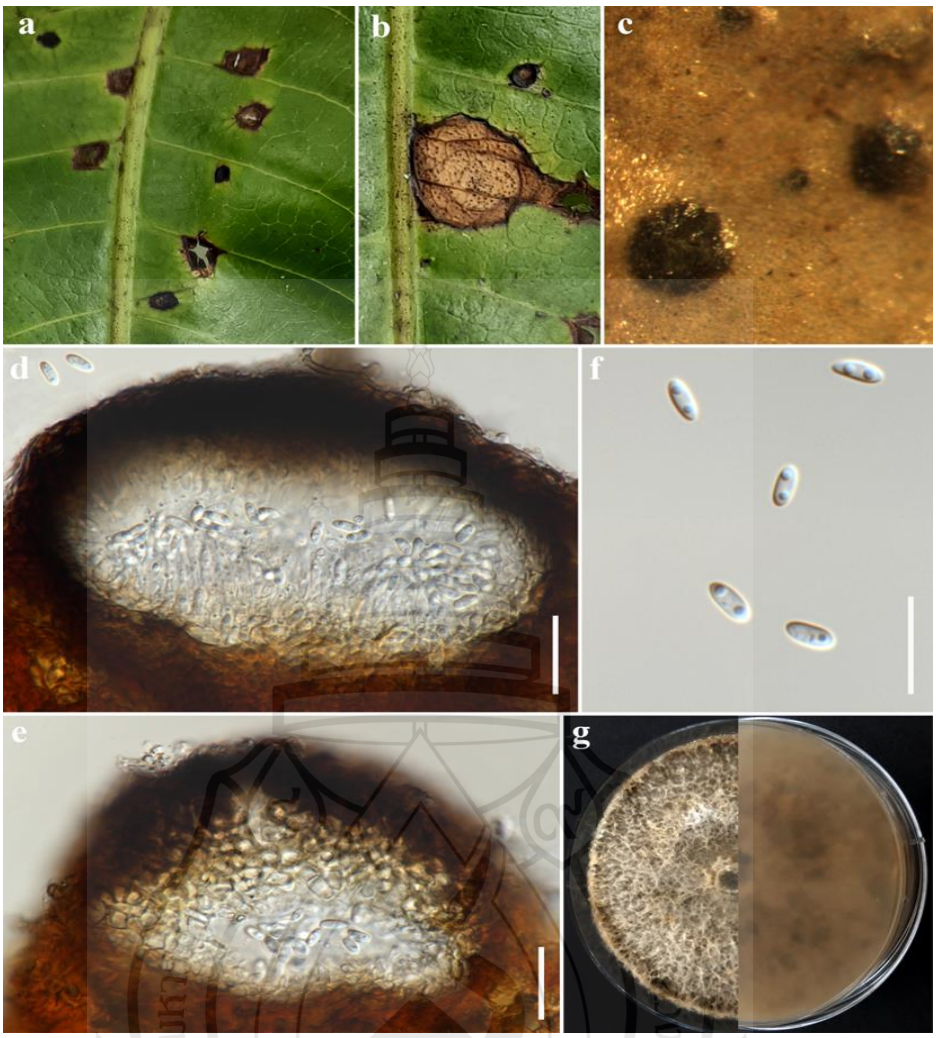

Note **a**, **b**. Symptomatic leaves **c**. Fruiting bodies produced on the leaf **d**, **e**. Cross section of pycnidia **f**. Alpha conidia **g**. Upper and reverse view of colonies on PDA; Scale bars: **d**, **e** = 20 µm, **e**, **f** = 10 µm

Figure 8.17 *Diaporthe rosae* (MFLU 20-0430)

Diaporthe siamensis Udayanga, Xing Z. Liu & K.D. Hyde (2012)

Index Fungorum: IF 800826; Facesoffungi: FoF 02398

Description: See Udayanga et al. (2012)

Material examined: Thailand, Chiang Rai Province, Mueang Chiang Rai District, Ban Du; on leaves of *Mangifera indica* (Anacardiaceae), 10 December 2022, M. Fallahi, MF15-5 (MFLU 24-0431; MFLUCC 24-0370, living culture).

Notes: *Diaporthe siamensis* is recognised for its broad host range and widespread distribution, particularly in tropical and subtropical regions, reported on various hosts,

including woody and herbaceous plants (Gomes et al., 2013). However, this species has not been reported on mango. The current study isolated and identified *D. siamensis* infesting mango leaves for the first time worldwide. The single strain MF15-5 (MFLUCC 24-0370) clustered together with the ex-type strain of *D. siamensis* with 100%/100%/1.00 (ML/MP/PP) support values (Figure 8.16). The strain showed 3/318 bp (0.9%) differences in *tef1-α*, 1/343 bp (0.3%) in *tub2*, and 1/467 bp (0.2%) in *cmdA*. The *his3* is not available for the ex-type strain, and there were no differences in the ITS region between our strain and ex-type strain. Morphological comparison was not feasible as our strain remained sterile on PDA and CLA media. To our knowledge, this is the first report of *Diaporthe siamensis* isolated from mango worldwide.

Diaporthe sojae Lehman 1923

Figure 8.18

Index Fungorum: IF 278338; Facesoffungi: FoF 06582

Description: See Lehman (1923)

Material examined: Thailand, Chiang Rai Province, Mueang Chiang Rai District, Ban Du; on leaves of *Mangifera indica* (Anacardiaceae), 10 December 2022, M. Fallahi, MF24-7 (MFLU 24-0432; MFLUCC 24-0371, living culture).

Notes: *Diaporthe subellipicola* was isolated from a non-living wood in China (Hyde et al., 2018c). It has been illustrated with its sexual morph, and the asexual morph was not observed in the original illustration. Sun et al. (2021) have introduced *Diaporthe heterostemmatis* from *Heterostemma grandiflorum* by its asexual morph in China, as sister clade of *D. subellipicola*. According to the multi-locus phylogenetic tree (Figure 8.16), the single strain MF24-7 (MFLUCC 24-0371) made a separate lineage, clustering as a sister lineage to *D. subellipicola* (KUMCC 17-0153) and *D. heterostemmatis* (SAUCC 194.85). However, all species in the clade B in the phylogenetic tree (Figure 8.16) representing *D. sojae* species complex, were recently considered as a single species, *Diaporthe sojae* (Dissanayake et al., 2024). Therefore, the strain MF24-7 was identified as *D. sojae*.

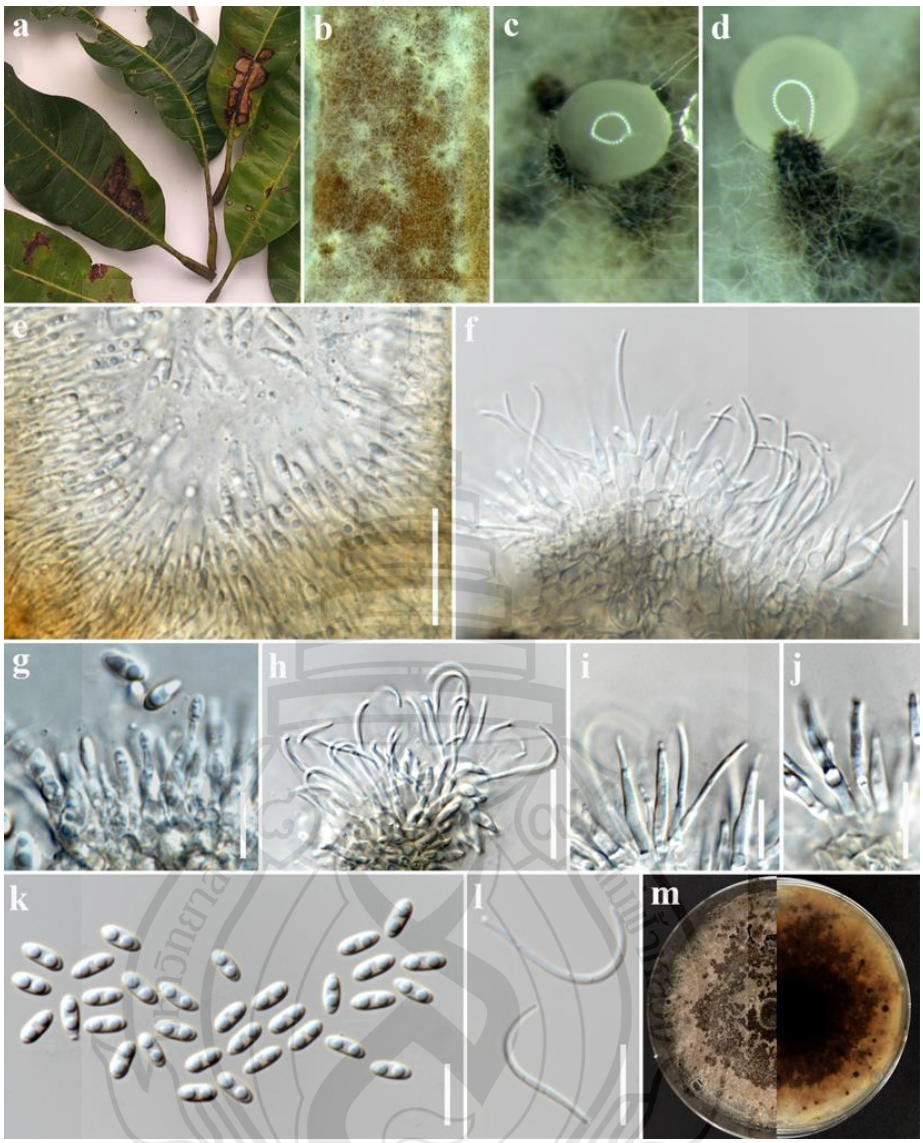

Note **a**. Symptomatic leaves **b**. Fruiting bodies produced on the CLA **c**, **d**. Pycnidia with conidial drop mass **e**. Cross section of pycnidium **f**–**j**. Conidiogenous cells **k**. Alpha conidia **l**. Beta conidia **m**. Upper and reverse view of colonies on PDA; Scale bars: **e**, **f** = 20 µm**, g** = 10 µm, **h** = 20 µm, **i**–**l**. 10 µm

Figure 8.18 *Diaporthe sojae* (MFLU 24-0432)

Diaporthe sp.

Figure 8.19

Pathogenic on mango leaves. Sexual morph: not observed. Asexual morph: *Conidiomata* pycnidial, subglobose or globose, dark brown to black, semi-immersed, erumpent, solitary, scattered on host leaf, *Conidiophores* hyaline, smooth, septate,

simple, densely aggregated, cylindrical, straight to flexuous, 10–13 × 1.7–2 µm. *Conidiogenous cells*, cylindrical, rarely ampuliform, phialidic, straight or flexuous, 5–9 × 1.8–2 µm. *Alpha conidia* abundant, hyaline, smooth, aseptate, bi-guttulate, one at each end, ellipsoid, rarely slightly curved, 5.2–6.5 × 2–2.8 µm ($\bar{x}$ = 5.7 × 2.3 µm, n = 30). *Beta conidia* and *gamma conidia* not observed.

Culture characteristics: Colonies on PDA reach 83–90 mm in diam. after 7 days at 25 ± 2 °C. Aerial mycelia feathery, white to pale grey on surface, becoming olivaceous black in age, same color on reverse.

Material examined: Thailand, Chiang Rai Province, Mueang Chiang Rai District, Mae Fah Luang University Campus, on leaves of *Mangifera indica* (Anacardiaceae), 12 December 2021, A. Armand, C27-1 (MFLU 24-0433, MFLUCC 24-0372R, living culture).

Notes: According to the phylogenetic tree based on the concatenated dataset (ITS + *tef1-α* + *tub2* + *cmdA* + *his3*), the strain C27-1 (MFLUCC 24-0372R) clustered within a clade containing the species *Diaporthe chinensis*, *D. pseudobauhiniae* (= *D. chiangraiensis*; Hongsanan et al., 2023), *D. eleutharrhenae*, and *D. yunnanensis*, with 75% ML bootstrap support. However, MP and PP analyses did not provide acceptable support for this clade (Figure 8.16). The two species which are closely related to our strain, *D. pseudobauhiniae* and *D. eleutharrhenae*, were also positioned within this clade but without strong bootstrap support. Additionally, no sequences are available for the type strain of *D. pseudobauhiniae* in the *tub2*, *cmdA*, and *his3* regions, and for *D. eleutharrhenae* in the *cmdA* and *his3* loci. Amplification of the *tef1-α* region for our strain also failed, making it difficult to confirm C27-1 as a new taxon. Nevertheless, strain C27-1 exhibited 1/436 bp (0.2%) nucleotide difference in ITS and 12/343 bp (3.5%) in *tub2* compared to *D. eleutharrhenae*. It also showed 6/435 bp (0.2%) polymorphisms in ITS compared to *D. pseudobauhiniae*, although other gene regions could not be compared due to the lack of data. Morphological comparison with *D. pseudobauhiniae* (= *Chiangraiomyces bauhiniae*) is not feasible, as it was illustrated by its sexual morph, and the asexual morph was represented only by beta conidia (Senanayake et al., 2017), whereas our strain (C27-1) did not produce beta and gamma conidia. Therefore, we refrain from introducing this strain as a new species, pending

further sample collection and amplification to improve the certainty of its placement within the clade.

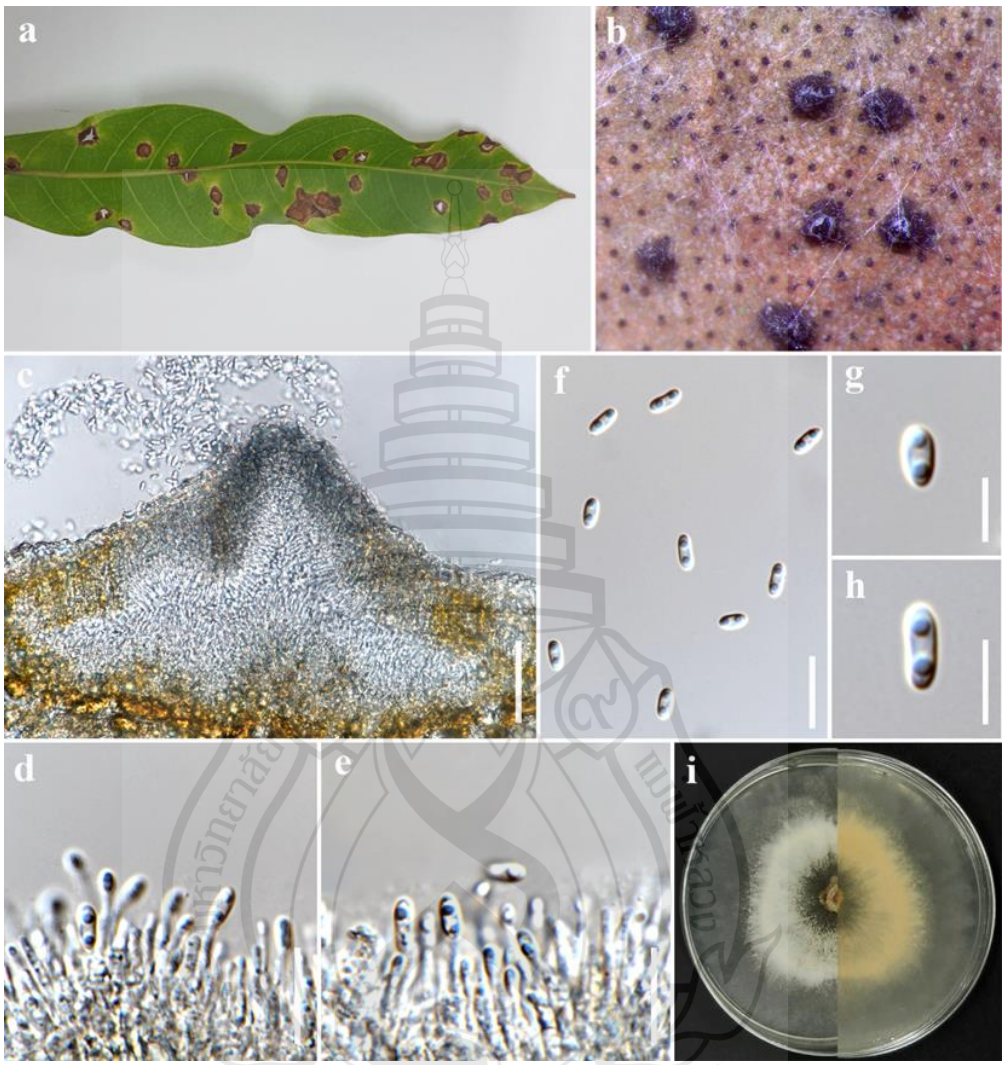

Note **a**. Symptomatic leaf **b**. Fruiting bodies produced on the leaf **c**. Cross section of pycnidia **d**, **e**. Conidiogenous cells and conidia **f–h**. Alpha conidia **i**. Upper and reverse view of colonies on PDA; Scale bars: **c** = 20 µm, **d–f** = 10 µm, **g**–**h** = 5 µm

Figure 8.19 *Diaporthe* sp. (MFLU 24-0433)

Diaporthe thunbergiicola Udayanga & K.D. Hyde (2015)

Figure 8.20

Index Fungorum: IF 551072; Facesoffungi: FoF 00472

Description: See Liu J. et al. (2015)

Material examined: Thailand, Chiang Rai Province, Mueang Chiang Rai District, Tha Sud, on leaves of *Mangifera indica* (Anacardiaceae), 16 October 2021, A. Armand, A4-3 (MFLU 24-0434; MFLUCC 24-0373, ex-type living culture).

Notes: In the phylogenetic tree resulting from the five-locus analysis, one strain clustered with the ex-type strain of *Diaporthe thunbergiicola*, supported by 72% ML and 0.97 PP values (Figure 8.16). *Diaporthe thunbergiicola* was originally described by Liu J. et al. (2015) based on ITS and *tef1-α* phylogenies as well as morphological characteristics. Morphologically, the strain differs from the ex-holotype of *D. thunbergiicola* by producing rare alpha conidia, which are smaller than those of *D. thunbergiicola* (5–6.5 μm long in strain A4-3 vs. 5.7–7.5 μm long in *D. thunbergiicola*). Additionally, beta conidia were not produced by the ex-holotype of *D. thunbergiicola*, whereas our strain produced abundant beta conidia (Figure 8.20). Pairwise nucleotide comparison between strain A4-3 and the ex-type strain of *D. thunbergiicola* revealed 7/436 bp (1.6%) differences in ITS, while sequences for *tub2*, *cmdA*, and *his3* were not available for *D. thunbergiicola*. However, *Diaporthe thunbergiicola* has been shown as a species with a high intraspecific variation, and many species were considered as synonyms of *D. thunbergiicola* (Dissanayake et al. 2024). Therefore, the strain A4-3 (MFLUCC 24-0373) was identified as *D. thunbergiicola* herein. To our knowledge, this is the first report of *D. thunbergiicola* infesting mangoes worldwide.

Note **a**. Symptomatic leaves **b**. Fruiting bodies produced on CLA (Carnation Leaf Agar) **c**. Conidiogenous cells **d**, **e**. Beta conidia **f**. Alpha conidia **g**. Upper and reverse view of colonies on PDA; Scale bars: **c** = 10 µm, **d** = 20 µm, **e**, **f** = 10 µm

Figure 8.20 *Diaporthe thunbergiicola* (MFLU 24-0434)

Neofusicoccum Crous, Slippers & A.J.L. Phillips, Stud. Mycol. 55: 247 (2006)

Neofusicoccum (Botryosphaeriaceae, Botryosphaeriales) was established by Crous et al. (2006b) to accommodate the species formerly included in *Fusicoccum*. Species of *Neofusicoccum* can be accurately identified using morphological

characterisation coupled with the phylogenetic analysis of ITS, *tef1-α*, *tub2*, and *rpb2* sequence data (Crous et al., 2006b; Zang et al., 2021). *Neofusicoccum* species are pathogens of woody plants and many species have an endophytic life stage (Phillips et al., 2013).

Neofusicoccum sinoeucalypti G.Q. Li & S.F. Chen (2017)

Figure 8.21

Index Fungorum: IF 822327; Facesoffungi: FoF 07477

Description: See Li et al. (2018)

Material examined: Thailand, Chiang Rai Province, Mae Sai District, Wat Ban Tham; on leaves of *Mangifera indica* (Anacardiaceae), 28 February 2022, A. Armand, P21-2 (MFLU 24-0435; MFLUCC 24-0374, living culture).

Notes: A single strain, P21-2 (MFLUCC 24-0374), was morphologically similar to *Neofusicoccum sinoeucalypti* (CGMCC3.18752, ex-type) in the shape and size of conidiogenous cells and conidia (Li et al. 2018). Phylogenetic analysis showed that this strain grouped with the type strain of *N. sinoeucalypti*, with 61% ML bootstrap support (Figure 8.22). Pairwise nucleotide comparison between our strain and the type strain revealed 1/208 bp (0.4%) difference in the *tef1-α* region, with no differences observed in the ITS, *tub2*, and *rpb2* regions. Based on these findings, the strain was identified as *Neofusicoccum sinoeucalypti*. This is the first report of this species occurring on mangoes worldwide.

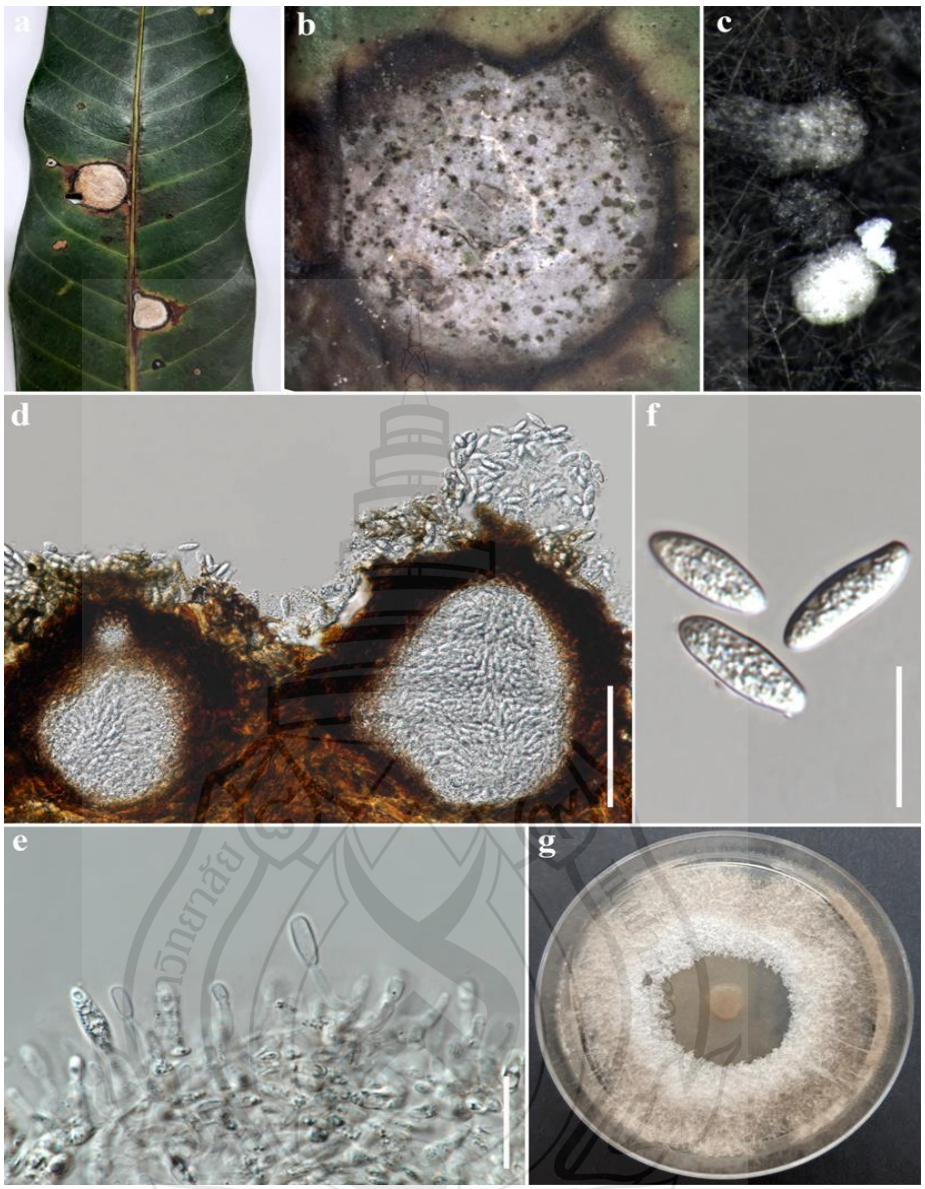

Note **a**. Symptomatic mango leaf **b**. Fruiting bodies produced on the leaf **c**. Immature pycnidia **d**. Cross section of mature pycnidia **e**. Conidiogenous cells and conidial attachment **f**. Conidia **g**. Upper view of colonies on PDA; Scale bars: **d** = 100 µm, **e**, **f** = 20 µm

Figure 8.21 *Neofusicoccum sinoeucalypti* (MFLU 24-0435)

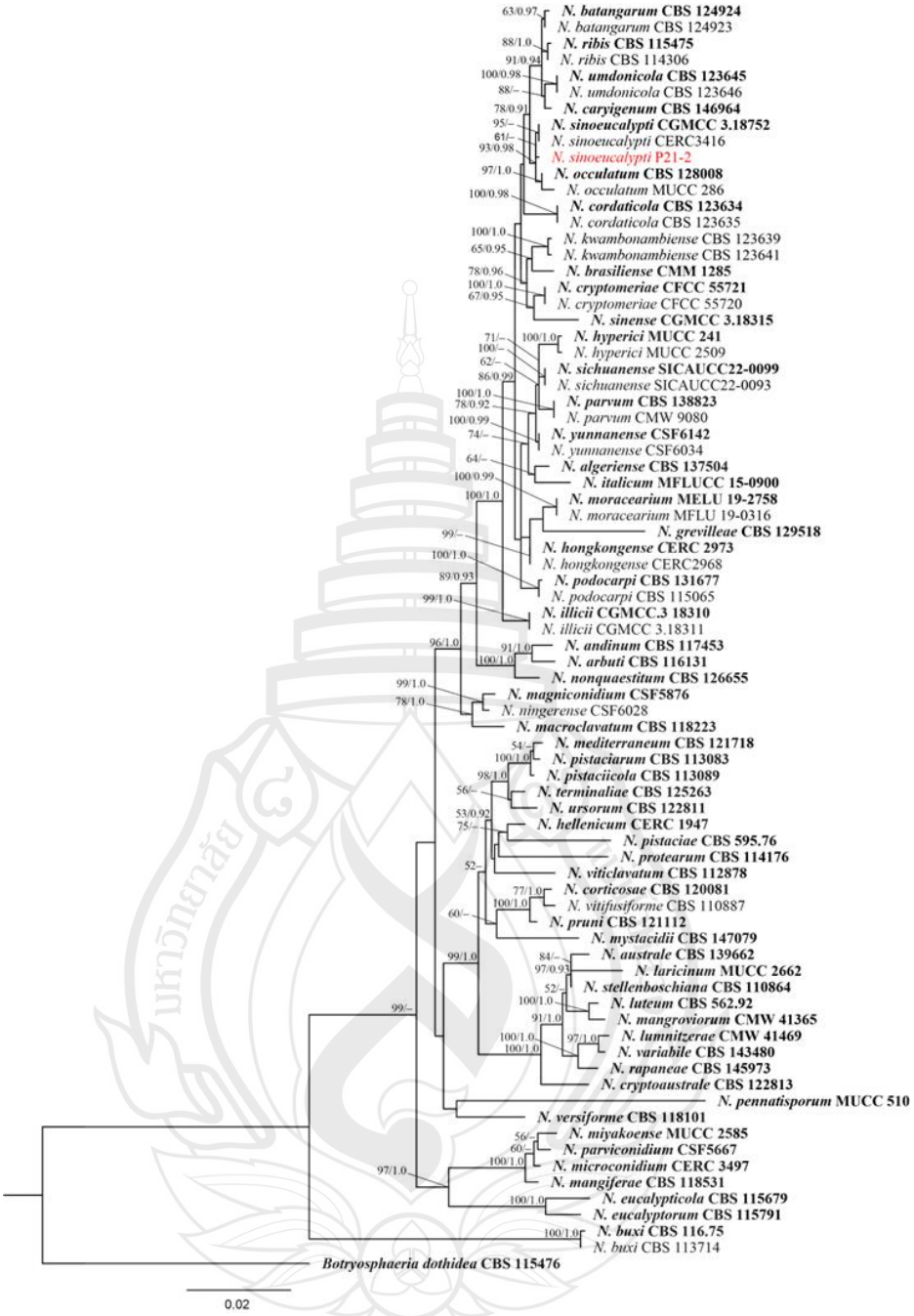

Note Maximum likelihood support values ≥ 50% and bayesian posterior probabilities ≥ 0.90 are shown near the nodes, respectively. The tree is rooted with *Botryosphaeria dothidea* (CBS 115476). Isolates from this study are in red, and ex-type strains are in bold

Figure 8.22 The Maximum Likelihood (ML) tree of *Neofusicoccum* based on the combined ITS, *EF1-α*, *tub2*, and *rpb2* sequence dataset

Neopestalotiopsis Maharachch., K.D. Hyde & Crous (2014)

Neopestalotiopsis (Sporocadaceae, Amphisphaeriales, Xylariomycetidae) was erected by Maharachchikumbura et al. (2014) to accommodate the species separated from *Pestalotiopsis* based on phylogenetic analysis and morphological characteristics. The species of *Neopestalotiopsis* are endophytes (Abdelhamid et al., 2024; Koutb et al., 2021) and pathogens, responsible for grey leaf spots (Shahriar et al., 2022), dieback (Fiorenza et al., 2022), root and crown rot (Obregón et al., 2018), stem lesion (Fiorenza et al., 2022), and stem rot (Santos et al., 2020). *Neopestalotiopsis* species were reported from a wide range of plants and crops, including strawberry (Obregón et al., 2018), avocado (Fiorenza et al., 2022), oil palm (Ismail et al., 2017), eucalyptus (Belisário et al., 2020; Diogo et al., 2021), macadamia (Akinsanmi et al., 2017), rubber tree (Pornsuriya et al., 2020), grapevine (Maharachchikumbura et al., 2016), and persimmon (Qin et al., 2023).

Neopestalotiopsis chrysea (Maharachch. & K.D. Hyde) Maharachch., K.D. Hyde & Crous (2014)

Figure 8.23

Index Fungorum: IF 809763; Facesoffungi: FoF 17010

Basionym: *Pestalotiopsis chrysea* Maharachch. & K.D. Hyde 2012

Description: See Maharachchikumbura et al. (2012, 2014)

Material examined: Chiang Rai Province, Mueang Chiang Rai District, Mae Fah Luang University Campus; on leaves of *Mangifera indica* (Anacardiaceae), 26 April 2023, A. Armand, AS-3 (MFLU 24-0436; MFLUCC 24-0375, living culture).

Notes: Phylogenetic analysis of a combined ITS, *tef1-α*, and *tub2* dataset revealed that strain AS-3 clustered with the type strain of *Neopestalotiopsis chrysea*, receiving 87% ML and 1.00 PP bootstrap support (Figure 8.24). Morphologically, strain AS-3 closely resembled *N. chrysea* (MFLU12-0411, holotype) in conidial shape, size, and appendage characteristics (Maharachchikumbura et al., 2012). Nucleotide comparison between strain AS-3 (MFLUCC 24-0375) and the ex-type strain showed 1/445 bp (0.2%) difference in the *tef1-α* region, while the ITS and *tub2* regions were 100% identical. This study represents the first global report of *Neopestalotiopsis chrysea* infesting mangoes.

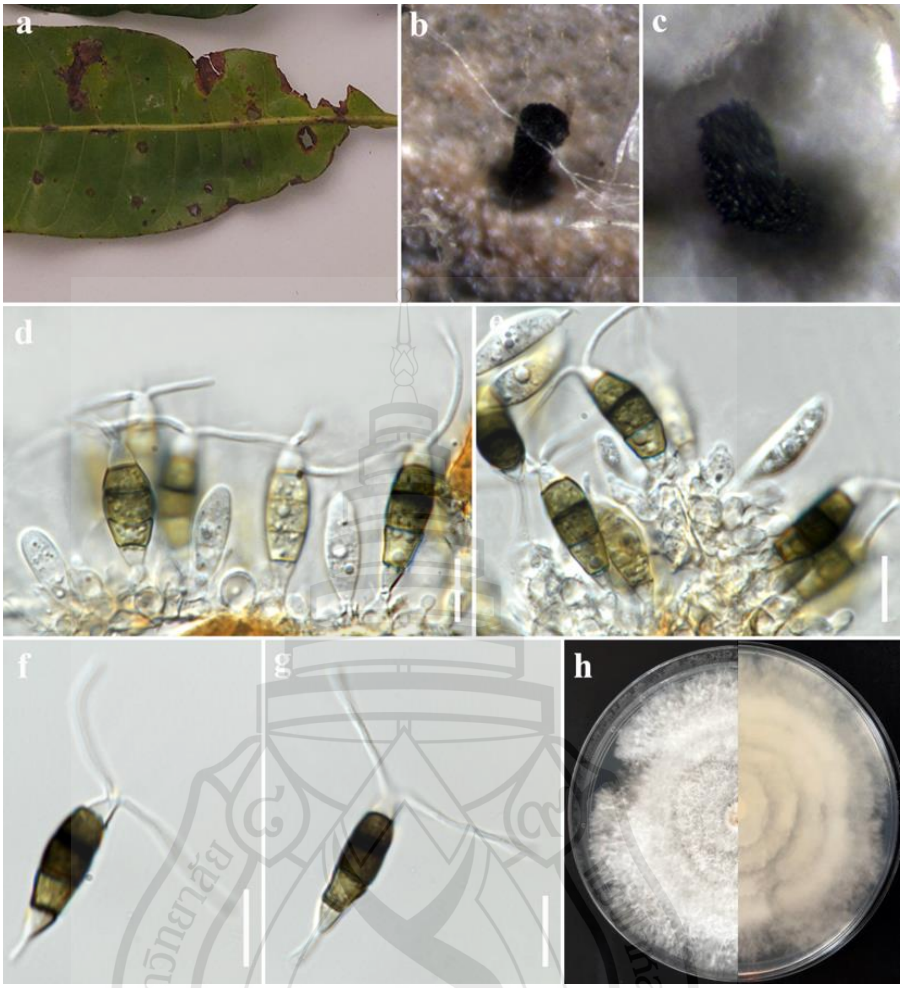

Note **a**. Symptomatic leaf **b**, **c**. Fruiting bodies and conidial mass **d**, **e**. Conidiogenous cells and immature conidia **f**, **g**. Conidia **h**. Upper and reverse view of colonies on PDA; Scale bars: **d**–**g** = 10 µm.

Figure 8.23 *Neopestalotiopsis chrysea* (MFLU 24-0436)

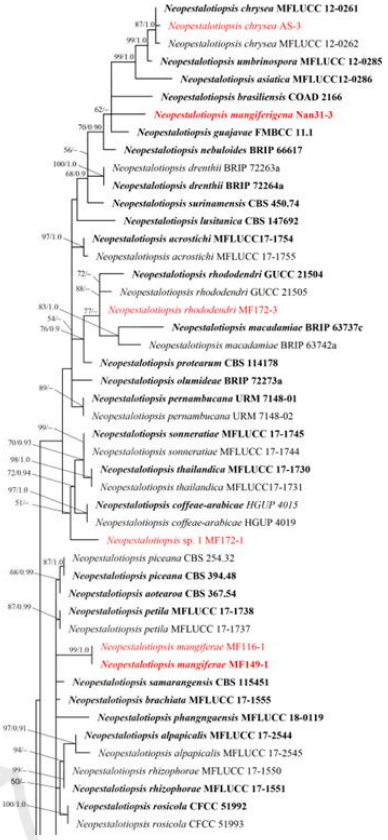

Note Maximum likelihood support values ≥ 50% and bayesian posterior probabilities ≥ 0.90 are shown near the nodes, respectively. The tree is rooted with *Pestalotiopsis trachicarpicola* (OP068) and *Pestalotiopsis diversiseta* (MFLUCC 12-0287). Isolates from this study are in red, and ex-type strains are in bold

Figure 8.24 Maximum likelihood (ML) tree of *Neopestalotiopsis* based on the combined ITS, *EF1-α*, and *tub2* sequence dataset

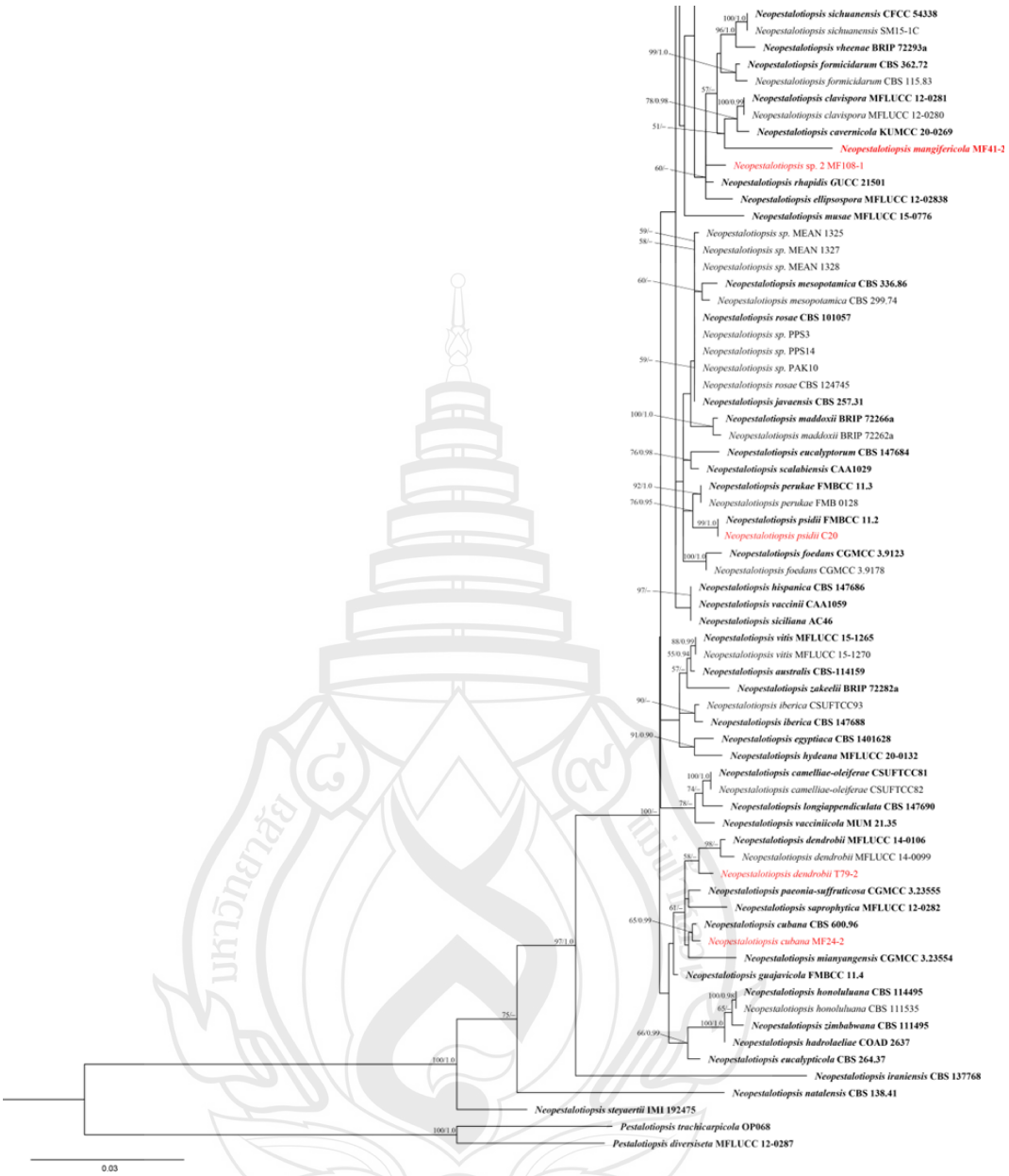

Figure 8.24 (continued)

Neopestalotiopsis cubana Maharachch., K.D. Hyde & Crous 2014

Figure 8.25

Index Fungorum: IF 809765; Facesoffungi: FoF 17011

Description: See Maharachchikumbura et al. (2014)

Material examined: Thailand, Chiang Rai Province, Mueang Chiang Rai District, Mae Fah Luang University Campus; on leaves of *Mangifera indica*

(Anacardiaceae), 24 November 2022, M. Fallahi, MF24-2 (MFLU 24-0437; MFLUCC 24-0376).

Notes: A single strain, MF24-2, grouped with the ex-type of *Neopestalotiopsis cubana*, showing 65% ML and 0.99 PP support values (Figure 8.24). Pairwise nucleotide comparison revealed 3/445 bp (0.4%) differences in the *tef1-α* region between MF24-2 and the ex-type strain, and there were no differences in the ITS and *tub2* regions. Morphologically, the strain was similar to the ex-type (CBS 600.96), and no conspicuous differences were observed. To our knowledge this is the first report of *Neopestalotiopsis cubana* causing disease on mango worldwide.

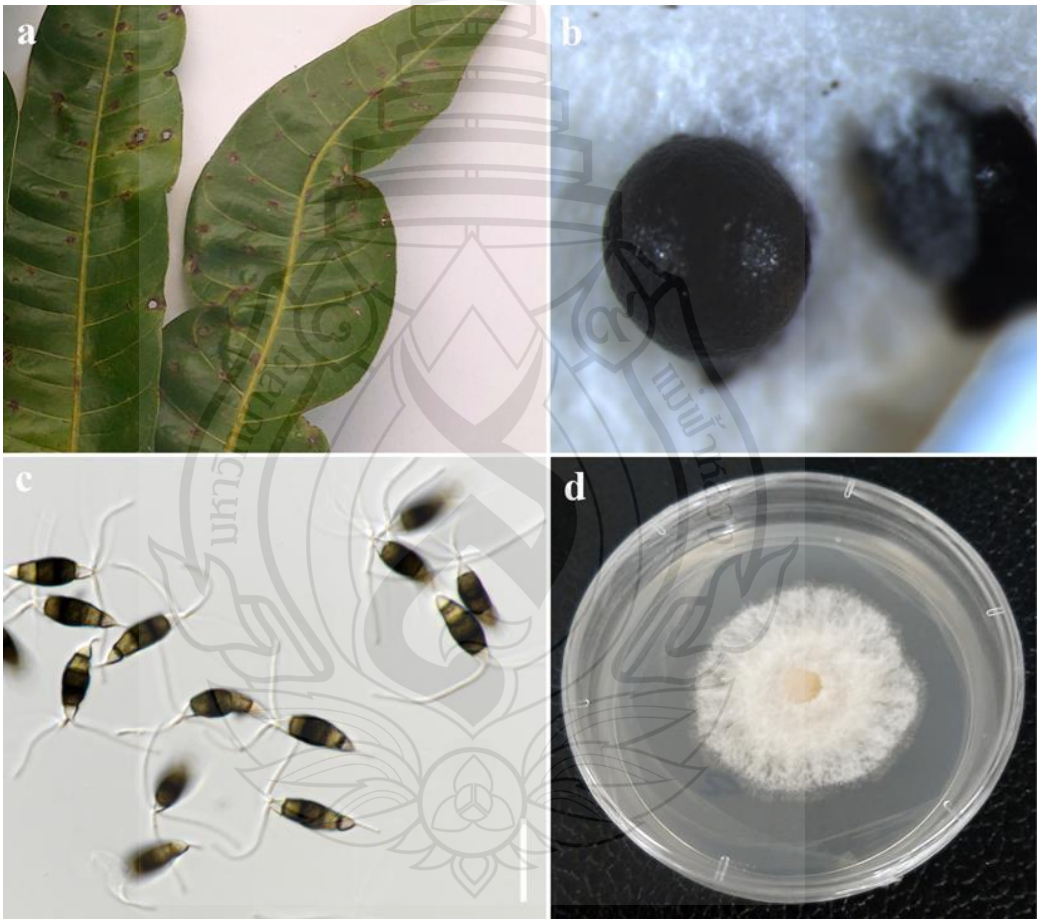

Note **a**. Symptomatic mango leaves **b**. Fruiting bodies and conidial mass **c**. Conidia **d**. Upper and reverse view of colonies on PDA; Scale bars: 20 µm.

Figure 8.25 *Neopestalotiopsis cubana* (MFLU 24-0437)

Neopestalotiopsis dendrobii X.Y. Ma, K.D. Hyde & J.C. Kang (2019)

Figure 8.26

Index Fungorum: IF 830981; Facesoffungi: FoF 17012

Description: See Ma et al. (2019)

Material examined: Thailand, Chiang Rai Province, Phan District, Mae Ao, Ang Kep Nam Huai Tonyang Reservoir; on leaves of *Mangifera indica* (Anacardiaceae), 27 September 2021, A. Armand, T79-2 (MFLU 24-0438; MFLUCC 24-0377, living culture).

Notes: Strain T79-2 (MFLUCC 24-0377) clustered with the type strain of *Neopestalotiopsis dendrobii*, along with the strain MFLUCC 14-0099, forming a distinct clade separate from other species, with 58% ML bootstrap support (Figure 8.24). Strain T79-2 formed a sister lineage to the other two strains of *N. dendrobii*; however, the *tef1-α* region in *N. dendrobii* (MFLUCC 14-0106, ex-type) and *N. dendrobii* (MFLUCC 14-0099) is notably shorter than the *tef1-α* sequence of our strain, resulting in a higher number of gaps in the *tef1-α* region between our strain and the other two. Nucleotide comparison with the ex-type strain revealed 1/461 bp (0.2%) difference in the ITS region, 2/234 bp (0.8%) in the *tef1-α* region, and 3/346 bp (0.8%) in the *tub2* region. Additionally, the morphological characteristics of our strain closely resemble those of the ex-type strain (Ma et al., 2019). Based on these findings, T79-2 was identified as *Neopestalotiopsis dendrobii*. This study repoerts *Neopestalotiopsis dendrobii* infesting mango leaves for the first time worldwide.

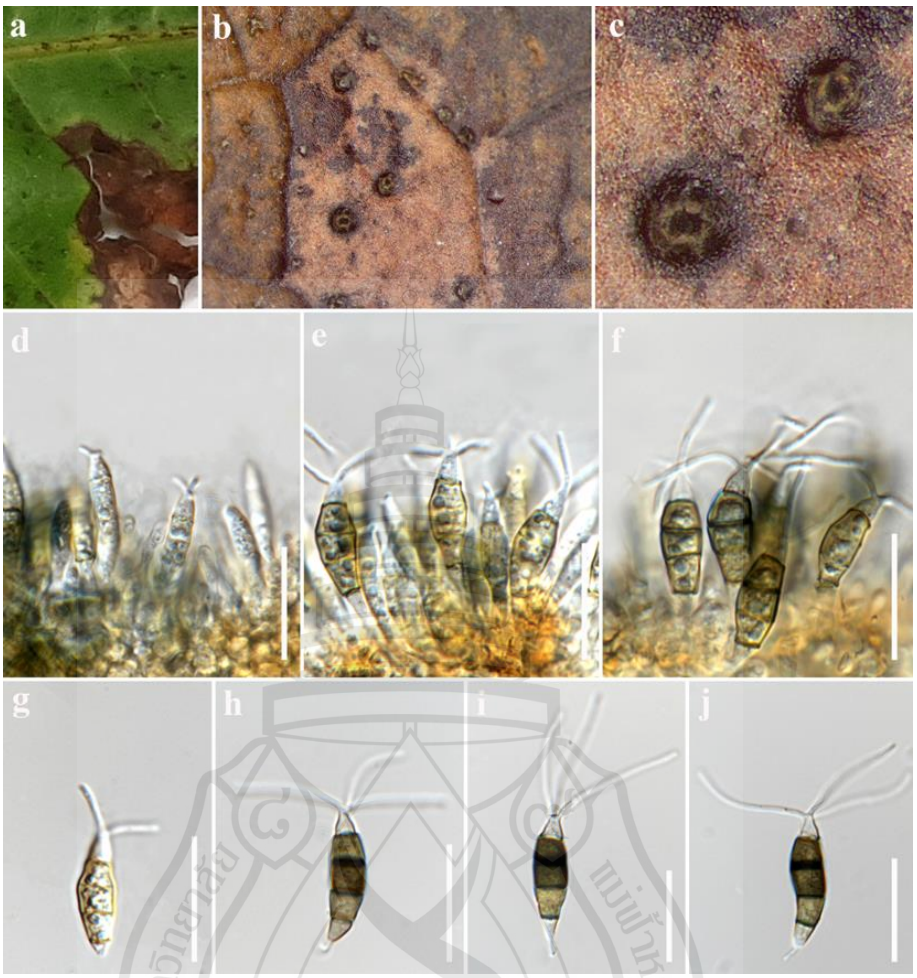

Note **a**. Symptomatic mango leaf **b**, **c**. Fruiting bodies produced on the leaf **d**, **e**. Conidiogenous cells and immature conidia **f**, **g**. Conidiogenous cells and mature conidia **h**. Upper and reverse view of colonies on PDA; Scale bars: **d**–**j** = 20 µm

Figure 8.26 *Neopestalotiopsis dendrobii* (MFLU 24-0438)

Neopestalotiopsis mangiferae A. Armand, Jayaward. & K.D. Hyde, sp. nov.

Figure 8.27

Index Fungorum: IF 903318; Facesoffungi: FoF 17013

Etymology: Named after the host plant genus, *Mangifera*.

Pathogenic on mango fruit. Sexual morph: not observed. Asexual morph: *Conidiomata* on PDA acervular, black, aggregated or scattered, semi-immersed, exuding black glistening conidial masses. *Conidiophores* indistinct and reduced to conidiogenous cells. *Conidiogenous cells* discrete, smooth-walled, hyaline, aseptate, simple, cylindrical to subcylindrical, or ampuliform, 6–10 × 3–5.5 µm ($\bar{x}$ = 7.5 × 3.5

µm, n = 10). *Conidia* fusoid to ellipsoid, straight or slightly curved, 4-septate, 17–23 × 6–8.3 µm ($\bar{x}$ = 20 × 7.5 µm, n = 20). *Basal cell* obconic to subcylindrical, hyaline to pale brown, smooth, 2.7–4.5 µm long. *Three median cells* doliiform, versicolored, verruculose, darker at the third septum from the base, 13.5–15 µm long ($\bar{x}$ = 14.3 µm, n = 20). *Second cell* from the base pale brown, 3.7–5 µm long ($\bar{x}$ = 4.3 µm, n = 20). *Third cell* dark brown, 4–5.7 µm long ($\bar{x}$ = 5 µm, n = 20). *Fourth cell* dark brown, 3.5–5.5 µm long ($\bar{x}$ = 4.7 µm, n = 20). *Apical cell* hyaline, conical to cylindrical, 3–4 µm long ($\bar{x}$ = 3.4 µm, n = 20), comprising 2–3 appendages (frequently 2). *Apical appendages* 23–35 µm long ($\bar{x}$ = 27 µm, n = 20), hyaline, tubular, arising from the apex of the apical cell. *Basal appendage* 4.5–8 µm long ($\bar{x}$ = 5.2 µm, n = 20), hyaline, filiform.

Culture characteristics: Colonies on PDA reach 80–90 mm in diam. after 7 days at 25 ± 2 °C, entire in margin. Aerial mycelia fluffy, white to pale rosy buff on surface, pale buff on reverse. Conidiomata produced after 10 days on PDA.

Material examined: Thailand, Sakon Nakhon, Mueang Sakon Nakhon, Soi, Chang Wat, That Na Weng, Bannongbuayai; on *Mangifera indica* (Anacardiaceae), 19 February 2023, Fallahi M., MF149-1 (MFLU 24-0439 holotype; MFLUCC 24-0378, ex-type living culture); Thailand, Chiang Rai Province, Phan District, Sai Khao, on *Mangifera indica* (Anacardiaceae), 03 February 2023, M. Fallahi, MF116-1 (MFLUCC 24-0379).

Notes: The phylogenetic analysis of the concatenated ITS, *tef1-α*, and *tub2* datasets revealed that the two strains, MF149-1 (MFLUCC 24-0378) and MF116-1 (MFLUCC 24-0379), clustered together with strong support values of 99% (ML) and 1.00 (PP) (Figure 8.24). These strains formed a distinct clade, separate from other species, although bootstrap values did not support close proximity to any particular species. The strains were isolated from specimens collected in two different provinces in northern Thailand. However, nucleotide comparison revealed identical sequences in the ITS, *tef1-α*, and *tub2* regions. Morphological comparison further confirmed the similarity between strains MF149-1 and MF116-1. These strains are distinguished by the production of long apical appendages (up to 35 µm, typically 2) and a darkened third septum located between the third and fourth cells. Based on multi-locus phylogeny

and morphological examination, *Neopestalotiopsis mangiferae* is introduced and illustrated as a new taxon, found infesting *Mangifera indica*.

Note **a**. Fruiting bodies Produced on MLA (Mango Leaf Agar) **b**. Conidial mass produced on PDA **c**. Conidial mass produced on WA **d**. Conidiogenous cells and immature conidia **e**, **f**. Mature conidia **g**. Upper and reverse view of colonies on PDA; Scale bars: **c** = 10 µm, **d**, **f** = 20 µm

Figure 8.27 *Neopestalotiopsis mangiferae* (MFLU 24-0439 holotype)

Neopestalotiopsis mangifericola A. Armand, R.S. Jayaward. & K.D. Hyde, sp. nov.

Figure 8.28

Index Fungorum: IF 903319; Facesoffungi: FoF 17014

Etymology: Named after the host plant genus, *Mangifera.*

Associated with the symptomatic mango. Sexual morph: not observed. Asexual morph: *Conidiomata* on PDA acervular, black, aggregated or scattered, semi-immersed, exuding black glistening conidial masses. *Conidiophores* indistinct and reduced to conidiogenous cells. *Conidiogenous cells* discrete, smooth-walled, hyaline, aseptate, simple, subcylindrical, ampuliform, or bottle-shaped, 6–17 × 4–6 µm ($\bar{x}$ = 10.5 × 4.5 µm, n = 10). *Conidia* cylindrical to subcylindrical, rarely fusoid, straight, 4-septate, 18–22 × 4.6–5.7 µm ($\bar{x}$ = 20.8 × 5.3 µm, n = 20). *Basal cell* obconic to subcylindrical, hyaline to pale brown, smooth, 3–4 µm long. *Three median cells* doliiform, smooth, versicolored or same, darker at the septa, 11.5–14 µm long ($\bar{x}$ = 12.5 µm, n = 20). *Second cell* from the base pale brown, 3.3–4.5 µm long ($\bar{x}$ = 3.8 µm, n = 20). *Third cell* brown, 3.8–4.4 µm long ($\bar{x}$ = 4 µm, n = 20). *Fourth cell* brown, 4–5 µm long ($\bar{x}$ = 4.3 µm, n = 20). *Apical cell* hyaline, conical to cylindrical, 2.4–3.6 µm long ($\bar{x}$ = 3.8 µm, n = 20), comprising 2–3 appendages. *Apical appendages* 14–18(–22) µm long ($\bar{x}$ = 16.5 µm, n = 20), hyaline, tubular, arising from the apex of the apical cell. *Basal appendage* 2.2–3.2 µm long ($\bar{x}$ = 2.7 µm, n = 20), hyaline, filiform.

Culture characteristics: Colonies on PDA reach 75–80 mm in diam. after 7 days at 25 ± 2 °C, entire in margin. Aerial mycelia fluffy, white on surface, pale buff on reverse. Conidiomata produced after 12 days on PDA.

Material examined: Thailand, Chiang Rai, Mueang Chiang Rai District, Ban Du; on *Mangifera indica* (Anacardiaceae), 10 December 2022, M. Fallahi, MF41-2 (MFLU 24-0440 holotype; MFLUCC 24-0380, ex-type living culture).

Notes: Phylogenetically, the single strain MF41-2 (MFLUCC 24-0380) grouped together with the type strain of *Neopestalotiopsis cavernicola* and *N. clavispora*. However, it was separated from the two species with 51% ML bootstrap value (Figure 8.24). *Neopestalotiopsis mangifericola* is differentiated from *N. clavispora* with 19/445 bp (4.2%) polymorphisms in *tef1-α* and 12/363 bp (3.3%) in *tub2*. It is also distinguished from *N. cavernicola* showing 17/393 bp (4.3%) polymorphisms in *tef1-α*

and 11/362 bp (3.0%) in the *tub2* region. Morphologically, *Neopestalotiopsis mangifericola* differs from *N. clavispora* (Maharachchikumbura et al., 2012) by its longer and thinner conidia (18–22 × 4.6–5.7 μm in *N. mangifericola* vs. 18–26 × 6.5–8.5 μm in *N. clavispora*). It was also different in the shape and colour of conidia (subcylindrical, rarely fusoid, pale brown to brown in *N. mangifericola* vs. clavate-fusiform, dark brown in *N. clavispora*). *Neopestalotiopsis mangifericola* differs from *N. cavernicola* by producing smaller conidia (10–30 × 5–10 μm in *N. cavernicola*) comprising up to 3 apical appendages, while *N. cavernicola* produced up to 4 apical appendages. Moreover, conidiogenous cells produced by *N. mangifericola* are ampuliform to bottle-shaped, while *N. cavernicola* produced narrowly cylindrical conidiogenous cells (Liu et al., 2021).

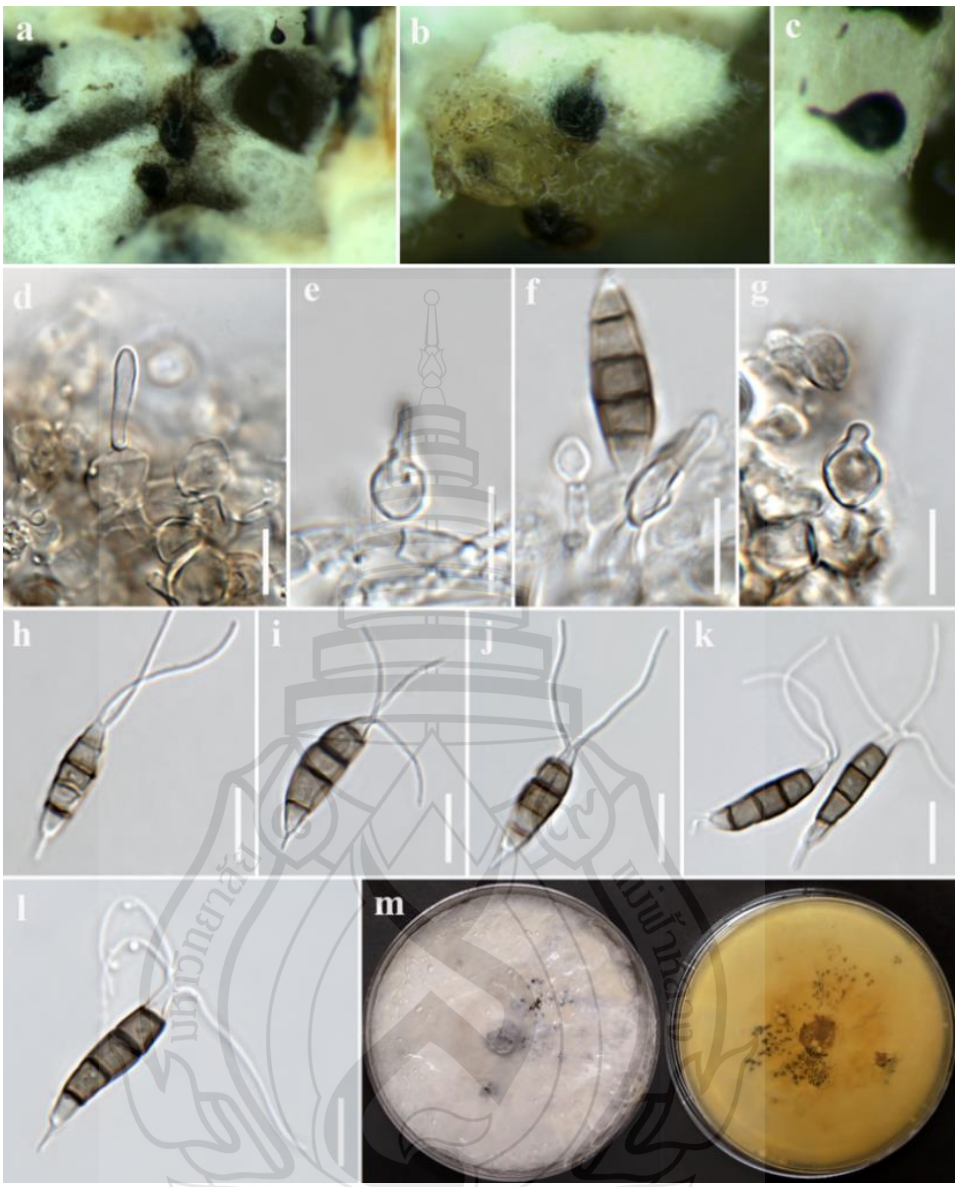

Note **a**, **b**. Fruiting bodies Produced on PDA **c**. Conidial mass produced on CLA **d**–**g**. Conidiogenous cells **h**, **l**. Conidia **m**. Upper and reverse view of colonies on PDA; Scale bars: **d**, **l** = 10 µm

Figure 8.28 *Neopestalotiopsis mangifericola* (MFLU 24-0440 holotype)

Neopestalotiopsis mangiferigena A. Armand, R.S. Jayaward. & K.D. Hyde, sp. nov.

Figure 8.29

Index Fungorum: IF 903320; Facesoffungi: FoF 17015

Etymology: Named after the host plant genus, *Mangifera.*

Pathogenic on mango leaves. Sexual morph: not observed. Asexual morph: *Conidiomata* on PDA acervular, black, aggregated or scattered, semi-immersed, exuding black glistening conidial masses. *Conidiophores* indistinct and reduced to conidiogenous cells. *Conidiogenous cells* discrete, smooth-walled, hyaline, aseptate, simple, ampuliform to bottle-shaped, 7–10 × 3.7–5 µm ($\bar{x}$ = 8.5 × 4.3 µm, n = 10). *Conidia* cylindrical to subcylindrical, straight, 4-septate, 23–27 × 6–7 µm ($\bar{x}$ = 25 × 5.3 µm, n = 20). *Basal cell* obconic to subcylindrical, hyaline to pale brown, smooth, 4.5–5.2 µm long. *Three median cells* doliiform, verruculose, versicolored, darker at the septa, 14–18 µm long *(*$\bar{x}$ = 16.5 µm, n = 20). *Second cell* from the base pale brown, 5–5.8 µm long ($\bar{x}$ = 5.3 µm, n = 20). *Third cell* dark brown, 4.8–5.6 µm long ($\bar{x}$ = 5 µm, n = 20). *Fourth cell* dark brown, 4.5–6 µm long ($\bar{x}$ = 5 µm, n = 20). *Apical cell* hyaline, conical to cylindrical, 2.5–4 µm long ($\bar{x}$ = 3.2 µm, n = 20), comprising 2–3 appendages. *Apical appendages* 17–23(–33) µm long ($\bar{x}$ = 21.5 µm, n = 20), hyaline, tubular, arising from the apex of the apical cell. *Basal appendage* 3.5–5 µm long ($\bar{x}$ = 4.2 µm, n = 20), hyaline, filiform.

Culture characteristics: Colonies on PDA reach 86–90 mm in diam. after 7 days at 25 ± 2 °C, entire in margin. Aerial mycelia fluffy, white on surface with concentric zonation, pale buff on reverse. Conidiomata produced after 15 days on PDA.

Material examined: Thailand, Nan Province, Phu Phiang District, Mueang Chang, on leaves of *Mangifera indica* (Anacardiaceae), 8 September 2022, A. Armand, Nan31-3 (MFLU 24-0441, holotype; MFLUCC 24-0381, ex-type living culture).

Notes: Strain Nan31-3 clustered within a clade comprising *N. chrysea*, *N. umbrinospora*, *N. asiatica*, *N. brasiliensis*, *N. guajavae*, and *N. neboloides*, showing 70%/0.90 (ML/PP) support values (Figure 8.24). While its position was not consistent in the vicinity of any species in this clade. Based on the pairwise nucleotide comparison, our strain showed nucleotide polymorphisms with the close species as follows: *N. chrysea* (0/488 bp in ITS, 12/444 bp (2.7%) in *tef1-α*, 5/326 bp (1.5%) in *tub2*); *N. umbrinospora* (0/488 bp in ITS, 10/444 bp (2.2%) in *tef1-α*, 6/346 bp (1.7%) in *tub2*); *N. asiatica* (0/488 bp in ITS, 18/444 bp (4.0%) in *tef1-α*, 3/346 bp (0.8%) in *tub2*); *N. brasiliensis* (3/450 bp (0.6%) in ITS, 12/444 bp (2.7%) in *tef1-α*, 0/346 bp in *tub2*); *N. guajavae* (1/481 bp (0.2) in ITS, 10/411 bp (2.4%) in *tef1-α*, 0/307 bp in *tub2*); and *N. nebuloides* (1/481 bp (0.2) in ITS, 11/444 bp (2.4%) in *tef1-α*, 0/346 in *tub2*). Given the

nucleotide differences from closely related species, the strain is introduced as a new species.

Note **a**. Symptomatic mango leaf **b**. Fruiting bodies and conidial mass produced on the leaf **c–f**. Conidiogenous cells and conidial attachment **g**, **h**. Conidia **i**. Upper and reverse view of colonies on PDA; Scale bars: **c**, **d** = 20 µm, **e**, **f** = 10 µm, **g**, **h** = 20 µm

Figure 8.29 *Neopestalotiopsis mangiferigena* (MFLU 24-0441 holotype)

Neopestalotiopsis psidii I.U. Haq, S. Ijaz & N.A. Khan (2021)

Figure 8.30

Index Fungorum: IF 840638; Facesoffungi: FoF 13404

Description: See Haq et al. (2021)

Material examined: Thailand, Chiang Rai Province, Mueang Chiang Rai District, Ban Du; on leaves of *Mangifera indica* (Anacardiaceae), 10 December 2022, A. Armand, C20 (MFLU 24-0442; MFLUCC 24-0382, living culture).

Notes: A single strain was identified as *Neopestalotiopsis psidii*, isolated from symptomatic mango leaves. Phylogenetic analysis showed that the strain clustered with the ex-type strain of *N. psidii* (FMBCC 11.2; Haq et al. 2021) with strong support values of 99% (ML) and 1.00 (PP) (Figure 8.24). Nucleotide comparison between our strain and the ex-type strain revealed no differences in the ITS, *tef1-α,* and *tub2* loci. Additionally, the strains were morphologically similar. Therefore, the strain was confirmed as *N. psidii*, based on morpho-molecular evidence. To our knowledge, this is the first report of *Neopestalotiopsis psidii* isolated from mangoes worldwide.

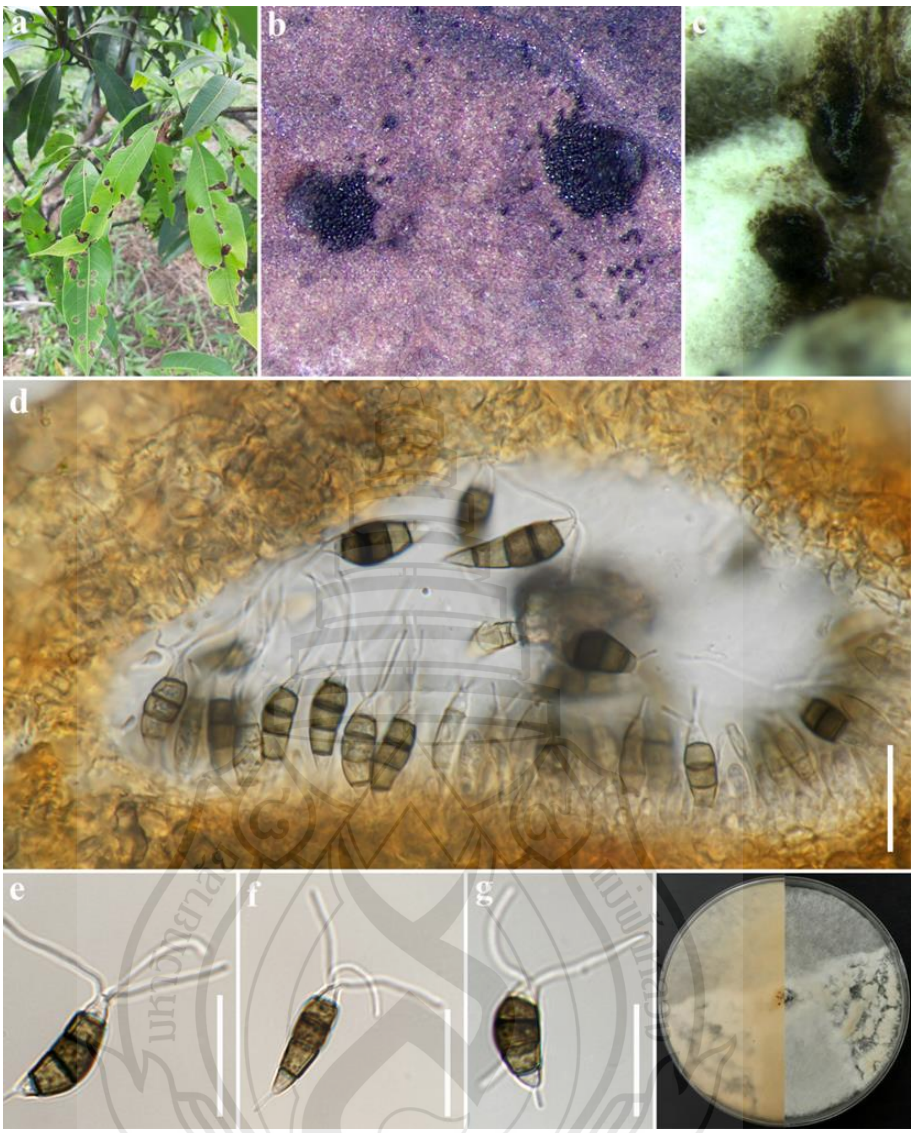

Note **a**. Symptomatic mango leaves **b**. Fruiting bodies and conidial mass produced on the leaf **c**. conidial mass produced on the PDA **d**. Cross section of acervolus **e**–**g**. Conidia **h**. Upper and reverse view of colonies on PDA; Scale bars: **d–g** = 20 µm

Figure 8.30 *Neopestalotiopsis psidii* (MFLU 24-0442)

Neopestalotiopsis rhododendri Qi Yang & Yong Wang bis (2021)

Figure 8.31

Index Fungorum: IF 840066; Facesoffungi: FoF 12918

Description: See Yang et al. (2021)

Material examined: Thailand, Kalasin Province, Kuchinarai District, Nong Hang; on *Mangifera indica* (Anacardiaceae), 20 February 2023, M. Fallahi, MF172-3 (MFLU 24-0443; MFLUCC 24-0383, living culture).

Notes: A single strain (MF172-3) clustered with *Neopestalotiopsis rhododendri* based on phylogenetic analysis of the combined ITS, *tef1-α*, and *tub2* dataset, with an ML bootstrap support value of 88% (Figure 8.24). Morphologically, it was similar to the ex-type strain, though our strain produced conidia that were slightly thicker than those of the ex-type strain. There were only two nucleotide polymorphisms in the *tef1-α* region (2/445 bp (0.4%)), while the ITS and *tub2* loci were identical. Therefore, the strain was identified as *N. rhododendri*. This study represents the first global report of *Neopestalotiopsis rhododendri* associated with mangoes.

Note **a–c**. Fruiting bodies and conidial mass produced on the PDA **d**. Conidia **e**. Upper and reverse view of colonies on PDA; Scale bars: 20 µm

Figure 8.31 *Neopestalotiopsis rhododendri* (MFLU 24-0443)

Neopestalotiopsis sp. 1

Figure 8.32

Associated with symptomatic mango. Sexual morph: not observed. Asexual morph: *Conidiomata* on PDA acervular, black, scattered, semi-immersed, exuding black glistening conidial masses. *Conidiophores* indistinct and reduced to conidiogenous cells. *Conidiogenous cells* discrete, smooth-walled, hyaline, aseptate, simple, subcylindrical, rarely bottle-shaped, 7.5–13 × 4–7 µm ($\bar{x}$ = 11 × 5.5 µm, n = 10). *Conidia* subcylindrical, to fusoid, straight or slightly curved, 4-septate, 16–20 × 4.5–5.2 µm ($\bar{x}$ = 17.5 × 5 µm, n = 20). *Basal cell* obconic to subcylindrical, hyaline to pale brown, smooth, 3.2–4 µm long. *Three median cells* doliiform, smooth, versicolored, darker at the septa, 11–13 µm long ($\bar{x}$ = 12 µm, n = 20). *Second cell* from the base pale brown, 4–4.8 µm long ($\bar{x}$ = 4.2 µm, n = 20). *Third cell* brown, 2.5–3.4 µm long ($\bar{x}$ = 2.7 µm, n = 20). *Fourth cell* brown, 3.2–3.7 µm long ($\bar{x}$ = 3.5 µm, n = 20). *Apical cell* hyaline, conical, 2–3.4 µm long ($\bar{x}$ = 3 µm, n = 20), comprising 2–4 appendages. *Apical appendages* 16–19(–26) µm long ($\bar{x}$ = 18.5 µm, n = 20), hyaline, tubular, arising from the apex of the apical cell. *Basal appendage* 2–3.2 µm long ($\bar{x}$ = 2.3 µm, n = 20), hyaline, filiform.

Culture characteristics: Colonies on PDA reach 70–77 mm in diam. after 7 days at 25 ± 2 °C, undulate in margin. Aerial mycelia fluffy, white to pale rosy buff on surface, pale buff on reverse. Conidiomata produced after 20 days on PDA.

Material examined: Thailand, Kalasin Province, Kuchinarai District, Nong Hang; on *Mangifera indica* (Anacardiacea), 20 February 2023, M. Fallahi, MF172-1 (MFLU 24-0444; MFLUCC 24-0384R, living culture).

Notes: Strain MF172-1 (MFLUCC 24-0384R) separated from the clade comprising species such as *Neopestalotiopsis sonneratiae*, *N. thailandica*, and *N. coffeae-arabicae*, but the ML bootstrap support for this lineage was 51%, and the PP support was very low (Figure 8.24). Nucleotide comparison between our strain and its closest relative, *N. coffeae-arabicae*, revealed 2/434 bp (0.4%) differences in the *tef1-α* region and 4/330 bp (1.2%) in the *tub2* region. Morphological examination did not reveal any distinguishing characteristics from *N. coffeae-arabicae*. Due to the low number of nucleotide polymorphisms and the low support values in both ML and PP

analyses, we refrain from introducing this strain as a new taxon, pending the acquisition of additional strains and further studies.

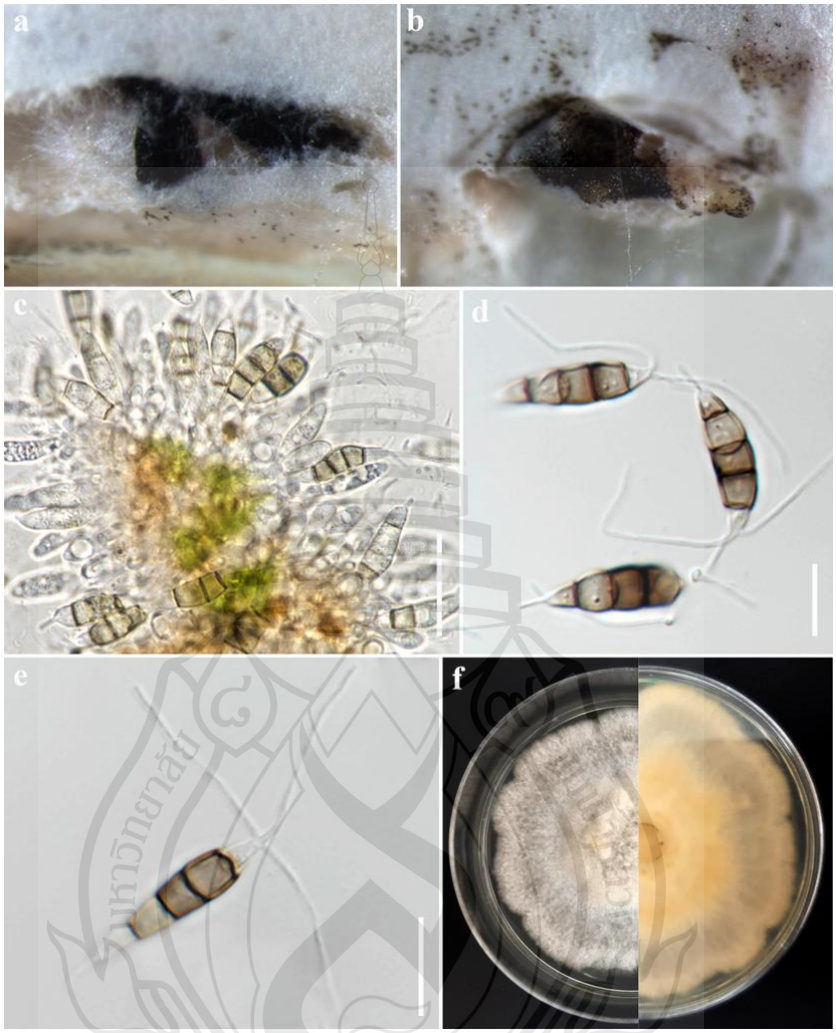

Note **a–b**. Fruiting bodies and conidial mass produced on the PDA **c**. Conidiogenous cells and conidia produced on host **d**, **e**. Conidia produced on the PDA **f**. Upper and reverse view of colonies on PDA; Scale bars: **c** = 20 µm, **d**, **e** = 10 µm

Figure 8.32 *Neopestalotiopsis* sp. 1 (MFLU 24-0444)

Neopestalotiopsis sp. 2

Associated with symptomatic mango. Sexual morph: not observed. Asexual morph: *Conidiomata* on PDA acervular, black, scattered, immersed or semi-immersed, exuding black glistening conidial masses. *Conidiophores* indistinct and reduced to conidiogenous cells. *Conidiogenous cells* discrete, smooth-walled, hyaline, aseptate, simple, subcylindrical, bottle-shaped or ampuliform, 5–10 × 3–5 µm ($\bar{x}$= 7.5 × 4.3 µm,

n = 10). *Conidia* fusoid, straight or slightly curved, 4-septate, 21–26 × 5–7 µm ($\bar{x}$ = 24 × 5.5 µm, n = 20). *Basal cell* obconic, hyaline to pale brown, smooth to verruculose, 3–5 µm long. *Three median cells* doliiform, smooth, versicolored, darker at the third septum from the base, 15.3–18.5 µm long ($\bar{x}$ = 16.3 µm, n = 20). *Second cell* from the base pale brown, 3.3–5 µm long ($\bar{x}$ = 3.7 µm, n = 20). *Third cell* dark brown, 4.6–5.5 µm long ($\bar{x}$ = 4.9 µm, n = 20). *Fourth cell* dark brown, 4.7–5.8 µm long ($\bar{x}$ = 5 µm, n = 20). *Apical cell* hyaline, conical, 2.8–4 µm long ($\bar{x}$ = 3.3 µm, n = 20), comprising 2–4 appendages. *Apical appendages* 13–17(–25) µm long ($\bar{x}$ = 15.5 µm, n = 20), hyaline, tubular, arising from the apex of the apical cell. *Basal appendage* 2–4.5 µm long ($\bar{x}$ = 2.8 µm, n = 20), hyaline, filiform.

Culture characteristics: Colonies on PDA reach 72–75 mm in diam. after 7 days at 25 ± 2 °C, undulate in margin. Aerial mycelia fluffy, white to pale rosy buff on surface, pale buff on reverse. Conidiomata produced after 22 days on PDA.

Material examined: Thailand, Chiang Rai Province, Phan District, Sai Khao; on leaves of *Mangifera indica* (Anacardiacea), 8 February 2023, M. Fallahi, MF108-1 (MFLU 24-0445; MFLUCC 24-0385R, living culture).

Notes: According to the phylogenetic tree (Figure 8.24), strain MF108-1 (MFLUCC 24-0385R) formed a distinct lineage, separate from any known species. However, the ML and PP analyses provided insufficient support for the placement of the strain, resulting in inconsistency within the tree. The strain exhibited 6/433 bp (1.3%) polymorphisms in the *tef1-α* locus compared to the closely related species, *Neopestalotiopsis rhapidis* (GUCC 21501), while the ITS and *tub2* regions were identical. Nevertheless, due to the low support values, the placement of the strain cannot be considered reliable, leading to an inconclusive identification. The strain remains unnamed, pending further sampling and analysis.

Note **a**. Symptomatic mango leaves **b**. Fruiting bodies and conidial mass produced on the PDA **c**, **d**. Conidiogenous cells **e**, **f**. Conidia produced on the PDA **g**. Upper and reverse view of colonies on PDA; Scale bars: **c** = 10 µm, **d** = 20 µm, **e**, **f** = 10 µm.

Figure 8.33 *Neopestalotiopsis* sp. 2 (MFLU 24-0445)

Neoscytalidium Crous & Slippers, Stud. Mycol. 55: 244 (2006)

Crous et al. (2006b) established *Neoscytalidium* typified by *Neoscytalidium dimidiatum*. The genus is characterised by conidia occurring in arthric chains in aerial mycelium, powdery to the touch, disarticulating, cylindrical–truncate, oblong–obtuse to doliiform, dark brown, hyphenate, 0–2-septate (Crous et al., 2006b). There are currently five legitimate species of *Neoscytalidium* listed in MycoBank (accessed on 30 September 2024). *Neoscytalidium dimidiatum* with a worldwide distribution, has

emerged as a substantial global ecological and agricultural threat in the last two decades (Kazemzadeh et al., 2015). It causes a broad range of diseases, such as canker, blight, dieback, leaf spot, root rot, and fruit rot, affecting diverse fruit trees, field crops, shrubs, and tree species (Derviş & Özer, 2023).

Neoscytalidium dimidiatum (Penz.) Crous & Slippers (2006)

Figure 8.34

Index Fungorum: IF 500869; Facesoffungi: FoF 11892

Basionym: *Torula dimidiata* Penz., Michelia 2: 466. 1882 (basionym; hyphomycete synanamorph)

= *Hendersonula toruloidea Nattrass*, Trans. Brit. Mycol. Soc. 18: 197. 1933 (coelomycete synanamorph).

Description: See Sutton & Dyko (1989); Crous et al. (2006b)

Material examined: Thailand, Chiang Rai Province, Mueang Chiang Rai District, Tha Sud, on leaves of *Mangifera indica* (Anacardiaceae), 16 December 2021, A. Armand, T82 (MFLU 24-0446; MFLUCC 24-0386 living culture).

Notes: *Neoscytalidium dimidiatum* has been associated with several synonyms (Syn: *Fusicoccum dimidiatum*, *Torula dimidiata*, *Scytalidium dimidiatum*, *Hendersonula toruloidea*) (Farr et al., 2005), due to producing two synanamorphs. The coelomycetous synanamorph produces pycnidia containing conidia that are two-septate, with a darkened central cell resembling fusicoccum-like conidia. While, the hyphomycetous synanamorph generates powdery, arthric disarticulating chains of conidia, resembling scytalidium-like conidia (Crous et al., 2006b; Farr et al., 2005; Nattrass, 1933). In this investigation, a strain has been identified as *Neoscytalidium dimidiatum* based on phylogenetic analysis of a combined ITS, *tef1-α*, and *tub2* dataset along with morphological examination. The phylogenetic tree showed that the strain clustered together with other strains of *N. dimidiatum*, showing 91%/0.99 (ML/PP) support values (Figure 8.35). Morphologically, the strain was similar to hyphomycetous synanamorph of *N. dimidiatum* (syn: *Torula dimidiata*) in producing arthric conidia described by Penzig (1882). Moreover, the coelomycetous synanamorph observed in our strain was similar to the pycnidial synanamorph described as *Hendersonula toruloidea* (synonym of *Neoscytalidium dimidiatum*). The species affects a broad range of woody perennial crops and ornamental plants (Bragard et al., 2023). *Neoscytalidium*

dimidiatum has also been isolated from mango in Australia (Ray et al., 2010), Brazil (Marques et al., 2013), Israel (Sharma et al., 2024), and Niger (Reckhaus, 1987). However, it has not been reported in Thailand until this study and this is the first report of *Neoscytalidium dimidiatum* causing leaf blight on mango in Thailand.

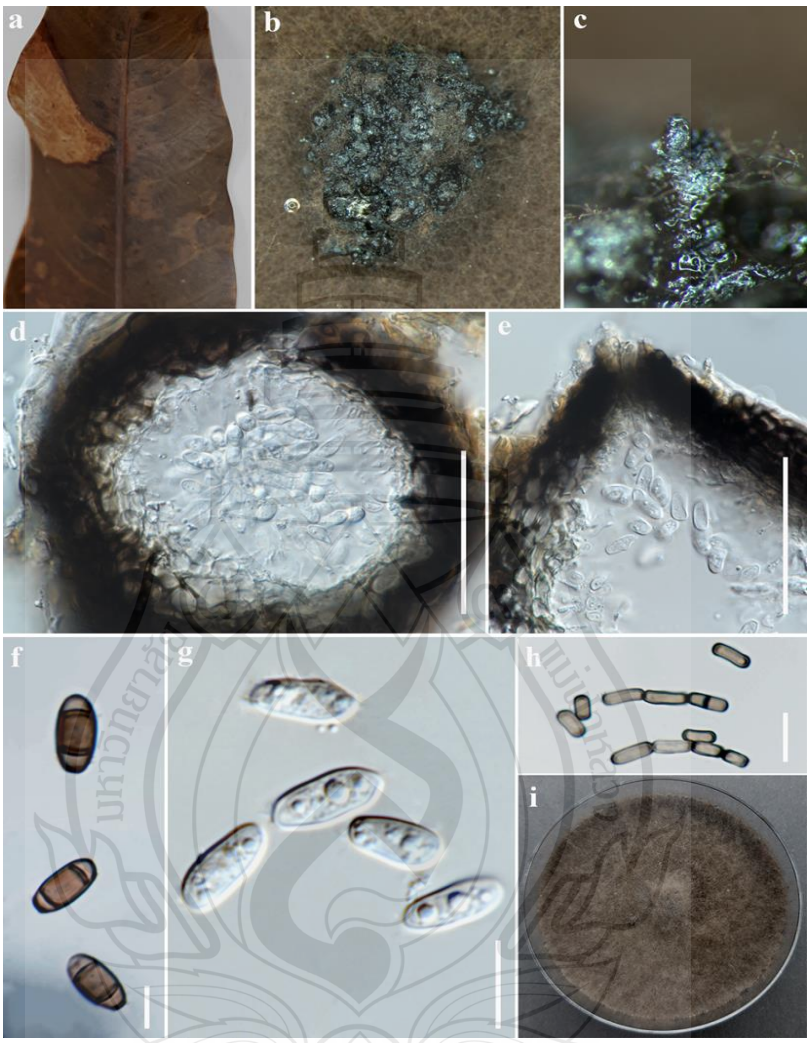

Note **a**. Symptomatic mango leaf **b**, **c**. Fruiting bodies produced on PDA **d**. Cross section of pycnidium **e**. Pycnidial wall and ostiole **f**. Conidia of coelomycete synanamorph produced on PDA **g**. Conidia of coelomycete synanamorph produced on natural substrate **h**. Arthroconidia (disarticulating aerial mycelium) produced on PDA **i**. Upper view of colonies on PDA; Scale bars: **d**, **e** = 50 µm, **f**–**h** = 10 µm

Figure 8.34 *Neoscytalidium dimidiatum* (MFLU 24-0446)

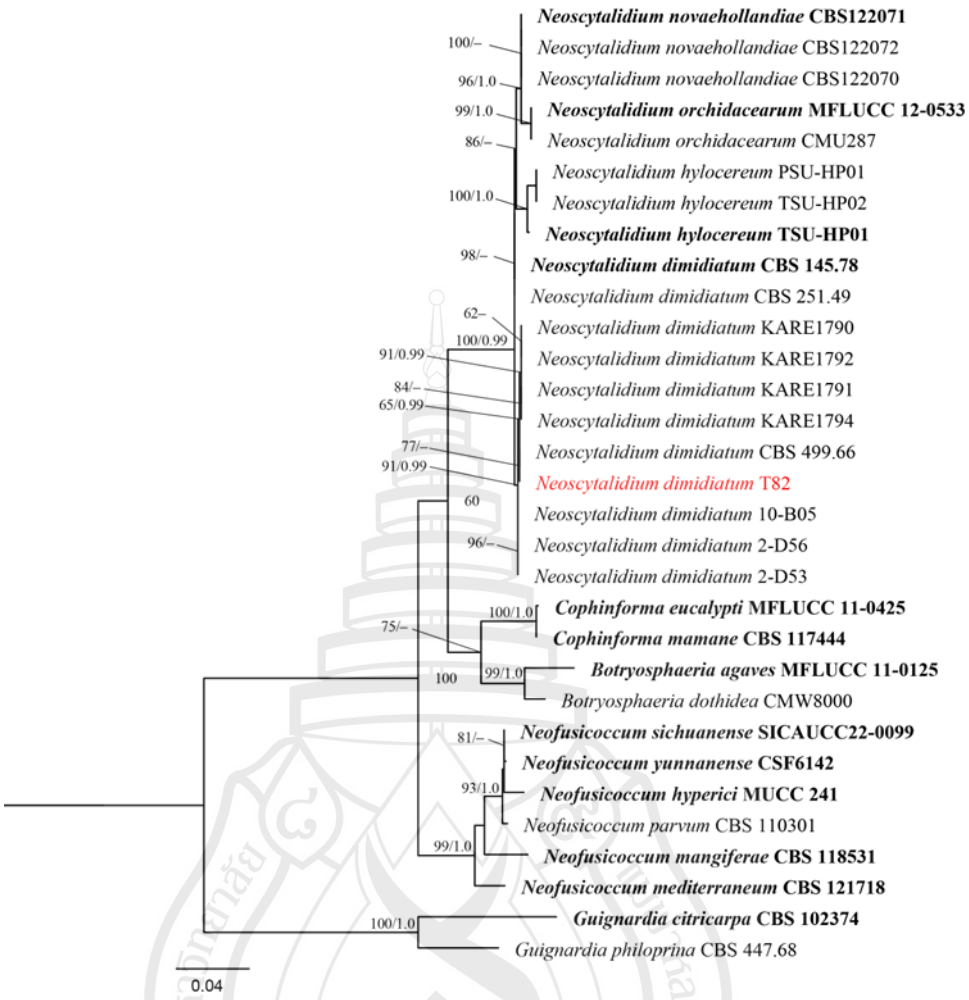

Note Maximum likelihood support values ≥ 50% and bayesian posterior probabilities ≥ 0.90 are shown near the nodes, respectively. The tree is rooted with *Guignardia citricarpa* (CBS 102374) and *Guignardia philoprina* (CBS 447.68). Isolates from this study are in red and ex-type strains are in bold

Figure 8.35 Maximum Likelihood (ML) tree of *Neoscytalidium* based on the combined ITS, *EF1-α*, and *tub2* sequence dataset

Pestalotiopsis Steyaert, Bull. Jard. bot. État Brux. 19: 300 (1949)

Based on the morphological characterisation, Steyaert (1949) established pestalotiopsis to accommodate species formerly classified within *Pestalotia*. However, Maharachchikumbura et al. (2014) re-evaluated *Pestalotiopsis* using both morphological characteristics and molecular analysis, leading to transferring many species into newly erected genera, *Neopestalotiopsis* and *Pseudopestalotiopsis*. Species

of *Pestalotiopsis* have endophytic, pathogenic, and saprobic life stages (Maharachchikumbura et al., 2011; Wu et al., 2022). As pathogens, the species cause various plant diseases, such as blight, leaf necrosis, leaf spots, fruit rot, dry flower disease, dieback disease, canker, and postharvest diseases (Akinsanmi et al., 2017; Chen et al., 2012; Ding et al., 2009; Keith, 2008; Palou et al., 2015; Ren et al., 2021; Sowndhararajan et al., 2013). *Pestalotiopsis* species have also gained attention due to their diverse and complex secondary metabolites production (Wu et al., 2022).

Pestalotiopsis humicola Maharachch., K.D. Hyde & Crous (2014)

Figure 8.36

Index Fungorum: IF 821661; Facesoffungi: FoF 17016

Description: See Maharachchikumbura et al. (2014)

Material examined: Thailand, Chiang Rai Province, Mueang Chiang Rai District, Mae Fal Luang University Campus, on leaves of *Mangifera indica* (Anacardiaceae), 16 October 2021, A. Armand, A4-2 (MFLU 24-0447; MFLUCC 24-0387, living culture).

Notes: In the current study, one strain was identified as *Pestalotiopsis humicola*, isolated from mango leaf blight. Phylogenetically, the strain clustered with the ex-type strain of *P. humicola*, with bootstrap support values of 71% ML and 0.93 PP (Figure 8.37). Morphologically, the strain was consistent with the ex-type strain described by Maharachchikumbura et al. (2014). Pairwise nucleotide comparisons revealed that strain A4-2 (MFLUCC 24-0387) exhibited 1/434 bp (0.2%) difference in the *tef1-α* and 4/475 bp (0.8%) nucleotide differences in the *tub2* locus compared to the ex-type strain. To our knowledge, this represents the first global report of *Pestalotiopsis humicola* causing leaf blight on *Mangifera indica*.

Note Symptomatic mango leaves **b**. Fruiting bodies and conidial mass produced on the PDA **c**. Conidiogenous cells **d**, **e**. Conidia **f**. Upper and reverse view of colonies on PDA; Scale bars: **c** = 10 µm, **d**, **e** = 20 µm

Figure 8.36 *Pestalotiopsis humicola* (MFLU 24-0447)

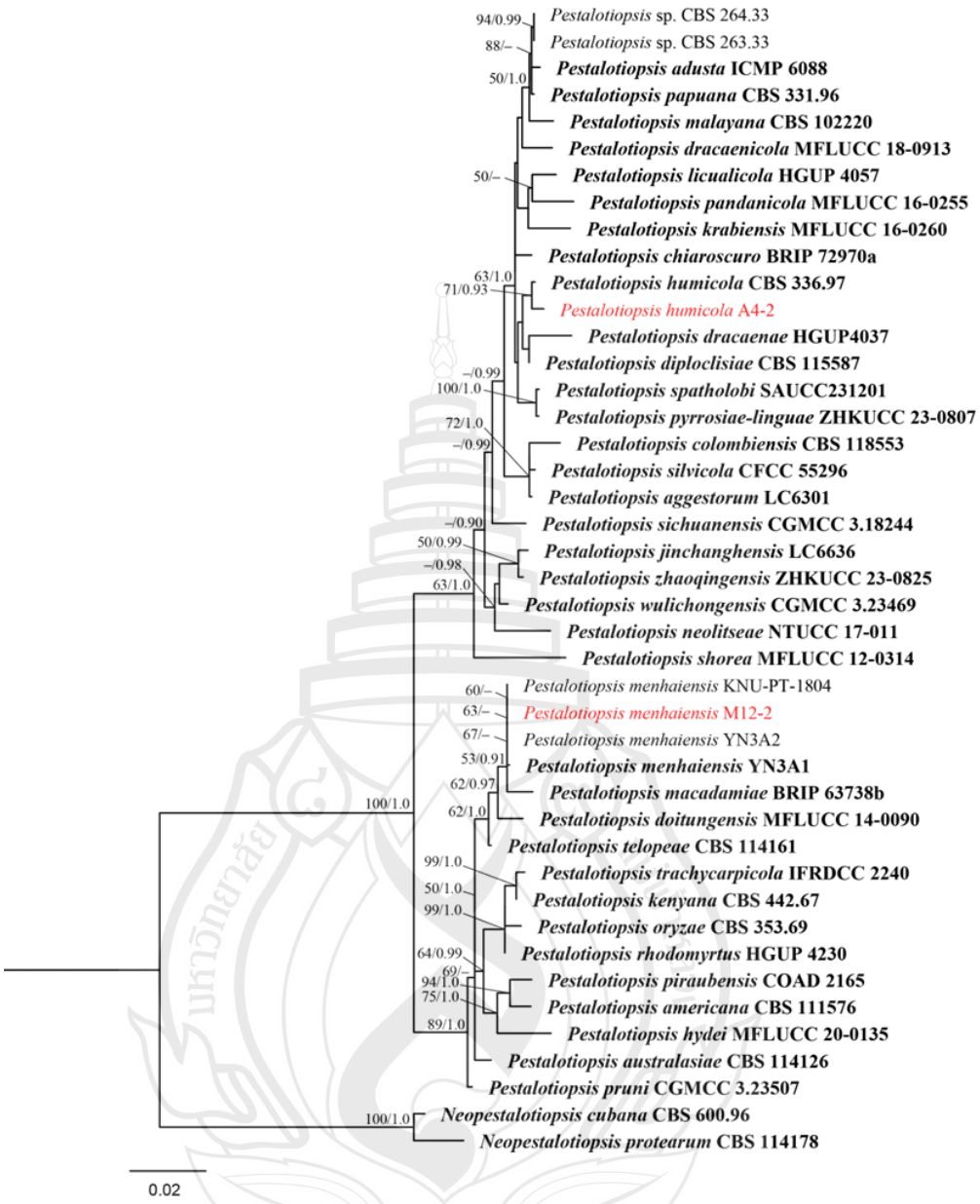

Note Maximum likelihood support values ≥ 50% and bayesian posterior probabilities ≥ 0.90 are shown near the nodes, respectively. The tree is rooted with *Neopestalotiopsis cubana* (CBS 600.96) and *Neopestalotiopsis protearum* (CBS 114178). Isolates from this study are in red, and ex-type strains are in bold

Figure 8.37 Maximum Likelihood (ML) tree of *Pestalotiopsis* based on the combined ITS, *EF1-α*, and *tub2* sequence dataset

Pestalotiopsis menhaiensis Y.C. Wang, X.C. Wang & Y.J. Yang (2019)

Figure 8.28

Index Fungorum: IF 827687; Facesoffungi: FoF 17017

Description: See Wang et al. (2019)

Material examined: Thailand, Chiang Rai Province, Mueang Chiang Rai District, Tha Sud, on leaves of *Mangifera indica* (Anacardiaceae), 26 April 2023, A. Armand, M12-2 (MFLU 24-0448; MFLUCC 24-0388, living culture).

Notes: The strain M12-2 (MFLUCC 24-0388) was grouped together with the ex-type strain of *Pestalotiopsis menhaiensis* with 67% ML bootstrap values (Figure 8.37). Morphological comparison showed that the strain M12-2 is similar to the type strain (CGMCC3.18250) (Wang et al. 2019). The newly isolated strain showed 1/526 BP (0.1%) nucleotide difference in ITS with the ex-type strain, and was identical with the ex-type strain in *tef1-α* and *tub2* regions. This is the first report of *Pestalotiopsis menhaiensis* isolated from mango leaf blight worldwide.

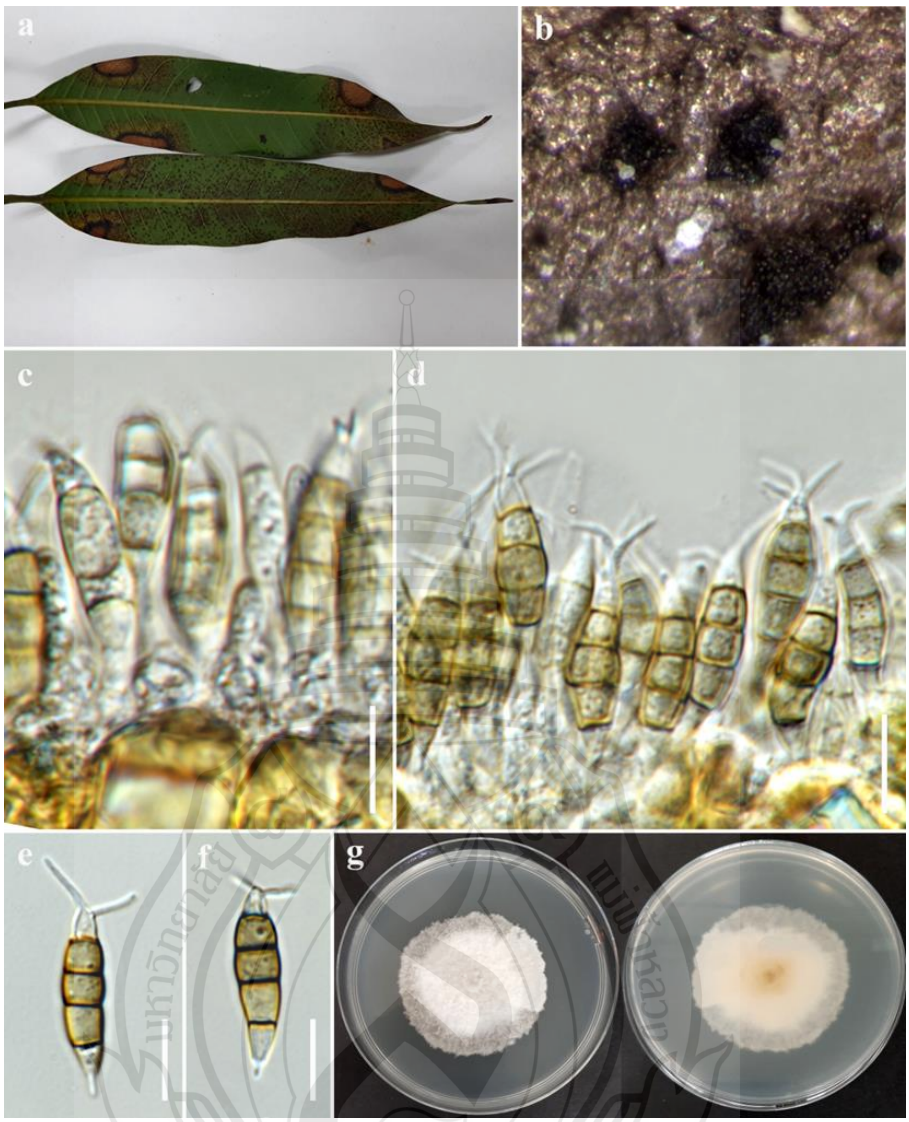

Note **a**. Symptomatic mango leaves **b**. Fruiting bodies produced on the leaf **c**, **d**. Conidiogenous cells, immature and mature conidia **e**, **f**. Conidia **g**. Upper and reverse view of colonies on PDA; Scale bars: **c**–**f** = 10 µm

Figure 8.38 *Pestalotiopsis menhaiensis* (MFLU 24-0448)

Pseudopallidocercospora A. Armand, Jayaward. & K.D. Hyde, gen. nov

Index Fungorum: IF 903315; Facesoffungi: FoF 17018

Etymology: Composed of "Pseudo-" meaning "false", combined with the genus name *Pallidocercospora.*

Type species: *Pseudopallidocercospora mangiferae* A. Armand, Jayaward. & K.D. Hyde.

Plant pathogenic, foliicolous. *Mycelia* immersed, rarely external. *Colonies* hypogenous. *Stromata* hypogenous, substomatal to intraepidermal, well-developed, sporodochial, textura globosa, pigmented. *Conidiophores* aseptate, i.e., conidiophores reduced to conidiogenous cells, arising from stromatic cells, caespitose, straight or flexuous, lageniform or pyriform, walls subhyaline to pale olivaceous, thin-walled and smooth, unilocal, determinate (not proliferating), apical conidiogenous locus not conspicuous, obtuse to subtruncate, locus wall neither thickened nor darkened. *Conidia* solitary, rarely in disarticulating chains, cylindrical, subcylindrical to obclavate, pale olivaceous, straight, flexuous to irregularly shaped, septa few, walls smooth, hila obtuse to subtruncate, neither thickened nor darkened.

Notes: *Pseudopallidocercospora* is morphologically intermediate between *Pallidocercospora* (pale olivaceous to olivaceous brown, thin-walled, smooth conidia and conidiophores, neither thickened nor darkened conidiogenous loci and hila; see Crous et al., 2004a, 2013) and *Scolecostigmina* (conidiophores formed in sporodochial conidiomata with well-developed stromata; see Braun et al., 1999; Crous et al., 2013). However, it is morphologically distinguished from both *Pallidocercospora* and *Scolecostigmina*. It differs from *Pallidocercospora* by forming well-developed sporodochial stromata, absence of red crystals in agar, and forming conidia in disarticulating chains in vivo. *Pseudopallidocercospora mangiferae* is differentiated from *Scolecostigmina* spp. by producing pale olivaceous fascicles of conidiophores, and pale, thin-walled, smooth conidia; while *Scolecostigmina* spp. form brown to dark brown fascicles, conidiophores, and conidia, which often have somewhat thickened and ornamented walls.

Pseudopallidocercospora mangiferae A. Armand, Jayaward. & K.D. Hyde, sp. nov.

Figure 8.39

Index Fungorum: IF 903316; Facesoffungi: FoF 17019

Etymology: Species epithet refers to the host genus from which the fungus was isolated.

Plant pathogenic, foliicolous. *In planta*: Sexual morph: not observed. Asexual morph: *Mycelium* immersed, rarely external. *Colonies* hypogenous, greenish olivaceous, *Stromata* hypogenous, substomatal to intraepidermal, well-developed,

semi-immersed, 50–73 µm diam., textura globosa, pale brown to brown. *Conidiophores* aseptate, reduced to conidiogenous cells, 5.5–9(–12) µm long, arising from stromatic cells, caespitose or sporodochial, or occurring singly, arising from superficial hyphae, pale olivaceous, straight to flexuous, lageniform or pyriform, cylindrical when occurring singly, aseptate, thin-walled, smooth, unilocal, determinate (non-proliferating) apical conidiogenous locus inconspicuous, obtuse to subtruncate, neither thickened nor darkened. *Conidia* solitary, cylindrical, subcylindrical to obclavate, subhyaline to pale olivaceous, flexuous or irregular in shape, rarely straight, guttulate, thin- and smooth-walled, 9.5–19 µm long ($\bar{x}$ = 13.7 µm), 2.5–3.7 µm wide ($\bar{x}$ = 3 µm), obtuse at the apex, 0–4-septate, hila obtuse to subtrunacte, 0.5–0.9 µm wide, neither thickened nor darkened.

Culture characteristics: Colonies on MEA reaching 10 mm in diam. after 20 days, with raised to convex surface, folded, and irregular undulate margin; aerial mycelia sparse; surface greenish olivaceous, reverse olivaceous black; growth rate 11–13 mm in 20 d. Colonies on PDA with raised to convex surface, folded, and with irregular undulate margin; aerial mycelia sparse; surface greenish olivaceous or olivaceous buff, reverse olivaceous black.

Material examined: Thailand, Chiang Rai Province, Mueang Chiang Rai District, Tha Sud, on leaves of *Mangifera indica* (Anacardiaceae), 8 March 2022, A. Armand, H2 (MFLU 24-0449 holotype; MFLUCC 24-0389, ex-type living culture); Thailand, Chiang Rai Province, Mueang Chiang Rai District, Tha Sud, on leaves of *Mangifera indica*, 08 March 2022, A. Armand, H2-2 (MFLUCC 24-0390).

Notes: The pairwise nucleotide comparison between *Pseudopallidocercospora mangiferae* and the type species of *Pallidocercospora*, *Pallidocercospora heimii* (CBS 110682), revealed 9/728 bp (2%; no gaps) differences in LSU, 7/452 bp (2%; no gaps) differences in ITS, and 90/880 bp (11%; no gaps) differences in *rpb2*. The pairwise nucleotide comparison between *Pseudopallidocercospora mangiferae* and type species of *Scolecostigmina*, *Scolecostigmina mangiferae* (CBS 125467, neotype), showed 11/728 bp (2%; no gaps) differences in LSU, 19/451 bp (5%; no gaps) differences in ITS, and 69/816 bp (9%; no gaps) differences in *rpb2*. The phylogenetic analysis of the combined sequence data of partial LSU, ITS, and *rpb2* supported the separation of *Pseudopallidocercospora* from allied genera, clustering in a separate clade from the

molecularly closest genus, *Scolecostigmina*, by 68%/55% (ML/MP) bootstrap values. The two obtained strains clustered together with 100%/100%/1.00 (ML/MP/PP) support values (Figure 8.40).

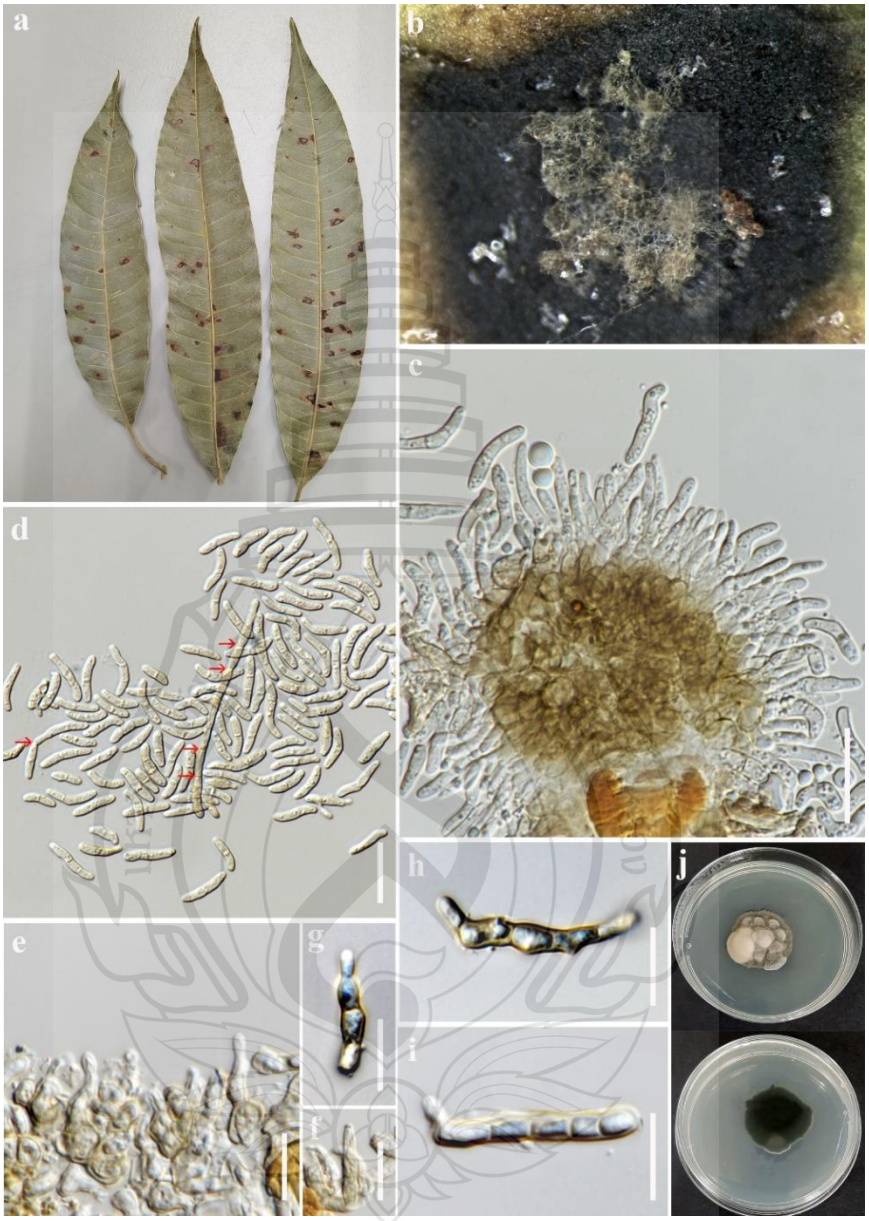

Note **a**. Symptoms **b**. Conidiomata formed on the underside of the leaf **c**. Stroma, conidiophores and conidial attachment **d**. Solitary conidia and the conidia formed in disarticulating chains (arrows) **e**. Conidiogenous cells **f**. Solitary conidiophore arising from a superficial hypha **g**–**i**. Germinating conidia **j**. Upper and reverse view of colonies on PDA; Scale bars: **c**, **d** = 20 µm, **e**, **i** = 10 µm

Figure 8.39 *Parapseudocercospora mangiferae* (MFLU 24-0449 holotype)

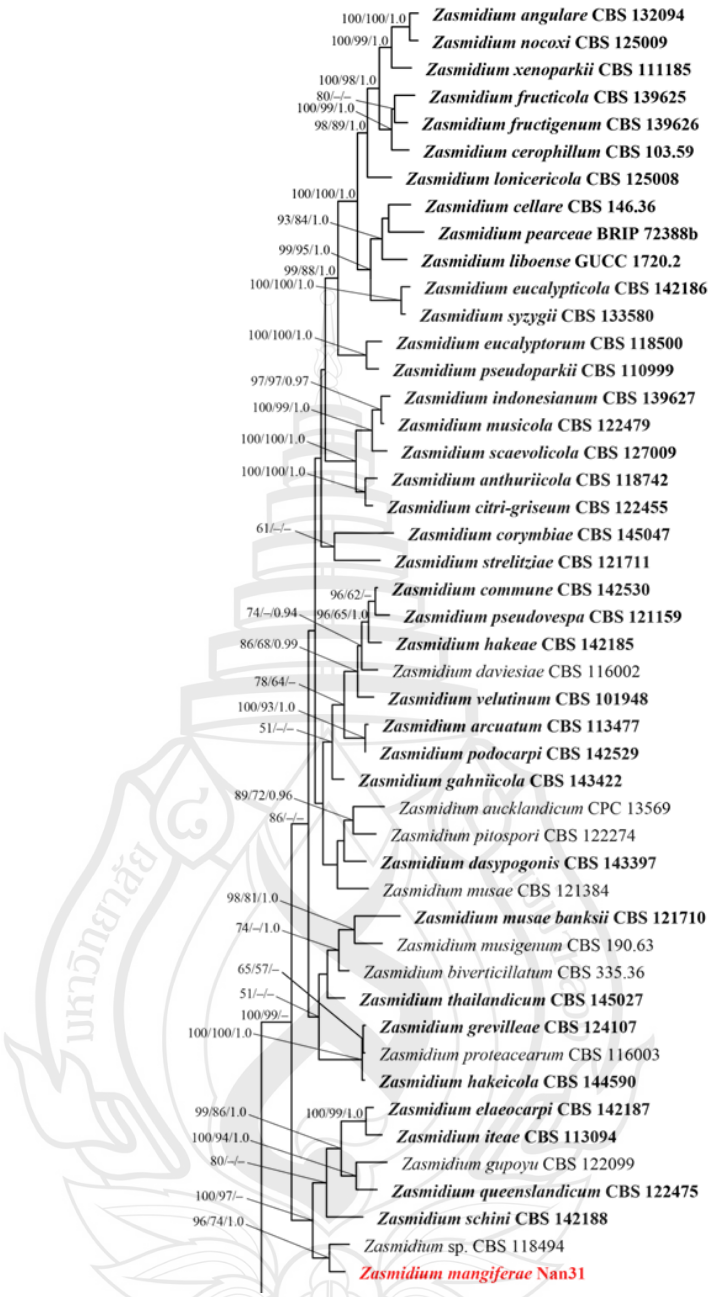

Note Maximum likelihood and maximum parsimony bootstrap support values ≥ 50% (BT) as well as bayesian posterior probabilities ≥ 0.90 (PP) are shown respectively near the nodes, respectively. The tree is rooted with *Cladosporium cladosporioides* (CBS 112388) and *Cladosporium ramotenellum* (CBS 133.29). Isolates from this study are in red, and ex-type strains are in bold

Figure 8.40 Maximum likelihood (ML) tree of *Zasmidium*, *Pseudopallidocercospora*, and allied genera based on the combined LSU, ITS, and *rpb2* sequence dataset

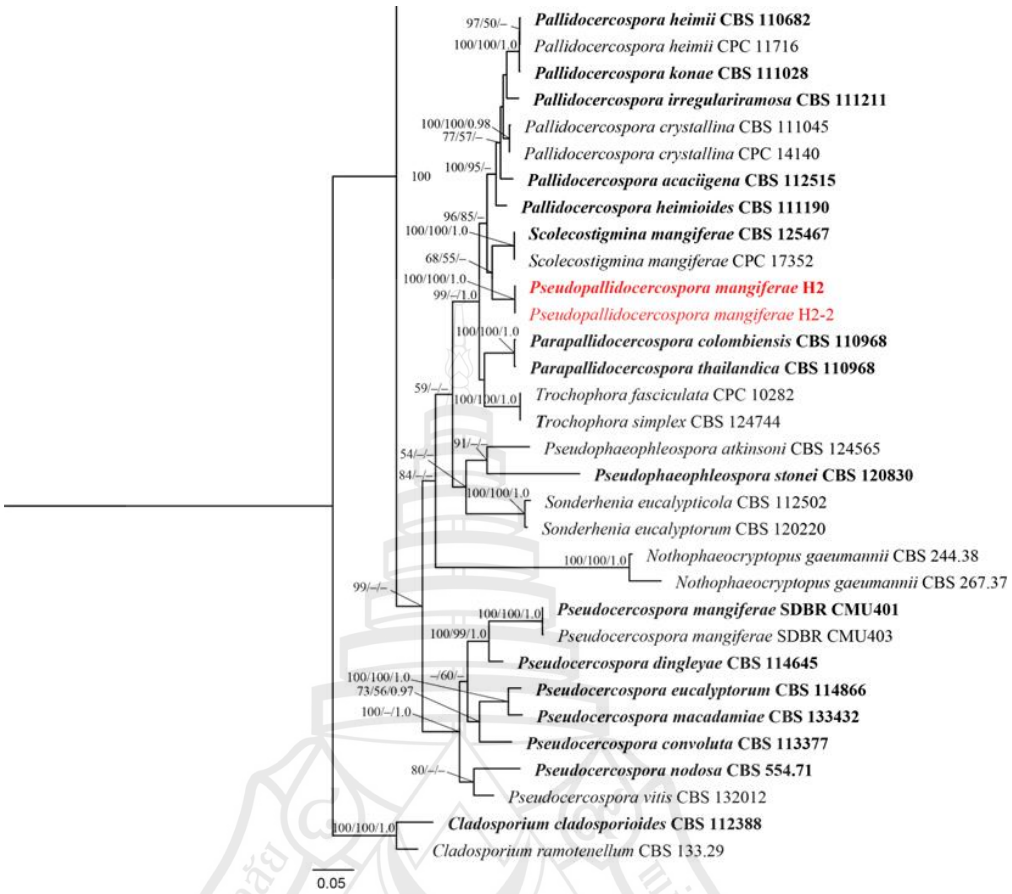

Figure 8.40 (continued)

Zasmidium Fr., Summa veg. Scand., Sectio Post. (Stockholm): 407 (1849)

Zasmidium was established by Fries in 1849. The type species of *Zasmidium*, *Z. cellare*, clusters in the Mycosphaerellaceae (Arzanlou et al., 2007). This genus is a Stenella-like hyphomycete; however, the type species of *Stenella*, *S. araguata*, belongs to Teratosphaeriaceae (Arzanlou et al., 2007). Broun et al. (2010) synonymized many species with *Zasmidium* which were formerly considered as *Stenella* and *Cercospora*, while confining *Stenella* s. str. (Teratosphaeriaceae) to *S. araguata*. *Zasmidium* species are mostly associated with leaf spots, and isolated from different plant families, such as Amaryllidaceae, Araliaceae, Asparagaceae, Asteraceae, Dioscoreaceae, Myrtaceae, Rosaceae, Convolvulaceae (Braun et al., 2010; Singh et al., 2014).

Zasmidium mangiferae A. Armand, Jayaward. & K.D. Hyde, sp. nov.

Figure 8.41

Index Fungorum: IF 903317; Facesoffungi: FoF 17020

Etymology: Named after the host plant genus, *Mangifera*.

Pathogenic on mango leaves. Sexual morph: Not observed. Asexual morph in vitro: On SNA hyphomycetous. *Hyphae* septate, branched, pale brown to brown, verruculose, 2–3.5 µm wide. *Stromata* superficial, dark brown, 67–81 µm diam. *Conidiophores* arising singly as lateral branches of superficial hyphae, or fasciculate, arising from stromata, macronematous, mononematous, straight, unbranched, thick-walled, smooth, 4–8-septate, swollen at the base, non-geniculate, brown at the below, becoming pale brown toward the apex, 35–83 µm long, 2.5–4 µm wide. *Conidiogenous cells* integrated, terminal, 12–20 µm long, proliferation sympodial, polyblastic, cylindrical, non-geniculate. *Conidiogenous loci* (scars) thickened and darkened, 0.5–1 µm wide. *Conidia* acropleurogenous, holoblastic, solitary, 1–6-septate, finely verrucose, guttulate, pale brown to brown, obclavate, straight, rarely slightly curved, (12–)20–43(–59) µm long and 4–6 µm wide, apex obtuse to rounded. *Hila* truncate or subtruncate, thickened and darkened, 1–1.5 µm wide.

Culture characteristics: Colonies on MEA raised or with convex surface, folded, and with irregular undulate margin; aerial mycelia rare; surface olivaceous greenish black, reverse olivaceous black; growth rate 14–15 mm in 20 d. Colonies on PDA raised or with convex surface, folded, and with irregular undulate margin; aerial mycelia sparse; surface greenish black, reverse olivaceous black; growth rate 13–14 mm in 20 d.

Material examined: Thailand, Nan Province, Phu Phiang District, Mueang Chang, on leaves of *Mangifera indica* (Anacardiaceae), 8 September 2022, A. Armand, Nan31 (MFLU 24-0450 holotype; MFLUCC 24-0391, ex-type living culture).

Notes: Based on the phylogenetic analysis of combined LSU, ITS, and *rpb2* sequence data, the strain Nan31 (MFLUCC 24-0391) constitutes a distinct clade, comprising *Zasmidium* sp. (CBS 118494), showing 96%/74%/1.00 (ML/MP/PP) support values (Figure 8.40). *Zasmidium* sp. (CBS 118494) was initially studied by Crous et al. (2006c) as *Mycosphaerella* sp. isolated from *Eucalyptus* sp. with unknown anamorph. Later, Videira et al. (2017) transferred it to *Zasmidium* based on multi-locus phylogenetic analysis of the LSU, ITS, and *rpb2* combined dataset. However, the strain was retained as *Zasmidium* sp. due to its sterility in culture and the absence of fungarium material. In the current study, the *rpb2* amplification for strain Nan31 was unsuccessful,

yet it differs from *Zasmidium* sp. (CBS 118494) by 17 nucleotide polymorphisms in the LSU region (17/728 bp (2.3%)) and 12 nucleotide differences in the ITS region (12/460 bp (2.6%)). Therefore, this strain is introduced as a new taxon herein.

Note **a**. Symptoms on the leaf **b**, **c**. Stromata produced on SNA **d**–**f**. Conidiophores and conidial arrangement **g**. Conidiophore **h**, **i**. Conidial attachment **j**. A conidiophore with thickened and darkened conidiogenous loci (scars) **k**, **l**. Conidia **m**. Upper and reverse view of colonies on PDA. Scale bars: **g**–**l** = 20 µm

Figure 8.41 *Zasmidium mangiferae* (MFLU 24-0450, holotype)

8.3.5 Haplotype Assignment and Networks of *Colletotrichum asianum*

The haplotype diversity and haplotype networks for *Colletotrichum asianum* were performed using single data sets of ITS. The ITS dataset consisted of 220 strains isolated from mango and 486 sites (excluding sites with gaps or missing data = 312). The ITS dataset yielded 8 haplotypes, and haplotype diversity (Hd) = 0.5936 (Figure 8.42). Based on the haplotype analyses, *C. asianum* did not show a clear grouping of isolates based on the countries from which they were reported. Analyses of the ITS sequence data showed that two haplotypes were most common (H1 and H2) (Figure 8.42). The H1 haplotype represents most of the *C. asianum* isolates from Australia, followed by Ghana and Thailand, while the H2 haplotype represents most of the *C. asianum* isolates from China, followed by Brazil. Additionally, only isolates from China were included in the H5 haplotype (Figure 8.42).

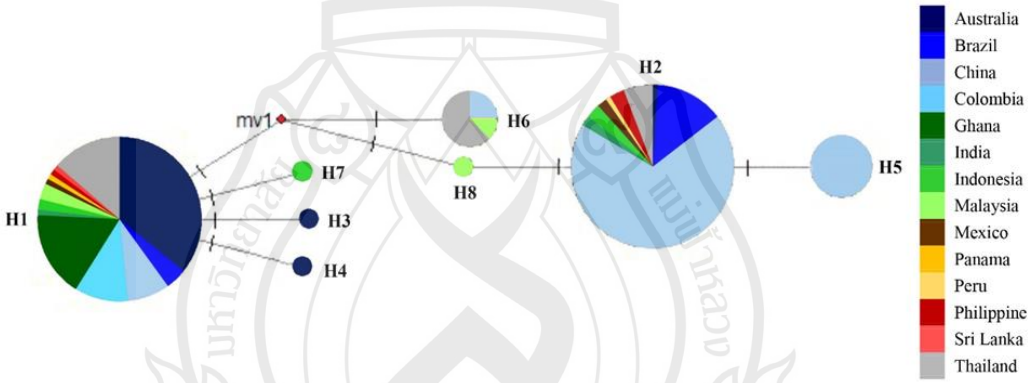

Note Circle sizes are proportional to haplotype frequency. Colours represent the different countries that *C. asianum* isolates were reported. H1–H8 represent the haplotypes. The figure legend shows the countries where *C. asianum* isolates were reported

Figure 8.42 Haplotype network generated for the ITS sequences data

8.3.6 Pathogenicity Testing

All tested isolates were pathogenic to wounded mango leaves and fruits except P20 on mango leaves, and M14-4, MF41-2, MF172-1, and MF172-3 on mango fruits. The aggressiveness of the tested isolates on mango fruits differed significantly (Figure 8.43, 8.44), with lesion diameters ranging from 0.11 cm to 2.83 cm. Among the 20 isolates tested on fruits, 8 (40%) isolates were strongly virulent, 7 (35%) isolates were

moderately virulent, 1 (5%) isolate was weakly virulent, and 4 (20%) isolates were non-virulent (Table A14). Among the 40 isolates tested on mango leaves, 12 (30%) isolates were strongly virulent, 22 (55%) isolates were moderately virulent, 5 (12.5%) isolates were weakly virulent, and 1 (2.5%) isolate was non-virulent (Table A14). The least virulent strains on fruits were MF172-1 and MF172-3, while the most virulent strain was M4 (Figure 8.44). The aggressiveness of the tested isolates on mango leaves was also significantly different (Figure 8.45, 8.46), and the diameters of disease lesions varied from 0.70 cm to 2.46 cm. The least virulent strain on leaves was T79-3, while the most virulent strain was P22-2 (Figure 8.46). Using the virulence scale, 20 isolates (33.33%) were strongly virulent, 29 isolates (48.33%) were moderately virulent, 6 isolates (10%) were weakly virulent, and 5 (8.33%) isolates were non-virulent.

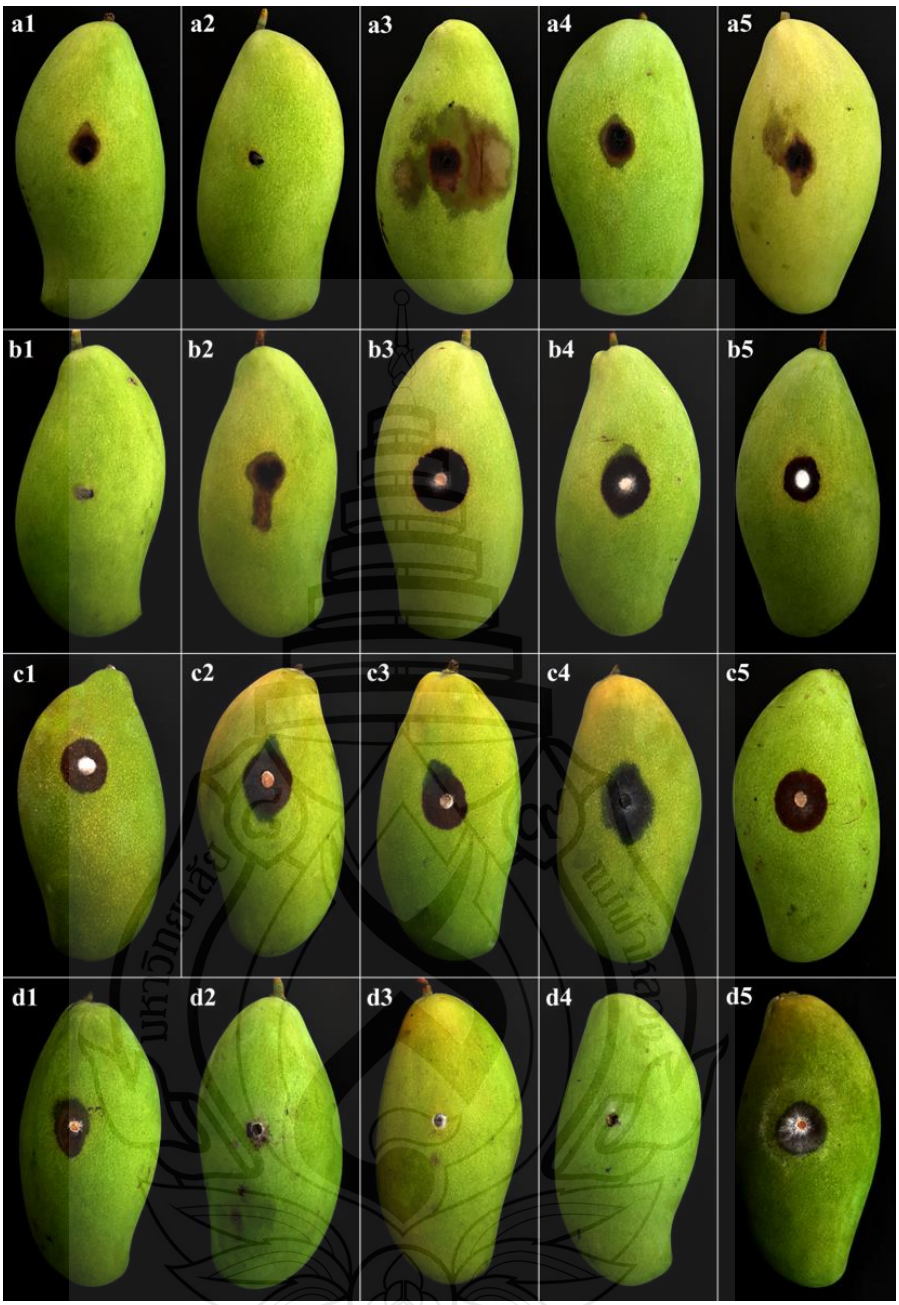

Note **a1**–**b1** *Botryosphaeria* spp.; **b2** *Neoscytalidium dimidiatum*; **b3**–**c5** *Colletotrichum* spp.; **d1**–**d5** *Neopestalotiopsis* spp.; Strains: **a1**: M10 **a2**: M10-2 **a3**: M14 **a4**: M14-2 **a5**: M14-3 **b1**: M14-4 **b2**: T82 **b3**: M4 **b4**: M4-2 **b5**: M13 **c1**: M18-2 **c2**: A20-2 **c3**: P25 **c4**: R35-2 **c5**: R50 **d1**: MF116-1 **d2**: MF41-2 **d3**: MF172-1 **d4**: MF172-3 **d5**: MF149-1

Figure 8.43 Pathogenicity testing on mango fruits, photographed 7 days post-incubation

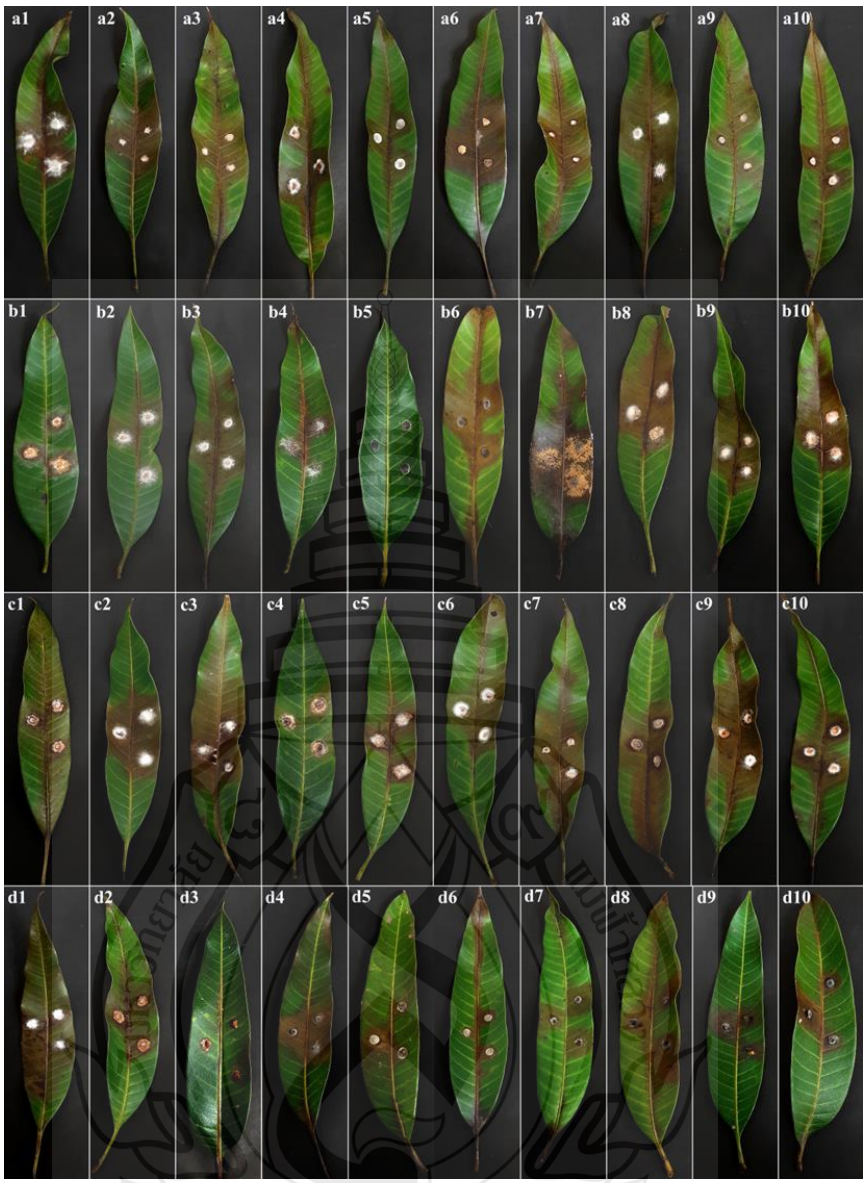

Note **a1**–**a8** *Neopestalotiopsis* spp.; **a9–c8** *Colletotrichum* spp.; **c9–d6** *Diaporthe* spp.; **d7** *Botryosphaeria* spp.; **d8** *Zasmidium mangiferae*; **d9**, **d10** *Pseudopallidocercospora mangiferae*); Strains: **a1**: M12-2 **a2**: Nan31-3 **a3**: T79-2 **a4**: AS-3 **a5**: C20 **a6**: A4-2 **a7**: MF108-1 **a8**: MF24-2 **a9**: As-1 **a10**: As-2 **b1**: P6 **b2**: P7-2 **b3**: P9 **b4**: P9-2 **b5**: P20 **b6**: P22 **b7**: P22-2 **b8**: P48 **b9**: P49 **b10**: P98 **c1**: P100 **c2**: A18 **c3**: A19 **c4**: MF15-4 **c5**: MF24-5 **c6**: T117 **c7**: T117-2 **c8**: C51-2 **c9**: A4-3 **c10**: MF15-5 **d1**: MF172-2 **d2**: MF24-7 **d3**: Nan32-2 **d4**: C27-1 **d5**: T79 **d6**: T79-3 **d7**: P21-2 **d8**: Nan31 **d9**: H2 **d10**: H2-2

Figure 8.44 Pathogenicity testing on mango leaves, photographed 7 days post-incubation

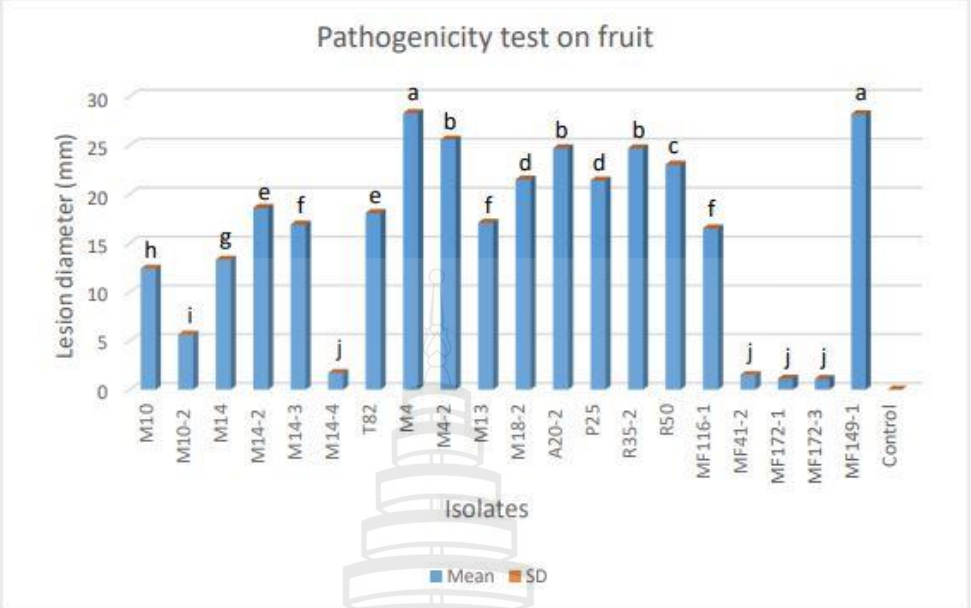

Note Mean is shown in blue and standard deviation is shown in orange. Significant variations in means are indicated by different letters above the bars ($p < 0.05$)

Figure 8.45 Lesion area (mm) progression of the tested strains on mango fruits at 7 days post-inoculation

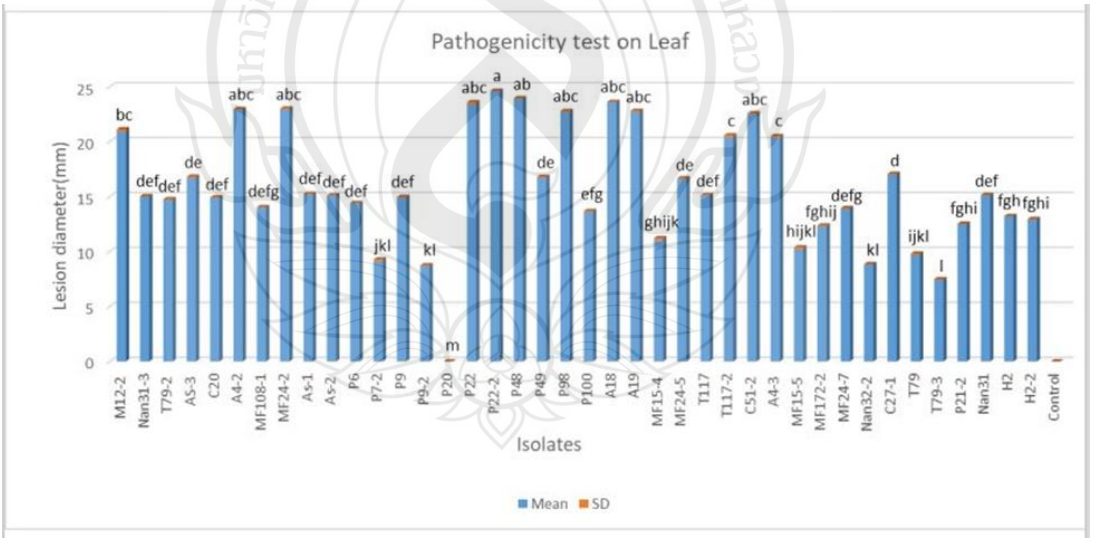

Note Mean is shown in blue and standard deviation is shown in orange. Significant variations in means are indicated by different letters above the bars s ($p < 0.05$)

Figure 8.46 Lesion area (mm) progression of the tested strains on mango leaves at 7 days post-inoculation

8.4 Discussion

High species diversity of pathogenic fungi was found associated with mango from four provinces in northern Thailand. *Botryosphaeria* and *Neofusicoccum* were only associated with fruit rot, while *Diaporthe* spp. were only isolated from symptomatic leaves. *Colletotrichum* and *Neopestalotiopsis* species were associated with both mango fruits and leaves. However, *Neopestalotiopsis* showed higher species diversity on mango leaves than those from mango fruits. *Colletotrichum* was the predominant genus, and *Colletotrichum asianum* was the most abundant species causing anthracnose, which was consistent with the studies conducted by Lima et al. (2013), Mo et al. (2018), Li et al. (2019). Phoulivong et al. (2010) demonstrated that *Colletotrichum gloeosporioides* is not a prevalent pathogen in tropical regions and is not responsible for causing anthracnose in mango in Laos and Thailand. Consistent with these findings, this study revealed that none of the *Colletotrichum* strains isolated from mango were identified as *C. gloeosporioides*.

Pathogenicity testing showed that the virulence of species and even different strains within a species is significantly different. For instance, *Botryosphaeria scharifii* (M14-4) was non-virulent on mango fruit, while *B. scharifii* (M14-2) was assessed as moderately virulent. Both *Pestalotiopsis* species demonstrated strong virulence on mango leaves. Of the four strains that were non-virulent on mango fruits, three were identified as *Neopestalotiopsis* species: MF172-1 (*Neopestalotiopsis* sp. 1), MF41-2 (*N. mangifericola*), and MF172-3 (*N. rhododendri*). *Colletotrichum asianum* and *Neopestalotiopsis mangiferae* were the most virulent species on mango fruits, while a greater number of species exhibited strong virulence on mango leaves. *Colletotrichum asianum* strains exhibited varying levels of virulence, ranging from moderately to strongly virulent, with the exception of one strain (P20), which was non-virulent.

The haplotype diversity and networks for *Colletotrichum asianum* were generated using ITS sequence. The data of genetic loci for *Colletotrichum asianum* were not available for the analysed strains or were found non-informative for the haplotype assignment. The dataset consisted of 220 strains of *Colletotrichum asianum*, which were identified using multi-locus phylogenetic analysis from 14 countries. The

calculated haplotype diversity of *C. asianum* was more than 0.5 (Hd > 0.5), suggesting that *C. asianum* has a high genetic diversity. The life cycle of *Colletotrichum* species comprises a sexual and an asexual stage (Wharton & Diéguez-Uribeondo, 2004). Therefore, a hypothesis for the high genetic diversity of *C. asianum* is the occurrence of sexual recombination between strains of the species. Another mechanism by which genetic diversity can be generated in *Colletotrichum* populations is through vegetative compatibility (Correll et al., 1994, 2004). Vegetative compatibility in fungi allows strains to fuse hyphae through anastomosis, forming heterokaryons when genetically distinct strains combine, with isolates capable of fusion belonging to the same vegetative compatibility group (VCG). VCGs help study population structures in fungi such as *Colletotrichum* by identifying groups that share a gene pool (Brooker et al., 1991; Chacko et al., 1994; Correll et al., 2000; Katan, 2000).

Phylogenetic analysis using multi-locus datasets, combined with morphological characterisation, revealed one new genus, five new species, twelve new host records, and six new geographical records of pathogenic fungi associated with mango in northern Thailand. This study highlights the potential for future investigations on pathogenic fungi associated with *Mangifera indica* to uncover additional new taxa and provide a deeper understanding of species diversity on this host.

Research on fungal species infecting mangoes in Thailand has largely focused on anthracnose caused by *Colletotrichum* spp. (Dinh et al., 2003; Laksanaphisut et al., 2019; Rattanakreetakul et al., 2023), while there have been no comprehensive investigations exploring the diversity of pathogenic genera and species diversity using the most reliable molecular markers and gene combinations, nor studies assessing their virulence on mango leaves and fruits. Therefore, this study represents the most comprehensive research to date on pathogenic fungal species associated with mango in Thailand. The findings have broad implications, particularly in the accurate identification of closely related species, which is crucial for mapping the geographical distribution of specific fungal pathogens, developing effective quarantine regulations, and understanding the epidemiology of mango diseases.

There have been no comprehensive studies focusing on endophytic fungi in mangoes from Thailand. Research from other countries has predominantly centred on the antagonistic activities of isolated endophytes, often overlooking modern methods

for precise species identification. The findings of this study suggest that there may be considerable species diversity associated with *Mangifera indica* in Thailand. Therefore, a comprehensive investigation into endophytic fungi associated with *Mangifera indica* is recommended, employing polyphasic approaches for species identification. Such methods could uncover high levels of cryptic species that may have been overlooked due to the isolation techniques used for pathogenic fungi. Furthermore, this approach may facilitate the discovery of endophytic fungal species with potential antagonistic properties against mango pathogens.

CHAPTER 9

FUNGAL FOOTPRINTS IN THE TROPICS: AN UPDATE ON SPECIES DIVERSITY LINKED TO DISEASED FRUIT CROPS AND ORNAMENTALS IN NORTHERN THAILAND

9.1 Introduction

Agriculture, encompassing horticulture and floriculture, is fundamental to the global economy, serving as a key driver of economic activity, environmental sustainability, and both social and economic development (Antle et al., 2020; Sarris, 2001). This is particularly significant in developing nations, where these sectors often form the backbone of the economy (Alvarado et al., 2021). Their importance is further emphasised by their role in promoting food security and fostering human development (Baba et al., 2010; Byerlee et al., 2009). In Thailand, where both agriculture and horticulture are crucial, approximately 54.4% of the population is involved in farming (Boonyanam, 2020). However, plant pathogenic fungi pose an ongoing threat to these sectors, impacting productivity (Jantasorn et al., 2016; Ristaino et al., 2021).

In 2020, the estimated area for cultivating ornamental plant species was 14,000 hectares (FAO: https://www.fao.org/family-farming/detail/en/c/1316738/). However, the actual production area is likely smaller, as some of this land was allocated for growing marigolds for feed ingredients and lotus for edible seeds. Widely cultivated crops include orchids, marigolds, roses, jasmine, lotus, and chrysanthemums. Of the total export value of 89.2 million USD in 2005, cut orchids accounted for the largest share at 63.5 million USD. Orchid plants and other plants followed in distant second and third places, generating 11.2 million USD and 6.6 million USD, respectively (Thammasiri, 2014; Wannakrairoj, 2007).

Phytopathogenic fungi pose significant challenges to agriculture and global food security, leading to considerable losses in both crops and postharvest produce

(Abeywickrama et al., 2022; Crous et al., 2016; Gould, 2009; Jayawardena et al., 2020; Udayanga et al., 2020). These fungal pathogens can cause diseases affecting all parts of the plant, including roots, pseudostems, leaves, inflorescences, and fruits (Anuagasi et al., 2017; Bhunjun et al., 2021b; Vujanovic et al., 2000; Zimowska, 2008). They employ a range of advanced strategies to effectively colonise their host plants, initiating pathogenic effects that are often marked by the formation of specialised infection structures and the strategic release of virulence factors (Doehlemann et al., 2017). With a wide host range, plant pathogenic fungi display various parasitic behaviours, including both obligate and facultative parasitism (Capote et al., 2012). Furthermore, these fungi can have catastrophic consequences if they extend beyond their native ranges and invade new hosts (Case et al., 2022; Fones et al., 2017).

While plant pathogenic fungi are essential components of ecosystems, our understanding of many species remains limited and fragmented (Jayawardena et al., 2021a), highlighting a lack of available data (Hawksworth, 2001; Hawksworth & Lücking, 2017; Mueller & Schmit, 2007; Schmit & Mueller, 2007). This gap in fundamental taxonomic diversity information has significant implications across various biological fields (Bass & Richards, 2011). The accurate use of taxonomic names is crucial for effectively communicating information about fungi, particularly in plant pathology, as these names serve as vital links to data on fungal biology, host-specificity, geographic distribution, and associated risks (Crous et al., 2015a). Consequently, extensive sampling and thorough investigations, especially in tropical regions, are necessary to resolve uncertainties in fungal taxonomy, enhancing our understanding of their biology, ecological niches, distribution, and potential invasiveness (Bhunjun et al., 2022; Crous et al., 2006a; Crowther et al., 2014; Hawksworth, 2012; Hyde et al., 2018b; Jayawardena et al., 2021a). Moreover, accurately identifying and delineating plant pathogenic species is vital for developing effective disease control strategies and mitigating their adverse effects on food security (Crous et al., 2016; Jayawardena et al., 2021b; Rossman & Palm-Hernández, 2008; Udayanga et al., 2020; Wijayawardene et al., 2012).

Various fungal diseases impact economically significant fruit crops in Thailand. Tropical fruits are particularly vulnerable to infections by *Colletotrichum* species, which commonly cause anthracnose disease during both pre- and post-harvest phases

(Talhinhas & Baroncelli, 2023; Zakaria, 2021, 2022; Zhang Y. et al., 2023). These fungi are responsible for anthracnose and fruit rot in several key fruits, including mango, lychee, papaya, dragon fruit, guava, and avocado, thereby presenting considerable challenges for their production and marketing (Zakaria, 2021, 2022; Zhang Q. et al., 2023). *Lasiodiplodia* species are linked to cankers, decline, dieback, and fruit rot diseases affecting a wide range of tropical fruits in Thailand, such as avocado, mango, longan, mangosteen, strawberry, and melon (Chang-ngern et al., 2010; Trakunyingcharoen et al., 2014, 2015a; Pipattanapuckdee et al., 2019; Suwannarach et al., 2020; Zakaria, 2022; Phetphan et al., 2023). The genus *Cercospora*, known for its destructive impacts, has also been identified as infecting various host plants in Thailand (To-Anun et al., 2011). Other significant pathogenic genera reported in Thailand include *Pestalotiopsis*, *Neopestalotiopsis*, *Diaporthe*, *Pseudocercospora*, *Alternaria*, and *Fusarium* (Cheewangkoon et al., 2021; Huanaluek et al., 2021; Sunpapao et al., 2022; Pongpisutta et al., 2023).

9.2 Materials & Methods

9.2.1 Sample Collection, Fungal Isolation and Purification

Sample collection was conducted from 2021 to 2023 across various important plant species in northern Thailand, particularly in Chiang Rai, Kalasin, Nan, and Sakon Nakhon Provinces. Plant leaves, twigs, and fruits exhibiting symptomatic features were collected for the isolation of causal fungi. Symptomatic fruits and plant tissues were examined using a LEICA-EZ4 stereomicroscope, and fungal structures were photographed with an OLYMPUS SZX16 stereomicroscope. Further morphological analysis was conducted using a Nikon DS-Ri2 camera-equipped optical microscope.

Fungal isolation employed both direct and indirect methods, including single-spore and hyphal-tip isolation, following protocols by Senanayake et al. (2020). Direct isolation was performed on specimens with visible fruiting bodies, where conidial suspensions were prepared by transferring mature fruiting bodies to sterile water. A portion of conidial suspensions was streaked onto potato dextrose agar (PDA) (Merck, Germany) for culture for single-spore isolation. For samples lacking visible fruiting

bodies, the tissue isolation method was utilised. Plant tissues were cut into 5 mm² fragments from healthy and infected margins, then surface sterilised in 70% alcohol and 10% NaOHCl solution, followed by washing in sterilised distilled water. The dried fragments were placed on PDA media, and after 2–3 days, emerging fungal mycelia were transferred to new plates. Cultures were maintained at room temperature (27°C ± 2°C) for over a month to promote conidia production. Key morphological characteristics, such as conidial shape, size, and pigmentation, were measured. Cultures were deposited in the Mae Fah Luang University Culture Collection (MFLUCC), and specimens were housed in the University Fungarium (MFLU).

9.2.2 DNA Extraction and PCR Amplification

Genomic DNA was extracted from 14-day-old fresh mycelia grown on potato dextrose agar (PDA) at room temperature (28 ± 2 °C) using the DNA Extraction Kit (Omega Bio-Tek), in accordance with the manufacturer's instructions. Amplification procedures were performed in a total volume of 25 µL, which included 12.5 µL of 2 × Power Taq PCR Master Mix, 1 µL of each primer (20 µM), 9.5 µL of deionised water, and 1 µL of template DNA (5–10 ng). Polymerase chain reactions (PCR) were conducted using an Eppendorf thermal cycler (Master Cycler X50s) to amplify specific gene regions necessary for phylogenetic analysis. Various markers along with their respective primers and thermal cycling conditions are detailed in supplementary information (Table A15).

9.2.3 Phylogenetic Analyses

The obtained genetic sequences were analysed using a BLASTn search on the NCBI platform, followed by retrieval of reference sequences from the GenBank database. Each dataset was aligned using MAFFT v. 7 (https://mafft.cbrc.jp/alignment/server/) (Katoh et al., 2019). Alignments were refined with BioEdit v. 7.0.9.0 (Hall, 1999) and automatically trimmed using TrimAl v. 1.2 (Capella-Gutiérrez et al., 2009) with either the -gapthreshold (0.8) or -gappyout option. The optimal evolutionary model for each gene region was determined using jModelTest 2 v.2.1.6 on XSEDE, as described by Darriba et al. (2012).

Maximum likelihood (ML) analyses were performed with RAxML (Stamatakis 2006) as implemented in raxmlGUI 1.3 (Silvestro & Michalak, 2012) using the ML + rapid bootstrap setting and the GTRGAMMA substitution model with 1000 bootstrap

replicates. Maximum Parsimony (MP) analyses were performed with PAUP v. 4.0a169 (Swofford, 2002). All molecular characters were unordered and given equal weight; analyses were performed with gaps treated as missing data; the COLLAPSE command was set to MINBRLEN. MP analysis of the combined multi-locus matrix was done using 1000 replicates of heuristic search with random addition of sequences and subsequent TBR branch swapping (MULTREES option in effect, steepest descent option not in effect). Bootstrap analyses with 1000 replicates were performed in the same way, but using 10 rounds of random sequence addition and subsequent branch swapping during each bootstrap replicate. Multi-locus concatenated sequence datasets were used to perform pairwise homoplasy index (PHI) tests using Splits Tree 4 (version 4.14.2) to determine the recombination level (Fu et al., 2019). The phylograms were visualised in FigTree v. 1.4.0 and annotated in Adobe Illustrator CC 22.0.0 (Adobe Systems, San Jose, CA, USA).

9.2.4 Species Recognition

Recommendations given by Chethana et al. (2021), Jayawardena et al. (2021b), and Maharachchikumbura et al. (2021) were followed in species recognition in this study. *Diaporthe* species recognition followed the system recommended by Dissanayake et al. (2024) and Pereira et al. (2023, 2024).

9.3 Results

9.3.1 Sample Collection and Fungal Isolation

Between 2021 and 2023, more than 300 samples were collected and examined from a range of economically significant crops and ornamental plants. These samples encompassed various plant parts, including leaves, branches, and fruits at both pre- and post-harvest stages. From these samples, a total of 131 fungal isolates were obtained, subsequently purified, and preserved in cryogenic tubes under refrigerated conditions for future analyses.

9.3.2 Phylogenetic analyses

The 131 obtained strains were phylogenetically classified into one phylum (Ascomycota), two classes (Dothideomycetes and Sordariomycetes), six orders

(Amphisphaeriales, Botryosphaeriales, Diaporthales, Glomerellales, Hypocreales, Mycosphaerellales), eight families (Botryosphaeriaceae, Diaporthaceae, Glomerellaceae, Mycosphaerellaceae, Nectriaceae, Phyllostictaceae, Pseudoplagiostomataceae, Sporocadaceae), 13 genera, and 50 taxa, comprising 12 new species and 38 known species (Table A16).

The phylogenetic tree of *Fusarium* and allied genera (*Albonectria*, *Bisifusarium*, and *Neocosmospora*) was obtained using combined sequences of *tef1*, *rpb1*, *rpb2*, and *cmdA*. The alignment for the Fusarium species comprised 94 taxa, including 92 ingroup taxa and two outgroup taxa. The best-scoring ML tree with final optimisation had a likelihood value of -24085.4757. The matrix consisted of 428 distinct alignment patterns. Estimated base frequencies were as follows: A = 0.253, C = 0.268, G = 0.242, T = 0.235, with substitution rates AC = 0.872259, AG = 3.157199, AT = 1.044864, CG = 0.582022, CT = 5.706009, GT = 1.000000. The Bayesian posterior probabilities analysis using Markov chain Monte Carlo (MCMC) was evaluated using a final average standard deviation of the split frequencies of 0.002361. The maximum parsimonious dataset comprised 1187 constant characters (proportion = 0.48449), 1141 parsimony-informative and 122 parsimony-uninformative characters. The parsimony analysis resulted in one parsimonious tree (tree length = 4571, Consistency Index (CI) = 0.492, Retention Index (RI) = 0.894, and Homoplasy Index (HI) = 0.508).

Based on concatenated sequences of ITS, *act*, *cmdA*, *gapdh*, *his3*, and *tef1*, the phylogenetic analyses of *Cercospora* species were conducted. The alignment comprised 143 taxa, including 142 ingroup taxa and one outgroup taxon. The best-scoring ML tree with final optimisation had a likelihood value of -20135.090. The matrix consisted of 943 distinct patterns, 569 parsimony-informative, 301 singleton sites, and 1539 constant sites. Estimated base frequencies were as follows: A = 0.211, C = 0.301, G = 0.259, T = 0.228, with substitution rates AC = 1.10228, AG = 3.24535, AT = 1.14988, CG = 0.85592, CT = 4.14156, GT = 1.00000, and the tree-length = 1.809. The Bayesian posterior probabilities analysis using Markov chain Monte Carlo (MCMC) was evaluated using a final average standard deviation of the split frequencies of 0.009042.

Based on combined sequences of ITS, *gapdh*, *chs-1*, *act*, and *tub2*, the phylogenetic trees of the *Colletotrichum gloeosporioides* species complex were generated. The final alignment comprised 115 taxa, including 113 ingroup taxa and two outgroup taxa. The best-scoring ML tree with final optimisation had a likelihood value of -12353.985. The matrix consisted of 980 distinct patterns, 447 parsimony-informative, 298 singleton sites, and 1143 constant sites. Estimated base frequencies were as follows: A = 0.230, C = 0.298, G = 0.243, T = 0.229, with substitution rates AC = 1.18415, AG = 2.82001, AT = 1.27553, CG = 1.00877, CT = 5.31432, GT = 1.00000, and the tree-length = 0.985. The Bayesian posterior probabilities analysis using Markov chain Monte Carlo (MCMC) was evaluated using a final average standard deviation of the split frequencies of 0.021810.

The phylogenetic tree of *Diaporthe* was obtained using combined sequences of ITS, *tef1*, *tub2*, *cmdA*, and *his3*. The alignment for *Diaporthe* species comprised 153 taxa, including 152 ingroup taxa and one outgroup taxon. The best-scoring ML tree with final optimisation had a likelihood value of -27159.27159. The matrix consisted of 248 distinct alignment patterns. Estimated base frequencies were as follows: A = 0.187, C = 0.386, G = 0.219, T = 0.206, with substitution rates AC = 0.759337, AG = 2.564258, AT = 1.377225, CG = 0.803735, CT = 4.683510, GT = 1.000000. The maximum parsimonious dataset comprised 1130 constant characters (proportion = 0.473398), 858 parsimony-informative and 399 parsimony-uninformative characters. The Bayesian posterior probabilities analysis using Markov chain Monte Carlo (MCMC) was evaluated using a final average standard deviation of the split frequencies of 0.005197. The parsimony analysis resulted in one parsimonious tree (tree length = 4719, Consistency Index (CI) = 0.436, Retention Index (RI) = 0.874, and Homoplasy Index (HI) = 0.564).

A combined dataset of ITS, *tef1*, *tub2*, and *rpb2* was used to generate phylogenetic trees of *Lasiodiplodia*. The final alignment consisted of 83 taxa, including 82 ingroup taxa and one outgroup taxon. The best-scoring ML tree with final optimisation had a likelihood value of -7224.128515. The matrix consisted of 472 distinct alignment patterns with 14.49% completely undetermined characters. Estimated base frequencies were as follows: A = 0.221221, C = 0.286350, G = 0.265949, T = 0.226481, with substitution rates AC = 0.992273, AG = 4.017018, AT =

1.436597, CG = 0.908896, CT = 7.910412, GT = 1.00000, and the tree-length = 0.749991. The Bayesian posterior probabilities analysis using Markov chain Monte Carlo (MCMC) was evaluated using a final average standard deviation of the split frequencies of 0.005805.

A combined dataset comprising ITS, *tef1*, *tub2*, and *rpb2* loci was utilised to construct phylogenetic trees for the genus *Neofusicoccum*. The final alignment included 80 taxa, consisting of 79 ingroup taxa and one outgroup taxon. The best-scoring maximum likelihood (ML) tree, after final optimisation, achieved a likelihood value of -8303.725. The dataset contained 594 unique patterns, with 306 parsimony-informative sites, 197 singleton sites, and 1265 constant sites. The estimated base frequencies were A = 0.215, C = 0.291, G = 0.275, and T = 0.218. Substitution rates were calculated as follows: AC = 1.09847, AG = 4.37496, AT = 0.85890, CG = 1.15011, CT = 8.07977, and GT = 1.00000, with a tree length of 0.655. Bayesian posterior probabilities were assessed using Markov chain Monte Carlo (MCMC), yielding a final average standard deviation of split frequencies of 0.002127.

Based on combined sequences of ITS, *tef1*, and *tub2*, the phylogenetic trees of the *Neopestalotiopsis* species were generated. The alignment for *Neopestalotiopsis* species comprised 114 taxa, including 112 ingroup taxa and two outgroup taxa. The best-scoring ML tree with final optimisation had a likelihood value of -7376.0288. The matrix consisted of 159 distinct alignment patterns. Estimated base frequencies were as follows: A = 0.246, C = 0.211, G = 0.202, T = 0.340, with substitution rates AC = 0.411979, AG = 1.396776, AT = 0.741015, CG = 0.387043, CT = 3.887079, GT = 1.000000. Bayesian posterior probabilities were calculated using Markov chain Monte Carlo (MCMC), resulting in a final average standard deviation of split frequencies of 0.004231. The maximum parsimonious dataset comprised 1077 constant characters (proportion = 0.713718), 288 parsimony-informative and 144 parsimony-uninformative characters. The parsimony analysis resulted in one parsimonious tree (tree length = 939, Consistency Index (CI) = 0.590, Retention Index (RI) = 0.734, Rescaled Consistency (RC) = 0.433, and Homoplasy Index (HI) = 0.410).

Phylogenetic analyses of *Phyllosticta* species were performed using concatenated sequences of ITS, LSU, *tef1*, *act*, and *gapdh* loci. The final alignment comprised 79 taxa, including 77 ingroup taxa and two outgroup taxa. The optimised

best-scoring maximum likelihood (ML) tree had a likelihood value of -11670.171. The dataset contained 751 distinct patterns, with 559 parsimony-informative sites, 133 singleton sites, and 1401 constant sites. Estimated base frequencies were A = 0.200, C = 0.301, G = 0.277, and T = 0.222. Substitution rates were calculated as AC = 0.83093, AG = 2.18463, AT = 0.92855, CG = 0.98146, CT = 5.41077, and GT = 1.00000, with a tree length of 1.070. Bayesian posterior probabilities were calculated using Markov chain Monte Carlo (MCMC), resulting in a final average standard deviation of split frequencies of 0.005553.

Phylogenetic analyses of *Pseudocercospora* species were conducted using concatenated sequences of the ITS, *act*, *tef1*, and *rpb2* loci. The final alignment consisted of 53 taxa, including 52 ingroup taxa and one outgroup taxon. The best-scoring maximum likelihood (ML) tree, following optimisation, achieved a likelihood value of -9466.324. The dataset included 607 distinct patterns, 265 parsimony-informative sites, 302 singleton sites, and 1333 constant sites. Estimated base frequencies were A = 0.234, C = 0.266, G = 0.256, and T = 0.245. Substitution rates were as follows: AC = 1.12528, AG = 2.95403, AT = 1.38346, CG = 1.12306, CT = 5.35152, and GT = 1.00000, with a tree length of 0.830. Bayesian posterior probabilities were inferred using Markov chain Monte Carlo (MCMC), resulting in a final average standard deviation of split frequencies of 0.0032280.

Phylogenetic analyses of *Pseudoplagiostoma* species were performed using concatenated sequences of the ITS, LSU, *tef1*, and *tub2* loci. The final alignment included 35 taxa, comprising 34 ingroup taxa and one outgroup taxon. The best-scoring maximum likelihood (ML) tree, following optimisation, achieved a likelihood value of -12272.735. The dataset consisted of 895 distinct patterns, 715 parsimony-informative sites, 204 singleton sites, and 1632 constant sites. Estimated base frequencies were A = 0.232, C = 0.261, G = 0.275, and T = 0.232. Substitution rates were as follows: AC = 1.91739, AG = 2.70804, AT = 1.85931, CG = 0.99608, CT = 5.77285, and GT = 1.00000, with a tree length of 0.971. Bayesian posterior probabilities were calculated using Markov chain Monte Carlo (MCMC), yielding a final average standard deviation of split frequencies of 0.004964.

9.3.3 Taxonomy

Ascomycota

Sordariomycetes

Hypocreales

Nectriaceae

Albonectria durionigenum A. Armand, Pourmoghaddam, Jayaward. & K.D. Hyde, *sp. nov.*

Figure 9.1

Index Fungorum:; MycoBank:

Etymology: The epithet name refers to the host plant from which the fungus was isolated.

Associated with fruit rot of Durian. Sexual morph: not observed. Asexual morph: *Sporodochia* and *Macroconidia* not produced neither on PDA nor CLA. *Aerial conidiophores* produced on SNA, single or branched, often reduced to single phialides. *Aerial conidiogenous cells* monophialidic, straight or slightly curved, simple cylindrical or rarely flask-shaped (15–)20–27(–40) × 2.5–3.5(–5) μm ($\bar{x}$ = 15 × 3 μm, n = 20), hyaline, smooth, thin-walled, periclinal thickening and collarette conspicuous. *Aerial microconidia* forming in chains on tips of phialides, smooth, thin-walled, straight, oblong oval to cylindrical, apex rounded, base obtuse or truncate, aseptate or 1-septate, hyaline, 8.5–12(–14) × 3.5–4.7 μm ($\bar{x}$ = 10.5 × 4.2 μm, n = 30). *Chlamydospores* smooth-walled, rounded, hyaline, 8–10 × 10–14 μm.

Culture characteristics: Colonies on PDA reach 37–40 mm diam. after 7 days at 25 ± 2 °C, dense, pale purplish grey, floccose, round, undulated in margin, reverse dark brick at the center, olivaceous buff at the margin. Colonies on SNA reaching 40 mm diam. after 7 days, pale pink, aerial mycelia sparse, margin entire, reverse pink. Pigment and odor absent.

Material examined: Thailand, Chiang Rai Province, Chang Wat Chiang Rai, Wiang Chai, Wiang Nuea, associated with fruit rot of *Durio zibethinus* (Malvaceae), 22 February 2022, A. Armand, N6-2 (MFLU 25-0048 holotype, MFLUCC 25-0041 ex-type living culture).

Notes: A single strain, MFLUCC 25-0041, formed a distinct lineage separated from the *Albonectria guizhouensis* clade, showing statistical support of 75%/–/– (ML/MP/PP) (Figure 9.2). A pairwise nucleotide comparison between our strain and the ex-type of *Albonectria guizhouensis* showed 99.34% (604/607 bp) sequence

similarity in *tef1*, 98.96% (478/483 bp) in *tub2*, 99.07% (214/216 bp) in *rpb1*, 99.22% (891/898 bp) in *rpb2*, and 99.64% (567/569 bp) in *cmdA*. Morphologically, *Albonectria durionigenum* differs from the ex-type of *A. guizhouensis* in the formation of microconidia (microconidia formed in chains in *A. durionigenum* vs. microconidia formed in false heads in *A. guizhouensis*), the number of septa in microconidia (0–1-septate in *A. durionigenum* vs. aseptate in *A. guizhouensis*), the shape of aerial conidiophores (branched in *A. durionigenum* vs. unbranched in *A. guizhouensis*), and the size of aerial conidiophores (20–27 µm in *A. durionigenum* vs. 4–34 µm *A. guizhouensis*). Additionally, *A. durionigenum* did not produce sporodochia and macroconidia, while these characters were observed in *A. guizhouensis* (Zhang N. et al., 2023).

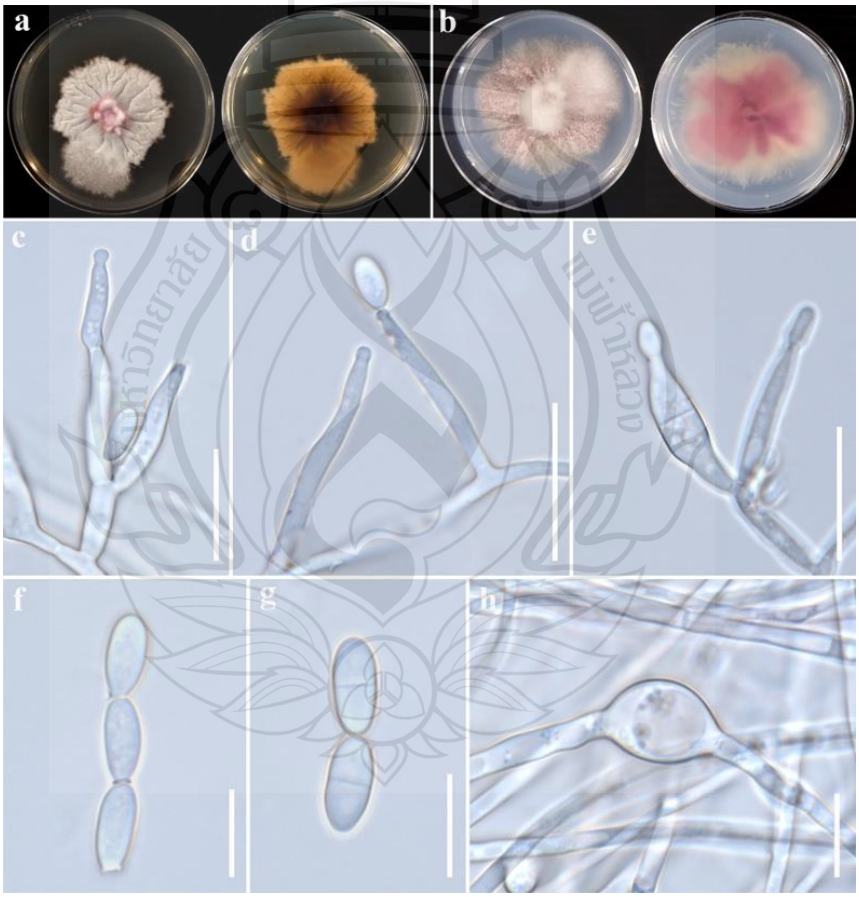

Note **a** Colonies on PDA after 7 days. **b** Colonies on SNA after 7 days, **c–e** Aerial conidiophores (phialides). **f**, **g** Microconidia forming in chain **h** Chlamydospore. Scale bars: **c**–**e** = 20 µm, **f**–**h** = 10 µm

Figure 9.1 *Albonectria durionigenum* (MFLU 25-0048 holotype)

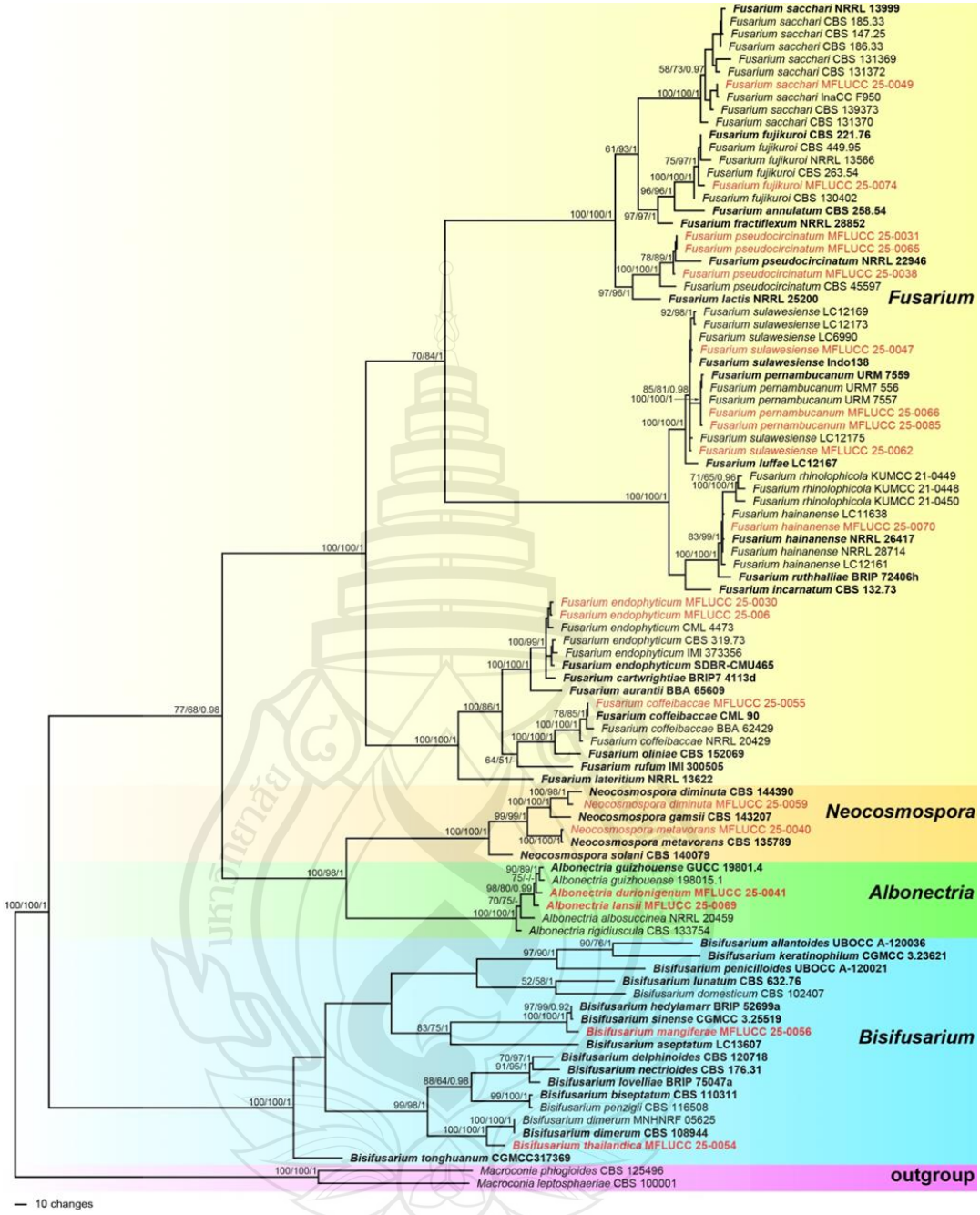

Note Maximum likelihood and maximum parsimony bootstrap values greater than 50% and bayesian posterior probabilities greater than 0.90 are shown near the nodes, respectively. The tree is rooted with *Macroconia phlogioides* (CBS 125496) and *M. leptosphaeriae* (CBS 100001). Type strains are indicated in bold, and newly sequenced taxa are highlighted in red

Figure 9.2 The most parsimonious tree obtained from a combined dataset of *tef1*, *rpb1*, *rpb2*, and *cmdA* sequences

Albonectria lansii A. Armand, Pourmoghaddam, Jayaward. & K.D. Hyde, *sp. nov.*

Figure 9.3

Index Fungorum:; MycoBank:

Etymology: The epithet name refers to the host plant from which the fungus was isolated.

Associated with fruit rot of Langsat. Sexual morph: not observed. Asexual morph: *Sporodochia* produced on both PDA and CLA, conidial mass cream to yellow. *Sporodochial conidiophores* reduced to phialides. *Sporodochial conidiogenous cells* monophialidic, cylindrical, hyaline, septate, simple or branched, smooth, straight to slightly curved, tapering towards the apex, periclinal thickening and collarette inconspicuous, 16–25(–45) × 3–4 μm ($\bar{x}$ = 22 × 3.3 μm, n = 30). *Sporodochial Macroconidia* curved, apical cell curved to blunt; basal cell papillate, poorly developed to well-developed, foot-shaped, 4–7-septate (mostly 7-septate), hyaline, smooth, thin-walled: 4-septate macroconidia 52–60 × 5–6 μm ($\bar{x}$ = 58 × 5.2 μm, n = 20) 5-septate macroconidia 55–68 × 5.5–6.5 μm ($\bar{x}$ = 66.5 × 6 μm, n = 30); 6-septate macroconidia 65–77 × 5.5–6 μm ($\bar{x}$ = 71 × 6.3 μm, n = 30); 7-septate macroconidia 70–80 × 6–6.5 μm ($\bar{x}$ = 78 × 6.2 μm, n = 30). *Aerial conidiophores* produced on SNA, single or branched, often reduced to single phialides. *Aerial conidiogenous cells* monophialidic, rarely polyphialidic, straight, cylindrical or flask-shaped to ampulliform, (5–)10–20(30) × 2–3(–6) μm ($\bar{x}$ = 15 × 2.5 μm, n = 20), hyaline, smooth, thin-walled, periclinal thickening and collarette inconspicuous. *Aerial microconidia* forming in chains on tips of phialides, smooth, thin-walled, straight, ellipsoid or oval to oblong oval, apex obtuse, base truncate, aseptate or rarely 1-septate, hyaline, 6.5–8(–10) × 3–4 μm ($\bar{x}$ = 7.5 × 3.5 μm, n = 30). *Chlamydospores* not observed.

Culture characteristics: Colonies on PDA reach 49–51 mm diam. after 7 days at 25 ± 2 °C, dense, pink, white at the margin, floccose, round, undulated in margin, aerial mycelia abundant, reverse dark peach, white at the margin. Colonies on SNA reaching 45 mm diam. after 7 days, white to pale pink, aerial mycelia sparse, margin entire, reverse pale pink to pink. Pigment and odor absent.

Material examined: Thailand, Chiang Rai Province, Mae Salong Nok; associated with fruit rot of *Lansium domesticum* (Meliaceae), 14 February 2022, A. Armand, P47-2 (MFLU 25-0049 holotype; MFLUCC 25-0069 ex-type living culture).

Notes: Phylogenetic analysis of combined *tef1*, *rpb1*, *rpb2*, and *cmdA* sequence data showed that the strain *Albonectria lansii* MFLUCC 25-0069 formed a distinct lineage from other close species, including *Albonectria guizhouensis* and *A. durionigenum*, receiving 98%/80%/0.99 (ML/MP/PP) support values (Figure 9.2). *Albonectria lansii* shares 99.47% (572/575 bp) sequence similarity with *A. durionigenum* in *tef1*, 98.75% (476/482 bp) in *tub2*, 99.22% (769/775 bp) in *rpb2*, and 99.41% (683/687 bp) in *cmdA*. Morphologically, *A. lansii* differs from *A. durionigenum* in the shape of aerial conidiophores (monophialidic, straight or slightly curved, simple cylindrical in *A. durionigenum* vs. monophialidic or polyphialidic, cylindrical with swollen at the base, or flask-shaped to ampulliform in *A. lansii*), the shape of microconidia (oblong oval to cylindrical in *A. durionigenum* vs. ellipsoid or oval to oblong oval in *A. lansii*), and the size of microconidia (8.5–12(–14) μm long (3.1 μm L/W) in *A. durionigenum* vs. 6.5–8(–10) μm long (2.1 μm L/W) in *A. lansii*). Moreover, *A. lansii* produced sporodochia and macroconidia, while they were not produced in *A. durionigenum*.

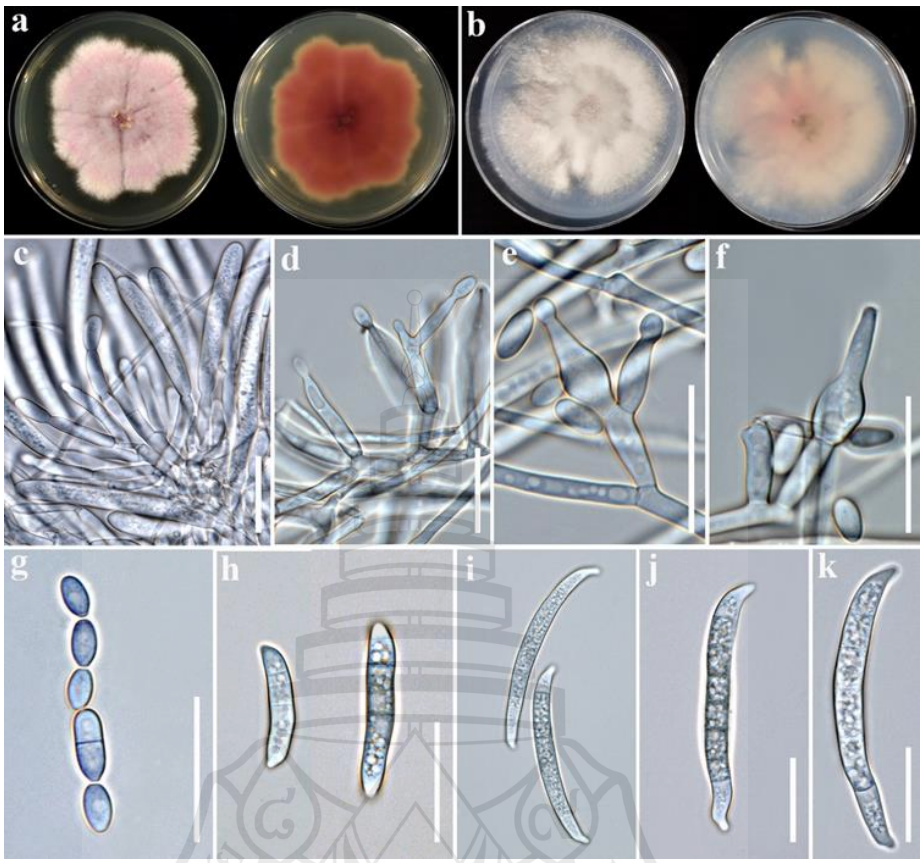

Note **a** Colonies on PDA after 7 days. **b** Colonies on SNA after 7 days, **c–f** Monophialides and polyphialides. **g** Microconidia forming in chain **h** Mesoconidia **i**–**k** Macroconidia. Scale bars: **c**–**k** = 20 µm

Figure 9.3 *Albonectria lansii* (MFLU 25-0049 holotype)

Bisifusarium mangiferae A. Armand, Pourmoghaddam, Jayaward. & K.D. Hyde, *sp. nov.*

Figure 9.4

Index Fungorum:; MycoBank:

Etymology: The epithet name refers to the host plant from which the fungus was isolated.

Associated with dieback of mango. Sexual morph: not observed. Asexual morph: Hyphae branched, septate, hyaline, smooth. *Sporodochia* produced on CLA, rosy buff to salmon. *Sporodochial conidiophores* reduced to phialides, produced in two types, cylindrical to clavate phialides abundant, monophialidic, simple or branched, aseptate, straight or slightly curved, tapering towards the apex, smooth, periclinal

thickening and collarette inconspicuous, 10–15 × 2–3 μm ($\bar{x}$ = 12 × 2.6 μm, n = 30), obpyriform phialides rare, monophialidic, simple, aseptate, periclinal thickening and collarette inconspicuous, 6–8 × 4–5 μm ($\bar{x}$ = 6.5 × 4.5 μm, n = 10). *Aerial conidiophores* abundant, monophialidic, cylindrical to clavate, simple or branched, septate, straight or slightly curved, tapering towards the apex, smooth, periclinal thickening and collarette inconspicuous, 12–25 × 2–3 μm ($\bar{x}$ = 18.5 × 2.5 μm, n = 30). *Macroconidia* aseptate to 2-septate, cylindrical or fusiform, obtuse to subacute at ends, straight or curved, 12–15 × 2.5–3.5 μm ($\bar{x}$ = 13.5 × 2.8 μm, n = 30). *Microconidia* aseptate, fusiform, subcylindrical to cylindrical, with obtuse ends, straight or curved 7–10 × 2.4–3 μm ($\bar{x}$ = 8.5 × 2.5 μm, n = 30), microconidia and macroconidia were homogenous. *Chlamydospores* abundant, produced in chains, circular to ellipsoid, hyaline, thick-walled.

Culture characteristics: Colonies on PDA reach 40–50 mm diam. after 7 days at 25 ± 2 °C, dense, salmon, round, entire in margin, aerial mycelia sparse, reverse same colour. Colonies on SNA reaching 27–30 mm diam. after 7 days, salmon to orange, aerial mycelia sparse, margin filiform, reverse salmon. Pigment and odor absent.

Material examined: Thailand, Chiang Rai Province, Phan District, Mae Ao, Ang Kep Nam Huai Tonyang Reservoir, on *Mangifera indica* (Anacardiaceae), 27 September 2021, A. Armand, T115-3 (MFLU 25-0050 holotype; MFLUCC 25-0056 ex-type living culture).

Notes*:* Phylogenetic analyses showed that the strain MFLUCC 25-0056 clustered as a distinct lineage from the two closest species, *Bisifusarium helylamarr* and *B. sinense*, showing 100%/100%/1.00 (ML/MP/PP) bootstrap support (Fig. 2). *Bisifusarium mangiferae* shares 96.17% (226/235 bp) sequence similarity in *tef1* to *B. helylamarr* and *B. sinense*, and 98.84% (768/777 bp) in *rpb2* (*rpb1* and *cmdA* sequences are missing). Morphologically, *B. mangiferae* is distinguished from *B. sinense* in the formation of phialides (two types in *B. mangiferae*, cylindrical to clavate and obpyriform phialides vs. simple cylindrical phialides in *B. sinense*), the number of septa in conidia (0–2 septate in *B. mangiferae* vs. 0–1-septate in *B. sinense*), and the size and shape of conidia (distinguishable in *B. mangiferae*, macroconidia 12–15 μm and microconidia 7–10 μm long vs. 3.5–13 μm long in *B. sinense*) (Zhang et al., 2024).

Morphological comparison with *B. helylamarr* was not feasible due to the absence of a morphological description for *B. helylamarr* (Tan & Shivas, 2023).

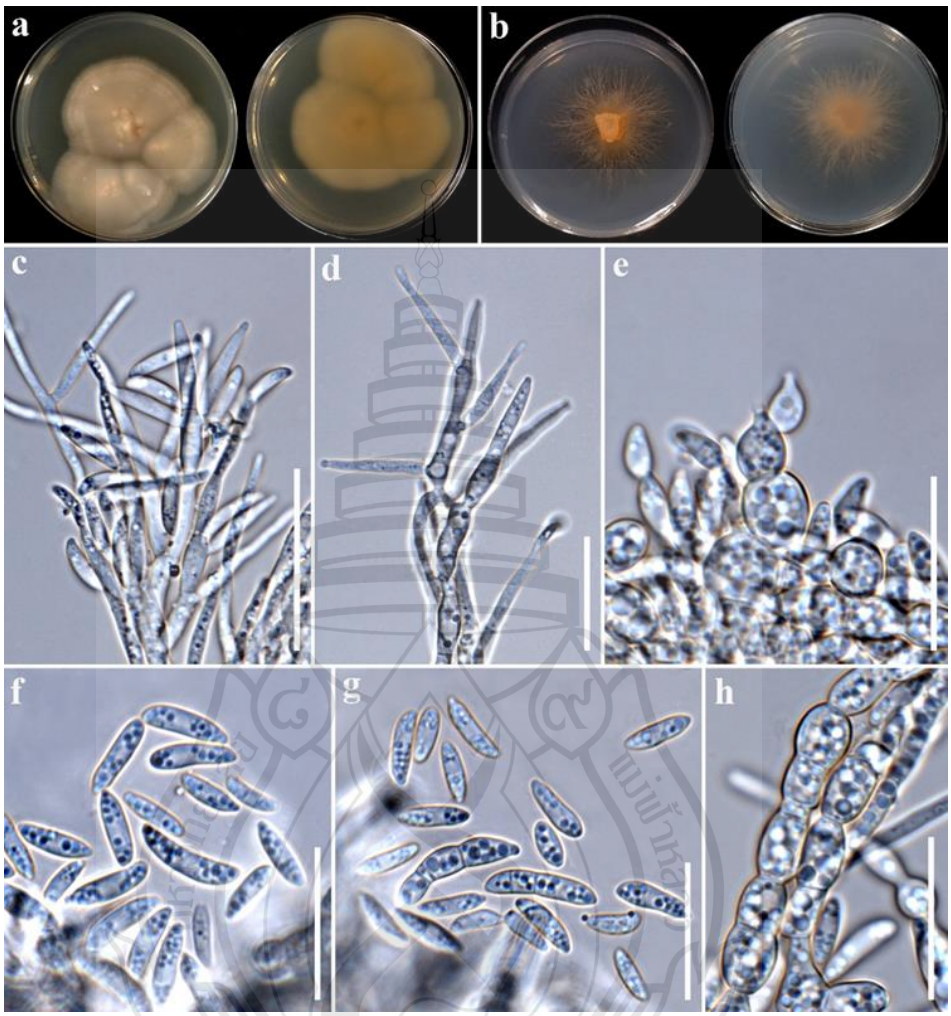

Note **a** Colonies on PDA after 7 days. **b** Colonies on SNA after 7 days, **c**, **d** Phialides produced on aerial hyphae. **e** Phialides produced on sporodochium **f**, **g** Micro and macroconidia. **h** Chlamydospores. Scale bars: **c**–**h** = 20 µm

Figure 9.4 *Bisifusarium mangiferae* (MFLU 25-0050 holotype)

Bisifusarium thailandica A. Armand, Pourmoghaddam, Jayaward. & K.D. Hyde, *sp. nov.*

Figure 9.5

Index Fungorum:; MycoBank:

Etymology: The epithet name refers to the country from which the fungus was isolated.

Associated with dieback of dragon fruit. Sexual morph: not observed. Asexual morph: Hyphae branched, septate, hyaline, smooth. *Sporodochia* produced on CLA, rosy buff. *Sporodochial conidiophores* reduced to phialides, cylindrical to ampuliform, monophialidic, simple or branched, aseptate, straight or slightly curved, tapering towards the apex, smooth, periclinal thickening and collarette inconspicuous, 11–16 × 2–3.5 μm ($\bar{x}$ = 13.5 × 2.5 μm, n = 30). *Aerial conidiophores* abundant, monophialidic or polyphialidic, cylindrical, simple or branched, septate, straight or slightly curved, tapering towards the apex, smooth, periclinal thickening and collarette inconspicuous, 8–20 × 2.5–3.5 μm ($\bar{x}$ = 18.5 × 3 μm, n = 30). *Macroconidia* produced on sporodochia, aseptate, fusiform, slightly curved, subacute to acute at the ends, 13–16 × 3–3.5 μm ($\bar{x}$ = 14.5 × 3.2 μm, n = 30). *Mesoconidia* produced on aerial conidiophores, 0–1-septate, cylindrical to allantoid, slightly to strongly curved, with obtuse ends, 6–10 × 3–3.5 μm ($\bar{x}$ = 7 × 3 μm, n = 30). *Microconidia* produced on aerial conidiophores, aseptate, ellipsoid, subcylindrical to cylindrical, straight or slightly curved, with obtuse ends, 4.5–8 × 2.5–3 μm ($\bar{x}$ = 5.5 × 2.7 μm, n = 30). *Chlamydospores* not observed.

Culture characteristics: Colonies on PDA reach 60–63 mm diam. after 7 days at 25 ± 2 °C, white, round, entire in margin, aerial mycelia sparse, reverse ochreous. Colonies on SNA reaching 25–27 mm diam. after 7 days, white, aerial mycelia medium sparse, entire in margin, reverse white to rosy buff. Pigment and odor absent.

Material examined: Thailand, Chiang Rai Province, Phan District, Mae Ao, Ang Kep Nam Huai Tonyang Reservoir, on *Selenicereus undatus* (Cactaceae), 27 September 2021, A. Armand, T74-2 (MFLU 25-0051 holotype; MFLUCC 25-0054 ex-type living culture).

Notes: Phylogenetic analyses revealed that the strain MFLUCC 25-0054 formed a distinct lineage from *Bisifusarium dimerum*, showing 100%/100%/1.00 (ML/MP/PP) bootstrap support (Figure 9.2). *Bisifusarium thailandica* shares 96.29% (598/621 bp) sequence similarity to the ex-type of *Bisifusarium dimerum* in *tef1*, 98.07% (766/781 bp) in *rpb2*, and 99.48% (578/581 bp) in *cmdA*. Morphologically, *B. thailandica* differs from *B. dimerum* in the number of septa in macroconidia (aseptate in *B. thailandica* vs. 1-septate in *B. dimerum*), formation of mesoconidia (common in *B. thailandica* vs. not observed in *B. dimerum*), formation of polyphialides (common in *B. thailandica* vs. not observed in *B. dimerum*), formation of lateral phialidic pegs (not observed in *B.*

thailandica vs. common in *B. dimerum*), and shape of microconidia (ellipsoid, subcylindrical to cylindrical in *B. thailandica* vs. broadly lunate to reniform in *B. dimerum*) (Schroers et al., 2009).

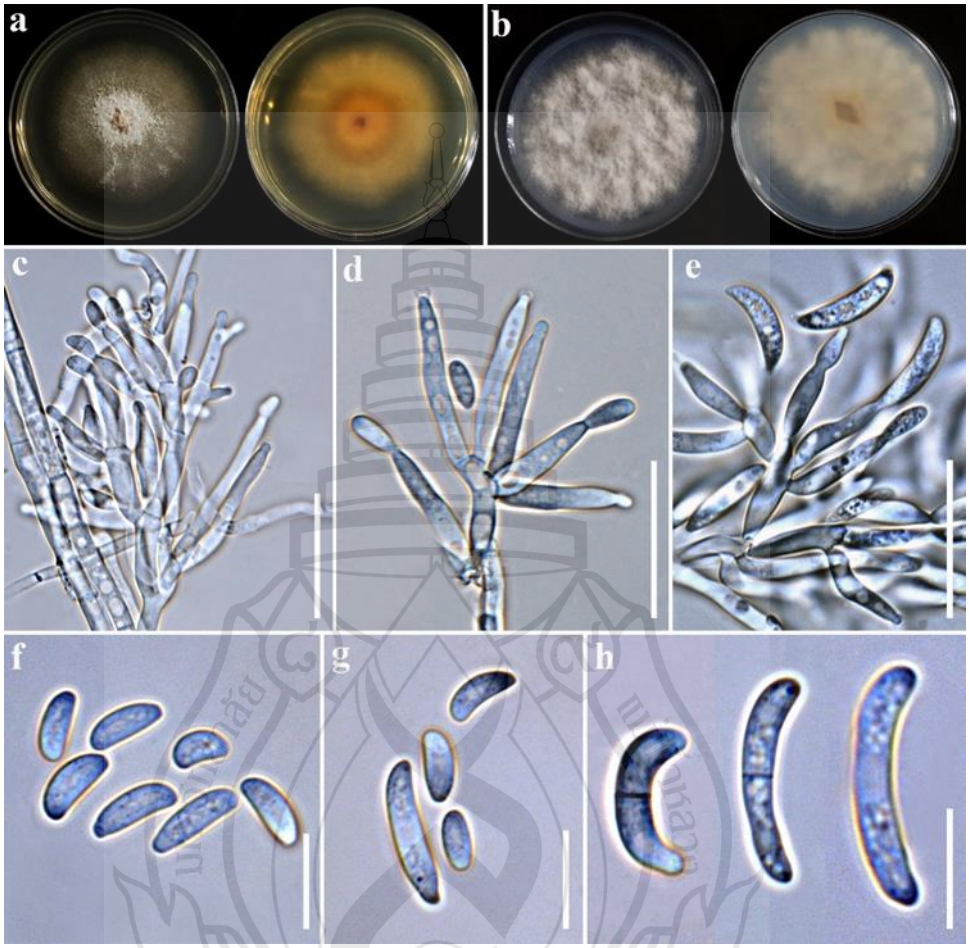

Note **a** Colonies on PDA after 7 days. **b** Colonies on SNA after 7 days. **c–d** Monophialides and polyphialides. **e** Sporodochial conidiophores and macroconidia. **f** Microconidia **g** Mesocnidia and microcnidia. **h** Mesoconidia. Scale bars: **c**, **e** = 20 µm, **f**, **g** = 10 µm, **h** = 5 µm

Figure 9.5 *Bisifusarium thailandica* (MFLU 25-0051 holotype)

Dothideomycetes

Mycosphaerellales

Mycosphaerellaceae

Cercospora alocasiicola A. Armand, Jayaward. & K.D. Hyde, *sp. nov.*

Figure 9.6

Index Fungorum:; MycoBank:

Etymology: The epithet name refers to the host plant from which the fungus was isolated.

Associated with leaf spots of *Alocasia cucullate*. Leaf spots circular, amphigenous, pale brown to brown, grey in the center, margin definite to irregular. Sexual morph: not observed. Asexual morph: Mycelium internal. *Caespituli* hypogenous, scattered, pale brown to grey. *Stromata* oval to globose, brown to dark brown, brown, composed of swollen hyphal cells, intraepidermal or substomatal, 38−68 μm diam. *Conidiophores* fasciculate, arising from stromata (6−23 per fascicle), straight or sinuous, geniculate, cylindrical smooth-walled, brown, paler toward the apex, 45−116 × 4.3−5.5 μm, 3−6-septate, distance between septa 9–33. *Conidiogenous cells* integrated, terminal, cylindrical, 18−34 μm long, pale brown. *Conidiogenous loci* conspicuous, subcircular to circular, thickened and darkened, multi-local, lateral and apical, 1.5–3 μm diam. *Conidia* solitary, obclavate-cylindrical, hyaline, acircular, straight or curved, subacute at the apex, truncate to slightly obconically truncate at the base, 6−12-septate, 90−143 × 3−4 μm; hila thickened and darkened, 2–3 μm diam.

Culture characteristics: Colonies on PDA reach 20–25 mm in diam. after 3 weeks at 25 ± 2 °C. moderate to dense, felty aerial mycelium, pale grey in the center, dark brown in the margin, margin branching, with no pigment diffusion into the agar. Conidia not formed in culture.

Material examined: Thailand, Chiang Rai Province, Mueang Chiang Rai District, Tha Sut; associated with leaf spots of *Alocasia cucullate* (Araceae), 04 July 2022, A. Armand, C33 (MFLU 25-0052 holotype; MFLUCC 25-0028 ex-type living culture).

Notes: Based on the multi-gene phylogenetic analysis, two strains (MFLUCC 25-0029 and MFLUCC 25-0028) clustered together with 100%/1.00 (ML/PP) bootstrap support, separated from other related species (Figure 9.7). The strains were associated with leaf spots of *Alocasia cucullata* and *Alocasia macrorrhizos*, respectively.

Note **a** Symptoms on the leaf. **b**, **c** Conidiomata. **d**–**f** Conidiophores **g**–**j** Conidia. Scale bars: **d**–**j** = 50 µm

Figure 9.6 *Cercospora alocasiicola* (MFLU 25-0052 holotype)

Cercospora capsici Heald & F.A. Wolf (1911)

Index Fungorum: IF 259712; MycoBank: MB 259712

Illustration and description: See Heald and Wolf (1911)

Known distribution: Worldwide, mostly distributed in the tropical and subtropical regions (Albu et al., 2016; Dahal et al., 1992; Gautam et al., 2020; Groenewald et al., 2013; Larter, 1943; Videira et al., 2017; This study).

Habitat & host range: The species is associate with leaf spots and fruit spots disease of *Capsicum* (Solanaceae), *Pandanus amaryllifolius* (Pandanaceae), *Piper* sp. (Piperaceae), (Hyde et al., 2018b; Nguanhom et al., 2015; Tibpromma et al., 2018; This study).

Notes: The species was reported from Thailand by Nguanhom et al. (2015). They utilised morphological characteristics and phylogenetic analysis of a concatenated ITS + *cmdA* sequence data to identify *Cercospora* species. Herein, *Cercospora capsici* was reported from fruit spots of *Capsicum annuum* in northern Thailand using phylogenetic analysis of a combined ITS, *act*, *cmdA*, *gapdh*, *his*, and *tef1* dataset (Figure 9.7).

Note Maximum likelihood bootstrap values greater than 50% and bayesian posterior probabilities greater than 0.90 are shown near the nodes, respectively. The tree is rooted with *Sphaerulina cercidis* (CBS 118910). The newly obtained strains are in red, and ex-type strains are in bold

Figure 9.7 The maximum likelihood (ML) tree of *Cercospora* based on the concatenated ITS, *act*, *cmdA*, *gapdh*, *his*, and *tef1* sequence dataset

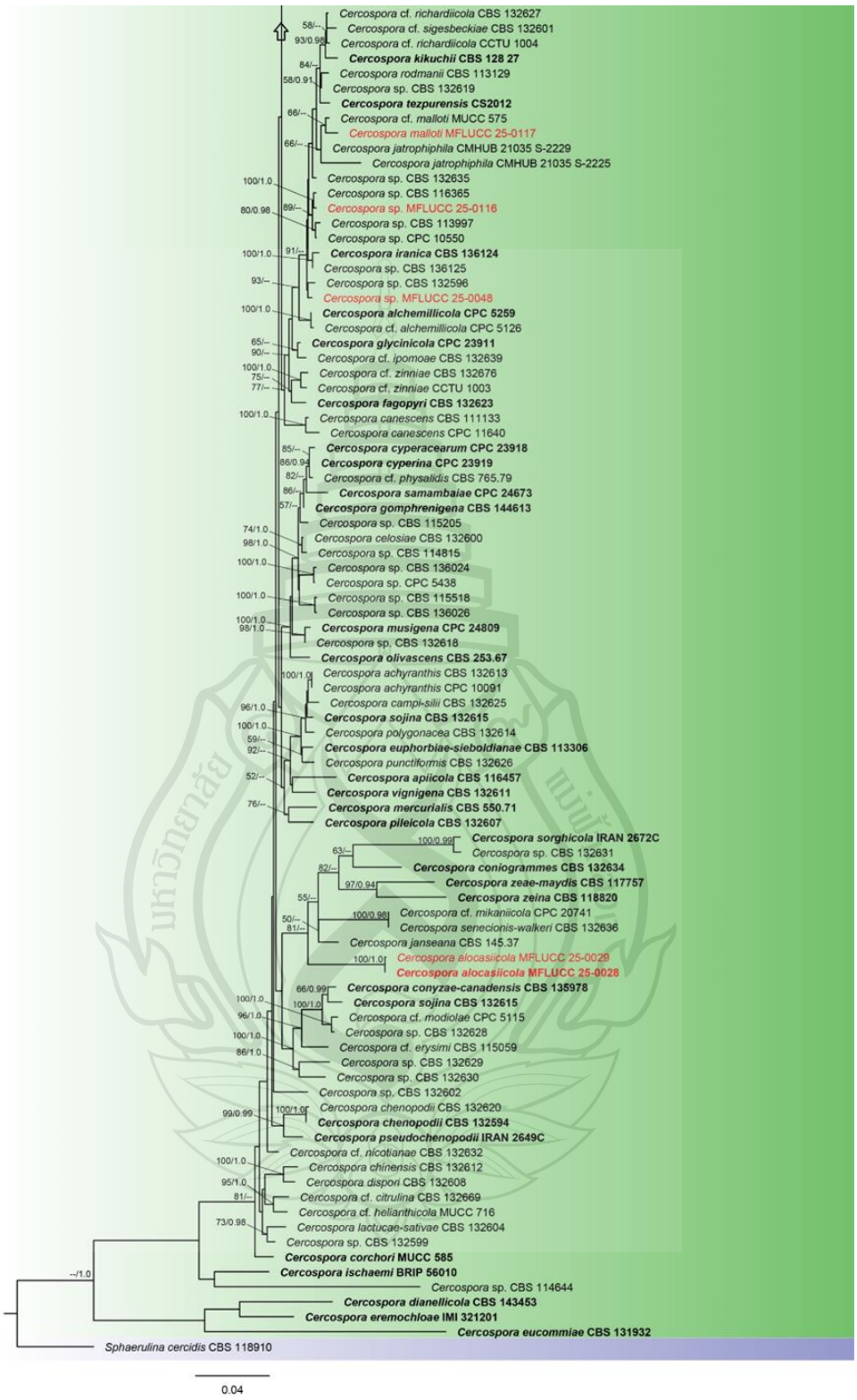

Figure 9.7 (continued)

Cercospora malloti Ellis & Everh. (1888)

Figure 9.8

Index Fungorum: IF 171671; MycoBank: MB 171671

Illustration and description: See Ellis and Everhart (1988); Groenewald et al. (2013).

Known distribution: China, Japan, Thailand, and United States (Phengsintham et al., 2012; This study).

Habitat & host range: Associated with leaf spots of different plant families such as Acanthaceae, Asteraceae, Brassicaceae, Cucurbitaceae, Euphorbiaceae, Malvaceae, Musaceae, Plantaginaceae, Polemoniaceae, Saururaceae, and Solanaceae (Groenewald et al., 2013; Nguanhom et al., 2015; This study).

Material examined: Thailand, Nan Province, Phu Phiang District, Mueang Chang, on leaves of *Durio zibethinus* (Malvaceae), 8 September 2022, A. Armand, Nan25-2 (MFLU 25-0053; MFLUCC 25-0117 living culture).

Notes: *Cercospora* species were investigated in Thailand by Nguanhom et al. (2015), and *Cercospora* cf. *malloti* was shown to be the most common species in northern Thailand, occurring on a wide host range. Sequences derived from several collections on various unrelated host species, including *Asystasia salicifiolia,* clustered in a clade tentatively denominated as *C.* cf. *malloti* in Groenewald et al. (2013). Herein, we provided gene sequence data for *C. malloti,* helping future studies to resolve this collection's confusion. Moreover, this is the first record of this species on *Durio zibethinus* (Malvaceae) worldwide (Figure 9.7). Two additional strains isolated in this study, MFLUCC 25-0116 and MFLUCC 25-0048, remained sterile in culture and were not identifiable to the species level (Figure 9.7).

Note **a** Symptoms on the leaf **b**, **c** Conidiomata **d**–**f** Conidiophores **g**–**j** Conidia. Scale bars: **d** = 50 µm. **e**, **f** = 25 µm. **g** = 50 µm, **h** = 25 µm

Figure 9.8 *Cercospora malloti* (MFLU 25-0053)

Sordariomycetes

Glomerellales

Glomerellaceae

Colletotrichum endophyticum Manamgoda, Udayanga, L. Cai & K.D. Hyde (2013)

Index Fungorum: IF 565248; MycoBank: MB 565248

Illustration and description: See Manamgoda et al. (2013).

Known distribution: Mostly distributed in tropical and subtropical regions (Liu et al., 2022; Talhinhas & Baroncelli, 2023; This study).

Habitat & host range: The species is responsible for the anthracnose, leaf spots, and fruit rots disease as well as endophyte of various crops in Arecacea, Poaceae, Anacardiaceae, Fabaceae, Malvaceae, Myrtaceae, Solanaceae, and Theaceae (Talhinhas & Baroncelli, 2023; This study).

Notes: Two strains identified as *C. endophyticum* clustered with the ex-type of the species with 95%/1.00 (ML/PP) bootstrap support (Figure 9.9). Strain MFLUCC 25-0131was isolated from *Psidium guajava* exhibiting leaf anthracnose, and strain MFLUCC 25-0130 was associated with leaf anthracnose on *Theobroma cacao*. Both represent new host records globally.

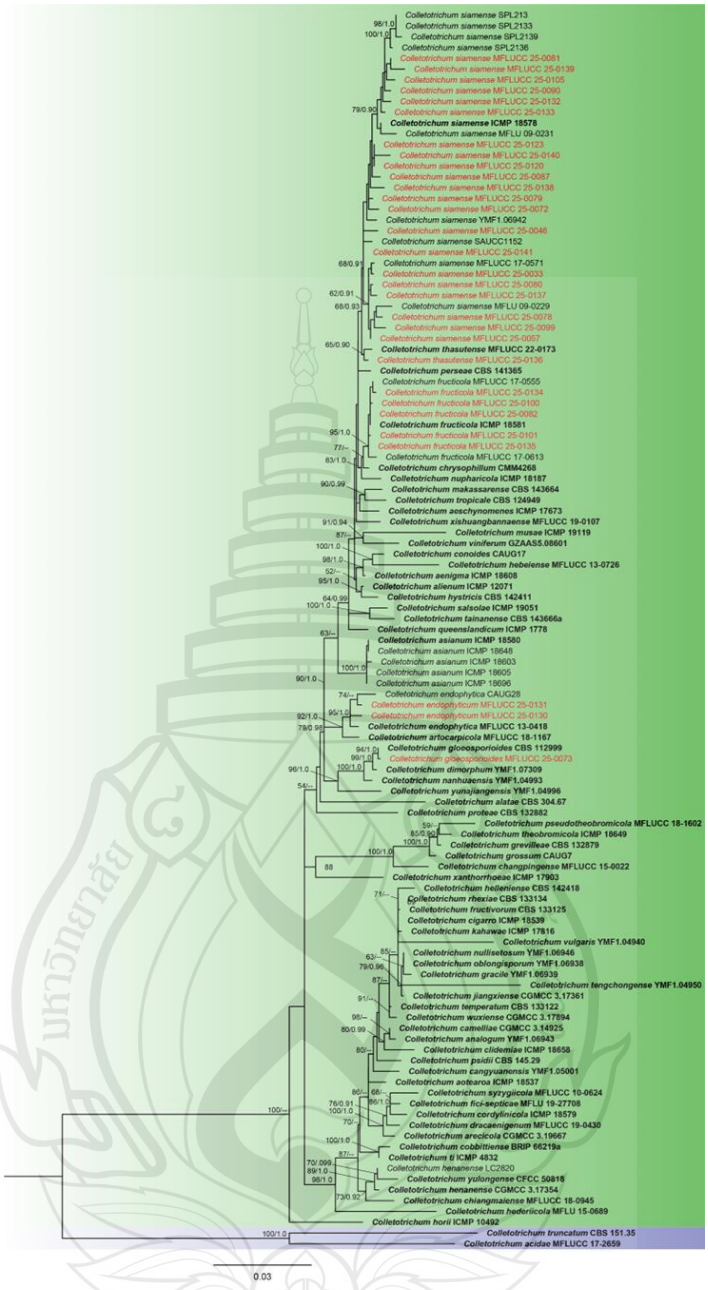

Note Maximum likelihood bootstrap values greater than 50% and bayesian posterior probabilities greater than 0.90 are shown near the nodes, respectively. The tree is rooted with *Colletotrichum truncatum* (CBS 151.35) and *C. acidae* (MFLUCC 17-2659). The newly obtained strains are in red, and ex-type strains are in bold

Figure 9.9 The maximum likelihood (ML) tree of *Colletotrichum gloeosporioides* species complex based on the concatenated ITS, *gapdh*, *chs-1*, *act*, and *tub2* sequence dataset

Colletotrichum fructicola Prihast., L. Cai & K.D. Hyde (2009)

Index Fungorum: IF 515409; MycoBank: MB 515409

Known distribution: Mostly distributed in tropical and sub-tropical regions (Hirayama et al., 2018; Liu et al., 2022; Lopes et al., 2021; Talhinhas & Baroncelli, 2021; Vithanage et al., 2021; Weir et al., 2012).

Habitat & host range: The species mostly occurs associated with anthracnose symptoms in a wide range of host plants, including Actinidiaceae, Altingiaceae, Anacardiaceae, Annonaceae, Apiaceae, Aquifoliaceae, Araceae, Araliaceae, Arecaceae, Asteraceae, Bignoniaceae, Brassicaceae, Burseraceae, Cactaceae, Caricaceae, Chrysobalanaceae, Cucurbitaceae, Dioscoreaceae, Ebenaceae, Euphorbiaceae, Fabaceae, Garryaceae, Hamamelidaceae, Hydrangeaceae, Juglandaceae, Lamiaceae, Lauraceae, Magnoliaceae, Malvaceae, Melanthiaceae, Moraceae, Musaceae, Myricaceae, Myrtaceae, Oleaceae, Orchidaceae, Oxalidaceae, Piperaceae, Plumbaginaceae, Poaceae, Pontederiaceae, Primulaceae, Proteaceae, Rhamnaceae, Rosaceae, Rubiaceae, Rutaceae, Sapindaceae, Sapotaceae, Schisandraceae, Solanaceae, Theaceae, Vitaceae, Zingiberaceae (Talhinhas and Baroncelli 2021, 2023). It has also been isolated as an endophyte in various plant hosts (Manamgoda et al., 2013; Vieira et al., 2014; Wu et al., 2022).

Notes: Five newly isolated strains, including MFLUCC 25-0134, MFLUCC 25-0135, MFLUCC 25-0100, MFLUCC 25-0101, and MFLUCC 25-0082, were obtained from *Manilkara zapota*, *Piper nigrum*, *Capsicum annuum*, and *Dimocarpus longan*, respectively. Phylogenetic analysis showed these strains clustering with the ex-type strain of *Colletotrichum fructicola*, supported by 95%/1.00 (ML/PP) bootstrap values (Figure 9.9). *Colletotrichum fructicola* has been previously reported from Thailand on *Dimocarpus longan* and *Capsicum annuum*; however, this is the first record of its association with *Manilkara zapota* and *Piper nigrum* worldwide.

Colletotrichum gloeosporioides (Penz.) Penz. & Sacc. (1884)

Index Fungorum: IF 158410; MycoBank: MB 158410

Illustration and description: See Cannon et al. (2008); Weir et al. (2012).

Known distribution: Mostly distributed in tropical and sub-tropical regions (Jayawardena et al., 2021a; Talhinhas & Baroncelli, 2021; Weir et al., 2012).

Habitat & host range: The species is commonly associated with plant diseases such as anthracnose and fruit rots, and has been reported from a wide range of plant families, including Actinidiaceae, Amaranthaceae, Amaryllidaceae, Anacardiaceae, Annonaceae, Aquifoliaceae, Araceae, Araliaceae, Arecaceae, Asparagaceae, Asteraceae, Bignoniaceae, Cannaceae, Caricaceae, Celastraceae, Cornaceae, Ebenaceae, Elaeocarpaceae, Ericaceae, Euphorbiaceae, Fabaceae, Fagaceae, Juglandaceae, Lardizabalaceae, Lauraceae, Lecythidaceae, Lythraceae, Magnoliaceae, Malvaceae, Moraceae, Musaceae, Myrtaceae, Oleaceae, Orchidaceae, Oxalidaceae, Paeoniaceae, Piperaceae, Poaceae, Proteaceae, Rhamnaceae, Rosaceae, Rubiaceae, Rutaceae, Salicaceae, Sapindaceae, Sapotaceae, Smilacaceae, Solanaceae, Theaceae, Viburnaceae, Vitaceae, Xanthorrhoeaceae, Zingiberaceae (Talhinhas and Baroncelli 2021, 2023). This species was also reported as endophytic fungi from various hosts (Chapla et al., 2014; Gangadevi & Muthumary, 2008; Zou et al., 2000).

Notes: A single strain, MFLUCC 25-0073, was obtained, which clustered with the ex-type of *C. gloeosporioides* with 94%/1.00 (ML/PP) bootstrap support (Figure 9.9). The single strain was obtained from *Citrus* sp. associated with leaf anthracnose. Najafiniya et al. (2024) reported *C. gloeosporioides* from *Citrus* sp. in northern Thailand. *Colletotrichum gloeosporioides* has been rarely identified from Thailand on tropical fruits (Phoulivong et al., 2010; Udayanga et al., 2013). We provide additional evidence to say that *C. gloeosporioides* is not a common species on tropical fruits.

Colletotrichum siamense Prihast., L. Cai & K.D. Hyde (2009)

Index Fungorum: IF 515410; MycoBank: MB 515410

Illustration and description: See Prihastuti et al. (2009)

Known distribution: Mostly distributed in tropical and sub-tropical regions (Jayawardena et al., 2021a; Liu et al., 2022; Talhinhas & Baroncelli, 2021).

Habitat & host range: The species mostly causes fruit or foliar disease on a variety of plant families such as Actinidiaceae, Amaryllidaceae, Anacardiaceae, Annonaceae, Apocynaceae, Aquifoliaceae, Araceae, Araliaceae, Arecaceae, Asparagaceae, Asteraceae, Bignoniaceae, Cactaceae, Caricaceae, Celastraceae, Chloranthaceae, Chrysobalanaceae, Commelinaceae, Convolvulaceae, Cornaceae, Cucurbitaceae, Dioscoreaceae, Droseraceae, Ebenaceae, Ericaceae, Euphorbiacea, Fabaceae, Garryaceae, Iridaceae, Juglandaceae, Magnoliaceae, Malvaceae, Meliaceae,

Moraceae, Musaceae, Myrtaceae, Lamiaceae, Lauraceae, Lythraceae, Nelumbonaceae, Oleaceae, Pandanaceae, Passifloraceae, Piperaceae, Poaceae, Primulaceae, Proteaceae, Rhamnaceae, Rosaceae, Rubiaceae, Rutaceae, Salicaceae, Santalaceae, Sapindaceae, Saururaceae, Schisandraceae, Solanaceae, Theaceae, Violaceae, Vitaceae, Xanthorrhoeaceae, Zingiberaceae, (Talhinhas and Baroncelli 2021, 2023); however, it also can be found as endophyte (Casas et al., 2021; do Espírito Santo et al., 2023; Liu et al., 2022; Silva Santos et al., 2022).

Notes: *Colletotrichum siamense* is a significant pathogen associated with anthracnose disease in chilli (*Capsicum* spp.), particularly in tropical and subtropical regions. In Thailand, where chilli cultivation is a major agricultural activity, anthracnose caused by *C. siamense* poses a serious threat to crop productivity (Than, 2008a, b). Twenty-one strains were identified as *Colletotrichum siamense*, clustering with the ex-type strain of *C. siamense* with 68%/0.91 (ML/PP) bootstrap support (Figure 9.9). These strains were isolated from a range of crops and ornamental plants. Among these, eight strains represent new host records, and five constitute new geographical records (Table A16).

Colletotrichum thasutense Armand, K.D. Hyde & Jayaward. (2022)

Index Fungorum: IF 900127; MycoBank: MB 900127

Illustration and description: See Jayawardena et al. (2022)

Known distribution: Thailand (Jayawardena et al., 2022; This study).

Habitat & host range: Associated with anthracnose of *Syngonium* sp. (Araceae), and *Theobroma cacao* (Malvaceae) (Jayawardena et al., 2022; This study)

Notes: The species was originally described as associated with anthracnose of *Syngonium* sp. from Thailand (Jayawardena et al., 2022). Herein, a single strain was isolated as a new host record, associated with leaf anthracnose of *Theobroma cacao*. The strain MFLUCC 25-0136 clustered with the ex-type of *C. thasutense* with 65%/0.90 (ML/PP) bootstrap support (Figure 9.9).

Sordariomycetes

Diaporthales

Diaporthaceae

Diaporthe arecae (H.C. Srivast., Zakia & Govindar.) R.R. Gomes, Glienke & Crous (2013)

Index Fungorum: IF 802924; MycoBank: MB 802924

Illustration and description: See Gomes et al. (2013); Pereira et al. (2023)

Known distribution: Distributed mostly in tropical and subtropical countries, including China (Huang et al., 2015), India (Dissanayake et al., 2017; Yang et al., 2018), Malaysia (Lim et al., 2019), and Thailand (This study).

Habitat & host range: Reported as endophyte, saprobe, and pathogen from different plat hosts, including *Areca catechu* (Arecaceae), *Citrus grandis* (Rutaceae), *Citrus* sp., *Citrus unshiu*, *Mangifera indica* (Anacardiaceae), and *Persea americana* (Lauraceae) (Farr & Rossman, 2024).

Notes: Pereira et al. (2023) conducted an integrative taxonomic study on the *Diaporthe arecae* species complex, identifying three well-defined subclades represented by *D. arecae*, *D. chiangmaiensis*, and *D. smilacicola*. They synonymised 52 species under *D. arecae*, confirming their conspecificity and sister relationship to *D. chiangmaiensis* and *D. smilacicola*. Pereira et al. (2024) further synonymised four additional species under *D. arecae*, confirming three well-supported subclades withing *D. arecae* species complex. Five strains isolated from fruit rot and leaf blight of *Durio zibethinus* (Malvaceae), leaf blight of *Acacia auriculiformis* (Fabaceae), and *Gomphrena globosa* (Amaranthaceae) clustered within the *D. arecae* species complex, grouping with those synonymised under *D. areca* (Figure 9.10). Therefore, the five strains were identified as *D. arecae*. This study reports three new host records of *D. arecae* from Thailand (Table A16).

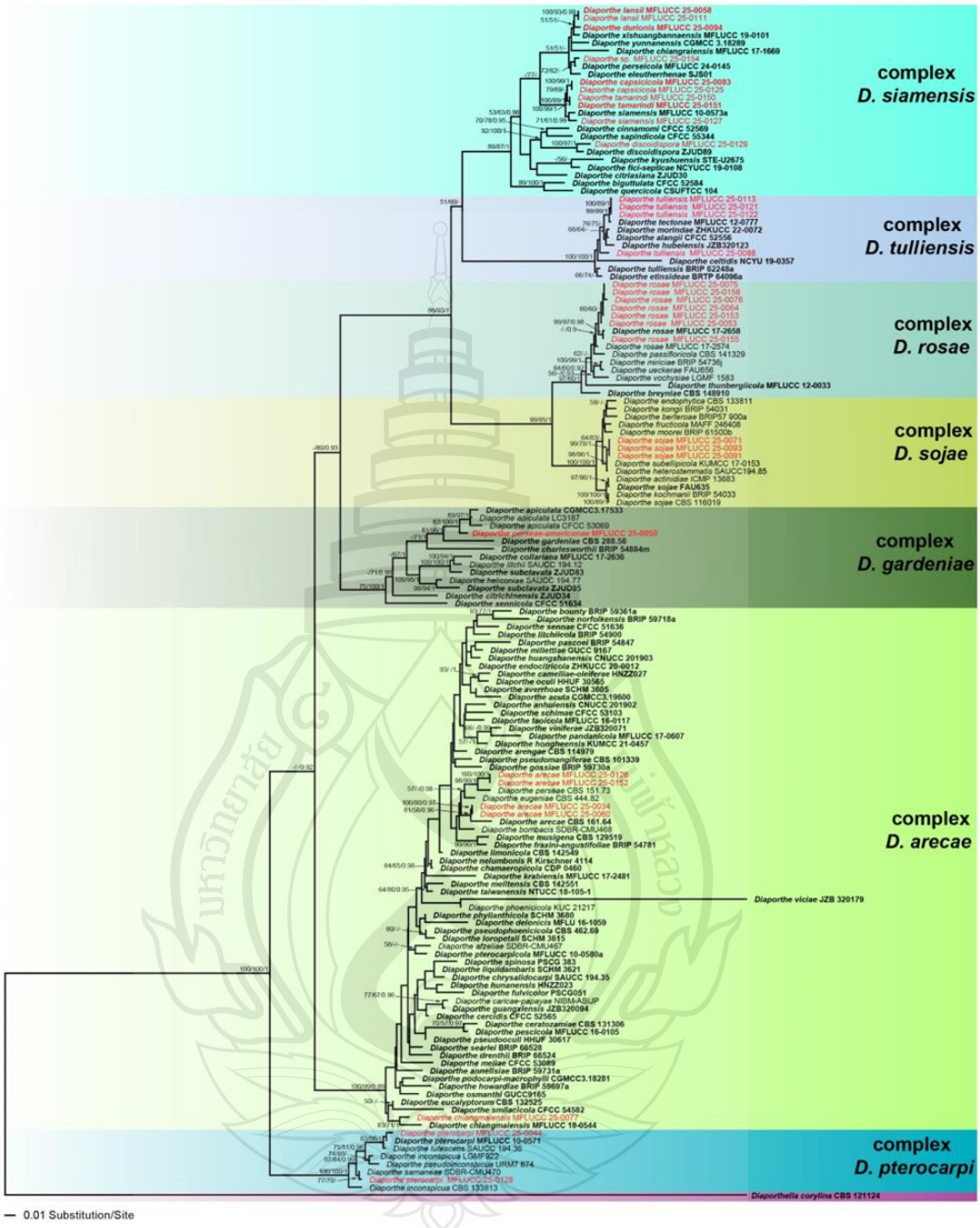

Note Maximum likelihood bootstrap values greater than 50% and bayesian posterior probabilities greater than 0.90 are shown near the nodes, respectively. The tree is rooted with *Diaporthella corylina* (CBS 121124). The newly obtained strains are in red, and ex-type strains are in bold

Figure 9.10 The maximum likelihood (ML) tree of *Diaporthe* based on the concatenated ITS, *tef1*, *tub*2, *cmdA*, and *his3* sequence dataset

Diaporthe capsicicola A. Armand, Pourmoghaddam, Jayaward. & K.D. Hyde, *sp. nov.*

Figure 9.11

Index Fungorum:; MycoBank:

Etymology: The epithet name refers to the host plant from which the fungus was isolated.

Associated with fruit rot of chili peppers. Sexual morph: not observed. Asexual morph: *Conidiomata* pycnidial, subglobose or globose, dark brown or dark grey to black, semi-immersed, erumpent, solitary or aggregated. *Conidiophores* reduced to conidiogenous cells. *Conidiogenous cells* densely aggregated, ampuliform, phialidic, straight or flexuous, 5–9 × 1.8–2 µm. *Alpha conidia* abundant, hyaline, smooth, aseptate, biguttulate or multiguttulate, fusiform, straight, apex rounded or acute, base acute, 6.4–7 × 2.3–3 µm ($\bar{x}$ = 6.8 × 2.5 µm, n = 30). *Beta conidia* abundant, hyaline, smooth, aseptate, filiform, straight or curved, tapering toward both ends, 16–23 × 1.5–2.5 µm ($\bar{x}$ = 21 × 2 µm, n = 30). *Gamma conidia* not observed.

Culture characteristics: Colonies on PDA reach 77–80 mm in diam. after 7 days at 25 ± 2 °C. Aerial mycelia fluffy, white on surface, becoming olivaceous buff after 10 days. Reverse same colour. Colony undulated in margin. Conidiomata produced after 20 days, irregularly distributed over the agar surface.

Material examined: Thailand, Chiang Rai Province, Mueang Chiang Rai District, associated with *Capsicum annuum* (Solanaceae) fruit rot, 04 July 2022, A. Armand, R36 (MFLU 25-0054 holotype; MFLUCC 25-0083 et-type living culture).

Notes: Phylogenetic analyses revealed that the strains MFLUCC 25-0083 and MFLUCC 25-0125 (isolated from *Capsicum annuum* and *Durio zibethinus*) clustered together in a distinct clade within the *Diaporthe siamensis* species complex, showing 100%/100%/1.00 (ML/MP/PP) bootstrap values (Figure 9.10). *Diaporthe capsicicola* was found to be the closest species to *D. tamarindi*. *Diaporthe capsicicola* shares 99.59% (488/490 bp) sequence similarity with *D. tamarindi* in ITS, 98.22% (498/507 bp) in *tub2*, and 99.76% (419/420 bp) in *his3*. Furthermore, the pairwise homoplasy index (PHI) test revealed that there is no significant recombination (p = 0.30) between *Diaporthe capsicicola* and *Diaporthe tamarindi* (Figure 9.12). Morphologically, *D. capsicicola* differs from *D. tamarindi* in the shape of alpha conidia (fusiform,

biguttulate, or multiguttulate in *D. capsicicola* vs. biguttulate and mostly ellipsoid in *D. tamarindi*), and the shape of beta conidia (narrowly filiform in *D. capsicicola* vs. strongly tapered toward the apex, swollen at the base in *D. tamarindi*). Moreover, gamma conidia were not observed in *D. capsicicola*, while they were present in *D. tamarindi*.

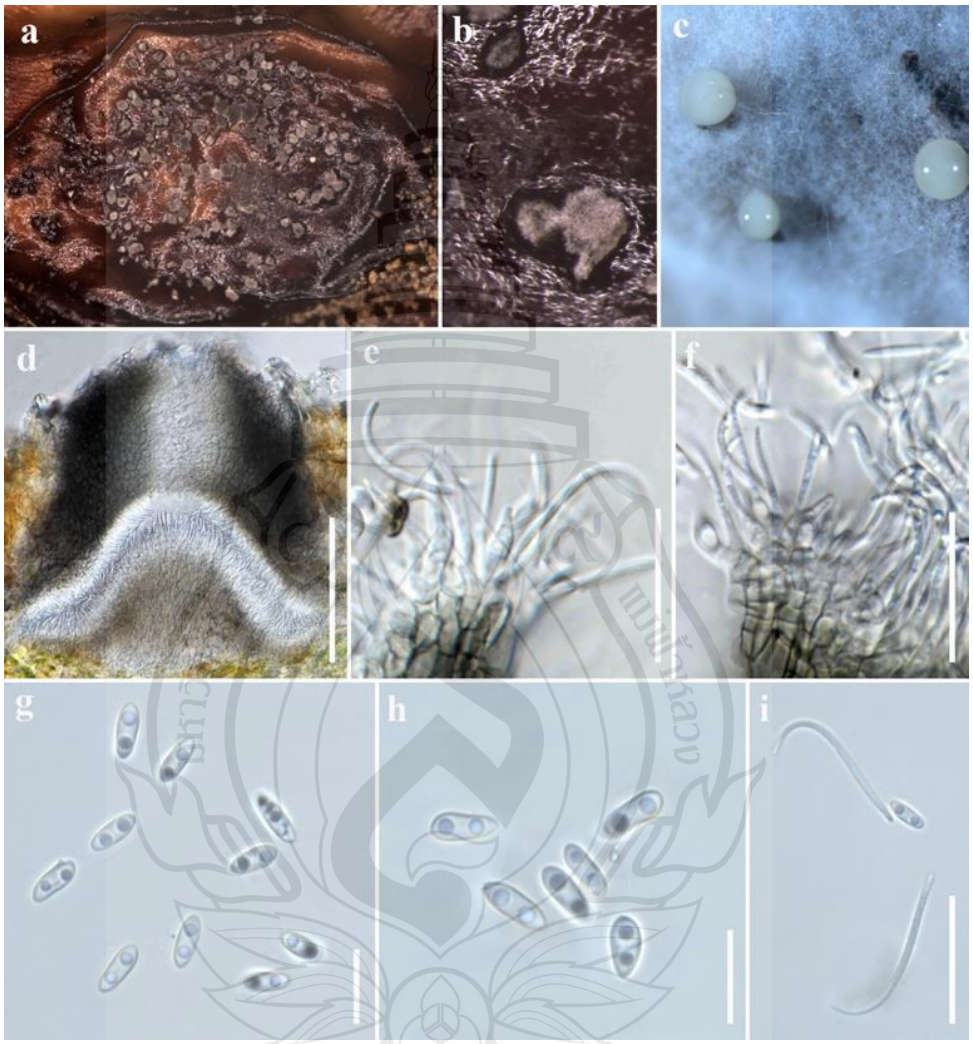

Note **a**, **b** Conidiomata produced on the host **c** Conidiomata and conidial masses produced on CLA **d.** Cross section of pycnidium **e**–**f** Conidiogenous cells **g**, **h** Alpha conidia **i** Beta conidia. Scale bars: **d** = 100 µm **e**, **f** = 20 µm **g**, **h** = 10 µm, **i** = 20 µm

Figure 9.11 *Diaporthe capsicicola* (MFLU 25-0054 holotype)

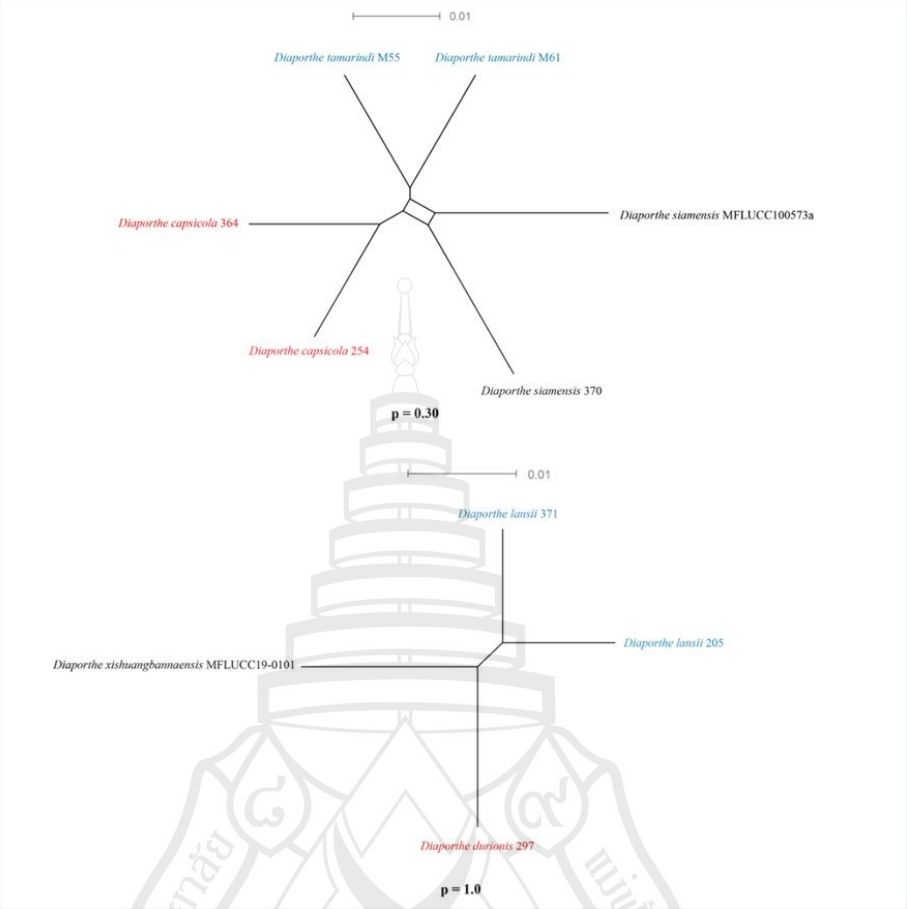

Note The pairwise homoplasy index (PHI) test was conducted using a five-loci sequence dataset. New taxa are printed in blue and red

Figure 9.12 The pairwise homoplasy index (PHI) test of new *Diaporthe* species and their closely related species in the *Diaporthe siamensis* species complex

Diaporthe chiangmaiensis N.I. de Silva, Lumyong & K.D. Hyde (2022)

Index Fungorum: IF 559527; MycoBank: MB 559527

Illustration and description: See De Silva et al. (2022); Pereira et al. (2024)

Known distribution: China (Luo et al., 2022), India (Gomes et al., 2013), Malaysia (Azuddin et al., 2021) and Thailand (De Silva et al., 2022, Seifollahi et al., 2023; This study).

Notes: Currently, three species are accepted within the *Diaporthe arecae* species complex, namely *D. arecae*, *D. chiangmaiensis*, and *D. smilacicola* (Pereira et al., 2023, 2024). The multi-locus phylogenetic tree showed that the strain MFLUCC 25-0077 clustered with the ex-type of *D. chiangmaiensis*, showing 83%/71%/1.00

(ML/MP/PP) bootstrap support (Figure 9.10). Therefore, the strain was identified as *D. chiangmaiensis*.

Diaporthe discoidispora F. Huang, K.D. Hyde & Hong Y. Li (2015)

Index Fungorum: IF 810580; MycoBank: MB 810580

Illustration and description: See Huang et al. (2015)

Known distribution: China and Thailand (Farr & Rossman, 2024; This study).

Habitat & host range: Isolated as endophyte and saprobe from *Camellia sinensis* (Theaceae), *Citrus reticulata* (Rutaceae), *Citrus sinensis*, *Citrus* sp., *Citrus unshiu*, and *Eugenia uniflora* (Myrtaceae) (Farr & Rossman, 2024; This study).

Notes: A single strain, MFLUCC 25-0129, was obtained in this study, clustered with the ex-type of *Diaporthe discoidispora* (Figure 9.10). This is the first report of *D. discoidispora* from leaf blight of *Eugenia uniflora* (Table A16).

Diaporthe durionis Armand, Pourmoghaddam, Jayaward. & K.D. Hyde, *sp. nov.*

Figure 9.13

Index Fungorum:; MycoBank:

Etymology: The epithet name refers to the host plant from which the fungus was isolated.

Associated with leaf blight of durian. Sexual morph: not observed. Asexual morph: *Conidiomata* pycnidial, globose, dark brown to black, semi-immersed, erumpent, solitary. *Conidiophores* hyaline, smooth, simple, 0–1 septate, cylindrical, straight or flexuous, 17–20 × 2–2.3 µm, or reduced to conidiogenous cells. *Conidiogenous cells* densely aggregated, subcylindrical to ampuliform, phialidic, straight or flexuous, 5–8 × 2–2.7 µm. *Alpha conidia* abundant, hyaline, smooth, aseptate, biguttulate, fusiform, straight, apex rounded or acute, base subacute to acute, 5.2–6.2 × 2–2.6 µm ($\bar{x}$ = 5.6 × 2.2 µm, n = 30). *Beta conidia* rare, hyaline, smooth, aseptate, filiform, straight or curved, tapering toward both ends, (15–)19–25 × 1.8–2.5 µm ($\bar{x}$ = 22.8 × 2 µm, n = 20). *Gamma conidia* rare, hyaline, smooth, aseptate, multiguttulate, fusiform, straight or curved, 11.5–13.5 × 1.9–2.3 µm.

Culture characteristics: Colonies on PDA reach 78–80 mm in diam. after 7 days at 25 ± 2 °C. Aerial mycelia fluffy, white on surface, becoming greyish sepia after 14

days. Reverse same colour. Colony entire in margin. Conidiomata produced after 10 days, irregularly distributed over the agar surface.

Material examined: Thailand, Chiang Rai Province, Wiang Chai District, associated with leaf blight of *Durio zibethinus* (Malvaceae) fruit rot, 04 July 2022, A. Armand, P134 (MFLU 25-0055 holotype; MFLUCC 25-0094 ex-type living culture).

Notes: A single strain, MFLUCC 25-0094, formed a distinct lineage, separate from *Diaporthe lansii* and *D. xishuangbannaensis* (Figure 9.10). *Diaporthe durionis* (MFLUCC 25-0094) shares 99.43% (532/535 bp) sequence similarity with *Diaporthe lansii* (MFLUCC 25-0058 and MFLUCC 25-0111)) in *tef1*, 96.90% (438/452 bp) in *tub2*, and 98.96% (477/482 bp) in *cmdA*. This species also shares 98.71% (308/312 bp) sequence similarity with *D. xishuangbannaensis* in *tef1*, 97.56% (441/452 bp) in *tub2*, and 96.29% (390/405 bp) in *cmdA*. Moreover, the PHI test indicated that there is no significant recombination ($p = 1.0$) among these species (Figure 9.12). Morphologically, *D. durionis* is distinguished from *D. xishuangbannaensis* in the size of alpha conidia (5.2–6.2 µm long (2.5 µm L/W) in *Diaporthe durionis* vs. 10–14 µm long (4.8 µm L/W) in *D. xishuangbannaensis*) (De Silva et al., 2021). *Diaporthe xishuangbannaensis* lacked both beta and gamma conidia, whereas they were produced by *Diaporthe durionis*.

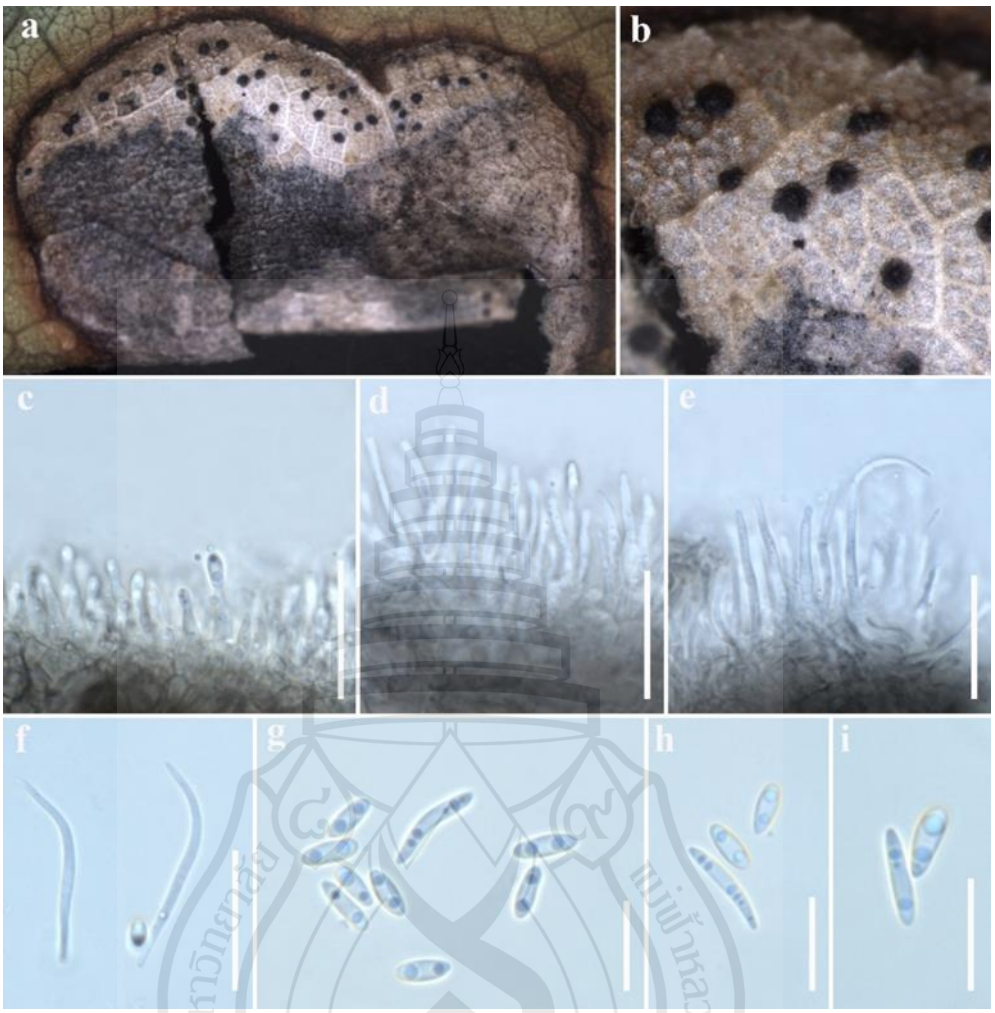

Note **a**, **b** Conidiomata produced the host leaves **c–e** Conidiophores and conidiogenous cells **f** Beta conidia **g**–**i** Alpha and gamma conidia. Scale bars: **c**–**f** = 20 µm, **g**–**i** = 10 µm

Figure 9.13 *Diaporthe durionis* (MFLU 25-0055 holotype)

Diaporthe lansii Armand, Pourmoghaddam, Jayaward. & K.D. Hyde, *sp. nov.*

Figure 9.14

Index Fungorum:; MycoBank:

Etymology: The epithet name refers to the host plant from which the fungus was isolated.

Associated with fruit rot of Langsat. Sexual morph: not observed. Asexual morph: *Conidiomata* pycnidial, subglobose or globose, dark brown or dark grey to black, semi-immersed, erumpent, solitary or aggregated. *Conidiophores* hyaline,

smooth, simple, 0–1 septate, cylindrical, straight or flexuous, 15–20 × 1.5–2.3 µm, or reduced to conidiogenous cells. *Conidiogenous cells* densely aggregated, subcylindrical to ampuliform, phialidic, straight or flexuous, 4.5–8 × 2–2.7 µm. *Alpha conidia* abundant, hyaline or brown, smooth, aseptate, biguttulate, rarely ellipsoid to fusiform, mostly spindle-like, straight or slightly curved, apex rounded or acute, base rounded or acute, 5.5–6.5 × 2.5–3.3 µm ($\bar{x}$ = 5.7 × 3 µm, n = 30). *Beta conidia* abundant, hyaline, smooth, aseptate, filiform, straight or curved, tapering toward both ends, 20–25 × 1.5–2.3 µm ($\bar{x}$ = 23.8 × 2 µm, n = 30). *Gamma conidia* not observed.

Culture characteristics: Colonies on PDA reach 83–90 mm in diam. after 7 days at 25 ± 2 °C. Aerial mycelia fluffy, white on surface, becoming isabelline to dark brick after 14 days. Reverse same colour. Colony entire in margin. Conidiomata produced after 20 days, irregularly distributed over the agar surface.

Material examined: Thailand, Chiang Rai Province, Mueang Chiang Rai District, Tha Sut, associated with *Lansium domesticum* (Meliaceae) fruit rot, 05 April 2023, A. Armand, M2-3 (MFLU 25-0056 holotype, MFLUCC 25-0058 ex-type living culture).

Notes: Two strains, MFLUCC 25-0058 and MFLUCC 25-0111, isolated from *Lansium domesticum* and *Psidium guajava*, clustered in a distinct clade, separate from *Diaporthe durionis* (Figure 9.10). *Diaporthe lansii* shares 99.43% (532/535 bp) sequence similarity with *D. durionis* in *tef1*, 96.90% (438/452 bp) in *tub2*, and 98.96% (477/482 bp) in *cmdA*. Furthermore, the PHI test indicated that there is no significant recombination (p = 1.0) among these species (Figure 9.12). Morphologically, *D. lansii* differs from *D. durionis* in the shape of alpha conidia (rarely ellipsoid to fusiform, mostly spindle-like in *D. lansii* vs. fusiform in *D. durionis*). *Diaporthe lansii* lacked gamma conidia, whereas gamma conidia were produced by *Diaporthe durionis*.

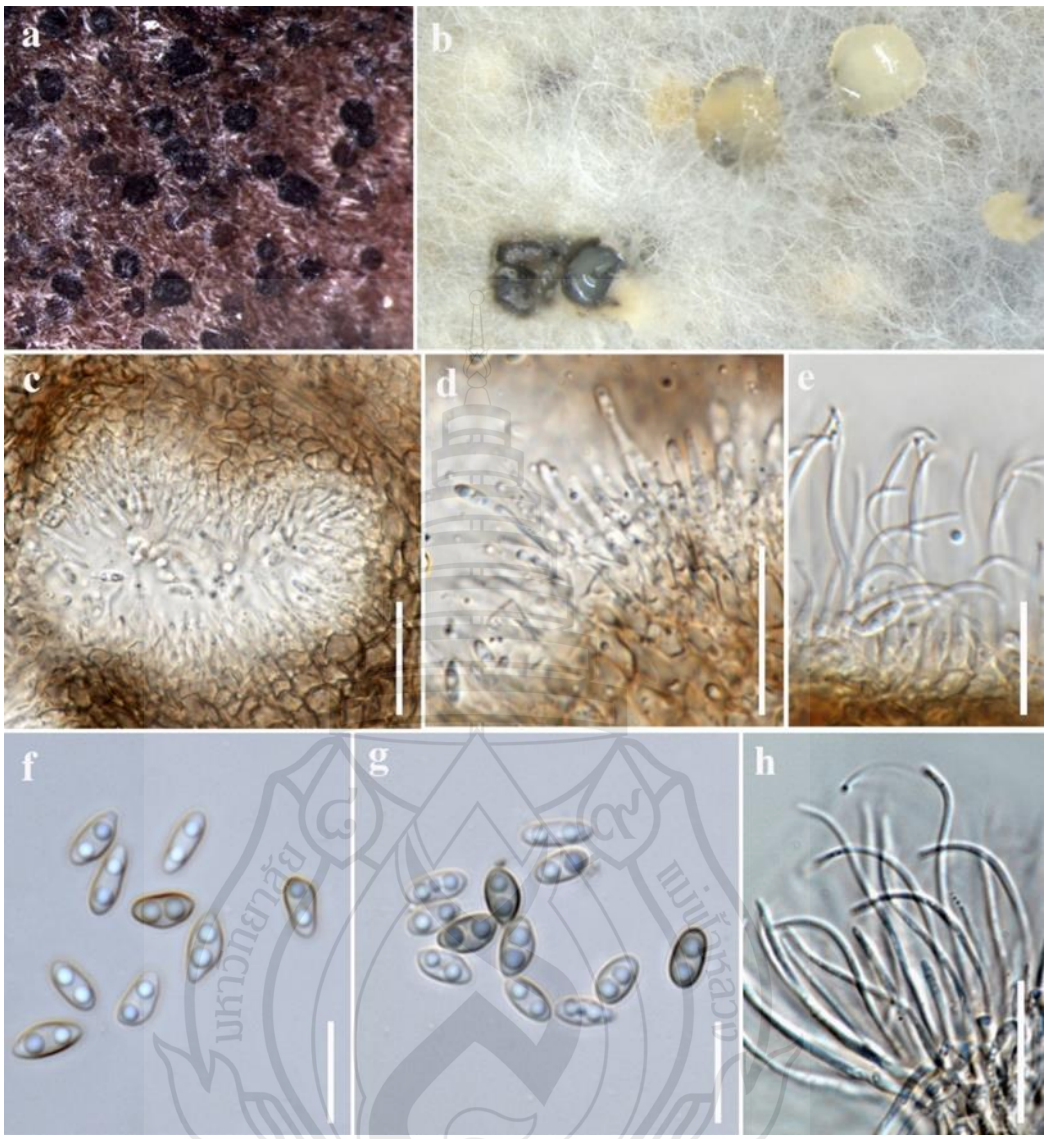

Note **a** Conidiomata produced the host leaf **b** Conidiomata and conidial mass produced on CLA **c** Cross section of pycnidium **d**, **e** Conidiophores and conidiogenous cells **f**, **g** Alpha conidia **h** Beta conidia. Scale bars: **c**–**e** = 20 µm, **f**, **g** = 10 µm, **h** = 20 µm

Figure 9.14 *Diaporthe lansii* (MFLU 25-0056 holotype)

Diaporthe perseae-americanae Armand, Pourmoghaddam, Jayaward. & K.D. Hyde, *sp. nov.*

Figure 9.15

Index Fungorum:; MycoBank:

Etymology: The epithet name refers to the host plant from which the fungus was isolated.

Associated with leaf blight of Avocado. Sexual morph: not observed. Asexual morph: *Conidiomata* pycnidial, subglobose or globose, brown to dark brown or dark grey, semi-immersed, erumpent, solitary or aggregated. *Conidiophores* hyaline, smooth, simple, aseptate, cylindrical, straight or flexuous, 11–15 × 2–2.5 µm, or reduced to conidiogenous cells. *Conidiogenous cells* densely aggregated, subcylindrical to ampuliform, phialidic, straight or flexuous, 3.5–6.5 × 2–2.5 µm. *Alpha conidia* abundant, hyaline, smooth, aseptate, biguttulate, fusiform, mostly straight, rarely slightly curved, apex rounded, base acute, 7.5–9 × 2.5–3 µm ($\bar{x}$ = 8.5 × 2.9 µm, n = 30). *Beta conidia* abundant, hyaline, smooth, aseptate, filiform, straight or curved, tapering toward the apex, 20–27 × 2–2.5 µm ($\bar{x}$ = 25.7 × 2.7 µm, n = 30). *Gamma conidia* rare, hyaline, smooth, aseptate, multiguttulate, narrowly fusiform, straight or slightly curved, 12.5–15 × 1.5–2 µm.

Culture characteristics: Colonies on PDA reach 77–83 mm in diam. after 7 days at 25 ± 2 °C. Aerial mycelia fluffy, white on surface, becoming pale luteous after 20 days. Reverse e brownish yellow. Colony entire in margin. Conidiomata produced after 20 days, irregularly distributed over the agar surface.

Material examined: Thailand, Chiang Rai Province, Mae Salong Nok, associated with leaf blight of *Persea americana* (Lauraceae), 14 February 2022, A. Armand, P5-2 (MFLU 25-0057 holotype; MFLUCC 25-0050 ex-type living culture).

Notes: A single strain, MFLUCC 25-0050, was isolated from *Persea americana* clustered as a distinct lineage, grouped as a sister group for *Diaporthe apiculata* in the *Diaporthe gardeniae* species complex, showing 82%/100%/1.00 (ML/MP/PP) bootstrap values (Figure 9.10). *Diaporthe perseae-americanae* shares 98.58% (431/436 bp) sequence similarity with *D. apiculata* (CGMCC3.17533) in ITS, 95.98% (263/274 bp) in *tef1*, and 99.44% (356/358 bp) in *tub2* (*cmdA* and *his3* sequence data are missing). Morphologically, *D. perseae-americanae* differs from *D. apiculata* (LC3418) in the shape of alpha conidia (fusiform, apex rounded, base acute *D. perseae-americanae* vs. apiculate or fusiform, tapering towards both ends in *D. apiculata*), and the size of beta conidia (20–27 µm long (20–27 µm long (9.5 µm L/W) in *D. perseae-americanae* vs. 25–39 µm long (14 µm L/W) in *D. apiculata*). Additionally, *D. perseae-*

americanae produced gamma conidia, which were not observed in *D. apiculata* (Gao et al., 2016).

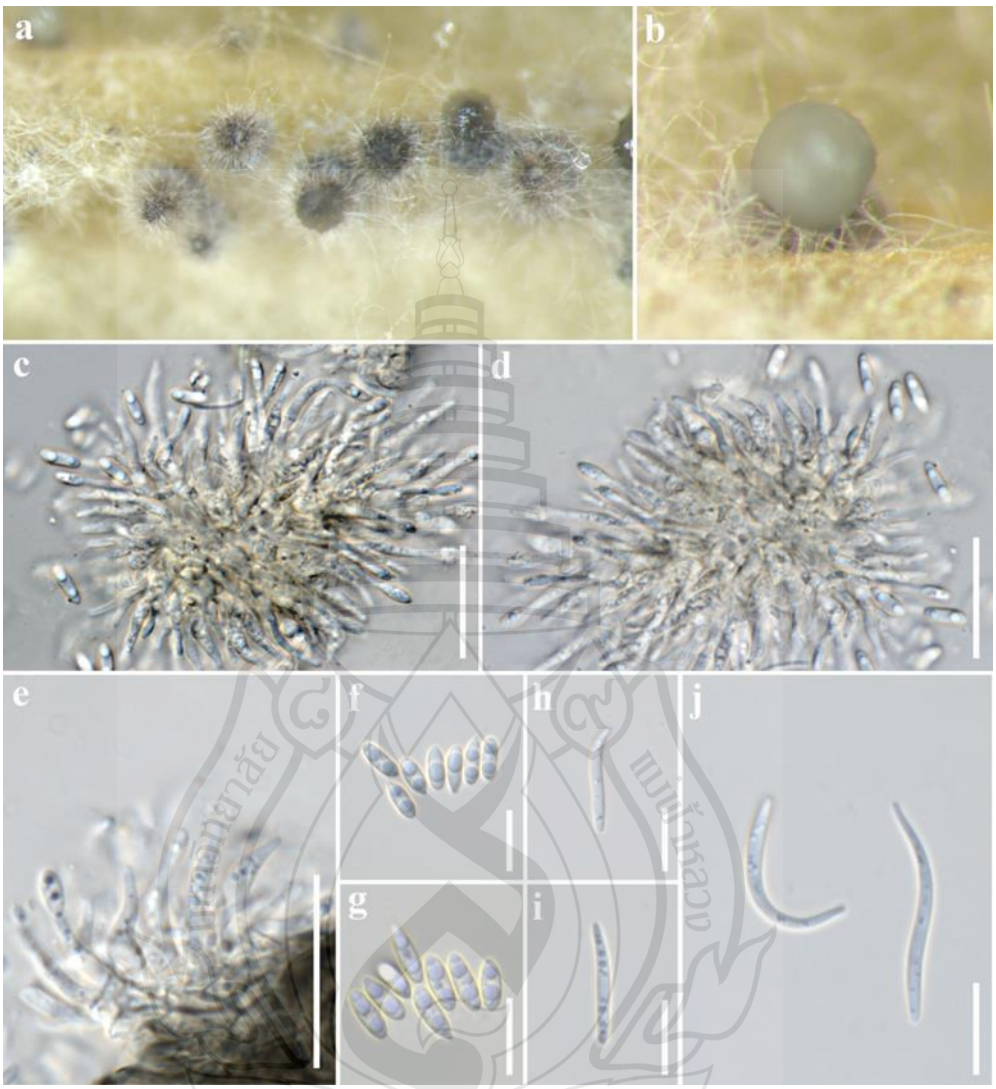

Note **a**, **b** Conidiomata and conidial mass produced on CLA **c-e** Conidiogenous cells **f, g** Alpha conidia **h**, **i** Gamma conidia **j** Beta conidia Scale bars: **c-e** = 20 µm, **f-j** = 10 µm

Figure 9.15 *Diaporthe perseae-americanae* (MFLU 25-0057 holotype)

Diaporthe pterocarpi (S. Hughes) Udayanga, Xing Z. Liu & K.D. Hyde (20120

Index Fungorum: IF 801055; MycoBank: MB 801055

Illustration and description: See Udayanga et al. (2012)

Known distribution: Distributed in Central and West Africa, Hong Kong, India, and Thailand (Farr & Rossman, 2024).

Habitat & host range: Reported from *Cucumis melo* (Cucurbitaceae), *Magnolia* sp. (Magnoliaceae), *Pterocarpus angolensis* (Fabaceae), *Pterocarpus erinaceus*, *Pterocarpus indicus*, *Pterocarpus santalinoides*, *Jatropha curcas* (Euphorbiaceae), and *Ougeinia dalbergioides* (Fabaceae) (Farr & Rossman, 2024).

Notes: The *Diaporthe pterocarpi* species complex was recently considered as a single species, *Diaporthe pterocarpi* (Dissanayake et al., 2024). Two strains were obtained from leaf blight of *Iris pseudacorus* and *Ziziphus mauritiana* identified as *Diaporthe pterocarpi* through multi-gene phylogenetic analysis (Fig. 10). This study reveals two new host records of *D. pterocarpi* from Thailand (Table A16).

Diaporthe rosae Samarak. & K.D. Hyde (2018)

Index Fungorum: IF 554072; MycoBank: MB 554072

Illustration and description: See Wanasinghe et al. (2018)

Known distribution: Thailand (Farr & Rossman, 2024).

Habitat & host range: Reported from *Magnolia champaca* (Magnoliaceae), *Nephelium lappaceum* (Sapindaceae), *Rosa* sp. (Rosaceae), and *Senna siamea* (Fabaceae) (Abeywickrama et al., 2023; Huanraluek et al., 2022; Farr & Rossman, 2024).

Notes: The *Diaporthe rosae* species complex was recently considered as a single species, *Diaporthe rosae* (Dissanayake et al. 2024). Seven strains were obtained from leaf blight of different plants identified as *D. rosae* through multi-gene phylogenetic analysis (Figure 9.10). This study provides six new host records of *D. rosae* from Thailand, as outlined in Table A16.

Diaporthe siamensis Udayanga, Xing Z. Liu & K.D. Hyde (2012)

Index Fungorum: IF 800826; MycoBank: MB 800826

Illustration and description: See Udayanga et al. (2012)

Known distribution: China (Cui et al., 2021) and Thailand (Hyde et al., 2018b; Udayanga et al., 2012).

Habitat & host range: Reported as endophyte and saprobe from *Dasymaschalon* sp. (Annonaceae), *Pandanus* sp. (Pandanaceae), and *Citrus sinensis* (Rutaceae) (Farr & Rossman, 2024).

Notes: Phylogenetic analyses showed that a single strain clustered with the ex-type of *D. siamensis*, showing 71%/61%/0.99 (ML/MP/PP) bootstrap support (Figure

9.10). This is a new host record of *D. siamensis* isolated from *Durio zibethinus* fruit rot (Table A16).

Diaporthe sojae Lehman (1923)

Index Fungorum: IF 278338; MycoBank: MB 278338

Illustration and description: See Lehman (1923)

Known distribution: Globally distributed (Farr & Rossman, 2024).

Habitat & host range: Associated with *Actinidia chinensis* (Actinidiaceae), *Actinidia deliciosa*, *Arachis hypogaea* (Fabaceae), *Arctium lappa* (Asteraceae), *Asparagus officinalis* (Asparagaceae), *Aster exilis* (Asteraceae), *Camellia oleifera* (Theaceae), *Caperonia palustris* (Euphorbiaceae), *Citrus limon* (Rutaceae), *Citrus reticulata*, *Citrus unshiu*, *Cucumis melo* (Cucurbitaceae), *Cyclopia subternata* (Fabaceae), *Euphorbia nutans* (Euphorbiaceae), *Glycine max* (Fabaceae), *Glycine soja*, *Helianthus annuus* (Asteraceae), *Phaseolus limensis* (Fabaceae), *Phaseolus vulgaris*, *Pyrus pyrifolia* (Rosaceae), *Stokesia laevis* (Asteraceae), *Vitis vinifera* (Vitaceae), *Abutilon theophrasti* (Malvaceae), and *Strophostyles helvola* (Fabaceae) (Farr & Rossman, 2024).

Notes: All species in the *Diaporthe sojae* species complex were recently considered as a single species, *Diaporthe sojae* (Dissanayake et al., 2024). Therefore, three strains clustered within the *Diaporthe sojae* species complex were identified as *Diaporthe sojae* (Figure 9.10). This study reports two new host records of *D. sojae* from Thailand (Table A16).

Diaporthe tamarindi Armand, Pourmoghaddam, Jayaward. & K.D. Hyde, *sp. nov*.

Figure 9.16

Index Fungorum:; MycoBank:

Etymology: The epithet name refers to the host plant from which the fungus was isolated.

Associated with leaf blight of tamarind. Sexual morph: not observed. Asexual morph: *Conidiomata* pycnidial, subglobose or globose, dark brown to black, semi-immersed or immersed, erumpent, solitary or aggregated. *Conidiophores* hyaline, smooth, simple, aseptate, cylindrical, straight, 13–18 × 1.5–2 μm, or reduced to conidiogenous cells. *Conidiogenous cells* densely aggregated, subcylindrical to

cylindrical, phialidic, straight, 6–9.5 × 1.8–2.5 µm. *Alpha conidia* abundant, hyaline, smooth, aseptate, biguttulate, ellipsoid to fusiform, straight, apex rounded, base rounded to acute, 5–8 × 2–2.5 µm ($\bar{x}$ = 6.2 × 2.3 µm, n = 30). *Beta conidia* rare, hyaline, smooth, aseptate, filiform, curved, strongly tapered toward the apex, base swollen, 16–23 × 1.5–2.5 µm ($\bar{x}$ = 21 × 2 µm, n = 20). *Gamma conidia* rare, hyaline, smooth, aseptate, biguttualte to multiguttulate, fusiform to subcylindrical, straight or slightly curved, 9–13 × 1.8–2.8 µm.

Culture characteristics: Colonies on PDA reach 69–75 mm in diam. after 7 days at 25 ± 2 °C. Aerial mycelia fluffy, white on surface, becoming greenish olivaceous after 14 days. Reverse same colour. Colony entire in margin. Conidiomata produced after 20 days, irregularly distributed over the agar surface.

Material examined: Thailand, Chiang Rai Province, Phan District, Sai Khao, associated with *Tamarindus indica* (Fabaceae) leaf blight, 08 February 2023, M. Fallahi, MF99-2 (MFLU 25-0058 holotype; MFLUCC 25-0151 ex-type living culture).

Notes: Based on multi-gene phylogenetic analyses, MFLUCC 25-0150 and MFLUCC 25-0151 clustered together in a distinct clade, closely related to *Diaporthe capsicola* and *D. siamensis* (Figure 9.10). These strains were associated with leaf blight of *Tamarindus indica* and fruit rot of *Nephelium lappaceum*. Molecular and morphological comparisons between *D. tamarindi* and *D. capsicola* have been discussed earlier (see the notes section under *Diaporthe capsicola*). *Diaporthe tamarindi* shares 96.48% (302/313 bp) sequence similarity with *D. siamensis* in *tef1*, and 98.76% (399/404 bp) in *tub2*. Moreover, the PHI test revealed that there is no significant recombination (p = 0.30) among *D. tamarindi*, *D. capsicola*, and *D. siamensis* (Figure 9.12).

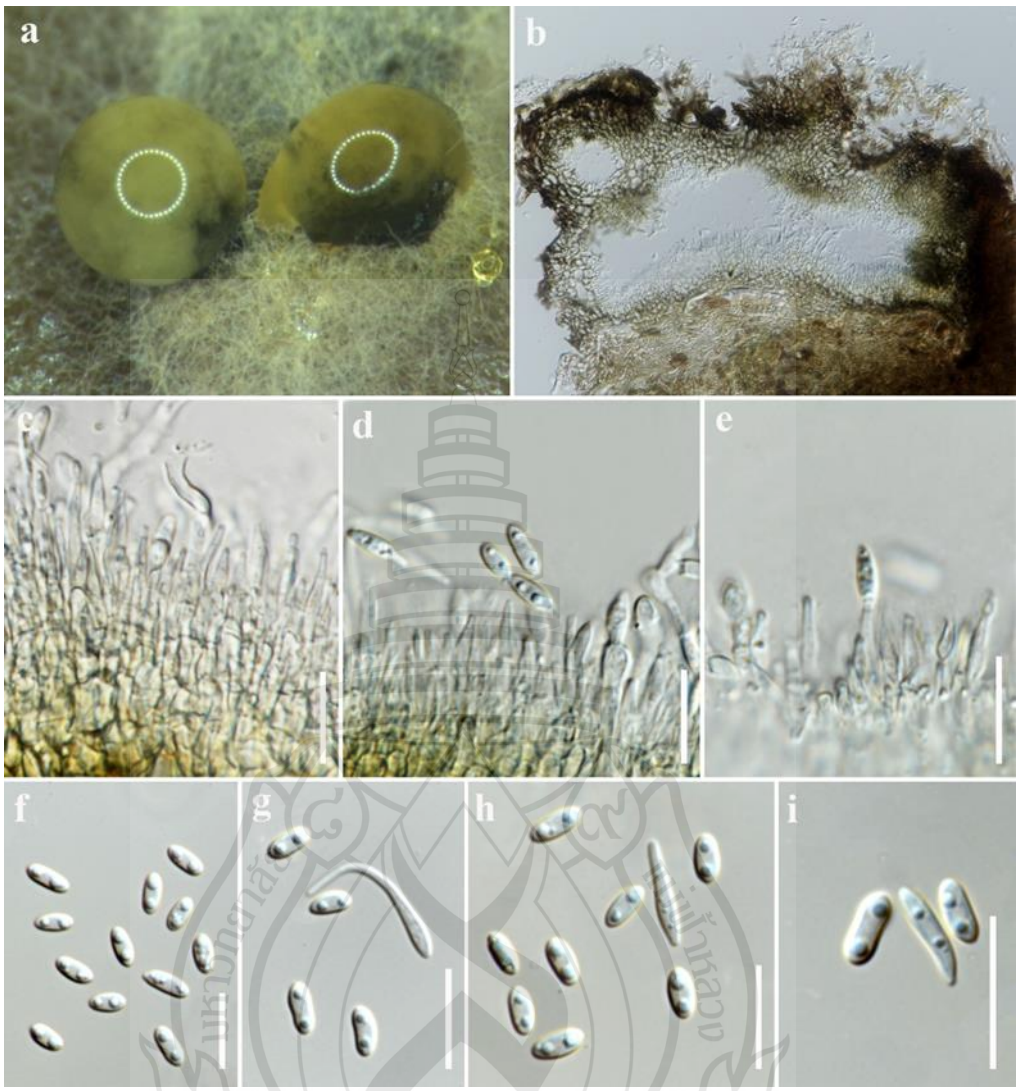

Note **a** Conidiomata and conidial mass produced on CLA **b** Cross section of pycnidium **c-e** Conidiophores and conidiogenous cells **f** Alpha conidia **g** Beta conidia **h**, **i** Alpha and gamma conidia Scale bars: **c–i** = 10 µm

Figure 9.16 *Diaporthe tamarindi* (MFLU 25-0058 holotype)

Diaporthe tulliensis R.G. Shivas, Vawdrey & Y.P. Tan (2015)

Index Fungorum: IF 812896; MycoBank: MB 812896

Illustration and description: See Crous et al. (2015b)

Known distribution: Australia (Dissanayake et al., 2017; Yang et al., 2018), China (Bai et al., 2017), and Thailand (This study).

Habitat & host range: Reported from *Actinidia chinensis* (Actinidiaceae), *Parthenocissus tricuspidate* (Vitaceae), and *Theobroma cacao* (Malvaceae) (Farr & Rossman, 2024).

Notes: The *Diaporthe tulliensis* species complex was recently considered as a single species, *Diaporthe tulliensis* (Dissanayake et al., 2024). Three strains clustered withing *Diaporthe tulliensis* were obtained from fruit rot of *Solanum lycopersicum* (Solanaceae), *Durio zibethinus* (Malvaceae), and *Litchi chinensis* (Sapindaceae) identified as *Diaporthe tulliensis* (Fig. 10). This study reports three new host records of *D. tulliensis* from Thailand (Table A16).

Sordariomycetes

Hypocreales

Nectriaceae

Fusarium coffeibaccae M.M. Costa, L.H. Pfenning, Sand.-Den. & Crous (2024)

Index Fungorum: IF 854633; MycoBank: MB 854633

Illustration and description: See Costa et al. (2024)

Known distribution: Brazil, China, Ethiopia, Guinea, Kenya, Malawi, New Caledonia, New Guinea, Nyasaland, Thailand, and Zimbabwe (Farr & Rossman, 2024; This study).

Habitat & host range: Associated with leaves, bark and stem of *Coffea arabica* (Rubiaceae) and *Coffea* sp. (Farr & Rossman, 2024).

Notes: A single strain obtained in this study clustered within *Fusarium coffeibaccae* clade, showing 100%/100%/1.00 (ML/MP/PP) bootstrap support (Figure 9.2). The species was discovered in 2024 from fruit of *Coffea arabica* (Costa et al., 2024). This is the first report of *F. coffeibaccae* associated with guajava fruit rot worldwide.

Fusarium endophyticum Suwannar. (2023)

Index Fungorum: IF 848095; MycoBank: MB 848095

Illustration and description: See Suwannarach et al. (2023)

Known distribution: Thailand (Suwannarach et al., 2023).

Habitat & host range: Endophytic of *Camellia sinensis* var. *assamica* (Theaceae) (Suwannarach et al., 2023).

Notes: Two strains obtained in this study clustered with the ex-type of *Fusarium endophyticum*, showing 100%/99%/1.00 (ML/MP/PP) bootstrap support (Figure 9.2). The species was identified in 2023 as an endophyte of *Camellia sinensis* (Suwannarach et al., 2023). This study reports two new host records of *F. endophyticum* from Thailand, associated with *Citrus* sp. and *Dimocarpus longan* (Sapindaceae) fruit rot (Table A16).

Fusarium fujikuroi Nirenberg (1976)

Index Fungorum: IF 314213; MycoBank: MB 314213

Illustration and description: See Han et al. (2023)

Known distribution: Distributed worldwide (Farr & Rossman, 2024).

Habitat & host range: Widely identified as causal agent of rice bakanae disease, rice spikelet rot, wheat crown rot, wheat scab, maize ear rot, and maize stalk rot (Duan et al., 2020; Han et al., 2023; Qiu et al., 2020). *Fusarium fujikuroi* was mostly reported from Poaceae, but also reported from Anacardiaceae, Bromeliaceae, Cucurbitaceae, Fabaceae, Juglandaceae, Liliaceae, Malvaceae, Musaceae, Pinaceae, Piperaceae, Solanaceae, and Vitaceae (Farr & Rossman, 2024).

Notes: A single strain was identified as *Fusarium fujikuroi* (Figure 9.2), reported from *Persea americana* (Lauraceae) for the first time worldwide (Table A16). Phylogenetic analyses showed that the strain MFLUCC 25-0074 clustered with *Fusarium fujikuroi*, showing 100%/99%/1.00 (ML/MP/PP) bootstrap support (Figure 9.2).

Fusarium hainanense M.M. Wang, Qian Chen & L. Cai (2019)

Index Fungorum: IF 829536; MycoBank: MB 829536

Illustration and description: See Wang et al. (2019)

Known distribution: China, Costa Rica, Cuba, and Thailand (Farr & Rossman, 2024; This study).

Habitat & host range: Associated with *Acacia* sp. (Fabaceae), *Musa* sp. (Musaceae), *Oryza* sp. (Poaceae) (Farr & Rossman, 2024).

Notes: A single strain was identified as *Fusarium hainanense* (Figure 9.2), isolated from *Mangifera indica* for the first time worldwide (Table A16). The strain MFLUCC 25-0070 clustered with *Fusarium hainanense* clade, showing 83%/99%/1.00 (ML/MP/PP) bootstrap support (Figure 9.2).

Fusarium pernambucanum A.C.S. Santos, C.S. Lima, P.V. Tiago & N.T. Oliveira (2019)

Index Fungorum: IF 825273; MycoBank: MB 825273

Illustration and description: See Santos et al. (2019)

Known distribution: Brazil, China, and Thailand (Farr & Rossman, 2024; This study).

Habitat & host range: The species was primarily identified associated with a whitefly in the family Aleyrodidae (*Aleurocanthus woglumi*) and a scale insect in the family Dactylopiidae (*Dactylopius opuntiae*). However, it has been reported from plant hosts, including *Cucumis melo* (Cucurbitaceae) (Medeiros Araujo et al., 2021), *Musa* sp. (Musaceae) (Lima et al., 2021), *Passiflora edulis* (Passifloraceae) (Liu Y. et al., 2021).

Notes: Two strains identified as *Fusarium pernambucanum* (Figure 9.2) were reported from *Carica papaya* and *Persea americana* for the first time worldwide (Table A16). Phylogenetic analyses showed that the strains MFLUCC 25-0066 and MFLUCC 25-0085 clustered with *Fusarium pernambucanum*, showing 100%/99%/1.00 (ML/MP/PP) bootstrap support (Figure 9.2).

Fusarium pseudocircinatum O'Donnell & Nirenberg (1998)

Index Fungorum: IF 444889; MycoBank: MB 444889

Illustration and description: See Nirenberg & O'Donnell (1998)

Known distribution: Reported from America (Cavalcanti et al., 2020; Montoya-Martínez et al., 2022; Nirenberg & O'Donnell, 1998), Caribbean (Garcia-Lopez et al., 2016), Oceania (Liew et al., 2016; Nirenberg & O'Donnell, 1998), South Asia (Farr & Rossman, 2024; Kee et al., 2020; Pinaria et al., 2010).

Habitat & host range: Reported from *Desmodium procumbens* (Fabaceae), *Handroanthus chrysotrichus* (Bignoniaceae), *Heteropsylla incisa* (Psyllidae), *Mangifera indica* (Anacardiaceae), *Musa acuminata* (Musaceae), *Pinus kesiya* (Pinaceae), *Sansevieria trifasciata* (Asparagaceae), *Sida rhombifolia* (Malvaceae), *Solanum* sp. (Solanaceae), *Swietenia macrophylla* (Meliaceae), *Tabebuia rosea* (Bignoniaceae), and *Vanilla planifolia* (Orchidaceae) (Farr & Rossman, 2024).

Notes: Three strains were identified as *Fusarium pseudocircinatum* based on multi-locus phylogenetic analysis. The strains clustered with *Fusarium*

pseudocircinatum, showing 78%/89%/1.00 (ML/MP/PP) bootstrap support (Figure 9.2). This study discovered the species associated with leaf blight of *Spathiphyllum* sp. (Araceae), and fruit rot of *Citrus* sp. (Rutaceae) and *Carica papaya* (Caricaceae) as three new host records (Table A16).

Fusarium sacchari (E.J. Butler) W. Gams (1971)

Index Fungorum: IF 314221; MycoBank: MB 314221

Illustration and description: See Han et al. (2023)

Known distribution: Globally distributed (Farr & Rossman, 2024).

Habitat & host range: *Fusarium sacchari* is pathogenic to diverse crops worldwide, including maize ear rot, wheat scab, rice spikelet rot and maize stalk rot (Duan et al., 2020; Farr & Rossman, 2024). This species was also reported from other plant hosts, such as *Musa* sp. (Musaceae), *Lycopersicon esculentum* (Solanaceae), *Ananas comosus* (Bromeliaceae), *Pinus radiata* (Pinaceae), *Linum usitatissimum* (Linaceae), and *Syzygium cordatum* (Myrtaceae). *Fusarium sacchari* is also known associated with insets, including *Pyrilla perpusilla* (Lophopidae), *Pulvinaria elongata* (Coccidae), *Emmalocera depressella* (Pyralidae), and *Chilo sacchariphagus-indicus* (Crambidae) (Farr & Rossman, 2024; Han et al., 2023).

Notes: A single strain was identified as *Fusarium sacchari*, isolated from *Musa* sp. (Musaceae) for the first time from Thailand (Table A16). Based on multi-locus phylogenetic analysis, the strain MFLUCC 25-0049 clustered with *Fusarium sacchari*, showing 100%/100%/1.00 (ML/MP/PP) bootstrap support (Figure 9.2).

Fusarium sulawesiense Maryani, Sand.-Den., L. Lombard, Kema & Crous (2019)

Index Fungorum: IF 830777; MycoBank: MB 830777

Illustration and description: See Maryani et al. (2019)

Known distribution: Reported from Brazil (Medeiros Araujo et al., 2021), China (Wang et al., 2019), Indonesia (Lima et al., 2021), Mexico (Montoya-Martínez et al., 2022), Pakistan (Kamran et al., 2020), and Thailand (Xia et al., 2019; This study).

Habitat & host range: *Fusarium sulawesiense* was reported from *Cucumis melo* (Cucurbitaceae), *Musa acuminata* (Musaceae), *Oryza sativa* (Poaceae), *Bixa orellana* (Bixaceae), *Capsicum* sp. (Solanaceae), *Citrus reticulata* (Rutaceae), *Colocasia esculenta* (Araceae), *Gossypium hirsutum* (Malvaceae), *Ipomoea aquatica*

(Convolvulaceae), *Ipomoea batatas*, *Luffa aegyptiaca* (Cucurbitaceae), *Sesamum indicum* (Pedaliaceae), *Sida rhombifolia* (Malvaceae), *Sorghum vulgare* (Poaceae), *Syngonium auritum* (Araceae), and *Zea* sp. (Poaceae) (Farr & Rossman, 2024).

Notes: Two strains were identified as *Fusarium sulawesiense*, marking the first global report of this species associated with fruit rot of *Dimocarpus longan* (Sapindaceae) and *Carica papaya* (Caricaceae) (Table A16). Based on the multi-locus phylogenetic tree, the strains MFLUCC 25-0062 and MFLUCC 25-0047 clustered with *Fusarium sulawesiense*, showing 85%/81%/0.98 (ML/MP/PP) bootstrap support (Figure 9.2).

Dothideomycetes

Botryosphaeriales

Botryosphaeriaceae

Lasiodiplodia brasiliensis M.S.B. Netto, M.W. Marques & A.J.L. Phillips 2014

Index Fungorum: IF 812566; MycoBank: MB 812566

Illustration and description: See Netto et al. (2014)

Known distribution: Australia, Brazil, China, Laos, Madagascar, Malaysia, Mexico, Peru, Puerto Rico, Thailand, and Turkey (Farr & Rossman, 2024).

Habitat & host range: Reported as saprobe and pathogen from *Adansonia madagascariensis* (Malvaceae), *Anacardium occidentale* (Anacardiaceae), *Annona squamosa* (Annonaceae), *Annona muricata*, *Carica papaya* (Caricaceae), *Cocos nucifera* (Arecaceae), *Eucalyptus* sp. (Myrtaceae), *Fragaria* × *ananassa* (Rosaceae), *Malus domestica* (Rosaceae), *Mangifera indica* (Anacardiaceae), *Spondias purpurea* (Anacardiaceae), *Tectona grandis* (Lamiaceae), *Vitis vinifera* (Vitaceae), *Aquilaria crassna* (Thymelaeaceae), *Citrus latifolia* (Rutaceae), *Dimocarpus longan* (Sapindaceae), *Gossypium hirsutum* (Malvaceae), *Manihot esculenta* (Euphorbiaceae), and *Sansevieria trifasciata* (Asparagaceae) (Farr & Rossman, 2024).

Notes: A single strain was identified as *Lasiodiplodia brasiliensis*, marking the first global report of this species associated with fruit rot of *Durio zibethinus* (Malvaceae) (Table A16). Phylogenetic analyses showed that the strain MFLUCC 25-0124 clustered with the ex-type of *Lasiodiplodia brasiliensis*, showing 73%/1.00 (ML/PP) bootstrap support (Figure 9.17).

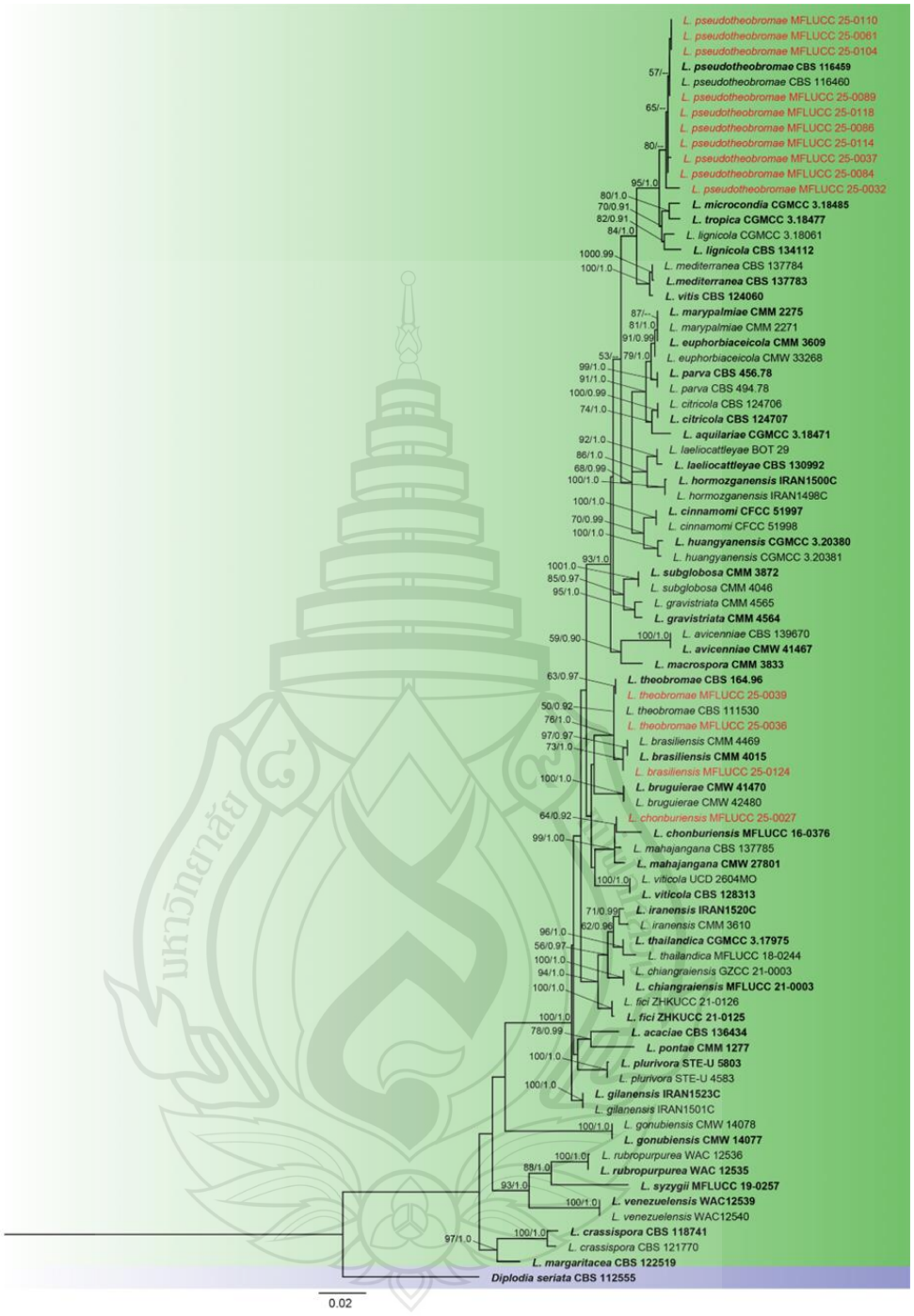

Note Maximum likelihood bootstrap values greater than 50% and bayesian posterior probabilities greater than 0.90 are shown near the nodes, respectively. The tree is rooted with *Diplodia seriata* (CBS 112555). The newly obtained strains are in red, and ex-type strains are in bold

Figure 9.17 The maximum likelihood (ML) tree of *Lasiodiplodia* based on the concatenated ITS, *tef1*, *tub*2, and *rpb2* sequence dataset

Lasiodiplodia chonburiensis Tibpromma & K.D. Hyde (2018)

Index Fungorum: IF 554472; MycoBank: MB 554472

Illustration and description: See Tibpromma et al. (2018)

Known distribution: Thailand (Hyde et al., 2018b; This study).

Habitat & host range: Associated with leaf blight in *Hevea brasiliensis* (Euphorbiaceae) (Pornsuriya et al., 2023) and saprobic on dead leaves of *Pandanus* sp. (Pandanaceae) (Tibpromma et al., 2018).

Notes: A single strain was identified as *Lasiodiplodia chonburiensis* represnting the first worldwide report of this species associated with leaf blight of *Morinda citrifolia* (Rubiaceae) (Table A16). The phylogenetic tree showed that the strain MFLUCC 25-0027 clustered with the ex-type of *Lasiodiplodia chonburiensis*, showing 64%/0.92 (ML/PP) bootstrap support (Figure 9.17).

Lasiodiplodia pseudotheobromae A.J.L. Phillips, A. Alves & Crous (2008)

Index Fungorum: IF 510941; MycoBank: MB 510941

Illustration and description: See Alves et al. (2008)

Known distribution: Distributed globally in tropical and subtropical regions (Farr & Rossman, 2024; Rathnayaka et al., 2023).

Habitat & host range: Reported as saprobe and pathogen from *Acacia* spp. (Acacia), *Adansonia digitata* (Malvaceae), *Albizia falcataria* (Fabaceae), *Anacardium* spp. (Anacardiaceae), *Annona* spp. (Annonaceae), *Aquilaria crassna* (Thymelaeaceae), *Bouea burmanica* (Anacardiaceae), *Bougainvillea spectabilis* (Nyctaginaceae), *Camellia sinensis* (Theaceae), *Cananga odorata* (Annonaceae), *Carica papaya* (Caricaceae), *Citrus* spp. (Rutaceae), *Coffea arabica* (Rubiaceae), *Cynometra malaccensis* (Fabaceae), *Dimocarpus longan* (Sapindaceae), *Diospyros kaki* (Ebenaceae), *Durio zibethinus* (Malvaceae), *Eucalyptus* spp. (Myrtaceae), *Ficus racemosa* (Moraceae), *Gmelina arborea* (Lamiaceae), *Gossypium hirsutum* (Malvaceae), *Hevea brasiliensis* (Euphorbiaceae), *Jatropha curcas* (Euphorbiaceae), *Juglans regia* (Juglandaceae), *Juniperus chinensis* (Cupressaceae), *Lagerstroemia indica* (Lythraceae), *Macadamia integrifolia* (Proteaceae), *Malus pumila* (Rosaceae), *Mangifera indica* (Anacardiaceae), *Mangifera sylvatica*, *Manihot esculenta* (Euphorbiaceae), *Morinda officinalis* (Rubiaceae), *Morus alba* (Moraceae), *Nephelium lappaceum* (Spindaceae), *Nopalea cochenillifera* (Cactaceae), *Ormosia pinnata*

(Fabaceae), *Osmanthus fragrans* (Oleaceae), *Pandanus* sp. (Pandanaceae), *Parkinsonia aculeata* (Fabaceae), *Paulownia fortune* (Paulowniaceae), *Persea americana* (Lauraceae), *Phyllanthus acidus* (Phyllanthaceae), *Pinus* sp. (Pinaceae), *Pistacia* sp. (Anacardiaceae), *Plukenetia volubilis* (Euphorbiaceae), *Prunus persica* (Rosaceae), *Psidium* sp. (Myrtaceae), *Pteridium aquilinum* (Dennstaedtiaceae), *Pterocarpus angolensis* (Fabaceae), *Rosa* sp. (Rosaceae), *Sansevieria trifasciata* (Asparagaceae), *Santalum album* (Santalaceae), *Schizolobium parahyba* (Fabaceae), *Senegalia mellifera* (Fabaceae), *Spondias purpurea* (Anacardiaceae), *Syzygium* spp. (Myrtaceae), *Tamarindus indica* (Fabaceae), *Tectona grandis* (Lamiaceae), *Terminalia* spp. (Combretaceae), *Theobroma cacao* (Malvaceae), *Vaccinium corymbosum* (Ericaceae), *Vachellia karroo* (Fabaceae), *Vitis vinifera* (Vitaceae), and *Zea mays* (Poaceae) (Farr & Rossman, 2024).

Notes: Ten strains obtained in this study clustered with the *Lasiodiplodia pseudotheobromae* clade, showing 80%/– (ML/MP) bootstrap support (Figure 9.17). The strains were associated with leaf blight of *Iris pseudacorus* (Iridaceae), *Elaeagnus pungens* (Elaeagnaceae), *Dimocarpus longan* (Sapindaceae), *Litchi chinensis* (Sapindaceae), and *Durio zibethinus* (Malvaceae), and fruit rot of *Dimocarpus longan*, *Persea americana* (Lauraceae), and *Durio zibethinus*. This study presents three new host records of *L. pseudotheobromae* from Thailand (Table A16).

Lasiodiplodia theobromae (Pat.) Griffon & Maubl. (1909)

Index Fungorum: IF 188476; MycoBank: MB 188476

Illustration and description: See Zhang et al. (2021)

Known distribution: Distributed globally in tropical and subtropical regions (Farr & Rossman, 2024; Rathnayaka et al., 2023).

Habitat & host range: Reported on almost all host families except for Dennstaedtiaceae, Phyllanthaceae, Podocarpaceae, Rhizophoraceae, and Salvadoraceae (Farr & Rossman, 2024; Rathnayaka et al., 2023).

Notes: Two strains were identified as *Lasiodiplodia theobromae*, representing a new geographical report of *L. theobromae* associated with fruit rot of *Musa* sp. (Musaceae) and a new host record from *Durio zibethinus* (Malvaceae) leaf blight (Table A16). Based on the phylogenetic tree, the strains MFLUCC 25-0039 and MFLUCC 25-

0036 clustered with the ex-type of *Lasiodiplodia theobromae*, showing 50%/0.92 (ML/PP) bootstrap support (Figure 9.17).

Sordariomycetes

Hypocreales

Nectriaceae

Neocosmospora diminuta Sand.-Den. & Crous (2019)

Index Fungorum: IF 831180 ; MycoBank: MB 831180

Illustration and description: See Sandoval-Denis et al. (2019)

Known distribution: The United States (Sandoval-Denis et al., 2019) and Thailand (This study).

Habitat & host range: Reported from *Coelocaryon preussi* (Myristicaceae) treated wood and bathroom sink.

Notes: A single strain was identified as *Neocosmospora diminuta* in this study, isolated from *Durio zibethinus* (Malvaceae) fruit rot for the first time worldwide (Table A16). Phylogenetic analyses revealed that the strain MFLUCC 25-0059 clustered with the ex-type of *Neocosmospora diminuta*, showing 100%/98%/1.00 (ML/MP/PP) bootstrap support (Figure 9.2).

Neocosmospora metavorans (Al-Hatmi, S.A. Ahmed & de Hoog) Sand.-Den. & Crous (2018)

Index Fungorum: IF 823687; MycoBank: MB 823687

Illustration and description: See Al-Hatmi eat al. (2018)

Known distribution: The United States, Greece, India, Italy, Spain, Turkey, and Thailand (Sandoval-Denis et al., 2019; This study).

Habitat & host range: Mostly isolated from human. Also isolated from plant (*Malus sylvestris*; Rosaceae) and insect (*Ceresa bubalus*; Membracidae) (Al-Hatmi et al., 2018; Sandoval-Denis et al., 2019).

Notes: A single strain was identified as *Neocosmospora metavorans*, isolated from *Persea americana* (Lauraceae) fruit rot for the first time worldwide (Table A16). Based on the phylogenetic tree, the strain MFLUCC 25-0040 grouped with the ex-type of *Neocosmospora metavorans*, representing 100%/100%/1.00 (ML/MP/PP) bootstrap support (Figure 9.2).

Dothideomycetes

Botryosphaeriales

Botryosphaeriaceae

Neofusicoccum parvum (Pennycook & Samuels) Crous, Slippers & A.J.L. Phillips (2006)

Index Fungorum: IF 500879; MycoBank: MB 500879

Illustration and description: See Crous et al. (2006b)

Known distribution: Globally distributed (Farr & Rossman, 2024).

Habitat & host range: Reported as endophyte, saprobe and pathogen, from *Ligustrum lucidum* (Oleaceae), *Lilium lancifolium* (Liliaceae), *Linus usitattisimum* (Linaceae), *Lumnitzera racemosa* (Combretaceae), *Macadamia integrifolia* (Proteaceae), *Magnifera indica* (Anacardiaceae), *Magnolia* sp. (Magnoliaceae), *Malania oleifera* (Olacaceae), *Malus* spp. (Rosaceae), *Maytenus hookeri* (Celastraceae), *Melia azedarach* (Meliaceae), *Metrosideros polymorpha* (Myrtaceae), *Musa* sp. (Musaceae), *Myrcianthes cisplatensis* (Myrtaceae), *Myrciaria tenella* (Myrtaceae), *Myristica fragrans* (Myristicaceae), *Nephelium lappaceum* (Spindaceae), *Nothapodytes nimmoniana* (Icacinaceae), *Olea* spp. (Oleaceae), *Osmanthus fragrans* (Oleaceae), *Persea americana* (Lauraceae), *Phoebe* spp. (Lauraceae), *Picea abies* (Pinaceae), Pinus spp. (Pinaceae), *Pistacia vera* (Anacardiaceae), *Pittosporum tobira* (Pittosporaceae), *Platanus* spp. (Platanaceae), *Platostoma palustre* (Lamiaceae), *Podocarpus henkelii* (Podocarpaceae), *Populus nigra* (Salicaceae), *Protea* spp. (Proteaceae), *Prunus* spp. (Rosaceae), *Psidium* spp. (Myrtaceae), *Punica granatum* (Punicaceae), *Pyrus* spp. (Rosaceae), *Quercus* spp. (Fagaceae), *Rhaphiolepis indica* (Rosaceae), *Rhizophora* spp. (Rhizophoraceae), *Rhododendron* spp. (Ericaceae), *Rhus* spp. (Anacardiaceae), *Ribes* sp. (Grossulariaceae), *Salix* sp. (Salicaceae), *Santalum album* (Santalaceae), *Scaevola taccada* (Goodeniaceae), *Schizolobium parahyba* (Fabaceae), *Senna siamea* (Caesalpinioideae), *Sequoia sempervirens* (Cupressaceae), *Sequoiadendron giganteum* (Cupressaceae), *Solanum melongena* (Solanaceae), *Syzygium* spp. (Myrtaceae), *Tamarix tenuissima* (Tamaricaceae), *Terminalia* spp. (Combretaceae), *Theobroma cacao* (Malvaceae), *Thuja* spp. (Cupressaceae), *Thujopsis* spp. (Cupressaceae), *Torilis arvensis*, (Apiaceae) *Vaccinium* spp. (Ericaceae), *Vitis* spp. (Vitaceae), *Wollemia nobilis* (Araucariaceae), *Xanthostemon* sp. (Myrtaceae), and *Zanthoxylum bungeanum* (Rutaceae) (Farr & Rossman, 2024).

Notes: Three strains were identified as *Neofusicoccum parvum*, representing a new geographical report of this species associated with fruit rot and leaf spots of *Persea americana* (Lauraceae) from Thailand (Table A16). Phylogenetic analyses showed that the strains clustered within *Neofusicoccum parvum*, representing 99%/1.00 (ML/PP) bootstrap support (Figure 9.18).

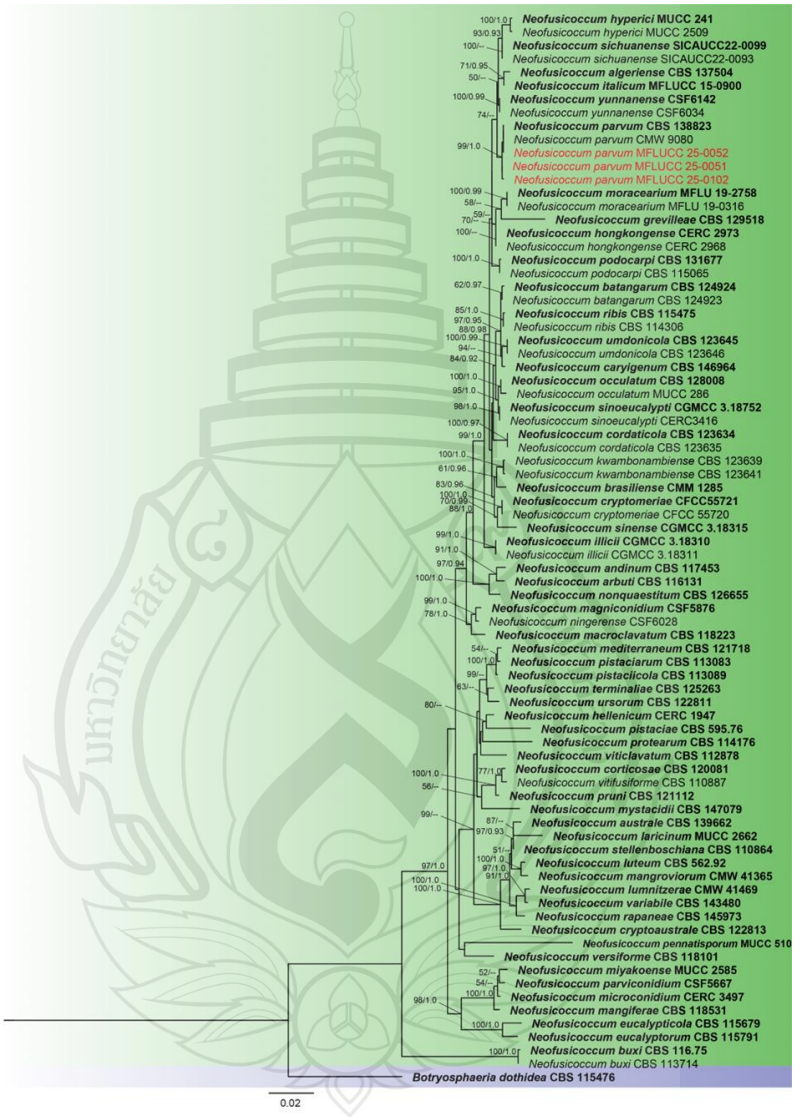

Note Maximum likelihood bootstrap values greater than 50% and bayesian posterior probabilities greater than 0.90 are shown near the nodes, respectively. The tree is rooted with *Botryosphaeria dothidea* (CBS 115476). The newly obtained strains are in red, and ex-type strains are in bold

Figure 9.18 The maximum likelihood (ML) tree of *Neofusicoccum* based on the concatenated ITS, *tef1*, *tub*2, and *rpb2* sequence dataset

Sordariomycetes

Amphisphaeriales

Sporocadaceae

Neopestalotiopsis cubana Maharachch., K.D. Hyde & Crous (2014)

Figure 9.19

Index Fungorum: IF 809765; MycoBank: MB 809765

Illustration and description: See Maharachchikumbura et al. (2014)

Known distribution: China (Li et al., 2021b), Cuba (Maharachchikumbura et al., 2014), Malaysia (Khoo et al., 2022), and Thailand (Pornsuriya et al., 2020; This study).

Habitat & host range: Isolated from *Camellia oleifera* (Theaceae), *Hevea brasiliensis* (Euphorbiaceae), *Ixora chinensis* (Rubiaceae), and an unknown leaf litter (Farr & Rossman, 2024).

Material examined: Thailand, Chiang Rai Province, Mae Salong Nok; associated with fruit rot of *Lansium domesticum* (Meliaceae); 17 February 2022, A. Armand, P46 (MFLU 25-0059; MFLUCC 25-0068 living culture).

Notes: Eight strains were isolated in this study (from fruit rot of langsat, rambutan, mangosteen, avocado, guava, and leaf spots of *Nyssa sylvatica* (tupelo)) clustered with the ex-type of *Neopestalotiopsis cubana*, showing 60%/–/– (ML/MP/PP) bootstrap support (Figure 9.20). The strains share 99.60% (511/513 bp) sequence similarity with *N. cubana* in ITS, 99.35% (459/462 bp) in *tef1*, and 99.13% (460/464 bp) in *tub2*. Morphologically, they resemble the ex-type of *N. cubana* (Maharachchikumbura et al., 2014), however, they show differences in the size of conidia (18–23 × 6.3–7 µm in our collection vs. 20–25(–27) × (7.5–)8–9.5(–10) µm in the ex-type) and apical appendages (25–32 µm long in our collection vs. (19–) 21–27(–28) µm long in the ex-type of *N. cubana*). This study revealed six new host records of *N. cubana*, occurring on important tropical fruits (Table A16).

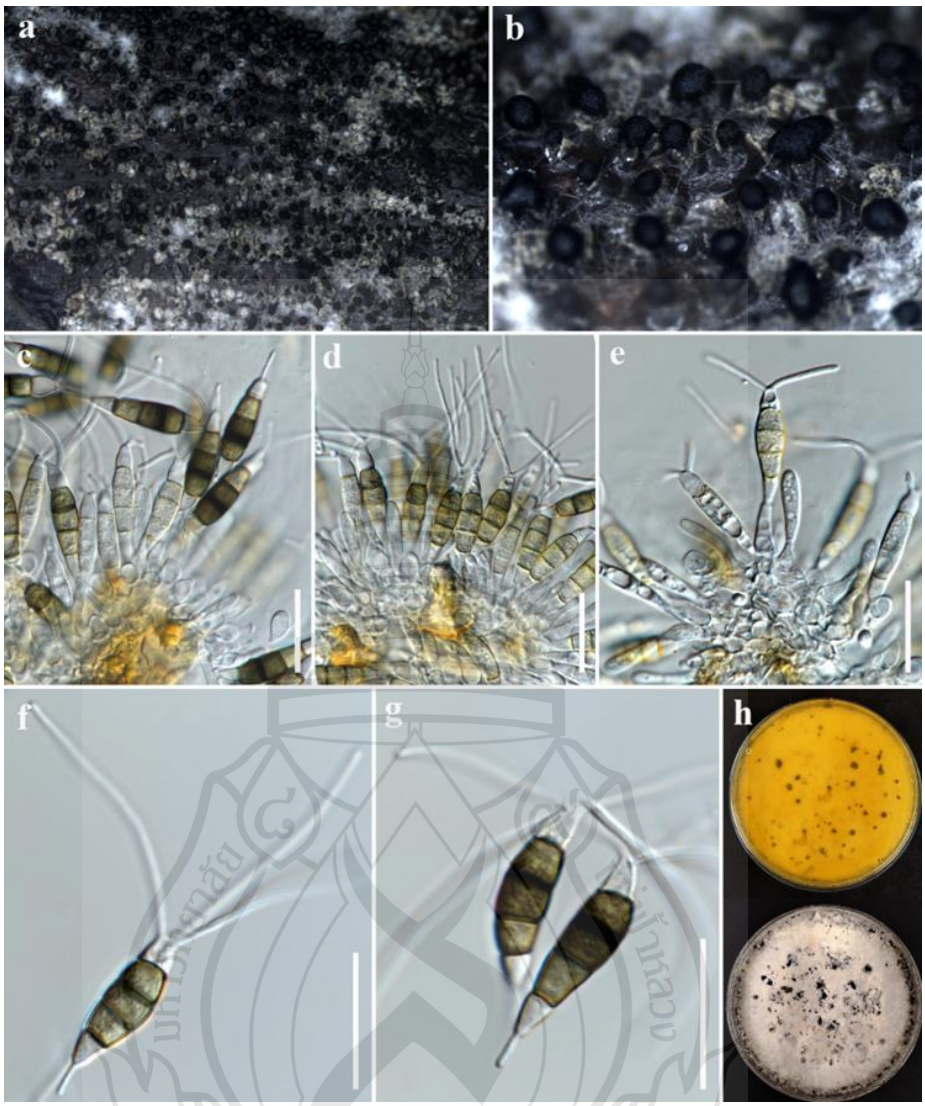

Note **a**, **b** Conidiomata and conidial mass produced on the host **c-e** Conidiogenous cells **f**, **g** Mature conidia **h** Upper and reverse view of the colonies on PDA. Scale bars: **d-i** = 20 µm. Scale bars: **c-g** = 20 µm

Figure 9.19 *Neopestalotiopsis cubana* (MFLU 25-0059)

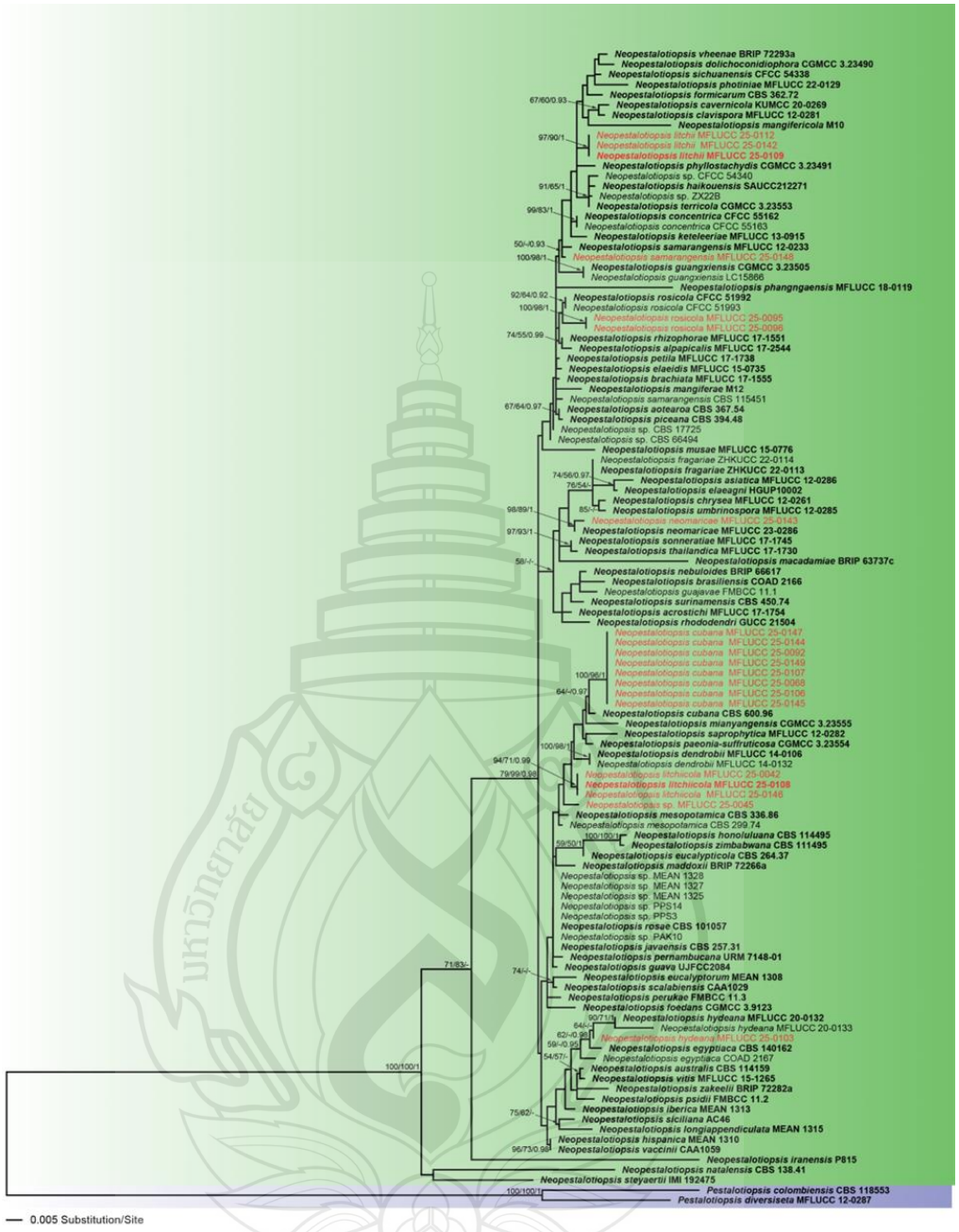

Note Maximum likelihood and maximum parsimony bootstrap values greater than 50% and bayesian posterior probabilities greater than 0.90 are shown near the nodes, respectively. The tree is rooted with *Pestalotiopsis colombiensis* (CBS 118553) and *P. diversiseta* (MFLUCC 12-0287). The newly obtained strains are in red, and ex-type strains are in bold

Figure 9.20 The maximum likelihood (ML) tree of *Neopestalotiopsis* based on the concatenated ITS, *tef1*, and *tub*2 sequence dataset

Neopestalotiopsis hydeana Huanraluek & Jayaward. (2021)

Figure 9.21

Index Fungorum: IF 558099; MycoBank: MB 558099

Illustration and description: See Huanaluek et al. (2021)

Known distribution: Thailand (Huanaluek et al. 2021; This study).

Habitat & host range: Associated with leaf spots of pteridophyte, *Artocarpus heterophyllus* (Moraceae), *Alpinia malaccensis* (Zingiberaceae), and *Alpinia galangal* (Zingiberaceae), and fruit rot *Annona squamosa* (Annonaceae), *Garcinia mangostana* (Clusiaceae), *Vitis vinifera* (Vitaceae), *Garcinia mangostana* (Clusiaceae), *Garcinia mangostana* (Clusiaceae), *Citrus* sp. (Rutaceae) (Farr & Rossman, 2024; Huanaluek et al., 2021).

Material examined: Thailand, Chiang Rai Province, Mueang Chiang Rai, Tha Sut, associated with fruit rot of *Persea americana* (Lauraceae); 10 May 2022, A. Armand, R34-3 (MFLU 25-0060; MFLUCC 25-0103 living culture).

Notes: A single strain was obtained from *Persea americana*, clustered with the ex-type of *Neopestalotiopsis hydeana* in a distinct clade, showing 74%/–/0.93 (ML/MP/PP) bootstrap support (Figure 9.20). Our collection shares 99.58% (477/479 bp) with *Neopestalotiopsis hydeana* in *tef1*, and 99.28% (414/417 bp) in *tub2*. Morphologically, our collection resembles *Neopestalotiopsis hydeana* (MFLUCC 20–0132) (Huanaluek et al., 2021). This is a new host record of *N. hydeana* occurring on *Persea americana.*

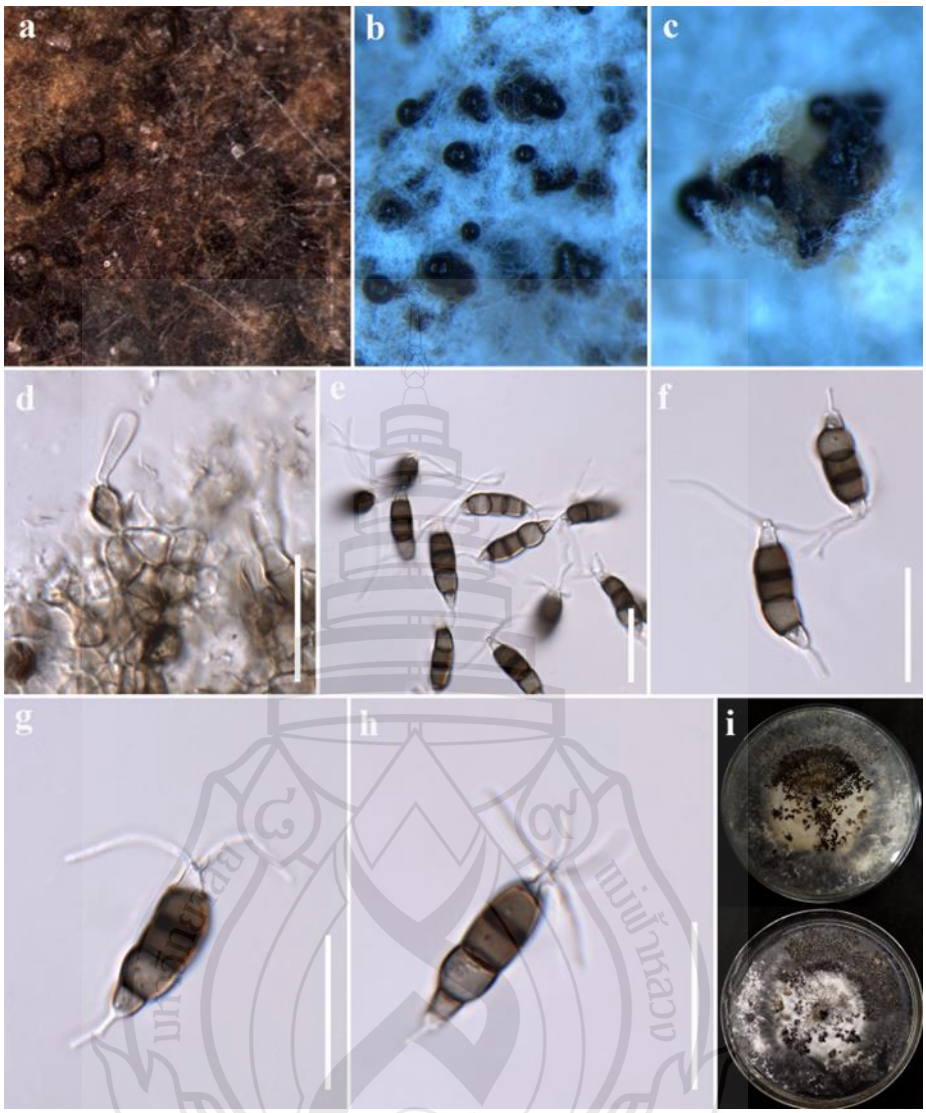

Note **a** Conidiomata produced on the host **b** Conidiomata and conidial mass produced on PDA **d** Conidiogenous cells **e-h** Mature conidia **j** Upper and reverse view of the colonies on PDA. Scale bars: **d-h** = 20 µm

Figure 9.21 *Neopestalotiopsis hydeana* (MFLU 25-0060)

Neopestalotiopsis sp.

Figure 9.22

Associated with *Iris pseudacorus* leaf blight. Sexual morph: not observed. Asexual morph: *Conidiomata* acervular, black, scattered, immersed to semi-immersed, exuding black glistening conidial masses. *Conidiophores* distinct or indistinct and reduced to conidiogenous cells, cylindrical to subcylindrical, hyaline, smooth-walled,

1–2 septate, branched, 12–20 × 3–4 µm. *Conidiogenous cells* discrete, smooth-walled, hyaline, aseptate, simple, lageniform or ampuliform, 7–12 × 4–5 µm ($\bar{x}$ = 10.5 × 4.4 µm, n = 10). *Conidia* cylindrical or ellipsoid, fusoid, straight or slightly curved, 4-septate, 16.5–18(–21) × 5–5.6 µm ($\bar{x}$ = 19.5 × 5.5 µm, n = 20). *Basal cell* conical to obconic, hyaline, smooth, 2–4 µm long. *Three median cells* doliiform, versicolored, smooth, 11–13 µm long ($\bar{x}$ = 12.6 µm, n = 20). *Second cell* from the base pale brown, 3.5–4.8 µm long ($\bar{x}$ = 4.4 µm, n = 20). *Third cell* brown to somewhat dark brown, 3.5–4 µm long ($\bar{x}$ = 3.7 µm, n = 20). *Fourth cell* brown, 3.8–4.3 µm long ($\bar{x}$ = 3.5 µm, n = 20). *Apical cell* hyaline, conical to subcylindrical, 2.7–3.2 µm long ($\bar{x}$ = 2.9 µm, n = 20), comprising 2–4 appendages (frequently 3). *Apical appendages* 12–19 µm long ($\bar{x}$ = 13.5 µm, n = 20), hyaline, tubular, arising from the apex of the apical cell. *Basal appendage* 1.7–3.7 µm long ($\bar{x}$ = 2.3 µm, n = 20), hyaline, filiform.

Culture characteristics: Colonies on PDA reach 33–35 mm in diam. after 7 days at 25 ± 2 °C, undulate in margin. Aerial mycelia fluffy, white to pale brown in the center, olivaceous in the margin, reverse same colour. Conidiomata acervular, aggregated, produced after 17 days on PDA.

Material examined: Thailand, Chiang Rai Province, Mueang Chiang Rai, Mae Fah Luang University premises, associated with *Iris pseudacorus* leaf blight (Iridaceae); 25 February 2022, A. Armand, C48 (MFLU 25-0061; MFLUCC 25-0045 living culture).

Notes: A single strain was obtained from *Iris pseudacorus* that formed a distinct lineage from *Neopestalotiopsis litchiicola* and *N. mesopotamica* (Figure 9.20). The strain shares 98.83% (507/513 bp) sequence similarity with *N. mesopotamica* in ITS, 99.32% (444/447 bp) in *tef1*, and 99.34% (457/460 bp) in *tub2*. It also shares 99.22% (509/513) sequence similarity with *N. litchiicola* in ITS, 99.32% (441/444 bp) in *tef1*, and 99.13% (456/460 bp) in *tub2*. Morphologically, the strain MFLUCC 25-0045 differs from *N. litchiicola* in the shape of conidia (cylindrical or ellipsoid, fusoid in MFLUCC 25-0045 vs. fusoid in *N. litchiicola*), the size of conidia (16.5–18 µm long in MFLUCC 25-0045 vs. 23–28 µm long in *N. litchiicola*), and the production of beta conidia (beta conidia were absent in MFLUCC 25-0045 vs. beta conidia were produced by *N. litchiicola*). Moreover, the strain MFLUCC 25-0045 is distinguished from *N. mesopotamica* in the size of conidia (16.5–18 µm long in MFLUCC 25-0045 vs. 26–32

μm long in *N. mesopotamica*) and the size of apical appendages (12–19 μm long in MFLUCC 25-0045 vs. 28–38 μm long in *N. mesopotamica*) (Maharachchikumbura et al., 2014). However, due to lack of strong bootstrap support to separate the strain from closely related species, we retrain introducing this strain as new species, pending for further strain collections.

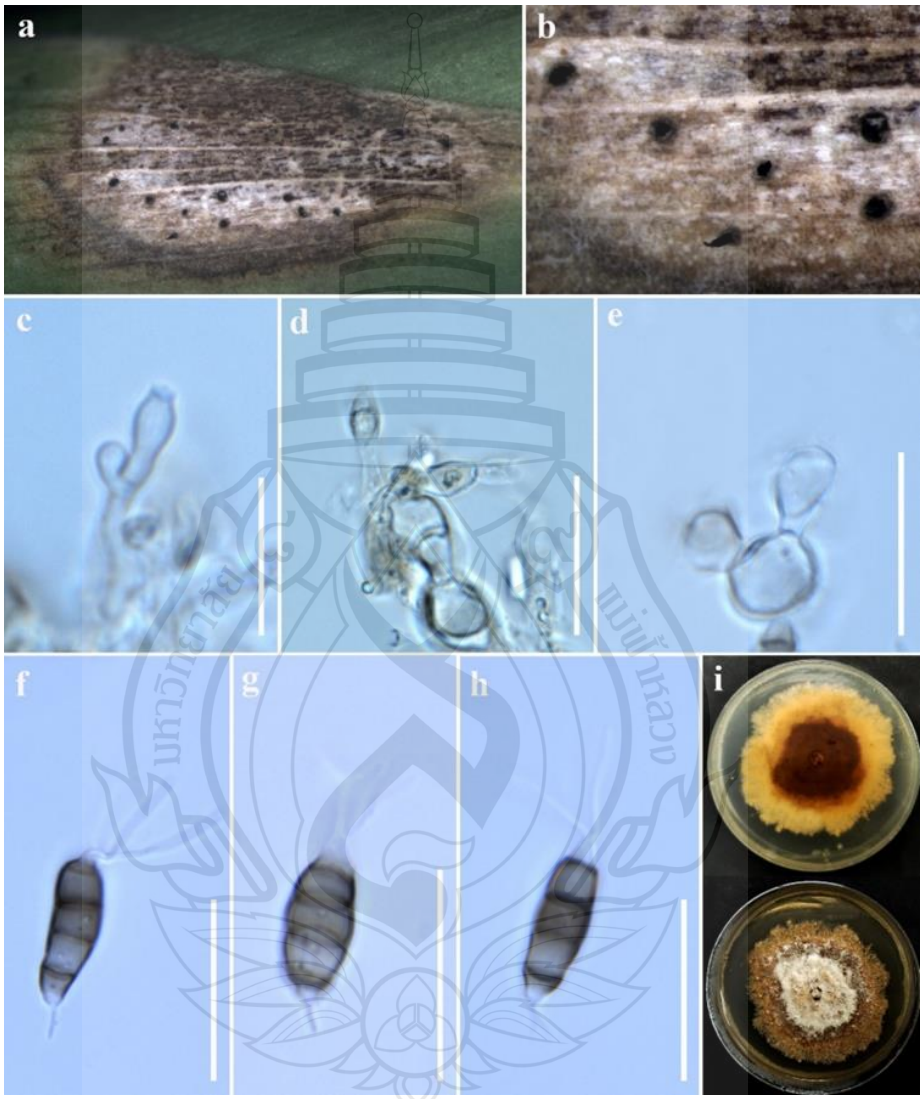

Note **a** Symptom caused by the fungus **b** Conidiomata and conidial mass produced on the host leaf **c** Conidiophores **d**, **e** Conidiogenous cells **f-h** Mature conidia **i** Upper and reverse view of the colonies on PDA. Scale bars: c = 10 μm, d-h = 20 μm

Figure 9.22 *Neopestalotiopsis* sp. (MFLU 25-0061)

Neopestalotiopsis litchii Armand, Pourmoghaddam, Jayaward. & K.D. Hyde, *sp. nov.*

Figure 9.23

Index Fungorum:; MycoBank:

Etymology: The epithet name refers to the host plant from which the fungus was isolated.

Associated with lychee fruit rot. Sexual morph: not observed. Asexual morph: *Conidiomata* acervular, black, aggregated or scattered, semi-immersed or immersed, exuding black glistening conidial masses. *Conidiophores* indistinct and reduced to conidiogenous cells. *Conidiogenous cells* discrete, smooth-walled, hyaline, aseptate, simple, ampuliform to lageniform, 5–9.5 × 3–5.5 µm ($\bar{x}$ = 8 × 3.5 µm, n = 10). *Conidia* subcylindrical, moniliform, straight or slightly curved, 4-septate, 22–28(–29) × 5.2–6.4 µm ($\bar{x}$ = 26 × 5.8 µm, n = 20). *Basal cell* obconic to subcylindrical, hyaline, slightly verruculose, 3.7–4.2 µm long. *Three median cells* doliiform, versicolored, verruculose, 14–17 µm long ($\bar{x}$ = 15.5 µm, n = 20). *Second cell* from the base pale brown, 4.5–6 µm long ($\bar{x}$ = 5 µm, n = 20). *Third cell* brown to somewhat dark brown, 4.3–5.8 µm long ($\bar{x}$ = 4.8 µm, n = 20). *Fourth cell* brown, 3.8–5.5 µm long ($\bar{x}$ = 5 µm, n = 20). *Apical cell* hyaline, conical to cylindrical, 3.9–5 µm long ($\bar{x}$ = 4.3 µm, n = 20), comprising 2–3 appendages (frequently 2). *Apical appendages* 9–16 µm long ($\bar{x}$ = 13.5 µm, n = 20), hyaline, tubular, arising from the apex of the apical cell. *Basal appendage* 1.4–2.3 µm long ($\bar{x}$ = 1.7 µm, n = 20), hyaline, filiform.

Culture characteristics: Colonies on PDA reach 55–58 mm in diam. after 7 days at 25 ± 2 °C, entire in margin. Aerial mycelia fluffy, white on surface, pale buff on reverse. Conidiomata acervular, aggregated or scattered, produced after 8 days on PDA.

Material examined: Thailand, Chiang Rai Province, Mueang Chiang Rai, local market, associated with fruit rot of *Litchi chinensis* (Sapindaceae); 18 July 2023, A. Armand, M26 (MFLU 25-0062 holotype; MFLUCC 25-0109 ex-type living culture).

Note: Phylogenetic analyses revealed that the strains MFLUCC 25-0112, MFLUCC 25-0142, and MFLUCC 25-0109 clustered together as a distinct clade from other species, showing 99%/92%/0.99 bootstrap values (Figure 9.20). The closest species to our species was *Neopestalotiopsis concentrica*. However, multi-locus phylogenetic analysis based on ITS, *tef1*, and *tub2* sequence data (Figure 9.20) clearly

distinguished our collections from *N. concentrica*. Our species shares 99.41% (508/511 bp) sequence similarity with *N. concentrica* in ITS, 98.69% (453/459 bp) in *tef1*, and 98.68% (451/457 bp) in *tub2*. Morphologically, *N. litchii* is distinguished from *N. concentrica* (BJFC-S1882) in the shape of conidia (moniliform in *N. litchii* vs. fusoid or ellipsoid in *N. concentrica*) and the size of conidia (22–28 µm long in *N. litchii* vs. 14–18.5 µm long in *N. concentrica*) (Peng et al., 2022).

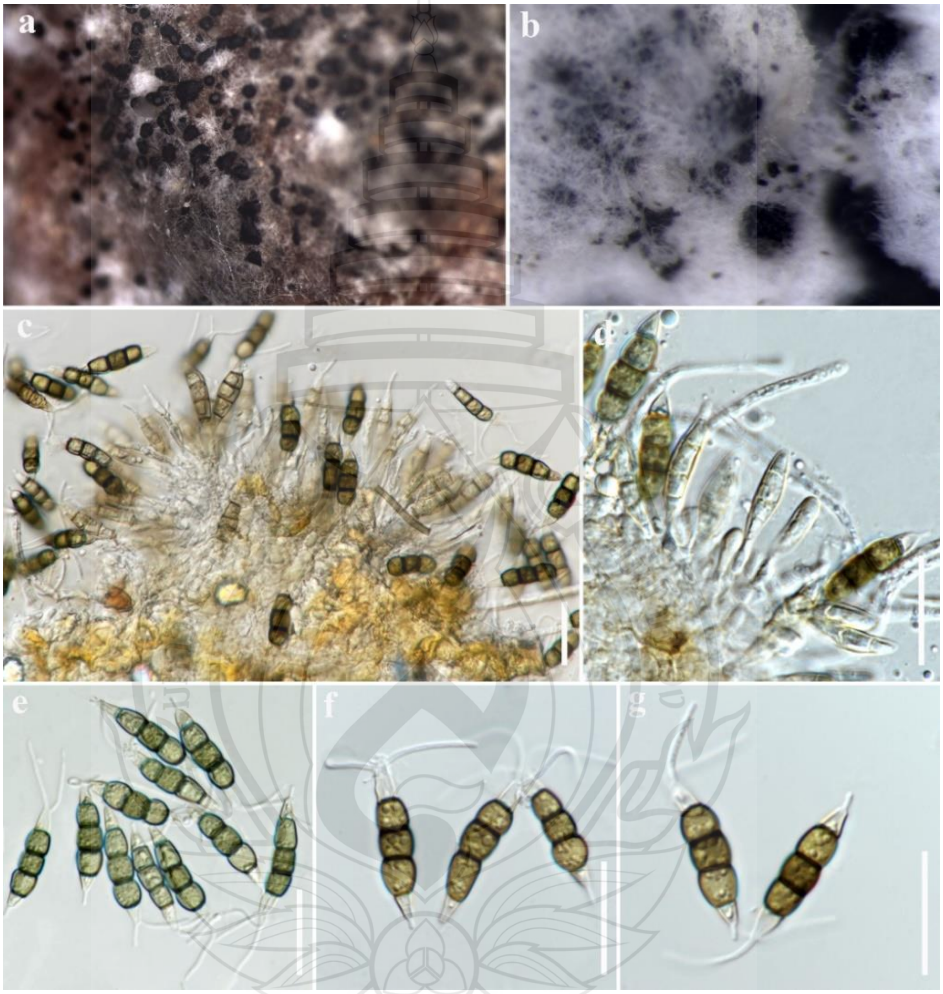

Note **a** Conidiomata and conidial mass produced on the host **b** Conidiomata and conidial mass produced on PDA **c-d** Conidiogenous cells **e**, **g** Mature conidia. Scale bars: **c-g** = 20 µm

Figure 9.23 *Neopestalotiopsis litchii* (MFLU 25-0062 holotype)

Neopestalotiopsis litchiicola Armand, Pourmoghaddam, Jayaward. & K.D. Hyde, *sp. nov.*

Figure 9.24

Index Fungorum:; MycoBank:

Etymology: The epithet name refers to the host plant from which the fungus was isolated.

Associated with lychee fruit rot. Sexual morph: not observed. Asexual morph: *Conidiomata* acervular, black, aggregated or scattered, immersed to semi-immersed, exuding black glistening conidial masses. *Alpha-conidiophores* indistinct and reduced to conidiogenous cells. *Alpha-conidiogenous cells* discrete, smooth-walled, hyaline, aseptate, simple, subcylindrical or ampuliform, 5–9 × 3.3–5.7 µm ($\bar{x}$ = 7.9 × 4 µm, n = 10). *Alpha-conidia* subcylindrical to fusoid, straight or slightly curved, 4-septate, 23–28 × 5–6.5 µm ($\bar{x}$ = 25.5 × 5.9 µm, n = 20). *Basal cell* obconic to subcylindrical, hyaline, smooth, 3.8–4.8 µm long. *Three median cells* doliiform, versicolored, verruculose, 16–18.3 µm long ($\bar{x}$ = 16.7 µm, n = 20). *Second cell* from the base pale brown, 4.4–6.2 µm long ($\bar{x}$ = 5.4 µm, n = 20). *Third cell* brown to somewhat dark brown, 5–5.5 µm long ($\bar{x}$ = 5 µm, n = 20). *Fourth cell* brown, 5–5.8 µm long ($\bar{x}$ = 5.3 µm, n = 20). *Apical cell* hyaline, conical to cylindrical, 3.4–5 µm long ($\bar{x}$ = 4.8 µm, n = 20), comprising 2–4 appendages (frequently 3). *Apical appendages* 18–23 µm long ($\bar{x}$ = 20.5 µm, n = 20), hyaline, tubular, arising from the apex of the apical cell. *Basal appendage* 0.9–2.5 µm long ($\bar{x}$ = 1.6 µm, n = 20), hyaline, filiform. *Beta-conidiophores* cylindrical to subcylindrical, smooth, hyaline, 1-septate, 11–13 µm long, or reduced to conidiogenous cells. *Beta-conidiogenous cells* discrete, hyaline, smooth, cylindrical, 8–10 µm long. *Beta-conidia* thread-like, curved, hyaline, apex subobtuse, base truncate.

Culture characteristics: Colonies on PDA reach 42–47 mm in diam. after 7 days at 25 ± 2 °C, undulate in margin. Aerial mycelia fluffy, white to pale yellow to buff on surface, pale buff on reverse. Conidiomata acervular, aggregated or scattered, produced after 10 days on PDA.

Material examined: Thailand, Chiang Rai Province, Mueang Chiang Rai, Tha Sut; associated with fruit rot of *Litchi chinensis* (Sapindaceae), 17 July 2023, A. Armand, M25 (MFLU 25-0063 holotype; MFLUCC 25-0108 ex-type living culture).

Notes: Phylogenetic analyses revealed that three strains (isolated from *Litchi chinensis*, *Chamaedorea seifrizii*, and *Nephelium lappaceum*) (Table A16) clustered together in a distinct clade, showing 95%/69%/0.99 (ML/MP/PP) bootstrap values (Figure 9.20). *Neopestalotiopsis litchiicola* is closely related to *N. dendrobii*. However, this species shares 98.75% (237/240 bp) sequence similarity with *N. dendrobii* in *tef1* and 98.55% (409/415 bp) in *tub2*. Morphologically, *N. litchiicola* is distinguished from *N. dendrobii* by producing beta conidia (lacked in *N. dendrobii*) and longer alpha conidia (23–28 µm long in *N. litchiicola* vs. 22–25 µm long in *N. dendrobii*) (Ma et al., 2019).

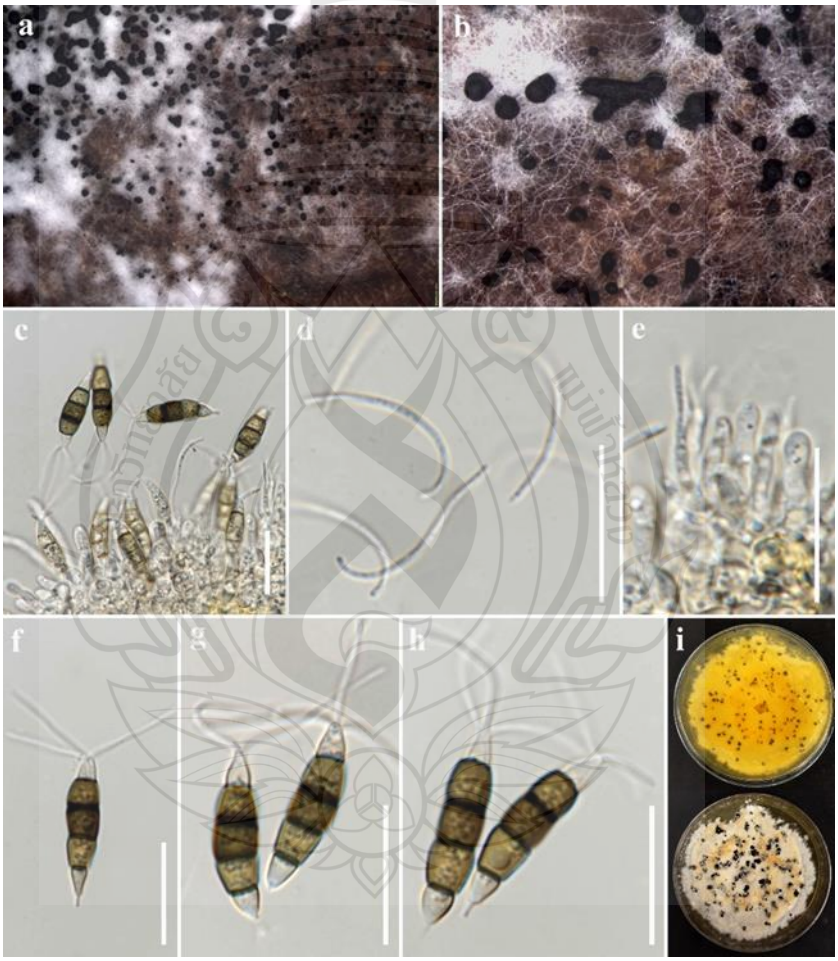

Note **a**, **b** Conidiomata and conidial mass produced on the host **c**, **d** Conidiogenous cells **e** Beta conidia **f-h** Mature conidia **i** Upper and reverse view of the colonies on PDA. Scale bars: **d-i** = 20 µm. Scale bars: **c-h** = 20 µm

Figure 9.24 *Neopestalotiopsis litchiicola* (MFLU 25-0063 holotype)

Neopestalotiopsis neomaricae Aumentado, Jayawardena & K.D. Hyde (2024)

Index Fungorum: IF 901464; MycoBank: MB 901464

Illustration and description: See Hyde et al. (2024b)

Known distribution: Thailand (Hyde et al. 2024b; This study).

Habitat & host range: Isolated from symptomatic leaves of *Neomarica longifolia* (Iridaceae) (Hyde et al., 2024b).

Notes: Phylogenetic analysis of a combined ITS, *tef1*, and *tub2* sequence dataset showed that a single strain, MFLUCC 25-0143 clustered with the ex-type of *Neopestalotiopsis neomaricae*, representing 98%/89%/1.00 (ML/MP/PP) bootstrap support (Figure 9.20). Additionally, our strain shares 100% (470/470 bp) with the ex-type of *N. neomaricae* in ITS, 99.56% (451/453 bp) in *tef1*, and 99.77% (449/450 bp) in *tub2*. *Neopestalotiopsis neomaricae* was originally reported from *Neomarica longifolia* (Iridaceae) from Thailand, and this is a new host record of this species isolated from *Casearia lasiophylla* (Salicaceae) (Table A16).

Neopestalotiopsis rosicola C.M. Tian & N. Jiang (2018)

Figure 9.25

Index Fungorum: IF 820879; MycoBank: MB 820879

Illustration and description: See Jiang et al. (2018)

Known distribution: China (Jiang et al., 2018), Italy (Aiello et al., 2024), and Thailand (This study).

Habitat & host range: Isolated from *Rosa chinensis* (Rosaceae), *Myrtus communis* (Myrtaceae) (Aiello et al., 2024; Jiang et al., 2018).

Material examined: Thailand, Chiang Rai Province, Mae Salong Nok, associated with *Cocos nucifera* (Arecaceae), 17 February 2022, A. Armand, P143 (MFLU 25-0064; MFLUCC 25-0096 living culture).

Notes: Two strains, MFLUCC 25-0095 and MFLUCC 25-0096, clustered together in a distinct clade, showing 99%/96%/1.00 (ML/MP/PP) bootstrap support (Figure 9.20). However, there was insufficient support to separate our collection from *Neopestalotiopsis rosicola*. The strains were associated with spadices dry rot of coconut (*Cocos nucifera*) and formed a clade with *Neopestalotiopsis rosicola*. Our collection shares 99.58% (477/479 bp) with the ex-type of *N. rosicola* in ITS, 99.55% (448/450 bp) in *tef1*, and 99.55% (447/449 bp) in *tub2*. Morphologically, our collection

resembles the ex-type of *N. rosicola*; however, they differ in the size of conidiogenous cells (5–10 µm long in our collection vs. 5−20 µm long in the ex-type) and the size of conidia (19–23 µm long in our collection vs. 20.2−25.5 long in the ex-type) (Jiang et al., 2018). This is a new host record of *N. rosicola* occurring on *Cocos nucifera* (Arecaceae) worldwide (Table A16).

Note **a–c** Conidiomata and conidial mass produced on the host **d–g** Conidiogenous cells **h**, **i** Mature conidia **j** Upper and reverse view of the colonies on PDA. Scale bars: **d–i** = 20 µm

Figure 9.25 *Neopestalotiopsis rosicola* (MFLU 25-0064)

Neopestalotiopsis samarangensis (Maharachch. & K.D. Hyde) Maharachch., K.D. Hyde & Crous (2014)

Index Fungorum: IF 809778; MycoBank: MB 809778

Illustration and description: See Maharachchikumbura et al. (2014)

Known distribution: Thailand (Maharachchikumbura et al., 2014; This study).

Habitat & host range: Isolated from *Syzygium samarangense* (Myrtaceae) (Maharachchikumbura et al., 2014).

Notes: Phylogenetic analysis of a combined ITS, *tef1*, and *tub2* sequence dataset showed that a single strain, MFLUCC 25-0148 clustered with the ex-type of *Neopestalotiopsis neomaricae*, representing 50%/–/0.93 (ML/MP/PP) bootstrap support (Figure 9.20). Our strain shares 100% (508/508 bp) with the ex-type of *N. samarangensis* in ITS, 99.77% (451/452 bp) in *tef1*, and 99.56% (457/459 bp) in *tub2*. *Neopestalotiopsis samarangensis* was originally reported from *Syzygium samarangense* (Myrtaceae) from Thailand, and this is a new host record of this species isolated from *Garcinia mangostana* (Clusiaceae) (Table A16).

Dothideomycetes

Botryosphaeriales

Phyllostictaceae

Phyllosticta capitalensis Henn. (1908)

Index Fungorum: IF 168326; MycoBank: MB 168326

Illustration and description: See Wikee et al. (2013)

Known distribution: Globally distributed (Farr & Rossman, 2024).

Habitat & host range: Recognised as endophyte and pathogen, reported from *Acacia crassicarpa* (Fabaceae), *Acer* sp. (Sapindaceae), *Aleurites fordii* (Euphorbiaceae), *Allamanda cathartica* (Apocynaceae), *Allophylus* sp. (Sapindaceae), *Alocasia* sp. (Araceae), *Amomum* sp. (Zingiberaceae), *Ampelopsis* sp. (Vitaceae), *Anacardium giganteum* (Anacardiaceae), *Anacardium* sp. (Anacardiaceae), *Anogeissus latifolia* (Combretaceae), *Anthocleista* sp. (Gentianaceae), *Anthurium* sp. (Araceae), *Artocarpus* sp. (Moraceae), *Arundina* spp. (Orchidaceae), *Aspidistra elatior* (Asparagaceae), *Aspidosperma polyneuron* (Apocynaceae), *Atropis distans* (Poaceae), *Baccaurea ramiflora* (Phyllanthaceae), *Banksia dryandroides* (Proteaceae), *Barringtonia racemosa* (Lecythidaceae), *Barringtonia* sp. (Lecythidaceae), *Bauhinia racemosa* (Fabaceae), *Bifrenaria harrisoniae* (Orchidaceae), *Botrychium* sp. (Ophioglossaceae), *Bowdichia nitida* (Fabaceae), *Bowdichia* sp. (Fabaceae), *Bumelia lycioides* (Sapotaceae), *Butea monosperma* (Fabaceae), *Caesalpinia* sp. (Fabaceae),

Calophyllum sp. (Calophyllaceae), *Camellia sinensis* (Theaceae), *Canthium* sp. (Rubiaceae), *Capsicum* sp. (Solanaceae), *Careya arborea* (Lecythidaceae), *Cariniana estrellensis* (Lecythidaceae), *Cassia fistula* (Fabaceae), *Cedrus deodara* (Pinaceae), *Cerbera* sp. (Apocynaceae), *Cercidiphyllum* spp. (Cercidiphyllaceae), *Cercis* spp. (Fabaceae), *Cinnamomum* sp. (Lauraceae), *Citrus* spp. (Rutaceae), *Cliffortia* sp. (Rosaceae), *Clutia* sp. (Peraceae), *Cocculus* sp. (Menispermaceae), *Codiaeum* sp. (Euphorbiaceae), *Coelogyne* sp. (Orchidaceae), *Combretum* sp. (Combretaceae), *Comocladia* sp. (Anacardiaceae), *Coprosma* sp. (Rubiaceae), *Cordia* spp. (Boraginaceae), *Cordyline fruticose* (Asparagaceae), *Crinum* spp. (Amaryllidaceae), *Croton* sp. (Euphorbiaceae), *Ctenomeria* sp. (Poaceae), *Curtisia* sp. (Cornaceae), *Cussonia* sp. (Araliaceae), *Cymbidium* sp. (Orchidaceae), *Cyphostemma* sp. (Vitaceae), *Dalbergia lanceolaria* (Fabaceae), *Davidia* spp. (Nyssaceae), *Dendrobium* spp. (Orchidaceae), *Dendropanax trifidus* (Araliaceae), *Dieffenbachia* sp. (Araceae), *Diospyros* spp. (Ebenaceae), *Dodonaea* sp. (Sapindaceae), *Dovyalis* sp. (Salicaceae), *Ekebergia* sp. (Meliaceae), *Elaeis guineensis* (Arecaceae), *Elaeodendron glaucum* (Celastraceae), *Encephalartos ferox* (Zamiaceae), *Enkianthus* sp. (Ericaceae), *Eriobotrya japonica* (Rosaceae), *Erythroxylum monogynum* (Erythroxylaceae), *Eucalyptus* spp. (Myrtaceae), *Euclea* sp. (Ebenaceae), *Euphorbia* spp. (Euphorbiaceae), *Ficus* spp. (Moraceae), *Fortunella* sp. (Rutaceae), *Gardenia* sp. (Rubiaceae), *Ginkgo* spp. (Ginkgoaceae), *Givotia rottleriformis* (Euphorbiaceae), *Glyptostrobus pensilis* (Cupressaceae), *Gmelina arborea* (Lamiaceae), *Grevillea* spp. (Proteaceae), *Grewia* spp. (Malvaceae), *Hebe* sp. (Plantaginaceae), *Hedera* sp. (Araliaceae), *Heliconia* sp. (Heliconiaceae), *Helicteres* spp. (Malvaceae), *Heptapleurum venulosum* (Araliaceae), *Hevea brasiliensis* (Euphorbiaceae), *Hibiscus* spp. (Malvaceae), *Hydrangea quercifolia* (Hydrangeaceae), *Ilex* sp. (Aquifoliaceae), *Ipomoea* sp. (Convolvulaceae), *Itea* sp. (Iteaceae), *Ixora* spp. (Rubiaceae), *Jacquiniella* sp. (Orchidaceae), *Kandelia* sp. (Rhizophoraceae), *Kydia calycina* (Malvaceae), *Lagerstroemia* spp. (Lythraceae), *Leucadendron* spp. (Proteaceae), *Leucospermum* spp. (Proteaceae), *Ligustrum* spp. (Oleaceae), *Litchi* sp. (Sapindaceae), *Lithocarpus* spp. (Fagaceae), *Livistona* sp. (Arecaceae), *Loxostylis* sp. (Anacardiaceae), *Mackaya* sp. (Acanthaceae), *Maerua* sp. (Capparaceae), *Magnolia* spp. (Magnoliaceae), *Mangifera indica* (Anacardiaceae), *Metasequoia glyptostroboides* (Cupressaceae), *Michelia* sp. (Magnoliaceae),

Monanthotaxis sp. (Annonaceae), *Morus* sp. (Moraceae), *Musa* spp. (Musaceae), *Myracrodruon* spp. (Anacardiaceae), *Naringi crenulata* (Rutaceae), *Nephelium lappaceum* (Sapindaceae), *Nerium* spp. (Apocynaceae), *Ocotea* sp. (Lauraceae), *Oncidium* sp. (Orchidaceae), *Ophiopogon* spp. (Asparagaceae), *Ougeinia oojeinensis* (Fabaceae), *Pandanus* sp. (Pandanaceae), *Paphiopedilum* spp. (Orchidaceae), *Philodendron* sp. (Araceae), *Piper* sp. (Piperaceae), *Pittosporum* spp. (Pittosporaceae), *Platostoma palustre* (Lamiaceae), *Podocarpus* sp. (Podocarpaceae), *Polyalthia* spp. (Annonaceae), *Protea* spp. (Proteaceae), *Prunus* sp. (Rosaceae), *Psidium guajava* (Myrtaceae), *Punica granatum* (Lythraceae), *Rhododendron* spp. (Ericaceae), *Ricinus communis* (Euphorbiaceae), *Robinia pseudoacacia* (Fabaceae), *Rubus chingii* (Rosaceae), *Saccharum officinarum* (Poaceae), *Sansevieria* spp. (Asparagaceae), *Schefflera venulose* (Araliaceae), *Schrebera* sp. (Oleaceae), *Sclerocarya* sp. (Anacardiaceae), *Scutia* sp. (Rhamnaceae), *Secamone* sp. (Apocynaceae), *Senegalia* spp. (Fabaceae), *Shorea robusta* (Dipterocarpaceae), *Spondias* sp. (Anacardiaceae), *Sterculia foetida* (Malvaceae), *Streblus* spp. (Moraceae), *Syzygium cumini* (Myrtaceae), *Tabebuia* spp. (Bignoniaceae), *Tamarindus indica* (Fabaceae), *Taxodium* spp. (Cupressaceae), *Tecomella* sp. (Bignoniaceae), *Terminalia* spp. (Combretaceae), *Tetradium glabrifolium* (Rutaceae), *Theobroma cacao* (Malvaceae), *Thuja* sp. (Cupressaceae), *Toona ciliata* (Meliaceae), *Trichilia* sp. (Meliaceae), *Tylophora* spp. (Apocynaceae), *Vaccinium* spp. (Ericaceae), *Vanda* spp. (Orchidaceae), *Viola* spp. (Violaceae), *Vitex* spp. (Lamiaceae), *Wikstroemia* sp. (Thymelaeaceae), *Xylosma* spp. (Salicaceae), *Zea mays* (Poaceae), *Ziziphus mauritiana* (Rhamnaceae), and *Ziziphus* spp. (Rhamnaceae) (Farr & Rossman, 2024).

Notes: Phylogenetic analyses revealed that four strains clustered with *Phyllosticta capitalensis*, showing 90%/1.00 (ML/MP) bootstrap support (Figure 9.26). The strains were isolated from leaf spots of *Diospyros virginiana* (Ebenaceae), *Dimocarpus longan* (Sapindaceae), and *Brassica oleracea* (Brassicaceae), and fruit rot of *Psidium guajava*. This study reveals two new host records and two new geographical records of *Ph. Capitalensis* from Thailand (Table A16).

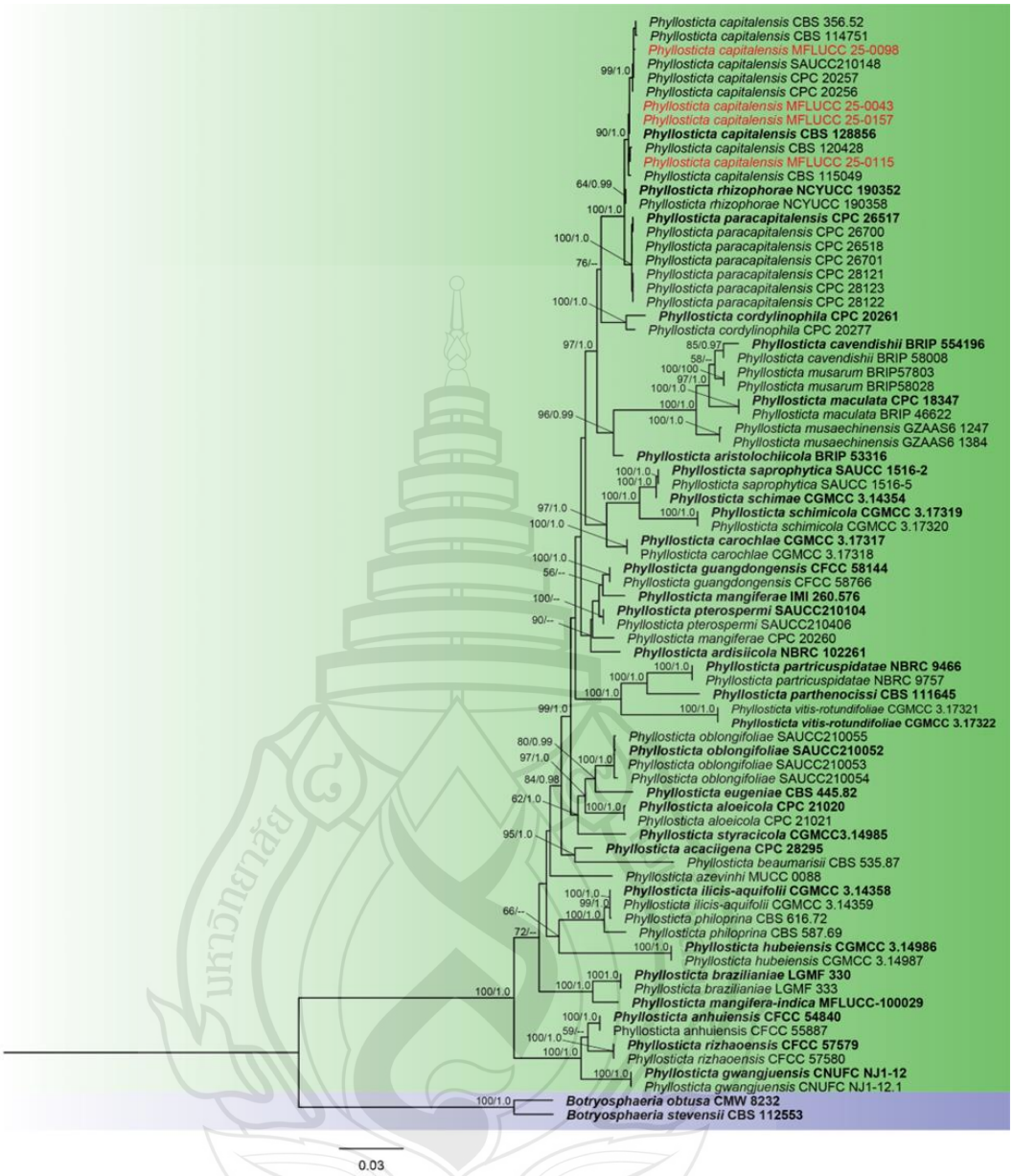

Note Maximum likelihood bootstrap values greater than 50% and bayesian posterior probabilities greater than 0.90 are shown near the nodes, respectively. The tree is rooted with *Botryosphaeria obtusa* (CMW 8232) and *B. stevensii* (112553). The newly obtained strains are in red, and ex-type strains are in bold

Figure 9.26 The maximum likelihood (ML) tree of *Phyllosticta* based on the concatenated ITS, LSU, *tef1*, *act*, and *gapdh* sequence dataset

Dothideomycetes

Mycosphaerellales

Mycosphaerellaceae

Pseudocercospora terengganuensis C. Nakash., Y. Hattori, Suhaizan & Nurul Faziha (2022)

Figure 9.27

Index Fungorum: IF 838267; MycoBank: MB 838267

Illustration and description: See Chen et al. (2022)

Known distribution: Malaysia (Chen et al., 2022).

Habitat & host range: Associated with leaf spots of *Hymenocallis speciosa* (Amaryllidaceae) (Chen et al., 2022).

Material examined: Thailand, Chiang Rai Province, Mueang Chiang Rai, Tha Sut, associated with *Hymenocallis speciosa* (Amaryllidaceae), 15 September 2022, A. Armand, A32 (MFLU 25-0065; MFLUCC 25-0097 living culture).

Notes: A single strain was obtained from leaf spots of *Hymenocallis speciosa*. Phylogenetic analysis of combined ITS, *act*, *tef1*, and *rpb*2 sequence data showed that the strain A32 clustered with the ex-type of *Pse. terengganuensis* with 100%/1.00 (ML/PP) bootstrap support (Figure 9.28). *Pseudocercospora terengganuensis* was originally isolated from the same host plant in Malaysia (Chen et al., 2022). However, this is the first record of *Pse. terengganuensis* from Thailand.

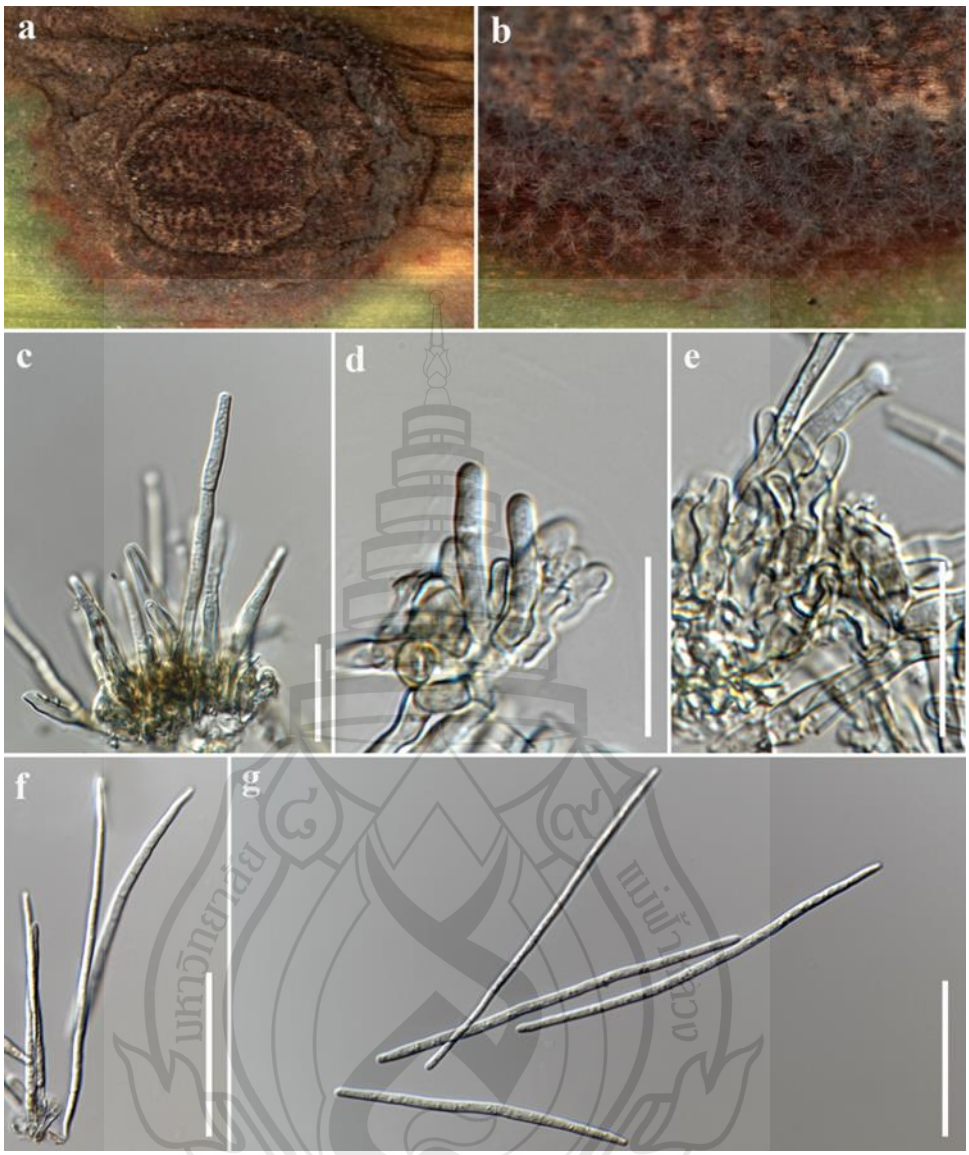

Note **a** Symptoms on the leaf. **b** Conidiomata. **c**-**e** Conidiophores **f**, **g** Conidia. Scale bars: **c**-**e** = 20 µm, **f**, **g** = 50 µm

Figure 9.27 *Pseudocercospora terengganuensis* (MFLU 25-0065)

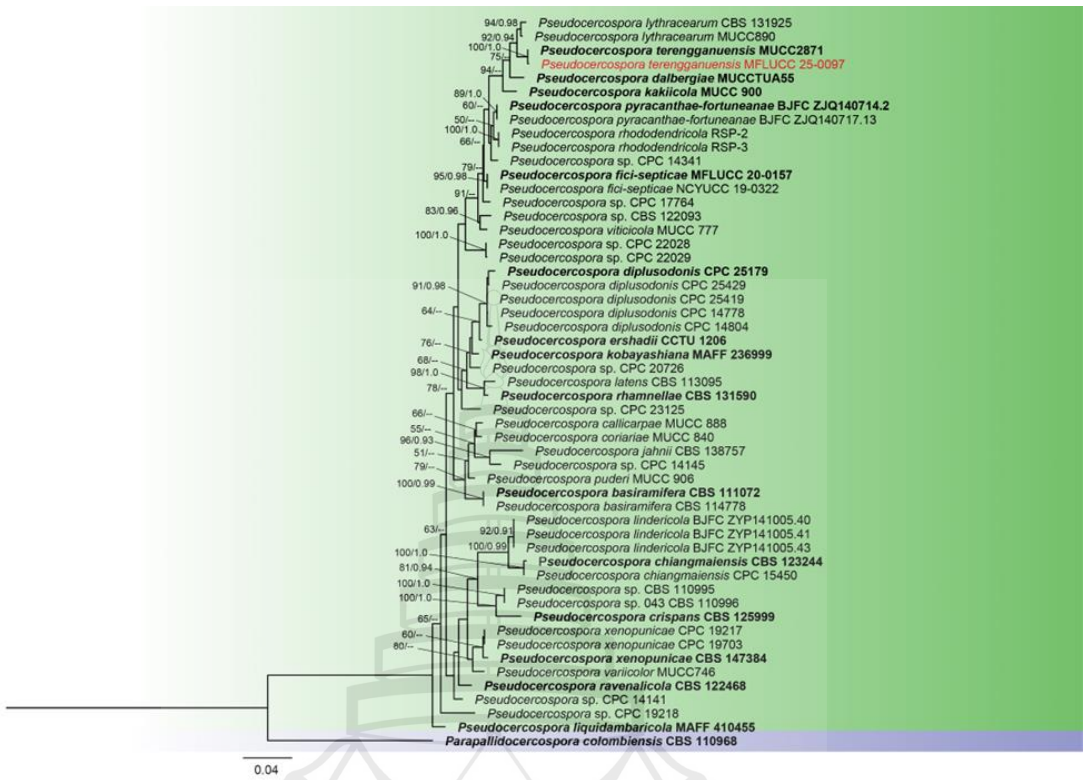

Note Maximum likelihood bootstrap values greater than 50% and bayesian posterior probabilities greater than 0.90 are shown near the nodes, respectively. The tree is rooted with *Parapallidocercospora colombiensis* (CBS 110968). The newly obtained strains are in red, and ex-type strains are in bold

Figure 9.28 The maximum likelihood (ML) tree of *Pseudocercospora* based on the concatenated ITS, *act*, *tef1*, and *rpb2* sequence dataset

Sordariomycetes

Diaporthales

Pseudoplagiostomataceae

Pseudoplagiostoma perseae C.J. Wu, J.L. Chen, S.S. Tzean & H.F. Ni (2024)

Figure 9.29

Index Fungorum: IF 839192; MycoBank: MB 839192

Illustration and description: See Wu et al. (2024)

Known distribution*:* Taiwan (Wu et al., 2024) and Thailand (This study).

Habitat & host range: Pathogenic to avocado, causing leaf spots. The species is known to reproduces sexually and asexually (Wu et al., 2024).

Material examined: Thailand, Nan Province, Phu Phiang District, Mueang Chang, on leaves of *Persea americana* (Lauraceae), 8 September 2022, A. Armand, Nan30 (MFLU 25-0066; MFLUCC 25-0119 living culture).

Notes: Wu et al. (2024) described *Pseudoplagiostoma perseae* using multi-locus phylogeny of ITS, LSU, and *tub* sequence data, causing leaf spots on *Persea americana* (Lauraceae). In this study, *P. perseae* was identified using phylogenetic analysis of a concatenated ITS, LSU, *tef1*, and *tub*. The species was isolated from the same host, associated with leaf spots from two provinces (Chiang Rai and Nan Provinces) in northern Thailand. Phylogenetic analysis showed the two newly isolated strains grouped within the *P. perseae* clade together with the ex-type strain (Figure 9.30). Morphologically, the strains resemble the holotype strain of *P. perseae* (Wu et al., 2024). This is a new geographical report of *P. perseae* from Thailand (Table A16).

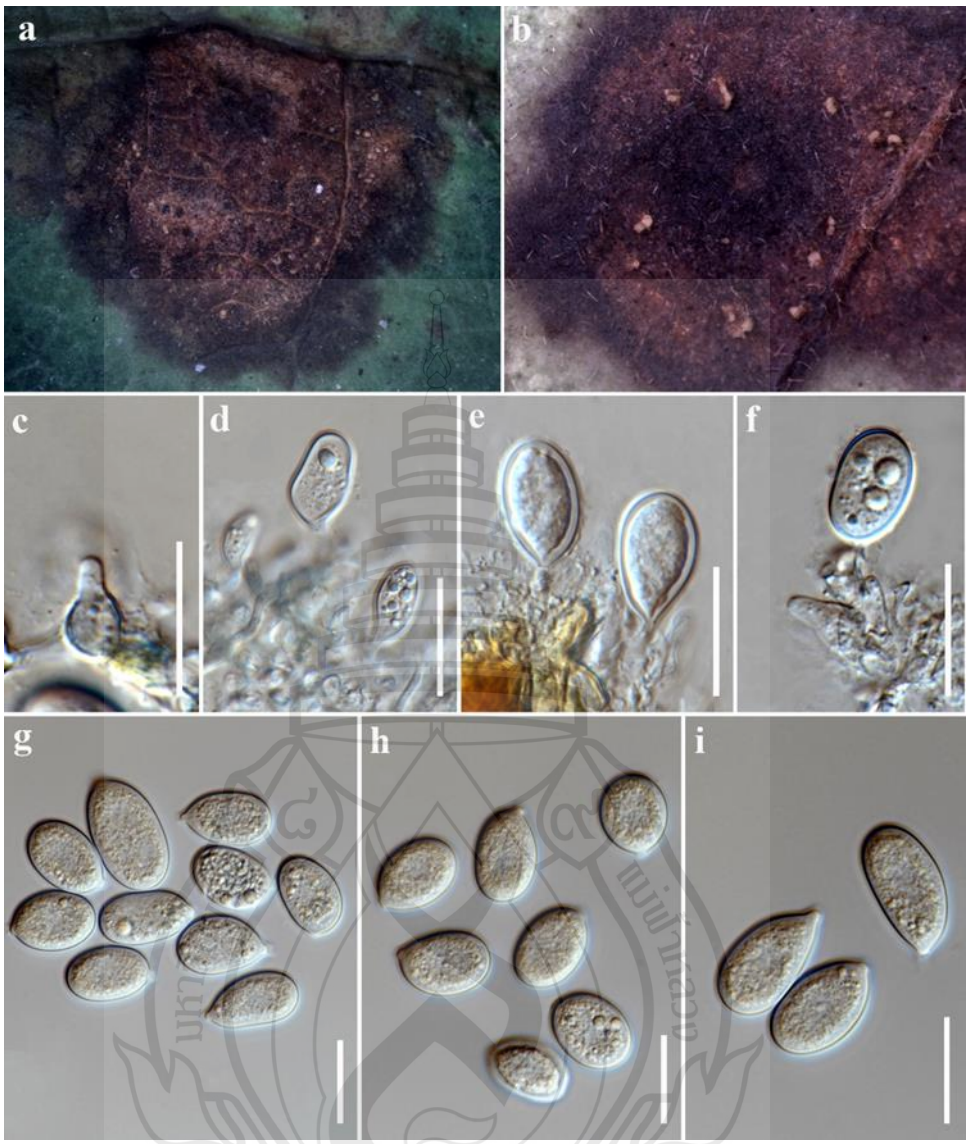

Note **a** Symptoms on avocado leaf. **b** Fruiting bodies produced on the leaf. **c** Conidiogenous cell. **d–f** Conidiogenous cells and conidial attachment. **g–i** Mature conidia. Scale bars: **c**–**i** = 20 µm

Figure 9.29 *Pseudoplagiostoma perseae* (MFLU 25-0066)

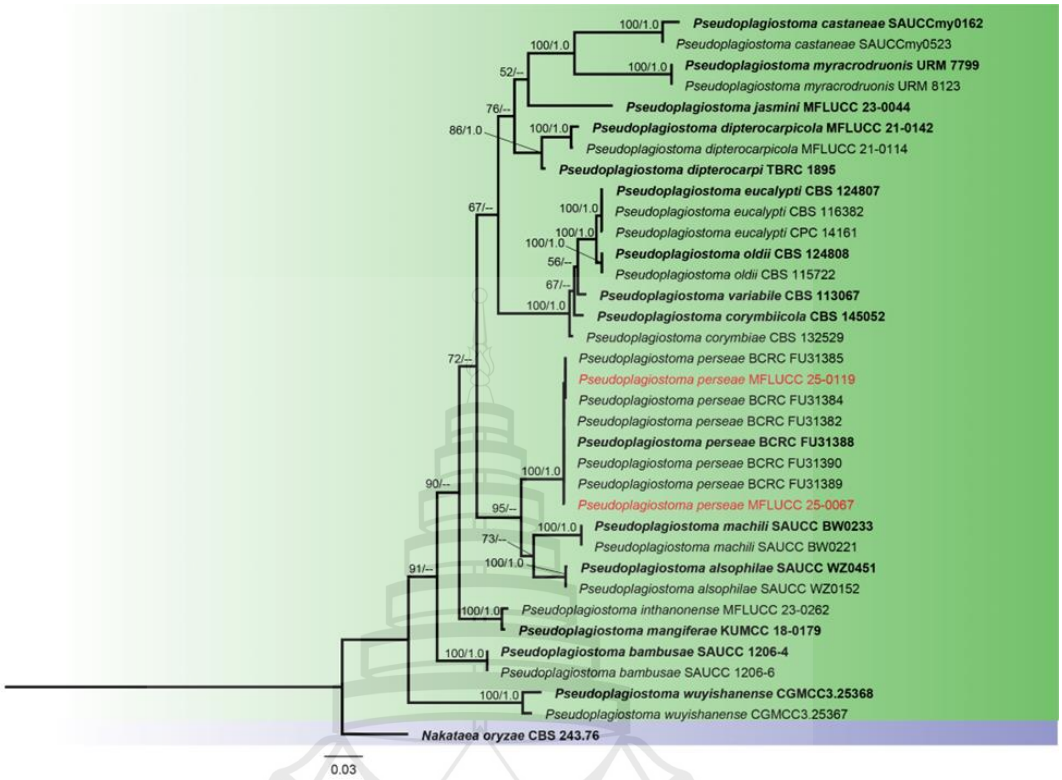

Note Maximum likelihood bootstrap values greater than 50% and bayesian posterior probabilities greater than 0.90 are shown near the nodes, respectively. The tree is rooted with *Nakataea oryzae* (CBS 243.76). The newly obtained strains are in red, and ex-type strains are in bold

Figure 9.30 The maximum likelihood (ML) tree of *Pseudoplagiostoma* based on the concatenated ITS, LSU, *tef1*, and *tub* sequence dataset

9.4 Discussion

Current knowledge of phytopathogens in Thailand primarily relies on morphological characteristics and host associations, resulting in the use of outdated or inappropriate names (Cheewangkoon et al., 2021; Ko et al., 2011). In many cases, identification processes have not employed multiple genetic markers, often focusing solely on the ITS region. As a result, the information obtained may not accurately reflect the true causal pathogens (Zakaria, 2021). To enhance our understanding of the evolutionary relationships among species and to advance plant pathology, it is crucial

to adopt a polyphasic approach that incorporates molecular data for species-level identification (Cheewangkoon et al., 2021; Ko et al., 2011). This approach should prioritise significant fungal pathogens affecting commercial crops and plants, thereby promoting agricultural productivity and sustainability (Cheewangkoon et al., 2021; Hyde et al., 2024a; Ko et al., 2011). Following the methodologies outlined in previous studies (Chethana et al., 2021; Hyde et al., 2009; Jayawardena et al., 2016, 2021b;), this research employed a multi-locus phylogenetic analysis integrated with morphological characterisation to facilitate accurate species identification.

A detailed investigation was conducted to identify pathogenic genera linked to infected avocado tissues in northern Thailand, encompassing leaves, fruits, branches, and stems. This study led to the identification of a novel species, *Diaporthe perseae-americanae,* found to be associated with leaf blight. Additionally, new records from Thailand included *Pseudoplagiostoma perseae*, associated with leaf spots, and *Neofusicoccum parvum,* linked to leaf blight and fruit rot. Furthermore, the research revealed globally new reports of fungal pathogens associated with infected avocado tissues, including *Neopestalotiopsis hydeana* (fruit rot), *Neocosmospora metavorans* (fruit rot), *Fusarium pernambucanum* (dieback), *Fusarium fujikuroi* (dieback), and *Diaporthe rosae* (leaf dieback).

A comprehensive survey of fresh durian fruits exhibiting rot symptoms, along with leaves and branches displaying spots, necrosis, and dieback, was conducted across multiple locations in northern Thailand. Previously, fungal species associated with *Durio zibethinus* (durian) in Thailand had been identified exclusively through morphological analysis or ITS sequence data (Farr & Rossman, 2024; Sangchote et al., 2012). This study identified a novel species, *Diaporthe durionis,* associated with leaf blight in durian. Additionally, *Lasiodiplodia theobromae* and *Lasiodiplodia brasiliensis* were recorded as new host associations linked to leaf blight and fruit rot on durian. Additional fungi, including *Diaporthe rosae*, *D. arecae, D. tulliensis*, and *D. siamensis,* were also documented as new host records for durian. Notably, prior to this research, only a single report of *Diaporthe* species associated with durian existed globally (Crous et al., 2020). Moreover, *Neocosmospora diminuta* was reported for the first time on durian, associated with fruit rot.

Moreover, the fungal species associated with diseased *Dimocarpus longan* (longan) tissues were also investigated in northern Thailand. Six new host records were identified: *Phyllosticta capitalensis*, *Fusarium sulawesiense, Fusarium endophyticum, Diaporthe sojae*, *Diaporthe rosae*, and *Colletotrichum siamense*. Additionally, *Lasiodiplodia pseudotheobromae* and *Colletotrichum fructicola* were isolated. *Phyllosticta capitalensis*, typically an endophyte (Wikee et al., 2013), was isolated from blighted leaves, suggesting its potential as an opportunistic pathogen. *Lasiodiplodia pseudotheobromae* was linked to both fruit rot and leaf blight, indicating a dual role as a fruit and foliar pathogen. *Fusarium sulawesiense* and *F. endophyticum* were associated with fruit rot, expanding the range of *Fusarium* species known to affect fruit crops. The isolation of *F. endophyticum* highlights its capacity to shift from an endophytic to a pathogenic state under favourable conditions, posing a potential threat to fruit quality and yield. *Diaporthe sojae* and *D. rosae* were associated with leaf dieback, illustrating the diversity of *Diaporthe* species affecting longan. The association of *Colletotrichum siamense* and *C. fructicola* with fruit rot and anthracnose underscores their economic impact on tropical fruit crops. These findings enhance our understanding of the diversity, distribution, and potential roles of fungal species in longan diseases.

This study investigated the occurrence and pathogenic associations of fungi on lychee (*Litchi chinensis*). Several fungi were identified as associated with various symptoms on leaves and fruits. *Colletotrichum siamense* was identified as associated with leaf anthracnose in lychee for the first time in Thailand. *Diaporthe tulliensis* was isolated as a new host record, associated with dieback in lychee trees. *Lasiodiplodia pseudotheobromae* was also documented as a new host record, linked to leaf blight in lychee. Two novel species of *Neopestalotiopsis*, designated *Neopestalotiopsis litchii* and *Neopestalotiopsis litchiicola*, were discovered and associated with fruit rot, which significantly impacts marketability and post-harvest quality. These findings expand the understanding of fungal pathogens affecting lychee in Thailand, offering valuable insights into their identification and pathology.

The present study sheds light on the species diversity associated with langsat (*Lansium domesticum*), particularly those linked to fruit rot, and broadens knowledge of their diversity and pathogenic associations. Four significant fungal species were

identified as associated with fruit rot: *Albonectria lansii* sp. nov., *Diaporthe lansii* sp. nov., *Neopestalotiopsis cubana*, and *Colletotrichum siamense*. These species were characterised using an integrative polyphasic approach, combining morphological traits and multi-locus phylogenetic analyses. Notably, *C. siamense* was reported for the first time globally on langsat, where it was isolated from fruits displaying anthracnose-like symptoms, characterised by dark, sunken lesions with sporulation.

The investigation highlights the diversity and pathogenic associations of fungal species linked to various symptoms on guava (*Psidium guajava*). *Colletotrichum endophyticum* and *C. siamense* were identified in association with anthracnose and leaf spots, representing new host and geographical records, respectively. *Diaporthe sojae* was documented as a new host record, associated with fruit rot and leaf dieback, demonstrating its adaptability and potential pathogenic versatility across different plant tissues. The discovery of *Fusarium coffeibaccae* associated with fruit rot in guava is particularly notable, as this species was previously known to affect *Coffea arabica* fruits (Costa et al., 2024). Multi-locus phylogenetic analysis confirmed its identification, marking *F. coffeibaccae* as an emerging pathogen on guava. Additionally, the detection of *Phyllosticta capitalensis* in guava fruit rot underscores its potential role as a latent pathogen, supporting the hypothesis that endophytic fungi can transition to pathogenicity under suitable conditions (Wikee et al., 2013).

This study provides a comprehensive documentation of newly identified fungal species and host records, emphasising their associations with diverse plant hosts and symptoms. *Neopestalotiopsis lansii* was isolated from fruit rot on mangosteen and rambutan, as well as from leaf spots on tupelo. Furthermore, *Colletotrichum endophyticum* and *C. thasutense* were identified in *Cocoa* leaf anthracnose, representing new global host records. *Cercospora alocasiicola* sp. nov. was identified from leaf spots on *Alocasia* spp., while *Cercospora capsici* was reported from fruit spots on *Capsicum annuum*. Two unidentified *Cercospora* species associated with leaf spot symptoms on durian and papaya remained sterile when cultured on PDA and SNA media. Two new *Bisifusarium* species, namely *Bisifusarium mangiferae* and *B. thailandica*, were discovered from *Mangifera indica* and *Selenicereus undatus*, respectively. *Neopestalotiopsis rosicola* was documented from coconut spadices with dry rot, a condition affecting coconut production in northern Thailand. Additional

Neopestalotiopsis litchiicola was associated with fruit rot in lychee and rambutan, as well as leaf spots on bamboo palm. Another *Neopestalotiopsis litchii* was identified in avocado fruit rot and leaf spots on pawpaw (*Asimina triloba*). The research also reported *Colletotrichum siamense* and *Lasiodiplodia chonburiensis* from *Morinda citrifolia*, marking new global host records. Moreover, *Lasiodiplodia pseudotheobromae* was identified in association with leaf blight on *Elaeagnus pungens* (thorny olive) and *Iris pseudacorus* (yellow iris), representing first global reports. These findings provide critical insights into fungal diversity and plant-fungal interactions, with significant implications for agriculture and plant health in Thailand. *Colletotrichum siamense* emerged as the predominant *Colletotrichum* species identified in this study. It was documented as a new geographical record associated with jackfruit, lychee, black pepper, guava, and hibiscus, and as a new host record from bamboo palm, Singapore daisy, vanilla, common persimmon, tomato, and langsat. Additionally, *Colletotrichum fructicola* was identified in association with leaf anthracnose on sapodilla and black pepper, representing new global host records (Table A16).

In conclusion, the findings of this study provide valuable insights for plant pathologists by enhancing the understanding of fungal pathogen diversity associated with various crops in Thailand and have implications for disease management and quarantine protocols. Recent years have seen the introduction of many new species (MycoBank, https://www.mycobank.org/page/Simple%20names%20search), with many potentially undiscovered species still remaining (Bhunjun et al., 2022; Hyde et al., 2018b). Additionally, numerous studies have reported new host associations for existing pathogenic species (Zhu et al., 2023), thus expanding their host and geographical ranges. Consequently, further investigations focused on isolating and identifying phytopathogenic species associated with key crops can enhance our understanding of fungal diversity and host range and may lead to the discovery of novel or emerging species.

CHAPTER 10

CONCLUSIONS

10.1 Overall Conclusions

In accordance with the methodologies recommended by previous research (Hyde et al., 2009; Jayawardena et al., 2016, 2021b; Chethana et al., 2021), this study utilised multi-locus phylogenetic analysis coupled with morphological characterisation for the species identification.

Paramyrothecium (*Stachybotryaceae*, *Hypocreales, Sordariomycetes*) was separated as a distinct genus from *Myrothecium* sensu lato, which contains 20 species. Among them many species have been reported as plant pathogens, causing leaf blight and leaf spots. This study revealed a new species *Paramyrothecium amorphophalli* from symptomatic leaves of elephant foot yam (*Amorphophallus* sp.), collected from Chiang Rai, Thailand based on distinct morphological characteristics and phylogenetic analyses. The isolate formed a distinct lineage from *Paramyrothecium eichhorniae* and *P. vignicola* based on maximum likelihood, maximum parsimony and Bayesian posterior probability analyses of ITS, *cmdA*, *rpb2* and *tub2* sequence data. Furthermore, pathogenicity assays confirmed that *P. amorphophalli* is pathogenic to the original host, causing leaf blight.

Pineapple is one of the most economically important fruits in tropical countries, particularly in Thailand. Canned pineapple is currently Thailand's main exported commodity to many countries, including the United States, Russia, Germany, Poland, and Japan. Fungal diseases are considered a permanent threat to fruits in the pre- and post-harvest stages, leading to considerable economic losses. Fungal disease is one of the primary causes of massive yield losses in pineapples around the world. *Colletotrichum* species are the most common fungal pathogens affecting different tropical fruits. Although there are many reports regarding *Colletotrichum* species associated with pineapple, they do not have molecular data to confirm species identification. However, the occurrence of *Colletotrichum* species on pineapple has not

been reported in Thailand so far. In this study, we isolated and identified *Colletotrichum fructicola* on pineapple in northern Thailand and have proven its pathogenicity to the host. This is the first report of the occurrence of *Colletotrichum* in pineapple, based on morpho-molecular approaches.

Colletotrichum is one of the most important plant pathogenic genera affecting different plant species, particularly tropical and sub-tropical crops and fruits. Species of the genus can cause many diseases, including fruit rots, crown rots, stem end rots, and anthracnose. The objective of the present study was to identify the *Colletotrichum* species associated with durian fruit rots in northern Thailand. Based on morphological study and phylogenetic analyses of five loci (internal transcribed spacer (ITS), actin (*ACT*), chitin synthase 1 (*CHS-1*), glyceraldehyde-3-phosphate dehydrogenase (*GAPDH*), and ß-tubulin (*TUB2*)), four species belonging to three complexes were identified and described. *Colletotrichum durionigenum* is introduced as a new species, and *C. gigasporum, C. pandanicola,* and *C. truncatum* are described and illustrated as new host records.

Avocado production is restricted globally by the anthracnose disease caused by *Colletotrichum* species. In Thailand, anthracnose symptoms can be found on avocado leaves and fruits, and it is an important postharvest disease, reducing the shelf life of the fruits and causing huge economic losses. Avocado leaves and fruits showing anthracnose disease were collected from Chiang Rai province, located in northern Thailand, and the *Colletotrichum* species isolated from the samples were identified based on morphological examination and multigene phylogenetic analyses. Phylogenetic analyses using five loci (ITS, *ACT*, *CHS-1, GAPDH* and *TUB2*) coupled with the morphology of 11 isolates showed that they belonged to four known species of *Colletotrichum*. *Colletotrichum endophyticum, C. fructicola* and *C. siamense* are illustrated as new geographical records, and *C. henanense* is characterized as a new host record. Furthermore, the pathogenicity of these species in avocado fruits and leaves (West Indian variety) has been proven. In addition, this study provides further evidence for the synonymization of *C. pandanicola* and *C. parvisporum* with *C. siamense*.

Plant pathogenic fungi are significant in agricultural ecosystems, causing substantial economic losses worldwide. Understanding their diversity and distribution by exploring the poorly studied niches is essential for agricultural and horticultural

production and effective disease management strategies. In this study, we conducted a comprehensive survey of plant pathogenic fungi on the Mae Fah Luang University premises, Thailand. Through morphological and multi-gene phylogenetic analyses, eight new fungus-host and five new geographical records are reported. Additionally, a new species, *Neopestalotiopsis iridis*, is illustrated and described. The survey revealed a diverse assemblage of fungal pathogens infecting various plant hosts, including economically important crops and ornamental plants. Our findings contribute to the knowledge of fungal biodiversity in northern Thailand and provide valuable insights into new niches of the species. This study underscores the importance of continued research efforts to monitor plant pathogenic fungi in different niches to increase our understanding of species diversity, distributions and evolutionary relationships.

This study also aimed to identify fungal pathogens responsible for diseases affecting mango orchards and fruits in the primary mango-growing regions of northern Thailand, and to evaluate their pathogenicity against mango. Mango leaves, branches, and fruits showing fruit and leaf anthracnose, leaf spots, fruit rot, stem-end rot, fruit decline, leaf and stem blight, and shoot dieback were collected and examined from Chiang Rai, Kalasin, Nan, and Sakon Nakhon provinces located in northern Thailand. The isolated fungi were identified based on morphological characteristics and multi-locus phylogenetic analysis based on the most reliable markers and loci combinations suggested for each genus. This study illustrates and describes nine pathogenic genera, including eight known genera and one new genus, *Pseudopallidocercospora*. *Botryosphaeria fabicerciana*, *B. scharifii*, *Colletotrichum asianum*, *C. gigasporum*, *C. guajavae*, *C. musae*, *C. plurivorum*, *C. siamense*, *Diaporthe rosae*, *D. siamensis*, *D. subellipicola*, *Neofusicoccum sinoeucalypti*, *Neopestalotiopsis chrysea*, *N. cubana*, *N. dendrobii*, *N. psidii*, *N. rhododendri*, *Neoscytalidium dimidiatum*, *Pestalotiopsis humicola* and *P. menhaiensis* were identified as known species. Five new species, including *Neopestalotiopsis mangiferae*, *N. mangifericola*, *N. mangiferigena*, *Pseudopallidocercospora mangiferae*, and *Zasmidium mangiferae* were fully illustrated and justified. Moreover, this study reports twelve globally new host-fungus occurrences and six new geographical records. Furthermore, pathogenicity assessment revealed that the majority of the isolates (91.6%) were pathogenic against mango, while their virulence was significantly different. *Colletotrichum asianum* was found to be the

predominant pathogenic species with a frequency of 31.6%. Haplotype networks generated using ITS sequence data for 220 *Colletotrichum asianum* strains isolated from mango across 14 countries revealed eight haplotypes, indicating high genetic diversity (Hd = 0.5936) within the species. However, the analysis did not reveal a clear grouping of isolates based on their country of origin.

Agriculture is a cornerstone of Thailand's economy. However, fungal species represent a major constraint on agricultural productivity, significantly affecting crops during both pre- and post-harvest stages. Despite the critical importance of understanding these species, a comprehensive investigation of fungal species associated with economically significant plants in Thailand remains lacking. This study provides a comprehensive survey of fungal species associated with diverse tropical fruit crops and economically important plants in northern Thailand, aimed to expand the understanding of fungal diversity, taxonomic novelties and new host or geographical records of main fungal species and their potential impacts on the crops. In this study, 131 fungal strains were collected and identified through morphological characterization combined with multi-locus phylogenetic analysis, enabling precise identification of species associated with crop diseases in Thailand. The obtained strains belonged to 13 genera and 50 species, comprising 12 new species viz. *Albonectria durionigenum*, *A. lansii*, *Bisifusarium mangiferae*, *B. thailandica*, *Cercospora alocasiicola*, *Diaporthe capsicicola*, *D. durionis*, *D. lansii*, *D. perseae-americanae*, *D. tamarindi*, *Neopestalotiopsis litchii*, and *N. litchiicola*. Moreover, this investigation provides 68 new host records worldwide, including *Cercospora*. cf. *malloti* (from *Durio zibethinus*), *Colletotrichum endophyticum* (from *Psidium guajava* and *Theobroma cacao*), *C. fructicola* (from *Sapodilla sapote* and *Piper nigrum*), *C. siamense* (from *Polyscias balfouriana*, *Diospyros virginiana*, *Solanum lycopersicum*, *Sphagneticola trilobata*, *Hibiscus rosa-sinensis*, *Dimocarpus longan*, *Artocarpus heterophyllus*, *Chamaedorea seifrizii*, *Syzygium jambos*, *Vanilla planifolia*, and *Lansium domesticum*), *C. thasutense* (from *Theobroma cacao*), *Diaporthe arecae* (from *Durio zibethinus* and *Acacia auriculiformis*) *D. chiangmaiensis* (from *Gomphrena globosa*), *D. discoidispora* (from *Eugenia uniflora*), *D. pterocarpi* (from *Iris pseudacorus* and *Ziziphus mauritiana*), *D. rosae* (from *Persea americana*, *Bougainvillea glabra*, *Durio zibethinus*, *Dimocarpus longan*, *Tabebuia aurea*, and *Cladrastis kentukea*), *D. siamensis* from (*Durio*

zibethinus), *D. sojae* (from *Dimocarpus longan* and *Psidium guajava*), *D. tulliensis* (from *Litchi chinensis*, *Solanum lycopersicum* and *Durio zibethinus*), *Fusarium coffeibaccae* (from *Psidium guajava*), *F. endophyticum* from (*Citrus* sp. and *Dimocarpus longan*), *F. fujikuroi* (from *Persea americana*), *F. hainanense* (from *Mangifera indica*), *F. pernambucanum* (from *Persea americana* and *Carica papaya*), *F. pseudocircinatum* (from *Citrus* sp., *Spathiphyllum* sp., and *Carica papaya*), *F. sulawesiense* (from *Dimocarpus longan* and *Carica papaya*), *Lasiodiplodia brasiliensis* (from *Durio zibethinus*), *L. chonburiensis* (from *Morinda citrifolia*), *L. pseudotheobromae* (from *Iris pseudacorus*, *Elaeagnus pungens*, and *Litchi chinensis*), *L. theobromae* (from *Durio zibethinus*), *Neocosmospora diminuta* (from *Durio zibethinus*), *N. metavorans* (from *Persea americana*), *Neopestalotiopsis cubana* (from *Lansium domesticum*, *Nephelium lappaceum*, *Garcinia mangostana*, *Nyssa sylvatica*, *Persea americana*, and *Psidium guajava*), *Neopestalotiopsis. hydeana* (from *Persea americana*), *N. neomaricae* (from *Casearia lasiophylla*), *N. rosicola* (from *Cocos nucifera*), *N. samarangensis* (from *Garcinia mangostana*), and *Phyllosticta capitalensis* (from *Diospyros virginiana*, *Brassica oleracea*, and *Dimocarpus longan*). Additionally, the present study revealed nine new geographical records in Thailand.

10.2 Research Advances

The present research study emphasizes the critical role of taxonomy and phylogeny in accurately identifying fungal pathogens affecting fruit crops, emphasizing on important fruit in Thailand. The study also investigated the pathogenicity of fungal isolates and assessed their aggressiveness and progression on fruits. The findings shed light on main microfungal species affecting economical important fruit crops in Thailand, their occurrence, frequency, and potential threats on fruits. These findings offer a deeper understanding of the behavior of the fungal pathogen and present valuable insights for future research and disease management approaches, emphasizing the importance of accurate pathogen identification through taxonomy and phylogeny in effectively protecting and mitigating the impact of these pathogens on fruit crops against evolving threats thereby securing agricultural productivity and food security.

10.3 Future Directions

Pathogenicity tests are crucial for confirming the causal relationship between fungi and observed plant symptoms, as they establish whether a specific fungal isolate is indeed responsible for the disease symptoms based on Koch's postulates. These tests also help differentiate between true pathogens, opportunistic colonisers, and endophytes, ensuring accurate identification of the disease-causing agent. Additionally, they contribute to understanding disease dynamics, host specificity, and virulence, which are vital for devising effective management strategies and ensuring scientific rigour in plant pathology research. However, due to time constraints, the vast number of host plants studied in this research, and the lack of access to certain host plants for experimental validation, pathogenicity tests could not be performed for some important crops in this study. As a result, the fungi isolated here are referred to as 'associated' with plant symptoms rather than confirmed causal agents. Future studies should incorporate pathogenicity tests to validate these findings and further elucidate the role of these fungi in plant disease development.

Molecular studies play a crucial role in understanding fungal pathogenicity by revealing the genetic and biochemical mechanisms that enable fungi to infect hosts. Future research should focus on genome-wide analyses, transcriptomics, and functional genomics to identify key pathogenicity-related genes, effector proteins, and resistance mechanisms. Investigating fungal lifestyle transitions, host adaptation, and stress responses at the molecular level can enhance disease management strategies. Additionally, integrating molecular tools such as CRISPR-Cas9 and RNA sequencing can provide deeper insights into fungal virulence and host-pathogen interactions, ultimately contributing to the development of targeted disease control measures.

Investigating endophytic fungi and bacteria is essential for developing sustainable fungal disease management strategies. Endophytic fungi can promote plant resistance by competing with pathogens, producing antifungal metabolites, or inducing host defence responses. Similarly, beneficial bacteria, such as plant growth-promoting rhizobacteria (PGPR) and antagonistic bacteria, can suppress fungal pathogens through mechanisms like antibiosis, nutrient competition, and biofilm formation. Future studies

should focus on metagenomic and metabolomic approaches to characterise the microbial communities associated with plants, identify potential biocontrol agents, and explore their interactions with pathogenic fungi. Understanding these microbial interactions can lead to innovative biological control strategies, reducing the reliance on chemical fungicides and promoting sustainable agriculture.

10.4 Publications Generated from the Dissertation

The data in this dissertation were generated from seven first-author (5 published, 2 submitted) publications and fourteen co-author publications in peer-reviewed journals as follows:

First author publications

Armand, A., Absalan, S., Khongphinitbunjong, K., Maharachchikumbura, S., & Jayawardena, R. S. (2024). New species and new records of plant pathogenic fungi from northern Thailand. *Asian Journal of Mycology*, *7*(2), 148–174.

Armand, A., & Jayawardena, R. S. (2023). Morpho-molecular identification and pathogenicity of *Colletotrichum* species associated with avocado anthracnose in northern Thailand. *Plant Pathology*, *73*, 186–197.

Armand, A., Hyde, K. D., Huanraluek, N., Wang, Y., & Jayawardena, R. S. (2023). Identification and characterization of *Colletotrichum* species associated with durian fruit in northern Thailand. *Mycosphere 14*(2), 107–129.

Armand, A., Hyde, K. D., & Jayawardena, R. S. (2023). First report of *Colletotrichum fructicola* causing fruit rot and leaf-tip dieback on pineapple in Northern Thailand. *Plants*, *12*(4), 971.

Armand, A., Bundhun, D., Bhunjun, C. S., Punyaboon, W., & Jayawardena, R. S. (2023). *Paramyrothecium amorphophalli* sp. nov., a causal agent of leaf blight on elephant foot yam in northern Thailand. *Current Research in Environmental & Applied Mycology (Journal of Fungal Biology)*, *13*(1), 57–67.

Armand, A., Fallahi, M., Absalan, S., Rathnayaka, A. R., Braun, U., Taylor, P.W.J., Khongphinitbunjong, K., McKenzie, E. H. C., Hyde, K. D., Al-Otibi F., & Jayawardena, R. S. (2025). Mango Microcosm: Unveiling the species diversity and pathogenic potential of fungi isolated from mango (*Mangifera indica*) in northern Thailand. *Fungal Biology* (in press)

Armand, A., Pourmoghaddam, M. J., Absalan, S., Fallahi, M., Wang, Y., Wang, Y., Li, L., Yang, H., Hyde, K. D., & Jayawardena, R. S., (2025). Fungal Footprints in the Tropics: Unveiling the species diversity of phytopathogenic genera associated with crops and ornamentals in northern Thailand. *Botanical Studies* (submitted)

REFERENCES

Abdelhamid, S. A., Abo Elsoud, M. M., El-Baz, A. F., Nofal, A. M., & El-Banna, H. Y. (2024). Optimisation of indole acetic acid production by *Neopestalotiopsis aotearoa* endophyte isolated from *Thymus vulgaris* and its impact on seed germination of *Ocimum basilicum*. *BMC biotechnology*, *24*(1), 46.

Abdollahzadeh, J., Zare, R., & Phillips, A. J. (2013). Phylogeny and taxonomy of *Botryosphaeria* and *Neofusicoccum* species in Iran, with description of *Botryosphaeria scharifii* sp. nov. *Mycologia*, *105*(1), 210–1220.

Abeywickrama, P. D., Camporesi, E., Jayawardena, R. S., Hyde, K. D., Yan, J., Zhang, W., & Li, X. (2022). Novel and surprising host associations of *Diaporthe* (Diaporthaceae, Diaporthales) species from Italy. *Chiang Mai J. Sci*, *49*, 223–247.

Abeywickrama, P. D., Jayawardena, R. S., Thakshila, S. A. D., Hyde, K. D., Yan, J., Zhang, W., & Li, X. (2023). Phyto-pathogenic fungi associated with tropical fruit crops in Thailand–1. *Current Research in Environmental & Applied Mycology*, *13*(1), 347–411.

Adikaram, N. K. B., & Yakandawala, D. M. D. (2020). A checklist of plant pathogenic fungi and Oomycota in Sri Lanka. *Ceylon Journal of Science*, *49*(1), 93–123.

Aiello, D., Gusella, G., Leonardi, G. R., Polizzi, G., & Voglmayr, H. (2024). Bottlebrush and Myrtle twig canker caused by *Neopestalotiopsis* species: an emerging canker-causing group of fungi in Italy. *MycoKeys*, *106*, 133–151.

Akinsanmi, O. A., Nisa, S., Jeff-Ego, O. S., Shivas, R. G., & Drenth, A. (2017). Dry flower disease of *Macadamia* in Australia caused by *Neopestalotiopsis macadamiae* sp. nov. and *Pestalotiopsis macadamiae* sp. nov. *Plant disease*, *101*(1), 45–53.

Albu, S., Schneider, R. W., Price, P. P., & Doyle, V. P. (2016). *Cercospora* cf. *flagellaris* and *Cercospora* cf. *sigesbeckiae* are associated with *Cercospora* leaf blight and purple seed stain on soybean in North America. *Phytopathology*, *106*(11), 1376–1385.

Al-Hatmi, A. M., Ahmed, S. A., Van Diepeningen, A. D., Drogari-Apiranthitou, M., Verweij, P. E., Meis, J. F., & De Hoog, G. S. (2018). *Fusarium metavorans* sp. nov.: the frequent opportunist 'FSSC6'. *Medical Mycology*, *56*, S144–S152.

Aliya, S. S. S., Nusaibah, S. A., Mahyudin, M. M., Yun, W. M., & Yusop, M. R. (2022). *Colletotrichum siamense* and *Pestalotiopsis jesteri* as potential pathogens of new rubber leaf spot disease via detached leaf assay. *Journal of Rubber Research*, *25*(3), 195–212.

Almeida, É. S., de Oliveira, D., & Hotza, D. (2019). Properties and applications of *Morinda citrifolia* (noni): A review. *Comprehensive Reviews in Food Science and Food Safety*, *18*(4), 883–909.

Alvarado, R., Ortiz, C., Jiménez, N., Ochoa-Jiménez, D., & Tillaguango, B. (2021). Ecological footprint, air quality and research and development: The role of agriculture and international trade. *Journal of Cleaner Production*, *288*, 125589.

Alves, A., Crous, P. W., Correia, A., & Phillips, A. J. L. (2008). Morphological and molecular data reveal cryptic speciation in *Lasiodiplodia theobromae*. *Fungal diversity*, *28*, 1–13.

Altendorf, S. (2018). Minor tropical fruits. *Food outlook*, *1*, 67–75.

Antle, J. M., Ray, S., Antle, J. M., & Ray, S. (2020). Economic development, sustainable development, and agriculture. *Sustainable Agricultural Development: An Economic Perspective*, 9–42.

Anuagasi, C. L., Onuorah, J. A., & Okigbo, R. N. (2017). Fungal pathogens affecting seedlings of *Gmelina arborea* Roxb and *Tectona grandis* Lf and effect of three plant extracts. *IJAT*, *13*, 307–330.

Apipatpapha, T., Ongkunaruk, P., & Chollakup, R. (2022, August). Pineapple leaf fiber supply chain analysis for the sustainability of community enterprise: a case study in Thailand. In *IOP Conference Series: Earth and Environmental Science* (Vol. 1074, No. 1, p. 012032). IOP Publishing.

Armand, A., Hyde, K. D., & Jayawardena, R. S. (2023a). First report of *Colletotrichum fructicola* causing fruit rot and leaf-tip dieback on pineapple in Northern Thailand. *Plants*, *12*(4), 971.

Armand, A., Hyde, K. D., Huanraluek, N., Wang, Y., & Jayawardena, R. S. (2023b). Identification and characterization of *Colletotrichum* species associated with durian fruit in northern Thailand. *Mycosphere*, *14*(2), 107–129.

Armand, A., & Jayawardena, R. S. (2024). Morphomolecular identification and pathogenicity of *Colletotrichum* species associated with avocado anthracnose in northern Thailand. *Plant Pathology*, *73*(1), 186–197.

Arnold, G. R. (1986). *Lista de hongos fitopatógenos de Cuba*. Ministerio de Cultura, Editorial Cientifico-Tecnica.

Arzanlou, M., Groenewald, J. Z., Gams, W., Braun, U., Shin, H. D., & Crous, P. W. (2007). Phylogenetic and morphotaxonomic revision of *Ramichloridium* and allied genera. *Studies in Mycology*, *58*(1), 57-93.

Athinuwat, D., Ruangwong, O. U., Harishchandra, D. L., Latehnuering, F., & Sunpapao, A. (2024). Morphology and molecular characterization of *Colltetotrichum siamense* associated with leaf spot disease of rubber tree (*Hevea brasiliensis*) in southern Thailand. *Physiological and Molecular Plant Pathology*, *130*, 102248.

Aumentado, H. D., & Balendres, M. A. (2022). Identification of *Paramyrothecium foliicola* causing crater rot in eggplant and its potential hosts under controlled conditions. *Journal of Phytopathology*, *170*(3), 148–157.

Ayvar-Serna, S., Díaz-Nájera, J. F., Vargas-Hernández, M., Plancarte-Galán, P. J., Alvarado-Gómez, O. G., Tejeda-Reyes, M. A., & Mena-Bahena, A. (2018). *Colletotrichum tropicale* causal agent of anthracnose on noni plants (*Morinda citrifolia*) in Guerrero, Mexico. *Plant Pathology & Quarantine*, *8*(2), 165–169.

Ayvar-Serna, S., Díaz-Nájera, J. F., Vargas-Hernández, M., Camacho-Tapia, M., Valencia-Rojas, G. A., Lima, N. B., & Tovar-Pedraza, J. M. (2021). First report of *Colletotrichum jiangxiense* causing avocado anthracnose in Mexico. *Plant Disease*, *105*(2), 502.

Azizi, R., Ghosta, Y., & Ahmadpour, A. (2020). New fungal canker pathogens of apple trees in Iran. *Journal of crop protection*, *9*(4), 669–681.

Azuddin, N. F., Mohd, M. H., Rosely, N. F. N., Mansor, A., & Zakaria, L. (2021). Molecular phylogeny of endophytic fungi from rattan (*Calamus castaneus* Griff.) spines and their antagonistic activities against plant pathogenic fungi. *Journal of Fungi*, *7*(4), 301.

Baba, S. H., Saini, A. S., Sharma, K. D., & Thakur, D. R. (2010). Impact of investment on agricultural growth and rural development in Himachal Pradesh: Dynamics of public and private investment. *Indian Journal of Agricultural Economics*, *65*(1).

Bai, Q., Wang, G. P., Hong, N., Guo, Y. S., & Fu, M. (2017). First report of *Diaporthe tulliensis* and *Diaporthe actinidiae* causing kiwifruit stem canker in Hubei and Anhui provinces, China. *Plant Disease*, *101*(3), 508–509.

Balendres, M. A., Mendoza, J., & Dela Cueva, F. (2020). Characteristics of *Colletotrichum musae* PHBN0002 and the susceptibility of popular banana cultivars to postharvest anthracnose. *Indian Phytopathology*, *73*(1), 57–64.

Bampenrat, A., Boonkitkoson, A., Seangwattana, T., Suttiarporn, P., & Sukkathanyawat, H. (2020, October). Kinetic analysis of durian rind pyrolysis using model-free method. In *IOP Conference Series: Earth and Environmental Science* (Vol. 586, No. 1, p. 012002). IOP Publishing.

Bandelt, H. J., Forster, P., & Röhl, A. (1999). Median-joining networks for inferring intraspecific phylogenies. *Molecular biology and evolution*, *16*(1), 37–48.

Baruwa, O. I. (2013). Profitability and constraints of pineapple production in Osun State, Nigeria. *Journal of Horticultural research*, *21*(2), 59–64.

Bass, D., & Richards, T. A. (2011). Three reasons to re-evaluate fungal diversity ‘on Earth and in the ocean’. *Fungal biology reviews*, *25*(4), 159–164.

Belisário, R., Aucique-Pérez, C. E., Abreu, L. M., Salcedo, S. S., Oliveira, W. D., & Furtado, G. Q. (2020). Infection by *Neopestalotiopsis* spp. occurs on unwounded eucalyptus leaves and is favoured by long periods of leaf wetness. *Plant Pathology*, *69*(2), 194–204.

Ben, H. Y., Qu, H. Y., Chen, L. X., Zhang, J. M., Ma, J., Zhang, X. Y., ... Huang, D. Y. (2017). First report of *Myrothecium roridum* causing leaf spot on *Petunia hybrida* in China. *Plant Disease*, *101*(11), 1956.

Benatar, G. V., & Wibowo, A. (2021). First report of *Colletotrichum asianum* associated with mango fruit anthracnose in Indonesia. *Crop Protection*, *141*, 105432.

Bhunjun, C. S., Jayawardena, R. S., Wei, D. P., Huanraluek, N., Abeywickrama, P. D., Jeewon, R., ... Hyde, K. (2019). Multigene phylogenetic characterisation of *Colletotrichum artocarpicola* sp. nov. from *Artocarpus heterophyllus* in northern Thailand. *Phytotaxa*, *418*(3), 273–286.

Bhunjun, C. S., Phillips, A. J., Jayawardena, R. S., Promputtha, I., & Hyde, K. D. (2021a). Importance of molecular data to identify fungal plant pathogens and guidelines for pathogenicity testing based on Koch's postulates. *Pathogens*, *10*(9), 1096.

Bhunjun, C. S., Phukhamsakda, C., Jayawardena, R. S., Jeewon, R., Promputtha, I., & Hyde, K. D. (2021b). Investigating species boundaries in *Colletotrichum*. *Fungal Diversity*, *107*, 107–127.

Bhunjun, C. S., Niskanen, T., Suwannarach, N., Wannathes, N., Chen, Y. J., McKenzie, E. H., ... Lumyong, S. (2022). The numbers of fungi: are the most speciose genera truly diverse?. *Fungal Diversity*, *114*(1), 387–462.

Bincader, S., Pongpisutta, R., & Rattanakreetakul, C. (2021). *Colletotrichum* species related to "Nam Dork Mai See Tong" mango in central Thailand and risk detection of Carbendazim-Resistant strains. *Research Square*.

Boonyanam, N. (2020). Agricultural economic zones in Thailand. *Land Use Policy*, *99*, 102774.

Borges, R. C., Rossato, M., Santos, M. D. M., dos Santos Vieira, W. A., Câmara, M. P., & Reis, A. (2023). Characterization of *Colletotrichum* isolates causing anthracnose on *Artocarpus heterophyllus* in Brazil. *Journal of Plant Pathology*, *105*(1), 299–305.

Boufleur, T. R., Castro, R. R. L. D., Rogério, F., Ciampi-Guillardi, M., Baroncelli, R., & Massola Junior, N. S. (2020). First report of *Colletotrichum musicola* causing soybean anthracnose in Brazil. *Plant Disease*, *104*(6), 1858.

Bragard, C., Dehnen-Schmutz, K., Di Serio, F., Gonthier, P., Jacques, … Milonas, P. (2021). Pest categorisation of *Colletotrichum* Fruct. *EFSA J*, *19*(8), e06803.

Bragard, C., Baptista, P., Chatzivassiliou, E., Di Serio, F., Gonthier, P., ... Reignault, P. L. (2023). Pest categorisation of *Neoscytalidium dimidiatum*. *EFSA Journal*, *21*(5), e08001.

Braun, U., Mouchacca, J., & McKenzie, E. H. C. (1999). Cercosporoid hyphomycetes from New Caledonia and some other South Pacific islands. *New Zealand Journal of Botany*, *37*(2), 297–327.

Braun, U., Crous, P. W., Schubert, K., & Shin, H. D. (2010). Some reallocations of *Stenella* species to *Zasmidium*. *Schlechtendalia*, *20*, 99-104.

Brooker, N. L., Leslie, J. F., & Dickman, M. B. (1991). Nitrate non-utilizing mutants of *Colletotrichum* and their use in studies of vegetative compatibility and genetic relatedness. *Phytopathology*, *81*(6), 672–677.

Bruen, T. C., Philippe, H., & Bryant, D. (2006). A simple and robust statistical test for detecting the presence of recombination. *Genetics*, *172*(4), 2665–2681.

Burdon, J. J., & Silk, J. (1997). Sources and patterns of diversity in plant-pathogenic fungi. *Phytopathology*, *87*(7), 664–669.

Bustamante, M. I., Osorio-Navarro, C., Fernández, Y., Bourret, T. B., Zamorano, A., & Henríquez-Sáez, J. L. (2022). First record of *Colletotrichum anthrisci* causing anthracnose on avocado fruits in Chile. *Pathogens*, *11*(10), 1204.

Byerlee, D., De Janvry, A., & Sadoulet, E. (2009). Agriculture for development: Toward a new paradigm. *Annu. Rev. Resour. Econ.*, *1*(1), 15–31.

Cagliari, R., Kremer, F. S., & da Silva Pinto, L. (2018). Bauhinia lectins: Biochemical properties and biotechnological applications. *International journal of biological macromolecules*, *119*, 811-820.

Cai, L., Hyde, K. D., Taylor, P. W. J., Weir, B., Waller, J., Abang, M. M., ... Shivas, R. G. (2009). A polyphasic approach for studying Colletotrichum. *Fungal Diversity*, *39*(1), 183–204.

Calabon, M. S., Hyde, K. D., Jones, E. G., Luo, Z. L., Dong, W., Hurdeal, V. G., ... Zeng, M. (2022). Freshwater fungal numbers. *Fungal Diversity*, *114*(1), 3–235.

Cannon, P. F., Bridge, P. D., Monte, E. (2000). Linking the past, present and future of *Colletotrichum* systematics. In D. Prusky, S. Freeman, & M. B. Dickman (Eds) *Colletotrichum: Host specificity, pathology and host-pathogen interaction* (pp. 1–20). APS Press.

Cannon, P. F., Buddie, A. G., & Bridge, P. D. (2008). The typification of *Colletotrichum gloeosporioides*. *Mycotaxon*, *104*, 189–120.

Cannon, P. F., Damm, U., Johnston, P. R., & Weir, B. S. (2012). *Colletotrichum*: current status and future directions. *Studies in mycology*, *73*(1), 181–213.

Capella-Gutiérrez, S., Silla-Martínez, J. M., & Gabaldón, T. (2009). trimAl: a tool for automated alignment trimming in large-scale phylogenetic analyses. *Bioinformatics*, *25*(15), 1972–1973.

Capote, N., Pastrana, A. M., Aguado, A., & Sánchez-Torres, P. (2012). Molecular tools for detection of plant pathogenic fungi and fungicide resistance. *Plant pathology*, *12*, 151-202.

Carbone, I., & Kohn, L. M. (1999). A method for designing primer sets for speciation studies in filamentous ascomycetes. *Mycologia*, *91*(3), 553–556.

Case, N. T., Berman, J., Blehert, D. S., Cramer, R. A., Cuomo, C., Currie, C. R., ... Cowen, L. E. (2022). The future of fungi: threats and opportunities. *G3*, *12*(11), 224.

Casas, L. L., Pereira, J. O., Costa-Neto, P. Q., Silva, J. F., Almeida, L. N., Bianco, R. A., & Azevedo, J. L. (2021). Endophytic *Colletotrichum siamense* for biocontrol and resistance induction in guarana seedlings. *International Journal of Microbiology*, *2021*(1), 1925226.

Castro, J. F., Millas, P., Cisterna-Oyarce, V., Carrasco-Fernández, J., Santelices, C., Muñoz, V., ... France, A. (2023). First report of *Colletotrichum fioriniae* causing anthracnose fruit rot on *Vaccinium corymbosum* in Chile. *Plant Disease*, *107*(3), 959.

Cavalcante, G. R., Barguil, B. M., Vieira, W. A., Lima, W. G., Michereff, S. J., Doyle, V. P., & Câmara, M. P. (2019). Diversity, prevalence, and virulence of *Colletotrichum* species associated with lima bean in Brazil. *Plant disease*, *103*(8), 1961–1966.

Cavalcanti, A. D., da Silva Santos, A. C., de Oliveira Ferro, L., Bezerra, J. D., Souza-Motta, C. M., & Magalhães, O. M. C. (2020). *Fusarium massalimae* sp. nov. (*F. lateritium* species complex) occurs endophytically in leaves of *Handroanthus chrysotrichus*. *Mycological Progress*, *19*, 1133–1142.

Chacko, R. J., Weidemann, G. J., Tebeest, D. O., & Correll, J. C. (1994). The use of vegetative compatibility and heterokaryosis to determine potential asexual gene exchange in *Colletotrichum gloeosporioides*. *Biological control*, *4*(4), 382–389.

Chai, A. L., Zhao, Q., Li, B. J., & Sinsiri, W. (2018). First report of anthracnose caused by *Colletotrichum brevisporum* on gac (*Momordica cochinchinensis*) in Thailand. *Plant disease*, *102*(11), 2378–2378.

Chaiwan, N., Gomdola, D., Wang, S., Monkai, J., Tibpromma, S., Doilom, M., ... Hyde, K. D. (2021). An online database providing updated information of microfungi in the Greater Mekong Subregion. *Mycosphere*, *12*, 1513–1526.

Chang-ngern, P., Sardsud, U., Pathomaree, W., Chantrasri, P., & Chukeatirote, E. (2010). Diversity of molds in fresh longan. *Agric Sci J*, *41*(1), 322–324.

Chantarasiri, A., & Boontanom, P. (2021). *Fusarium solani* and *Lasiodiplodia pseudotheobromae*, fungal pathogens causing stem rot disease on durian trees (*Durio zibethinus*) in Eastern Thailand. *New Disease Reports*, *44*(1).

Chapla, V. M., Zeraik, M. L., Leptokarydis, I. H., Silva, G. H., Bolzani, V. S., Young, M. C. M., ... Araújo, A. R. (2014). Antifungal compounds produced by *Colletotrichum gloeosporioides*, an endophytic fungus from *Michelia champaca*. *Molecules*, *19*(11), 19243–19252.

Charoensumran, P., Pratumyot, K., Vilaivan, T., & Praneenararat, T. (2021). Investigation of key chemical species from durian peduncles and their correlations with durian maturity. *Scientific Reports*, *11*(1), 13301.

Cheek, M., Nic Lughadha, E., Kirk, P., Lindon, H., Carretero, J., Looney, B., ... Niskanen, T. (2020). New scientific discoveries: Plants and fungi. *Plants, People, Planet*, *2*(5), 371–388.

Chen, Q., Bakhshi, M., Balci, Y., Broders, K. D., Cheewangkoon, R., Chen, S. F., ... Crous, P. W. (2022). Genera of phytopathogenic fungi: GOPHY 4. *Studies in Mycology*, *101*, 417.

Chen, S., Pavlic, D., Roux, J., Slippers, B., Xie, Y., Wingfield, M. J., & Zhou, X. D. (2011). Characterization of *Botryosphaeriaceae* from plantation-grown *Eucalyptus* species in South China. *Plant Pathology*, *60*(4), 739–751.

Chen, S., Wang, Y., Schnabel, G., Peng, C. A., Lagishetty, S., Smith, K., ... Yuan, H. (2018). Inherent resistance to 14α-demethylation inhibitor fungicides in *Colletotrichum truncatum* is likely linked to CYP51A and/or CYP51B gene variants. *Phytopathology*, *108*(11), 1263–1275.

Chen, X. R., Xing, Y. P., Zhang, T. X., Zheng, J. T., Xu, J. Y., Wang, Z. R., & Tong, Y. H. (2012). First report of *Pestalotiopsis sydowiana* causing leaf necrosis of *Myrica rubra* in China. *Plant Disease*, *96*(5), 764–764.

Chen, Y., Ran, S. F., Dai, D. Q., Wang, Y., Hyde, K. D., Wu, Y. M., & Jiang, Y. L. (2016). Mycosphere essays 2. *Myrothecium*. *Mycosphere*, *7*(1), 64–80.

Chen, Y., Fu, D., Wang, W., Gleason, M. L., Zhang, R., Liang, X., & Sun, G. (2022). Diversity of *Colletotrichum* species causing apple bitter rot and *Glomerella* leaf spot in China. *Journal of Fungi*, *8*(7), 740.

Chen, Y. C., Li, Z., Zhao, Y. X., Gao, M., Wang, J. Y., Liu, K. W., ... Wang, Y. D. (2020). The *Litsea* genome and the evolution of the laurel family. *Nature Communications*, *11*(1), 1675.

Chen, Y. P., Wu, T., Tian, W. H., Ilyukhin, E., Hyde, K. D. & Maharachchikumbura S. S. N. (2022) Comparative 1231 genomics provides new insights into the evolution of *Colletotrichum*. *Mycosphere*, *13*(2), 134–187.

Chen, Z. D., Li, P. L., Chai, A. L., Guo, W. T., Shi, Y. X., Xie, X. W., & Li, B. J. (2018). Crown canker caused by *Paramyrothecium roridum* on greenhouse muskmelon (*Cucumis melo*) in China. *Canadian Journal of Plant Pathology*, *40*(1), 115–120.

Cheng, Y. J., Wu, Y. J., Lee, F. W., Ou, L. Y., Chen, C. N., Chu, Y. Y., & Kuan, Y. C. (2022). Impact of storage condition on chemical composition and antifungal activity of pomelo extract against *Colletotrichum gloeosporioides* and anthracnose in post-harvest mango. *Plants*, *11*(15), 2064.

Cheewangkoon, R., Kodsueb, R., Monkhung, S., Karunarathna, K. V. A., Wongwan, T., Withee, P., ... Tamakeaw, N. (2021). Phytopathogenic fungi identification in Thailand: current trends and future perspectives. *Chiang Mai Journal of Science*, *48*(3), 726–759.

Chethana, K. T., Manawasinghe, I. S., Hurdeal, V. G., Bhunjun, C. S., Appadoo, M. A., Gentekaki, E., ... Hyde, K. D. (2021). What are fungal species and how to delineate them?. *Fungal Diversity*, *109*(1), 1–25.

Chomchalow, N., Somsri, S., & Songkhla, P. N. (2008). Marketing and export of major tropical fruits from Thailand. *Assumption university Journal of technology*, *11*(3), 133–143.

Correll, J. C., Rhoads, D. D., & Guerber, J. C. (1994). Genetic and molecular diversity of populations of *Glomerella cingulata*, *Colletotrichum gloeosporioides*, and *C. acutatum* from apple fruit (Abstr.). *5th Int. Mycol. Congr., Vancouver, Canada*, 77.

Correll, J. C., Guerber, J. C., Wasilwa, L. A., Sherrill, J. F., & Morelock, T. E. (2000). Inter-and intra-species variation in Colletotrichum and mechanisms which affect population structure. *Colletotrichum: host Specificity, pathology, and host-Pathogen interaction*, 145–179.

Costa, M. M., Sandoval-Denis, M., Moreira, G. M., Kandemir, H., Kermode, A., Buddie, A. G., ... Crous, P. W. (2024). Known from trees and the tropics: new insights into the *Fusarium lateritium* species complex. *Studies in Mycology*, *109*: 403–450.

Crous, P. W., Groenewald, J. Z., Mansilla, J. P., Hunter, G. C., & Wingfield, M. J. (2004a). Phylogenetic reassessment of *Mycosphaerella* spp. and their anamorphs occurring on Eucalyptus. *Studies in Mycology*, *50*(1), 195-214.

Crous, P. W., Groenewald, J. Z., Risède, J. M., Simoneau, P., & Hywel-Jones, N. L. (2004b). *Calonectria* species and their *Cylindrocladium* anamorphs: species with sphaeropedunculate vesicles. *Studies in mycology*, *50*, 415–430.

Crous, P. W., Rong, I. H., Wood, A., Lee, S., Glen, H., Botha, W., ... Hawksworth, D. L. (2006a). How many species of fungi are there at the tip of Africa?. *Studies in mycology*, *55*, 13–33.

Crous, P. W., Slippers, B., Wingfield, M. J., Rheeder, J., Marasas, W. F., Philips, A. J., ... & Groenewald, J. Z. (2006b). Phylogenetic lineages in the *Botryosphaeriaceae*. *Studies in mycology*, *55*(1), 235–253.

Crous, P. W., Wingfield, M. J., Mansilla, J. P., Alfenas, A. C., & Groenewald, J. Z. (2006c). Phylogenetic reassessment of *Mycosphaerella* spp. and their anamorphs occurring on *Eucalyptus*. II. *Studies in Mycology*, *55*(1), 99–131.

Crous, P. W., Schoch, C. L., Hyde, K. D., Wood, A. R., Gueidan, C., De Hoog, G. S., & Groenewald, J. Z. (2009). Phylogenetic lineages in the Capnodiales. *Studies in mycology*, *64*(1), 17–47.

Crous, P. W., Braun, U., Hunter, G. C., Wingfield, M. J., Verkley, G. J. M., Shin, H. D., ... & Groenewald, J. Z. (2013). Phylogenetic lineages in *Pseudocercospora*. *Studies in Mycology*, *75*(1), 37–114.

Crous, P. W., Hawksworth, D. L., & Wingfield, M. J. (2015a). Identifying and naming plant-pathogenic fungi: past, present, and future. *Annual Review of Phytopathology*, *53*(1), 247–267.

Crous, P. W., Wingfield, M. J., Le Roux, J. J., Richardson, D. M., Strasberg, D., Shivas, R. G., ... Groenewald, J. Z. (2015b). Fungal Planet description sheets: 371–399. *Persoonia-Molecular Phylogeny and Evolution of Fungi*, *35*(1), 264–327.

Crous, P. W., Groenewald, J. Z., Slippers, B., & Wingfield, M. J. (2016). Global food and fibre security threatened by current inefficiencies in fungal identification. *Philosophical Transactions of the Royal Society B: Biological Sciences*, *371*(1709), 20160024.

Crous, P. W., Wingfield, M. J., Chooi, Y. H., Gilchrist, C. L., Lacey, E., Pitt, J. I., ... Venzhik, A. S. (2020). Fungal Planet description sheets: 1042–1111. *Persoonia: Molecular Phylogeny and Evolution of Fungi*, *44*, 301.

Crowther, T. W., Maynard, D. S., Crowther, T. R., Peccia, J., Smith, J. R., & Bradford, M. A. (2014). Untangling the fungal niche: the trait-based approach. *Frontiers in microbiology*, *5*, 579.

Cui, M. J., Wei, X., Xia, P. L., Yi, J. P., Yu, Z. H., Deng, J. X., & Li, Q. L. (2021). *Diaporthe taoicola* and *D. siamensis*, two new records on *Citrus sinensis* in China. *Mycobiology*, *49*(3), 267–274.

Dahal, G., Amatya, P., Manandhar, & H.K. (1992). Plant diseases in Nepal. *Review of Plant Pathology*, *71*(11), 797–807.

Daiuto, É. R., Vieites, R. L., Tremocoldi, M. A., Carvalho, L. R. D. & Fumes, J. G. F. (2013) Postharvest of 'Hass' avocados submitted to UV-C radiation. *Revista Colombiana de Ciências Hortícolas*, *7*, 149–160.

Darriba, D., Taboada, G. L., Doallo, R., & Posada, D. (2012). jModelTest 2: more models, new heuristics and high-performance computing. *Nature methods*, *9*(8), 772.

Damm, U., Woudenberg, J. H. C., Cannon, P. F., & Crous, P. W. (2009). *Colletotrichum* species with curved conidia from herbaceous hosts. *Fungal Diversity*, *39*, 45.

Damm, U., Cannon, P. F., Woudenberg, J. H. C., & Crous, P. W. (2012). The *Colletotrichum acutatum* species complex. *Studies in mycology*, *73*, 37–113.

Damm, U., Sato, T., Alizadeh, A., Groenewald, J. Z., & Crous, P. W. (2019). The *Colletotrichum dracaenophilum*, *C. magnum* and *C. orchidearum* species complexes. *Studies in mycology*, *92*(1), 1–46.

Darge, W. A., & Woldemariam, S. S. (2021). *Botryosphaeria* tree fungal pathogens and their diversity. *International Journal of Phytopathology*, *10*(1), 49–56.

Darriba, D., Taboada, G. L., Doallo, R., & Posada, D. (2012). jModelTest 2: more models, new heuristics and high-performance computing. *Nature methods*, *9*(8), 772.

Dayarathne, M. C., Thambugala, K. M., Daranagama, D. A., Mridha, A. U., Dissanayake, A. J., Dissanayake, L. S., ... Lumyong, S. (2023). Global challenges in identifying plant pathogenic fungi: an overview with suggestions for the way forward. *Chiang Mai Journal of Science*, *50*(4), 1–17

Dela Cueva, F. M., Laurel, N. R., Dalisay, T. U., & Sison, M. L. J. (2021). Identification and characterisation of *Colletotrichum fructicola*, *C. tropicale* and *C. theobromicola* causing mango anthracnose in the Philippines. *Archives of Phytopathology and Plant Protection*, *54*, 1989–2006.

Derviş, S., & Özer, G. (2023). Plant-associated *neoscytalidium dimidiatum*—Taxonomy, host range, epidemiology, virulence, and management strategies: A comprehensive review. *Journal of Fungi*, *9*(11), 1048.

De Silva, D. D., Groenewald, J. Z., Crous, P. W., Ades, P. K., Nasruddin, A., Mongkolporn, O., & Taylor, P. W. (2019). Identification, prevalence and pathogenicity of *Colletotrichum* species causing anthracnose of Capsicum annuum in Asia. *IMA fungus*, *10*, 1–32.

De Silva, N. I., Maharachchikumbura, S. S. N., Thambugala, K. M., Bhat, D. J., Karunarathna, S. C., Tennakoon, D. S., ... Hyde, K. D. (2021). Morpho-molecular taxonomic studies reveal a high number of endophytic fungi from *Magnolia candolli* and *M. garrettii* in China and Thailand. *Mycosphere*, *12*(1), 163–237.

De Silva, N. I., Hyde, K. D., Lumyong, S., Phillips, A. J. L., Bhat, D. J., Maharachchikumbura, S. S. N., ... Karunarathna, S. C. (2022). Morphology, phylogeny, host association and geography of fungi associated with plants of *Annonaceae*, *Apocynaceae* and *Magnoliaceae*. *Mycosphere*, *13*, 955–1076.

Diao, Y. Z., Zhang, C., Liu, F., Wang, W. Z., Liu, L., Cai, L., & Liu, X. L. (2017). Colletotrichum species causing anthracnose disease of chili in China. *Persoonia-Molecular Phylogeny and Evolution of Fungi*, *38*(1), 20–37.

Dianda, O. Z., Wonni, I., Ouédraogo, L., Sankara, P., Tollenaere, C., Del Ponte, E. M., & Fernandez, D. (2023). *Lasiodiplodia* species associated with mango (*Mangifera indica* L.) decline in Burkina Faso and influence of climatic factors on the disease distribution. *Physiological and Molecular Plant Pathology*, *126*, 102041.

Dieye, C., MBAYE, N., & Diédhiou P. M. (2020). Distribution of the mango malformation disease in southern Senegal. *International Journal of Science, Environment and Technology*, *9*, 362–372.

Ding, G., Zheng, Z., Liu, S., Zhang, H., Guo, L., & Che, Y. (2009). Photinides A− F, cytotoxic benzofuranone-derived γ-Lactones from the plant endophytic fungus *Pestalotiopsis photiniae*. *Journal of Natural Products*, *72*(5), 942–945.

Dinh, S. Q., Chongwungse, J., Pongam, P., & Sangchote, S. (2003). Fruit infection by *Colletotrichum gloeosporioides* and anthracnose resistance of some mango cultivars in Thailand. *Australasian Plant Pathology*, *32*, 533–538.

Diogo, E., Gonçalves, C. I., Silva, A. C., Valente, C., Bragança, H., & Phillips, A. J. (2021). Five new species of *Neopestalotiopsis* associated with diseased *Eucalyptus* spp. in Portugal. *Mycological Progress*, *20*(11), 1441–1456.

Dissanayake, A. J. (2017). Molecular phylogenetic analysis reveals seven new *Diaporthe* species from Italy. *Mycosphere*, *8*(5), 853–877.

Dissanayake, D. M. S., Adikaram, N. K. B., Yakandawala, D. M. D., & Jayasinghe, L. (2021). Molecular phylogeny-based identification of *Colletotrichum endophytica* and *C. siamense* as causal agents of avocado anthracnose in Sri Lanka. *Ceylon Journal of Science*, *50*(4), 449–458.

Dissanayake, A. J., Zhu, J. T., Chen, Y. Y., Maharachchikumbura, S. S., Hyde, K. D., & Liu, J. K. (2024). A re-evaluation of *Diaporthe*: refining the boundaries of species and species complexes. *Fungal Diversity*, *126*(1), 1–125.

Doehlemann, G., Ökmen, B., Zhu, W., & Sharon, A. (2017). Plant pathogenic fungi. *The fungal kingdom*, 701–726.

do Espírito Santo, B. C., Oliveira, J. A. D. S., Ribeiro, M. A. D. S., Schoffen, R. P., Polli, A. D., Polonio, J. C., ... Pamphile, J. A. (2023). Antitumor and antibacterial activity of metabolites of endophytic *Colletotrichum siamense* isolated from coffee (*Coffea arabica* L. cv IAPAR-59). *Brazilian Journal of Microbiology*, *54*(4), 2651–2661.

Ellis, J. B., & Everhart, B. M. (1888). New species of fungi from various localities (continued). *The Journal of Mycology*, *4*(6), 49–59.

Farr, D. F., Elliott, M., Rossman, A. Y., & Edmonds, R. L. (2005). *Fusicoccum arbuti* sp. nov. causing cankers on Pacific madrone in western North America with notes on *Fusicoccum dimidiatum*, the correct name for *Scytalidium dimidiatum* and *Nattrassia mangiferae*. *Mycologia*, *97*(3), 730–741.

Farr D. F., & Rossman A. Y. (2024). Fungal Databases, U.S. National Fungus Collections, ARS, USDA. https://nt.ars-grin.gov/fungaldatabases/

Farr, D. F., & Rossman, A. Y. (2022) Fungal Databases; Systematic Mycology Microbiology Laboratory, *USDA-ARS: Beltsville, MD, USA, 12*.

Feng, W., Li, M., Li, L., He, Y., Yang, J., Sun, J., ... Hu, M. (2023). First report of stem-end rot caused by *Botryosphaeria fabicerciana* on mango fruits in China. *Plant Disease*, *107*(9), 2880.

Fiorenza, A., Gusella, G., Aiello, D., Polizzi, G., & Voglmayr, H. (2022). *Neopestalotiopsis siciliana* sp. nov. and *N. rosae* causing stem lesion and dieback on avocado plants in Italy. *Journal of Fungi*, *8*(6), 562.

Fones, H. N., Fisher, M. C., & Gurr, S. J. (2017). Emerging fungal threats to plants and animals challenge agriculture and ecosystem resilience. *The fungal kingdom*, 787–809.

Fries, E. M. (1849). *Summa Vegetabilium Scandinaviae 2. HolmiaeA., Bonnier*, pp. 259–572.

Fu, M., Crous, P. W., Bai, Q., Zhang, P. F., Xiang, J., Guo, Y. S., ... Wang, G. P. (2019). *Colletotrichum* species associated with anthracnose of *Pyrus* spp. in China. *Persoonia-Molecular Phylogeny and Evolution of Fungi*, *42*(1), 1–35.

Fuentes-Aragón, D., Silva-Rojas, H. V., Guarnaccia, V., Mora-Aguilera, J. A., Aranda-Ocampo, S., Bautista-Martínez, N., & Téliz-Ortíz, D. (2020a). *Colletotrichum* species causing anthracnose on avocado fruit in Mexico: Current status. *Plant Pathology*, *69*(8), 1513–1528.

Fuentes-Aragón, D., Guarnaccia, V., Rebollar-Alviter, A., Juárez-Vázquez, S. B., Aguirre-Rayo, F., & Silva-Rojas, H. V. (2020b). Multilocus identification and thiophanate-methyl sensitivity of *Colletotrichum gloeosporioides* species complex associated with fruit with symptoms and symptomless leaves of mango. *Plant Pathology*, *69*(6), 1125–1138.

Galsurker, O., Diskin, S., Maurer, D., Feygenberg, O., & Alkan, N. (2018). Fruit stem-end rot. *Horticulturae*, *4*(4), 50.

Gangadevi, V., & Muthumary, J. (2008). Isolation of *Colletotrichum gloeosporioides*, a novel endophytic taxol-producing fungus from the leaves of a medicinal plant, Justicia gendarussa. *Mycologia balcanica*, *5*(1), 1–4.

Gao, Y., Liu, F., & Cai, L. (2016). Unravelling *Diaporthe* species associated with *Camellia*. *Systematics and Biodiversity*, *14*(1), 102–117.

Garcia-Lopez, E. L. V. I. S., Mora-Aguilera, J. A., Nava-Diaz, C., Villegas-Monter, A. N. G. E. L., Tovar-Pedraza, J. M., Serra, C., & Batista-Marte, C. M. (2016). First report of *Fusarium pseudocircinatum* causing mango malformation disease in Dominican Republic. *Plant Disease*, *100*(7), 1501–1501.

Garud, A. B. (1968) An anthracnose disease of pineapple in India. *Plant Disease Report*, *52*, 436–437.

Gautam, A. K., Avasthi, S., Prasher, I. B., & Verma, R. K. (2020). Diversity and distribution of cercosporoid fungi in Himachal Pradesh: an annotated checklist. *Studies in Fungi*, *5*(1), 17–49.

Geremu, M. A., Welelaw, E., Tamirat, S., & Kidane, B. (2022). Associated fungal pathogens and causes of postharvest losses in the avocado value chain in Hossana town market, Ethiopia. *African Journal of Food, Agriculture, Nutrition and Development*, *22*(6), 20646–20667.

Giatgong, P. (1978). *Host Index of Plant Diseases in Thailand*. Mycology Branch, Plant Pathology and Microbiology Division, Ministry of Agriculture and Cooperative, Bangkok, Thailand. 118.

Giblin, F. R., Tan, Y. P., Mitchell, R., Coates, L. M., Irwin, J. A. G., & Shivas, R. G. (2018). *Colletotrichum* species associated with pre-and post-harvest diseases of avocado and mango in eastern Australia. *Australasian Plant Pathology*, *47*, 269–276.

Glass, N. L., & Donaldson, G. C. (1995). Development of primer sets designed for use with the PCR to amplify conserved genes from filamentous ascomycetes. *Applied and environmental microbiology*, *61*(4), 1323–1330.

Glez-Peña, D., Gomez-Blanco, D., Reboiro-Jato, M., Fdez-Riverola, F., Posada, D. (2010). ALTER: program-oriented conversion of DNA and protein alignments. *Nucleic Acids Research*, *38*, 14–18.

Gold, S. E., García-Pedrajas, M. D., & Martínez-Espinoza, A. D. (2001). New (and used) approaches to the study of fungal pathogenicity. *Annual review of phytopathology*, *39*(1), 337–365.

Gomdola, D., Bhunjun, C. S., Hyde, K. D., Jeewon, R., Pem, D., & Jayawardena, R. S. (2022). Ten important forest fungal pathogens: a review on their emergence and biology. *Mycosphere*, *13*, 612–671

Gomes, R. R., Glienke, C., Videira, S. I. R., Lombard, L., Groenewald, J. Z., & Crous, P. W. (2013). *Diaporthe*: a genus of endophytic, saprobic and plant pathogenic fungi. *Persoonia-Molecular Phylogeny and Evolution of Fungi*, *31*(1), 1–41.

Gould, A. B. (2009). Fungi: plant pathogenic. In *Encyclopedia of microbiology* (pp. 457–477). Elsevier Inc..

Groenewald, J. Z., Nakashima, C., Nishikawa, J., Shin, H. D., Park, J. H., Jama, A. N., ... & Crous, P. W. (2013). Species concepts in *Cercospora*: spotting the weeds among the roses. *Studies in Mycology*, *75*(1), 115-170.

Guarnaccia, V., Vitale, A., Cirvilleri, G., Aiello, D., Susca, A., Epifani, F., ... & Polizzi, G. (2016). Characterisation and pathogenicity of fungal species associated with branch cankers and stem-end rot of avocado in Italy. *European Journal of Plant Pathology*, *146*, 963–976.

Guarnaccia, V., Gilardi, G., Martino, I., Garibaldi, A., & Gullino, M. L. (2019). Species diversity in *Colletotrichum* causing anthracnose of aromatic and ornamental Lamiaceae in Italy. *Agronomy*, *9*(10), 613.

Guindon, S., Dufayard, J. F., Lefort, V., Anisimova, M., Hordijk, W., & Gascuel, O. (2010). New algorithms and methods to estimate maximum-likelihood phylogenies: assessing the performance of PhyML 3.0. *Systematic biology*, *59*(3), 307–321.

Hall, T. A. (1999, January). BioEdit: a user-friendly biological sequence alignment editor and analysis program for Windows 95/98/NT. In *Nucleic acids symposium series*, *41*(41), 95–98.

Han, S. L., Wang, M. M., Ma, Z. Y., Raza, M., Zhao, P., Liang, J. M., ... Cai, L. (2023). *Fusarium* diversity associated with diseased cereals in China, with an updated phylogenomic assessment of the genus. *Studies in Mycology*, *104*(1), 87–148.

Haq, I., Ijaz, S., & Khan, N. A. (2021). Genealogical concordance of phylogenetic species recognition-based delimitation of *Neopestalotiopsis* species associated with leaf spots and fruit canker disease affected guava plants. *Pakistan Journal of Agricultural Sciences*, *58*(4).

Hariharan, G., & Prasannath, K. (2021). Recent advances in molecular diagnostics of fungal plant pathogens: a mini review. *Frontiers in Cellular and Infection Microbiology*, *10*, 600234.

Hasan, S., Hasan, S. S., Saha, S., & Islam, M. R. (2022). Identify problems and suggest possible solutions for safe pineapple production in Madhupur tract. *European Journal of Agriculture and Food Sciences*, *4*(5), 68–74.

Hawksworth, D. L. (2001). The magnitude of fungal diversity: the 1.5 million species estimate revisited. *Mycological research*, *105*(12), 1422–1432.

Hawksworth, D. L. (2012). Global species numbers of fungi: are tropical studies and molecular approaches contributing to a more robust estimate?. *Biodiversity and conservation*, *21*, 2425–2433.

Hawksworth, D. L., & Lücking, R. (2017). Fungal diversity revisited: 2.2 to 3.8 million species. *Microbiology spectrum*, *5*(4), 10–1128.

Heald, F. D., & Wolf, F. A. (1911). New species of Texas fungi. *Mycologia*, *3*(1), 5–22.

Hemung, B. O., Sompholkrang, M., Wongchai, A., Chanshotikul, N., & Ueasin, N. (2022). A study of the potential of by-products from pineapple processing in Thailand. *Int. J. Health Sci*, *6*, 12605–12615.

Hilário, S., Santos, L., & Alves, A. (2021). *Diaporthe amygdali*, a species complex or a complex species?. *Fungal biology*, *125*(7), 505–518.

Hirayama, Y., Asano, S., Okayama, K. O., Ohki, S. T., & Tojo, M. (2018). Weeds as the potential inoculum source of *Colletotrichum fructicola* responsible for strawberry anthracnose in Nara, Japan. *Journal of general plant pathology*, *84*, 12–19.

Hofer, K. M., Braithwaite, M., Braithwaite, L. J., Sorensen, S., Siebert, B., Pather, V., ... Toome-Heller, M. (2021). First report of *Colletotrichum fructicola*, *C. perseae*, and *C. siamense* causing anthracnose disease of avocado (*Persea americana*) in New Zealand. *Plant disease*, *105*(05), 1564.

Honger, J. O., Offei, S. K., Oduro, K. A., Odamtten, G. T., & Nyaku, S. T. (2014). Identification and species status of the mango biotype of *Colletotrichum gloeosporioides* in Ghana. *European Journal of Plant Pathology*, *140*, 455–467.

Hongsanan, S., Norphanphoun, C., Senanayake, I. C., Jayawardena R. S., Manawasinghe, I. S., Abeywickrama, P. D., … Bhunjun, C. S. (2023). Annotated notes on *Diaporthe* species. *Mycosphere*, *14*(1), 918–1189.

Hossain, M. F., Akhtar, S., & Anwar, M. (2015). Nutritional value and medicinal benefits of pineapple. *International Journal of Nutrition and Food Sciences*, *4*(1), 84–88.

Huaman-Pilco, A. F., Huaman-Pilco, J., Torres-de la Cruz, M., Oliva-Cruz, S. M., & Díaz-Valderrama, J. R. (2023). First report of *Paramyrothecium roridum* causing leaf spot and stem rot diseases on *Coffea arabica* in Peru. *Plant Disease*, *107*(1), 221.

Huang, F., Chen, G. Q., Hou, X., Fu, Y. S., Cai, L., Hyde, K. D., & Li, H. Y. (2013). Colletotrichum species associated with cultivated citrus in China. *Fungal Diversity*, *61*, 61–74.

Huanraluek, N., Jayawardena, R. S., Maharachchikumbura, S. S., & Harishchandra, D. L. (2021). Additions to pestalotioid fungi in Thailand: *Neopestalotiopsis hydeana* sp. nov. and *Pestalotiopsis hydei* sp. nov. *Phytotaxa*, *479*(1), 23–43.

Huanraluek, N., Phunyaboon, W., & Jayawardena, R. S. (2022). A new host record of *Diaporthe rosae* on Rambutan (*Nephelium lappaceum* L.). *Phytotaxa*, *567*(2), 162–172.

Hunupolagama, D. M., Wijesundera, R. L. C., Chandrasekharan, N. V., Wijesundera, W. S. S., Kathriarachchi, H., & Fernando, T. H. P. S. (2015). Characterization of *Colletotrichum* isolates causing avocado anthracnose and first report of *C. gigasporum* infecting avocado in Sri Lanka. *Plant Pathology & Quarantine*, *5*(2), 132–143.

Huo, J. F., Yao, Y. R., Ben, H. Y., Tian, T., Yang, L. J., Wang, Y., ... Wang, W. L. (2021). First report of *Paramyrothecium foliicola* causing stem canker of cucumber (*Cucumis sativus*) seedlings in China. *Plant Disease*, *105*(6), 1859.

Huo, J. F., Yao, Y. R., Ben, H. Y., Yang, L. J., Yang, X. R., Sun, B. B., ... Wang, W. L. (2023). First report of leaf spot caused by *Paramyrothecium foliicola* on tomato (*Solanum lycopersicum*) in China. *Plant Disease*, *107*(1), 220.

Hou, L. W., Liu, F., Duan, W. J., & Cai, L. (2016). *Colletotrichum aracearum* and *C. camelliae-japonicae*, two holomorphic new species from China and Japan. *Mycosphere*, *7*(8), 1111–1123.

Huson, D. H. (1998). SplitsTree: analyzing and visualizing evolutionary data. *Bioinformatics (Oxford, England)*, *14*(1), 68–73.

Huson, D. H., & Bryant, D. (2006). Application of phylogenetic networks in evolutionary studies. *Molecular biology and evolution*, *23*(2), 254–267.

Hyde, K. D., Cai, L., McKenzie, E. H. C., Yang, Y. L., Zhang, J. Z., & Prihastuti, H. (2009). *Colletotrichum*: a catalogue of confusion. *Fungal Diversity*, *39*(1), 1–17.

Hyde, K. D., Udayanga, D., Manamgoda, D. S., Tedersoo, L., Larsson, E., Abarenkov, K., ... Nilsson, H. R. (2013). Incorporating molecular data in fungal systematics: a guide for aspiring researchers. *Current Research on Environtal and Applied Mycology*, *3*, 1–32.

Hyde, K. D., Nilsson, R. H., Alias, S. A., Ariyawansa, H. A., Blair, J. E., Cai, L., ... Zhou, N. (2014). One stop shop: backbones trees for important phytopathogenic genera: I (2014). *Fungal Diversity*, *67*, 21–125.

Hyde, K. D., Al-Hatmi, A. M., Andersen, B., Boekhout, T., Buzina, W., Dawson, T. L., ... Tsui, C. K. (2018a). The world's ten most feared fungi. *Fungal Diversity*, *93*, 161–194.

Hyde, K. D., Norphanphoun, C., Chen, J., Dissanayake, A. J., Doilom, M., Hongsanan, S., ... Stadler, M. (2018b). Thailand's amazing diversity: up to 96% of fungi in northern Thailand may be novel. *Fungal diversity*, *93*, 215–239.

Hyde, K. D., Chaiwan, N., Norphanphoun, C., Boonmee, S., Camporesi, E., Chethana, K. W. T., ... Zhao, Q. (2018c). Mycosphere notes 169–224. *Mycosphere*, *9*(2), 271–430.

Hyde, K. D., Tennakoon, D. S., Jeewon, R., Bhat, D. J., Maharachchikumbura, S. S., Rossi, W., ... Doilom, M. (2019). Fungal diversity notes 1036–1150: taxonomic and phylogenetic contributions on genera and species of fungal taxa. *Fungal diversity*, *96*, 1–242.

Hyde, K. D., Noorabadi, M. T., Thiyagaraja, V., Mq, H., Johnston, P. R., Wijesinghe, S. N., ... Dianese, J. (2024a). The 2024 Outline of Fungi and fungus-like taxa. *Mycosphere*, *15*(1), 5146–6239.

Hyde, K. D., Wijesinghe, S. N., Afshari, N., Aumentado, H. D., Bhunjun, C. S., Boonmee, S., ... Zhang, J. Y. (2024b). Mycosphere Notes 469–520. *Mycosphere 15*(1), 1294–1454.

Illana, A., Rodriguez-Romero, J., & Sesma, A. (2013). Major plant pathogens of the *Magnaporthaceae* family. In *Genomics of Soil-and Plant-Associated Fungi* (pp. 45–88). Springer Berlin Heidelberg.

International Trade Centre Trade Map: List of exporters for product. Pineapples in 2020 Trade Map. Retrieved December 10, 2022, from https: //www.trademap.org.

Iqbal, S., Khan, M. A., Atiq, M., Rajput, N. A., Usman, M., Nawaz, A., ... Ahmad, H. (2022). Mango anthracnose: Global status and the way forward for disease management. *Journal of Innovative Sciences*, *8*(2), 222–235.

Ismail, S. I., Zulperi, D., Norddin, S., & Ahmad-Hamdani, S. (2017). First report of *Neopestalotiopsis saprophytica* causing leaf spot of oil palm (*Elaeis guineensis*) in Malaysia. *Plant Disease*, *101*(10), 1821.

Jantasorn, A., Moungsrimuangdee, B., & Dethoup, T. (2016). In vitro antifungal activity evaluation of five plant extracts against five plant pathogenic fungi causing rice and economic crop diseases. *Journal of Biopesticides*, *9*(1), 1.

Jayasiri, S. C., Hyde, K. D., Ariyawansa, H. A., Bhat, J., Buyck, B., Cai, L., ... Promputtha, I. (2015). The Faces of Fungi database: fungal names linked with morphology, phylogeny and human impacts. *Fungal diversity*, *74*, 3–18.

Jayawardena, R. S., Hyde, K. D., Damm, U., Cai, L., Liu, M., Li, X. H., ... Yan, J. Y. (2016). Notes on currently accepted species of *Colletotrichum*. *Mycosphere*, *7*(8), 1192–1260.

Jayawardena, R. S., Hyde, K. D., Jeewon, R., Ghobad-Nejhad, M., Wanasinghe, D. N., Liu, N., ... Kang, J. C. (2019). One stop shop II: taxonomic update with molecular phylogeny for important phytopathogenic genera: 26–50 (2019). *Fungal Diversity*, *94*, 41–129.

Jayawardena, R. S., Hyde, K. D., Chen, Y. J., Papp, V., Palla, B., Papp, D., ... Wang, Y. (2020). One stop shop IV: taxonomic update with molecular phylogeny for important phytopathogenic genera: 76–100 (2020). *Fungal Diversity*, *103*, 87–218.

Jayawardena, R. S., Bhunjun, C. S., Hyde, K. D., Gentekaki, E., & Itthayakorn, P. (2021a). *Colletotrichum*: Lifestyles, biology, morpho-species, species complexes and accepted species. *Mycosphere*, *12*, 519–669.

Jayawardena, R. S., Hyde, K. D., de Farias, A. R. G., Bhunjun, C. S., Ferdinandez, H. S., Manamgoda, D. S., ... Thines, M. (2021b). What is a species in fungal plant pathogens?. *Fungal Diversity*, *109*(1), 239–266.

Jayawardena, R. S., Hyde, K. D., Wang, S., Sun, Y. R., Suwannarach, N., Sysouphanthong, P., ... Wang, Y. (2022). Fungal diversity notes 1512–1610: Taxonomic and phylogenetic contributions on genera and species of fungal taxa. *Fungal Diversity*, *117*(1), 1–272.

Jeewon, R., & Hyde, K. D. (2016). Establishing species boundaries and new taxa among fungi: recommendations to resolve taxonomic ambiguities. *Mycosphere, 7*(11), 1669–1677.

Jiang, N., Bonthond, G., Fan, X. L., & Tian, C. M. (2018). *Neopestalotiopsis rosicola* sp. nov. causing stem canker of *Rosa chinensis* in China. *Mycotaxon*, *133*(2), 271–283.

John, N., Anjanadevi, I. P., & Jeeva, M. L. (2014). Efficacy of cassava by-products as carrier materials of Trichoderma harzianum, a biocontrol agent against Sclerotium rolfsii causing collar rot in Amorphophallus. *Journal of Root Crops*, *40*(1), 74–79.

Johnston, A. A. (1960). supplement to a host list of plant diseases in Malaya. *Mycological Papers*, *77*, 1–30.

Johnson, D. A., Carris, L. M., & Rogers, J. D. (1997). Morphological and molecular characterization of *Colletotrichum nymphaeae* and *C. nupharicola* sp. nov. on water-lilies (*Nymphaea* and *Nuphar*). *Mycological Research*, *101*(6), 641–649.

Joy, P. P. (2010). Benefits and uses of pineapple. *Pineapple Research Station (Kerala Agricultural University), Vazhakulam-686*, *670*.

Kader, A., Hossain, F. M. J., Islam, M. M., Kabir, G., Sarkar, S. K., & Absar, N. (2010). A comparative analysis on the nutritional contents of two varieties of pineapple of Chittagong region. *Chittagong University Journal of Biological Sciences*, 105–112.

Kaewchai, S., Paopradit, P., Pornsuriya, C., Jayawarrdena, R. S., & Hyde, K. D. (2024). Pathogenicity and molecular phylogenetic analysis reveal *Colletotrichum siamense* as causal agent of leaf fall disease in rubber trees (*Hevea brasiliensis*) in southern Thailand. *Agriculture and Natural Resources*, *58*(1).

Kaewjan, P., Sittikul, C., Cheewangkoon, R., Hyde, K. D., & Akarapisan, A. (2012). *Mycosphaerella* and other fungi associated with banana leaf diseases from northern Thailand. *Chiang Mai University Journal of Natural Sciences*, *11*(1), 25–32.

Kalyaanamoorthy, S., Minh, B. Q., Wong, T. K., Von Haeseler, A., & Jermiin, L. S. (2017). ModelFinder: fast model selection for accurate phylogenetic estimates. *Nature methods*, *14*(6), 587–589.

Kamran, M., Ullah, I., Ehetisham ul Haq, M., Iqbal, M., Abbas, H., Nazir, S., ... Idrees, M. (2020). First report of *Fusarium sulawesiensis* (FIESC-16) associated with stem rot of sesame in Pakistan. *Plant Disease*, *104*(5), 1554–1554.

Katan, T. (2000). Vegetative compatibility in *Colletotrichum*. In D. Prusky, S. Freeman, & M. B. Dickman (Eds.), *Colletotrichum: Host Specificity, Pathology, and Host-Pathogen Interaction* (pp. 145–179). The American Phytopathological Society.

Katoh, K., Rozewicki, J., & Yamada, K. D. (2019). MAFFT online service: multiple sequence alignment, interactive sequence choice and visualization. *Briefings in bioinformatics*, *20*(4), 1160–1166.

Kazemzadeh Chakusary, M., Mohammadi, H., & Khodaparast, S. A. (2019). Diversity and pathogenicity of *Botryosphaeriaceae* species on forest trees in the north of Iran. *European Journal of Forest Research*, *138*, 685–704.

Kee, Y. J., Zakaria, L., & Mohd, M. H. (2020). Morphology, phylogeny and pathogenicity of *Fusarium* species from *Sansevieria trifasciata* in Malaysia. *Plant pathology*, *69*(3), 442–454.

Keith, L. M. (2008). First report of *Pestalotiopsis virgatula* causing *Pestalotiopsis* fruit rot on Rambutan in Hawaii. *Plant Disease*, *92*(5), 835–835.

Khoo, Y. W., Tan, H. T., Khaw, Y. S., Li, S. F., & Chong, K. P. (2022). First report of *Neopestalotiopsis cubana* causing leaf blight on *Ixora chinensis* in Malaysia. *Plant Disease*, *106*(10), 2747.

Khuna, S., Kumla, J., Thitla, T., & Suwannarach, N. (2023a). First report of Anthracnose on giant *Philodendron* caused by *Colletotrichum siamense* in Thailand. *Plant Disease*, *107*(10), 3301.

Khuna, S., Kumla, J., Thitla, T., Lumyong, S., & Suwannarach, N. (2023b). First report of rose apple leaf spot caused by *Colletotrichum siamense* in Thailand. *Plant Disease*, *107*(5), 1625.

Khuna, S., Kumla, J., & Suwannarach, N. (2024). First report of post-harvest fruit rot on watermelon caused by *Lasiodiplodia theobromae* in northern Thailand. *Canadian Journal of Plant Pathology*, *46*(3), 265-274.

Ko, T. W. K., McKenzie, E. H. C., Bahkali, A. H., To-Anun, C., Chukeatirote, E., Promputtha, I., ... Hyde, K. D. (2011). The need for re-inventory of Thai phytopathogens. *Chiang Mai Journal of Science*, *38*(4), 625–637.

Koutb, M. M., Hassan, E. A., El-Sokkary, G. H., Saber, S. H., & Hussein, N. A. (2021). Paclitaxel production by endophytic fungus, *Neopestalotiopsis clavispora* KY624416 and subsequent extraction of chitosan from fungal biomass wastes. *Global Nest Journal*, *23*(3), 370–380.

Kumar, K., Singh, D. R., Amaresan, N., & Madhuri, K. (2012). Isolation and pathogenicity of *Colletotrichum* spp. causing anthracnose of Indian mulberry (Morinda citrifolia) in tropical islands of Andaman and Nicobar, India. *Phytoparasitica*, *40*(5), 485–491.

Laksanaphisut, S., Songkumarn, P., & Receiv, S. S. (2019). Characterizations of *Colletotrichum* spp., pathogens on mango fruits (*Mangifera indica* L. cv.'Nam Dok Mai'). *Thai Agricultural Research Journal*, *37*(2), 197–215.

Lenne JM. (1990). A world list of fungal diseases of tropical pasture species. *Phytopathology*. *31*, 1–162.

Larran, S., Bahima, J. V., Bello, G. D., Franco, E., & Balatti, P. (2015). *Colletotrichum siamense* causing anthracnose in *Bauhinia forficata* subsp. *pruinosa* in Argentina. *Australasian Plant Disease Notes*, *10*, 1–2.

Larsson, A. (2014). AliView: a fast and lightweight alignment viewer and editor for large datasets. *Bioinformatics*, *30*(22), 3276–3278.

Larter, L. N., Martyn, E.B. (1943). A preliminary list of plant diseases in Jamaica. *Mycological Papers*, *8*, 16.

Lehman, G. (1923). Pod and stem blight of soybean. *Annals of the Missouri Botanical Garden*, *10*(2), 111–178.

Li, G. Q., Liu, F. F., Li, J. Q., Liu, Q. L., & Chen, S. F. (2018). *Botryosphaeriaceae* from Eucalyptus plantations and adjacent plants in China. *Persoonia-Molecular Phylogeny and Evolution of Fungi*, *40*(1), 63–95.

Li, J. X., Schieberle, P., & Steinhaus, M. (2012). Characterization of the major odor-active compounds in Thai durian (*Durio zibethinus* L.'Monthong') by aroma extract dilution analysis and headspace gas chromatography–olfactometry. *Journal of agricultural and food chemistry*, *60*(45), 11253–11262.

Li, L., Mohd, M. H., & Zakaria, L. (2020). *Colletotrichum* species associated with mango (*Mangifera indica* L.) stem-end rot. *Journal of Plant Pathology*, *102*, 505–509.

Li, L., Mohd, M. H., Mohamed Nor, N. M. I., Subramaniam, S., & Latiffah, Z. (2021a). Identification of *Botryosphaeriaceae* associated with stem-end rot of mango (*Mangifera indica* L.) in Malaysia. *Journal of Applied Microbiology*, *130*(4), 1273–1284.

Li, L., Yang, Q., & Li, H. (2021b). Morphology, phylogeny, and pathogenicity of pestalotioid species on *Camellia oleifera* in China. *Journal of Fungi*, *7*(12), 1080.

Li, L., & Li, H. (2022). First report of *Colletotrichum aeschynomenes* causing anthracnose on *Camellia oleifera* in China. *Forest Pathology*, *52*(5), e12770.

Li, M., Feng, W., Yang, J., Gao, Z., Zhang, Z., Zhang, W., ... Hu, M. (2022). First report of anthracnose caused by *Colletotrichum siamense* on avocado fruits in China. *Crop Protection*, *155*, 105922.

Li, P. L., Liu, D., Zheng, X. J., Chen, H. B., Gong, G. S., Zhang, M., & Wang, X. G. (2016). First report of *Colletotrichum gloeosporioides* causing anthracnose on *Bauhinia blakeana*. *Plant Disease*, *100*(10), 2165–2165.

Li, Q., Bu, J., Shu, J., Yu, Z., Tang, L., Huang, S., ... Hsiang, T. (2019). *Colletotrichum* species associated with mango in southern China. *Scientific reports*, *9*(1), 18891.

Liang, J., Li, G., Zhou, S., Zhao, M., & Cai, L. (2019). Myrothecium-like new species from turfgrasses and associated rhizosphere. *MycoKeys*, *51*, 29.

Liang, L., Li, S., Han, S., Qiao, T., Li, S., & Zhu, T. (2023). First report of *Colletotrichum endophyticum*, a causal agent of leaf spot of *Bauhinia blakeana*, in Southwest China. *Plant Disease*, *107*(3), 956.

Liew, E. C. Y., Laurence, M. H., Pearce, C. A., Shivas, R. G., Johnson, G. I., Tan, Y. P., ... Summerell, B. A. (2016). Review of *Fusarium* species isolated in association with mango malformation in Australia. *Australasian Plant Pathology*, *45*, 547–559.

Lim, L., Mohd, M. H., & Zakaria, L. (2019). Identification and pathogenicity of Diaporthe species associated with stem-end rot of mango (Mangifera indica L.). *European Journal of Plant Pathology*, *155*, 687-696.

Lim, T. K., & Sangchote, S. (2003). Diseases of durian. *Diseases of tropical fruit crops*, 241–251.

Lima, E. N., Oster, A. H., Bordallo, P. N., Araújo, A. A., Silva, D. E., & Lima, C. S. (2021). A novel lineage in the *Fusarium incarnatum-equiseti* species complex is one of the causal agents of *Fusarium* rot on melon fruits in northeast Brazil. *Plant Pathology*, *70*(1), 133–143.

Lima, N. B., de A. Batista, M. V., De Morais, M. A., Barbosa, M. A., Michereff, S. J., Hyde, K. D., & Câmara, M. P. (2013). Five *Colletotrichum* species are responsible for mango anthracnose in northeastern Brazil. *Fungal Diversity*, *61*, 75-88.

Liu, F., Cai, L., Crous, P. W., & Damm, U. (2014). The *Colletotrichum gigasporum* species complex. *Persoonia-Molecular Phylogeny and Evolution of Fungi*, *33*(1), 83-97.

Liu, F., Weir, B. S., Damm, U., Crous, P. W., Wang, Y., Liu, B., ... Cai, L. (2015). Unravelling *Colletotrichum* species associated with *Camellia*: employing ApMat and GS loci to resolve species in the *C. gloeosporioides* complex. *Persoonia-Molecular Phylogeny and Evolution of Fungi*, *35*(1), 63–86.

Liu, F., Ma, Z. Y., Hou, L. W., Diao, Y. Z., Wu, W. P., Damm, U., ... Cai, L. (2022). Updating species diversity of *Colletotrichum*, with a phylogenomic overview. *Studies in Mycology*, *101*(1), 1–56.

Liu, J. K., Hyde, K. D., Jones, E. G., Ariyawansa, H. A., Bhat, D. J., Boonmee, S., ... Camporesi, E. (2015). Fungal diversity notes 1–110: taxonomic and phylogenetic contributions to fungal species. *Fungal diversity*, *72*, 1–197.

Liu, L. P., Shu, J., Zhang, L., Hu, R., Chen, C. Q., Yang, L. N., ... Hsiang, T. (2017). First report of post-harvest anthracnose on mango (*Mangifera indica*) caused by *Colletotrichum siamense* in China. *Plant Disease*, *101*(5), 833–833.

Liu, X., Tibpromma, S., Zhang, F., Xu, J., Chethana, K. W. T., Karunarathna, S. C., & Mortimer, P. E. (2021). *Neopestalotiopsis cavernicola* sp. nov. from Gem Cave in Yunnan Province, China. *Phytotaxa*, *512*(1), 1–27.

Liu, Y., Tang, J., & Zhou, Y. (2021). Identification and description of a new pathogen causing flower dry rot on *Passiflora edulis* in China. *Plant Disease*, *105*(7), 1967–1975.

Lombard, L., Houbraken, J., Decock, C., Samson, R. A., Meijer, M., Réblová, M., ... & Crous, P. W. (2016). Generic hyper-diversity in Stachybotriaceae. *Persoonia-Molecular Phylogeny and Evolution of Fungi*, *36*(1), 156–246.

Lopes, L. H. R., Boiteux, L. S., Rossato, M., Aguiar, F. M., Fonseca, M. E., Oliveira, V. R., & Reis, A. (2021). Diversity of *Colletotrichum* species causing onion anthracnose in Brazil. *European Journal of Plant Pathology*, *159*, 339–357.

Luo, M., Guo, W., Zhao, M., Manawasinghe, I. S., Guarnaccia, V., Liu, J., ... You, C. (2022). Endophytic *Diaporthe* associated with *Morinda officinalis* in China. *Journal of Fungi*, *8*(8), 806.

Ma, X., Nontachaiyapoom, S., Jayawardena, R. S., Gentekaki, E., Zhou, S., Qian, Y., ... Kang, J. (2018). Endophytic *Colletotrichum* species from *Dendrobium* spp. in China and northern Thailand. *MycoKeys*, *43*, 23–57.

Ma, X. Y., Maharachchikumbura, S. S., Chen, B. W., Hyde, K. D., Mckenzie, E. H., Chomnunti, P., & Kang, J. C. (2019). Endophytic pestalotiod taxa in *Dendrobium* orchids. *Phytotaxa*, *419*(3), 268-286.

Maharachchikumbura, S. S., Guo, L. D., Chukeatirote, E., Bahkali, A. H., & Hyde, K. D. (2011). *Pestalotiopsis*—morphology, phylogeny, biochemistry and diversity. *Fungal diversity*, *50*, 167–187.

Maharachchikumbura, S. S., Guo, L. D., Cai, L., Chukeatirote, E., Wu, W. P., Sun, X., ... Hyde, K. D. (2012). A multi-locus backbone tree for *Pestalotiopsis*, with a polyphasic characterization of 14 new species. *Fungal Diversity*, *56*, 95–129.

Maharachchikumbura, S. S., Hyde, K. D., Groenewald, J. Z., Xu, J., & Crous, P. W. (2014). *Pestalotiopsis* revisited. *Studies in Mycology*, *79*(1), 121–186.

Maharachchikumbura, S. S., Larignon, P., Hyde, K. D., Al-Sadi, A. M., & Liu, Z. Y. (2016). Characterization of *Neopestalotiopsis*, *Pestalotiopsis* and *Truncatella* species associated with grapevine trunk diseases in France. *Phytopathologia Mediterranea*, 380–390.

Maharachchikumbura, S. S., Chen, Y., Ariyawansa, H. A., Hyde, K. D., Haelewaters, D., Perera, R. H., ... Stadler, M. (2021). Integrative approaches for species delimitation in Ascomycota. *Fungal Diversity*, *109*(1), 155–179.

Manamgoda, D. S., Udayanga, D., Cai, L., Chukeatirote, E., & Hyde, K. D. (2013). Endophytic *Colletotrichum* from tropical grasses with a new species *C. endophytica*. *Fungal Diversity*, *61*, 107–115.

Manawasinghe, I. S., Dissanayake, A. J., Li, X., Liu, M., Wanasinghe, D. N., Xu, J., ... Yan, J. (2019). High genetic diversity and species complexity of *Diaporthe* associated with grapevine dieback in China. *Frontiers in Microbiology*, *10*, 1936.

Mapook, A., Hyde, K. D., McKenzie, E. H., Jones, E. G., Bhat, D. J., Jeewon, R., ... Purahong, W. (2020). Taxonomic and phylogenetic contributions to fungi associated with the invasive weed *Chromolaena odorata* (Siam weed). *Fungal Diversity*, *101*, 1–175.

Marais, L. J. (2004). Avocado diseases of major importance worldwide and their management. In *Diseases of Fruits and Vegetables: Volume II: Diagnosis and Management* (pp. 1–36). Springer Netherlands.

Marques, M. W., Lima, N. B., de Morais, M. A., Michereff, S. J., Phillips, A. J., & Câmara, M. P. (2013). *Botryosphaeria*, *Neofusicoccum*, *Neoscytalidium* and *Pseudofusicoccum* species associated with mango in Brazil. *Fungal Diversity*, *61*, 195–208.

Maryani, N., Sandoval-Denis, M., Lombard, L., Crous, P. W., & Kema, G. H. J. (2019). New endemic *Fusarium* species hitch-hiking with pathogenic *Fusarium* strains causing Panama disease in small-holder banana plots in Indonesia. *Persoonia-Molecular Phylogeny and Evolution of Fungi*, *43*(1), 48–69.

Medeiros Araujo, M. B., Moreira, G. M., Nascimento, L. V., Nogueira, G. D. A., Nascimento, S. R. D. C., Pfenning, L. H., & Ambrósio, M. M. D. Q. (2021). *Fusarium* rot of melon is caused by several *Fusarium* species. *Plant Pathology*, *70*(3), 712–721.

Meeboon, J., Hidayat, I., & To-anun, C. (2007). An annotated list of cercosporoid fungi in Northern Thailand. *Journal of Agricultural Technology*, *3*(1), 51–63.

Meetum, P., Leksomboon, C., & Kanjanamaneesathian, M. (2015). First report of *Colletotrichum aenigma* and *C. siamense*, the causal agents of anthracnose disease of dragon fruit in Thailand. *Journal of Plant Pathology*, *97*(2).

Mendes, M. A. S. (1998). *Fungos em plantas no Brasil*. Serviço de Produção de Informação.

Miller, M. A., Pfeiffer, W., & Schwartz, T. (2011, July). The CIPRES science gateway: a community resource for phylogenetic analyses. In *Proceedings of the 2011 TeraGrid Conference: extreme digital discovery* (pp. 1–8).

Minh, B. Q., Schmidt, H. A., Chernomor, O., Schrempf, D., Woodhams, M. D., Von Haeseler, A., & Lanfear, R. (2020). IQ-TREE 2: new models and efficient methods for phylogenetic inference in the genomic era. *Molecular biology and evolution*, *37*(5), 1530–1534.

Mo, J., Zhao, G., Li, Q., Solangi, G. S., Tang, L., Guo, T., Huang, S., Hsiang, T. (2018). Identification and characterization of *Colletotrichum* species associated with mango anthracnose in Guangxi, China. *Plant disease*, *102*(7), 1283–1289.

Monkai, J., Hongsanan, S., Bhat, D. J., Dawoud, T. M., & Lumyong, S. (2023). Integrative taxonomy of novel *Diaporthe* species associated with medicinal plants in Thailand. *Journal of Fungi*, *9*(6), 603.

Montoya-Martínez, A. C., O'Donnell, K., Busman, M., Vaughan, M. M., McCormick, S. P., Santillán-Mendoza, R., ... Rodríguez-Alvarado, G. (2022). Weeds harbor *Fusarium* species that cause malformation disease of economically important trees in Western Mexico. *Plant Disease*, *106*(2), 612–622.

Mueller, G. M., & Schmit, J. P. (2007). Fungal biodiversity: what do we know? What can we predict?. *Biodiversity and conservation*, *16*, 1–5.

Mukherjee, S. K., & Litz, R. E. (2009). Introduction: botany and importance. In *The mango: Botany, production and uses* (pp. 1–18). Wallingford UK: CABI.

Najafiniya, M., de Farias, A. R. G., Armand, A., Jungkhun, N., & Jayawardena, R. (2024). Characterization of *Colletotrichum* species obtained from citrus in northern Thailand and introducing a new host record for *C. plurivorum*. *Plant Pathology*. *73*, 1349–1362

Nath, O., Fletcher, S. J., Hayward, A., Shaw, L. M., Masouleh, A. K., Furtado, A., ... Mitter, N. (2022). A haplotype resolved chromosomal level avocado genome allows analysis of novel avocado genes. *Horticulture Research*, *9*, uhac157.

Nattrass, R. M. (1933). A new species of *Heudersonula* (*H. toruloidea*) on deciduous trees in Egypt. *Transactions of the British Mycological Society*, *18*(3), 189–198.

Nelson, S. C. (2008). Mango anthracnose (*Colletotrichum gloeosporiodes*). *Plant Disease*, PD–48.

Netto, M. S., Assunção, I. P., Lima, G. S., Marques, M. W., Lima, W. G., Monteiro, J. H., ... Câmara, M. P. (2014). Species of *Lasiodiplodia* associated with papaya stem-end rot in Brazil. *Fungal Diversity*, *67*, 127–141.

Nguanhom, J., Cheewangkoon, R., Groenewald, J. Z., Braun, U., To-Anun, C., & Crous, P. W. (2015). Taxonomy and phylogeny of *Cercospora* spp. from northern Thailand. *Phytotaxa*, *233*(1), 27–48.

Nigar, Q., Cadle-Davidson, L., Gadoury, D. M., & Hassan, M. U. (2023). First report of *Colletotrichum fioriniae* causing grapevine anthracnose in New York. *Plant Disease*, *107*(1), 223.

Nirenberg, H. I., & O'Donnell, K. (1998). New *Fusarium* species and combinations within the *Gibberella fujikuroi* species complex. *Mycologia*, *90*(3), 434–458.

Noireung, P., Phoulivong, S., Liu, F., Cai, L., Mckenzie, E. H., Chukeatirote, E., ... Hyde, K. D. (2012). Novel species of *Colletotrichum* revealed by morphology and molecular analysis. *Cryptogamie, Mycologie*, *33*(3), 347–362.

Noor, N. M., & Zakaria, L. (2018). Identification and characterization of *Colletotrichum* spp. associated with chili anthracnose in peninsular Malaysia. *European Journal of Plant Pathology*, *151*, 961–973.

Norphanphoun, C., Jayawardena, R. S., Chen, Y., Wen, T. C., Meepol, W., & Hyde, K. D. (2019). Morphological and phylogenetic characterization of novel pestalotioid species associated with mangroves in Thailand. *Mycosphere*, *10*, 531–578.

Norphanphoun, C., Gentekaki, E., Hongsanan, S., Jayawardena, R., Senanayake, I. C., Manawasinghe, I. S., ... Hyde, K. D. (2022). *Diaporthe*: Formalizing the species-group concept. *Mycosphere*, *13*(1), 752–819.

Obregón, V. G., Meneguzzi, N. G., Ibañez, J. M., Lattar, T. E., & Kirschbaum, D. S. (2018). First report of *Neopestalotiopsis clavispora* causing root and crown rot on strawberry plants in Argentina. *Plant disease*, *102*(9), 1856–1856.

O'Donnell, K., Kistler, H. C., Cigelnik, E., & Ploetz, R. C. (1998). Multiple evolutionary origins of the fungus causing Panama disease of banana: concordant evidence from nuclear and mitochondrial gene genealogies. *Proceedings of the National Academy of Sciences*, *95*(5), 2044–2049.

O'Donnell, K., Nirenberg, H. I., Aoki, T., & Cigelnik, E. (2000). A multigene phylogeny of the Gibberella fujikuroi species complex: detection of additional phylogenetically distinct species. *Mycoscience*, *41*(1), 61–78.

O'Donnell, K., Sarver, B. A., Brandt, M., Chang, D. C., Noble-Wang, J., Park, B. J., ... Ward, T. J. (2007). Phylogenetic diversity and microsphere array-based genotyping of human pathogenic Fusaria, including isolates from the multistate contact lens-associated US keratitis outbreaks of 2005 and 2006. *Journal of clinical microbiology*, *45*(7), 2235–2248.

Pacheco-Esteva, M. C., Soto-Castro, D., Vásquez-López, A., Lima, N. B., & Tovar-Pedraza, J. M. (2022). First report of *Colletotrichum chrysophilum* causing papaya anthracnose in Mexico. *Plant Disease*, *106*(12), 3213.

Pakdeeniti, P., Tamakaew, N., Suwannarach, N., Senwanna, C., Haituk, S., Withee, P., ... Cheewangkoon, R. (2022). First report of *Colletotrichum theobromicola* causing centro anthracnose leaf spot in Thailand. *Plant Disease*, *106*(4), 1306.

Palou, L., Montesinos-Herrero, C., Tarazona, I., Besada, C., & Taberner, V. (2015). Incidence and etiology of postharvest fungal diseases of persimmon (*Diospyros kaki* Thunb. cv. Rojo Brillante) in Spain. *Plant Disease*, *99*(10), 1416–1425.

Pardo-De la Hoz, C. J., Calderón, C., Rincón, A. M., Cárdenas, M., Danies, G., López-Kleine, L., ... Jiménez, P. (2016). Species from the *Colletotrichum acutatum*, *Colletotrichum boninense* and *Colletotrichum gloeosporioides* species complexes associated with tree tomato and mango crops in Colombia. *Plant Pathology*, *65*(2), 227–237.

Pariona, A. (2018). *The top mango producing countries in the world Diakses melalui*. https://www. worldatlas. com/articles/the-top-mango-producing-countries-in-the-world.

Pappachan, A., Tabiyo, K., Rahul, K., & Trivedy, K. (2019). Isolation and molecular identification of potential bacterial antagonist for the management of brown leaf spot of mulberry. *Journal of Pharmacognosy and Phytochemistry*, *8*(3), 4098–4103.

Peng, C., Crous, P. W., Jiang, N., Fan, X. L., Liang, Y. M., & Tian, C. M. (2022). Diversity of Sporocadaceae (pestalotioid fungi) from Rosa in China. *Persoonia-Molecular Phylogeny and Evolution of Fungi*, *49*(1), 201–260.

Penzig, O. (1882). *Funghi agrumicoli: contribuzione allo studio dei funghi parassiti degli agrumi*. P. Fracanzani.

Pereira, D. S., Hilário, S., Gonçalves, M. F., & Phillips, A. J. (2023). *Diaporthe* species on palms: Molecular re-assessment and species boundaries delimitation in the *D. arecae* species complex. *Microorganisms*, *11*(11), 2717.

Pereira, D. S., & Phillips, A. J. L. (2024). *Diaporthe* species on palms–integrative taxonomic approach for species boundaries delimitation in the genus *Diaporthe*, with the description of *D. pygmaeae* sp. nov. *Studies in Mycology*, *109*(1), 487–594.

Perera, R. H., Hyde, K. D., Dissanayake, A. J., Jones, E. B. G., Liu, J. K., Wei, D., & Liu, Z. Y. (2018a). *Diaporthe collariana* sp. nov., with prominent collarettes associated with *Magnolia champaca* fruits in Thailand. *Studies in Fungi*, *3*(1), 141–151.

Perera, R. H., Hyde, K. D., Peršoh, D., Jones, E. B. G., Liu, J. K., & Liu, Z. Y. (2018b). Additions to wild seed and fruit fungi 1: The sexual morph of *Diaporthe rosae* on *Magnolia champaca* and *Senna siamea* fruits in Thailand. *Mycosphere*, *9*(2), 256–270.

Pérez-Jiménez, R. M. (2008). Significant avocado diseases caused by fungi and oomycetes. *European Journal of Plant Science Biotechnology*, *2*(1), 1–24.

Perkins, M. L., Joyce, D. C., & Coates, L. M. (2019). Possible contribution of impact injury at harvest to anthracnose expression in ripening avocado: A review. *Scientia Horticulturae*, *246*, 785–790.

Phengsintham, P., Chukeatirote, E., McKenzie, E. H., Moslem, M. A., Hyde, K. D., & Braun, U. (2012). Fourteen new records of cercosporoids from Thailand. *Maejo International Journal of Science and Technology*, *6*(1), 47.

Phengsintham, P., Braun, U., McKenzie, E. H. C., Chukeatirote, E., Cai, L., & Hyde, K. D. (2013). Monograph of cercosporoid fungi from Thailand. *Plant Pathology & Quarantine*, *3*(2), 67–138.

Phetphan, C., Supakitthanakorn, S., Phuakjaiphaeo, C., Pipattanapuckdee, A., Kunasakdakul, K., & Ruangwong, O. U. (2023). Biological and molecular characterization of *Lasiodiplodia theobromae* causing dieback disease of strawberry in Thailand. *Journal of Phytopathology*, *171*(7-8), 285–290.

Phillips, A. J. L., Alves, A., Abdollahzadeh, J., Slippers, B., Wingfield, M. J., Groenewald, J. Z., & Crous, P. W. (2013). The *Botryosphaeriaceae*: genera and species known from culture. *Studies in mycology*, *76*(1), 51–167.

Photita, W., Lumyong, S., Lumyong, P., McKenzie, E. H. C., & Hyde, K. D. (2004). Are some endophytes of *Musa acuminata* latent pathogens. *Fungal Diversity*, *16*, 131–140.

Photita, W., Taylor, P. W., Ford, R., Hyde, K. D., & Lumyong, S. (2005). Morphological and molecular characterization of *Colletotrichum* species from herbaceous plants in Thailand. *Fungal Diversity*, *18*(2), 117–133.

Phoulivong, S., Cai, L., Chen, H., McKenzie, E. H., Abdelsalam, K., Chukeatirote, E., & Hyde, K. D. (2010). *Colletotrichum gloeosporioides* is not a common pathogen on tropical fruits. *Fungal Diversity*, *44*, 33–43.

Phoulivong, S., Cai, L., Parinn, N., Chen, H., Abd-Elsalam, K. A., Chukeatirote, E., & Hyde, K. D. (2011). A new species of *Colletotrichum* from *Cordyline fruticosa* and Eugenia javanica causing anthracnose disease. *Mycotaxon*, *114*(1), 247–257.

Phoulivong, S., McKenzie, E. H. C., & Hyde, K. D. (2012). Cross infection of *Colletotrichum* species; a case study with tropical fruits. *Current Research in Environmental & Applied Mycology*, *2*(2), 99–111.

Pinaria, A. G., Liew, E. C. Y., & Burgess, L. W. (2010). *Fusarium* species associated with vanilla stem rot in Indonesia. *Australasian Plant Pathology*, *39*, 176–183.

Pinruan, U., Unartngam, J., Unartngam, A., Piyaboon, O., Sommai, S., & Khamsuntorn, P. (2022). *Paramyrothecium eichhorniae* sp. nov., causing leaf blight disease of water hyacinth from Thailand. *Mycobiology*, *50*(1), 12–19.

Pipattanapuckdee, A., Boonyakait, D., Tiyayon, C., Seehanam, P., & Ruangwong, O. U. (2019). Lasiodiplodia pseudotheobromae causes postharvest fruit rot of longan in Thailand. *Australasian Plant Disease Notes*, *14*, 1–7.

Ploetz, R. C. (2003). Diseases of mango. *Diseases of tropical fruit crops*, 327–363.

Pongpisutta, R., Keawmanee, P., Sanguansub, S., Dokchan, P., Bincader, S., Phuntumart, V., & Rattanakreetakul, C. (2023). Comprehensive investigation of die-back disease caused by *Fusarium* in durian. *Plants*, *12*(17), 3045.

Popluechai, S., Onto, S., & Eungwanichayapant, P. D. (2007). Relationships between some Thai cultivars of pineapple (*Ananas comosus*) revealed by RAPD analysis. *Songklanakarin Journal of Science & Technology*, *29*(6).

Pornsuriya, C., Chairin, T., Thaochan, N., & Sunpapao, A. (2020). Identification and characterization of *Neopestalotiopsis* fungi associated with a novel leaf fall disease of rubber trees (*Hevea brasiliensis*) in Thailand. *Journal of Phytopathology*, *168*, 416–427.

Pornsuriya, C., Thaochan, N., Chairin, T., & Sunpapao, A. (2023). Morphological and phylogenetic evidences reveal *Lasiodiplodia chonburiensis* and *L. theobromae* associated with leaf blight in *Hevea brasiliensis* in Southern Thailand. *Diversity*, *15*(9), 961.

Prasad, L., Javeria, S., Kumar, B., & Sharma, P. (2017). First report of anthracnose of elephant foot yam caused by *Colletotrichum siamense* in India. *New Diseae Report*, *36*(21), 2044–0588.

Prihastuti, H., Cai, L., Chen, H., McKenzie, E. H. C., & Hyde, K. D. (2009). Characterization of *Colletotrichum* species associated with coffee berries in northern Thailand. *Fungal Diversity*, *39*(1), 89–109.

Prusky, D., Kobiler, I., Miyara, I., & Alkan, N. (2009). Fruit diseases. In *The mango: botany, production and uses* (pp. 210-230). Wallingford UK: CABI.

Py, C.; Lacoevilhe, J.J.; Teisson, C. (1987). Pineapple, cultivation and uses. *Techniques Agricoles et Productions Tropicales*; *P. Maisonneuve Et Larose: Paris, France*, 205.

Qin, R., Li, Q., Huang, S., Chen, X., Mo, J., Guo, T., ... Yu, Z. (2023). Fruit rot on persimmon caused by *Neopestalotiopsis saprophytica* and *Neopestalotiopsis ellipsospora* in Guangxi, China. *Plant Disease*, *107*(8), 2531.

Qiu, J., Lu, Y., He, D., Lee, Y. W., Ji, F., Xu, J., & Shi, J. (2020). *Fusarium fujikuroi* species complex associated with rice, maize, and soybean from Jiangsu province, China: phylogenetic, pathogenic, and toxigenic analysis. *Plant Disease*, *104*(8), 2193–2201.

Quaedvlieg, W., Binder, M., Groenewald, J. Z., Summerell, B. A., Carnegie, A. J., Burgess, T. I., & Crous, P. W. (2014). Introducing the consolidated species concept to resolve species in the *Teratosphaeriaceae*. *Persoonia-Molecular Phylogeny and Evolution of Fungi*, *33*(1), 1–40.

Rakotoniriana, E. F., Scauflaire, J., Rabemanantsoa, C., Urveg-Ratsimamanga, S., Corbisier, A. M., Quetin-Leclercq, J., ... Munaut, F. (2013). *Colletotrichum gigasporum* sp. nov., a new species of *Colletotrichum* producing long straight conidia. *Mycological Progress*, *12*, 403–412.

Rapilly, F. (2001). Plant fungi: the first pathogenic agents recognized in the history of science. *Comptes Rendus de L'academie des sciences. Serie III, Sciences de la vie*, *324*(10), 893–898.

Rathnayaka, A. R., Chethana, K. W. T., Manawasinghe, I. S., Wijesinghe, S. N., de Silva, N. I., Tennakoon, D. S., ... Jones, E. B. G. (2023). *Lasiodiplodia*: Generic revision by providing molecular markers, geographical distribution and haplotype diversity. *Mycosphere*, *14*(1), 1254–1339.

Rattanakreetakul, C., Keawmanee, P., Bincader, S., Mongkolporn, O., Phuntumart, V., Chiba, S., & Pongpisutta, R. (2023). Two newly identified *Colletotrichum* species associated with mango anthracnose in central Thailand. *Plants*, *12*(5), 1130.

Rattanapanone, N., Chongsawat, C., & Chaiteep, S. (2000). Fresh-cut fruits in Thailand. *HortScience*, *35*(4), 543–546.

Ray, J. D., Burgess, T., & Lanoiselet, V. M. (2010). First record of *Neoscytalidium dimidiatum* and *N. novaehollandiae* on *Mangifera indica* and *N. dimidiatum* on *Ficus carica* in Australia. *Australasian Plant Disease Notes*, *5*(1), 48-50.

Razaghi, P., Raza, M., Han, S. L., Ma, Z. Y., Cai, L., Zhao, P., ... Liu, F. (2024). Sporocadaceae revisited. *Studies in Mycology*, *109*, 155.

R Core Team. (2014) R: a language and environment for statistical computing. Available from: http://www.r-project.org/ [Accessed 18th July 2023].

Reckhaus, P., & Adamou, I. (1987). *Hendersonula* dieback of mango in Niger. *Plant Disease*, *71*(11), 1045.

Reina-Pinto, J. J., & Yephremov, A. (2009). Surface lipids and plant defenses. *Plant Physiology and Biochemistry*, *47*(6), 540–549.

Ren, H., Wu, Y., Ahmed, T., Qi, X., & Li, B. (2021). Response of resistant and susceptible bayberry cultivars to infection of twig blight pathogen by histological observation and gibberellin related genes expression. *Pathogens*, *10*(4), 402.

Richardson MJ. 1990 – *An Annotated List of Seed-Borne Diseases*. Fourth Edition. International Seed Testing Association, Zurich.

Ristaino, J. B., Anderson, P. K., Bebber, D. P., Brauman, K. A., Cunniffe, N. J., Fedoroff, N. V., ... Wei, Q. (2021). The persistent threat of emerging plant disease pandemics to global food security. *Proceedings of the National Academy of Sciences*, *118*(23), e2022239118.

Ronquist, F., Teslenko, M., Van Der Mark, P., Ayres, D. L., Darling, A., Höhna, S., ... Huelsenbeck, J. P. (2012). MrBayes 3.2: efficient Bayesian phylogenetic inference and model choice across a large model space. *Systematic biology*, *61*(3), 539-542.

Rossman, A. Y., & Palm-Hernández, M. E. (2008). Systematics of plant pathogenic fungi: why it matters. *Plant disease*, *92*(10), 1376–1386.

Rozas, J., Ferrer-Mata, A., Sánchez-DelBarrio, J. C., Guirao-Rico, S., Librado, P., Ramos-Onsins, S. E., & Sánchez-Gracia, A. (2017). DnaSP 6: DNA sequence polymorphism analysis of large data sets. *Molecular biology and evolution*, *34*(12), 3299–3302.

RStudio Team. (2015) RStudio: integrated development for R. Boston, MA: RStudio, Inc. Available from: http://www.rstudio.com/ [Accessed 18th July 2023].

Sabahi, F., Mirtalebi, M., & Banihashemi, Z. (2022). *Paramyrothecium foliicola* causes crown dry rot of melon (*Cucumis melo*) in Iran. *Journal of Phytopathology*, *170*(9), 655–660.

Sahoo, B., Nedunchezhiyan, M., & Acharyya, P. (2016). Incidence of collar rot in elephant foot yam [*Amorphophallus paeoniifolius* (Dennst.) Nicolson] as influenced by varied nutrient regimes in east and south-eastern coastal plain zone of Odisha.

Sakalidis, M. L., Ray, J. D., Lanoiselet, V., Hardy, G. E. S., & Burgess, T. I. (2011). Pathogenic *Botryosphaeriaceae* associated with *Mangifera indica* in the Kimberley region of Western Australia. *European journal of plant pathology*, *130*, 379–391.

Samarakoon, M. C., Peršoh, D., Hyde, K. D., Bulgakov, T. S., Manawasinghe, I. S., Jayawardena, R. S., & Promputtha, I. (2018). *Colletotrichum acidae* sp. nov.

from northern Thailand and a new record of *C. dematium* on *Iris* sp. *Mycosphere*, *9*(3), 583–597.

Samarakoon, B. C., Samarakoon, M. C., Wanasinghe, D. N., Jayawardena, R. S., Hyde, K. D., & Chomnunti, P. (2024). Taxonomic and phylogenetic assessment of selected fungal pathogens associated with banana fruits in the local markets of northern Thailand. *European Journal of Plant Pathology*, 1–20.

Sandoval-Denis, M., & Crous, P. W. (2018). Removing chaos from confusion: assigning names to common human and animal pathogens in *Neocosmospora*. *Persoonia-Molecular Phylogeny and Evolution of Fungi*, *41*(1), 109–129.

Sandoval-Denis, M., Lombard, L., & Crous, P. W. (2019). Back to the roots: a reappraisal of *Neocosmospora*. *Persoonia-Molecular Phylogeny and Evolution of Fungi*, *43*(1), 90–185.

Sangchote, S., Jaisong, S., & Sangsiri, T. (2012, February). Fruit rot disease on durian, pathogen resistance to fungicide and control. In *Proceedings of the 10th National Plant Protection Conference, Kum Phukam Resident, Chiang Mai, Thailand*, 22–24.

Sangdit, P., Leksomboon, C., & Lertsrutaiyotin, R. (2014). Cultural, morphological and pathological characterization of *Colletotrichum falcatum* causing red rot disease of sugarcane in Thailand. *Agriculture and Natural Resources*, *48*(6), 880–892.

Sangpueak, R., Phansak, P., & Buensanteai, N. (2018). Morphological and molecular identification of *Colletotrichum* species associated with cassava anthracnose in Thailand. *Journal of Phytopathology*, *166*(2), 129–142.

Santos, A. C. D. S., Trindade, J. V. C., Lima, C. S., Barbosa, R. D. N., da Costa, A. F., Tiago, P. V., & de Oliveira, N. T. (2019). Morphology, phylogeny, and sexual stage of *Fusarium caatingaense* and *Fusarium pernambucanum*, new species of the *Fusarium incarnatum-equiseti* species complex associated with insects in Brazil. *Mycologia*, *111*(2), 244–259.

Santos, G. S., Mafia, R. G., Aguiar, A. M., Zarpelon, T. G., Damacena, M. B., Barros, A. F., & Ferreira, M. A. (2020). Stem rot of eucalyptus cuttings caused by *Neopestalotiopsis* spp. in Brazil. *Journal of Phytopathology*, *168*(6), 311–321.

Sapak, Z., Mohd Faisol Mahadeven, A. N., Nurul Farhana, M. H., Norsahira, S., & Mohd Zafri, A. W. (2021). A review of common diseases of pineapple: The causal pathogens, disease symptoms, and available control measures. *Food Res*, *5*(4), 1–14.

Sarris, A. (2001) The role of agriculture in economic development and poverty reduction: an empirical and conceptual foundation, World Bank Group. United States of America. https://policycommons.net/artifacts/1440181/the-role-of-agriculture-in-economic-development-and-poverty-reduction/2068020/ on 06 Feb 2024.

SAS Institute. (2016). *Statistical Analysis Software (SAS) User's Guide Version 9.4*. SAS Institute, Inc.

Savatin, D. V., Gramegna, G., Modesti, V., & Cervone, F. (2014). Wounding in the plant tissue: the defense of a dangerous passage. *Frontiers in plant science*, *5*, 470.

Schmit, J. P., & Mueller, G. M. (2007). An estimate of the lower limit of global fungal diversity. *Biodiversity and conservation*, *16*, 99–111.

Schroers, H. J., O'Donnell, K., Lamprecht, S. C., Kammeyer, P. L., Johnson, S., Sutton, D. A., ... Summerbell, R. C. (2009). Taxonomy and phylogeny of the *Fusarium dimerum* species group. *Mycologia*, *101*(1), 44–70.

Seifollahi, E., de Farias, A. R. G., Jayawardena, R. S., & Hyde, K. D. (2023). Taxonomic Advances from fungal flora associated with ferns and fern-like hosts in Northern Thailand. *Plants*, *12*(3), 683.

Senanayake, I. C., Crous, P. W., Groenewald, J. Z., Maharachchikumbura, S. S., Jeewon, R., Phillips, A. J., ... Hyde, K. D. (2017). Families of Diaporthales based on morphological and phylogenetic evidence. *Studies in Mycology*, *86*, 217–296.

Senanayake, I. C., Jeewon, R., Chomnunti, P., Wanasinghe, D. N., Norphanphoun, C., Karunarathna, A., ... Karunarathna, S. C. (2018). Taxonomic circumscription of Diaporthales based on multigene phylogeny and morphology. *Fungal Diversity*, *93*, 241–443.

Senanayake, I. C., Rathnayaka, A. R., Marasinghe, D. S., Calabon, M. S., Gentekaki, E., Lee, H. B., ... Xiang, M. M. (2020). Morphological approaches in studying fungi: Collection, examination, isolation, sporulation and preservation. *Mycosphere*, *11*(1), 2678–2754.

Senanayake, I. C., Pem, D., Rathnayaka, A. R., Wijesinghe, S. N., Tibpromma, S., Wanasinghe, D. N., ... Xie, N. (2022). Predicting global numbers of teleomorphic ascomycetes. *Fungal Diversity*, *114*(1), 237–278.

Serrato-Diaz, L. M., Rivera-Vargas, L. I., Goenaga, R., Verkley, G. J. M., & French-Monar, R. D. (2011). First report of a *Lasmenia* sp. causing rachis necrosis, flower abortion, fruit rot, and leaf spots on rambutan in Puerto Rico. *Plant Disease*, *95*(10), 1313–1313.

Shahriar, S. A., Nur-Shakirah, A. O., & Mohd, M. H. (2022). *Neopestalotiopsis clavispora* and *Pseudopestalotiopsis camelliae-sinensis* causing grey blight disease of tea (*Camellia sinensis*) in Malaysia. *European Journal of Plant Pathology*, 1–16.

Sharma, G., Kumar, N., Weir, B. S., Hyde, K. D., & Shenoy, B. D. (2013). The ApMat marker can resolve *Colletotrichum* species: a case study with Mangifera indica. *Fungal Diversity*, *61*, 117–138.

Sharma, G., & Shenoy, B. D. (2014). *Colletotrichum fructicola* and *C. siamense* are involved in chilli anthracnose in India. *Archives of Phytopathology and Plant protection*, *47*(10), 1179–1194.

Sharma, G., Gryzenhout, M., Hyde, K. D., Pinnaka, A. K., & Shenoy, B. D. (2015). First report of *Colletotrichum asianum* causing mango anthracnose in South Africa. *Plant Disease*, *99*(5), 725–725.

Sharma, G., Maymon, M., & Freeman, S. (2017). Epidemiology, pathology and identification of *Colletotrichum* including a novel species associated with avocado (*Persea americana*) anthracnose in Israel. *Scientific Reports*, *7*(1), 15839.

Sharma, G., Elazar, M., Maymon, M., Meshram, V., & Freeman, S. (2024). Identification and pathogenicity of *Lasiodiplodia* and *Neoscytalidium* species associated with mango (*Mangifera indica*) dieback disease in Israel. *Phytoparasitica*, *52*(1), 8.

Shenoy, B. D., Jeewon, R., Lam, W. H., Bhat, D. J., Than, P. P., Taylor, P. W., & Hyde, K. D. (2007). Morpho-molecular characterisation and epitypification of *Colletotrichum capsici* (*Glomerellaceae*, Sordariomycetes), the causative agent of anthracnose in chilli. *Fungal Diversity*, *27*(1), 197–211.

Shivas, R. G., Tan, Y. P., Edwards, J., Dinh, Q., Maxwell, A., Andjic, V., ... & Weir, B. S. (2016). *Colletotrichum* species in Australia. *Australasian Plant Pathology*, *45*, 447–464.

Si, Y. Z., Sun, J. W., Wan, Y., Chen, Y. N., He, J., Li, W. Z., ... Zhu, L. H. (2023). *Neofusicoccum cryptomeriae* sp. nov. and *N. parvum* cause stem basal canker of *Cryptomeria japonica* in China. *Journal of Fungi*, *9*(4), 404.

Silva Santos, S. D., Silva, A. A. D., Polonio, J. C., Polli, A. D., Orlandelli, R. C., Oliveira, J. A. D. S., ... Pamphile, J. A. (2022). Influence of plant growth-promoting endophytes *Colletotrichum siamense* and *Diaporthe masirevici* on tomato plants (*Lycopersicon esculentum* Mill.). *Mycology*, *13*(4), 257–270.

Silvestro, D., & Michalak, I. (2012). raxmlGUI: a graphical front-end for RAxML. *Organisms Diversity & Evolution*, *12*, 335–337.

Singh, R., Singh, A., Kumar, S., Upadhyaya, P. P., & Castañeda-Ruíz, R. F. (2014). Two new species of *Zasmidium* from northeastern Uttar Pradesh, India. *Nova Hedwigia*, *98*(1-2), 257–263.

Siriphanich, J. (2011). Durian (*Durio zibethinus* Merr.). In *Postharvest biology and technology of tropical and subtropical fruits* (pp. 80-116e). Woodhead Publishing.

Slippers, B., Johnson, G. I., Crous, P. W., Coutinho, T. A., Wingfield, B. D., & Wingfield, M. J. (2005). Phylogenetic and morphological re-evaluation of the *Botryosphaeria* species causing diseases of *Mangifera indica*. *Mycologia*, *97*(1), 99–110.

Soares, M. G., Alves, E., Silveira, A. L., Pereira, F. D., & Guimarães, S. S. (2021). *Colletotrichum siamense* is the main aetiological agent of anthracnose of avocado in south-eastern Brazil. *Plant Pathology*, *70*(1), 154–166.

Sodjinou, M. K., Assouma-Imorou, A., & Olounlade, A. O. (2022). Technical efficiency of pineapple production and challenges in Southern Benin. *African Journal of Agricultural. Research*, *18*, 522–534.

Somsri, S. (2011). Tropical and Subtropical Fruit Production in Thailand: GAP. In *International Symposium on Tropical and Subtropical Fruits 1024* (pp. 25–37).

Song, Y. U., Geng, K. U. N., Hyde, K. D., Zhao, W. S., Wei, J. G., Kang, J. C., & Wang, Y. (2013). Two new species of *Pestalotiopsis* from Southern China. *Phytotaxa*, *126*(1), 22–32.

Sowndhararajan, K., Marimuthu, S., & Manian, S. (2013). Biocontrol potential of phylloplane bacterium *Ochrobactrum anthropi* BMO-111 against blister blight disease of tea. *Journal of Applied Microbiology*, *114*(1), 209–218.

Stamatakis, A. (2006). RAxML-VI-HPC: maximum likelihood-based phylogenetic analyses with thousands of taxa and mixed models. *Bioinformatics*, *22*(21), 2688–2690.

Steyaert, R. L. (1949). Contribution à l'étude monographique de Pestalotia de Not. et Monochaetia Sacc.(*Truncatella* gen. nov. et *Pestalotiopsis* gen. nov.). *Bulletin du Jardin botanique de l'Etat, Bruxelles/Bulletin van den Rijksplantentuin, Brussel*, 285–347.

Su, Y. Y., Noireung, P., Liu, F., Hyde, K. D., Moslem, M. A., Bahkali, A. H., ... Cai, L. (2011). Epitypification of *Colletotrichum musae*, the causative agent of banana anthracnose. *Mycoscience*, *52*(6), 376–382.

Sun, W., Huang, S., Xia, J., Zhang, X., & Li, Z. (2021). Morphological and molecular identification of *Diaporthe* species in south-western China, with description of eight new species. *MycoKeys*, *77*, 65.

Sun, J. E., Meng, C. R., Phillips, A. J. L., & Wang, Y. (2022). Two new *Botryosphaeria* (*Botryosphaeriales, Botryosphaeriaceae*) species in China. *MycoKeys 94*: 1–16.

Sunpapao, A., Suwannarach, N., Kumla, J., Dumhai, R., Riangwong, K., Sanguansub, S., ... Arikit, S. (2022). Morphological and molecular identification of plant pathogenic fungi associated with dirty panicle disease in coconuts (*Cocos nucifera*) in Thailand. *Journal of Fungi*, *8*(4), 335.

Sutton, B. C. (1980). The Coelomycetes. Commonwealth Mycological Institute. *Kew, Srrey, England*, *643*.

Sutton, B. C., & Dyko, B. J. (1989). Revision of *Hendersonula*. *Mycological Research*, *93*(4), 466–488.

Suwannarach, N., Khuna, S., Kumla, J., Tanruean, K., & Lumyong, S. (2020). First report of *Lasiodiplodia theobromae* causing fruit rot on melon (*Cucumis melo*) in Thailand. *Plant Disease*, *104*(1), 280–280.

Suwannarach, N., Khuna, S., Kumla, J., Thitla, T., Hongsanan, S., Nuangmek, W., & Lumyong, S. (2023). *Fusarium endophyticum* sp. nov.(Nectriaceae, Hypocreales), a new endophytic fungus from northern Thailand. *Phytotaxa*, *606*(1), 43–53.

Suwannarat, S., Steinkellner, S., Songkumarn, P., & Sangchote, S. (2017). Diversity of *Colletotrichum* spp. isolated from chili pepper fruit exhibiting symptoms of anthracnose in Thailand. *Mycological Progress*, *16*, 677–686.

Swofford, D. L. (1993). PAUP, phylogenetic analysis using parsimony. *version 3.1. Computer program distributed by the Illinois Natural History Survey*.

Swofford, D. L. (2002) PAUP*. Phylogenetic Analysis Using Parsimony (* and Other Methods). Ver. 4.0b10. *Sinauer Associates*.

Swofford, D. L., & Sullivan, J. (2003). Phylogeny inference based on parsimony and other methods using PAUP*. *The phylogenetic handbook: a practical approach to DNA and protein phylogeny*, *7*, 160–206.

Talhinhas, P., & Baroncelli, R. (2021). *Colletotrichum* species and complexes: geographic distribution, host range and conservation status. *Fungal Diversity*, *110*(1), 109–198.

Talhinhas, P., & Baroncelli, R. (2023). Hosts of *Colletotrichum*. *Mycosphere*, *14*, 158–261.

Tamakaew, N., Karunarathna, A., Pakdeeniti, P., Withee, P., Senwanna, C., Haituk, S., & Cheewangkoon, R. (2022). New species of Cercosporoid on mango in Thailand. *Chiang Mai J. Sci*, *49*, 684–1692.

Tan, Y. P., & Shivas, R. G. (2022). Nomenclatural novelties. *Index of Australian Fungi 1*, 1–18.

Teh, B. T., Lim, K., Yong, C. H., Ng, C. C. Y., Rao, S. R., Rajasegaran, V., ... Tan, P. (2017). The draft genome of tropical fruit durian (*Durio zibethinus*). *Nature genetics*, *49*(11), 1633–1641.

Templeton, M. D., Rikkerink, E. H., Solon, S. L., & Crowhurst, R. N. (1992). Cloning and molecular characterization of the glyceraldehyde-3-phosphate dehydrogenase-encoding gene and cDNA from the plant pathogenic fungus *Glomerella cingulata*. *Gene*, *122*(1), 225–230.

Teodoro, N. G. (1937).*"An enumeration of Philippine fungi.". Tech. Bull. Philipp. Dep. Agric.*, 585.

Than, P. P., Jeewon, R., Hyde, K. D., Pongsupasamit, S., Mongkolporn, O., & Taylor, P. W. J. (2008a). Characterization and pathogenicity of *Colletotrichum* species associated with anthracnose on chilli (*Capsicum* spp.) in Thailand. *Plant pathology*, *57*(3), 562–572.

Than, P. P., Prihastuti, H., Phoulivong, S., Taylor, P. W., & Hyde, K. D. (2008b). Chilli anthracnose disease caused by *Colletotrichum* species. *Journal of Zhejiang University Science B*, *9*, 764–778.

Thammasiri, K. (2014, February). Current status of orchid production in Thailand. In *II International Orchid Symposium 1078* (pp. 25–33).

Tibpromma, S., Hyde, K. D., Bhat, J. D., Mortimer, P. E., Xu, J., Promputtha, I., ... Karunarathna, S. C. (2018). Identification of endophytic fungi from leaves of Pandanaceae based on their morphotypes and DNA sequence data from southern Thailand. *MycoKeys*, (33), 25.

To-Anun, C., Hidayat, I., & Meeboon, J. (2011). Genus *Cercospora* in Thailand: taxonomy and phylogeny (with a dichotomous key to species). *Plant Pathology & Quarantine*, *1*(1), 11–87.

Tovar-Pedraza, J. M., Mora-Aguilera, J. A., Nava-Diaz, C., Lima, N. B., Michereff, S. J., Sandoval-Islas, J. S., ... Leyva-Mir, S. G. (2020). Distribution and pathogenicity of *Colletotrichum* species associated with mango anthracnose in Mexico. *Plant disease*, *104*(1), 137–146.

Trakunyingcharoen, T., Cheewangkoon, R., & To-anun, C. (2013). Phylogeny and pathogenicity of fungal species in the family *Botryosphaeriaceae* associated with mango (*Mangifera indica*) in Thailand. *Journal of Agricultural Technology*, *9*(6):1535–1543.

Trakunyingcharoen, T., Cheewangkoon, R., To-Anun, C., Crous, P. W., Van Niekerk, J. M., & Lombard, L. (2014). *Botryosphaeriaceae* associated with diseases of mango (*Mangifera indica*). *Australasian Plant Pathology*, *43*, 425–438.

Trakunyingcharoen, T., Cheewangkoon, R., & To-Anun, C. (2015a). Phylogenetic study of the *Botryosphaeriaceae* species associated with avocado and para rubber in Thailand. *Chiang Mai Journal of Science*, *42*(1), 104–116.

Trakunyingcharoen, T., Lombard, L., Groenewald, J. Z., Cheewangkoon, R., To-Anun, C., & Crous, P. W. (2015b). Caulicolous Botryosphaeriales from Thailand. *Persoonia-Molecular Phylogeny and Evolution of Fungi*, *34*(1), 87–99.

Trkulja, V., Perviz, M., Mitrović, P., Vojvodić, M., & Bulajić, A. (2020). Species of the genus *Alternaria* pathogens of vegetable and spice plants from the family Apiaceae. *Biljni lekar*, *48*(6), 586-609.

Tukey, J.W. (1951). Components in regression. *Biometrics 7*, 33–69.

Udayanga, D., Liu, X., McKenzie, E. H., Chukeatirote, E., Bahkali, A. H., & Hyde, K. D. (2011). The genus *Phomopsis*: biology, applications, species concepts and names of common phytopathogens. *Fungal diversity*,*50*, 189–225.

Udayanga, D., Liua, X., Mckenzie, E. H., Chukeatirote, E., & Hyde, K. D. (2012). Multi-locus phylogeny reveals three new species of *Diaporthe* from Thailand. *Cryptogamie, Mycologie*, *33*(3), 295–309.

Udayanga, D., Manamgoda, D. S., Liu, X., Chukeatirote, E., & Hyde, K. D. (2013). What are the common anthracnose pathogens of tropical fruits?. *Fungal Diversity*, *61*, 165–179.

Udayanga, D., Castlebury, L. A., Rossman, A. Y., & Hyde, K. D. (2014). Species limits in *Diaporthe*: molecular re-assessment of *D. citri*, *D. cytosporella*, *D. foeniculina* and *D. rudis*. *Persoonia-Molecular Phylogeny and Evolution of Fungi*, *32*(1), 83–101.

Udayanga, D., Miriyagalla, S. D., Herath, I. S., Castlebury, L. A., Ferdinandez, H. S., & Manamgoda, D. S. (2020). Foliar pathogenic fungi: Growing threats to global food security and ecosystem health. *Ceylon Journal of Science 49 (Special Issue)*, 337–353.

Umi, H. N., Tricahya, R. A., & Farid, A. M. (2020, March). Performance analysis of drip and sprinkler irrigation on pineapple cultivation. *IOP Conference Series: Earth and Environmental Science*, *451*(1), 012034.

Vásquez-López, A., Palacios-Torres, R. E., Camacho-Tapia, M., Granados-Echegoyen, C., Lima, N. B., Vera-Reyes, I., ... Leyva-Mir, S. G. (2019). *Colletotrichum brevisporum* and *C. musicola* causing leaf anthracnose of taro (*Colocasia esculenta*) in Mexico. *Plant Disease*, *103*(11), 2963–2963.

Videira, S. I. R., Groenewald, J. Z., Nakashima, C., Braun, U., Barreto, R. W., de Wit, P. J., & Crous, P. W. (2017). *Mycosphaerellaceae*–chaos or clarity?. *Studies in mycology*, *87*, 257-421.

Vieira, W. A., Michereff, S. J., de Morais, M. A., Hyde, K. D., & Câmara, M. P. (2014). Endophytic species of *Colletotrichum* associated with mango in northeastern Brazil. *Fungal diversity*, *67*, 181–202.

Vilgalys, R., & Hester, M. (1990). Rapid genetic identification and mapping of enzymatically amplified ribosomal DNA from several *Cryptococcus* species. *Journal of bacteriology*, *172*(8), 4238-4246.

Vithanage, I. K., Yakandawala, D. M. D., Maharachchikumbura, S. S. N., Jayasinghe, L., & Adikaram, N. K. B. (2021). *Colletotrichum* species causing anthracnose disease in *A. andraeanum*, manifested as spathe rot also in addition to spadix rot and leaf spot. *European Journal of Plant Pathology*, *161*, 837–846.

Vujanovic, V., St-Arnaud, M., & Neumann, P. J. (2000). Susceptibility of cones and seeds to fungal infection in a pine (*Pinus* spp.) collection. *Forest Pathology*, *30*(6), 305–320.

Wanasinghe, D. N., Phukhamsakda, C., Hyde, K. D., Jeewon, R., Lee, H. B., Gareth Jones, E. B., ... Karunarathna, S. C. (2018). Fungal diversity notes 709–839: taxonomic and phylogenetic contributions to fungal taxa with an emphasis on fungi on Rosaceae. *Fungal diversity*, *89*, 1–236.

Wannakrairoj, S. (2007, January). Status of ornamental plants in Thailand. In *International Workshop on Ornamental Plants 788* (pp. 29–36).

Wang, H., Jiang, F., Lan, Y., & Han, X. (2021). First record of *Paramyrothecium roridum* causing leaf spot on *Physostegia virginiana* in China. *Plant Disease*, *105*(2), 505.

Wang, M. M., Chen, Q., Diao, Y. Z., Duan, W. J., & Cai, L. (2019). *Fusarium incarnatum-equiseti* complex from China. *Persoonia-Molecular Phylogeny and Evolution of Fungi*, *43*(1), 70–89.

Wang, Q. H., Fan, K., Li, D. W., Han, C. M., Qu, Y. Y., Qi, Y. K., & Wu, X. Q. (2020). Identification, virulence and fungicide sensitivity of *Colletotrichum gloeosporioides* ss responsible for walnut anthracnose disease in China. *Plant disease*, *104*(5), 1358–1368.

Wang, X., Zhang, W., Peng, J., Manawasinghe, I. S., Wu, L., Li, Y., ... Yan, J. (2024). Lifestyle changes in *Botryosphaeriaceae* as evidenced by ancestral genome expansion and horizontal gene transfer. *Fungal Diversity*, *125*(1), 221-241.

Wang, Y., Xiong, F., Lu, Q., Hao, X., Zheng, M., Wang, L., ... Yang, Y. (2019). Diversity of Pestalotiopsis-like species causing gray blight disease of tea plants (*Camellia sinensis*) in China, including two novel *Pestalotiopsis* species, and analysis of their pathogenicity. *Plant Disease*, *103*(10), 2548–2558.

Wang, Y., Jia, W., Zhu, X., Mi, Z., Wang, E., Chang, G., ... He, S. (2023). First report of *Colletotrichum aenigma* causing anthracnose of tree peony in China. *Plant Disease*, *107*(4), 1242.

Wei, S., Yuan, H., Lei, T., & Chen, S. (2023). First Report of Anthracnose Caused by *Colletotrichum kahawae* and *Colletotrichum horii* on Tea-Oil Tree in China. *Plant Disease*, *107*(6), 1944.

Weir, B. S., Johnston, P. R., & Damm, U. (2012). The *Colletotrichum gloeosporioides* species complex. *Studies in mycology*, *73*, 115–180.

Wharton, P. S., & Diéguez-Uribeondo, J. (2004, June). The biology of *Colletotrichum* acutatum. In *Anales del jardín botánico de Madrid*, *61*, 3–22.

White, T. J. (1990). Amplification and direct sequencing of fungal ribosomal RNA genes for phylogenetics. *PCR Protocols: A guide to methods and applications*, 315–322.

Wijayawardene, N. N., Mckenzie, E. H., Chukeatirote, E., Wang, Y., & Hyde, K. D. (2012). Coelomycetes. *Cryptogamie, Mycologie*, *33*(3), 215–244.

Wijayawardene, N. N., Hyde, K. D., Al-Ani, L. K. T., Tedersoo, L., Haelewaters, D., Rajeshkumar, K. C., ... Castañeda-Ruiz, R. F. (2020). Outline of Fungi and fungus-like taxa. *Mycosphere Online: Journal of Fungal Biology*, *11*(1), 1060–1456.

Williams, P. A., Crespo, O., Atkinson, C. J., & Essegbey, G. O. (2017). Impact of climate variability on pineapple production in Ghana. *Agriculture & Food Security*, *6*, 1–14.

Wikee, S., Lombard, L., Crous, P. W., Nakashima, C., Motohashi, K., Chukeatirote, E., ... Hyde, K. D. (2013). *Phyllosticta capitalensis*, a widespread endophyte of plants. *Fungal Diversity*, *60*, 91–105.

Withee, P., Haituk, S., Senwanna, C., Karunarathna, A., Tamakaew, N., Pakdeeniti, P., ... Cheewangkoon, R. (2022). Identification and pathogenicity of *Paramyrothecium* species associated with leaf spot disease in northern Thailand. *Plants*, *11*(11), 1445.

Worldatlas, (2019). *The top mango producing countries in the world*. https://www.worldatlas.com/articles/thetop-mango-producing-countries-in-the-world.html

Woudenberg, J. H. C., Aveskamp, M. M., De Gruyter, J., Spiers, A. G., & Crous, P. W. (2009). Multiple *Didymella* teleomorphs are linked to the *Phoma clematidina* morphotype. *Persoonia-Molecular Phylogeny and Evolution of Fungi*, *22*(1), 56-62.

Woudenberg, J. H. C., Truter, M., Groenewald, J. Z., & Crous, P. W. (2014). Large-spored *Alternaria* pathogens in section Porri disentangled. *Studies in Mycology*, *79*, 1–47.

Wrona, C. J., Mohankumar, V., Schoeman, M. H., Tan, Y. P., Shivas, R. G., Jeff-Ego, O. S., & Akinsanmi, O. A. (2020). *Phomopsis* husk rot of macadamia in Australia and South Africa caused by novel *Diaporthe* species. *Plant Pathology*, *69*(5), 911–921.

Wu, C., Wang, Y., & Yang, Y. (2022). *Pestalotiopsis* diversity: Species, dispositions, secondary metabolites, and bioactivities. *Molecules*, *27*(22), 8088.

Wu, C. J., Chen, H. K., & Ni, H. F. (2020). Identification and characterization of *Colletotrichum* species associated with mango anthracnose in Taiwan. *European journal of plant pathology*, *157*, 1–15.

Wu, C. J., Lin, M. C., & Ni, H. F. (2023). *Colletotrichum* species causing anthracnose disease on avocado fruit in Taiwan. *European Journal of Plant Pathology*, *165*(4), 629–647.

Wu, C. J., Chen, J. L., Tzean, S. S., & Ni, H. F. (2024). *Pseudoplagiostoma perseae* sp. nov. causes leaf spot disease on avocado leaves in Taiwan. *European Journal of Plant Pathology*, 1–13.

Wu, W. W., Zhu, M. F., Liang, Y., Bai, X. H., Lu, Y., Xi, J. G., ... Yi, K. X. (2021). First report of *Paramyrothecium breviseta* causing leaf spot disease of *Coffea canephora* in China. *Plant Disease*, *105*(11), 3752.

Xia, J. W., Sandoval-Denis, M., Crous, P. W., Zhang, X. G., & Lombard, L. (2019). Numbers to names-restyling the *Fusarium incarnatum-equiseti* species complex. *Persoonia-Molecular Phylogeny and Evolution of Fungi*, *43*(1), 186–221.

Yang, Q., Fan, X. L., Guarnaccia, V., & Tian, C. M. (2018). High diversity of *Diaporthe* species associated with dieback diseases in China, with twelve new species described. *MycoKeys*, *39*, 97.

Yang, Q., Zeng, X. Y., Yuan, J., Zhang, Q., He, Y. K., & Wang, Y. (2021). Two new species of *Neopestalotiopsis* from southern China. *Biodiversity Data Journal*, *9*.

Yao-ling, L., Rong-hua, D., Ni, C., Juan, P., & Jie, P. (2013). Review of konjac glucomannan: isolation, structure, chain conformation and bioactivities. *Organization (WHO)*, *4*(8).

Yoshida, K., Burbano, H. A., Krause, J., Thines, M., Weigel, D., & Kamoun, S. (2014). Mining herbaria for plant pathogen genomes: back to the future. *PLoS pathogens*, *10*(4), e1004028.

Yu, Z., Jiang, X., Zheng, H., Zhang, H., & Qiao, M. (2022). Fourteen new species of foliar *Colletotrichum* associated with the invasive plant *Ageratina adenophora* and surrounding crops. *Journal of fungi*, *8*(2), 185.

Yu, J., Li, Q., Zhang, W., Bai, P., Huo, J., Liu, Y., & Gao, W. (2023). First report of *Colletotrichum truncatum* causing anthracnose of green foxtail (*Setaria viridis*) in China. *Plant Disease*, *107*(3), 939.

Zakaria, L. (2021). Diversity of *Colletotrichum* species associated with anthracnose disease in tropical fruit crops—A review. *Agriculture*, *11*(4), 297.

Zakaria, L. (2022). Fungal and oomycete diseases of minor tropical fruit crops. *Horticulturae*, *8*(4), 323.

Zhang, H., Zeng, Y., Wei, T. P., Jiang, Y. L., & Zeng, X. Y. (2023). Endophytic *Fusarium* and allied fungi from *Rosa roxburghii* in China. *Mycosphere*, *14*(1), 2092–2207.

Zhang, N., Yuan, S. L., Zhu, Y. N., Wang, B. Y., Xu, Y. Y., Hu, T. L., & Yang, W. X. (2023). First report of anthracnose on chili Pepper caused by *Colletotrichum sojae* in Hebei Province, China. *Plant Disease*, *107*(5), 1633.

Zhang, Q., Nizamani, M. M., Feng, Y., Yang, Y. Q., Jayawardena, R. S., Hyde, K. D., Wang, Y., & Li, C. (2023). Genome-scale and multi-gene phylogenetic analyses of *Colletotrichum* spp. host preference and associated with medicinal plants. *Mycosphere 14*(2), 1–106.

Zhang, W., Groenewald, J. Z., Lombard, L., Schumacher, R. K., Phillips, A. J. L., & Crous, P. W. (2021). Evaluating species in Botryosphaeriales. *Persoonia-Molecular Phylogeny and Evolution of Fungi*, *46*(1), 63–115.

Zhang, Y. X., Chen, J., Manawasinghe, I. S., Lin, Y. H., Jayawardena, R. S., Mckenzie, E. H. C., ... Xiang, M. M. (2023). Identification and characterization of *Colletotrichum* species associated with ornamental plants in Southern China. *Mycosphere*, *14*, 262–302.

Zhang, Z. Y., Pan, H., Tao, G., Li, X., Han, Y. F., Feng, Y., ... Ding, C. Y. (2024). Culturable Mycobiota from Guizhou Wildlife Park in China. *Mycosphere*, *15*(1), 654–763.

Zhu, Z. X., Dong, Z. X., Mo, R. L., Zhang, C., Zuo, Y. Y., Yu, C., & Hu, X. M. (2023). First report of *Colletotrichum aenigma* causing anthracnose on mulberry leaves in China. *Plant Disease*, *107*(2), 571.

Zimowska, B. E. A. T. A. (2008). Biodiversity of fungi colonizing and damaging selected parts of motherwort (*Leonurus cardiaca* L.). *Herba Pol*, *54*(2), 30–40.

Zou, W. X., Meng, J. C., Lu, H., Chen, G. X., Shi, G. X., Zhang, T. Y., & Tan, R. X. (2000). Metabolites of *Colletotrichum gloeosporioides*, an endophytic fungus in *Artemisia mongolica*. *Journal of natural products*, *63*(11), 1529–1530.

APPENDIX A

IDENTIFICATION AND CHARACTERIZATION OF *Colletotrichum* SPECIES ASSOCIATED WITH DURIAN FRUIT IN NORTHERN THAILAND

Table A1 Taxa with their respective GenBank accession numbers used in the phylogenetic analyses

Taxa	**Strains**	**GenBank accession numbers**				
		ITS	***GAPDH***	***CHS-1***	***ACT***	***TUB***
Colletotrichum Acidae	MFLUCC 17-2659*	MG996505	MH003691	MH003694	MH003697	MH003700
C. acidae	MFLU 18-0233	MG996506	MH003692	MH003695	MH003698	MH003701
C. aenigma	ICMP 18608*	JX010244	JX010044	JX009774	JX009443	JX010389
C. aeschynomenes	ICMP 17673*, ATCC 201874	JX010176	JX009930	JX009799	JX009483	JX010392
C. alatae	CBS 304.67*, ICMP 17919	JX010190	JX009990	JX009837	JX009471	JX010383
C. alienum	ICMP 12071*	JX010251	JX010028	JX009882	JX009572	JX010411
C. aotearoa	ICMP 18537*	JX010205	JX010005	JX009853	–	JX010420

Table A1 (continued)

Taxa	Strains	GenBank accession numbers				
		ITS	***GAPDH***	***CHS-1***	***ACT***	***TUB***
C. artocarpicola	MFLUCC 18-1167*	MN415991	MN435568	MN435569	MN435570	MN435567
C. arxii	CBS 132551*	KF687716	KF687843	KF687780	KF687802	KF687881
C. arxii	CBS 169.59, IMI 304050, IMI 309371	KF687717	KF687824	KF687781	KF687784	KF687868
C. asianum	ICMP 18580*	JX010196	JX010053	JX009867	JX009584	JX010406
C. analogum	YMF1.0694	OK030860	OK513663	OK513559	OK513599	OK513629
C. camelliae	3* LC1364*	KJ955081	KJ954782	MZ799255	KJ954363	KJ955230
C. cangyuanensis	YMF1.0500	OK030864	OK513667	OK513563	OK513603	OK513633
C. changpingense	1* CGMCC 3.17582*, SA0016, MFLUCC 15-0022	KP683152	KP852469	KP852449	KP683093	KP852490
C. chiangmaiense	MFLUCC 18-0945*	MW346499	MW548592	MW623653	MW655578	–
C. chrysophilum	URM 7368, CMM4268*	KX094252	KX094183	KX094083	KX093982	KX094285
C. cigarro	ICMP 18539*	JX010230	JX009966	JX009800	JX009523	JX010434

Table A1 (continued)

Taxa	Strains	GenBank accession numbers				
		ITS	***GAPDH***	***CHS-1***	***ACT***	***TUB***
C. clidemiae	ICMP 18658*	JX010265	JX009989	JX009877	JX009537	JX010438
C. cobbittiense	BRIP 66219*	MH087016	MH094133	MH094135	MH094134	MH094137
C. conoides	CGMCC 3.17615, CAUG17, LC6226*	KP890168	KP890162	KP890156	KP890144	KP890174
C. cordylinicola	MFLUCC 090551*, ICMP 18579	JX010226	JX009975	JX009864	HM470234	JX010440
C. crousii	LC13858, MH0588*	MZ595876	MZ664059	MZ799281	MZ664174	MZ673995
C. crousii	LC13860, MH0592	MZ595878	MZ664061	MZ799282	MZ664176	MZ673997
C. curcumae	IMI 288937*	GU227893	GU228285	GU228383	GU227991	GU228187
C. dimorphum	YMF1.0730 9*	OK030867	OK513670	OK513566	OK513606	OK513636
C. dracaenigenum	MFLUCC 19-0430*	MN921250	MT215577	MT215575	MT313686	–
C. durionigenum	**MFLUCC 22-0111***	**OP740244**	**OP744505**	**OP744504**	**OP744503**	**OP744506**
C. endophytica	MFLUCC 13-0418, LC0324*	KC633854	KC832854	MZ799261	KF306258	MZ673954
C. fici-septicae	MFLU 19- 2770*	MW114367	MW183774	MW177701	MW151585	–

Table A1 (continued)

Taxa	Strains	GenBank accession numbers				
		ITS	***GAPDH***	***CHS-1***	***ACT***	***TUB***
C. fructicola	ICMP 18581*, CBS 130416	JX010165	JX010033	JX009866	FJ907426	JX010405
C. fructivorum	CBS 133125*	JX145145	MZ664047	MZ799259	MZ664126	JX145196
C. fusiforme	MFLU 13- 0291*	KT290266	KT290255	KT290253	KT290251	KT290256
C. gigasporum	CBS 133266, MUCL 44947*	KF687715	KF687822	KF687761	–	KF687866
C. gigasporum	CBS 101881	KF687736	KF687841	KF687777	KF687797	KF687886
C. gigasporum	CBS 181.52	KF687734	KF687838	KF687775	KF687799	KF687885
C. gigasporum	CBS 109355	KF687729	KF687827	KF687774	KF687798	KF687870
C. gigasporum	CBS 125385	KF687732	KF687835	KF687764	KF687787	KF687872
C. gigasporum	CBS 125387	KF687733	KF687834	KF687765	KF687788	KF687873
C. gigasporum	CBS 125730	KF687735	KF687840	KF687770	KF687793	KF687878
C. gigasporum	CBS 125476	KF687728	KF687833	KF687767	KF687790	KF687875
C. gigasporum	CBS 124947	KF687731	KF687828	KF687763	KF687786	KF687871
C. gigasporum	CBS 125731	KF687727	KF687837	KF687771	KF687794	KF687879

Table A1 (continued)

Taxa	Strains	GenBank accession numbers				
		ITS	***GAPDH***	***CHS-1***	***ACT***	***TUB***
C. gigasporum	CBS 132884	KF687730	KF687830	KF687773	KF687796	–
C. gigasporum	CBS 125475	KF687723	KF687836	KF687766	KF687789	KF687874
C. gigasporum	CBS 132881	KF687725	KF687829	KF687772	KF687795	KF687880
C. gigasporum	CBS 159.75	KF687726	KF687839	KF687776	KF687783	KF687884
C. gigasporum	**MFLUCC 22-0108**	**OP740245**	**OP744509**	**OP744508**	**OP744507**	**OP744510**
C. gloeosporioides	IMI 356878*	JQ005152	JQ005239	JQ005326	JQ005500	JQ005587
C. gracile	YMF1.06939*	OK030868	OK513671	OK513567	OK513607	OK513637
C. grevilleae	CPC 15481*	KC297078	KC297010	KC296987	KC296941	KC297102
C. grossum	CGMCC3.1 7614, CAUG7, LC6227*	KP890165	KP890159	KP890153	KP890141	KP890171
C. hebeiense	MFLUCC 13-0726*	KF156863	KF377495	KF289008	KF377532	KF288975
C. hederiicola	MFLU 15-0689*	MN631384	–	MN635794	MN635795	–
C. helleniense	CBS 142418, CPC 26844*	KY856446	KY856270	KY856186	KY856019	KY856528
C. henanense	LC3030, CGMCC 3.17354*	KJ955109	KJ954810	MZ799256	KM023257	KJ955257

Table A1 (continued)

Taxa	Strains	GenBank accession numbers				
		ITS	***GAPDH***	***CHS-1***	***ACT***	***TUB***
C. horii	NBRC 7478*, ICMP 10492, MTCC 10841	GQ329690	GQ329681	JX009752	JX009438	JX010450
C. hystricis	CBS 142411, CPC 28153*	KY856450	KY856274	KY856190	KY856023	KY856532
C. jiangxiense	CGMCC 3.17363*	KJ955201	KJ954902	–	KJ954471	KJ955348
C. jishouense	GMBC 0209*, GZU_HJ2_G3	MH482929	MH681658	–	MH708135	MH727473
C. jishouense	GZU_HJ2_G2	MH482931	MH681657	–	MH708134	MH727472
C. jishouense	GZU_HJ2_G4	MH482932	MH681659	–	MH708136	MH727474
C. jishouense	GZU_HJ3_ J5	MH482930	MH492706	–	MH708137	–
C. kahawae	IMI 319418*, ICMP 17816	JX010231	JX010012	JX009813	JX009452	JX010444
C. magnisporum	CBS 398.84*	KF687718	KF687842	KF687782	KF687803	KF687882
C. makassarense	CBS 143664*	MH728812	MH728820	MH805850	MH781480	MH846563
C. mengyinense	SAUCC200 702*	MW786742	–	MW883686	MW883695	MW888970
C. musae	CBS 116870*	HQ596292	HQ596299	JX009896	HQ596284	HQ596280
C. nanhuaensis	YMF1.04993*	OK030870	OK513673	OK513569	OK513609	OK513639

Table A1 (continued)

Taxa	Strains	GenBank accession numbers				
		ITS	***GAPDH***	***CHS-1***	***ACT***	***TUB***
C. nullisetosum	YMF1.0694 6*	OK030872	OK513675	OK513571	OK513611	OK513641
C. nupharicola	CBS 470.96*, ICMP 18187	JX010187	JX009972	JX009835	JX009437	JX010398
C. oblongisporum	YMF1.0693 8*	OK030874	OK513677	OK513573	–	OK513643
C. parvisporum	YMF1.0694 2*	OK030876	OK513679	OK513575	OK513613	OK513645
C. pandanicola	MFLUCC 17-0571*	MG646967	MG646934	MG646931	MG646938	MG646926
C. pandanicola	**MFLUCC 22-0109**	**OP740246**	**OP744513**	**OP744512**	**OP744511**	**OP744514**
C. perseae	CBS 141365*, GA100	KX620308	KX620242	MZ799260	KX620145	KX620341
C. proteae	CBS 132882*	KC297079	KC297009	KC296986	KC296940	KC297101
C. pseudomajus	CBS 571.88*	KF687722	KF687826	KF687779	KF687801	KF687883
C. pseudotheobromicola	MFLUCC 18-1602*	MH817395	MH853675	MH853678	MH853681	MH853684
C. psidii	CBS 145.29*, ICMP 19120	JX010219	JX009967	JX009901	JX009515	JX010443
C. queenslandicum	ICMP 1778*	JX010276	JX009934	JX009899	JX009447	JX010414
C. radicis	CBS 529.93*	KF687719	KF687825	KF687762	KF687785	KF687869

Table A1 (continued)

Taxa	Strains	GenBank accession numbers				
		ITS	***GAPDH***	***CHS-1***	***ACT***	***TUB***
C. rhexiae	Coll1026, BPI 884112, CBS 133134*	JX145128	MZ664046	MZ799258	MZ664127	JX145179
C. salsolae	ICMP 19051*	JX010242	JX009916	JX009863	JX009562	JX010403
C. serranegrense	COAD 2100*	KY400111	–	KY407894	KY407892	KY407896
C. siamense	ICMP 18578*, CBS 130417	FJ972613	FJ972575	JX009865	FJ907423	FJ907438
C. siamense	HSI-3	OM654563	OM831360	OM831354	OM831342	OM831384
Colletotrichum. sp.	CBS 159.50	KF687724	KF687823	KF687778	KF687800	KF687867
C. subacidae	LC13857, LH01*	MZ595846	MZ664068	MZ799307	MZ664144	MZ673967
C. subacidae	NN054605	MZ595893	MZ664075	MZ799309	MZ664191	MZ674011
C. subvariabile	LC13876, NN040649*	MZ595883	MZ664054	MZ799343	MZ664181	MZ674001
C. syzygiicola	DNCL021, MFLUCC 10-0624*	KF242094	KF242156	–	KF157801	KF254880
C. tainanense	CBS 143666*	MH728818	MH728823	MH805845	MH781475	MH846558
C. temperatum	CBS 133122*, Coll883, BPI 884100	JX145159	MZ664045	MZ799254	MZ664125	JX145211
C. tengchongense	YMF 1.04950*	OL842169	OL981264	OL981290	OL981238	–

Table A1 (continued)

Taxa	Strains	GenBank accession numbers				
		ITS	***GAPDH***	***CHS-1***	***ACT***	***TUB***
C. theobromicola	CBS 124945*, ICMP 18649	JX010294	JX010006	JX009869	JX009444	JX010447
C. ti	ICMP 4832*	JX010269	JX009952	JX009898	JX009520	JX010442
C. tropicale	CBS 124949*, ICMP 18653, MTCC 11371	JX010264	JX010007	JX009870	JX009489	JX010407
C. truncatum	CBS 151.35*	GU227862	GU228254	GU228352	GU227960	GU228156
C. truncatum	CBS 120709	GU227877	GU228269	GU228367	GU227975	GU228171
C. truncatum	CBS 141.79	GU227873	GU228265	GU228363	GU227971	GU228167
C. truncatum	IMI 135524	GU227874	GU228266	GU228364	GU227972	GU228168
C. truncatum	CBS 710.70	GU227864	GU228256	GU228354	GU227962	GU228158
C. truncatum	**MFLUCC 22-0110**	**OP740247**	**OP744517**	**OP744516**	**OP744515**	**OP744518**
C. variabile	LC13875, NN040656*	MZ595884	MZ664055	MZ799344	MZ664182	MZ674002
C. vietnamense	CBS 125478, LD16 (L2)*	KF687721	KF687832	KF687769	KF687792	KF687877
C. vietnamense	CBS 125477, BMT25 (L3)	KF687720	KF687831	KF687768	KF687791	KF687876
C. viniferum	GZAAS 5.08601*, yg1	JN412804	JN412798	–	JN412795	JN412813

Table A1 (continued)

Taxa	Strains	GenBank accession numbers				
		ITS	***GAPDH***	***CHS-1***	***ACT***	***TUB***
C. vulgaris	YMF 1.04940*	OL842170	OL981265	OL981291	OL981239	–
C. wuxiense	CGMCC 3.17894*	KU251591	KU252045	KU251939	KU251672	KU252200
C. xanthorrhoeae	BRIP 45094*, ICMP 17903,	JX010261	JX009927	JX009823	JX009478	JX010448
C. xishuangbannaense	MFLUCC 19-0107*	MW346469	MW537586	MW660832	MW652294	–
C. yulongense	CFCC 50818*	MH751507	MK108986	MH793605	MH777394	MK108987
C. yunajiangensis	YMF1.0499 6*	OK030885	OK513686	OK513583	OK513620	OK513649
C. zhaoqingense	LC13877, NN058985*	MZ595905	MZ664065	MZ799304	MZ664203	MZ674023
C. zhaoqingense	LC13878, NN071035	MZ595906	MZ664066	MZ799305	MZ664204	MZ674024

Note "*" indicates type strains and the newly generated sequences are in bold

APPENDIX B

MORPHOMOLECULAR IDENTIFICATION AND PATHOGENICITY OF *Colletotrichum* SPECIES ASSOCIATED WITH AVODADO ANTHRACNOSE IN NORTHERN THAILAND

Table A2 Strains and respective GenBank accession numbers used in this study

Taxa	**Strains**	**GenBank accession numbers**				
		ITS	***GAPDH***	***CHS-1***	***ACT***	***TUB***
Colletotrichum acidae	MFLUCC 17-2659*	MG996505	MH003691	MH003694	MH003697	MH003700
C. aenigma	ICMP 18608*	JX010244	JX010044	JX009774	JX009443	JX010389
C. aeschynomenes	ICMP 17673*, ATCC 201874	JX010176	JX009930	JX009799	JX009483	JX010392
C. alatae	CBS 304.67*, ICMP 17919	JX010190	JX009990	JX009837	JX009471	JX010383
C. alienum	ICMP 12071*	JX010251	JX010028	JX009882	JX009572	JX010411
C. aotearoa	ICMP 18537*	JX010205	JX010005	JX009853	—	JX010420
C. arecicola	CGMCC 3.19667*	MK914635	—	MK935541	MK935374	MK935498
C. artocarpicola	MFLUCC 18-1167*	MN415991	MN435568	MN435569	MN435570	MN435567
C. asianum	ICMP 18580*, CBS 130418	JX010196	JX010053	JX009867	JX009584	JX010406

Table A2 (continued)

Taxa	Strains	GenBank accession numbers				
		ITS	***GAPDH***	***CHS-1***	***ACT***	***TUB***
C. asianum	IMI 313839, ICMP 18696	JX010192	JX009915	JX009753	JX009576	JX010384
C. asianum	MAFF 306627, ICMP 18603	JX010195	JX009938	JX009825	JX009579	—
C. asianum	CBS 124960, ICMP 18648	JX010193	JX010017	JX009871	JX009546	—
C. asianum	HKUCC 10862, ICMP 18605	JX010194	JX010021	JX009787	JX009465	—
C. analogum	YMF1.06943*	OK030860	OK513663	OK513559	OK513599	OK513629
C. camelliae	CGMCC 3.14925, LC1364*	KJ955081	KJ954782	MZ799255	KJ954363	KJ955230
C. cangyuanensis	YMF1.05001*	OK030864	OK513667	OK513563	OK513603	OK513633
C. changpingense	CGMCC 3.17582*, SA0016, MFLUCC 15-0022	KP683152	KP852469	KP852449	KP683093	KP852490
C. chiangmaiense	MFLUCC 18-0945*	MW346499	MW548592	MW623653	MW655578	—
C. chrysophilum	URM 7368, CMM4268*	KX094252	KX094183	KX094083	KX093982	KX094285
C. cigarro	ICMP 18539*	JX010230	JX009966	JX009800	JX009523	JX010434
C. clidemiae	ICMP 18658*	JX010265	JX009989	JX009877	JX009537	JX010438
C. cobbittiense	BRIP 66219*	MH087016	MH094133	MH094135	MH094134	MH094137
C. fici-septicae	MFLU 19-2770*	MW114367	MW183774	MW177701	MW151585	—
C. fructicola	ICMP 18581*, CBS 130416	JX010165	JX010033	JX009866	FJ907426	JX010405
C. fructicola	MFLUCC 17-0555	MG646969	MG646936	MG646932	MG646944	MG646928
C. fructicola	MFLUCC 17-0613	MG646968	MG646935	MG646933	MG646939	MG646927
C. fructicola	**P11-2, MFLUCC 23-0012**	**OQ513191**	**OQ605852**	**OQ605841**	**OQ535385**	**OQ605859**

Table A2 (continued)

Taxa	Strains	GenBank accession numbers				
		ITS	***GAPDH***	***CHS-1***	***ACT***	***TUB***
C. fructivorum	Coll1414, BPI 884103, CBS133125*	JX145145	MZ664047	MZ799259	MZ664126	JX145196
C. gloeosporioides	IMI 356878*, ICMP 17821, CBS 112999	JQ005152	JQ005239	JQ005326	JQ005500	JQ005587
C. gracile	YMF1.06939*	OK030868	OK513671	OK513567	OK513607	OK513637
C. grevilleae	CBS 132879, CPC 15481*	KC297078	KC297010	KC296987	KC296941	KC297102
C. grossum	CGMCC3.17614, CAUG7, LC6227*	KP890165	KP890159	KP890153	KP890141	KP890171
C. hebeiense	MFLUCC 13-0726*	KF156863	KF377495	KF289008	KF377532	KF288975
C. hederiicola	MFLU 15-0689*	MN631384		MN635794	MN635795	
C. helleniense	CBS 142418, CPC 26844*	KY856446	KY856270	KY856186	KY856019	KY856528
C. henanense	LC3030, CGMCC 3.17354, LF238*	KJ955109	KJ954810	MZ799256	KM023257	KJ955257
C. henanense	LC2820, LF24	KM610182	KM610178	—	KM610172	KM610184
C. henanense	LC2821, LF25	KM610183	KM610179	—	KM610173	KM610185
C. henanense	**A28, MFLUCC 23-0006**	**OQ513190**	**OQ605851**	**OQ605840**	**OQ535384**	**OQ605863**
C. horii	NBRC 7478*, ICMP 10492, MTCC 10841	GQ329690	GQ329681	JX009752	JX009438	JX010450
C. hystricis	CBS 142411, CPC 28153*	KY856450	KY856274	KY856190	KY856023	KY856532

Table A2 (continued)

Taxa	Strains	GenBank accession numbers				
		ITS	***GAPDH***	***CHS-1***	***ACT***	***TUB***
C. jiangxiense	CGMCC 3.17363*	KJ955201	KJ954902	—	KJ954471	KJ955348
C. kahawae	IMI 319418*, ICMP 17816	JX010231	JX010012	JX009813	JX009452	JX010444
C. makassarense	CBS 143664*	MH728812	MH728820	MH805850	MH781480	MH846563
C. musae	CBS 116870*, ICMP 19119, MTCC 11349	HQ596292	HQ596299	JX009896	HQ596284	HQ596280
C. nanhuaensis	YMF1.04993*	OK030870	OK513673	OK513569	OK513609	OK513639
C. nullisetosum	YMF1.06946*	OK030872	OK513675	OK513571	OK513611	OK513641
C. nupharicola	CBS 470.96*, ICMP 18187	JX010187	JX009972	JX009835	JX009437	JX010398
C. oblongisporum	YMF1.06938*	OK030874	OK513677	OK513573	—	OK513643
C. parvisporum	YMF1.06942*	OK030876	OK513679	OK513575	OK513613	OK513645
C. pandanicola	MFLUCC 17-0571*	MG646967	MG646934	MG646931	MG646938	MG646926
C. pandanicola	SAUCC200204	MW786641	MW846239	MW883685	MW883694	MW888969
C. pandanicola	SAUCC1152	MW786746	MW876478	MW883693	MW883702	MW888977
C. perseae	CBS 141365*, GA100	KX620308	KX620242	MZ799260	KX620145	KX620341
C. proteae	CBS 132882*	KC297079	KC297009	KC296986	KC296940	KC297101
C. pseudotheobromicola	MFLUCC 18-1602*	MH817395	MH853675	MH853678	MH853681	MH853684
C. psidii	CBS 145.29*, ICMP 19120	JX010219	JX009967	JX009901	JX009515	JX010443

Table A2 (continued)

Taxa	Strains	GenBank accession numbers				
		ITS	***GAPDH***	***CHS-1***	***ACT***	***TUB***
C. queenslandicum	ICMP 1778*	JX010276	JX009934	JX009899	JX009447	JX010414
C. siamense	BML-I15, MFLU 090231	FJ972614	FJ972574	—	FJ907422	FJ907437
C. siamense	SPL213	LC604495	LC604555	LC604607	LC604581	LC604527
C. siamense	SPL2133	LC604496	LC604556	LC604608	LC604582	LC604528
C. siamense	SPL2136	LC604497	LC604557	LC604609	LC604583	LC604529
C. siamense	SPL2139	LC604498	LC604558	LC604610	LC604584	LC604530
C. siamense	**A6, MFLUCC 23-0005**	**OQ513184**	**OQ605845**	**OQ605834**	**OQ535378**	**OQ605853**
C. siamense	**S1-2, MFLUCC 23-0007**	**OQ513185**	**OQ605846**	**OQ605835**	**OQ535379**	**OQ605854**
C. siamense	**S1-3, MFLUCC 23-0008**	**OQ513186**	**OQ605847**	**OQ605836**	**OQ535380**	**OQ605855**
C. siamense	**P4, MFLUCC 23-0010**	**OQ513187**	**OQ605848**	**OQ605837**	**OQ535381**	**OQ605856**
C. siamense	**P39-2, MFLUCC 23-0014**	**OQ513188**	**OQ605849**	**OQ605838**	**OQ535382**	**OQ605857**
C. siamense	**P39-3, MFLUCC 23-0015**	**OQ513189**	**OQ605850**	**OQ605839**	**OQ535383**	**OQ605858**
C. syzygiicola	DNCL021, MFLUCC 10-0624*	KF242094	KF242156	—	KF157801	KF254880
C. tainanense	CBS 143666*	MH728818	MH728823	MH805845	MH781475	MH846558
C. temperatum	CBS 133122*, Coll883, BPI 884100	JX145159	MZ664045	MZ799254	MZ664125	JX145211
C. tengchongense	YMF 1.04950*	OL842169	OL981264	OL981290	OL981238	—
C. theobromicola	CBS 124945*, ICMP 18649	JX010294	JX010006	JX009869	JX009444	JX010447
C. ti	ICMP 4832*	JX010269	JX009952	JX009898	JX009520	JX010442

Table A2 (continued)

Taxa	Strains	GenBank accession numbers				
		ITS	***GAPDH***	***CHS-1***	***ACT***	***TUB***
C. tropicale	CBS 124949*, ICMP 18653, MTCC 11371	JX010264	JX010007	JX009870	JX009489	JX010407
C. truncatum	CBS 151.35*	GU227862	GU228254	GU228352	GU227960	GU228156
C. viniferum	GZAAS 5.08601*, yg1	JN412804	JN412798	—	JN412795	JN412813
C. vulgaris	YMF 1.04940*	OL842170	OL981265	OL981291	OL981239	—
C. wuxiense	CGMCC 3.17894*	KU251591	KU252045	KU251939	KU251672	KU252200
C. xanthorrhoeae	BRIP 45094*, ICMP 17903, CBS 127831	JX010261	JX009927	JX009823	JX009478	JX010448
C. xishuangbannaense	MFLUCC 19-0107*	MW346469	MW537586	MW660832	MW652294	—
C. yulongense	CFCC 50818*	MH751507	MK108986	MH793605	MH777394	MK108987
C. yunajiangensis	YMF1.04996*	OK030885	OK513686	OK513583	OK513620	OK513649

Note Type strains are indicated with "*", and the newly sequenced strains are in bold

APPENDIX C

STATISTICAL ANAYSES OF PATHOGENICITY TESTS ON AVOCADO FRUITS AND LEAVES

Table A3 Comparison of mean symptom diameter between wounded and non-wound methods on avocado fruits

Day	Treatment											
	M1		**P4-2**		**A28**		**P11-2**		**P39-2**		**S1-2**	
	W	**NW**	**W**	**NW**	**W**	**NW**	**W**	**NW**	**W**	**NW**	**W**	**NW**
1	0.6	0	0.6	0	1.3 [a]	0 [b]	1.3 [a]	0 [b]	1.3	0.6	0.3	0
SEM	0.21		0.21		0.33		0.33		0.26		0.17	
P-value	0.116		0.116		0.016		0.016		0.230		0.374	
2	3.6 [a]	1.3 [b]	1.3	1.0	4.3 [a]	1.0 [b]	7.6 [a]	1.0 [b]	3.6	3.0	1.3	0.6
SEM	0.56		0.16		0.76		1.50		0.42		0.26	
P-value	0.008		0.374		0.001		0.001		0.492		0.230	
3	7.3 [a]	2.3 [b]	2.3	1.3	8.0 [a]	2.6 [b]	11.0 [a]	1.3 [b]	6.3 [a]	4.3 [b]	2.6 [a]	1.0 [b]
SEM	1.14		0.31		1.23		2.18		0.49		0.40	
P-value	0.001		0.101		0.001		0.001		0.013		0.007	
4	10.0 [a]	4.0 [b]	6.0	4.6	11.0 [a]	4.3 [b]	14.0 [a]	2.0 [b]	11.0 [a]	7.0 [b]	8.6 [a]	2.3 [b]
SEM	1.34		0.49		1.52		2.69		0.96		1.43	
P-value	0.001		0.205		0.001		0.001		0.008		0.001	

Table A3 (continued)

Day	Treatment											
	M1		**P4-2**		**A28**		**P11-2**		**P39-2**		**S1-2**	
	W	**NW**	**W**	**NW**	**W**	**NW**	**W**	**NW**	**W**	**NW**	**W**	**NW**
5	15.6 [a]	4.3 [b]	12.3 [a]	6.0 [b]	16.6 [a]	5.0 [b]	18.6 [a]	3.3 [b]	13.6	13.3	11.0 [a]	2.6 [b]
SEM	2.54		1.45		2.61		3.43		0.34		1.87	
P-value	0.001		0.001		0.001		0.001		0.678		0.001	
6	19.6 [a]	5.6 [b]	19.6 [a]	13.3 [b]	20.6 [a]	6.6 [b]	23.6 [a]	6.3 [b]	18.0	17.3	18.3 [a]	5.6 [b]
SEM	3.14		1.48		3.16		3.90		0.33		2.84	
P-value	0.001		0.002		0.001		0.001		0.374		0.001	
7	24.3 [a]	10.3 [b]	23.3 [a]	17.0 [b]	25.6 [a]	11.6 [b]	30.3 [a]	7.6 [b]	23.0	22.6	20.3 [a]	8.3 [b]
SEM	3.15		1.45		3.14		5.07		0.16		2.69	
8	30.6 [a]	12.0 [b]	29.0 [a]	24.6 [b]	31.6 [a]	13.6 [b]	35.6 [a]	9.3 [b]	28.0	26.6	26.0 [a]	10.6 [b]
SEM	4.17		1.01		4.03		5.89		0.42		3.44	
P-value	0.001		0.003		0.001		0.001		0.116		0.001	
9	37.3 [a]	13.6 [b]	35.3 [a]	26.3 [b]	38.3 [a]	21.0 [b]	42.3 [a]	11.0 [b]	33.0 [a]	28.6 [b]	30.3 [a]	11.3 [b]
SEM	5.29		2.02		3.88		7.01		1.01		4.25	
P-value	0.001		0.001		0.001		0.001		0.003		0.001	
10	47.6 [a]	16.0 [b]	44.3 [a]	31.3 [b]	52.0 [a]	23.6 [b]	56.3 [a]	12.6 [b]	42.0 [a]	30.3 [b]	32.3 [a]	13.6 [b]
SEM	7.08		2.94		6.34		9.77		2.65		4.18	
P-value	0.001		0.002		0.001		0.001		0.004		0.001	

Table A4 Comparison of mean symptom diameter between wounded and non-wound methods on avocado leaves

Day	Treatment											
	M1		**P4-2**		**A28**		**P11-2**		**P39-2**		**S1-2**	
	W	**NW**	**W**	**NW**	**W**	**NW**	**W**	**NW**	**W**	**NW**	**W**	**NW**
1	0.0	0.0	1.0 [a]	0.0 [b]	0.0	0.0	0.0	0.0	0.0	0.0	0.0	0.0
SEM	0		0.22		0		0		0		0	
P-value	.		0.001		.		.		.		.	
2	0.0	0.0	1.3 [a]	0.0 [b]	0.0	0.0	0.0	0.0	0.0	0.0	0.0	0.0
SEM	0		0.22		0		0		0		0	
P-value	.		0.016		.		.		.		.	
3	2.0 [a]	0.0 [b]	2.0 [a]	0.0 [b]	1.0 [a]	0.0 [b]	1.6 [a]	0.0 [b]	1.3 [a]	0.0 [b]	1.3 [a]	0.0 [b]
SEM	0.51		0.45		0.22		0.40		0.33		0.33	
P-value	0.026		0.001		0.001		0.001		0.016		0.016	
4	5.3 [a]	0.0 [b]	4.0 [a]	0.0 [b]	3.3 [a]	0.0 [b]	3.3 [a]	0.0 [b]	3.0 [a]	0.0 [b]	3.3 [a]	0.0 [b]
SEM	0.52		0.45		0.22		0.40		0.33		0.33	
P-value	0.001		0.002		0.001		0.001		0.001		0.001	
5	7.0 [a]	0.0 [b]	5.0 [a]	0.0 [b]	4.0 [a]	0.0 [b]	5.0 [a]	0.0 [b]	4.6 [a]	0.0 [b]	5.0 [a]	0.0 [b]
SEM	1.56		1.12		0.89		1.12		1.05		1.12	
P-value	0.001		0.001		0.001		0.001		0.001		0.001	
6	9.6 [a]	0.0 [b]	6.6 [a]	0.0 [b]	5.6 [a]	0.0 [b]	7.6 [a]	0.0 [b]	7.0 [a]	0.0 [b]	7.0 [a]	0.0 [b]
SEM	1.56		1.12		0.89		1.12		1.05		1.12	

Table A4 (continued)

Day	Treatment											
	M1		**P4-2**		**A28**		**P11-2**		**P39-2**		**S1-2**	
	W	**NW**	**W**	**NW**	**W**	**NW**	**W**	**NW**	**W**	**NW**	**W**	**NW**
SEM	1.56		1.12		0.89		1.12		1.05		1.12	
P-value	0.001		0.001		0.001		0.001		0.001		0.001	
7	11.0 [a]	0.0 [b]	7.0 [a]	0.0 [b]	9.6 [a]	0.0 [b]	11.6 [a]	0.0 [b]	8.3 [a]	0.0 [b]	11.0 [a]	0.0 [b]
SEM	2.98		1.94		2.76		3.59		2.01		3.08	
P-value	0.001		0.001		0.001		0.001		0.001		0.001	
8	13.3 [a]	0.0 [b]	8.6 [a]	0.0 [b]	12.3 [a]	0.0 [b]	16.0 [a]	0.0 [b]	9.0 [a]	0.0 [b]	13.6 [a]	0.0 [b]
SEM	2.47		1.56		2.16		2.61		1.86		2.50	
P-value	0.001		0.001		0.001		0.001		0.001		0.001	
9	14.3 [a]	0.0 [b]	11.3 [a]	0.0 [b]	14.3 [a]	0.0 [b]	16.6 [a]	0.0 [b]	10.0 [a]	0.0 [b]	16.6 [a]	0.0 [b]
SEM	2.99		1.94		2.76		3.59		2.01		3.081	
P-value	0.001		0.001		0.001		0.001		0.001		0.001	
10	16.3 [a]	0.0 [b]	13.3 [a]	0.0 [b]	16.0 [a]	0.0 [b]	19.3 [a]	0.0 [b]	10.6 [a]	0.0 [b]	18.3 [a]	0.0 [b]

Table A4 (continued)

Day	Treatment											
	M1		**P4-2**		**A28**		**P11-2**		**P39-2**		**S1-2**	
	W	**NW**	**W**	**NW**	**W**	**NW**	**W**	**NW**	**W**	**NW**	**W**	**NW**
SEM	3.22		2.55		3.21		3.73		2.23		3.73	
P-value	0.001		0.001		0.001		0.001		0.001		0.001	
11	17.3 [a]	0.0 [b]	17.3 [a]	0.0 [b]	20.3 [a]	0.0 [b]	21.3 [a]	0.0 [b]	12.3 [a]	0.0 [b]	20.6 [a]	0.0 [b]
SEM	3.66		3.00		3.59		4.32		2.39		4.10	
P-value	0.001		0.001		0.001		0.001		0.001		0.001	
12	18.3 [a]	0.0 [b]	23.3 [a]	0.0 [b]	23.6 [a]	0.0 [b]	24.6 [a]	0.0 [b]	12.6 [a]	0.0 [b]	24.6 [a]	0.0 [b]
SEM	4.10		5.22		5.30		5.52		2.83		5.52	
P-value	0.001		0.001		0.001		0.001		0.001		0.001	
13	22.3 [a]	0.0 [b]	24.3 [a]	0.0 [b]	24.6 [a]	0.0 [b]	26.3 [a]	0.0 [b]	13.3 [a]	0.0 [b]	25.6 [a]	0.0 [b]
SEM	4.99		5.44		5.52		5.89		2.98		5.74	
P-value	0.001		0.001		0.001		0.001		0.001		0.001	
14	25.3 [a]	0.0 [b]	25.3 [a]	0.0 [b]	27.0 [a]	0.0 [b]	28.6 [a]	0.0 [b]	14.0 [a]	0.0 [b]	28.0 [a]	0.0 [b]
SEM	5.66		5.66		6.04		6.41		3.13		6.26	
P-value	0.001		0.001		0.001		0.001		0.001		0.001	
15	29.3 [a]	0.0 [b]	27.6 [a]	0.0 [b]	30.0 [a]	0.0 [b]	29.6 [a]	0.0 [b]	14.6 [a]	0.0 [b]	29.6 [a]	0.0 [b]
SEM	6.56		6.19		6.71		6.63		3.28		6.63	
P-value	0.001		0.001		0.001		0.001		0.001		0.001	

Table A5 Comparison of mean symptom diameter among strains in the wounded method on the fruits

Day	Treatment						SEM	*P*-value
	M1	P4-2	A28	P11-2	P39-2	S1-2		
	W	W	W	W	W	W		
1	0.6	0.6	1.3	1.3	0.6	0.3	0.14	0.261
2	3.6 ^{b}	1.3 ^{c}	4.3 ^{b}	7.6 ^{a}	3.0 ^{bc}	1.3 ^{c}	0.54	0.001
3	7.3 ^{b}	2.3 ^{c}	8.0 ^{b}	11.0 ^{a}	4.3 ^{c}	2.6 ^{c}	0.77	0.001
4	10.0 ^{bc}	6.0 ^{e}	11.0 ^{b}	14.0 ^{a}	7.0 ^{de}	8.6 ^{cd}	0.66	0.001
5	15.6 ^{b}	12.3 ^{cd}	16.6 ^{b}	18.6 ^{a}	13.6 ^{c}	11.0 ^{d}	0.64	0.001
6	19.6 ^{bc}	19.6 ^{bc}	20.6 ^{b}	23.6 ^{a}	17.3 ^{c}	18.3 ^{bc}	0.52	0.001
7	24.3 ^{bc}	23.3 ^{c}	25.6 ^{b}	30.3 ^{a}	23.0 ^{c}	20.3 ^{d}	0.75	0.001
8	30.6 ^{bc}	29.0 ^{cd}	31.6 ^{b}	35.6 ^{a}	28.0 ^{de}	26.0 ^{e}	0.76	0.001
9	37.3 ^{b}	35.3 ^{c}	38.3 ^{b}	42.3 ^{a}	33.0 ^{d}	30.3 ^{e}	0.94	0.001
10	47.6 ^{c}	44.3 ^{d}	52.0 ^{b}	56.3 ^{a}	42.0 ^{d}	32.3 ^{e}	1.86	0.001

Note The values are presented as the mean of replicates, and statistically significant differences are indicated by lowercase letters alongside the values

Table A6 Comparison of mean symptom diameter among strains in the non-wounded method on avocado fruits

Day	Treatment						SEM	*P*-value
	M1	P4-2	A28	P11-2	P39-2	S1-2		
	NW	NW	NW	NW	NW	NW		
1	0.0 ^{b}	0.0 ^{b}	0.0 ^{b}	0.0 ^{b}	1.3 ^{a}	0.0 ^{b}	0.13	0.001
2	1.3 ^{b}	1.0 ^{b}	1.0 ^{b}	1.0 ^{b}	3.6 ^{a}	0.6 ^{b}	0.27	0.001
3	2.3 ^{bc}	1.3 ^{bc}	2.6 ^{b}	1.3 ^{bc}	6.3 ^{a}	1.0 ^{c}	0.45	0.001
4	4.0 ^{bc}	4.6 ^{b}	4.3 ^{b}	2.0 ^{d}	11.0 ^{a}	2.3 ^{cd}	0.73	0.001
5	4.3 ^{bc}	6.0 ^{b}	5.0 ^{bc}	3.3 ^{cd}	13.3 ^{a}	2.6 ^{d}	0.87	0.001
6	5.6 ^{c}	13.3 ^{b}	6.6 ^{c}	6.3 ^{c}	18.0 ^{a}	5.6 ^{c}	1.16	0.001
7	10.3 ^{cd}	17.0 ^{b}	11.6 ^{c}	7.3 ^{e}	22.6 ^{a}	8.3 ^{de}	1.31	0.001
8	12.0 ^{d}	24.6 ^{b}	13.6 ^{c}	9.3 ^{e}	26.6 ^{a}	10.6 ^{de}	1.67	0.001
9	13.6 ^{d}	26.3 ^{b}	21.0 ^{c}	11.0 ^{e}	28.3 ^{a}	11.3 ^{e}	1.72	0.001
10	16.0 ^{c}	31.3 ^{a}	23.6 ^{b}	12.6 ^{d}	30.0 ^{a}	13.6 ^{d}	1.85	0.001

Note The values are presented as the mean of replicates, and statistically significant differences are indicated by lowercase letters alongside the values

Table A7 Comparison of mean symptom diameter among strains in the wounded method on avocado leaves

Day	Treatment						SEM	*P*-value
	M1	P4-2	A28	P11-2	P39-2	S1-2		
	W	W	W	W	W	W		
1	0.0 [b]	1.0 [a]	0.0 [b]	0.0 [b]	0.0 [b]	0.0 [b]	0.09	0.001
2	0.0 [b]	1.3 [a]	0.0 [b]	0.0 [b]	0.0 [b]	0.0 [b]	0.13	0.001
3	2.0	2.0	1.0	1.6	1.3	1.3	0.14	0.271
4	5.3 [a]	4.0 [ab]	3.3 [b]	3.3 [b]	3.0 [b]	3.3 [b]	0.22	0.007
5	7.0 [a]	5.0 [b]	4.0 [c]	5.0 [b]	4.6 [b]	5.0 [b]	0.23	0.001
6	9.6 [a]	6.6 [bc]	5.6 [c]	7.6 [b]	7.0 [bc]	7.0 [bc]	0.32	0.001
7	11.0 [a]	7.0 [c]	9.6 [ab]	11.6 [a]	8.3 [bc]	11.0 [a]	0.44	0.001
8	13.3 [b]	8.6 [c]	12.3 [b]	16.0 [a]	9.0 [c]	13.6 [b]	0.65	0.001
9	14.3 [b]	11.3 [c]	14.3 [b]	16.6 [a]	10.0 [c]	16.6 [a]	0.62	0.001
10	16.3 [b]	13.3 [c]	16.0 [b]	19.3 [a]	10.6 [d]	18.3 [ab]	0.73	0.001
11	17.3 [b]	17.3 [b]	20.3 [a]	21.3 [a]	12.3 [c]	20.6 [a]	0.76	0.001
12	18.3 [b]	23.3 [a]	23.6 [a]	24.6 [a]	12.6 [c]	24.6 [a]	1.07	0.001
13	22.3 [c]	24.3 [b]	24.6 [b]	26.3 [a]	13.3 [d]	25.6 [ab]	1.07	0.001
14	25.3 [c]	25.3 [c]	27.0 [b]	28.6 [a]	14.0 [d]	28.0 [ab]	1.20	0.001
15	29.3 [ab]	27.6 [b]	30.0 [a]	29.6 [a]	14.6 [c]	29.6 [a]	1.34	0.001

APPENDIX D

NEW SPECIES AND NEW RECORDS OF PLANT PATHOGENIC FUNGI FROM NORTHERN THAILAND

Table A8 Primers and respective conditions used in the current research

Primer	PCR Condition	Reference
act (ACT-512F/ACT-783R)	95 °C: 5 min, (95 °C: 30 s, 55 °C: 50 s, 72 °C: 1 min) ×40 cycles, 72 °C: 10 min	Carbone & Kohn 1999
chs-1 (CHS79F/CHS345 R)	94 °C: 5 min, (94 °C: 50 s, 58 °C: 30 s, 72 °C: 1:30 min) ×35 cycles, 72 °C: 10 min	Carbone & Kohn 1999
gapdh (GDF/GDR)	95 °C: 5 min, (95 °C: 50 s, 58 °C: 50 s, 72 °C: 1 min) ×40 cycles, 72 °C: 10 min	Templeton et al. 1992
ITS (ITS4/ITS5)	95 °C: 5 min, (95 °C: 45 s, 53 °C: 45 s, 72 °C: 2 min) ×40 cycles, 72 °C: 10 min	White et al. 1990
LSU (LR0R/LR5)	94 °C: 3 min, (94 °C: 30 s, 55 °C: 50 s, 72 °C: 1 min) ×35 cycles, 72 °C: 10 min	Rehner & Samuels 1994; Vilgalys & Hester 1990
rpb2 (fRPB2-5f2/fRPB2-7cr)	94 °C: 3 min, (94 °C: 30 s, 58 °C: 1 min, 72 °C: 1:20 min) ×40 cycles, 72 °C: 10 min	Liu et al. 1999
tef1 (EF1-728F/EF1-986R)	94 °C: 3 min, (94 °C: 30 s, 58 °C: 1:30 min, 72 °C: 1:20 min) ×40 cycles, 72 °C: 10 min	Carbone & Kohn 1999
tub2 (Btub2Fd/Btub4Rd)	94 °C: 3 min, (94 °C: 30 s, 58 °C: 1:30 min, 72 °C: 1:20 min) ×40 cycles, 72 °C: 10 min	Glass & Donaldson 1995

Table A9 The best evolutionary models selected by jModelTest

Dataset/ Species Complex	**Gene**						
	ITS	***gapdh***	***chs-1***	***act***	***tub2***	***tef1***	***rpb2***
Colletotrichum dracaenophilum	TrN+I+G	TPM3uf+G	TIM2ef	HKY+I	HKY+G	—	—
C. gloeosporioides	TIM1+G	TrN+I	TIM1+G	TPM1uf+G	TIM3ef+G	—	—
C. orchidearum and *C. magnum*	GTR+G	TPM3uf+G	TrNef+I+G	HKY+G	HKY+G	—	—
C. truncatum	TIM1ef+I	HKY+I	TrNef+I	TPM1uf+I	TPM3uf+G	—	—
Lasiodiplodia	TIM2ef+I+G	—	—	—	TIM1+G	HKY+G	TIM3+G
Neopestalotiopsis	TPM3uf+I	—	—	—	TPM2uf+G	TIM2+G	—

Table A10 Information of the isolates obtained in the current research

Species	Strain	Host	GenBank accession number					
			ITS	*tef1*	*gapdh*	*chs-1*	*act*	*tub2*
Colletotrichum fructicola	A9; MFLUCC 24-0210	*Ficus religiosa*	PP960250	—	PP982589	PP982575	PP975282	PP982559
C. fructicola	C42; MFLUCC 24-0214	*Bauhinia* sp.	PP960248	—	PP982587	PP982573	PP975280	PP982557
C. musae	C26; MFLUCC 24-0207	*Musa* sp.	PP960245	—	PP982584	PP982570	PP975277	PP982554
C. musicola	C30; MFLUCC 24-0206	*Lagerstroemia* sp.	PP960252	—	PP982591	PP982577	PP975284	PP982561
C. siamense	A3; MFLUCC 24-0203	*Asplenium nidus*	PP960243	—	PP982583	PP982568	PP975275	PP982552
C. siamense	A14; MFLUCC 24-0202	*Dendrobium* sp.	PP960242	—	PP982582	PP982567	PP975274	PP982551
C. siamense	C3; MFLUCC 24-0200	*Anthurium andraeanum*	PP960239	—	PP982579	PP982564	PP975271	PP982548
C. siamense	C4; MFLUCC 24-0201	*Artocarpus heterophyllus*	PP960241	—	PP982581	PP982566	PP975273	PP982550
C. siamense	C11; MFLUCC 24-0209	*Dracaena fragrans*	PP960244	—	—	PP982569	PP975276	PP982553

Table A10 (continued)

Species	Strain	Host	GenBank accession number					
			ITS	*tef1*	*gapdh*	*chs-1*	*act*	*tub2*
C. siamense	C29-2; MFLUCC 24-0208	*Bauhinia* sp.	PP960240	—	PP982580	PP982565	PP975272	PP982549
C. siamense	C36-1; MFLUCC 24-0204	*Morinda citrifolia*	PP960246	—	PP982585	PP982571	PP975278	PP982555
C. siamense	C36-2; MFLUCC 24-0205	*Morinda citrifolia*	PP960247	—	PP982586	PP982572	PP975279	PP982556
C. siamense	C45; MFLUCC 24-0215	*Ficus* sp.	PP960249	—	PP982588	PP982574	PP975281	PP982558
C. tropicicola	C41; MFLUCC 24-0213	*Citrus maxima*	PP960251	—	PP982590	PP982576	PP975283	PP982560
C. truncatum	A9-2; MFLUCC 24-0211	*Ficus religiosa*	PP960253	—	PP982592	PP982578	PP975285	—
Lasiodiplodia theobromae	C38; MFLUCC 24-0212	*Ficus* sp.	PP960254	PP982593	—	—	—	PP982562
Neopestalotiopsis iridis	C1; MFLUCC 24-0199^{T}	*Iris pseudacorus*	PP960255	PP982594	—	—	—	PP982563

Note Type strains are indicated with "^{T}"

APPENDIX E

MANGO MICROCOSM: UNVEILING THE SPECIES DIVERSITY AND PATHOGENIC POTENTIAL OF FUNGI ISOLATED FROM MANGO (*Mangifera indica*) IN NORTHERN THAILAND

Table A11 Details of loci, primers, and PCR conditions used in this research

Locus	Primers	PCR condition	Fungal genus	Reference
Internal transcribed spacer (ITS)	ITS5/ITS4; ITS1/ITS4	95 °C: 5 min, (95 °C: 45 s, 53 °C: 45 s, 72 °C: 2 min) ×40 cycles, 72 °C: 10 min	All genera	White et al. (1990)
Actin (*act*)	ACT-512F/ACT-783R	95 °C: 5 min, (95 °C: 30 s, 55 °C: 50 s, 72 °C: 1 min) ×40 cycles, 72 °C: 10 min	*Colletotrichum*, *Pseudopallidocercospora*, *Zasmidium*	Carbone & Kohn (1999)
Calmadulin (*cmdA*)	CL1/CL2A; CAL228F/CAL737R	95°C: 5 min, (95°C: 30 s, 54°C: 50 s, 72°C: 1 min) ×40 cycles, 72°C: 10 min	*Diaporthe*	O'Donnell et al. (2000); Carbone & Kohn (1999)

Table A11 (continued)

Locus	Primers	PCR condition	Fungal genus	Reference
Chitin synthase (*chs-1*)	CHS79F/CHS345R	94 °C: 5 min, (94 °C: 50 s, 58 °C: 30 s, 72 °C: 1:30 min) ×35cycles, 72 °C: 10 min	*Colletotrichum*	Carbone & Kohn (1999)
Glyceraldehyde-3-phosphate dehydrogenase (*gapdh*)	GDF/GDR	95 °C: 5 min, (95 °C: 50 s, 58 °C: 50 s, 72 °C: 1 min) ×40cycles, 72 °C: 10 min	*Colletotrichum*	Templeton et al. (1992)
Histone 3 (*his3*)	CYLH3F/H3-1b	94 °C: 3 min, (95 °C: 30 s, 57 °C: 30 s, 72 °C: 1 min) ×40 cycles, 72 °C: 10 min	*Diaporthe*	Crous et al. (2004b|); Glass & Donaldson, (1995)
Large subunit ribosomal RNA (LSU)	1Fd/LR5	95 °C: 3 min, (95 °C: 30 s, 53 °C: 30 s, 72 °C: 60 s) ×35cycles, 72 °C: 10 min	*Pseudopallidocercospora*, *Zasmidium*	Crous et al. (2009); Vilgalys & Hester (1990)
RNA polymerase II (*rpb2*)	5f2/fRPB2-7cR	95 °C: 5 min, (95 °C: 45 s, 54 °C: 45 s, 72 °C: 2 min) ×40cycles, 72 °C: 10 min	*Neofusicoccum*, *Pseudopallidocercospora*	Alves et al. (2008)

Table A11 (continued)

Locus	Primers	PCR condition	Fungal genus	Reference
Translation elongation factor 1 (*tef1-α*)	EF-728F/EF2	94 °C: 3 min, (94 °C: 30 s, 58 °C: 1:30 min, 72 °C: 1:20 min) ×40 cycles, 72 °C: 10 min	*Diaporthe*, *Pestalotiopsis*, *Neopestalotiopsis*, *Neoscytalidium*, *Pseudopallidocercospora* *Zasmidium*	O'Donnell et al. (1998); Carbone & Kohn (1999)
Translation elongation factor 1 (*tef1-α*)	EF1-728F/EF1-986R; EF1-688F/EF1-986R	94 °C: 3 min, (94 °C: 30 s, 58 °C: 1:30 min, 72 °C: 1:20 min) ×40 cycles, 72 °C: 10 min	*Botryosphaeria*, *Neofusicoccum*	Carbone & Kohn (1999); Alves et al. (2008)
β-tublin 2 (*tub2*)	BT-2Fd BT-4Rd	94 °C: 3 min, (94 °C: 30 s, 58 °C: 90 s, 72 °C: 80 s) ×40cycles, 72 °C: 10 min	*Colletotrichum*, *Diaporthe*, *Pestalotiopsis*, *Neopestalotiopsis*, *Neoscytalidium*	Woudenber et al. (2009)

Table A11 (continued)

Locus	Primers	PCR condition	Fungal genus	Reference
	Bt2a/Bt2b	94 °C: 3 min, (94 °C: 30 s, 58 °C: 1:30 min, 72 °C: 1:20 min) ×40 cycles, 72 °C: 10 min	*Botryosphaeria*, *Neofusicoccum*, *Pestalotiopsis*, *Neopestalotiopsis*	Glass & Donaldson (1995)

Table A12 Genera, respective gene regions amplified, and models used in the phylogenetic analysis

Genus/ Complex	**Loci**	**Evolutionary model**
Botryosphaeria	ITS	TrN+I
	tef1-α	TPM3uf
	tub2	GTR+I
Colletotrichum/ acutatum	ITS	TIM3ef+I
	gapdh	TPM1uf+G
	chs-1	TIM2ef+I
	act	TIM2+G
	tub2	TPM2uf+G
Colletotrichum/ gigasporum	ITS	TrN+I+G
	gapdh	TPM1uf+I
	chs-1	TrNef+I+G
	act	HKY+G
	tub2	TIM3+G
Colletotrichum/ gloeosporioides	ITS	TIM2ef+I+G
	gapdh	HKY+I
	chs-1	TrNef+I+G
	act	TPM1uf+G
	tub2	TrNef+I+G
Colletotrichum/ orchidearum	ITS	TIM3+I
	gapdh	HKY

Table A12 (continued)

Genus/ Complex	Loci	Evolutionary model
	chs-1	TrN+G
	act	HKY+I
Diaporthe	ITS	TIM2+I+G
	tef1-α	TIM2+I+G
	tub2	TPM2uf+I+G
	cmdA	TPM2uf+G
Neofusicoccum	ITS	TIM3+I+G
	rpb2	TIM3+G
	tef1-α	TPM2uf+G
Neopestalotiopsis	ITS	TPM2uf+I
	tef1-α	TPM3uf+G
Neoscytalidium	ITS	TIM1+G
	tef1-α	HKY+G
	tub2	HKY+G
Pseudopallidocercospora, Zasmidium	ITS	TIM2+I+G
	LSU	GTR+I+G
	rpb2	TIM2+I+G

Table A13 Details of obtained isolates and their respective GenBank accession numbers

Species	**Strain**	**Isolation source**	**GenBank accession numbers**		
Botryosphaeria			ITS	*tef1*	*tub*
B. fabicerciana	M10; MFLUCC 24-0333	Fruit	PQ632434	PQ659792	PQ659969
B. fabicerciana	M10-2; MFLUCC 24-0334	Fruit	PQ632435	PQ659793	PQ659970
B. scharifii	M14; MFLUCC 24-0337	Fruit	PQ632436	PQ659794	PQ659971
B. scharifii	M14-2; MFLUCC 24-0336	Fruit	PQ632437	–	PQ659972

Table A13 (continued)

Species	Strain	Isolation source	GenBank accession numbers				
Botryosphaeria					ITS	*tef1*	*tub*
B. scharifii	M14-4; MFLUCC 24-0335	Fruit			PQ632438	PQ659795	PQ659973
Colletotrichum			ITS	*gapdh*	*chs-1*	*act*	*tub*
C. asianum	A18; MFLUCC 24-0339	Leaf	PQ632517	PQ659814	PQ659839	PQ659864	PQ659891
C. asianum	A19; MFLUCC 24-0340	Leaf	PQ632518	PQ659815	PQ659840	PQ659865	PQ659892
C. asianum	M4; MFLUCC 24-0341	Fruit	PQ632521	PQ659818	PQ659843	PQ659868	PQ659894

Table A13 (continued)

Species	Strain	Isolation source	GenBank accession numbers				
Colletotrichum			ITS	*gapdh*	*chs-1*	*act*	*tub*
C. asianum	MF15-4; MFLUCC 24-0345	Leaf	PQ632519	PQ659816	PQ659841	PQ659866	PQ659893
C. asianum	P6; MFLUCC 24-0346	Leaf	PQ632506	PQ659803	PQ659828	PQ659853	PQ659880
C. asianum	P7-2; MFLUCC 24-0347	Leaf	PQ632507	PQ659804	PQ659829	PQ659854	PQ659881
C. asianum	P9; MFLUCC 24-0338	Leaf	PQ632508	PQ659805	PQ659830	PQ659855	PQ659882

Table A13 (continued)

Species	Strain	Isolation source	GenBank accession numbers				
Colletotrichum			ITS	*gapdh*	*chs-1*	*act*	*tub*
C. asianum	P9-2; MFLUCC 24-0348	Leaf	PQ632509	PQ659806	PQ659831	PQ659856	PQ659883
C. asianum	P20; MFLUCC 24-0349	Leaf	PQ632510	PQ659807	PQ659832	PQ659857	PQ659884
C. asianum	P22; MFLUCC 24-0350	Leaf	PQ632511	PQ659808	PQ659833	PQ659858	PQ659885
C. asianum	P22-2; MFLUCC 24-0351	Leaf	PQ632512	PQ659809	PQ659834	PQ659859	PQ659886
C. asianum	P48; MFLUCC 24-0352	Leaf	PQ632513	PQ659810	PQ659835	PQ659860	PQ659887

Table A13 (continued)

Species	Strain	Isolation source	GenBank accession numbers				
Colletotrichum			ITS	*gapdh*	*chs-1*	*act*	*tub*
C. asianum	P49; MFLUCC 24-0353	Leaf	PQ632514	PQ659811	PQ659836	PQ659861	PQ659888
C. asianum	P98; MFLUCC 24-0354	Leaf	PQ632515	PQ659812	PQ659837	PQ659862	PQ659889
C. asianum	P100; MFLUCC 24-0355	Leaf	PQ632516	PQ659813	PQ659838	PQ659863	PQ659890
C. asianum	R35-2; MFLUCC 24-0356	Fruit	PQ632527	PQ659824	PQ659848	PQ659873	PQ659900

Table A13 (continued)

Species	Strain	Isolation source	GenBank accession numbers				
Colletotrichum			ITS	*gapdh*	*chs-1*	*act*	*tub*
C. gigasporum	T117-2; MFLUCC 24-0357	Leaf	PQ632505	PQ659799	PQ659827	PQ659876	PQ659903
C. guajavae	A20-2; MFLUCC 24-0358	Fruit	PQ632504	PQ659798	PQ659826	PQ659875	PQ659902
C. musae	R50; MFLUCC 24-0359	Fruit	PQ632528	PQ659825	PQ659849	PQ659874	PQ659901
C. plurivorum	AS-1; MFLUCC 24-0360	Leaf	PQ632529	PQ659800	PQ659850	PQ659877	PQ659904

Table A13 (continued)

Species	Strain	Isolation source	GenBank accession numbers				
Colletotrichum			ITS	*gapdh*	*chs-1*	*act*	*tub*
C. plurivorum	AS-2; MFLUCC 24-0361	Leaf	PQ632530	PQ659801	PQ659851	PQ659878	PQ659905
C. plurivorum	T117; MFLUCC 24-0362	Leaf	PQ632531	PQ6598002	PQ659852	PQ659879	PQ659906
C. siamense	C51-2; MFLUCC 24-0364	Leaf	PQ632525	PQ659822	PQ659846	PQ659871	PQ659898
C. siamense	MF24-5; MFLUCC 24-0365	Leaf	PQ632520	PQ659817	PQ659842	PQ659867	–

Table A13 (continued)

Species	Strain	Isolation source	GenBank accession numbers				
Colletotrichum			ITS	*gapdh*	*chs-1*	*act*	*tub*
C. siamense	P25; MFLUCC 24-0363	Fruit	PQ632526	PQ659823	PQ659847	PQ659872	PQ659899
Diaporthe			ITS	*tef1*	*tub*	*cal*	*his*
D. arecae	MF172-2; MFLUCC 24-0366	Leaf	PQ632534	PQ659933	PQ659925	PQ659912	PQ659917
D. arecae	T79-3; MFLUCC 24-0367	Leaf	PQ632539	PQ659937	PQ659930	PQ659914	PQ659922
D. arecae	Nan32-2; MFLUCC 24-0368	Leaf	PQ632536	PQ659935	PQ659927	PQ659913	PQ659919

Table A13 (continued)

Species	Strain	Isolation source	GenBank accession numbers				
Diaporthe			ITS	*tef1*	*tub*	*cal*	*his*
D. rosae	T79; MFLUCC 24-0369	Leaf	PQ632538	PQ659936	PQ659928	PQ659911	PQ659921
D. siamensis	MF15-5; MFLUCC 24-0370	Leaf	PQ632533	PQ659932	PQ659924	PQ659908	PQ659916
D. sojae	MF24-7; MFLUCC 24-0371	Leaf	PQ632535	PQ659934	PQ659926	PQ659909	PQ659918
Diaporthe sp.	C27-1; MFLUCC 24-0372R	Leaf	PQ632537	–	PQ659928	PQ659910	PQ659920

Table A13 (continued)

Species	Strain	Isolation source	GenBank accession numbers				
Diaporthe			ITS	*tef1*	*tub*	*cal*	*his*
D. thunbergiicola	A4-3; MFLUCC 24-0373	Leaf	PQ632532	PQ659931	PQ659923	PQ659907	PQ659915
Neofusicoccum			ITS	*tef1*	*tub*	*rpb2*	
N. sinoeucalypti	P21-2; MFLUCC 24-0374	Leaf	PQ633202	PQ659938	PQ659939	PQ659940	
Neopestalotiopsis			ITS	*tef1*	*tub*		
N. dendrobii	T79-2; MFLUCC 24-0377	Leaf		PQ639957	PQ659949	PQ659960	

Table A13 (continued)

Species	Strain	Isolation source	GenBank accession numbers		
Neopestalotiopsis			ITS	*tef1*	*tub*
N. mangiferae	**MF149-1**; **MFLUCC 24-0378**	Fruit	PQ639955	PQ659947	PQ659958
N. mangiferae	MF116-1; MFLUCC 24-0379	Fruit	PQ639951	PQ659943	PQ659954
N. mangifericola	**MF41-2**; **MFLUCC 24-0380**	Fruit	PQ639952	PQ659944	PQ659955
N. mangiferigena	**Nan31-3**; **MFLUCC 24-0381**	Leaf	PQ639956	PQ659948	PQ659959

Table A13 (continued)

Species	Strain	Isolation source	GenBank accession numbers		
Neopestalotiopsis			ITS	*tef1*	*tub*
N. psidii	C20; MFLUCC 24-0382	Leaf	PQ639959	PQ659951	PQ659962
N. rhododendri	MF172-3; MFLUCC 24-0383	Fruit	PQ639954	PQ659946	PQ659957
Neopestalotiopsis sp. 1	MF172-1; MFLUCC 24-0384R	Fruit	PQ639953	PQ659945	PQ659956
Neopestalotiopsis sp. 2	MF108-1; MFLUCC 24-0385R	Leaf	PQ639949	PQ659941	PQ659952

Table A13 (continued)

Species	Strain	Isolation source	GenBank accession numbers		
Neoscytalidium			ITS	*tef1*	*tub*
N. dimidiatum	T82; MFLUCC 24-0386	Fruit	PQ633294	PQ659964	PQ659963
Pestalotiopsis			ITS	*tef1*	*tub*
P. humicola	A4-2; MFLUCC 24-0387	Leaf	PQ633351	PQ659965	PQ659967
P. menhaiensis	M12-2; MFLUCC 24-0388	Leaf	PQ633352	PQ659966	PQ659968

Table A13 (continued)

Species	Strain	Isolation source	GenBank accession numbers		
Pseudopallidocercospora			LSU	ITS	*rpb2*
Pse. mangiferae	**H2, MFLUCC 24-0389**	Leaf	PQ638519	PQ639271	PQ659796
Pseudopallidocercospora			LSU	ITS	*rpb2*
Pse. mangiferae	H2-2, MFLUCC 24-0390	Leaf	PQ638520	PQ639272	PQ659797
Zasmidium				LSU	ITS
Z. mangiferae	**Nan31, MFLUCC 24-0391**	Leaf		PQ638521	PQ639273

Note Type strains are in bold

Table A14 Virulence measurement and evaluation on mango fruits and leaves

Species	**Strain code**	**Lesion diameter on fruits (Mean±SD, cm)[1]**	**Lesion diameter on leaves (Mean±SD, cm)[2]**	**Virulence**
Botryosphaeria fabicerciana	M10	1.24±0.01		mv[3]
Botryosphaeria fabicerciana	M10-2	0.56±0.05		wv[4]
Botryosphaeria scharifii	M14	1.33±0.03		mv
Botryosphaeria scharifii	M14-2	1.86±0.03		mv
Botryosphaeria scharifii	M14-3	1.69±0.02		mv
Botryosphaeria scharifii	M14-4	0.17±0.02		nv[5]
Colletotrichum asianum	A18		2.36±0.01	sv[6]
Colletotrichum asianum	A19		2.27±0.11	sv
Colletotrichum asianum	M4	2.83±0.02		sv
Colletotrichum asianum	M4-2	2.56±0.01		sv
Colletotrichum asianum	M13	1.71±0.01		mv
Colletotrichum asianum	M18-2	2.15±0.03		sv
Colletotrichum asianum	MF15-4		1.10±0.22	mv
Colletotrichum asianum	P6		1.44±0.02	mv
Colletotrichum asianum	P7-2		0.91±0.18	wv
Colletotrichum asianum	P9		1.49±0.06	mv
Colletotrichum asianum	P9-2		0.87±0.05	wv
Colletotrichum asianum	P20		0	nv
Colletotrichum asianum	P22		2.34±0.19	sv

Table A14 (continued)

Species	Strain code	Lesion diameter on fruits (Mean±SD, cm)[1]	Lesion diameter on leaves (Mean±SD, cm)[2]	Virulence
Colletotrichum asianum	P22-2		2.46±0.03	sv
Colletotrichum asianum	P48		2.39±0.05	sv
Colletotrichum asianum	P49		1.67±0.09	mv
Colletotrichum asianum	P98		2.27±0.08	sv
Colletotrichum asianum	P100		1.36±0.08	mv
Colletotrichum asianum	R35-2	2.47±0.02		sv
Colletotrichum gigasporum	T117-2		2.04±0.18	sv
Colletotrichum mangifericola	A20-2	2.47±0.03		sv
Colletotrichum musae	R50	2.30±0.05		sv
Colletotrichum plorivorum	AS-1		1.52±0.04	mv
Colletotrichum plorivorum	AS-2		1.51±0.02	mv
Colletotrichum plorivorum	T117		1.51±0.03	mv
Colletotrichum siamense	C51-2		2.25±0.09	sv
Colletotrichum siamense	MF24-5		1.66±0.07	mv
Colletotrichum siamense	P25	2.14±0.03		sv
Diaporthe arecae	MF172-2		1.23±0.07	mv
Diaporthe arecae	T79-3		0.74±0.08	wv
Diaporthe arecae	Nan32-2		0.88±0.05	wv
Diaporthe rosae	T79		0.97±0.11	wv

Table A14 (continued)

Species	Strain code	Lesion diameter on fruits (Mean±SD, cm)[1]	Lesion diameter on leaves (Mean±SD, cm)[2]	Virulence
Diaporth siamensis	MF15-5		1.02±0.19	mv
Diaporthe sojae	MF24-7		1.39±0.05	mv
Diaporthe sp.	C27-1		1.70±0.06	mv
Diaporhte thunbergiicola	A4-3		2.04±0.19	sv
Neofusicoccum sinoeucalypti	P21-2		1.25±0.03	mv
Neopestalotiopsis chrysea	AS-3		1.67±0.11	mv
Neopestalotiopsis cubana	MF24-2		2.29±0.12	sv
Neopestalotiopsis dendrobii	T79-2		1.47±0.07	mv
Neopestalotiopsis mangiferae	MF149-1	2.82±0.02		sv
Neopestalotiopsis mangiferae	MF116-1	1.65±0.03		mv
Neopestalotiopsis mangifericola	MF41-2	0.15±0.02		nv
Neopestalotiopsis mangiferigena	Nan31-3		1.50±0.04	mv
Neopestalotiopsis psidii	C20		1.49±0.03	mv
Neopestalotiopsis rhododendri	MF172-3	0.11±0.01		nv
Neopestalotiopsis sp. 1	MF172-1	0.11±0.02		nv
Neopestalotiopsis sp. 2	MF108-1		1.40±0.04	mv
Neoscytalidium dimidiatum	T82	1.81±0.01		mv

Table A14 (continued)

Species	Strain code	Lesion diameter on fruits (Mean±SD, cm)[1]	Lesion diameter on leaves (Mean±SD, cm)[2]	Virulence
Pestalotiopsis humicola	A4-2		2.29±0.07	sv
Pestalotiopsis menhaiensis	M12-2		2.09±0.22	sv
Pseudopallidocercospora mangiferae	H2		1.32±0.02	mv
Pseudopallidocercospora mangiferae	H2-2		1.29±0.06	mv
Zasmidium mangiferae	Nan31		1.51±0.04	mv

Note 1=The virulence of the isolates was evaluated by measuring lesion length at 7 days post inoculation (DPI) in two perpendicular directions on fruits; 2=The virulence of the isolates was evaluated by measuring lesion length at 7 days post inoculation (DPI) in two perpendicular directions on leaves; 3mv = Moderately virulent; 4wv = Weakly virulent; 5nv = Non-virulent; 6sv = Strongly virulent

APPENDIX F

FUNGAL FOOTPRINTS IN THE TROPICS: AN UPDATE ON SPECIES DIVERSITY LINKED TO DISEASED FRUIT CROPS AND ORNAMENTALS IN NORTHERN THAILAND

Table A15 Primers and respective PCR condition used in this study

Genera	Primers	PCR condition
Cercospora	ITS(ITS4/ITS5)	94°C: 3 min, (94°C: 30 s, 56°C: 50 s, 72°C: 1 min) ×32 cycles, 72°C: 10 min
	GAPDH (Gpd1-LM/Gpd2-LM)	95°C: 5 min, (95°C: 1 min, 56°C: 1 min, 72°C: 1 min) ×30 cycles, 72°C: 10 min
	TEF (EF1-728F/EF2)	94°C: 3 min, (94°C: 30 s, 58°C: 1:30 min, 72°C: 1:20 min) ×40 cycles, 72°C: 10 min
	Actin (ACT-512F/ACT-783R	95°C: 5 min, (95°C: 30 s, 52°C: 50 s, 72°C: 1 min) ×40 cycles, 72°C: 10 min
	CaM (CAL-228F/CAL2Rd)	95°C: 5 min, (95°C: 30 s, 54°C: 50 s, 72°C: 1 min) ×40 cycles, 72°C: 10 min
	Histone (CYLH3F/CYLH3R)	94°C: 3 min, (95°C: 30 s, 57°C: 30 s, 72°C: 1 min) ×40 cycles, 72°C: 10 min
Colletotrichum	ITS(ITS4/ITS5)	94°C: 3 min, (94°C: 30 s, 56°C: 50 s, 72°C: 1 min) ×32 cycles, 72°C: 10 min
	GAPDH (GDF/GDR)	95°C: 5 min, (95°C: 50 s, 57°C: 50 s, 72°C: 1 min) ×40 cycles, 72°C: 10 min
	Chitin (CHS79F/CHS345 R)	94°C: 5 min, (94°C: 50 s, 58°C: 30 s, 72°C: 1:30 min) ×35cycles, 72°C: 10 min
	Actin (ACT-512F/ACT-783R)	95°C: 5 min, (95°C: 30 s, 52°C: 50 s, 72°C: 1 min) ×40 cycles, 72°C: 10 min
	β-tubulin (Btub2Fd/Btub4Rd)	94°C: 3 min, (94°C: 30 s, 58°C: 1:30 min, 72°C: 1:20 min) ×40 cycles, 72°C: 10 min

Table A15 (continued)

Genera	Primers	PCR condition
	Tub (Bt-2a/Bt-2b)	94°C: 3 min, (94°C: 30 s, 58°C: 1:30 min, 72°C: 1:20 min) ×40 cycles, 72°C: 10 min
Diaporthe	ITS (ITS4/ITS5)	94°C: 3 min, (94°C: 30 s, 56°C: 50 s, 72°C: 1 min) ×32 cycles, 72°C: 10 min
	CaM (CAL228F/CAL737R)	95°C: 5 min, (95°C: 30 s, 54°C: 50 s, 72°C: 1 min) ×40 cycles, 72°C: 10 min
	CaM (CL1/CL2A)	95°C: 5 min, (95°C: 30 s, 54°C: 50 s, 72°C: 1 min) ×40 cycles, 72°C: 10 min
	his3 (CYLH3F/H3-1b)	94°C: 3 min, (95°C: 30 s, 57°C: 30 s, 72°C: 1 min) ×40 cycles, 72°C: 10 min
	β-tubulin (Btub2Fd/Btub4Rd)	94°C: 3 min, (94°C: 30 s, 58°C: 1:30 min, 72°C: 1:20 min) ×40 cycles, 72°C: 10 min
Lasiodiplodia	ITS (ITS4/ITS5)	94°C: 3 min, (94°C: 30 s, 56°C: 50 s, 72°C: 1 min) ×32 cycles, 72°C: 10 min
	TEF1 (EF1-728F/EF1-986R)	94 °C 5 min, (94 °C, 45 s, 58 °C 30 s, 72 °C, 90 s) × 40 cycles, 72 °C, 7 min
	TUB2 (Bt-2a/Bt-2b)	94 °C 5 min, (94 °C, 45 s, 52 °C 30 s, 72 °C, 60 s) × 40 cycles, 72 °C, 7 min
	rbp2 (RPB2-5f2/fRPB2-7cR)	initial denaturation (95 C, 5 min), touch-down amplification (5 cycles of 95 C for 45 s, 60 C for 45 s, and 72 C for 120 s; 5 cycles of 95 C for 45 s, 58 C for 45 s, and 72 C for 120 s; and 30 cycles of 95 C for 45 s, 54 C for 45 s, and 72 C for 120 s), and final elongation at 72 C for 8 min
Neofusicoccum	ITS (ITS4/ITS5)	94°C: 3 min, (94°C: 30 s, 56°C: 50 s, 72°C: 1 min) ×32 cycles, 72°C: 10 min
	rpb2 (RPB2-5f2/fRPB2-7cR)	95°C，5 min, (95°C，45 s，54°C，45 s，72°C，120 s）x30 cycles，72°C，8 min
	TUB2 (Bt-2a/Bt-2b)	94 °C 5 min, (94 °C, 45 s, 52 °C 30 s, 72 °C, 60 s) × 40 cycles, 72 °C, 7 min
	TEF1 (EF1-728F/EF1-986R)	94 °C 5 min, (94 °C, 45 s, 52 °C 30 s, 72 °C, 90 s) × 40 cycles, 72 °C, 7 min

Table A15 (continued)

Genera	Primers	PCR condition
Neopestalotiopsis	ITS (ITS4/ITS5)	94°C: 3 min, (94°C: 30 s, 56°C: 50 s, 72°C: 1 min) ×32 cycles, 72°C: 10 min
	TEF (EF-728F/EF2)	95 °C 5 min, (95 °C, 30 s, 48 °C 30 s, 72 °C, 1 min) × 35 cycles, 72 °C, 7 min
Phyllosticta	β-tubulin (Btub2Fd/Btub4Rd)	94°C: 3 min, (94°C: 30 s, 58°C: 1:30 min, 72°C: 1:20 min) ×40 cycles, 72°C: 10 min
	ITS (ITS4/ITS5)	94°C: 3 min, (94°C: 30 s, 56°C: 50 s, 72°C: 1 min) ×32 cycles, 72°C: 10 min
	ACT (ACT-512F/ACT-783R)	95°C: 5 min, (95°C: 30 s, 52°C: 50 s, 72°C: 1 min) ×40 cycles, 72°C: 10 min
	TEF (EF1-728F/EF2)	94°C: 3 min, (94°C: 30 s, 58°C: 1:30 min, 72°C: 1:20 min) ×40 cycles, 72°C: 10 min
	LSU (LROR/LR5)	94°C: 5 min, (94°C: 30 s, 54°C: 50 s, 72°C: 1 min) ×35 cycles, 72°C: 10 min
	GPDH (GPD1-LM/GPD2-LM)	95°C: 5 min, (95°C: 1 min, 56°C: 1 min, 72°C: 1 min) ×30 cycles, 72°C: 10 min.
Pseudocercospora	ITS (ITS4/ITS5)	94°C: 3 min, (94°C: 30 s, 56°C: 50 s, 72°C: 1 min) ×32 cycles, 72°C: 10 min
	Actin (ACT-512F/ACT-783R)	95°C: 5 min, (95°C: 30 s, 52°C: 50 s, 72°C: 1 min) ×40 cycles, 72°C: 10 min
	TEF (EF1-728F/EF2)	95 °C 5 min, (95 °C, 30 s, 48 °C 30 s, 72 °C, 1 min) × 35 cycles, 72 °C, 7 min
	TEF1 (EF1-728F/EF1-986R)	94 °C 5 min, (94 °C, 45 s, 52 °C 30 s, 72 °C, 90 s) × 40 cycles, 72 °C, 7 min
Pseudocercospora	rpb2 (RPB2-5f2/fRPB2-7cR)	initial denaturation (95 C, 5 min), touch-down amplification (5 cycles of 95 C for 45 s, 60 C for 45 s, and 72 C for 120 s; 5 cycles of 95 C for 45 s, 58 C for 45 s, and 72 C for 120 s; and 30 cycles of 95 C for 45 s, 54 C for 45 s, and 72 C for 120 s), and final elongation at 72 C for 8 min
Pseudoplagiostoma	ITS (ITS4/ITS5)	94°C: 3 min, (94°C: 30 s, 56°C: 50 s, 72°C: 1 min) ×32 cycles, 72°C: 10 min

Table A15 (continued)

Genera	Primers	PCR condition
	TEF (EF-728F/EF2)	95 °C 5 min, (95 °C, 30 s, 48 °C 30 s, 72 °C, 1 min) × 35 cycles, 72 °C, 7 min
	LSU (LROR/LR5)	94°C: 5 min, (94°C: 30 s, 54°C: 50 s, 72°C: 1 min) ×35 cycles, 72°C: 10 min
	TUB2 (Bt-2a/Bt-2b)	94 °C 5 min, (94 °C, 45 s, 52 °C 30 s, 72 °C, 60 s) × 40 cycles, 72 °C, 7 min
Fusarium, Albonectria, Bisifusarium, Neocosmospora	ITS (ITS4/ITS5)	94°C: 3 min, (94°C: 30 s, 56°C: 50 s, 72°C: 1 min) ×32 cycles, 72°C: 10 min
	rpb2 (RPB2-5f2/fRPB2-7cR)	95°C，5 min, (95°C，45 s，54°C，45 s，72°C，120 s）×30 cycles，72°C，8 min
	LSU (LROR/LR5)	94°C: 5 min, (94°C: 30 s, 51°C: 50 s, 72°C: 1 min) ×35 cycles, 72°C: 10 min
	TEF (EF-728F/EF2)	95 °C 5 min, (95 °C, 30 s, 48 °C 30 s, 72 °C, 1 min) × 35 cycles, 72 °C, 7 min
	LSU (LROR/LR5)	94°C: 5 min, (94°C: 30 s, 54°C: 50 s, 72°C: 1 min) ×35 cycles, 72°C: 10 min
	TUB2 (Bt-2a/Bt-2b)	94 °C 5 min, (94 °C, 45 s, 52 °C 30 s, 72 °C, 60 s) × 40 cycles, 72 °C, 7 min
Fusarium, Albonectria, Bisifusarium, Neocosmospora	ITS (ITS4/ITS5)	94°C: 3 min, (94°C: 30 s, 56°C: 50 s, 72°C: 1 min) ×32 cycles, 72°C: 10 min
	rpb2 (RPB2-5f2/fRPB2-7cR)	95°C，5 min, (95°C，45 s，54°C，45 s，72°C，120 s）×30 cycles，72°C，8 min
	LSU (LROR/LR5)	94°C: 5 min, (94°C: 30 s, 51°C: 50 s, 72°C: 1 min) ×35 cycles, 72°C: 10 min
	TUB (T1//Bt-2b)	95°C: 4 min, (95°C: 30 s, 55°C: 30 s, 72°C: 1 min) ×35 cycles, 72°C: 10 min
	tef1 (EF-983/EF2218R)	94°C: 3 min, (94°C: 30 s, 58°C: 1:30 min, 72°C: 1:20 min) ×40 cycles, 72°C: 10 min

Table A16 Details of species isolated from crops and ornamental plants in this study

Species	strain	Host	Record status		GenBank Numbers		
Albonectria				***tef1***	***rpb1***	***rpb2***	***cmdA***
A. durionigenum	N6-2; MFLUCC 25-0041^{T}	Durian (*Durio zibethinus*)		PV130599	PV130601	PV130603	PV130605
A. lansii	P47-2; MFLUCC 25-0069^{T}	Langsat (*Lansium domesticum*)		PV130600	PV130602	PV130604	PV130606
Bisifusarium				***tef1***	***rpb1***	***rpb2***	***cmdA***
B. mangiferae	T115-3; MFLUCC 25-0056^{T}	Mango (*Mangifera indica*)		PV130612	PV130607	PV130609	PV130613
B. thailandica	T74-2; MFLUCC 25-0054^{T}	Dragon fruit (*Selenicereus undatus*)		PV130611	PV130608	PV130610	PV130614
Cercospora			**ITS**	***act***	***cmdA***	***gapdh***	***his3/tef1***
Cer. alocasiicola	C33; MFLUCC 25-0028^{T}	Chinese taro (*Alocasia cucullate*)	PV072645	PV130573	PV130579	PV130582	PV130588/ PV130594
Cer. alocasiicola	C28; MFLUCC 25-0029	Giant taro (*Alocasia macrorrhizos*)	PV072644	PV130572	PV130578	PV130581	PV130587/ PV130593
Cer. capsici	N3-3; MFLUCC 25-0035	Chilli (*Capsicum* sp.)	None PV072646	PV130574	–	PV130583	PV130589/ PV130595
Cer. malloti	Nan25-2; MFLUCC 25-0117	Durian (*Durio zibethinus*)	New host PV072648	PV130576	–	PV130585	PV130591/ PV130597

Table A16 (continued)

Species	strain	Host	Record status	GenBank Numbers				
Cercospora				**ITS**	***act***	***cmdA***	***gapdh***	***his3/tef1***
Cercospora sp.	Nan24; MFLUCC 25-0116	Durian (*Durio zibethinus*)		PV072647	PV130575	–	PV130584	PV130590/ PV130596
Cercospora sp.	R19-5; MFLUCC 25-0048	Papaya (*Carica papaya*)		PV072649	PV130577	PV130578	PV130586	PV130592/ PV130598
Colletotrichum				**ITS**	***gapdh***	***chs-1***	***act***	***tub2***
C. endophyticum	MF16-3; MFLUCC 25-0131	Guava (*Psidium guajava*)	New host	PV069419	PV085931	PV085901	PV085871	PV085960
C. endophyticum	MF2-5; MFLUCC 25-0130	Cocoa (*Theobroma cacao*)	New host	PV069417	PV085929	PV085899	PV085869	PV085958
C. fructicola	MF10-3; MFLUCC 25-0134	Sapodilla (*Sapodilla sapote*)	New host	PV069422	PV085934	PV085904	PV085874	PV085963
C. fructicola	MF21-2; MFLUCC 25-0135	Pepper (*Piper nigrum*)	New host	PV069423	PV085935	PV085905	PV085875	PV085964
C. fructicola	P89-3; MFLUCC 25-0082	Longan (*Dimocarpus longan*)	None	PV069409	PV085921	PV085891	PV085861	PV085951
C. fructicola	R26; MFLUCC 25-0100	Chilli (*Capsicum* sp.)	None	PV069415	PV085927	PV085897	PV085867	PV085956
C. fructicola	R27; MFLUCC 25-0101	Chilli (*Capsicum* sp.)	None	PV069416	PV085928	PV085898	PV085868	PV085957

Table A16 (continued)

Species	strain	Host	Record status	GenBank Numbers				
Colletotrichum				**ITS**	***gapdh***	***chs-1***	***act***	***tub2***
C. gloeosporioides	P146-2a; MFLUCC 25-0073	*Citrus* sp.	None	PV069413	PV085925	PV085895	PV085865	PV085955
C. siamense	N10; MFLUCC 25-0081	Lychee (*Litchi chinensis*)	New geographic	PV069408	PV085920	PV085890	PV085860	PV085950
C. siamense	MF30-1; MFLUCC 25-0139	*Polyscias balfouriana*	New host	PV069426	PV085938	PV085908	PV085878	PV085967
C. siamense	M22; MFLUCC 25-0105	Avocado (*Persea americana*)	None	PV069404	PV085916	PV085886	PV085856	PV085946
C. siamense	P106; MFLUCC 25-0090	*Citrus* sp.	None	PV069411	PV085923	PV085893	PV085863	PV085953
C. siamense	MF4-3; MFLUCC 25-0132	Common Persimmon (*Diospyros virginiana*)	New host	PV069420	PV085932	PV085902	PV085872	PV085961
C. siamense	MF54-3; MFLUCC 25-0133	Common Persimmon (*Diospyros virginiana*)		PV069421	PV085933	PV085903	PV085873	PV085962
C. siamense	M30; MFLUCC 25-0120	Tomato (*Solanum lycopersicum*)	New host	PV069405	PV085917	PV085887	PV085857	PV085947
C. siamense	M30-4; MFLUCC 25-0123	Tomato (*Solanum lycopersicum*)		PV069406	PV085918	PV085888	PV085858	PV085948

Table A16 (continued)

Species	strain	Host	Record status	GenBank Numbers				
Colletotrichum				**ITS**	***gapdh***	***chs-1***	***act***	***tub2***
C. siamense	MF53-2; MFLUCC 25-0140	*Sphagneticola trilobata*	New host	PV069427	PV085939	PV085909	PV085879	PV085968
C. siamense	P102; MFLUCC 25-0087	Pepper (*Piper nigrum*)	New geographic	PV069410	PV085922	PV085892	PV085862	PV085952
C. siamense	MF23-2; MFLUCC 25-0138	*Hibiscus rosa-sinensis*	New host	PV069425	PV085937	PV085907	PV085877	PV085966
C. siamense	A34; MFLUCC 25-0079	Longan (*Dimocarpus longan*)	New host	PV069401	PV085913	PV085883	PV085853	PV085943
C. siamense	A33-2; MFLUCC 25-0078	Longan (*Dimocarpus longan*)		PV069400	PV085912	PV085882	PV085852	PV085942
C. siamense	P144-3; MFLUCC 25-0072	Guava (*Psidium guajava*)	New geographic	PV069412	PV085924	PV085894	PV085864	PV085954
C. siamense	R25; MFLUCC 25-0099	Guava (*Psidium guajava*)		PV069414	PV085926	PV085896	PV085866	–
C. siamense	C49-2; MFLUCC 25-0046	Jackfruit (*Artocarpus heterophyllus*)	New host	PV069402	PV085914	PV085884	PV085854	PV085944
C. siamense	MF40-2; MFLUCC 25-0141	Bamboo Palm (*Chamaedorea seifrizii*)	New host	PV069428	PV085940	PV085910	PV085880	PV085969

Table A16 (continued)

Species	strain	Host	Record status	GenBank Numbers				
Colletotrichum				**ITS**	***gapdh***	***chs-1***	***act***	***tub2***
C. siamense	N9-3; MFLUCC 25-0080	Bamboo Palm (*Chamaedorea seifrizii*)		PV069407	PV085919	PV085889	PV085859	PV085949
C. siamense	A15; MFLUCC 25-0033	Rose apple (*Syzygium jambos*)	New host	PV069399	PV085911	PV085881	PV085851	PV085941
C. siamense	MF88-2; MFLUCC 25-0137	Vanilla (*Vanilla planifolia*)	New host	PV069424	PV085936	PV085906	PV085876	PV085965
C. siamense	M2-2; MFLUCC 25-0057	Langsat (*Lansium domesticum*)	New host	PV069403	PV085915	PV085885	PV085855	PV085945
C. thasutense	MF2-1; MFLUCC 25-0136	Cocoa (*Theobroma cacao*)	New host	PV069418	PV085930	PV085900	PV085870	PV085959
Diaporthe				**ITS**	***tef1***	***tub2***	***cmdA***	***his3***
D. arecae	Ch-4; MFLUCC 25-0126	Durian (*Durio zibethinus*)	New host	PV072676				PV166077
D. arecae	N7-5; MFLUCC 25-0034	Durian (*Durio zibethinus*)		PV072651				PV166075
D. arecae	N7-3; MFLUCC 25-0060	Durian (*Durio zibethinus*)		PV072652				PV166076
D. arecae	MF192-3; MFLUCC 25-0152	Earleaf acacia (*Acacia auriculiformis*)	New host	PV072677				PV166078

Table A16 (continued)

Species	strain	Host	Record status	GenBank Numbers				
Diaporthe				**ITS**	***tef1***	***tub2***	***cmdA***	***his3***
D. capsicicola	R36; MFLUCC 25-0083^{T}	Chilli (*Capsicum annuum*)		PV072669				PV166097
D. capsicicola	Ch-3; MFLUCC 25-0125	Durian (*Durio zibethinus*)		PV072670				PV166098
D. chiangmaiensis	A31-4; MFLUCC 25-0077	Globe amaranth (*Gomphrena globosa*)	New host	PV072668				–
D. discoidispora	MF17-2; MFLUCC 25-0129	*Eugenia uniflora*	New host	PV072682				PV166105
D. durionis	P134; MFLUCC 25-0094^{T}	Durian (*Durio zibethinus*)		PV072672				PV166102
D. lansii	M2-3; MFLUCC 25-0058^{T}	Langsat (*Lansium domesticum*)		PV072663				PV166095
D. lansii	P144-4; MFLUCC 25-0111	Guava (*Psidium guajava*)		PV072664				PV166096
D. perseae-americanae	P5-2; MFLUCC 25-0050^{T}	Avocado (*Persea americana*)		PV072655				PV166101
D. pterocarpi	C47; MFLUCC 25-0044	Yellow iris (*Iris pseudacorus*)	New host	PV072653				PV166093

Table A16 (continued)

Species	strain	Host	Record status	GenBank Numbers				
Diaporthe				**ITS**	***tef1***	***tub2***	***cmdA***	***his3***
D. pterocarpi	MF36-4; MFLUCC 25-0128	Common Jujube (*Ziziphus mauritiana*)	New host	PV072654				PV166094
D. rosae	P31; MFLUCC 25-0075	Avocado (*Persea americana*)	New host	PV072656				PV166079
D. rosae	MF61-2; MFLUCC 25-0156	Paperflower (*Bougainvillea glabra*)	New host	PV072660				PV166083
D. rosae	P35; MFLUCC 25-0053	Durian (*Durio zibethinus*)	New host	PV072657				PV166080
D. rosae	P35-2; MFLUCC 25-0076	Durian (*Durio zibethinus*)		PV072658				PV166081
D. rosae	P89; MFLUCC 25-0064	Longan (*Dimocarpus longan*)	New host	PV072659				PV166082
D. rosae	MF150-1; MFLUCC 25-0155	*Tabebuia aurea*	New host	PV072661				PV166084
D. rosae	MF171-1; MFLUCC 25-0153	*Cladrastis kentukea*	New host	PV072662				PV166085
D. siamensis	Ch-6; MFLUCC 25-0127	Durian (*Durio zibethinus*)	New host	PV072678				PV166103

Table A16 (continued)

Species	strain	Host	Record status	GenBank Numbers				
Diaporthe				**ITS**	***tef1***	***tub2***	***cmdA***	***his3***
D. sojae	P90-1; MFLUCC 25-0071	Longan (*Dimocarpus longan*)	New host	PV072665				PV166090
D. sojae	P112; MFLUCC 25-0093	Guava (*Psidium guajava*)	New host	PV072667				PV166092
D. sojae	P111-1; MFLUCC 25-0091	Guava (*Psidium guajava*)		PV072666				PV166091
Diaporthe sp.	MF58-1; MFLUCC 25-0154	Cape Jasmine (*Gardenia jasminoides*)	None	PV072681				PV166104
D. tamarindi	MF99-2; MFLUCC 25-0151^{T}	Tamarind (*Tamarindus indica*)		PV072680				PV166100
D. tamarindi	L1-1; MFLUCC 25-0150	Rambutan (*Nephelium lappaceum*)		PV072679				PV166099
D. tulliensis	Nan2-2; MFLUCC 25-0113	Lychee (*Litchi chinensis*)	New host	PV072673				PV166087
D. tulliensis	M30-2; MFLUCC 25-0121	Tomato (*Solanum lycopersicum*)	New host	PV072674				PV166088
D. tulliensis	M30-3; MFLUCC 25-0122	Tomato (*Solanum lycopersicum*)		PV072675				PV166089

Table A16 (continued)

Species	strain	Host	Record status	GenBank Numbers			
Diaporthe				**ITS**	***tef1***	***tub2***	***cmdA***	***his3***
D. tulliensis	P103-5; MFLUCC 25-0088	Durian (*Durio zibethinus*)	New host	PV072671				PV166086
Fusarium					***tef1***	***rpb1***	***rpb2***	***cmdA***
F. coffeibaccae	T106-4; MFLUCC 25-0055	Guava (*Psidium guajava*)	New host		PV130645	PV130629	PV130637	PV130653
F. endophyticum	A7-1; MFLUCC 25-0030	*Citrus* sp.	New host		PV130639	PV130623	PV130631	PV130647
F. endophyticum	P85; MFLUCC 25-0063	Longan (*Dimocarpus longan*)	New host		PV130640	PV130624	PV130632	PV130648
F. fujikuroi	P3(165); MFLUCC 25-0074	Avocado (*Persea americana*)	New host		PV130644	PV130628	PV130636	PV130652
F. hainanense	P79; MFLUCC 25-0070	Mango (*Mangifera indica*)	New host		PV130669	PV130657	PV130662	PV130672
F. pernambucanum	P28; MFLUCC 25-0066	Avocado (*Persea americana*)	New host		PV130665	PV130655	PV130660	PV130670
F. pernambucanum	R15; MFLUCC 25-0085	Papaya (*Carica papaya*)	New host		PV130666	PV130658	PV130663	PV130673

Table A16 (continued)

Species	strain	Host	Record status	GenBank Numbers			
Fusarium				***tef1***	***rpb1***	***rpb2***	***cmdA***
F. pseudocircinatum	A7-2; MFLUCC 25-0031	*Citrus* sp.	New host	PV130643	PV130627	PV130635	PV130651
F. pseudocircinatum	A1; MFLUCC 25-0038	*Spathiphyllum* sp.	New host	PV130642	PV130626	PV130634	PV130650
F. pseudocircinatum	R19-2; MFLUCC 25-0065	Papaya (*Carica papaya*)	New host	PV130641	PV130625	PV130633	PV130649
F. sacchari	T24-3; MFLUCC 25-0049	Banana (*Musa* sp.)	New geographic	PV130646	PV130630	PV130638	PV130654
F. sulawesiense	P76-2; MFLUCC 25-0062	Longan (*Dimocarpus longan*)	New host	PV130667	PV130656	PV130661	PV130671
F. sulawesiense	R17; MFLUCC 25-0047	Papaya (*Carica papaya*)	New host	PV130668	PV130659	PV130664	PV130674
Lasiodiplodia				**ITS**	***tef1***	***tub2***	***rpb2***
L. brasiliensis	Ch-2; MFLUCC 25-0124	Durian (*Durio zibethinus*)	New host	PV069460	PV086024	PV130680	PV130694
L. chonburiensis	C35-1; MFLUCC 25-0027	Morinda (*Morinda citrifolia*)	New host	PV069457	PV086021	PV130677	PV130691
L. pseudotheobromae	C73; MFLUCC 25-0110	Yellow iris (*Iris pseudacorus*)	New host	PV069459	PV086023	PV130679	PV130693

Table A16 (continued)

Species	strain	Host	Record status	GenBank Numbers			
Lasiodiplodia				**ITS**	***tef1***	***tub2***	***rpb2***
L. pseudotheobromae	C44; MFLUCC 25-0084	Thorny olive (*Elaeagnus pungens*)	New host	PV069458	PV086022	PV130678	PV130692
L. pseudotheobromae	P41; MFLUCC 25-0061	Avocado (*Persea americana*)	None	PV069466	PV086030	PV130686	PV130700
L. pseudotheobromae	M21-2; MFLUCC 25-0104	Avocado (*Persea americana*)		PV069461	PV086025	PV130681	PV130695
L. pseudotheobromae	A8; MFLUCC 25-0032	Avocado (*Persea americana*)		PV069456	PV086020	PV130676	PV130690
L. pseudotheobromae	P103-6; MFLUCC 25-0089	Durian (*Durio zibethinus*)	None	PV069468	–	PV130688	PV130702
L. pseudotheobromae	N7-4; MFLUCC 25-0037	Durian (*Durio zibethinus*)		PV069463	PV086027	PV130683	PV130697
L. pseudotheobromae	Nan5; MFLUCC 25-0114	Lychee (*Litchi chinensis*)	New host	PV069464	PV086028	PV130684	PV130698
L. pseudotheobromae	Nan27; MFLUCC 25-0118	Longan (*Dimocarpus longan*)	None	PV069465	PV086029	PV130685	PV130699
L. pseudotheobromae	P95; MFLUCC 25-0086	Longan (*Dimocarpus longan*)		PV069467	PV086031	PV130687	PV130701

Table A16 (continued)

Species	strain	Host	Record status	GenBank Numbers			
Lasiodiplodia				**ITS**	***tef1***	***tub2***	***rpb2***
L. theobromae	A5; MFLUCC 25-0039	Banana (*Musa* sp.)	New geographic	PV069455	PV086019	PV130675	PV130689
L. theobromae	N6; MFLUCC 25-0036	Durian (*Durio zibethinus*)	New host	PV069462	PV086026	PV130682	PV130696
Neocosmospora				***tef1***	***rpb1***	***rpb2***	***cmdA***
N. diminuta	N6-4; MFLUCC 25-0059	Durian (*Durio zibethinus*)	New host	PV130619	PV130615	PV130617	PV130621
N. metavorans	S1-1; MFLUCC 25-0040	Avocado (*Persea americana*)	New host	PV130620	PV130616	PV130618	PV130622
Neofusicoccum				**ITS**	***tef1***	***tub2***	***rpb2***
Neo. parvum	P10; MFLUCC 25-0051	Avocado (*Persea americana*)	New geographic	PV069473	PV086010	PV086013	PV086016
Neo. parvum	P10-3; MFLUCC 25-0052	Avocado (*Persea americana*)		PV069474	PV086011	PV086014	PV086017
Neo. parvum	R34; MFLUCC 25-0102	Avocado (*Persea americana*)		PV069475	PV086012	PV086015	PV086018
Neopestalotiopsis					**ITS**	***tef1***	***tub2***
N. cubana	P46; MFLUCC 25-0068	Langsat (*Lansium domesticum*)	New host		PV084818	PV085994	PV085974

Table A16 (continued)

Species	strain	Host	Record status	GenBank Numbers		
Neopestalotiopsis				**ITS**	***tef1***	***tub2***
N. cubana	L2-6; MFLUCC 25-0147	Rambutan (*Nephelium lappaceum*)	New host	PV084822	PV085998	PV085978
N. cubana	L3-8; MFLUCC 25-0145	Mangosteen (*Garcinia mangostana*)	New host	PV084824	PV086000	PV085980
N. cubana	L3-5; MFLUCC 25-0144	Mangosteen (*Garcinia mangostana*)		PV084823	PV085999	PV085979
N. cubana	MF216-1; MFLUCC 25-0149	Black tupelo (*Nyssa sylvatica*)	New host	PV084825	PV086001	PV085981
N. cubana	M22-2; MFLUCC 25-0106	Avocado (*Persea americana*)	New host	PV084820	PV085996	PV085976
N. cubana	M23; MFLUCC 25-0107	Avocado (*Persea americana*)		PV084821	PV085997	PV085977
N. cubana	P111-2; MFLUCC 25-0092	Guava (*Psidium guajava*)	New host	PV084819	PV085995	PV085975
N. hydeana	R34-3; MFLUCC 25-0103	Avocado (*Persea americana*)	New host	PV084828	PV086004	PV085984
N. litchii	M26; MFLUCC 25-0109^{T}	Lychee (*Litchi chinensis*)		PV084830	PV086006	PV085986

Table A16 (continued)

Species	strain	Host	Record status	GenBank Numbers		
Neopestalotiopsis				**ITS**	***tef1***	***tub2***
N. litchii	MF170-2; MFLUCC 25-0142	Common pawpaw (*Asimina triloba*)		PV084831	PV086007	PV085987
N. litchii	R34-4; MFLUCC 25-0112	Avocado (*Persea americana*)		PV084829	PV086005	PV085985
N. litchiicola	M25; MFLUCC 25-0108^{T}	Lychee (*Litchi chinensis*)		PV084815	PV085991	PV085971
N. litchiicola	L2-4; MFLUCC 25-0146	Rambutan (*Nephelium lappaceum*)		PV084816	PV085992	PV085972
N. litchiicola	N9-2; MFLUCC 25-0042	Bamboo Palm (*Chamaedorea seifrizii*)		PV084814	PV085990	PV085970
N. neomaricae	MF182-1; MFLUCC 25-0143	*Casearia lasiophylla*	New host	PV084832	PV086008	PV085988
N. rosicola	P143; MFLUCC 25-0096	Coconut (*Cocos nucifera*)	New host	PV084827	PV086003	PV085983
N. rosicola	P142; MFLUCC 25-0095	Coconut (*Cocos nucifera*)		PV084826	PV086002	PV085982

Table A16 (continued)

Species	strain	Host	Record status			GenBank Numbers	
Neopestalotiopsis						**ITS**	***tef1***	***tub2***
N. samarangensis	MF177-2; MFLUCC 25-0148	Mangosteen (*Garcinia mangostana*)	New host			PV084833	PV086009	PV085989
Neopestalotiopsis. sp.	C48; MFLUCC 25-0045	Yellow iris (*Iris pseudacorus*)				PV084817	PV085993	PV085973
Phyllosticta				**ITS**	**LSU**	***tef1***	***act***	***gapdh***
Ph. capitalensis	MF54-2; MFLUCC 25-0157	Common Persimmon (*Diospyros virginiana*)	New host	PV069472	PV077004	PV130709	PV130713	PV130717
Ph. capitalensis	N1-2; MFLUCC 25-0043	Cabbage (*Brassica oleracea*)	New host	PV069469	PV077001	PV130707	PV130710	PV130714
Ph. capitalensis	Nan18; MFLUCC 25-0115	Guava (*Psidium guajava*)	New geographic	PV069470	PV077002	–	PV130711	PV130715
Ph. capitalensis	P90-3; MFLUCC 25-0098	Longan (*Dimocarpus longan*)	New host	PV069471	PV077003	PV130708	PV130712	PV130716
Pseudocercospora					**ITS**	***act***	***tef1***	***rpb2***
Pse. terengganuensis	A32; MFLUCC 25-0097	Beach spider lily (*Hymenocallis littoralis*)	New geographic		PV072650	PV130718	PV130719	PV130720
Pseudoplagiostoma					**ITS**	**LSU**	***tef1***	***tub2***

Table A16 (continued)

Species	strain	Host	Record status	GenBank Numbers			
Pseudoplagiostoma				**ITS**	**LSU**	***tef1***	***tub2***
P. perseae	Nan30; MFLUCC 25-0119	Avocado (*Persea americana*)	New geographic	PV076959	PV076999	PV130705	PV130703
P. perseae	P39-1; MFLUCC 25-0067	Avocado (*Persea americana*)		PV076960	PV077000	PV130706	PV130704

Note Type strains are in indicated with "[T]"

APPENDIX G

PUBLICATIONS

Current Research in Environmental & Applied Mycology (Journal of Fungal Biology)
13(1): 57–67 (2023) ISSN 2229-2225
www.creamjournal.org
Article
Doi 10.5943/cream/13/1/4

Paramyrothecium amorphophalli sp. nov., a causal agent of leaf blight on elephant foot yam in northern Thailand

Armand A[1,2], Bundhun D[1,2], Bhunjun CS[1,2], Punyaboon W[1] and Jayawardena RS[1,2*]

[1]*Center of Excellence in Fungal Research, Mae Fah Luang University, Chiang Rai 57100, Thailand*
[2]*School of Science, Mae Fah Luang University, Chiang Rai 57100, Thailand*

Armand A, Bundhun D, Bhunjun CS, Punyaboon W, Jayawardena RS 2023 – *Paramyrothecium amorphophalli* sp. nov., a causal agent of leaf blight on elephant foot yam in northern Thailand. Current Research in Environmental & Applied Mycology (Journal of Fungal Biology) 13(1), 57–67, Doi 10.5943/cream/13/1/4

Abstract

Paramyrothecium was introduced in 2016 containing 20 species and many species have been reported as plant pathogens, causing leaf blight and leaf spots on different plant species. This study revealed a new species *Paramyrothecium amorphophalli* from symptomatic leaves of elephant foot yam (*Amorphophallus* sp.), collected from Chiang Rai, Thailand based on distinct morphological characteristics and phylogenetic analyses. The isolate formed a distinct lineage from *Paramyrothecium eichhorniae* and *P. vignicola* based on maximum likelihood, maximum parsimony and Bayesian posterior probability analyses of ITS, *cmdA*, *rpb2* and *tub2* sequence data. Furthermore, pathogenicity assays confirmed that *P. amorphophalli* is pathogenic to the original host, causing leaf blight.

Keywords – 1 new species – multi-locus phylogeny – plant pathogen – taxonomy – yam

Introduction

Elephant foot yam is a tropical tuber crop that belongs to *Amorphophallus*. It is a significant edible tuberous crop extensively cultivated in tropical and subtropical regions, especially in China and India (John et al. 2014, Prasad et al. 2017). Konjac Glucomannan (KGM) extracted from the tuber of *Amorphophallus konjac*, is used as a medicinal ingredient and nutritional supplement (Yao-ling et al. 2013). Among the significant health advantages of KGMs are those related to lowering cholesterol, regulating triglyceride levels, enhancing sugar levels, and promoting human immunological and intestinal functions (Yao-ling et al. 2013). Among plant pathogens, fungi are considered devastating agents responsible for economic losses in the agriculture circle and threatening food security (Hyde et al. 2018, Gomdola et al. 2022, Withee et al. 2022). Prasad et al. (2017) reported *Colletotrichum siamense* from India causing anthracnose on elephant foot yam. *Sclerotium rolfsii* is a devastating soil-borne disease which causes collar rot on this plant (Sahoo et al. 2016). As the correct identification is the first and vital step in disease management, it becomes imperative to consider a proper taxonomic identification and understanding of fungi to undertake appropriate strategies for managing plant diseases (Bhunjun et al. 2021, Jayawardena et al. 2021).

Paramyrothecium (*Stachybotryaceae*, *Hypocreales*, *Sordariomycetes*) (Wijayawardene et al. 2022) was introduced to accommodate taxa earlier included in *Myrothecium sensu lato* (Lombard et al. 2016). According to morphological characteristics and molecular analyses, Lombard et al.

Submitted 11 October 2022, Accepted 30 January 2022, Published 14 February 2023
Corresponding Author: Ruvishika S. Jayawardena – e-mail – ruvishika.jay@mfu.ac.th

plants

MDPI

Brief Report

First Report of *Colletotrichum fructicola* Causing Fruit Rot and Leaf-Tip Dieback on Pineapple in Northern Thailand

Alireza Armand [1,2], Kevin David Hyde [1,2,3] and Ruvishika Shehali Jayawardena [1,2,*]

[1] Center of Excellence in Fungal Research, Mae Fah Luang University, Chiang Rai 57100, Thailand
[2] School of Science, Mae Fah Luang University, Chiang Rai 57100, Thailand
[3] Innovative Institute for Plant Health, Zhongkai University of Agriculture and Engineering, Guangzhou 510225, China
* Correspondence: ruvishika.jay@mfu.ac.th

Abstract: Pineapple is one of the most economically important fruits in tropical countries, particularly in Thailand. Canned pineapple is currently Thailand's main exported commodity to many countries, including the United States, Russia, Germany, Poland, and Japan. Fungal diseases are considered a permanent threat to fruits in the pre- and post-harvest stages, leading to considerable economic losses. Fungal disease is one of the primary causes of massive yield losses in pineapples around the world. *Colletotrichum* species are the most common fungal pathogens affecting different tropical fruits. Although there are many reports regarding *Colletotrichum* species associated with pineapple, they do not have molecular data to confirm species identification. However, the occurrence of *Colletotrichum* species on pineapple has not been reported in Thailand so far. In this study, we isolated and identified *Colletotrichum fructicola* on pineapple in northern Thailand and have proven its pathogenicity to the host. This is the first report of the occurrence of *Colletotrichum* in pineapple, based on morpho-molecular approaches.

Keywords: *Ananas comosus*; phylogeny; plant pathogen; new record; taxonomy; tropical fruit

check for updates

Citation: Armand, A.; Hyde, K.D.; Jayawardena, R.S. First Report of *Colletotrichum fructicola* Causing Fruit Rot and Leaf-Tip Dieback on Pineapple in Northern Thailand. *Plants* **2023**, *12*, 971. https://doi.org/10.3390/plants12040971

Academic Editor: Vincent G.M. Bert

Received: 20 December 2022
Revised: 9 February 2023
Accepted: 13 February 2023
Published: 20 February 2023

Copyright: © 2023 by the author. Licensee MDPI, Basel, Switzerland. This article is an open access article distributed under the terms and conditions of the Creative Commons Attribution (CC BY) license (https://creativecommons.org/licenses/by/4.0/).

1. Introduction

Pineapple (*Ananas comosus* (L.) Merr.) is one of the edible and nutritious fruits of the Bromeliaceae, grown in tropical and subtropical countries [1]. Asia, South Central America, and Africa are the world's leading areas producing this fruit [2]. Pineapple is the second largest tropical crop in the world [2] and the third most consumed fruit worldwide [3]. Brazil, China, Costa Rica, India, the Philippines, and Thailand are the top pineapple-producing countries [1]. Pineapple could be eaten as a fresh fruit or selected as a basic raw ingredient used in the confectionery industry [4–6]. The fruit contains immense nutrients and is abundant in vitamins A, C, B1, and B6 [7–9]. It also has proteins, carbohydrates, fiber, copper, manganese, and several minerals [8,10].

In Thailand, pineapple products have been regarded as economic commodities for export [11]. Thailand is currently the second-largest supplier of processed pineapple fruit in the world. Production areas for pineapple in Thailand have been divided into northern, northeastern, central, and southern parts [12]. Most cultivated areas are in Prachuap Khiri Khan, Rayong, Ratchaburi, and Chonburi provinces [11]. Pineapple is classified into five groups based on the morphology of the leaf and fruit, namely Abacaxi, Cayenne, Maipure or Perolera, Queen, and Spanish [13]. Among these, Cayenne, Queen, and Spanish are cultivated in Thailand [14]. Nang Lae district in Chiang Rai province is the most pineapple-cultivating area, and Nang Lae (Cayenne group) and Phu Lae (Queen group) are the most common varieties in northern Thailand (http://www.doa.go.th/; https://www.saio.co.th/; accessed on 12 December 2022). The pineapple-growing area in Thailand is around 72,656 hectares, with an annual production of 1,680,884 metric tons. The total canned pineapples exported from Thailand were 290,524 metric tons in 2020, valued at about 345 million US dollars [15].

Mycosphere 14(2): 107–129 (2023) www.mycosphere.org ISSN 2077 7019
Article
Doi 10.5943/mycosphere/14/si2/2

Identification and characterization of *Colletotrichum* species associated with durian fruit in northern Thailand

Armand A[1,2], Hyde KD[1,2,3], Huanraluek N[1], Wang Y[4*] and Jayawardena RS[1,2*]

[1]*Center of Excellence in Fungal Research, Mae Fah Luang University, Chiang Rai 57100, Thailand*
[2]*School of Science, Mae Fah Luang University, Chiang Rai 57100, Thailand*
[3]*Innovative Institute for Plant Health, Zhongkai University of Agriculture and Engineering, Guangzhou 510225, P.R. China*
[4]*Department of Plant Pathology, Agriculture College, Guizhou University, Guiyang, 550025, China*

Armand A, Hyde KD, Huanraluek N, Wang Y, Jayawardena RS 2023 – Identification and characterization of *Colletotrichum* species associated with durian fruit in northern Thailand. Mycosphere 14(2), 107–129, Doi 10.5943/mycosphere/14/si2/2

Abstract

Colletotrichum is one of the most important plant pathogenic genera affecting different plant species, particularly tropical and sub-tropical crops and fruits. Species of the genus can cause many diseases, including fruit rots, crown rots, stem end rots, and anthracnose. The objective of the present study was to identify the *Colletotrichum* species associated with durian fruit rots in northern Thailand. Based on morphological study and phylogenetic analyses of five loci (internal transcribed spacer (ITS), actin (*ACT*), chitin synthase 1 (*CHS-1*), glyceraldehyde-3-phosphate dehydrogenase (*GAPDH*), and ß-tubulin (*TUB2*)), four species belonging to three complexes were identified and described. *Colletotrichum durionigenum* is introduced as a new species, and *C. gigasporum*, *C. pandanicola*, and *C. truncatum* are described and illustrated as new host records.

Keywords – 1 new species – Diversity – *Durio* spp. – Glomerellaceae – Phylogeny – Phytopathogen

Introduction

Durian (*Durio* sp., Malvaceae) is a tropical fruit native to Southeast Asia and one of the most popular fruits in Thailand (Teh et al. 2017). This fruit is known as the 'king of fruits' for its formidable spiny husk, unique overwhelming flavor and odor (Bampenrat et al. 2020, Li et al. 2012). The three leading durian-producing countries are Thailand, Malaysia, and Indonesia. Thailand is the main durian producer in the world. Thailand's commercial durian production was 1,111.93 thousand metric tons in 2020 (National Agricultural Big Data Center; OAE 2021).

Durian is one of the most economically important exported fruits in Thailand (Charoensumran et al. 2021). Thailand's most popular cultivars for consumption and export include 'Chanee', 'Gaan Yaow', 'Gradumtong', 'Nok Yib', 'Puang Mani' and 'Monthong' (Lim and Sangchote 2003). Sweeter cultivars with a mild odor are popular in Thailand (Monthong), whereas pungent and bitter varieties are popular in Malaysia and Singapore (Musang King) (Teh et al. 2017). The complexity of different cultivars and distinctive odors is due to differences in sulfur volatiles, esters, alcohol, and acid percentages (Siriphanich 2011). A draft genome assembly of *D. zibethinus* was provided by Teh et al. (2017).

Durian is also subjected to different kinds of fungal diseases: fruit rots, stem cankers and root rots, resulting in low yield and quality. Among these diseases, fruit rots are a serious problem in

Submitted 13 January 2023, Accepted 10 February 2023, Published 23 March 2023
Corresponding Author: Ruvishika Shehali Jayawardena – e-mail – ruvishika.jay@mfu.ac.th,
Yong Wang – e-mail – yongwangbis@aliyun.com

Received: 30 March 2023 | Accepted: 24 July 2023
DOI: 10.1111/ppa.13792

Plant Pathology WILEY

ORIGINAL ARTICLE

Morphomolecular identification and pathogenicity of *Colletotrichum* species associated with avocado anthracnose in northern Thailand

Alireza Armand[1,2] | Ruvishika S. Jayawardena[1,2,3]

[1]Center of Excellence in Fungal Research, Mae Fah Luang University, Chiang Rai, Thailand
[2]School of Science, Mae Fah Luang University, Chiang Rai, Thailand
[3]Kyung Hee University, Seoul, South Korea

Correspondence
Ruvishika S. Jayawardena, Center of Excellence in Fungal Research, Mae Fah Luang University, Chiang Rai 57100, Thailand.
Email: ruvishika.jay@mfu.ac.th

Funding information
National Science, Research and Innovation Fund: Thailand Science Research Innovation (Basic Research Fund 2021) "Biodiversity, taxonomy, phylogeny and evolution of Colletotrichum on Avocado, Citrus, Durian and Mango in northern Thailand", Grant/Award Number: 652A01003

Abstract

Avocado production is restricted globally by the anthracnose disease caused by *Colletotrichum* species. In Thailand, anthracnose symptoms can be found on avocado leaves and fruits, and it is an important postharvest disease, reducing the shelf life of the fruits and causing huge economic losses. Avocado leaves and fruits showing anthracnose disease were collected from Chiang Rai province, located in northern Thailand, and the *Colletotrichum* species isolated from the samples were identified based on morphological examination and multigene phylogenetic analyses. Phylogenetic analyses using five loci (ITS, *ACT*, *CHS-1*, *GAPDH* and *TUB2*) coupled with the morphology of 11 isolates showed that they belonged to four known species of *Colletotrichum*. *Colletotrichum endophytica*, *C. fructicola* and *C. siamense* are illustrated as new geographical records, and *C. henanense* is characterized as a new host record. Furthermore, the pathogenicity of these species in avocado fruits and leaves (West Indian variety) has been proven. In addition, this study provides further evidence for the synonymization of *C. pandanicola* and *C. parvisporum* with *C. siamense*.

KEYWORDS
anthracnose, Colletotrichum, new records, pathogenicity, poly-approach identification

1 | INTRODUCTION

The commercial avocado (*Persea americana*) is a member of the flowering plant family Lauraceae (Chen et al., 2020) and is divided into Mexican, Guatemalan and West Indian landraces (Nath et al., 2022). Mexican types are small and cold-hardy, whereas the West Indian race is not cold-hardy (Marais, 2004). It is one of the most economically important crops in the tropical and subtropical regions as an export fruit (Geremu et al., 2022; Perkins et al., 2019; Sharma et al., 2017). Avocado was deemed a "heart-healthy" food and was recommended as a dietary source of monounsaturated fatty acids by the Australian Heart Foundation. As a unique fruit, it contains excellent nutrients, oils, proteins, vitamins and carbohydrates (Daiuto et al., 2013; Pérez-Jiménez, 2008). Avocado is cultivated in more than 60 countries in the world, with 33 major avocado-producing countries, including Mexico, the United States, the Dominican Republic, Brazil, Israel, Indonesia, Haiti, Venezuela, Colombia, South Africa and Australia (Marais, 2004; Pérez-Jiménez, 2008). The world production of avocados was estimated at around 5,924,398 tonnes in 2017 (http://www.fao.org/).

In Thailand, avocado plants were initially cultivated in Nan province in the northern part about 90 years ago, and the planted area of avocado in Thailand increases every year, concentrated in the northern and north-eastern regions. It is an important fruit in Thailand and is exported to other Asian countries, including Hong Kong, Japan and Singapore (Traklumyingcharoen et al., 2015).

Avocado trees are attacked by various fungal pathogens that cause serious damage to roots, leaves, fruits, branches and trunks (Fuentes-Aragón et al., 2020; Guarnaccia et al., 2019). Anthracnose is a destructive disease that affects avocados worldwide,

Asian Journal of Mycology 7(2): 148–174 (2024)
www.asianjournalofmycology.org
ISSN 2651-1339
Article
Doi 10.5943/ajom/7/2/10

New species and new records of plant pathogenic fungi from northern Thailand

Armand A[1,2], Absalan S[2,3], Khongphinitbunjong K[1], Maharachchikumbura S[5], Kevin D. Hyde[2] and Jayawardena RS[1,2,4]

[1]*School of Science, Mae Fah Luang University, Chiang Rai 57100, Thailand*
[2]*Centre of Excellence in Fungal Research, Mae Fah Luang University, Chiang Rai 57100, Thailand*
[3]*Department of Biology, Faculty of Science, Chiang Mai University, Chiang Mai 50200, Thailand*
[4]*Kyung Hee University, 26 Kyungheedae-ro, Dongdaemun-gu, Seoul 02447, South Korea*
[5]*School of Life Science and Technology, University of Electronic Science and Technology, China*

Armand A, Absalan S, Khongphinitbunjong K, Maharachchikumbura S, Hyde KD, Jayawardena RS 2024 – New species and new records of plant pathogenic fungi from northern Thailand. Asian Journal of Mycology 7(2), 148–174, Doi 10.5943/ajom/7/2/10

Abstract

Plant pathogenic fungi are significant in agricultural ecosystems, causing substantial economic losses worldwide. Understanding their diversity and distribution by exploring the poorly studied niches is essential for agricultural and horticultural production and effective disease management strategies. In this study, we conducted a comprehensive survey of plant pathogenic fungi on the Mae Fah Luang University premises, Thailand. Through morphological and multi-gene phylogenetic analyses, eight new fungus-host and five new geographical records are reported. Additionally, a new species, *Neopestalotiopsis iridis*, is illustrated and described. The survey revealed a diverse assemblage of fungal pathogens infecting various plant hosts, including economically important crops and ornamental plants. Our findings contribute to the knowledge of fungal biodiversity in northern Thailand and provide valuable insights into new niches of the species. This study underscores the importance of continued research efforts to monitor plant pathogenic fungi in different niches to increase our understanding of species diversity, distributions and evolutionary relationships.

Keywords – *Bauhinia* sp. – *Iris pseudacorus* – Jack fruit – *Morinda citrifolia* – Niches – Phytopathogens

Introduction

Plant pathogenic fungi are a significant concern in agriculture, forestry, and natural ecosystems, causing diseases that lead to severe ecological problems and economic losses (Dayarathne et al. 2023). Determining the dynamic of interactions between plants and fungi in a particular ecological niche and creating efficient disease management plans requires an understanding of the diversity of plant pathogenic fungi (Burdon & Silk 1997). In the tropical setting of Thailand, with its unique climatic and ecological conditions, the prevalence and impact of plant pathogenic fungi necessitate detailed investigation (Ko et al. 2011, Withee et al. 2022).

Historically, the identification and characterization of plant pathogenic fungi have relied on classical morphological methods. However, recent advancements in molecular techniques have revolutionised fungal taxonomy, enabling more accurate identification and classification (Hariharan

Submitted 11 September 2024, Accepted 6 December 2024, Published 18 December 2024
Corresponding Author: Ruvishika S. Jayawardena – e-mail – ruvishika.jay@mfu.ac.th

CURRICULUM VITAE

NAME Alireza Armand

EDUCATIONAL BACKGROUND

2017–2020	Master of Bioscience Plant pathology Faculty of Agricultural Science, University of Guilan, Iran.
2013–2017	Bachelor of Bioscience Plant protection Faculty of Agricultural Science, University of Guilan, Iran.

WORK EXPERIENCE

2022–2024	Reaserch assistant Center of Excellence in Fungal Reseach
2019–2020	Reaserch assistant Mycology lab, University of Guilan, Iran.
2019–2020	Teaching Assistant Plant Pathology Lab, Department of Plant Protection, University of Guilan, Iran.

SCHOLARSHIP

2021-2024 (6 Semester)	Graduate division

PUBLICATION

Armand, A., Absalan, S., Khongphinitbunjong, K., Maharachchikumbura, S., & Jayawardena, R. S. (2024). New species and new records of plant pathogenic fungi from northern Thailand. *Asian Journal of Mycology*, *7*(2), 148–174.

Armand, A., & Jayawardena, R.S. (2023). Morpho-molecular identification and pathogenicity of *Colletotrichum* species associated with avocado anthracnose in northern Thailand. *Plant Pathology*, *73*, 186–197.

Armand, A., Hyde, K. D., Huanraluek, N., Wang, Y., & Jayawardena, R. S. (2023). Identification and characterization of *Colletotrichum* species associated with durian fruit in northern Thailand. *Mycosphere 14*(2), 107–129.

Armand, A., Hyde, K. D., & Jayawardena, R. S. (2023). First report of *Colletotrichum fructicola* causing fruit rot and leaf-tip dieback on pineapple in Northern Thailand. *Plants*, *12*(4), 971.

Armand, A., Bundhun, D., Bhunjun, C. S., Punyaboon, W., & Jayawardena, R. S. (2023). *Paramyrothecium amorphophalli* sp. nov., a causal agent of leaf blight on elephant foot yam in northern Thailand. *Current Research in Environmental & Applied Mycology (Journal of Fungal Biology)*, *13*(1), 57–67.

Armand, A., Fallahi, M., Absalan, S., Rathnayaka, A. R., Braun, U., Taylor, P.W.J., Khongphinitbunjong, K., McKenzie, E. H. C., Hyde, K. D., Al-Otibi F., & Jayawardena, R. S. (2025). Mango Microcosm: Unveiling the species diversity and pathogenic potential of fungi isolated from mango (*Mangifera indica*) in northern Thailand. *Fungal Biology* (in press).

Armand, A., Pourmoghaddam, M. J., Absalan, S., Fallahi, M., Wang, Y., Wang, Y., Li, L., Yang, H., Hyde, K. D., & Jayawardena, R. S., (2025). Fungal Footprints in the Tropics: Unveiling the species diversity of phytopathogenic genera associated with crops and ornamentals in northern Thailand. *Botanical Studies* (submitted).

Co-authorship

Absalan, S., Armand, A., Jayawardena, R. S., McKenzie, E. H., Hyde, K. D., & Lumyong S. (2024). Diversity of pleosporalean fungi isolated from rice (*Oryza sativa* L.) in northern Thailand and descriptions of five new species. *Journal of Fungi*, *10*(11), 763.

Aumentado, H. D. R., Armand, A., Phukhamsakda, C., Chetana, K. W. T., Norphanphoun, C., Hyde, K. D. … Jayawardena, R. S. (2024). Novel species, host records, and pathogenicity of *Allophoma* (*Didymellacaeae*) causing leaf spots on true mangroves and mangrove associates in Thailand. *Plant Pathology*, *73*(7), 1730–1748.

Aumentado, H. D. R., Armand, A., Phukhamsakda, C., Hyde, K. D., Jones, E. G., & Jayawardena, R. S. (2024). Polyphasic identification of two novel *Colletotrichum* species causing leaf spots on mangroves in Thailand. *European Journal of Plant Pathology*, *169*, 1–27.

Chethana, K. W. T., Rathnayaka, A. R., Samarakoon, B. C., Wu, N., Wijesinghe, S. N., Yasanthika, W. A. E., ... Hyde, K. D. (2023). AJOM new records and collections of fungi: 151–200. *Asian Journal of Mycology*, *6*(2), 89–243.

Fallahi, M., Armand, A., Jayawardena, R. S., & Hyde, K. D. (2024). Main pathogenic fungi and new related species affecting annual and perennial crops in northern Thailand. *MycoKeys* (submitted).

Hyde, K. D., Noorabadi, M. T., Thiyagaraja, V., He, M. Q., Johnston, P. R., Wijesinghe, S. N., Armand, A., … Zvyagina, E. (2024). The 2024 Outline of Fungi and fungus-like taxa. *Mycosphere*,*15*(1), 5146–6239.

Hyde, K. D., Abdel-Wahab, M. A., Abdollahzadeh, J., Abeywickrama, P. D., Absalan, S., Afshari, N., ... Ertz, D. (2023). Global consortium for the classification of fungi and fungus-like taxa. *Mycosphere*, *14*(1), 1960–2012.

Jayawardena, R. S., Hyde, K. D., Wang, S., Sun, Y. R., Suwannarach, N., Sysouphanthong, P., ... Wang, Y. (2022). Fungal diversity notes 1512–1610: Taxonomic and phylogenetic contributions on genera and species of fungal taxa. *Fungal Diversity*, *117*(1), 1–272.

Najafiniya, M., de Farias, A. R., Armand, A., Jungkhun, N., & Jayawardena, R. S. (2024). Characterization of *Colletotrichum* species obtained from citrus in northern Thailand and introducing a new host record for *C. plurivorum*. *Plant Pathology*, *73*(6), 1349–1362.